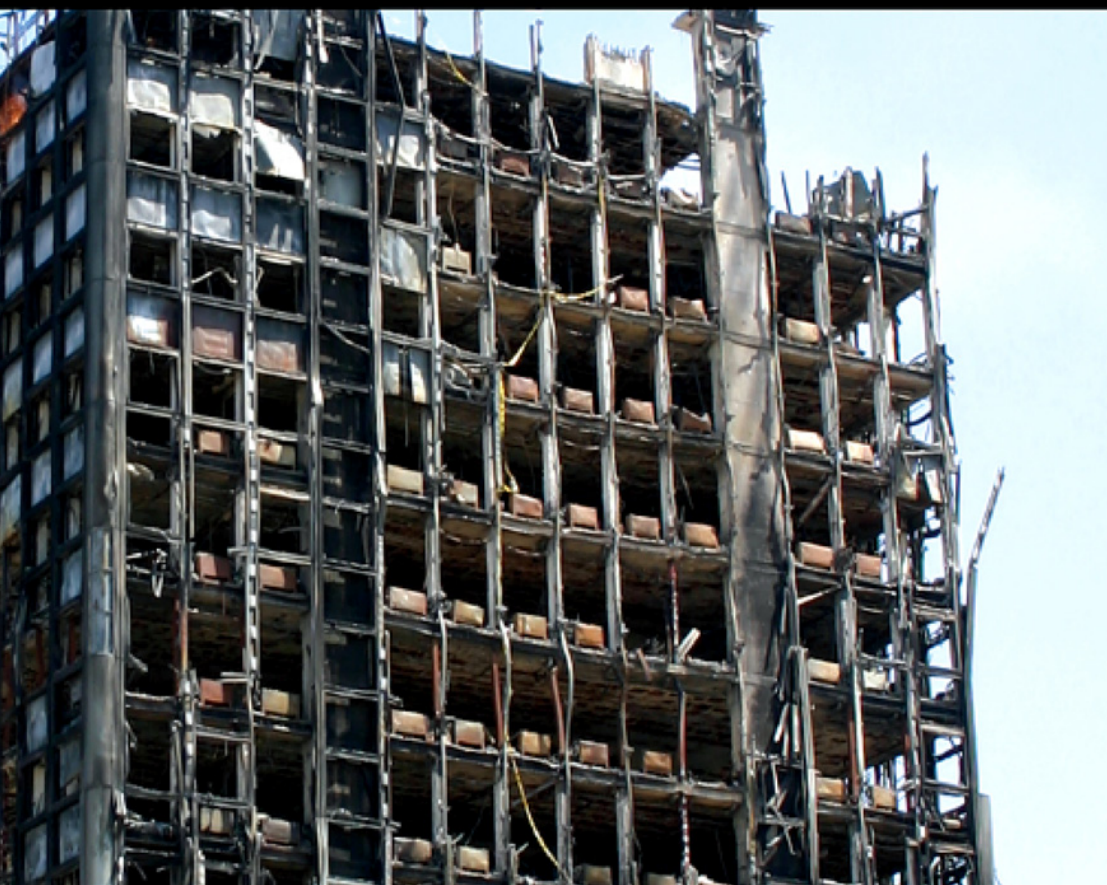


**SECOND EDITION**

**J. A. PURKISS**



# **FIRE SAFETY ENGINEERING**

**DESIGN OF STRUCTURES**

**B  
H**

# Fire Safety Engineering Design of Structures

**This page intentionally left blank**

# Fire Safety Engineering Design of Structures

---

Second Edition

John A. Purkiss  
BSc(Eng), PhD

Consultant,  
Formerly Lecturer,  
School of Engineering and Applied Science,  
Aston University, UK



ELSEVIER

Amsterdam • Boston • Heidelberg • London • New York • Oxford  
Paris • San Diego • San Francisco • Singapore • Sydney • Tokyo

Butterworth-Heinemann is an imprint of Elsevier



Butterworth-Heinemann is an imprint of Elsevier  
Linacre House, Jordan Hill, Oxford OX2 8DP, UK  
30 Corporate Drive, Suite 400, Burlington, MA 01803, USA

First edition 1996

Second edition 2007

Copyright © 2007 Elsevier Ltd. All rights reserved

No part of this publication may be reproduced, stored in a retrieval system or transmitted in any form or by any means electronic, mechanical, photocopying, recording or otherwise without the prior written permission of the publisher. Permissions may be sought directly from Elsevier's Science & Technology Rights Department in Oxford, UK: phone (+44) (0) 1865 843830; fax (+44) (0) 1865 853333; email: [permissions@elsevier.com](mailto:permissions@elsevier.com). Alternatively you can submit your request online by visiting the Elsevier web site at <http://elsevier.com/locate/permissions>, and selecting Obtaining permission to use Elsevier material

#### Notice

No responsibility is assumed by the publisher for any injury and/or damage to persons or property as a matter of products liability, negligence or otherwise, or from any use or operation of any methods, products, instructions or ideas contained in the material herein. Because of rapid advances in the medical sciences, in particular, independent verification of diagnoses and drug dosages should be made

#### **British Library Cataloguing in Publication Data**

A catalogue record for this book is available from the British Library

#### **Library of Congress Cataloging-in-Publication Data**

A catalog record for this book is available from the Library of Congress

For information on all Butterworth-Heinemann publications visit our web site at <a href="http://books.elsevier.com">books.elsevier.com</a>
---

Printed and bound in Great Britain  
07 08 09 10 10 9 8 7 6 5 4 3 2 1

ISBN-13: 978-0-7506-6443-1  
ISBN-10: 0-7506-6443-6

# Contents

---

<i>Preface to the second edition</i>	xiii
<i>Acknowledgements</i>	xvii
<i>Notation</i>	xxi
<b>Chapter 1: Fire safety engineering</b>	<b>1</b>
1.1 Design concerns	2
1.1.1 Control of ignition	3
1.1.1.1 Control of flammability	3
1.1.1.2 Control of growth of fire	3
1.1.1.3 Fire safety management	4
1.1.2 Means of escape	4
1.1.3 Detection and control of the fire	6
1.1.3.1 Fire detection	6
1.1.3.2 Smoke control	7
1.1.3.3 Fire-fighting systems	8
1.1.4 Compartmentation	9
1.1.5 Fire spread between structures	10
1.1.6 Structure collapse	10
1.2 Regulatory control	11
1.3 Fire precautions during construction and maintenance	11
1.4 Summary	12
1.4.1 Active measures	13
1.4.2 Passive measures	13
<b>Chapter 2: Design philosophies</b>	<b>14</b>
2.1 Ambient limit state design	14
2.2 Fire limit states	16
2.2.1 Load-bearing capacity criterion	17
2.2.2 Insulation criterion	18
2.2.3 Determination of partial safety factors	18

2.3	Assessment models	20
2.3.1	Assessment method – level 1	20
2.3.2	Assessment method – level 2	21
2.3.3	Assessment method – level 3	21
2.3.4	Practical considerations	21
2.4	Applicability of assessment levels	22
2.5	Interaction between active and passive measures	24
<b>Chapter 3: Prescriptive approach</b>		<b>26</b>
3.1	Standard fire test	26
3.2	Drawbacks to the fire test	32
3.2.1	Expense	32
3.2.2	Specimen limitations	33
3.2.3	Effect of restraint or continuity	33
3.2.4	Confidentiality of results	35
3.2.5	Loading	35
3.2.6	Failure modes	35
3.2.7	Reproducibility	36
3.3	Prescriptive determination of fire resistance	37
3.3.1	Concrete	39
3.3.2	Structural steelwork	40
3.3.3	Masonry	41
3.3.4	Timber	41
<b>Chapter 4: Behaviour of natural fires</b>		<b>43</b>
4.1	Development of compartment fires	43
4.1.1	Pre-flashover period	43
4.1.2	Post-flashover period	44
4.1.3	Decay phase	45
4.2	Factors affecting the growth phase	45
4.3	Calculation of compartment temperature–time responses	46
4.3.1	Basic formulation	46
4.3.1.1	Rate of heat release ( $\dot{h}_C$ )	47
4.3.1.2	Rate of heat loss by radiation through the openings ( $\dot{h}_R$ )	48
4.3.1.3	Rate of heat loss due to convection ( $\dot{h}_L$ )	48
4.3.1.4	Rate of heat loss through the compartment walls ( $\dot{h}_W$ )	48
4.3.1.5	Compartment temperature–time characteristics	48

4.3.2	Modifications to allow for other compartment configurations	50
4.3.2.1	Multiple vertical openings	50
4.3.2.2	Horizontal openings	50
4.3.2.3	Compartment construction	51
4.3.3	Calculation of fire load	51
4.3.3.1	Full calculation	52
4.3.3.2	Generic data	53
4.3.4	Parametric equation approach	53
4.3.4.1	Formulation due to Lie (1974)	54
4.3.4.2	EN 1991-1-2 approach	55
4.4	Estimation of fire characteristics	57
4.5	Fire severity and time equivalence	61
4.5.1	Fire severity	61
4.5.2	Time equivalence	62
4.5.2.1	Temperature base	62
4.5.2.2	Normalized heat load base	65
4.6	Localized fires	77
4.6.1	Plume fires	77
4.6.2	5 MW design fire	77
<b>Chapter 5: Properties of materials at elevated temperatures</b>		<b>78</b>
5.1	Thermal data	78
5.1.1	Steel	79
5.1.1.1	Density	79
5.1.1.2	Specific heat	79
5.1.1.3	Thermal conductivity	80
5.1.1.4	Thermal diffusivity	81
5.1.2	Concrete	81
5.1.2.1	Density	82
5.1.2.2	Specific heat	82
5.1.2.3	Thermal conductivity	84
5.1.2.4	Thermal diffusivity	86
5.1.3	Masonry	86
5.1.3.1	Density	87
5.1.3.2	Specific heat	87
5.1.3.3	Thermal conductivity	87
5.1.4	Timber	88
5.1.5	Aluminium	89
5.1.5.1	Density	89
5.1.5.2	Specific heat	89
5.1.5.3	Thermal conductivity	89

5.2	Materials data	90
5.2.1	Testing régimes	90
5.2.2	Steel	92
5.2.2.1	Strength characteristics	92
5.2.2.2	Unrestrained thermal expansion	93
5.2.2.3	Isothermal creep	96
5.2.2.4	Anisothermal creep data	96
5.2.3	Concrete	98
5.2.3.1	Stress–strain data	98
5.2.3.2	Creep	101
5.2.3.3	Free thermal expansion	102
5.2.3.4	Transient tests	104
5.2.3.5	Tensile strength of concrete at elevated temperature	106
5.2.3.6	Bond strength	106
5.2.3.7	High-strength (HSC) and self-compacting (SCC) concretes	106
5.2.3.8	Fibre concretes	110
5.2.3.9	Multi-axial behaviour	113
5.2.4	Timber	113
5.2.4.1	Rate of charring	114
5.2.4.2	Strength and elasticity loss	115
5.2.5	Masonry	117
5.2.6	Aluminium	117
5.2.6.1	Strength data	117
5.2.6.2	Thermal expansion	119
5.3	Constitutive stress–strain laws	119
5.3.1	Steel	121
5.3.1.1	Elastic strain	121
5.3.1.2	Creep	124
5.3.1.3	Design curves	127
5.3.2	Concrete	129
5.3.2.1	Anderberg and Thelandersson	132
5.3.2.2	Diederichs	134
5.3.2.3	Khoury and Terro	135
5.3.2.4	Khennane and Baker	136
5.3.2.5	Schneider	138
5.3.2.6	Li and Purkiss	140
5.3.3	Design code provisions for stress–strain behaviour	140
<b>Chapter 6: Calculation approach</b>		<b>142</b>
6.1	Thermal analysis	143
6.1.1	Governing equation and boundary conditions	143
6.1.2	Finite element solution of the heat transfer problem	147

6.2	Calculation of temperature in timber element	154
6.3	Structural analysis	154
6.3.1	Calculation of structural responses using simple approaches	155
6.3.2	Calculation of structural responses using finite element analysis packages	158
6.4	Examples	161
<b>Chapter 7: Design of concrete elements</b>		<b>168</b>
7.1	Calculation of temperatures	169
7.1.1	Graphical data	169
7.1.1.1	The ISE and Concrete Society design guide (1978)	169
7.1.1.2	FIP/CEB report (1978)	169
7.1.1.3	EN 1992-1-2	169
7.1.2	Empirical methods	170
7.1.2.1	Wickström's method	170
7.1.2.2	Hertz's method	171
7.1.3	Values of thermal diffusivity	173
7.1.4	Position of the 500°C isotherm	174
7.2	Simple calculation methods	175
7.2.1	Calculation of load effects	175
7.2.1.1	Direct calculation	175
7.2.1.2	Indirect calculation	175
7.2.2	Materials' partial safety factors	176
7.2.3	Methods of determining section capacity	176
7.2.3.1	Reduced section method (500°C isotherm)	176
7.2.3.2	Method of slices (zone method)	180
7.3	Columns	191
7.4	Comparisons between the methods of calculation	196
7.5	Design and detailing considerations	197
7.5.1	Shear	197
7.5.2	Bond	197
7.5.3	Spalling	198
7.5.3.1	Moisture content	198
7.5.3.2	Concrete porosity and permeability	198
7.5.3.3	Stress conditions	199
7.5.3.4	Aggregate type	200
7.5.3.5	Section profile and cover	200
7.5.3.6	Heating rate	200
7.5.3.7	Concrete strength	201
7.5.4	High strength concrete and self-compacting concrete	201
7.5.5	Detailing	201

<b>Chapter 8: Design of steel elements</b>	<b>203</b>
8.1 Calculation of temperatures	203
8.1.1 Basic principles	203
8.1.2 Heat flow in uninsulated steelwork	205
8.1.3 Heat flow in insulated steelwork	206
8.1.3.1 ECCS method of calculation	206
8.1.3.2 EN 1993-1-2 approach	207
8.1.4 Effect of moisture	208
8.1.4.1 Effective density of insulation	208
8.1.4.2 Delay time	208
8.1.5 Empirical approach for the calculation of temperatures	209
8.1.5.1 Bare steelwork	209
8.1.5.2 Protected steelwork	209
8.1.6 Calculation of $A_m/V$	210
8.1.7 Thermal properties of insulation materials	210
8.2 Design of non-composite steelwork	220
8.2.1 Determination of structural load in the fire limit state	220
8.2.2 EN 1993-1-2 approach for the determination of structural fire capacity	220
8.2.2.1 Background to the EuroCode method	220
8.2.2.2 EuroCode methods	222
8.3 Other steelwork constructions	241
8.3.1 External steelwork	241
8.3.2 Shelf angle floors	241
8.4 Stainless steel	247
8.5 Methods of protection	247
8.5.1 Types of protection	247
8.5.1.1 Board systems	247
8.5.1.2 Spray protection	248
8.5.1.3 Intumescent paints	248
8.5.1.4 Brickwork/blockwork	248
8.5.1.5 Concrete encasement	248
8.5.1.6 Manufacturer's data	249
8.5.2 Connections	250
8.5.3 Ageing of and partial loss of protection	251
8.5.3.1 Ageing effects	251
8.5.3.2 Partial loss of protection	252
<b>Chapter 9: Composite construction</b>	<b>253</b>
9.1 Composite slabs	253
9.1.1 Insulation requirement	253
9.1.1.1 Calculation approach	254
9.1.1.2 Effective thickness	254

9.1.2	Load-bearing capacity	255
9.1.2.1	Calculation of moment capacity	256
9.2	Composite beams	266
9.2.1	Critical temperature approach	267
9.2.2	Full moment calculation	267
9.3	Composite steel and concrete columns	275
9.3.1	Concrete filled rolled hollow steel columns	275
9.3.1.1	EN 1994-1-2	275
9.3.1.2	Empirical methods	276
9.3.2	Web-infilled columns	277
<b>Chapter 10:</b>	<b>Design of timber elements</b>	<b>278</b>
10.1	Design to EN 1995-1-2	278
10.1.1	Depth of charring	278
10.1.1.1	Exposure to the standard furnace curve	278
10.1.1.2	Charring to parametric exposure (Annex A)	279
10.1.2	Calculation of structural capacity	281
10.1.2.1	Effective section method	281
10.1.2.2	Reduced strength and stiffness method	281
10.2	Empirical approaches	286
10.2.1	Approach developed by Ödeen	286
10.2.2	Approach developed by Lie for beams	288
10.2.3	Empirical determination of fire endurance for columns	289
10.2.4	Approach developed by Stiller	291
10.2.4.1	Beams	292
10.2.4.2	Columns	292
10.3	Timber floors and protected timber systems	294
10.3.1	Timber floors	294
10.3.2	Protected timber systems	294
<b>Chapter 11:</b>	<b>Masonry, aluminium, plastics and glass</b>	<b>297</b>
11.1	Masonry	297
11.1.1	Insulation requirements of masonry construction	297
11.1.2	Thermal bowing	298
11.1.3	Load-bearing cavity walls	299
11.2	Aluminium	300
11.3	Plastics and plastic-based composites	301
11.4	Glass	302

<b>Chapter 12: Frames</b>	<b>303</b>
12.1 Tests on isolated frames and connections	303
12.1.1 Frame tests	303
12.1.2 Fire tests on beam and column assemblies	304
12.2 Tests on the large frame structures at Cardington	305
12.2.1 Timber frame structure	305
12.2.2 Concrete frame structures	306
12.2.3 Composite steel frames	308
12.3 Pitched roof portals	316
<b>Chapter 13: Assessment and repair of fire-damaged structures</b>	<b>323</b>
13.1 Visual inspection	323
13.1.1 Stability	323
13.1.2 Estimation of fire severity	324
13.2 Damage assessment	326
13.2.1 Structural survey	326
13.2.2 Materials testing	327
13.2.2.1 Concrete	327
13.2.2.2 Steel	335
13.3 Strength assessment of the structure	335
13.3.1 Residual properties	336
13.3.1.1 Concrete	336
13.3.1.2 Structural steel	339
13.3.1.3 Reinforcing and pre-stressing steels	340
13.3.1.4 Cast and wrought iron	340
13.3.1.5 Masonry	341
13.3.2 Determination of temperatures within an element	341
13.4 Methods of repair	343
13.5 Demolition of fire-damaged structures	345
<b>Chapter 14: Postscript</b>	<b>347</b>
<b>References</b>	<b>349</b>
<b>Author index</b>	<b>377</b>
<b>Subject index</b>	<b>383</b>

## Preface to the second edition

---

Since the publication of the First Edition of this book, substantial progress has occurred in Structural Fire Safety Engineering which has necessitated the production of a Second Edition. However, the author must report the death of two personally influential figures noted in the acknowledgements to the first edition, namely Bill Malhotra and Tony Morris, and the retirement of the third, Bob Anchor.

The intention behind this text remains provision to those involved in aspects of the design of structures to withstand the accidental effects due to fire occurring within part or the whole of the structure and of the tools required to enable such a design to be carried out. One of the major revisions is that the author has concentrated on the European Design Codes rather than British Standards which will in the course of the next five years become effectively obsolete. However, the designer should still be aware that any design code is subject to revision or amendment and that it is essential that the most recent edition be used, and that where this produces a discrepancy between this text and the Code, the Code must be taken as the final arbiter.

The second major revision has been due to the impact of the large-scale fire tests carried out at Cardington. This has meant there has had to be a re-assessment of the behaviour of composite steel–concrete frame structures, in that the whole structure performance markedly outweighs that of single elements. Equally, there are a number of guides produced by either the Institution of Structural Engineers or the Building Research Establishment promoting Structural Fire Safety Engineering.

The best available texts were used for the EuroCode material as some of the EuroCodes had not at the time when this text was prepared been finally approved or released by CEN (Comité Européen de Normalisation) for publication by the appropriate National Standards Organization. It is thus possible that there might be discrepancies between this text and the final published EN versions of the EuroCodes. It is hoped such variations are slight and will mostly be concerned with interpretive matters or notation and not basic principles.

For the EuroCodes no account has been taken directly of National Annexes, i.e. any nationally determined parameters are taken at recommended values and not amended to conform to a particular country's National Annex. The user of this text is presumed to have knowledge of structural mechanics and a background in the methods of structural design at ambient conditions since the design of structures at the fire limit state either uses modified ambient design methods or requires data such as member capacities from the ambient design. Some knowledge of the thermodynamics of heat transfer will also be useful. A series of worked examples has been included to provide a feel for the type of calculations possible. To assist in gaining a better understanding of the principles and procedures involved in fire safety engineering an extensive reference section is found at the rear of the text.

It has to be recognized that fire design must be envisaged as part of the overall design of the structure and not an item to be considered at the very end. To help the designer to obtain a full picture of the full design decisions required, the first chapter provides an overview of the complete field.

Certain acronyms appear with a high degree of regularity in the text. It was felt that these needed clarification, and that the preface was the most appropriate place:

ASCE	American Society of Civil Engineers
ASFP	Association for Specialist Fire Protection
BRE	Building Research Establishment (Garston, England)
CEB	Comité Euro-International du Béton
CIB	Conseil Internationale du Bâtiment pour la Recherche l'Étude et la Documentation (International Council for Building Research Studies and Documentation)
CIRIA	Construction Industry Research and Information Association (London)
ECCS	European Convention for Construction Steelwork
FIP	Fédération Internationale de la Précontrainte
ISE	Institution of Structural Engineers (London)
ISO	Organisation Internationale de Normalisation (International Organization for Standardization)
RILEM	Réunion Internationale des Laboratoires d'Essais et de Recherches sur les Matériaux et les Constructions (International Union of Testing and Research Laboratories for Materials and Structures)
SCI	Steel Construction Institute

### **Note on Temperature Units**

The conventional unit for temperature, namely the degree Celsius, has been used rather than the absolute measure (the degree Kelvin). This generally causes no problem except in heat transfer calculations when for the radiation component the degree Kelvin must be used. Also there are some empirical formulae which require the use of the degree Kelvin.

**This page intentionally left blank**

# Acknowledgements

---

The author would like to thank H.L. (Bill) Malhotra, W.A. Morris and R.D. Anchor for their valuable support and advice over many years. Thanks are also extended to Colin Bailey, Tom Lennon and Gerald Newman for their advice and encouragement.

The author would like to thank his colleague L-Y Li for writing Chapter 6.

Gratitude is also expressed to his Post-doctoral Research Fellow, Rosen Tenchev, and various Postgraduate Research Students, Sarah Guise, Bahjat Khalafallah, Raymond Connolly, Kamal Mustapha, Abderahim Bali and Nick Weeks who have assisted, often unwittingly, by discovering references, providing ideas and stimuli or by commenting on early versions of the text of the first edition.

His thanks are also expressed to Dr J.W. Dougill without whom this book would not have been possible, as many years ago John was responsible for kindling the flames as a research supervisor.

Thanks are also due to many individuals, too many to name individually, working in the field who have given their time and experience to deal with queries and questions.

The usual disclaimer must be made that in the final event any opinions expressed herein are entirely those of the author and that he alone is responsible for sins of either omission or commission.

The author also wishes to thank the following for graciously granting permission for material to be incorporated in this text:

- American Concrete Institute (Figs 5.15, 5.16, 5.24 and 13.5)
- American Society of Civil Engineers (Figs 5.23 and 5.34)
- The American Society of Testing and Materials (Figs 5.9 and 5.10)
- British Standards Institution

Code	BSI Ref	Book Ref
EN 1991-1-2	Table E5	Table 4.4
	Table F2	Table 4.7

EN 1992-1-2	Table 3.1 Fig B.2	Table 5.8 Fig 7.1
EN 1993-1-2	Fig 3.1 Table 3.1	Fig 5.31, Table 5.3 Table 5.6
EN 1994-1-2	Table 3.3 Fig D.1 Fig D.2 Fig D.3 a&b Table D.5 Table D.6	Table 5.8 Fig 9.1 Fig 9.3 Fig 9.4 Table 9.2 Table 9.1
EN 1995-1-2	Table 3.1 Table E.2	Table 10.1 Table 10.3
BS 5950: Part 8	Fig C.1 Fig C.2 Table C.1	Fig 8.8 Fig 8.8 Table 8.4
PD 7974-3	Table 4	Table 4.7

- British Steel (now Corus) Technical (Swinden Laboratories) (Fig. 13.4)
- Building Research Establishment (copyright material reproduced by permission of the Controller of HMSO) (Figs 4.6, 6.1, 5.15 and 13.5; Tables 4.5, 13.1 and 13.3)
- Chapman and Hall (Design of Structures against Fire (1986), originally published by Elsevier Applied Science) (Figs 8.5 and 8.76)
- Messrs Dunod Publishers (Matériaux et Constructions) (Figs 5.7 and 5.8)
- Elsevier Sequoia: Fire Safety Journal: Figs 3.4, 4.2, 5.14, 8.5 and 12.2; Tables 2.1, 4.2, 4.3, 4.6 and 9.3  
Solids and Structures: Fig. 7.6  
Engineering Structures: Fig. 6.6
- The Institution of Mechanical Engineers (by permission of Council) (Fig. 5.27)
- The Institution of Structural Engineers (Structural Engineer and 1978 Design Guide) (Fig. 5.11; Table 12.1)
- Lund Institute of Technology (Figs 5.10, 5.19, 5.21 and 5.33)
- H.L. Malhotra (Design of Fire Resisting Structures (1982), Surrey University Press) (Figs 5.1, 5.2 and 5.6; Table 8.1)
- National Research Council of Canada (Canadian Journal of Civil Engineering) (Table 10.2)
- Norwegian Institute of Technology (Fig. 6.9)
- Portland Cement Association (Fig. 5.16)

- RILEM (with special thanks to the Editors of the two Reports on High Temperature Properties; Yngve Anderberg and Ulrich Schneider) (Figs 5.3, 5.4, 5.5, 5.12, 5.13, 5.20 and 5.22; Tables 5.3 and 5.7)
- Society of Wood Science and Technology (Wood and Fiber Science) (Fig. 5.25),
- Swedish Institute of Steel Construction (Figs 4.4, 4.5 and 5.2; Table 4.1),
- Technical University of Denmark (Table 7.1)
- John Wiley and Sons (Fire and Materials) (Fig. 5.16)
- J. Witteveen BRE (1983) (Fig. 2.2)
- Thomas Telford Limited (Magazine of Concrete Research Figs 5.5 and 13.5, Table 13.3)

Whilst the author has made every attempt to contact possible copyright holders and authors, he apologizes if material has been included for which copyright clearance was for whatever reason overlooked. He would be grateful to receive details in order that such omissions can be corrected in any future editions.

**This page intentionally left blank**

# Notation

---

$A$	Roof pitch parameter, steel creep parameter, stress parameter (Khennane and Baker)
$A_c$	Area of concrete cross section
$A_f$	Area of floor of a compartment
$A_h$	Area of horizontal openings
$A_m$	Area of steel protection per unit length exposed to fire
$A_r$	Area of reinforcement, area of residual timber section
$A_s$	Area of tension steel, air space
$A_{s1}$	Area of tension steel resisting concrete compression
$A_{s2}$	Area of tension steel resisting steel compression
$A_t$	Total internal area of a compartment
$A_v$	Shear area, area of vertical openings
$a$	Axis distance from concrete surface to centroid of reinforcing bar(s), thermal diffusivity
$a_a$	Thermal diffusivity of steel
$a_c$	Thermal diffusivity of concrete
$a_w$	Thermal diffusivity of wood
$a_z$	Width of damage zone
$a_1$ to $a_6$	Parameters for determination of protection thicknesses
$B$	Parametric length, steel creep parameter, stress parameter (Khennane and Baker), width of section
$B_e$	Width of bottom flange of a shelf angle floor
$b$	Reduced width, thermal inertia, width of concrete compression stress block, flange width
$b_{eff}$	Effective width of slab on composite beam
$b_{fi}$	Temperature modified width of concrete compression stress block
$b_v$	Parameter dependant on openings ratio ( $\alpha_v$ )
$b_w$	Depth of web

xxii *Notation*

$b_1$	Width of bottom flange of steel beam
$b_2$	Width of top flange of steel beam
$C$	Constant, roof pitch parameter, steel creep parameter, temperature–time dependant boundary parameter (Hertz)
$C_1, C_2$ and $C_3$	Creep parameters (Schneider)
$\mathbf{C}$	Global capacitance matrix
$\mathbf{C}_e$	Element capacitance matrix
$c$	Parameter for equivalent fire resistance, specific heat, web depth, flange outstand
$c_a$	Specific heat of steel
$c_{al}$	Specific heat of aluminium
$c_c$	Specific heat of concrete
$c_p$	Specific heat of combustion gases, specific heat of protection
$c_{p,peak}$	Peak value allowing for moisture of specific heat of concrete
$c_{pm}$	Specific heat of masonry
$c_{pw}$	Specific heat of timber
$c_v$	Volumetric specific heat
$D$	Depth of compartment, overall section depth, steel creep parameter, temperature–time dependant boundary parameter (Hertz)
$D_e$	Height to underside of slab (shelf angle floor)
$d$	Depth, effective depth, shear stud diameter
$d_{char}$	Depth of charring
$d_{char,b}$	Depth of charring on the bottom of a beam (Stiller)
$d_{char,col}$	Depth of charring on a column (Stiller)
$d_{char,s}$	Depth of charring on the side of a beam (Stiller)
$d_{char,n}$	Depth of charring for multi-face exposure
$d_{char,0}$	Depth of charring for single-face exposure
$d_{fi}$	Temperature modified effective depth
$d_{ef}$	Effective reduced section
$d_{fi}$	Temperature modified effective depth
$d_p$	Protection or insulation thickness
$d_{wall}$	Wall thickness
$d_0$	Additional reduction in section dimensions
$E$	Height of stanchion, Young's Modulus, temperature–time dependant boundary parameter (Hertz)
$E_c$	Young's Modulus of concrete
$E_{c,\theta}$	Temperature affected Young's Modulus of concrete
$E_{cm}$	Young's Modulus for concrete
$E_{cm,\theta}$	Temperature affected Young's Modulus of concrete

$E_c^*$	Slope of descending branch of concrete stress–strain curve
$E_d$	Design effect
$E_{fi,d}$	Design effect of a fire
$E_{fi,d,t}$	Design effect of a fire at time $t$
$E_r$	Young’s Modulus of reinforcement
$E_s$	Young’s Modulus of steel
$E_{s,\theta}$	Young’s Modulus of steel at temperature $\theta$
$E_{stat,\theta}$	Static Young’s Modulus for concrete at elevated temperature
$E_{dyn,\theta}$	Dynamic Young’s Modulus for concrete at elevated temperature
$E_t$	Slope of linear section of stress–strain curve at time $t$ (Khennane and Baker)
$e$	Enhancement factor due to membrane action
$e_w$	Thickness of web
$e_1$	Thickness of bottom flange of steel beam
$e_2$	Thickness of top flange of steel beam
$F$	Force, steel creep parameter, surface area exposed to fire
$F_f$	Axial load in the fire limit state
$F_i$	Thermal forces ( $i = 1, 2, 3$ )
$F_s$	Tensile force in reinforcement
$f$	Overdesign factor for timber members
$f_{amax,\theta cr}$	Steel strength at critical design temperature
$f_{amax,\theta w}$	Temperature-reduced steel strength of web
$f_{amax,\theta 1}$	Temperature-reduced steel strength of top flange of steel beam
$f_{amax,\theta 2}$	Temperature-reduced steel strength of bottom flange of steel beam
$f_{ay,20^\circ C}$	Ambient steel design strength
$f_{c,20^\circ C}$	Ambient cylinder strength of concrete
$f_{c,\theta}$	Temperature dependant concrete strength, stress applied to concrete at start of heating
$f_{cd}$	Concrete design strength based on cylinder strength
$f_{ck}$	Characteristic strength of concrete at ambient (also $f_{ck,20}$ )
$f_k$	Characteristic strength, modification factor for compartment boundary conditions or horizontal openings
$f_{mean}$	Mean strength
$f_{sd,fi}$	Temperature-reduced tension reinforcement strength
$f_{scd,fi}$	Temperature-reduced compression reinforcement strength
$f_t$	Partial derivative of strain with respect to time
$f_u$	Ultimate strength of steel

$f_y, f_{yk}$	Characteristic or yield strength of reinforcement (also $f_{yk,20}$ )
$f_\theta$	Partial derivative of strain with respect to temperature
$f_\sigma$	Partial derivative of strain with respect to stress
$f_1, f_2$ and $f_3$	Temperature–time coordinate functions (Hertz)
$G$	Distance between ends of haunches in a portal frame, shear modulus, temperature gradient parameter
$G_k$	Characteristic permanent structural load
$g$	Temperature-dependant stress function (Schneider), acceleration due to gravity
$g_0$	Parameter defined by depth of compression block
$g_{2,\theta}$	Parameter for strength reduction of stainless steel
$H$	Height of windows or vertical openings, horizontal reaction, steel creep parameter
$H_t$	Strain hardening parameter at time $t$ (Khennane and Baker)
$H_{u,i}$	Calorific value of compartment fire load
$h$	Overall section depth, height
$h_c$	Overall slab depth
$h_{cr}$	Limiting depth to 250°C isotherm for a composite slab
$h_{eff}$	Effective (equivalent) depth of a profiled concrete composite deck
$h_u$	Depth of concrete stress block in a composite slab
$h_w$	Overall height of web
$h_{wall}$	Height of wall
$h_1$	Depth of trough for profile sheet decking, vertical distance between horizontal opening and mid-height of vertical opening
$h_2$	Depth of concrete above trough in a composite deck
$h_B$	Heat stored in the gas
$\dot{h}_c$	Rate of heat release from compartment
$\dot{h}_L$	Rate of heat loss due to convection
$\dot{h}_R$	Rate of heat loss through openings
$\dot{h}_W$	Rate of heat loss through walls
$\dot{h}_{net}$	Net design heat flow due to convection and radiation at the boundary
$\dot{h}_{net,c}$	Net rate of heat transmission at boundary due to convection
$\dot{h}_{net,r}$	Net rate of heat transmission at boundary due to radiation
$\bar{h}'$	Normalized heat load in a compartment
$\bar{h}''$	Normalized heat load in a furnace
$I$	Second moment of area
$I_a$	Second moment of area of steel section

$I_c$	Second moment of area of concrete
$I_r$	Second moment of area of reinforcement
<b>I</b>	Identity matrix
$i$	Radius of gyration
$J(\theta, \sigma)$	Unit stress compliance function (Schneider)
$K$	Coefficient of overall heat transfer, concrete buckling parameter, constant of proportionality in equivalent fire duration, parameter in the Ramburg–Osgood equation, portal frame parameter dependant on number of bays
<b>K</b>	Global matrix
$\mathbf{K}_c$	Global conductance matrix
$\mathbf{K}_{ce}$	Element conductance matrix ( $i = 1, 2, 3$ )
$K_{ij}$	Matrix coefficients ( $i, j = 1, 2, 3$ )
$k$	Ratio between strength and induced stress, constant of proportionality between transient and free thermal strain, parameter, property ratio, timber buckling parameter
$k_{E,\theta}$	Temperature reduction factor for Young's Modulus of steel
$k_{LT}$	Moment correction factor for lateral torsional buckling
$k_{amax,\theta}$	Temperature modification factor for steel strength
$k_b$	Factor dependant on compartment thermal boundaries
$k_c$	Temperature modification factor for concrete strength, correction factor for time equivalence on unprotected steelwork, timber strut buckling parameter
$k_{c,m}$	Reduction factor for mean concrete strength
$k_{mod,f}$	Modification factors applied to timber strengths and elastic modulus
$k_s$	Strength reduction factor due to temperature for steel
$k_{shadow}$	Shadow factor for determination of steel temperatures on bare steelwork
$k_y$	Moment correction factor
$k_{y,\theta}$	Reduction factor on yield strength due to temperature
$k_z$	Moment correction factor
$k_1$	Constant relating loss in UPV and strength
$k_2$	Constant of proportionality between transient and free thermal strain, constant relating loss in UPV and strength
$L$	Span, temperature dependant boundary condition parameter for the cooling period (Hertz)
$LITS$	Load induced thermal strain (Khoury)
$\bar{L}_e$	Effective or system length
$L_{f,d}$	Design fire load in kg of wood per unit floor area
$L_{fi,k}$	Total design fire load in kg of wood equivalent

$L_r$	Heated perimeter for profile decking
$l_1, l_2, l_3$	Dimensions of profile sheet steel decking
$l_\theta$	Effective length in the fire limit state
$M$	Bending moment, moisture content, number of elements in the solution domain
$M_{b,fi,t,d}$	Design bending strength in the fire limit state
$M_{fi,Rd}$	Design resistance moment in the fire limit state
$M_{fi,\theta,d}$	Applied design moment in the fire limit state
$M_{fr}$	Moment capacity in the fire limit state
$M_{k,i}$	Characteristic mass
$M_{pl}$	Plastic moment capacity
$M_y$	Bending moment about the $zz$ axis
$M_z$	Bending moment about the $yy$ axis
$M_{Rd}$	Moment of resistance
$M_{Sd}$	Ambient design moment
$M_{Ed,fi}$	Applied moment in the fire limit state
$M_U$	Moment capacity in the fire limit state of concrete in flexure
$M_{U1}$	Moment capacity in the fire limit state of the tensile reinforcement for concrete in flexure
$M_{U2}$	Moment capacity in the fire limit state of the compression reinforcement for concrete in flexure
$M_{y,fi,Ed}$	Moment applied about the $zz$ axis
$M_{z,fi,Ed}$	Moment applied about the $yy$ axis
$m$	Fuel load factor
$m_{p\theta}$	Temperature reduced moment capacity of slab
$m_\theta$	Strain hardening parameter
$m_F$	Rate of mass flow of outflow gases
$N$	Number of shear studs per half length of beam
$\mathbf{N}$	Interpolation matrix
$N_{fi,cr}$	Axial design resistance based on buckling
$N_{fi,Rd}$	Axial design resistance
$N_{fi,pl,Rd}$	Axial plastic load capacity in the fire limit state
$N_{fi,\theta,d}$	Required axial load capacity in the fire limit state
$N_i$	Interpolation function defined at node $i$
$N_x$	Axial membrane force
$N_{Rd}$	Axial capacity or resistance
$n$	Exponent, parameter in Popovics equation, parameter in Ramburg–Osgood equation, number of slices, number of nodes in an element, normal of the surface
$n_w$	Time-dependant parameter (Wickström)
$n_x, n_y$	Distance (coordinate) parameter (Wickström)
$\hat{n}$	Normal of the element boundary
$O$	Opening factor

$P_{fi,Rd}$	Shear stud capacity in the fire limit state
$P_{or}$	Initial concrete porosity
$p$	Moisture content in per cent by weight, perimeter of residual timber section
$p_{2,\theta}$	Temperature reduced 2% proof strength of stainless steel
$p_{0,2proof,\theta}$	Temperature reduced 0,2% proof strength of stainless steel
$Q_{fi,k}$	Total characteristic fire load
$Q_k$	Characteristic load
$Q_{k,I}$	Characteristic variable load
$Q_{mean}$	Mean load
$\mathbf{Q}$	Heat flow vector
$q$	Uniformly distributed load, vector of heat flux per unit area
$q_{p\theta,slab}$	Load carried by slab
$q_{p\theta,udl}$	UDL supported by the beam
$q_{fi,d}$	Uniformly distributed load in the fire limit state
$q_{f,d}$	Design fire load per unit floor area
$q_{f,k}$	Generic fire load
$q_t$	Fire load per unit area of compartment
$q_{t,d}$	Design fire load per unit area of compartment boundary
$q_x$	Axial distributed load
$q_y$	Transversely distributed load in $y$ -direction
$q_z$	Transversely distributed load in $z$ -direction
$q_{sd}$	Plastic distributed load in the fire limit state
$q_{sd,el}$	Elastic design distributed load in the fire limit state
$R$	Rate of burning in kg of wood equivalent per second, resistance
$R_d$	Design resistance effect
$R_{fi,d}$	Design resistance effect in the fire limit state
$R_1$	Length of portal frame rafter
$\mathbf{R}$	Global nodal vector
$\mathbf{R}_Q$	Global nodal vector of internal heat source
$\mathbf{R}_{Qe}$	Element nodal vector of internal heat source
$\mathbf{R}_q$	Global nodal vector of heat flow
$\mathbf{R}_{qe}$	Element nodal vector of heat flow
$r$	Radius of arris, fillet radius
$S$	Frame spacing, specific gravity of timber, initial water saturation
$S_d$	Fire effect due to structural loads (actions)
$SIG1$	Changeover stress for calculating steel creep
$T$	Tensile force resultant in a composite beam
$t$	Time
$t_d$	Fire duration based on design fire load

xxviii *Notation*

$t_{eff}$	Effective thickness of a masonry wall
$t_{e,d}$	Equivalent fire duration
$t_f$	Flange thickness
$t_{fi,d}$	Calculated fire resistance based on member performance
$t_{fi,requ}$	Design or required fire performance based on a classification system
$t_j$	Time at step $j$ ( $j = k, k + 1, \beta$ )
$t_{lim}$	Limiting value of $t_{max}$ due to fire type
$t_{max}$	Time to maximum temperature for a parametric fire
$t_{spall}$	Time to spalling
$t_v$	Delay time to allow for moisture
$t_w$	Web thickness
$t_0$	Time to maximum charring under parametric conditions
$t^*$	Parametric time for determining compartment temperature–time response
$t_d^*$	Parametric fire duration
$t_{max}^*$	Maximum value of $t^*$
$\bar{t}$	Time shift
$\bar{t}_{E,d}$	Mean test result
$U$	Creep activation energy
$U_{c,20}$	Ambient ultrasonic pulse velocity
$U_{c,\theta}$	Temperature modified ultrasonic pulse velocity
$U_{s,\theta}$	Temperature-reduced ultimate strength of stainless steel
$u$	Axial displacement
$u_x$	Correction factor for non-standard concrete diffusivity (Wickström)
$u_1, u_2, u_3$	Distances to reinforcement from face of trough of steel decking
$V$	Shear force, vertical reaction, volume of steel
$V_{fi,t,d}$	Design shear capacity in the fire limit state
$V_{Rd}$	Shear resistance
$V_i$	Volume of steel per unit length
$v$	Deflection in $y$ -direction
$W$	Compartment width, water content
$W_{el}$	Elastic section modulus
$W_{fi,d}$	Design structural fire load
$W_{pl}$	Plastic section modulus
$w$	Compartment geometry factor, moisture content percentage by weight, half width of section, deflection in $z$ -direction
$w_f$	Ventilation factor
$X_1$	Distance to end of haunch
$X_2$	Distance to centroid of loading on the haunch

$x$	Cartesian coordinate, depth of neutral axis (reinforced concrete), distance, factor dependant upon $t_{max}$ and $t_{lim}$
$x_n$	Depth to centroidal axis
$x_{spall}$	Depth of spalling
$Y$	Height to end of haunch
$y$	Cartesian coordinate, distance
$y_T$	Height to line of action of tensile force
$Z$	State function, Zener–Hollomon parameter
$z$	Cartesian coordinate, distance parameter, lever arm (tension steel)
$z'$	Lever arm (compression steel)
$\alpha$	Angle of rotation of stanchion, coefficient of total heat transfer, interpolation parameter, modification factor for shear stud capacity, ratio of ultimate strength at elevated temperature to ambient strength for timber, coefficient of thermal expansion, aspect ratio (<1,0), angle of decking
$\alpha_c$	Coefficient of convective heat transfer
$\alpha_{cc}$	Concrete load duration factor
$\alpha_{eff}$	Coefficient of effective heat transfer
$\alpha_h$	Ratio of horizontal compartment openings to floor area
$\alpha_m$	Coefficient of thermal expansion of masonry, surface absorption
$\alpha_r$	Coefficient of radiative heat transfer
$\alpha_v$	Ratio of area of vertical openings in a compartment to the floor area
$\beta$	Interpolation parameter, statistical acceptance/rejection limit, algorithm parameter
$\beta_c$	Imperfection factor for timber strut buckling
$\beta_n$	Charring rate including an allowance for arris rounding
$\beta_{par}$	Charring rate due to parametric exposure
$\beta_{M,LT}$	Moment gradient correction factor
$\beta_{M,y}$	Moment gradient correction factor
$\beta_{M,z}$	Moment gradient correction factor
$\beta_0$	Uniform charring rate of timber
$\Gamma$	Parameter to calculate parametric compartment temperature–time response
$\Gamma_e$	Boundary of the element
$\Gamma_{max}$	Maximum value of $\Gamma$ due to fire load restrictions
$\gamma_c$	Concrete materials partial safety factor
$\gamma_f$	Partial safety factor applied to loads or actions
$\gamma_G$	Partial safety factor applied to dead loads (permanent actions)

$\gamma_M$	Partial safety factors applied to design strengths
$\gamma_{M,fi}$	Materials partial safety factor in the fire limit state
$\gamma_{M,fi,a}$	Materials partial safety factor for structural steel
$\gamma_{M,fi,c}$	Materials partial safety factor for concrete in composite construction
$\gamma_{M,fi,v}$	Materials partial safety factor for shear studs
$\gamma_Q$	Partial safety factor applied to imposed loads (variable actions)
$\gamma_s$	Partial safety factor applied to steel design strengths
$\gamma_w$	Moisture dependant parameter (Schneider)
$\gamma_0$	Constant (Schneider)
$\delta$	Deflection, parametric measure of fuel energy lost through openings
$\delta_b$	Deflection due to flexure
$\delta_{bow,b}$	Thermal bowing calculated for a beam
$\delta_{bow,c}$	Thermal bowing calculated for a cantilever
$\delta_n$	Factor to allow for presence of active fire protection
$\delta_{q1}$	Partial safety factor dependant upon consequences of failure
$\delta_{q2}$	Partial safety factor dependant upon type of occupancy
$\varepsilon$	Strain, local buckling parameter
$\varepsilon_c$	Concrete strain
$\varepsilon_{c,\theta}$	Concrete strain at elevated temperature
$\varepsilon_{c,20}$	Concrete strain at ambient
$\varepsilon_{cr}$	Creep strain
$\varepsilon_{cr,c}$	Concrete creep strain
$\varepsilon_{cr,s}$	Steel creep strain
$\varepsilon_{cr,s,0}$	Creep intercept (Dorn model)
$\varepsilon_{cu}$	Ultimate concrete strain
$\varepsilon_f$	Emissivity of the fire or furnace
$\varepsilon_m$	Emissivity of surface
$\varepsilon_{p,c,\theta}$	Effective concrete plastic strain (Khennane and Baker)
$\varepsilon_{res}$	Resultant or effective emissivity
$\varepsilon_s$	Steel strain
$\varepsilon_{s,fi}$	Reinforcement strain in the fire limit state
$\varepsilon_{th}$	Free thermal strain
$\varepsilon_{th,c}$	Free thermal strain for concrete
$\varepsilon_{th,s}$	Free thermal strain for steel
$\varepsilon_{tot}$	Total strain
$\varepsilon_{tot,c}$	Total strain for concrete
$\varepsilon_{tot,s}$	Total strain for steel
$\varepsilon_{tr}$	Transient strain
$\varepsilon_{tr,c}$	Transient strain for concrete
$\varepsilon_{y,s}$	Yield strain for steel

$\varepsilon_{y,s,\theta}$	Yield strain for steel at temperature $\theta$
$\varepsilon_{0,c}$	Peak concrete strain
$\varepsilon_{1,c}$	Changeover strain between parabola and linear descending branch (Anderberg and Thelandersson)
$\varepsilon_{\sigma}$	Elastic strain
$\varepsilon_{\sigma,c}$	Elastic strain for concrete
$\varepsilon_{\sigma,s}$	Elastic strain for steel
$\eta$	Compartment geometry factor, imperfection coefficient for timber strut buckling, load ratio, strength reduction factor for rectangular stress block
$\eta_{fi}$	Ratio between the action effects from the fire and ambient limit states
$\eta_{fi,t}$	Ratio between the action effects from the fire and ambient limit states at time $t$
$\Theta$	Temperature compensated time (Dorn model)
$\Theta_0$	Temperature compensated time changeover point between primary and secondary creep
$\theta$	Elasto-plastic redistribution factor, rafter sag angle, temperature
$\theta_a$	Steel temperature, ambient temperature
$\theta_{a,t}$	Structural steel temperature at time $t$
$\theta_c$	Concrete temperature
$\theta_{cr}$	Critical steel temperature
$\theta_{cr,d}$	Critical design temperature
$\theta_{cw}$	Temperature at wood-char interface
$\theta_d$	Calculated design temperature
$\theta_e$	Vector of element nodal temperatures
$\theta_{f,max}$	Maximum temperature of a fire in compartment related solely to geometry
$\theta_g$	Creep temperature parameter (Schneider), furnace or gas temperature
$\theta_i$	Temperature of internal surface, temperature at node $i$
$\theta_{lim}$	Limiting temperature
$\theta_M$	Mean temperature
$\theta_m$	Temperature of masonry, temperature of the surface exposed to a fire
$\theta_{max}$	Maximum temperature reached at the duration of the fire
$\theta_R$	Reference temperature for a shelf angle floor
$\theta_s$	Reinforcing steel temperature
$\theta_t$	Fire temperature at time $t$
$\theta_w$	Wood temperature
$\theta_0$	Ambient or reference temperature, rafter angle at ambient

$\theta_1 \theta_2 \theta_8 \theta_{64}$	Curve fitting parameters for property reduction curves
$\bar{\theta}$	Prescribed temperature at a boundary
$\kappa$	Adaptation factor, non-linearity factor (Schneider)
$\kappa_{xy}$	Curvature in the $xy$ -plane
$\kappa_{xz}$	Curvature in the $xz$ -plane
$\kappa_1 \kappa_2$	Adaptation factors
$\lambda$	Slenderness ratio, thermal conductivity, concrete strength dependant stress block depth factor
$\lambda$	Thermal conductivity tensor
$\lambda_a$	Thermal conductivity of steel
$\lambda_{al}$	Thermal conductivity of aluminium
$\lambda_c$	Thermal conductivity of steel
$\lambda_i$	Thermal conductivity of compartment boundary
$\lambda_m$	Largest eigenvalue
$\lambda_p$	Thermal conductivity of protection material
$\lambda_{rel}$	Normalized slenderness ratio
$\lambda_0$	Dry thermal conductivity for masonry
$\lambda'$	Moisture modified thermal conductivity for masonry
$\bar{\lambda}$	Normalized strut buckling parameter
$\bar{\lambda}_\theta$	Temperature-dependant normalized strut buckling parameter
$\bar{\lambda}_{LT}$	Normalized lateral torsional buckling parameter
$\bar{\lambda}_{LT,\theta,com}$	Temperature-dependant normalized lateral torsional buckling parameter with respect to the temperature in the compression flange
$\mu_{LT}$	Correction factor dependant upon loading
$\mu_y$	Correction factor dependant upon loading
$\mu_z$	Correction factor dependant upon loading
$\mu_0$	Utilization factor
$\xi$	Reduction factor applied to permanent loads
$\xi_{cm}$	Mean strength reduction factor for concrete
$\xi_{s,02}$	Temperature-dependant modification factor for steel strength based on the 0,2% proof strength
$\xi_{\theta,x}, \xi_{\theta,y}$	Non-dimensional uniaxial temperature rise parameters (Hertz)
$\xi(\theta)$	Change in property at elevated temperature
$\rho$	Density
$\rho_a$	Density of structural steel
$\rho_{air}$	Density of air
$\rho_p$	Density of insulation
$\rho'_p$	Moisture modified density of insulation
$\sigma$	Stefan–Boltzmann constant
$\sigma_c$	Concrete stress

$\sigma_{c,\theta}$	Concrete strength at a temperature $\theta$
$\sigma_{c,20}$	Concrete strength at ambient conditions
$\sigma_d$	Design strength for timber
$\sigma_E$	Euler buckling stress
$\sigma_f$	Standard deviation of strengths
$\sigma_{h'}$	Standard deviation of the normalized heat flow in a compartment
$\sigma_{h''}$	Standard deviation of the normalized heat flow in a furnace
$\sigma_L$	Standard deviation of the compartment fuel load
$\sigma_{par}$	Strength parallel to grain
$\sigma_Q$	Standard deviation of the applied loading
$\sigma_{s,f}$	Temperature modified steel strength
$\sigma_t$	Standard deviation in the results from furnace tests
$\sigma_{w,t}$	Axial compressive strength of timber
$\sigma_{y,s}$	Steel yield strength
$\sigma_{y,s,\theta}$	Temperature modified steel yield stress
$\sigma_{y,20}$	Yield strength at ambient
$\sigma_{0,c}$	Peak concrete strength
$\sigma_{1,c,\theta}$	Changeover stress between the linear and elliptic part of curve (Khennane and Baker)
$\Phi$	Configuration factor for radiation, creep function (Schneider), insulation heat capacity factor, ventilation factor related to mass inflow, view factor for profile sheet decking
$\phi$	Creep function (Schneider)
$\phi_\theta$	Temperature-dependant strut buckling parameter
$\phi_{LT,\theta,com}$	Temperature-dependant lateral torsional buckling parameter
$\chi_{fi}$	Strength reduction factor due to strut buckling in the fire limit state
$\chi_{LT,fi}$	Strength reduction factor due to lateral torsional buckling in the fire limit state
$\psi$	Fire load density factor, end moment ratio
$\psi_{fi}$	Value of load reduction factor appropriate to the fire limit state
$\psi_0 \psi_1 \psi_2$	Load combination factors
$\Omega$	Solution domain
$\Omega_e$	Element domain
$\omega_k$	Mechanical reinforcement ratio
$\nabla$	Grad operator
$\Delta E_t$	Incremental in linear slope of stress–strain curve at time $t$ (Khennane and Baker)

$\Delta E_t$	Incremental in linear slope of strain hardening parameter at time $t$ (Khennane and Baker)
$\Delta H/R$	Activation energy
$\Delta H_c$	Heat of combustion of wood (18,8 J/kg)
$\Delta p$	Plastic strain semi axis (Khennane and Baker)
$\Delta t$	Time increment
$\Delta t_{cr}$	Critical value of time step
$\Delta x$	Layer thickness, nodal spacing
$\Delta y$	Nodal spacing
$\Delta \varepsilon_{th,c}$	Free thermal strain increment
$\Delta \varepsilon_{tot,c}$	Total strain increment
$\Delta \varepsilon_{th,c}$	Transient strain increment
$\Delta \theta$	Temperature gradient, temperature increment
$\Delta \theta_{a,t}$	Incremental increase in steel temperature
$\Delta \theta_g$	Increase in furnace (gas) temperature over ambient
$\Delta \theta_{lim}$	Increase in limiting temperature
$\Delta \sigma_c$	Concrete stress increment
$\Delta(.)$	Increment of variable (.)

**Note:**

The following subscripts are employed extensively throughout the text

$a$	structural steel (acier)
$c$	concrete
$fi$	fire
$Rd$	resistance
$Sd$ or $Ed$	design (applied)
$s$	reinforcing steel, general reference to steel
$e$	element
$el$	elastic
$pl$	plastic
$-$	hogging moment
$+$	sagging moment
$d$	design
$0$	refers to the peak values of stress or strain for concrete
$20$ or $20^\circ\text{C}$	refers to ambient conditions

# 1 Fire safety engineering

---

Before setting the groundwork for the complete subject of fire safety engineering and its influence on the overall planning, design and construction of building structures, it is necessary to attempt to define what is meant by 'fire safety engineering'. There is, as yet, no absolute definition, although the following may be found acceptable:

*Fire safety engineering* can be defined as the application of scientific and engineering principles to the effects of fire in order to reduce the loss of life and damage to property by quantifying the risks and hazards involved and provide an optimal solution to the application of preventive or protective measures.

The concepts of fire safety engineering may be applied to any situation where fire is a potential hazard. Although this text is mainly concerned with building structures, similar principles are equally applicable to the problems associated with oil or gas installations or other structures such as highway bridges. The additional hazards from gas and oil installations are primarily caused by the far more rapid growth of fire and the associated faster rates of temperature rise. This has been recognized by considering the testing of material response under heating regimes other than those associated with the more conventional cellulosic fires. The design methods used are, however, similar to those for the situation covered by the more normal cellulosic-based fires.

With any non-building structure, there can be a risk of fire damage, but the fact that this risk is extraordinarily low means that such a contingency can normally be ignored. However, in the case of, say, highway bridges where a tanker carrying a highly combustible cargo such as petrol collides with part of the supporting structure, the resultant damage from the fire can be large, often necessitating replacement of the original structure (Anon, 1990; Robbins, 1991).

The largest area of risk from fire damage is low-rise domestic housing which generally does not require sophisticated design methods as it is not a structural collapse which tends to be the problem, but the spread of smoke and toxic gases, and the resultant inability of the occupants to escape (Malhotra, 1987).

## 2 *Fire Safety Engineering Design of Structures*

Certainly within the UK for a long period, with the possible exception of the period 1939–1945 (during the Second World War), there have been very few, if any, recorded cases of death of the occupants in a fire caused directly by the collapse of the structure. There have been unfortunate cases, however, of the fire fighters being trapped by a collapse of the structure, well after the completion of occupant evacuation. This relatively low incidence of deaths resulting from collapse does not imply that structural integrity (load-bearing response) is unimportant, but is rather a testimony to the soundness of structural design, detailing and construction over that period. It has already been noted that the general cause of deaths is asphyxiation, i.e. being overcome by smoke and gases, or by being trapped and then being unable to escape and then being exposed to the effects of heat. It is therefore extremely important to consider all the issues which can play a part in ensuring life safety in a fire affected structure.

### 1.1 DESIGN CONCERNS

Elements within the discipline of fire safety engineering can be readily identified which relate both to life and property safety. These areas are not mutually exclusive as an action which increases life safety may also increase property safety. The key areas can be identified as follows:

#### 1. **Control of ignition**

This can be done by controlling the flammability of materials within the structure, by maintenance of the structure fabric and finishes, or by fire safety management in, say, imposing a ban on smoking or naked flames.

#### 2. **Control of means of escape**

This can be forced either by the imposition of statutory requirements on provision of suitable escape facilities or by the education of occupants.

#### 3. **Detection**

This covers the installation of methods whereby the fire may be detected, preferably at the earliest possible stage.

#### 4. **Control of the spread of fire**

Here, concern is the spread of the fire, either within the building or to adjacent properties. This control may either be effected by in-built features (such as compartmentation) or control of distance between buildings or by mechanical means (such as venting, smoke screens or sprinklers).

#### 5. **Prevention of structure collapse**

This covers the imposition of load-bearing capacity and integrity on the structure as a whole or in part during a fire.

Each of these can now be considered in greater depth.

### **1.1.1 Control of ignition**

This needs considering under three subheadings; the first two are concerned with spread of flame and the third with management and maintenance of the structure. Ignition can occur through a variety of mechanisms. Generally, these are accidental, e.g. lighted cigarette ends, electrical faults or overheating of mechanical or electrical plant. However, deliberate actions or arson cannot be discounted.

#### ***1.1.1.1 Control of flammability***

There have been too many cases where fire has spread rapidly owing to the unsuitable nature of the linings of a structure, thus any material used in the finishes on any part of the structure should be such that the spread of flame or flammability must be limited. This in general is controlled by the imposition of tests on flammability or flame spread by any relevant national or international standards, e.g. in the UK the relevant sections of the Fire Test Standard (BS 476: Parts 3, 6 and 7 or their equivalent European standards).

It is also essential to ensure that materials used in the contents of the structure should reduce any hazard. It is clearly impractical to insist that the contents of any structure make no contribution to the combustible fire load in a structure, but it is necessary to ensure that those contents produce as least a hazard as possible. This means that the surface coatings should not be easily ignitable, nor, as happened in recent cases in the UK with domestic fires involving foam-filled furniture, should certain foams which produce large quantities of highly toxic smoke on ignition be allowed. This latter has led to the use of such foams being controlled by legislation.

#### ***1.1.1.2 Control of growth of fire***

One classic means of controlling fire spread is by the use of vertical or horizontal fire compartments. However, these compartments are only satisfactory if there is no possible route for smoke or flame through the compartment boundary. Fire spread can also occur within a room or to a compartment beyond its point of origin if the original fire boundary is incapable of containing it due to unsatisfactory closures to the room of origin (Hopkinson, 1984). A more recent case of fire spread, attributed to lack of fire stopping following replacement of the original façade, was the Torre Windsor Tower in Madrid (Dowling, 2005; Redfern, 2005; Pope, 2006). There were additional problems in this case, namely what appeared to be longer than normal for the fire brigade to actually start fighting the fire, and steel columns above the 17th floor was not fire protected (Arup, 2005).

## 4 *Fire Safety Engineering Design of Structures*

An additional problem may arise where, although the compartment boundary is satisfactory when the civil (or structural) part of the construction sequence is complete, the installation of services may either destroy this fire break or not replace the fire break to a satisfactory standard. This situation can also arise when subsequent modifications are made, forced either by changes to the use of the structure or by repairs to, or replacements of, existing services.

A further problem can occur due to failure to clear away accumulations of combustible rubbish which can either be ignited by fire as at Bradford (Anon, 1985, 1986) or can gradually cause flashover by very slow fire growth, i.e. smouldering (Anon, 1987, 1988).

Such problems can be reduced by ensuring that a fully effective fire safety management policy is in place.

### **1.1.1.3 *Fire safety management***

In single occupancies, it is relatively easy to set up procedures to ensure that, in the event of a fire, all personnel are aware of the proper procedures and that there are suitable people to act as marshals and direct the fire brigade as required. In multiple occupancies, especially where the occupancy changes frequently and there is a large transient population, such as shopping malls, this is more difficult and it is therefore essential that the owners, often corporate bodies, set up a fire safety management strategy and ensure that there is a responsible group of persons on duty at all times to take full control in the case of an outbreak of fire. Note that this function can be taken by the staff employed for normal day-to-day security provided, they are fully and properly trained. It is also essential that full records of the fire detection, fire control and fire-fighting systems are kept and that a full check is made on any occupancy to ensure that no action is allowed to be taken which will negate any part of those systems. It is essential that where a fire engineering approach to building design is approved and adopted, the measures contained in that design are retained at all times and that financial exigencies are not allowed to compromise fire safety.

### **1.1.2 *Means of escape***

There are generally statutory requirements for the provision of escape routing in all except the simplest single-storey structures. Such requirements are based on the concept of the maximum length of escape route to a safe place, be it an external fire door or a protected fire-escape stairwell. The maximum lengths are based on the type of occupancy and are also dependant on the method of escape, i.e. whether along a corridor or

through the fire compartment. For multi-storey structures, it may well be possible to make use of the concept of phased evacuation where initially only a reduced number of storey adjacent to the fire affected zone are cleared, with other floors being cleared subsequently if needed.

There will also be requirements on the total number of fire-escapes and the dimensions of escape routes which are normally functions of the building type, the number of people expected within the building at any one time and the potential mobility of such persons. The escape routes are sized to give complete evacuation from the fire compartment into either a protected area or the outside of the structure in some 2,5 min with a basic travel velocity on staircases of approximately 150 persons per minute per metre width of escape route. It should however be recognized that staircases are built in discrete widths and that doubling the staircase width will not double the throughput as an individual person requires finite space, and that minimum widths also need to be specified. The above design figures are for able-bodied persons and need modification when there is a likelihood of disabled persons being part of the building occupancy (Shields, 1993).

The historical background to the reasons for imposing requirements on escape routes and evacuation is given in Read and Morris (1993). This imposition followed a series of disastrous fires over a period of some 50 years from 1881, when a theatre fire in Vienna was responsible for some 450 people being killed, to a fire in Coventry in 1931. Much of the background to current legislation in the UK is given in a Ministry of Works Report (1952) which was based on then current international practice.

All escape routes must also be lined with non-flammable, non-toxic materials. It should be noted that the fire doors opening on to escape routes may have a lower fire resistance performance requirement than the structure itself as they are only required to be effective in the very early stages of the fire where the major concern is with evacuation rather than structural stability. It has to be pointed out that fire doors propped open, even by fire extinguishers, are totally ineffective!

It is regrettable that there have been too many cases where, although the requisite number of escape routes have been provided, the escape routes have not been kept clear as the fire doors at the end of the escape routes were inoperative due to their being locked and unable to be opened. Examples of this occurred at Summerland (Anon, 1973) and the Dublin (Stardust) Disco fire (Anon, 1983).

It is equally important that the occupants of the structure are educated to respond to the warnings of any fire. In domestic situations, where the occupants are in a familiar situation, response may be faster than that in an unknown situation. There is still a large amount to be learnt concerning human behaviour in a fire (Canter, 1985; Proulx, 1994). Any warning

system must, to use a colloquial phrase, be 'user friendly'. It has still not been determined satisfactorily whether alarm bells or sirens should be implemented by broadcast instructions or graphical displays on the best manner of exit. It is, in any case, essential that all escape routes are fully illuminated with self-contained emergency lighting and all signs are also supplied by the emergency power supplies.

The number of stories, some, one suspects, apocryphal, whereby people have totally ignored warnings to continue whatever they were doing before the alarm are legion; for example, the restaurant user who insisted on continuing to eat the meal that had been paid for in spite of the large quantities of smoke gradually engulfing the individual concerned. Evidence suggests that individuals will carry on as long as possible behaving as if the fire did not exist or there were no warnings (Proulx, 1994).

The educational process must also extend to the owners and lessees of any structural complex. This process must form a part of any fire safety management policy adopted. For buildings where the occupancy is controlled, part of the educational process can take the form of fire drill procedure. This, however, must be treated with caution as it is the author's experience that more people who know when the drills are to take place, the more likely it is that the drill will be circumvented and its efficacy lost. The author has even noted the individuals going in the opposite direction to the flow of evacuees to collect items from offices, and when questioned glibly respond with words to the effect that it is only a drill!

### **1.1.3 Detection and control of the fire**

In order to ensure life safety through evacuation, it is necessary to ensure that means are available for detection and control of the fire. Control of the fire is needed both to reduce the production of smoke allowing more efficient evacuation and to keep temperatures down in the structure to reduce subsequent damage.

#### **1.1.3.1 Fire detection**

Systems installed for fire detection may be manual or automatic or a combination of these.

#### **1. Manual systems**

Manual systems, such as the traditional frangible glass panel, which when broken automatically sets off the fire alarm system, can be relatively simple. However, they require a human response to realize the existence of a fire and to perceive and determine its severity. Thus, such

systems may be of only limited use especially in situations where the presence of individuals cannot be certain.

## 2. Automatic systems

These rely either on the incidence of excessive amounts of heat or smoke being monitored by a sensor which either directly activates the fire-fighting system, as in the fusible head of a sprinkler, or indirectly activates any fire control and evacuation system. Recent developments in automatic systems include the use of low-power lasers or infra-red sensors to monitor the presence of smoke.

Many automatic systems rely on combinations of heat and smoke detection sensors, as the positioning of either type can be very sensitive to normal ambient conditions and the usage of the building in which they are situated. Kitchens or areas where smoking is allowed can be particularly problematic, although the level of problems formerly associated with such areas have been very much reduced with the advent of computer control.

In all cases, other than for small low-occupancy structures, any detection devices should be linked into a system to indicate either the source of the fire or the point at which the alarm was sounded, to initiate control of the fire by the operation of roller shutter doors to seal off compartments, smoke curtains or automatic venting systems, and to initiate any evacuation procedures together with the automatic registering of the outbreak of the fire at the local fire brigade station.

### 1.1.3.2 Smoke control

It is absolutely essential that during evacuation, any build-up of smoke is such that a clear visibility is granted to the evacuees, and that the bottom level of smoke is not allowed to fall below a level of about 2.5–3 m above floor level during, say, the first 15 min of the fire (Building Research Establishment, 1987; Morgan and Gardner, 1991). There may also be a requirement to keep the smoke temperatures below a critical value. The requirement on smoke control is in part due to problems caused by any toxic material within the smoke and in part due to the totally disorientating effect caused by loss of visibility. In general, either forced venting a fire to control smoke generation will be necessary or, in the early stages, smoke curtains can be used to form reservoirs and contain smoke.

Only in very few cases where natural venting of the fire occurs very early in the fire, notably in single-storey construction where the roofing material is given no specific fire resistance requirement or designed to fail and therefore collapses early during the fire, does no consideration need to be given to smoke control. However, for warehouses where the contents can be such that the toxic smoke can be emitted in the early stages

of the fire, such smoke will need to be contained in specific areas before the roof self-vents. Such containment need only be for a sufficient period to ensure full visibility during evacuation. This period is likely to be very short because of the relatively low numerical levels of human occupancy and the existence of direct level access being generally available to fire exits. Smoke control must be employed where compartment volumes are large or there are long escape routes.

These problems become much more severe in large open-plan building structures, notably large shopping malls or atrium structures. The levels of smoke production and the amount of ventilation required can be determined (Morgan and Gardner, 1991; Marshall, 1992; Marshall and Morgan, 1992; Hansell and Morgan, 1994). In such structures, the installation of an automatic smoke venting system initiated when the fire is detected is a *sine qua non*. Any such venting system must be automatic and can either rely on natural or forced draft ventilation. In both cases, the effect of access points needed by the fire brigade and also the possibility of part of the cladding falling in must be considered. In the case of a forced draft ventilation system, a completely reliable standby power supply must be available.

### **1.1.3.3 Fire-fighting systems**

In sensitive areas, automatic fire-fighting devices initiated either manually or by the fire detection system will be installed. Such automatic devices will vary depending on the type of fire to be expected but they generally operate by smothering the fire and denying the fire any source of oxygen. Sprinklers effectively act by reducing the temperature of the burning contents. Any fire-fighting system installed as part of the fabric of the structure will be supplemented by the supply of both suitable portable fire extinguishers and by, now rarely, hose reels for local fire fighting.

A large number of structures are also likely to have sprinkler systems installed either at the prompting of the insurance company to reduce property losses, or as part of the trade-off between active and passive systems allowed by some regulatory bodies, e.g. England and Wales Building Regulations, Approved Document B (Department of the Environment, 1992a). Such sprinkler systems are operated automatically by the melting of fusible elements or frangible glass in the head of the sprinkler. A drawback with water sprinkler systems is that a substantial amount of damage may be caused on floors other than those in which the fire occurs by the seepage of water through the structure. A sprinkler system also has the advantage that the amounts of smoke are much reduced giving increased opportunity for evacuation. In tests carried out after the Woolworth's fire (Anon, 1980; Stirland, 1981) the maximum temperatures

at ceiling level with sprinklers would have been 190°C compared to 940°C without sprinklers, the volume of smoke and gases in the first 7 min produced with sprinklers was 1500 m<sup>3</sup> and without some 10 000–20 000 m<sup>3</sup>, with only some 10% of the fire load consumed with sprinklers operative compared to that without as the fire size would have been reduced. It was also estimated that with sprinklers an extra minute would have been available for evacuation and that the fire would have been brought under full control in 22 min.

There has been concern expressed in some quarters at the efficiency of sprinkler systems in a fire as there have been cases where they have not operated. The evidence is not completely clear-cut. Stirland (1981) suggests that such concern is unnecessary.

There can also be inherent problems caused by the interaction between venting systems and sprinkler systems. The problems identified by Heselden (1984) are caused by the effect of water cooling the smoke plume and thereby destroying its upward buoyancy, and as a result there has been a series of tests carried out (Hinkley and Illingworth, 1990; Hinkley *et al.*, 1992) and design guidance published (Morgan, 1993). The problem caused by the interaction between smoke venting and sprinklers is either that the smoke plume does not rise and therefore causes a loss in visibility during evacuation, or that the upward velocity due to the vents causes a loss of effect of the water droplets descending from the sprinkler heads. Day (1994) indicates where both systems are fitted then for storage areas the sprinklers should operate before smoke vents, but in other areas where evacuation is important, then both may operate together.

Unless the fire is small or can be contained within a localized area by in-built fire-fighting systems, it is generally only by the prompt arrival at the scene of a fire by the fire brigade, that complete evacuation can be checked and control of the fire both within the structure and the avoidance of spread to adjacent structures be affected. To check evacuation from the building and to fight the fire, access must be provided by protected shafts containing either stairs or lifts. It is now generally a statutory requirement to provide adequate access for fire fighting.

#### 1.1.4 Compartmentation

Any large structure will need to be divided into compartments vertically, horizontally or a combination of the two. This requirement is to limit the spread of fire to the whole structure, and may also be imposed to allow the phased evacuation of any multi-storey structure, whereby only the floors contained within the fire affected compartment are initially evacuated, and the remaining floors either above or below the fire affected areas are evacuated at a later stage. The rules governing compartmentation are

generally unclear on the reasons why the values, expressed either as a maximum floor area or volume, limiting compartment sizes have been selected. It is probable that most of the criteria are historically based on long past experience which may be no longer valid with improved fire-fighting methods (Malhotra, 1993). The issue of fire spread between horizontal compartments due to failure of glazed curtain wall façades needs to be considered. This is partially due to the use of aluminium within such systems. Glazed curtain wall systems need either sprinkler protection or intumescent protection (Morris and Jackman, 2003). It is important to ensure that compartmentation is maintained following repairs, remedial work or renovation within a building.

### **1.1.5 Fire spread between structures**

There will also be an imposed restriction to limit the spread of fire across boundaries from one structure to another. Limits can be imposed on the lateral spacing of structures, the fire resistance requirements of any closures to openings in the structure, and to the materials used for the cladding (Read, 1991; LPC, ABI, FPA, 2000).

### **1.1.6 Structure collapse**

Quite clearly there must be no total collapse of the structure during the evacuation phase nor preferably during the fire-fighting phase. Provided the occupants are sufficiently mobile and aware of the situation, evacuation should be relatively fast, as the escape routes either to protected staircases or directly out of the building are designed to permit complete evacuation of the fire compartment in some 2,5 min. Fire fighting may extend over a substantial period and thus there should be a sufficiently long period before the structure shows any sign of collapse. There is, in the UK, a statutory requirement to provide safe access to the building to enable the fire services to carry out fire fighting. Collapse of the structure before a given period, conventionally defined as the fire resistance of the structure, can be avoided either by designing the structure such that although weakened and deformable, it is still capable of sustaining a reasonable level of applied load for the whole period (passive approach), or measures can be designed to ensure that the fire is contained or that temperatures do not reach a level that will cause mechanical distress to the structure (active approach). Unfortunately there have recently been cases, notably the World Trade Centre Towers and the Pentagon fire in 2001, where (partial) collapse occurred during a fire. It should be remembered that in both these cases, the fires were deliberately caused by fully laden aircraft being flown into the buildings. In the case of the world Trade

Centre towers, it is now thought that the aircraft impact was not a major cause of the collapse, but the fact that the fire protection on the original structure became dislodged due to the impact as the fire load was of a similar magnitude to that of a typical office fire load density (Dowling, 2005). The Pentagon building suffered only partial collapse – this was due to its being an *in situ* reinforced concrete frame structure (ISE, 2002; Mlakar *et al.*, 2003).

In reality, a structure is designed to have both approaches operative, although traditionally they were considered separately. It is only recently that it has been recognized, in the UK at least, that the two systems are interdependent and that one can be used to reduce or modify the needs of the other. This interaction is often referred to as 'trade-off'. Proposed changes to Approved Document B (Kirby *et al.*, 2004) are likely to reinforce this position.

Many of the measures to detect, control or contain the fire within a building are imposed by either legislation at a national or local level, or other statutory regulatory bodies. In certain cases, the insurance company for the building may impose additional constraints.

## 1.2 REGULATORY CONTROL

This has come about over a large period to protect the public and to ensure that a framework can be put into place to ensure that if a disastrous fire occurs, then the likelihood of a repetition of such a fire will be small. Such regulatory control can either be imposed through national or international standards, or by legislation. In the UK, much of the requirements for structures of different type or occupancy is covered in various parts of the Standard on Fire Precautions in the Design, Construction and Use of Buildings (BS 5588). Legislative control generally takes the form of either national or local building regulations or specific legal requirements. Some degree of control may also be imposed by the Insurance Companies. The current situation in the UK is covered by Read and Morris (1993) to which reference should be made. Guidance is also published by the Department of the Environment (1992b).

It has become apparent that it is not only the completed structures that require consideration to be given to fire safety, but also there is an increasing need to consider structures under construction or repair.

## 1.3 FIRE PRECAUTIONS DURING CONSTRUCTION AND MAINTENANCE

The situation during construction (execution), and indeed maintenance or repair, can be inherently more severe than for completed structures since

there can be a substantial amount of often highly combustible materials stored on the site, that some site processes involve the use of applied heat often with naked flame, that the active or passive fire protection systems may not be completed or operative, that the ventilation characteristics of any compartment will be different owing to cladding or walling not being in place, that compartmentation or fire stops may not be complete and that access to certain areas may be hindered by the construction process itself. It is also necessary to consider the possible requirement of a full security system linked to any fire detection procedure (Muirhead, 1993).

These problems have been highlighted when the severe damage caused to the Broadgate Centre (Phase 8) (Robbins, 1990), Minster Court (Bishop, 1991), London Underwriting Centre (Rosato, 1992), Pavilion of Discovery (Expo '92) (Byrd, 1992a, b) is considered, since all these buildings were under construction at the time of fire damage.

The problems outlined above on new constructions become even more important during reconstruction, repair or renovation of buildings which may be of supreme historical importance, such as Windsor Castle (Fowler and Doyle, 1992; Cockcroft, 1993), the Wiener Hofburg (Anon, 1993) or Torre Windsor (Madrid) (Pope, 2006). In the case of Windsor Castle, the situation was exacerbated by the lack of fire stopping in concealed cavities and the roof voids.

Fires in buildings under either construction or repair are clearly expensive for the Insurance Companies, if indeed the structures concerned are insured, and as a result has led to substantial increase in insurance costs and to the imposition, in the UK, of a Code of Practice (Building Employers Federation and Loss Prevention Council, 1992) although previously the Department of the Environment had issued a similar document relating to Crown works (Department of the Environment, 1991). It should be noted that most of the contents of these documents represent common sense and delineate what should be a good site practice. Both documents emphasize the need for fire safety management on any construction site.

Having briefly outlined the areas within fire safety engineering applied to both completed buildings and buildings under construction, it is useful to provide a brief summary before outlining the content of the remainder of this text.

### **1.4 SUMMARY**

The summary assigns the considerations involved in fire safety engineering under the two headings of active and passive provisions (Malhotra, 1986).

#### **1.4.1 Active measures**

- Provision of alarm systems,
- Provision of smoke control systems,
- Provision of in-built fire fighting or fire control systems,
- Control of hazardous contents,
- Provision of access for external fire fighting,
- Provision of a fire safety management system.

#### **1.4.2 Passive measures**

- Adequate compartmentation,
- Control of flammability of the structure fabric,
- Provision of fixed escape routes,
- Provision of adequate structural performance.

It is the last of these which forms the area of concern in this book. The remaining chapters outline the philosophy behind the concepts of structural fire safety engineering, the use of prescriptive methods to satisfy fire resistance requirements, the temperature–time response in a fire compartment and the basis behind calculation methods to satisfy fire resistance requirements. The next sections deal progressively with the materials data required and the methods of calculation for the common structural materials, both as structural elements and complete structures. The final section of the text considers the problems with fire damaged structures.

# 2 Design philosophies

---

This chapter is concerned with the theoretical justification for the methods that are available to determine the performance of structures or structural elements when accidentally subjected to the effects of fire. Much of the material in this chapter is derived from the CIB W14 Workshop Report (1983) which laid down some of the basic principles behind the methods that can be adopted to determine fire resistance.

However, before considering these, it is appropriate to review the concepts of limit state design applied at ambient conditions.

## 2.1 AMBIENT LIMIT STATE DESIGN

A limit state can be simply defined as the expression of a particular design criterion, e.g. flexural capacity or deflection. When possible design criteria are considered as a total package, it is recognized that some are more relevant to being determined on the basis of a 'failure' calculation (e.g. flexural capacity), whilst others (such as deflection) are more relevant to conditions pertaining through the total working or service life of the structure. Thus, two main categories of limit states are recognized; ultimate and serviceability.

The *ultimate limit state* is concerned with the determination of the member, or structure, capacity at actual or incipient failure. The *serviceability limit state* is concerned with the performance of the structure during its life time under normal conditions. Other limit states can also be recognized such as response to accidental loading or actions.

Serviceability conditions are necessarily checked under the application of working or service loads (actions) on a structure; these service loads are the characteristic loads (actions) multiplied by partial safety factors that can normally be taken as no greater than unity, thus the failure or ultimate conditions must be checked on loading greater than the service loads, i.e. load factors greater than unity are applied to the characteristic loads. Since both loads and material properties are subject to statistical uncertainties in their values, then the average value of the load or strength properties cannot be used, but characteristic values based on a 5% acceptance

limit on loads and a 5% rejection limit on material strengths. This means that the design is based on loading which has a 5% probability of being exceeded and strengths which have a 95% chance of being met. Thus, assuming a gaussian distribution of both load and strength variability, the characteristic loads or strengths may be written in terms of the mean and standard deviation.

For loads:

$$Q_k = Q_{mean} + 1,64\sigma_Q \quad (2.1)$$

where  $Q_k$  is the characteristic load,  $Q_{mean}$  is the mean or average load,  $\sigma_Q$  is the standard deviation of the load and the factor of 1,64 relates to the area under the gaussian distribution curve to give a 5% limit;

For strengths:

$$f_k = f_{mean} - 1,64\sigma_f \quad (2.2)$$

where  $f_k$  is the characteristic strength,  $f_{mean}$  is the mean strength and  $\sigma_f$  is the standard deviation.

Then, if the load effect  $S_d$  that is required to be resisted, e.g. bending (flexure), is calculated from the characteristic loading and the resistance effect  $R_d$  that is required to be satisfied, e.g. flexural strength, is calculated from the characteristic strengths, then the satisfaction of the ultimate limit state may be written as

$$\gamma_f S_d \leq \frac{R_d}{\gamma_m} \quad (2.3)$$

where  $\gamma_f$  is the partial safety factor applied to the loads or actions, and  $\gamma_m$  is a partial safety factor applied to the strengths. It should be noted that whilst the partial safety factors applied to loads (actions) are generally explicitly stated in design codes. The partial safety factors applied to material strengths will also be explicit except where the phenomena can only be described by empirical equations (such as shear in reinforced concrete).

Partial safety factors are set:

- to cover uncertainties in calculation methods in the analyses to determine both load and resistance effects;
- to cover variations, other than statistical variations, in assumed data;
- to ensure that the materials in the structure behave in a sensibly linear manner during service conditions and thus ensure that continued

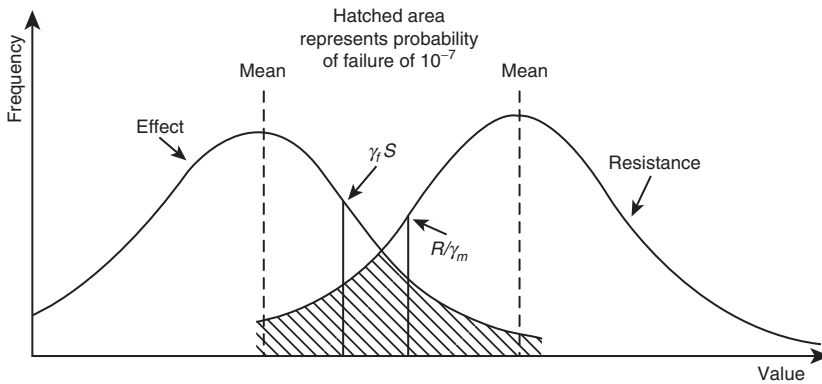


**Figure 2.1** Failure envelope for ultimate limit state design.

removal and application of imposed or variable loading does not cause irreversible deformations and

- to give an acceptable probability against failure.

It is impossible and extremely uneconomic to set the partial safety factors to give a zero failure probability. The generally acceptable probability is around  $10^{-7}$  (Fig. 2.1). This low probability of failure and the ensuing choice of partial safety factors also have the effect of ensuring that most designs which satisfy the ultimate limit state will also satisfy most structural service limit states such as deflection.

Where the concern is with accidental loading, there is clearly no requirement to satisfy any service limit states since there is no need to control, for example, deflection. It is only necessary to consider strength, thus the partial safety factors applied to the loading can essentially be reduced to unity, i.e. to values corresponding to service loading. Equally, the partial safety factors applied to the characteristic strengths can also be generally reduced to unity as there is no concern with materials being strained either beyond yield or into a non-linear region. This concept of limit state design can be extended into the situation when the effect of fire is concerned, as fire can be considered an accidental load.

## 2.2 FIRE LIMIT STATES

From the standard fire, or furnace, test a series of failure criteria were identified:

1. The element under test should have sufficient strength (load-bearing capacity) to resist the applied loading over the required duration of the test.

2. The temperatures on the unexposed face should be low enough not to cause initiation of combustion of materials stored against that face.
3. There should be no possibility of flame being able to reach the unexposed face through any weakness or loss of integrity in the construction either inherent in the construction itself or due to excessive deformation during the test.

These failure criteria can be simply identified as load-bearing capacity ( $L$ ), insulation ( $I$ ) and integrity ( $E$ ). The last of these is not amenable to calculation and can only be determined by physical testing and will not, therefore, be considered further. The other two criteria are capable of being assessed on a calculation basis and thus can be expressed mathematically as follows using state functions  $Z$  which are defined as the algebraic difference between calculated response and the minimum required value of that response.

### 2.2.1 Load-bearing capacity criterion

This can be expressed in one of the three ways.

- On a time base:

$$Z = t_{fi,d} - t_{fi,requ} \geq 0 \quad (2.4)$$

where  $t_{fi,d}$  is the calculated time to failure and  $t_{fi,requ}$  is the required time to failure ( $t_{fi,requ}$  may be replaced by the equivalent time  $t_{e,d}$ ).

- On a strength base:

$$Z = R_{fi,d} - E_{fi,d} \geq 0 \quad (2.5)$$

where  $R_{fi,d}$  is the load resistance and  $E_{fi,d}$  is the load effect, both evaluated with the application of suitable appropriate partial safety factors, over the required time period.

- On a temperature base:

$$Z = \theta_{cr,d} - \theta_d \geq 0 \quad (2.6)$$

where  $\theta_{cr,d}$  is the critical design temperature and  $\theta_d$  is the calculated design temperature of the member. This last criterion is applicable only to the load-bearing capacity when a member is exposed to the standard temperature–time curve.

### 2.2.2 Insulation criterion

This may also be expressed by Eq. (2.6) but with the temperatures defined as those on the surface of the member and not exposed to the fire.

### 2.2.3 Determination of partial safety factors

The partial safety factors used to determine the inequalities of Eqs (2.4)–(2.6) must be set to give an acceptable probability of failure. This probability should be allowed to be a function of the use and size of the structure (Table 2.1 after CIB W14 Report).

The partial safety factors are also governed to a certain extent by the fact that fire is seen in an emotive light, in which it is perceived that only a zero risk of fatal human involvement is desirable.

This is clearly impossible. It is therefore, necessary to consider risks that are acceptable to society as a whole. These risks should be a function of the type and usage of the structure under consideration (Rasbash, 1984/5).

These partial safety factors can be evaluated by a series of methods of decreasing complexity.

The most complex is to use a form of Monte Carlo simulation to assess the effect of random variation in all the parameters concerned to

**Table 2.1** Allowable probabilities of failure in the fire limit state

Occupancy	Load-bearing capacity		Insulation and integrity
	Single-storey	Multi-storey	
Dwelling	$10^{-4}$	$10^{-6}$	$10^{-4}$
Schools	$10^{-4}$	$10^{-5}$	$10^{-4}$
Hôtels	$10^{-6}$	$10^{-7}$	$10^{-6}$
Hospitals	$10^{-6}$	$10^{-7}$	$10^{-6}$
Elderly homes	$10^{-6}$	$10^{-7}$	$10^{-6}$
Theatres	$10^{-7}$	$10^{-8}$	$10^{-7}$
Shops	$10^{-4}$	$10^{-5}$	$10^{-4}$
Offices	$10^{-4}$	$10^{-5}$	$10^{-4}$
Factories, etc.	$10^{-3}$	$10^{-4}$	$10^{-3}$

The probabilities given above are for primary structural members. It may be justifiable to reduce these probabilities for secondary and minor structural elements by factors of 10 and 100, respectively.

Source: CIB W14 Report (1983) by permission

evaluate the possible outcomes and the distribution of such outcomes. Whilst, this is not a practical proposition for design methods, it is capable of being used to assess the relative importance of specific variables in a problem and can therefore be used to determine the critical areas of design or further research (Kordina and Henke, 1987; Purkiss, Claridge and Durkin, 1989).

The next possible method is to use a first-order reliability analysis on the mean and standard deviations of the state function  $Z$  to determine the reliability index of the state function and to set this to an appropriate value. Unfortunately, this method becomes complex unless the state function  $Z$  is a simple linear function of two variables. In the fire situation, both the required performance level and the calculated performance level will be non-linear multi-variable functions.

Thus, for all practical purposes, the evaluation of the partial safety factors needed in the calculations are set using a certain degree of common sense and the need to link in with conventional ambient limit state design in the use of, for example, characteristic loads and strengths.

For the structural fire loading, the quasi-permanent portion of the variable load is used, i.e. the variable load is multiplied by  $\psi_2$  from EN 1990. EN 1991-1-2, however, also allows the load (action) effect required to be resisted in a fire to be set equal to a proportion of the ambient load (action) effect, thus

$$E_{fi,d} = \eta_{fi} E_d \quad (2.7)$$

where  $E_d$  is the design effect at ambient and  $\eta_{fi}$  is the reduction factor, values of which are given in the relevant materials design codes. Typically  $\eta_{fi}$  takes values of around 0,6–0,7 depending upon the type of construction.

It should be noted that the materials partial safety factors for use in the fire design sections are generally lower than those specified for accidental damage or actions in the main sections of the design codes. Part of the reason why the materials partial safety factors are lower in the fire design case is that an acceptance/rejection limit of greater than 5% may be permissible.

All numerical examples in this text have been carried out with the recommended values of partial safety factors or load ratios. It is thus essential that the relevant National Annexes are consulted to verify if such values have been amended.

Having established the mechanisms by which the partial safety factors to be used can be determined, it is necessary to consider the methods whereby a structure or structural element can be assessed when exposed to fire.

2.3 ASSESSMENT MODELS

There are three heating and three structural models available each of which are with increasing complexity and are illustrated in Fig. 2.2 (Witteveen, 1983). The assessment method used to evaluate fire performance is related to the heating or temperature exposure model rather than the structural model.

2.3.1 Assessment method – level 1

This relates the heating model to exposure to the temperature–time relationship generated in the standard fire, or furnace, test and allows assessment of either simple structural elements or subassemblies by test or by calculation with the duration determined from regulations or codes. Historically, this method has been used to determine the fire resistance of structural elements and to provide the prescriptive data that have been

Model for structure / Model for thermal exposure		S <sub>1</sub>	S <sub>2</sub>	S <sub>3</sub>
		Element	Substructure	Complete structure
H <sub>1</sub>	<p>ISO-834</p>	<p>Test or calculation (deterministic)</p>	<p>Calculation exceptionally testing (deterministic)</p>	
H <sub>2</sub>	<p>ISO-834</p>	<p>Test or calculation (probabilistic)</p>	<p>Calculation exceptionally testing (probabilistic)</p>	<p>Calculation (probabilistic) should be avoided</p>
H <sub>3</sub>	<p>Real fire</p>	<p>Calculation (probabilistic)</p>	<p>Calculation (probabilistic)</p>	<p>Calculation (probabilistic) in special cases and for research</p>

Figure 2.2 Matrix of assessment models for structural fire safety design (by kind permission of Witteveen, 1983).

the cornerstone of most regulatory procedures and to provide the tabular material in various design codes of practice (Chapter 3). This method has also been used to provide a data bank to calibrate some of the available calculation models.

The combination of level 1 heating régime (standard furnace curve) and complete structures (Model type S<sub>3</sub>) is not considered by Witteveen owing to the large discrepancy between the levels of sophistication of the models. Since in real structures the cooling phase may well be important, as was demonstrated in the Cardington tests (see Chapter 12), it is the author's view that Witteveen's view remains correct.

### 2.3.2 Assessment method – level 2

At this level, the thermal model is that of exposure to the standard furnace curve but the duration of that exposure is determined by the equivalent fire duration time related to the actual fire characteristics of the compartment in which the structural element or subassembly is contained. For a full discussion of equivalent duration of fire exposure, reference should be made to section 4.5.2.

### 2.3.3 Assessment method – level 3

In this case, the temperature–time response used in the thermal model is one generated from the actual characteristics of the compartment, i.e. its fire load (combustible fuel), the available ventilation sources and the thermal characteristics of its boundaries. In *lieu* of a full calculation of such a response, it is permissible to use parametric equations to determine the compartment temperature–time response (Lie, 1974; EN 1991-1-2). The time of exposure is taken as the minimum which causes any of the appropriate limit states of load-bearing capacity or insulation to be no longer satisfied. The relevant failure criteria for various member types are given in Table 2.2.

Although some testing has been carried out with a natural fire exposure, it is intended that this level of assessment should only be used for calculation. The determination of the compartment temperature–time response is dealt with in Chapter 4.

### 2.3.4 Practical considerations

In general, only levels 1 and 2 will be required for most structures. It is only for innovative or complex structures that recourse is likely to be

**Table 2.2** Design criteria for structural members

Member type	Design criterion		
	Load bearing	Insulation	Integrity
Beam	<i>L</i>	<i>I</i>	–
Slab	<i>L</i>	<i>I</i>	<i>E</i>
Column	<i>L</i>	–	–
Wall	( <i>L</i> )	<i>I</i>	<i>E</i>

A wall requires only insulation and integrity, unless it is load bearing.

needed to a level 3 assessment. However, in certain circumstances, a level 3 assessment can show the need for a much reduced level of fire protection as the temperatures reached and the actions induced in the fire will not be sufficient to cause loss of load-bearing capacity.

Although EN 1991-1-2 covering the calculation of actions during fire exposure allows any of the three determination levels to be used, most of the codes for calculation of member resistances to applied actions appear only to allow calculation using level 1 assessment, or level 2 assessment using equivalent fire durations, as many of the design equations are related implicitly to the standard furnace temperature–time curve, since most of the data for calibrating such equations have been derived from furnace tests. Thus many of the resulting design aids available also correspond to a level 1 assessment. This may not be always apparent in the design code.

## 2.4 APPLICABILITY OF ASSESSMENT LEVELS

Owing to the fact that most regulatory authorities use standard gradings to determine the required fire resistance of a building, structural fire resistance has been based on standard periods or gradings of fire resistance of 30, 60, 90, 120 and 240 min determined from element tests. For ease of application these gradings have, traditionally, been related solely to the size of the structure (height, floor area or volume as appropriate) and to its usage (and by implication the combustible fire load) (Ministry of Works, 1946). These parameters were expressed in terms of broad-based categories. Until recently, no account was generally taken of the existence of automatic active fire protection methods such as sprinkler systems in the determination of the required fire grading (section 2.5). It should also be pointed out that, in the past, the required fire gradings have often been based on obsolete data from buildings now with outmoded forms of

construction, and therefore response in changes to these gradings to take account of new methods or materials of construction was often slow. To a certain extent, this innate conservatism of approach can be explained as fire and its effects tend to be the subject of an emotive rather than a rational response. However, this conservatism may also lead to the situation whereby developments are held back.

Gradually, it appears that some countries are coming to terms with the need to consider a more rational approach in determining the required duration of fire resistance for a structure, either by allowing a limited calculation using risk analysis (Kersken-Bradley, 1986) or by acknowledging, or indeed in certain cases specifying, the existence of active measures as has recently occurred in England and Wales (Department of the Environment, 1992a).

Equally, regulatory bodies are moving away from a prescriptive approach to fire resistance performance, by telling the designer what must be done to provide a specific method of construction with its required fire resistance to a functional approach in which the designer is told what must be achieved rather than how, i.e. the concept of fire safety engineering has been recognized as a legitimate design tool. Thus a much more flexible approach in terms of the use of calculation methods either on individual elements or the whole structure is available. Under certain circumstances, the designer can adopt a more flexible approach on the use of heating regimes other than the standard furnace curve. It is to be emphasized that there are a large number of uncertainties with the application of full calculation methods of which the designer needs to be aware (Purkiss, 1988), even though to a certain extent these uncertainties are covered by partial safety factors and the inherent conservatism in the design values used for various parameters needed in such calculations.

However, this freedom to use a full level 3 assessment is unlikely to be available for most structures since, whilst it may be possible to determine the fire load and ventilation characteristics for the structure as designed and built, any change of use during the life of the structure may alter both the fire load and/or ventilation giving totally different compartment temperature–time responses, and thus a totally different need for fire protection or fire design. As it is possible that such a change of use may need not to be notified to any regulatory authorities, or, worse, may fail to be notified, the need for change to the fire design may not be realized. This problem may be mitigated by the existence of a proper fire safety management policy. However, alterations to the fire safety design imposed by the change of use could be prohibitively expensive. It is therefore only really possible to design the structure for either exposure to the standard temperature–time curve on a time equivalent basis, or to a natural fire response where the structure is such that its use cannot change during its life. Examples of this type of structure include bus or railway stations,

sports stadia, airport terminals or large shopping complexes (Kirby, 1986; Kirby, undated).

It should also be pointed out that, for some structures, it may not be economic to consider the calculation methods even when the standard furnace curve is used as the thermal exposure model. This will be especially true when the required fire resistance period is low, say 30 min, when for reinforced concrete, for example, the cover required to satisfy durability will be far higher than that required to provide adequate fire performance.

## 2.5 INTERACTION BETWEEN ACTIVE AND PASSIVE MEASURES

Traditionally, structural fire performance has always been achieved by the provision of passive measures such as the provision of adequate cover to reinforcing steels or the provision of a given thickness of protection on a steel beam in order to achieve a specified regulatory fire resistance. Equally, the insurers of a structure have either insisted on, or have offered financial inducements in terms of reduced insurance costs for, the provision of active fire prevention measures commonly in the form of sprinkler systems. The insurer's motive is clearly to reduce the amount of damage caused to the property and contents in the case of a fire, but if the active system successfully controls the fire by either preventing its spread or controlling the temperature of the fire to such an extent so as to keep temperatures below those needed to cause structural damage, then the question can be raised as to whether the provision of such active measures should not be allowed to contribute to the overall fire resistance requirements. This argument has led to a discussion on possible 'trade-offs' between the two approaches as to the possibility of whether the provision of active measures can lead to a reduction of the passive requirements (Stirland, 1981; Read, 1985).

The solution to this problem is essentially statistical and has been addressed by Baldwin and Thomas (1973) and Baldwin (1975), when it was demonstrated that depending on relative costs and an assessment of the probability of failure of the sprinkler system, that the fire resistance grading required for an office block could be reduced by about 1 h if sprinklers are fitted over that period required if no sprinklers were to be fitted.

It is thus seen that there is a benefit from trade-off although the benefits gained may not yet have been fully utilized in that with a fully operative sprinkler system the fire may well be contained or indeed extinguished before any structural damage occurs. There is, however, still the need to consider the possibility of the fire occurring when for whatever reason the sprinkler system is inoperative. Thus, until further guidance becomes

available, it may well be prudent only to consider trade-off in terms of reduced fire resistance periods recognizing that one of the prime functions of fire resistance is to allow evacuation to proceed safely. The situation would appear that whilst the version of Approved Document B current when this text was written does allow some 'trade-off', the new proposed version will enhance the situation (Kirby *et al.*, 2004).

Having outlined the basic philosophy behind structural fire safety engineering design, it is still necessary to consider the role that traditional test methods and the prescriptive approach to fire resistance design that ensued have to play.

# 3 Prescriptive approach

---

Chapter 2 presented the rationale behind the concept of calculation methods applied to the design of structures to resist the effects of fire. These methods use an extension of the limit state approach which was originally formulated to deal with structural design at ambient conditions, in order to give the structure as a whole a uniform factor of safety against collapse. However, such calculation methods are not currently developed in such a manner that they can be applied to all structures. Also, such calculation methods can be too cumbersome to be used on simple structures where, for example, low periods of fire resistance are required, and it should be noted that the calculation methods may give solutions which are unacceptable for other design criteria, i.e. for reinforced concrete, calculations may produce covers to the reinforcement which are below those required to satisfy durability requirements.

It is therefore necessary to consider methods which can be used where the calculation approach cannot be justified due to the nature of the problem or where appropriate methods do not exist. These methods are essentially prescriptive in that the designer is told what parameter values to use rather than being able to calculate these values. It should be noted that the prescriptive approach historically preceded the calculation approach. The data used in the prescriptive approach are obtained by interpreting the results from the standard fire test. For a history of the development of the standard fire test, reference should be made to Malhotra (1982a, 1994), or Babrauskas and Williamson (1978a, b).

## 3.1 STANDARD FIRE TEST

The basic principle of the standard fire test which should perhaps, more properly, be known as the *standard furnace test*, is that a structural element is loaded so as to produce the same stresses in the element that would be induced in that element when in place in the structure of which it is considered a representative part. The element is then heated under load with the measured temperature régime in the furnace following

a prescribed temperature–time relationship until failure of the element occurs. Traditionally, beams and slabs are heated from beneath, while columns are heated on all four sides with walls being heated from one side only (Fig. 3.1).

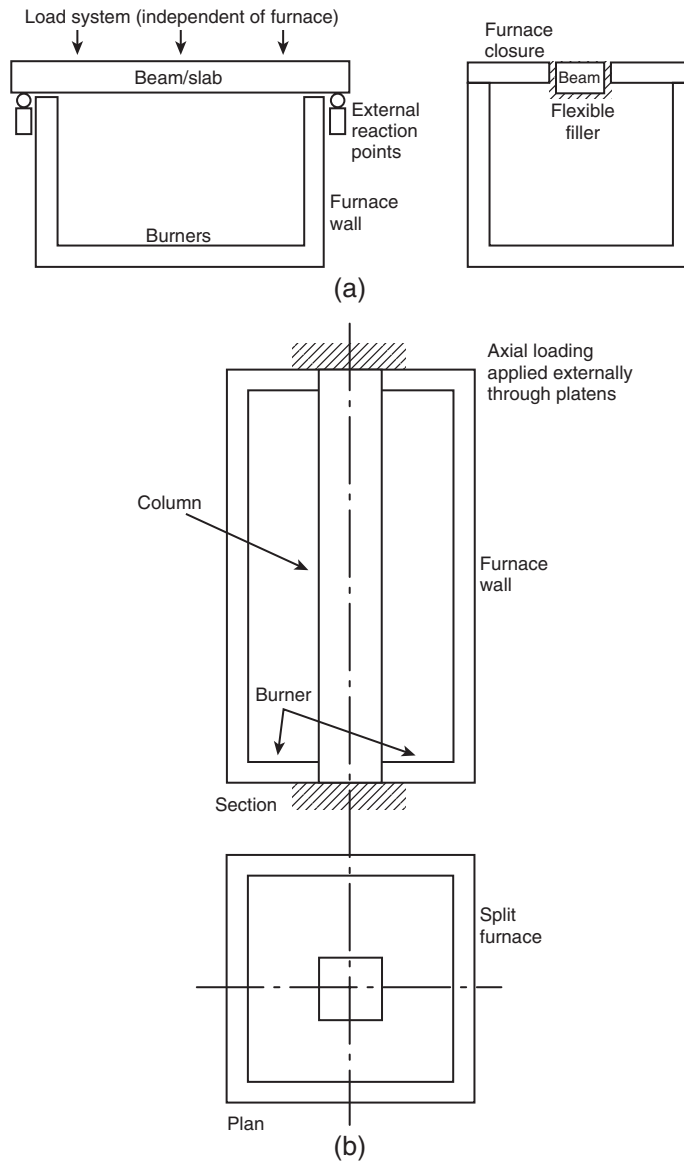


Figure 3.1 Standard furnace test layout: (a) beam and (b) column.

The standard furnace test is regulated on an international basis by ISO 834 (1975) which has been subject to amendments since 1975. National bases tend to be in essential agreement with the international standard, although there may be slight variations in the detail of the test. In the UK the current British Standard was BS 476 Parts 20–22 (1987), although it should be noted that much of the data contained within British Standard Codes of Practice and other relevant statutory standard documents were obtained from tests carried out to an earlier version of the standard, BS 476 Part 8 (1972). BS 476 has now been replaced by BS EN 1363.

The remainder of this section is specifically written in terms of the requirements of BS EN 1363 and BS EN 13501.

Traditionally, most building structure fires have been considered to occur with the bulk of the combustible material taken as cellulosic and the resultant standard furnace temperature–time curve being established on this basis. For such fire tests, the temperature–time curve specified for the furnace is

$$\theta_g = 20 = 345 \log(8t + 1) \quad (3.1)$$

where  $\theta_g$  is the furnace temperature ( $^{\circ}\text{C}$ ) and  $t$  is the time (minutes). Equation (3.1) is plotted in Fig. 3.2. The standard curve gives temperatures of  $842^{\circ}\text{C}$  at 30 min,  $945^{\circ}\text{C}$  at 60 min and  $1049^{\circ}\text{C}$  at 120 min.

It should be noted that whilst Eq. (3.1) is mathematically concise, it is not ideal for calculating analytically explicit solutions to the heat transfer equations (section 5.1) when an element is exposed to the standard furnace curve on one or more boundaries. Thus several alternative expressions were derived.

### 1. One due to Williams-Leir (1973):

$$\theta_g = \theta_0 + 532(1 - e^{-0,01t}) - 186(1 - e^{-0,05t}) + 820(1 - e^{-0,2t}) \quad (3.2)$$

or,

$$\theta_g = \theta_0 + 186[2,86(1 - e^{-0,01t}) - (1 - e^{-0,05t}) + 4,41(1 - e^{-0,20t})] \quad (3.3)$$

where  $t$  is in minutes, and  $\theta_0$  is the ambient temperature.

### 2. One due to Fackler (1959):

$$\theta_g = \theta_0 + 774(1 - e^{-0,49\sqrt{t}}) + 22,2\sqrt{t} \quad (3.4)$$

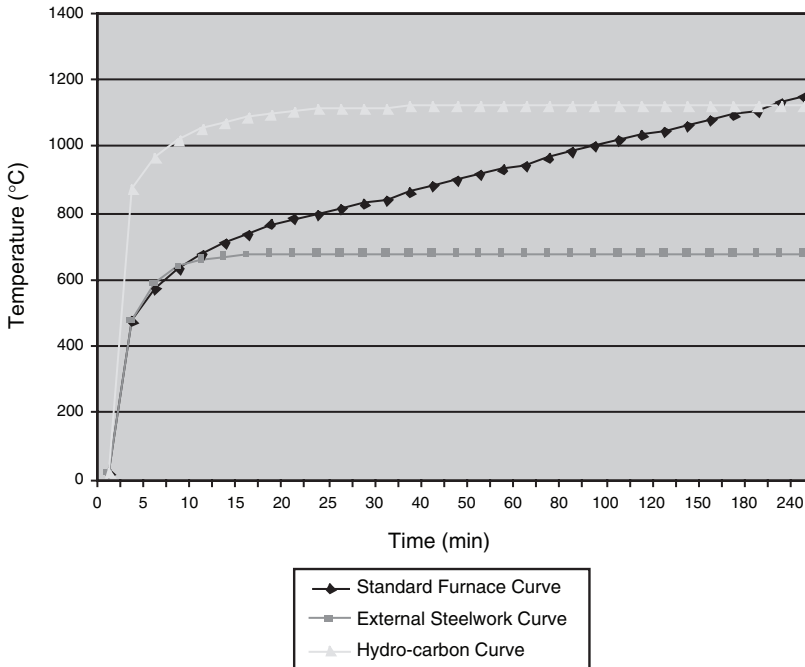


Figure 3.2 Standard temperature–time responses.

It should be further noted that whereas BS EN 1363 considers the fire temperature to be related to a base temperature of 20°C, and thus needs to set out resultant limits on the variations in ambient conditions which are acceptable during a fire test, ISO 834 (1975) relates the fire temperature to a measured ambient temperature  $\theta_0$ :

$$\theta_g = \theta_0 + 345 \log (8t + 1) \tag{3.5}$$

A revision of ISO 834 was proposed to bring it into line with BS 476 by adopting a fixed base temperature of 20°C. That draft revision also gave an alternative exponential form of the temperature–time curve as

$$\theta_g = 20 + 1325(1 - 0,325e^{-0,2t} - 0,204e^{-1,7t} - 0,471e^{-19t}) \tag{3.6}$$

This equation corresponds to the parametric curve for natural fire exposure given in EN 1992-1-2 with the parameter  $\Gamma$  defining the degree of exposure set equal to unity, i.e.  $t^* = t$ .

The temperature–time relationship given by Eqs (3.1)–(3.6) relate to members exposed to the full effect of a standard fire. This exposure is considered too severe for load-carrying members in a façade external to a structure and the following temperature–time relationship has been proposed (EN 1991-1-2):

$$\theta_g = 20 + 660 \left( 1 - 0,687e^{-0,32t} - 0,313e^{-3,8t} \right) \quad (3.7)$$

Equation (3.7) is also plotted in Fig. 3.2.

With the advent of an increasing use of petrochemicals and plastics, it was recognized that the cellulosic curve alone was no longer satisfactory since the temperature rise in a petrochemical fire is much faster and an additional curve was required. Thus, where an element is exposed in an environment of which the predominant constituent is of petrochemical origin, then a more appropriate temperature–time curve is given by:

$$\theta_g = 20 + 1100 \left[ 1 - 0,325e^{-0,1667t} - 0,204e^{-1,417t} - 0,471e^{-15,833t} \right] \quad (3.8)$$

The hydrocarbon curve Eq. (3.8) is designed to give a very rapid temperature rise. In 10 min, the temperature reaches 1052°C, with the limiting temperature of 1120°C effectively being reached at 40 min. Equation (3.8) is also plotted in Fig. 3.2. It is suggested (Varley and Both, 1999) that the standard hydrocarbon curve is not severe enough to represent fires in tunnels and that either the RABT curve which rises to around 1200°C in 10 min and remains constant until 60 min before a linear cooling phase, or the Rijkswaterstaat curve which rises to 1350°C at 60 min before cooling to 1200°C at 120 min.

The standard furnace test, whether conducted under the temperature–time régime imposed by either the cellulosic or hydrocarbon curve continues until failure occurs due to any one of the following criteria (or limit states) being met:

**1. Insulation (denoted as D):**

The average temperature on an unexposed face achieves a temperature of 140°C or a local value exceeds 180°C.

**2. Integrity (denoted as E):**

Cracks or openings occur in a separating element such that ignition can occur on the unexposed face.

**3. Load-bearing capacity (denoted as R):**

The element being tested loses load-bearing capacity when the element is no longer able to carry the applied loading. In practice, however,

deflection limits are imposed, partly in recognition of the fact that at collapse, large deflections occur due to the formation of plastic hinges in beams or slabs, or due to incipient buckling in walls or columns and partly to avoid the specimen collapsing into the furnace with possible consequential damage to the furnace and loading system.

For any members such limits should not be applied until the deflection reaches  $L/30$ . Then for

- **Flexural members:**

Limiting deflection is  $L^2/400d$  (mm) or rate of deflection  $L^2/9000d$  (mm/min)

where  $d$  is the depth of the member and  $L$  the span, both in mm.

- **Vertically loaded members:**

Limiting vertical contraction is  $h/100$  (mm) or rate of contraction  $3h/1000$  (mm/min)

where  $h$  is the initial height of the member (mm).

It is to be stressed that the deformation or, rate of deformation, limits ONLY apply to performance in the standard furnace test and NOT to elements within a structure.

The result from the fire test is quoted in time units of minutes when each of the limiting criteria  $R$ ,  $E$  or  $I$ , if appropriate to the element of construction being tested, is reached. The final test grading is then expressed as the least time for any of the criteria rounded down to the nearest appropriate classification, i.e. 30, 60, 90, 120, 180 or 240 min.

A fire test can be carried out for one of the three reasons:

1. to determine the fire resistance grading for a given method of construction to enable that method of construction to be accepted by regulatory bodies;
2. to assist in the development of new products or methods as initially it is more appropriate to accept results from tests rather than from calculations especially, where those calculations may need test results to provide justification for the assumptions used therein; or
3. to enable research on the influence of specific variables in a form of construction to be studied in order that a better understanding of the performance of structural elements or materials can be established. There can be substantial problems with this, especially, where phenomena such as spalling occurs (Purkiss, Morris and Connolly, 1996). This was also borne out in a set of tests reported by Aldea, Franssen and Dotreppe (1997) on reinforced concrete columns, of which the results are given in Table 3.1. The columns were 290 mm square and 2,10 m long. The actual concrete strengths are not quoted although

**Table 3.1** Fire resistance column test results

Concrete grade	Reinforcement	
	8D12 (1,08%)	4D25 (2,33%)
C20	3 h 54 min	3 h 13 min
C50	2 h 32 min	3 h 29 min
C90	1 h 46 min <sup>a</sup>	1 h 29 min <sup>b</sup>

<sup>a</sup> Spalling started at 8 min into the test.

<sup>b</sup> Spalling started at 12 min into the test.

Source: Aldea, Franssen and Dotreppe (1997) by permission

in all cases, the loading was 50% of the design load. The high performance columns did not contain polypropylene fibres. It is quite clear from these results that for the C20 and C50 concrete columns, there is no correlation between steel area and fire endurance. The high performance concrete column behaviour is dominated by spalling which prevents the columns reaching their full endurance period.

In recent years, the use of the standard furnace test to determine parametric variations has tended to become redundant with the advent of computer simulation.

It is, however, this use of the fire test that has provided much of the tabular data currently in design codes such as EN 1992-1-2, or other similar documents such as the FIP/CEB Report (1978) for concrete construction.

Although the fire test has provided a very useful amount of data, the test itself has a series of inherent drawbacks stemming in part from the very nature of the test and in part due to the uses of the test.

## 3.2 DRAWBACKS TO THE FIRE TEST

### 3.2.1 Expense

The fire test, especially if a full four-hour rating were required, is very expensive both in terms of the specimen preparation and the cost of the actual test. It should also be noted that the data obtained from a particular test are only applicable to that test. If a test does not give the required result in, say, that the desired fire resistance period was 60 min and the test gave 59 min fire resistance then its classified result would be 30 min,

and a new test following modifications would be necessary to establish the desired rating.

### 3.2.2 Specimen limitations

As test furnaces are restricted in size, it is generally impossible to test large elements of construction and thus 'representative' specimens are tested. Such restrictions (in the case of columns a maximum height of around 3 m and for beams and slabs, a maximum span of 4 m and a maximum width of around 4 m) mean that it is difficult to test realistic multi-span beams or slender columns, since any reduction in member size to achieve the required slenderness will give erroneous results as it is, in general, difficult to apply scaling to fire test results.

The availability or design of furnaces can also restrict the type of test that can be carried out. For example, in the case of columns, the most critical situation is likely to be when a column is subjected to moments both due to the applied loading and the thermal gradients induced by non-symmetric heating. However, most available column test furnaces can only heat columns on all four sides whilst the column is under the influence of axial load only.

### 3.2.3 Effect of restraint or continuity

Again owing to both the limitations of the loading arrangements in most furnaces and the limitation on specimen size mentioned above, it is generally only possible to test specimens with idealized end conditions, i.e. beams and slabs with simply supported ends and columns with some indeterminate degree of fixity arising from the loading platens in the test rig. Clearly, structural elements do not exist in isolation and, in practice, where a fire is restricted to part of a structure only, there will be some load redistribution away from the fire affected zones to those unaffected by the fire. This redistribution will generally have the effect of enhancing the fire performance of a member (Fig. 3.3). This has been shown by the tests that have been carried out to examine the effects of restraint (Selvaggio and Carlson, 1963; Ashton, 1966; Bahrends, 1966; Ehm and von Postel, 1966; Issen, Gustaferrero and Carlson, 1970; Lawson, 1985; Cooke and Latham, 1987). For example, Ashton indicates that whilst restraint may not significantly alter the load-carrying capacity, the deflections will be substantially reduced. It should be noted that in the tests reported by Ashton, the restraint applied was higher than that likely to apply in practice. The research undertaken in America reported that a moderate degree of restraint would enhance the fire performance of a pre-stressed

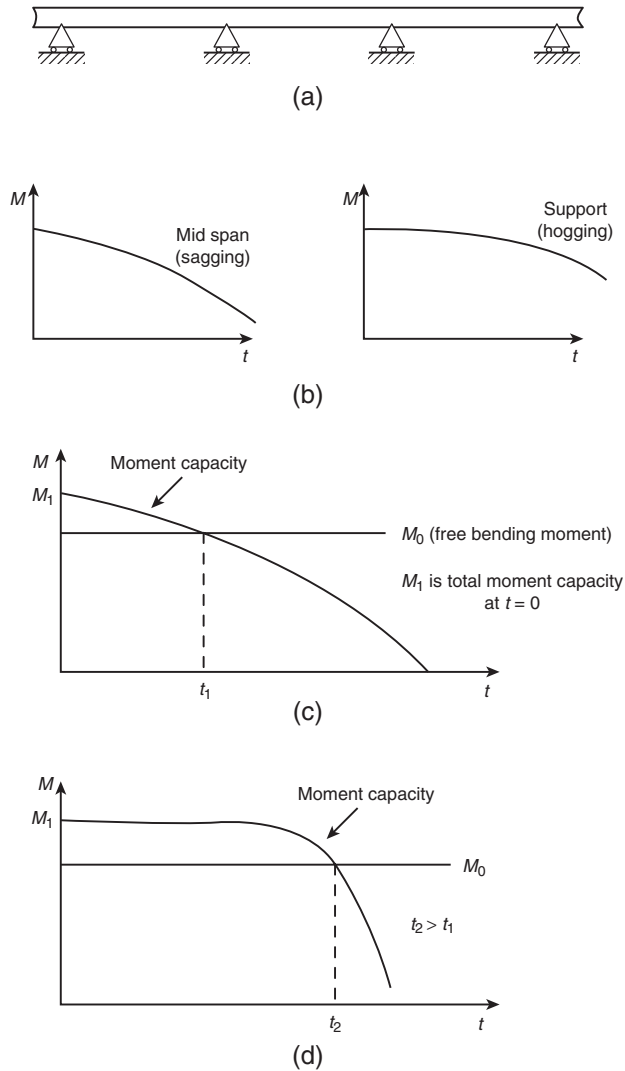


**Figure 3.3** Effect of member continuity on the fire affected performance of flexural members: (a) basic structure; (b) decrease of moment capacity with time; (c) no hogging moment and (d) hogging and sagging.

concrete slab, whereas a high degree of restraint would only give a similar fire performance to that where no restraint existed (Selvaggio and Carlson, 1963; Issen, Gustafsson and Carlson, 1970).

In the case of columns the existence of restraint will have two effects. The first is to lessen potential losses in strength and elasticity owing to

the presence of additional forces induced by the resistance to the free thermal expansion. The second is that the failure mode of the column may change from a sudden buckling collapse to one in which progressively larger deformations occur, when the load capacity is limited by strain capacity (Dougill, 1966). Dougill continues by questioning the relevance of the result on a single column in a furnace test to its performance in a stiff structure.

### **3.2.4 Confidentiality of results**

While, from a manufacturer's point of view, confidentiality of any result is absolutely essential, it also means that any data obtained from such tests are unavailable for the purposes of research and therefore cannot be used to provide additional or supplementary data for improved calibration of calculations on fire performance.

### **3.2.5 Loading**

For routine fire testing, the loading is specified as that causing the same stresses in the members to which they would be subjected under normal service or working loads. The fire testing of members under service loading led to the observation that, for concrete beams or slabs when tested as simply supported, the beam or slab was unable to continue to carry the applied loading when either the reinforcing or prestressing steel reached a temperature of around 500–550°C. A similar observation was made for steel beams. Thus, the concept of the existence of a critical failure temperature in the steel, be it reinforcement or structural, was adumbrated.

Early work using the fire test to provide data on the performance of reinforced and pre-stressed concrete structural elements under loading other than service loading generally, concentrated on loading greater than the service load to determine the effect of overload (Thomas and Webster, 1953; Ashton and Bate, 1960). It is not until much more recently that the effect of load levels lower than service loads have been considered (Robinson and Latham, 1986; Robinson and Walker, 1987). It was this latter work that finally led to the abandonment of the concept of a fixed critical temperature for structural steelwork (section 8.2.1).

### **3.2.6 Failure modes**

The standard furnace test is only capable of studying the failure mode of a single structural element and cannot therefore be used to investigate

failure modes of complete structure. It has been observed that, for example, in concrete structures failure of columns can be by shear caused by the expansion of the structure (Malhotra, 1978; Beitel and Iwankiw, 2005).

### 3.2.7 Reproducibility

There are two areas of concern here. The first is due to the fact that replicate tests are rarely undertaken, partly since the relevant test standards only specify the need for a single test and partly due to sheer expense. Dotreppe, Franssen and Vanderzeypen (1995) report the results on a pair of identical reinforced concrete columns tested in the same furnace, one gave a fire endurance of 84 min, the other 138 min. The authors indicated that a computer analysis predicted 85 min. It is not clear why the anomaly occurred, but the results do indicate the possible dangers of relying on single tests to establish code data.

The use of single tests is a situation rarely condoned in other fields of structural testing but the effect is, to a certain extent mitigated by the use of a classification scheme for expressing the results.

The second area of concern is that of reproducibility of results from different test furnaces. To assess this effect, a series of tests on steel rolled hollow sections was carried out (Witteveen and Twilt, 1981/2), the results from which are presented in Fig. 3.4, where it will be seen that there are

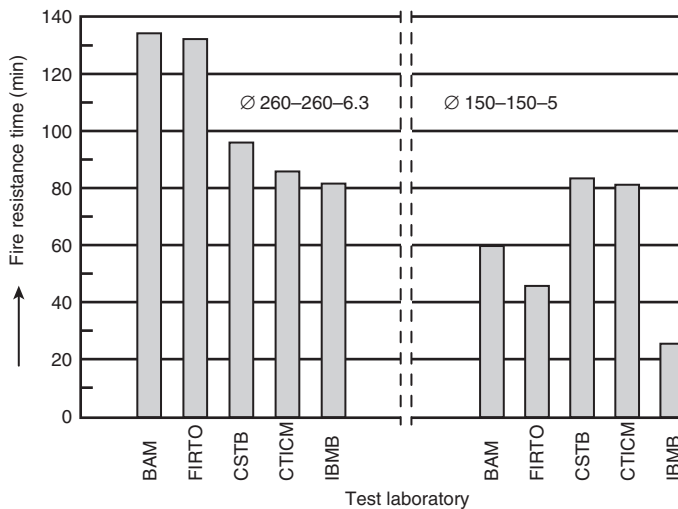


**Figure 3.4** Effect of furnace characteristics on fire test results (by permission, Witteveen and Twilt, 1981/2).

substantial differences in the behaviour obtained. It is likely that were such a test series to be carried out now, the differences between furnaces would be smaller.

Some of these differences are due to the loading arrangements, in that it is very difficult to provide either a pure pin end or pure fixed end at the loading platens. The actual condition is likely to be somewhere between the two, and will be somewhat variable depending on the actual load applied and the construction of the loading system which will therefore vary from furnace to furnace, even though most furnaces use hydraulic load application. Another difference is caused by the furnace itself since the test specifies only the temperature of the furnace at any time and not the heat flux falling on the specimen. The rate of temperature rise in the specimen will depend on the incident heat flux, which will be a function of the thermal characteristics of the furnace in terms of its thermal inertia (Harmathy, 1969), and of the method used to fire the furnace with respect to both the position of burners and the type of fuel (oil or gas) as this will affect the emissivity of the surface of the member. The results of measurements on three American furnaces indicating the differences between measured convective, radiative and total heat fluxes are presented in Fig. 3.5 (Castle, 1974). All three furnaces were operating in the standard furnace curve and were within the tolerance limits set down in the relevant test codes. With these differences it is, perhaps, not surprising that variations in test results occur between different furnaces. To help mitigate these differences, BS EN 1363-1 indicates that the furnace linings shall consist of materials with densities less than  $1000 \text{ kg/m}^3$  with a minimum thickness of 50 mm comprising at least 70% of the internally exposed surface.

In spite of these drawbacks, the furnace test has provided a substantial data bank of results on which the prescriptive method of determining the fire resistance of structures was based, and still provides a convenient and necessary method of providing comparisons between the performance of two different types of construction; it also provides data where calculation methods are neither applicable nor possible.

### **3.3 PRESCRIPTIVE DETERMINATION OF FIRE RESISTANCE**

The prescriptive approach for determining the fire resistance of a structure, or more correctly, the assemblage of the elements comprising the structure considered on an individual basis, can be defined in the flow diagram in Fig. 3.6, where the element is detailed to provide the fire resistance required by the appropriate regulatory guidelines. It should be noted that this method is still permissible under most design codes including the Eurocodes.

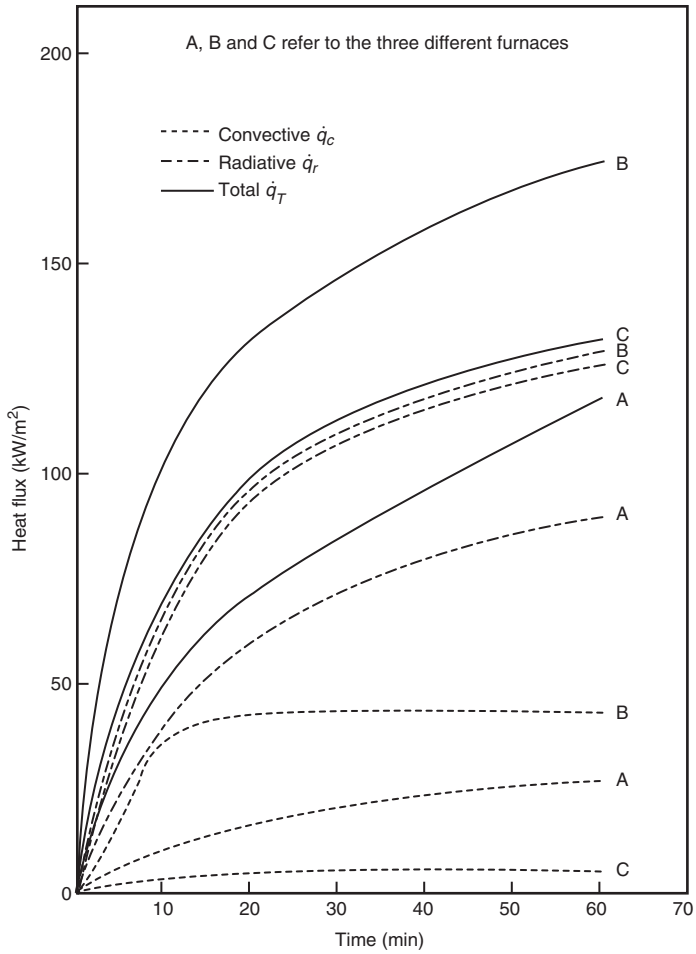


Figure 3.5 Variability of heat flux between different furnaces (Castle, 1974).

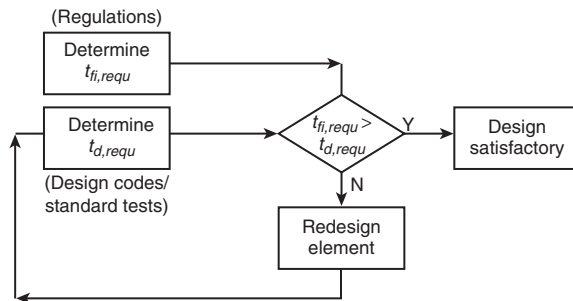


Figure 3.6 Prescriptive approach for determining the fire resistance of structural elements.

The prescriptive method is essentially very quick, but is not likely to be economic, in that calculations may show that thinner members with lower cover, in the case of concrete, or lower amounts of fire protection, or indeed no fire protection, in the case of structural steelwork, can provide the requisite fire performance. In order to provide examples of the prescriptive method, it is convenient to consider each of the construction materials separately.

### **3.3.1 Concrete**

The two main variables to be considered here are the specification of minimum overall dimensions of the member and the minimum axis distance to the main reinforcement. The minimum overall dimensions are specified, either in the case of walls or slabs to keep the temperature on the unexposed face below the insulation limit of 140°C, or to ensure that spalling will not be severe enough to cause either the web of a beam or rib in a slab or a column to lose an amount of concrete such that the member can no longer carry its design loading. The minimum axis distance is specified to keep the temperature of the main reinforcement, which can be either the bottom flexural steel in a beam or slab or the vertical compression reinforcement in a column or wall, below a critical value generally considered as being around 500–550°C, as it is at around this temperature that the strength of the reinforcement drops to a value equal to the stresses induced by service loading (which is the loading generally applied in fire testing). The values of member dimensions and axis distance are dependant on the type of aggregate within the concrete (siliceous or calcareous in normal-weight concrete or lightweight) and on the fire resistance period. For columns, the effect of load level on these dimensions is also considered. For beams and slabs, there may also be some allowance for continuous members in comparison with simply supported members by a slight reduction in axis distances and overall depth values, in recognition that there is a degree of redistribution of moments away from areas of sagging moment to areas of hogging moment during a fire (Fig. 3.7).

Additional requirements where spalling is considered to be critical may also be specified such as the provision of supplementary reinforcement in the form of light mesh in the concrete or the use of polypropylene fibres where axis distances exceed certain values or the concrete is high strength or self-compacting.

As indicated in the previous paragraph, axis distances to reinforcement rather than covers are specified. This is actually more scientifically correct as it is observed in computer-based heat transfer calculations that the temperatures at the centre of a reinforcing bar are identical to those at

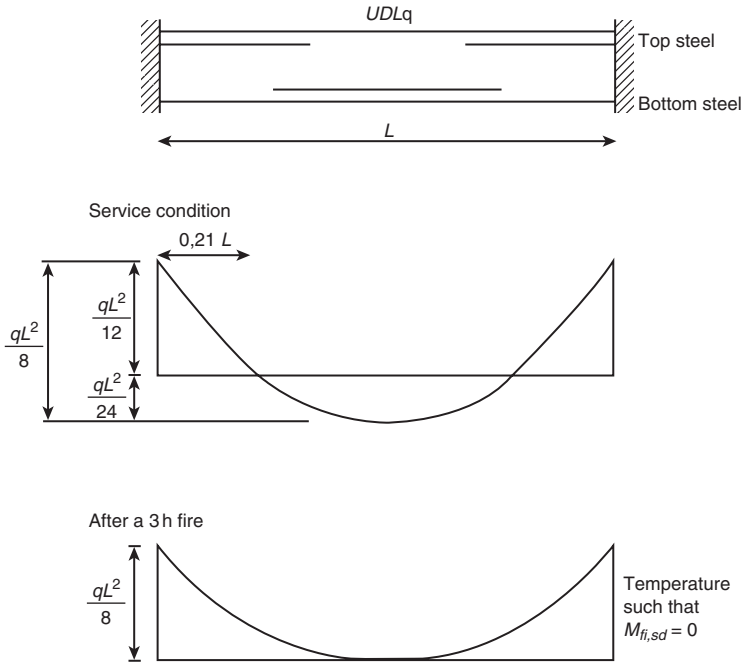


Figure 3.7 Redistribution of moments from midspan to support in a fire.

the same position in plain concrete (Ehm, 1967). Becker, Bizri and Bresler (1974) indicate that this is only correct for a reinforcement area less than 4% of the gross section. Where the main reinforcement is in more than one layer, then the effective axis distance is used to determine the fire resistance requirement.

### 3.3.2 Structural steelwork

In the case of steelwork, it is far more difficult to employ a prescriptive approach; this is partly due to the diversity of protection systems available and partly due to the fact that a calculation approach for steelwork is much simpler and much less restrictive than that for concrete. Because of the diversity of systems available, prescriptive data can only apply to generic categories and not to specific products. In addition, the fire performance is generally determined on a single-sized member (in the UK for beams a 406×178×60 UB (universal beam) and for columns a 203×203×52 UC (universal column) rather than a range of member sizes (Morris, Read and Cooke, 1988). Thus the results strictly should only

be applied to members of that size, but applied to alternative sizes, the results will be conservative when applied to larger sections and unsafe to smaller. Also, it should be noted that deflections (or surface strains) may be higher in an actual design over and above those in the representative test. This could give problems with stickability of the fire protection.

The situation has been partially remedied by manufacturers providing data on their own particular protection system allowing the thickness of the protection system to be related to the section size and the required fire resistance. In the UK, a convenient compendium of such data exists in the form of a document produced by the Association of Specialist Fire Protection Contractors and Manufacturers Limited, the Steel Construction Institute and the Fire Test Study Group (2004). It should be noted that, currently, the data in the compendium are based on a 'failure' temperature in the steel of 550°C for columns and 620°C for beams, and therefore these data make no allowance for the load intensity applied to the member. The difference between the two failure temperatures is that board and spray systems are generally tested on columns which are noted to 'fail' when the section attains a mean temperature of 550°C, when tested under full-service loading, whereas intumescent paint systems are generally tested on beams which when loaded to full-service loads fail at a slightly higher temperature, because of the thermal gradient induced by the heat sink effect of the non-composite cover slabs on the top flange of the beam.

### **3.3.3 Masonry**

Since, generally, masonry is usually used non-structurally, in that its vertical load-carrying capacity is not used, the essential requirement is that of insulation, i.e. the temperature on the unexposed face being kept below 140°C. This means it is relatively simple to use a prescriptive approach. Tables of required wall thicknesses to achieve a required fire resistance are given in ENV 1996-1-2.

### **3.3.4 Timber**

Owing to the fact that exposed timber is rarely used in situations requiring other than notional fire resistance there are few data available for a prescriptive approach, although some experimental data exist on the fire performance of stud partition walls (Meyer-Ottens, 1969). Where exposed timber is required to provide fire resistance, it is relatively simple to perform the necessary calculations, as the core of the timber member inside

the charred zone is little affected by temperature, and normal ambient design methods may then be used.

Before considering the possible methods of determining the performance of structures or structural elements in a fire by calculation, it is useful first to consider the character of fires and their relationship to the standard fire test.

# 4 Behaviour of natural fires

---

Unlike the temperature–time response in a furnace test which is imposed by the standard to which the test is being carried out, the temperature–time response in a fire compartment is a function of the compartment size, the type of compartment together with the available combustible material and the air supply available for combustion. This situation is often referred to as a *natural* or *real fire* (the former term is preferred here, although EN 1991-1-2 uses the term *parametric fire*), i.e. it is one in which the heat generated can be calculated from basic principles. However, attempts have been made to represent the solution to the natural compartment temperature–time response by empirical curves; one such is given in EN 1991-1-2.

The temperature–time curve generated from the standard furnace test is often referred to as a ‘pseudo’ fire as the temperature characteristic cannot be generated from basic principles. It is, however, possible to link the two types of response either by the concepts of fire severity and equivalent fire period or through parametric curves.

## 4.1 DEVELOPMENT OF COMPARTMENT FIRES

The development of compartment fires can be broken down into three phases: pre-flashover (also known as the growth period); post-flashover (fully developed fire) and the decay period (Fig. 4.1).

### 4.1.1 Pre-flashover period

In the pre-flashover period, any combustion is restricted to small areas of the compartment; therefore, only localized rise in temperature can occur which, it should be noted, may still be substantial. The overall or average rise in temperature within the bounded fire compartment will be very small and indeed at this stage there may be no obvious signs of

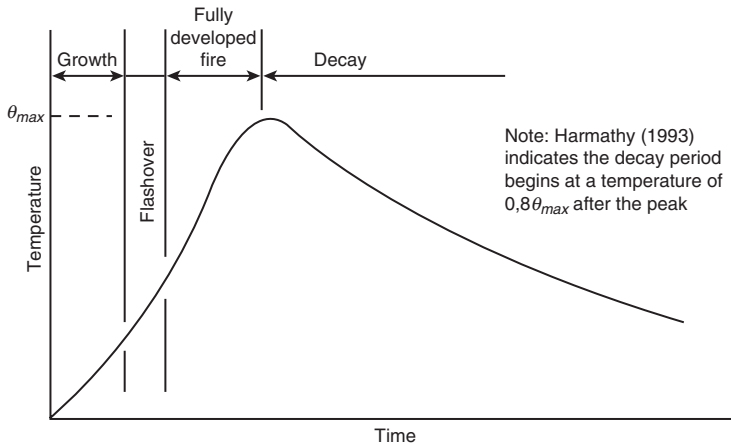


**Figure 4.1** Phases in a fully developed fire.

a fire. A large number of incipient fires never get beyond the stage of pre-flashover since there may be neither sufficient fire load nor air supply (ventilation) to allow the fire to grow beyond this stage. It should be noted that in many cases it is human intervention which causes flashover by, say, opening a door or window and thereby suddenly increasing the air supply. The pre-flashover stage is often ignored in the calculations of the compartment temperature–time response since the overall effect on the compartment is small even though the pre-flashover period can be long compared to the subsequent stages of the fire.

Flashover occurs when the fire ceases to be a local phenomenon within the compartment and spreads to all the available fuel within the compartment. Propagation of flames through any unburnt gases and vapours which have collected at ceiling level then ensues.

#### 4.1.2 Post-flashover period

In this period, the rate of temperature rise throughout the compartment is high as the rate of heat release within the compartment reaches a peak. In compartment fires, maximum temperatures of over  $1000^{\circ}\text{C}$  are possible. The rate of temperature rise continues until the rate of generation of volatiles from the fuel bed begins to decrease as the rate of fuel consumption decreases, or when there is insufficient heat available to generate such volatiles.

It is during the post-flashover or growth period that structural elements are exposed to the worst effects of the fire and where collapse or loss of

integrity is likely. Once the rate of temperature rise reaches a peak, the fire continues into its decay phase.

### 4.1.3 Decay phase

As its name suggests, the temperature in the compartment now starts to decrease as the rate of fuel combustion decreases. It should be noted that owing to thermal inertia, the temperature in the structure will continue to increase for a short while in the decay period, i.e. there will be a time lag before the structure starts to cool.

## 4.2 FACTORS AFFECTING THE GROWTH PHASE

Early work (Kawagoe, 1958) suggested the burning rate of wood cribs, which are conventionally used as the test fuel in compartment fire tests, was proportional to  $A_v\sqrt{h}$ , where  $A_v$  is the area of openings in the side of the compartment and  $h$  is the height of the ventilation opening. A fire of this nature is said to be *ventilation controlled* since it is the availability of the air supply that governs the fire. The fire temperatures will not continue to increase indefinitely as the ventilation is increased, as a limiting value, of ventilation beyond which the fire temperatures will not increase, exists. Beyond this point, the compartment temperatures are dependant entirely on the quantity of fuel available. After the limiting value of ventilation is reached, the fire is then said to be *fuel controlled*. Although the concept of a ventilation factor was originally deduced empirically, it is possible to derive from first principles the dependence of a ventilation controlled fire on the  $A_v\sqrt{h}$  factor based on the mass flow rate of air to the fire (Drysdale, 1998).

The other major factor is obviously the amount of available fuel. As pointed out, above tests are usually, but not always, carried out using wood cribs to simulate the combustible contents of a compartment. This is reasonable since in general the contents of most buildings are of a cellulosic nature and thus most materials can be expressed as an equivalent calorific value of wood cribs. It should be noted, however, that with the advent of plastics this practice is less applicable, thus care must be taken as plastics and other hydro-carbon based materials give off heat far quicker, although over a shorter period, and also emit substantial amounts of dense, possibly toxic, smoke (Latham, Kirby and Thompson, 1987). A comparison between the compartment temperature–time response for a purely cellulosic compartment fire and one in which the fuel is combination of part cellulosic material and part plastic material is given in Fig. 4.2.

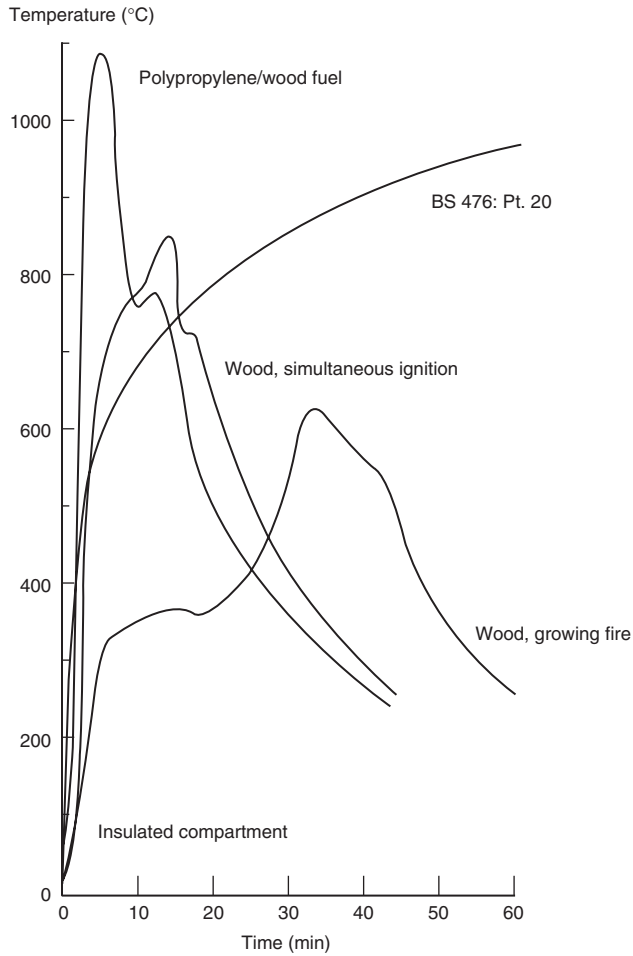


**Figure 4.2** Comparison between the temperature–time response in a compartment due to cellulosic and hydrocarbon combustibles (by permission Latham, Kirby and Thompson, 1987).

### 4.3 CALCULATION OF COMPARTMENT TEMPERATURE–TIME RESPONSES

#### 4.3.1 Basic formulation

Much of the work in this area was carried out in Sweden by Pettersson, Magnusson and Thor and forms the basis of a Swedish Institute of Steel

Construction Report (1976). It is this report, together with the outline given in Drysdale (1998), that forms the basis of this section of text.

The following assumptions were made to simplify the calculation model.

1. Combustion is complete and occurs entirely within the boundaries of the compartment.
2. There is no temperature gradient within the compartment.
3. The compartment walls can be characterized by a single set of heat transfer characteristics which is known as the thermal inertia  $b$  and is defined as  $\sqrt{(\lambda\rho c)}$  where  $\lambda$  is the thermal conductivity,  $\rho$  is the density and  $c$  is the specific heat.
4. All the fire load is ignited instantaneously.
5. The heat flow through the walls is assumed to be unidirectional.

The model is essentially generated by the solution of the compartment heat balance equation (Fig. 4.3)

$$\dot{h}_c = \dot{h}_L + \dot{h}_W + \dot{h}_R + \dot{h}_B \quad (4.1)$$

Each term of Eq. (4.1) may be considered separately. Note, the heat stored in the gas  $\dot{h}_B$  is negligible and may be ignored.

#### 4.3.1.1 Rate of heat release ( $\dot{h}_C$ )

It is assumed that the fire is fuel controlled, i.e. the rate of heat release is proportional to the ventilation factor, or

$$\dot{h}_C = 0,09A_V\sqrt{h}\Delta H_C \quad (4.2)$$

where  $\Delta H_C$  is the heat of combustion of wood (18,8 MJ/kg).

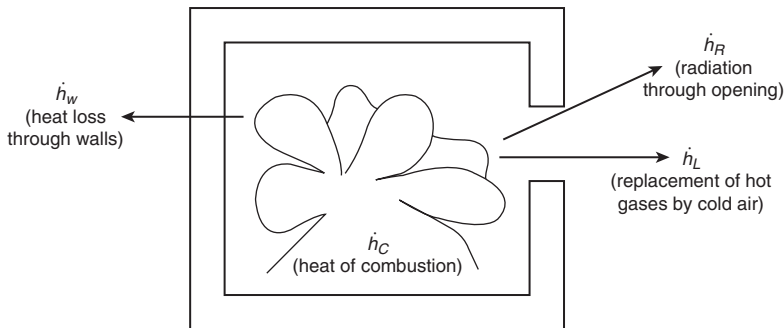


Figure 4.3 Heat balance terms for a compartment fire.

**4.3.1.2 Rate of heat loss by radiation through the openings ( $\dot{h}_R$ )**

This is calculated using the Stefan–Boltzmann law assuming the external temperature is negligible compared with the gas temperature within the compartment

$$\dot{h}_R = A_V \varepsilon_f \sigma \theta_g^4 \quad (4.3)$$

where  $\theta_g$  is the gas temperature,  $\sigma$  is the Stefan–Boltzmann constant and  $\varepsilon_f$  is the effective emissivity of the gases.

**4.3.1.3 Rate of heat loss due to convection ( $\dot{h}_L$ )**

$$\dot{h}_L = \dot{m}_F c_p (\theta_g - \theta_0) \quad (4.4)$$

where  $\dot{m}_F$  is the rate of outflow of gases,  $c_p$  is the specific heat of the gases and  $\theta_0$  is the external temperature.

**4.3.1.4 Rate of heat loss through the compartment walls ( $\dot{h}_W$ )**

This will depend on both the gas temperature and the temperature of the internal surface  $\theta_i$ , the effective thermal conductivity of the compartment boundary  $\lambda_i$  and the heat transfer coefficient (both convective and radiational) of the internal boundary  $\alpha$ .

$$\dot{h}_W = \frac{(A_t - A_v) (\theta_g - \theta_i)}{\frac{1}{\alpha} + \frac{\Delta x}{2\lambda_i}} \quad (4.5)$$

where  $A_t - A_v$  is the net internal area of the compartment allowing for ventilation openings and  $\Delta x$  is thickness of the layer used to solve the heat transfer equation through the compartment walls.

**4.3.1.5 Compartment temperature–time characteristics**

From the above formulations for the rates of heat flow, Eq. (4.1) may now be solved for the gas temperature  $\theta_g$  and graphs or tables prepared for varying values of the fuel load per unit area of the compartment boundary  $q_t$  (MJ/m<sup>2</sup>) and a modified ventilation factor  $O$  defined as  $A_v \sqrt{h} / A_t$  (m<sup>0.5</sup>). Typical results from Pettersson, Magnusson and Thor are given in Fig. 4.4 for a compartment with walls constructed from brickwork or concrete. For comparison the standard furnace curve from BS 476: Part 20 (or ISO 834 or EN 13501) is also plotted. For large compartments combustion will

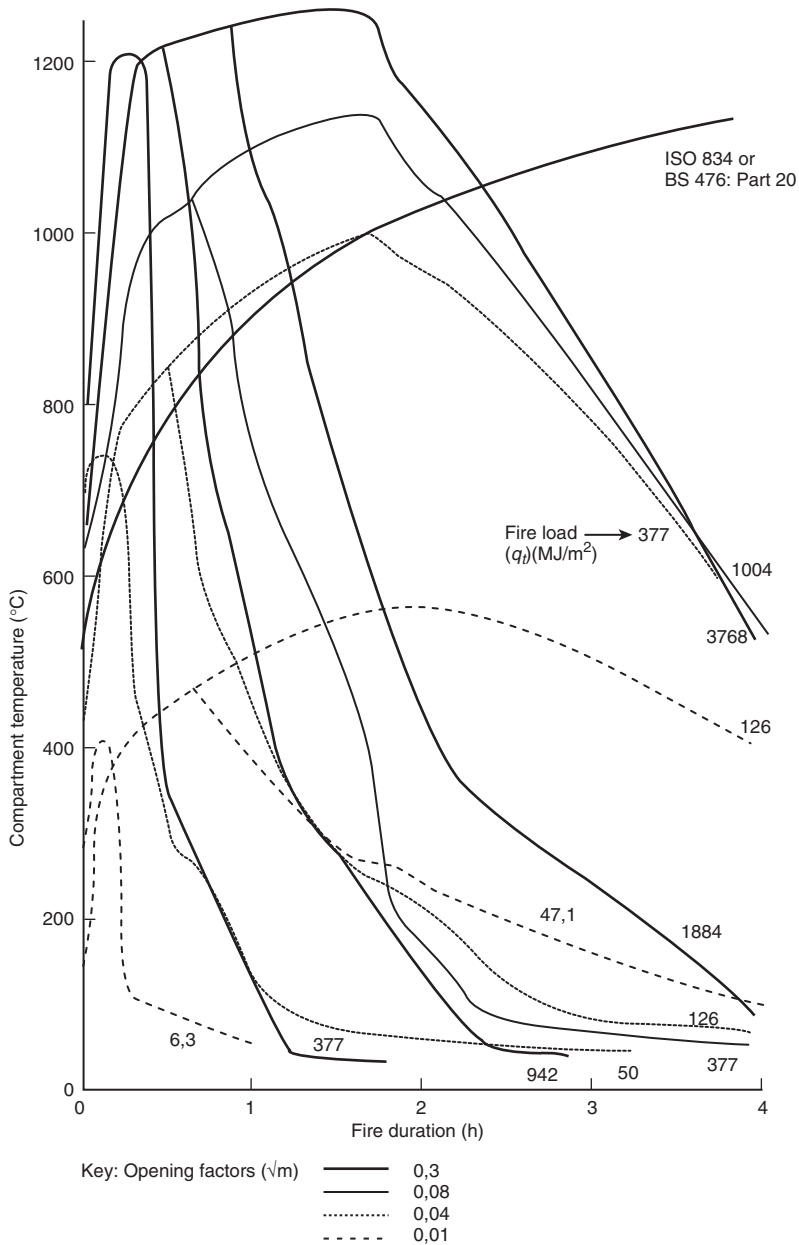


**Figure 4.4** Temperature–time response curves for a compartment fire with varying fuel loads and ventilation (Pettersson, Magnusson and Thor, 1976, reproduced by permission; © Swedish Institute of Steel Construction).

gradually spread through the compartment, but it has been shown that the peak temperatures measured at various points in the compartment occur at different times but have a similar peak value (Kirby *et al.*, 1994).

Where the compartment has multiple vertical openings, horizontal openings in the roof or where the compartment is of a different construction to the standard or reference compartment, the results from the analysis for compartment temperatures need modifying.

### 4.3.2 Modifications to allow for other compartment configurations

#### 4.3.2.1 Multiple vertical openings

In this case, the modified ventilation factor should be calculated using  $A_v$  as the total area of vertical openings and  $h_{eq}$  as the weighted average of the heights of the openings defined by

$$h_{eq} = \frac{\sum A_{v,i} h_i}{\sum A_{v,i}} \quad (4.6)$$

where  $A_{v,i}$  and  $h_i$  are the area and height of the  $i$ th opening, and the summations are taken over all the vertical openings.

#### 4.3.2.2 Horizontal openings

The effect of substantial horizontal openings is for all the combustion gases to be vented through the roof rather than the windows. When this happens the flow becomes unstable and therefore not able to be predicted using a simple model. The effect of horizontal openings is to move the neutral layer having zero pressure with respect to atmospheric pressure from the centre of the vertical opening towards the top of the opening.

Horizontal openings are treated by applying a modification factor  $f_k$  to the opening factor calculated on the basis of the vertical openings only.

The nomogram (from Pettersson, Magnusson and Thor) for calculating  $f_k$  is given in Fig. 4.5. The nomogram requires values of  $A_h \sqrt{h_1} / A_v \sqrt{h}$  and  $A_h / A_v$  where  $A_h$  is the area of the horizontal opening,  $h_1$  is the vertical distance between the horizontal opening and the mid-height of the vertical opening,  $A_v$  is the area of the vertical opening and  $h$  its height. To ensure that the horizontal opening is not dominant, i.e. the assumptions made in the calculation of the compartment temperature–time response still hold, limits are placed on the values of  $A_h \sqrt{h_1} / A_v \sqrt{h}$  for various compartment temperatures. Thus, for a compartment temperature of 1000°C the limiting value of  $A_h \sqrt{h_1} / A_v \sqrt{h}$  is 1,76 and for 500°C, 1,37. If the curves are approximated by straight lines and therefore the distinction between fire

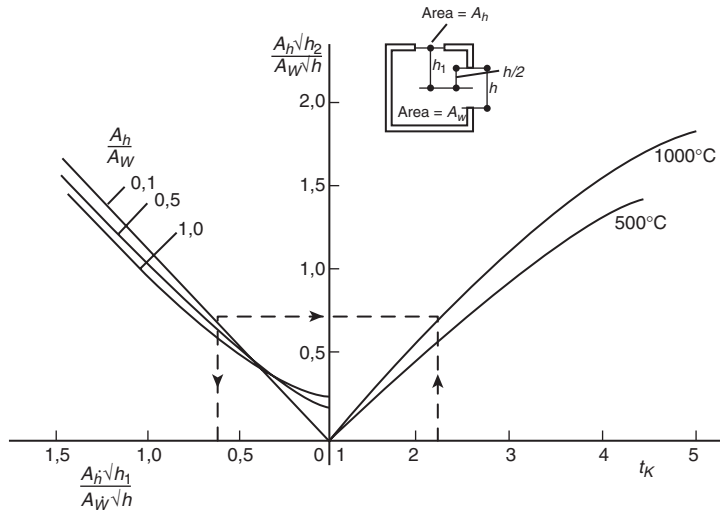


**Figure 4.5** Nomogram for calculating  $f_k$  for horizontal openings (Pettersson, Magnusson and Thor, 1976, reproduced by permission; © Swedish Institute of Steel Construction).

compartment values are removed, Buchanan (2001) gives the following equation for calculating the equivalent total vertical openings as

$$\left[ A_v \sqrt{h_v} \right]_{equiv} = A_v \sqrt{h_v} + 2,3 A_h \sqrt{h_1} \quad (4.7)$$

and is only applicable for  $0,3 \leq A_h \sqrt{h_1} / A_v \sqrt{h_v} \leq 1,5$ .

#### 4.3.2.3 Compartment construction

To allow for the effects of differing compartment construction, the values of both the fire load density and the ventilation factor should both be multiplied by a modification factor  $k_f$ . Values of  $k_f$  are dependant on both the materials of construction and the actual opening factor. Typical values are given in Table 4.1.

To use the above model to calculate the compartment temperature-time response the design fire load must be calculated.

#### 4.3.3 Calculation of fire load

This can be achieved in one of three ways: by full calculation on the contents of the compartment, by generic data or by empirical relationships.

**Table 4.1** Transformation parameter  $k_f$  for various compartments

Compartment boundary	Opening factor ( $A_v\sqrt{h_{eq}}/A_t$ )					
	0,02	0,04	0,06	0,08	0,10	0,12
$\lambda = 0,81 \text{ W/mC};$ $\rho c = 1,67 \text{ MJ/m}^3\text{C}^{(*)}$	1,00	1,00	1,00	1,00	1,00	1,00
Concrete	0,85	0,85	0,85	0,85	0,85	0,85
Aerated concrete ( $\rho = 500 \text{ kg/m}^3$ )	3,00	3,00	3,00	3,00	3,00	2,50
50% concrete; 50% aerated concrete	1,35	1,35	1,35	1,50	1,55	1,65
50% aerated concrete; 33% concrete; remainder brickwork <sup>(†)</sup>	1,65	1,50	1,35	1,50	1,75	2,00
20% concrete; 80% sheet steel <sup>(‡)</sup>	1,00	1,00	0,80	0,70	0,70	0,70
20% concrete; 80% plasterboard <sup>(§)</sup>	1,50	1,45	1,35	1,25	1,15	1,05
Sheet steel <sup>(¶)</sup>	3,00	3,00	3,00	3,00	3,00	3,00

(\*) This is taken as the reference compartment with  $\sqrt{\rho c \lambda} = 19,4 \text{ Wh}^{0,5}/\text{m}^2\text{C}$ .

(†) The actual remainder is 13 mm plasterboard ( $790 \text{ kg/m}^3$ ), 100 mm diabase wool ( $50 \text{ kg/m}^3$ ) and 200 mm brickwork ( $1800 \text{ kg/m}^3$ ) from interior to exterior.

(‡) The values quoted are for a fire load density of  $60 \text{ MJ/m}^2$  (or less). For a fire load of  $500 \text{ MJ/m}^2$  (or greater) all the coefficients are 0,50. For intermediate fire load densities, linear interpolation may be used.

(§) The plasterboard comprises a skin of 2 by 13 mm thick boards ( $790 \text{ kg/m}^3$ ) with an air gap of 100 mm.

(¶) The sheet steel is a sandwich panel enclosing 100 mm of diabase wool ( $50 \text{ kg/m}^3$ ).

Source: Pettersson, Magnusson and Thor (1976) (© Swedish Institute of Steel Construction by permission)

#### 4.3.3.1 Full calculation

In this method, the quantity and calorific value of each item in the compartment is identified, and then the total fire load in the compartment is established.

$$Q_{f_i,k} = \sum M_{k,i} H_{u,i} \quad (4.8)$$

where  $Q_{f_i,k}$  is the fire load and  $M_{k,i}$  and  $H_{u,i}$  are the mass and calorific value of the  $i$ th piece of contents within the compartment. The value of the fire load per unit area of either the whole compartment or the floor area may then be determined as appropriate. Typical values of  $H_{u,i}$  are given in Table 4.2.

**Table 4.2** Calorific value of common combustible materials

Material	Calorific value ( $H_{ui}$ ) (MJ/kg)
Acetylene	48,2
Acrylic	37–29
Alcohol	27–33
Celluloid	17–20
Cellulose	15–18
Coal	28–34
Foam rubber	34–40
Gasoline	43–44
Grain	16–18
Hydrogen	119,7
Methane	50,0
Paper, cardboard	13–21
Paraffin	40–42
Polyethylene	43–44
PTFE	5,00
PVC	16–17
Rubber tyres	31–33
Wood	17–20
Wool	21–26

*Source:* CIB W14 Report (1983) by permission

Clearly this method is extremely laborious for all but the simplest compartment and it is generally acceptable to use generic data.

#### **4.3.3.2 Generic data**

Given a large degree of experience, it has proved possible to provide typical data on the mean and standard deviation of the fire loads for a given type of structure or occupancy. A substantial quantity of such data is given in the CIB W14 Workshop Report (1983). Typical values are presented in Table 4.3.

#### **4.3.4 Parametric equation approach**

One disadvantage with the data on compartment temperature–time response from the results of Pettersson, Magnusson and Thor is that

**Table 4.3** Generic fire load data

Occupancy	Fire load (MJ/m <sup>2</sup> )		
	Average	Standard deviation	Coefficient of variation
Dwelling	140–150	20,1–24,7	14,5–16,5
Offices	102–124	31,4–39,4	25,3–35,6
Schools	61,1–96,7	14,2–20,5	16,9–30,1
Hospitals	116	36	31,0
Hôtels	67	19,3	28,8

The fire load density is calculated on the total area of the bounding fire compartment. The values quoted for dwellings, offices and schools are ranges, and it is not implied that, for example, the lowest standard deviation necessarily corresponds to the lowest mean. *Source:* CIB W14 Report (1983) by permission

they were presented in either tabular or graphical form. This formulation is not ideal if such data are required for further calculations on the thermal response of structural elements within the compartment. One possible solution to this difficulty is to determine empirical parametric equations relating the variables concerned. Although, originally there may have been a theoretical background to these parametric equations, they have, over the course of their development, been tweaked to give better correlation with measured compartment fires.

#### 4.3.4.1 *Formulation due to Lie (1974)*

This gives a series of parametric equations derived from the heat balance equation and involving the opening factor and the thermal boundaries of the compartment. The model consists of a non-linear characteristic up to the maximum temperature reached during the fire, followed by a linear decay curve and then a constant residual temperature. The parameters needed are the opening factor  $O$  defined as  $A_v \sqrt{h_{eq}} / A_t$  ( $m^{0,5}$ ), the fuel load per unit area of the compartment  $q_{t,d}$  ( $MJ/m^2$ ) and the fire duration  $t_d$  (minutes). The first two parameters are the same as those used in the work by Pettersson, Magnusson and Thor.

The compartment temperature  $\theta_g$  is given by

$$\theta_g = 20 + 250 (10O)^{\frac{0,1}{0,3}} e^{-\frac{O^2 t}{60}} \times \left[ 3 \left( 1 - e^{-0,01t} \right) - \left( 1 - e^{-0,05t} \right) + 4 \left( 1 - e^{-0,2t} \right) \right] + C \sqrt{\frac{600}{O}} \quad (4.9)$$

$C$  is a constant which takes a value of zero for heavyweight compartment boundary materials ( $\rho \geq 1600 \text{ kg/m}^3$ ) and unity for lightweight materials ( $\rho < 1600 \text{ kg/m}^3$ ).

Equation (4.9) is only valid for a value of  $t$  less than that defined by Eq. (4.10)

$$t \leq \frac{4,8}{O} + 60 \quad (4.10)$$

If  $t$  is greater than the value given by Eq. (4.10), then  $t$  should be set equal to the right-hand side of Eq. (4.10).

The duration of the fire  $t_d$ , in minutes, is given by

$$t_d = \frac{q_{t,d}}{5,5O} \quad (4.11)$$

Note, both Lie and Pettersson, Magnusson and Thor use a constant of proportionality of 0,09 rather than 0,1 in the equation to calculate the fire duration.

In the decay phase, i.e. when  $t > t_d$ , the gas temperature is given by

$$\theta_g = \theta_{max} - 600 \left( \frac{t}{t_d} - 1 \right) \geq 20 \quad (4.12)$$

where  $\theta_{max}$  is the temperature reached at  $t_d$ .

These parametric equations are valid for  $0,01 \leq O \leq 0,15$ . If  $F$  exceeds 0,15 it should be set equal to 0,15.

#### 4.3.4.2 EN 1991-1-2 approach

The background theory to this approach was proposed by Wickström (1981/2, 1985a) who suggested that the compartment temperature–time relationship was dependant entirely on the ratio of the opening factor  $A_v \sqrt{h_{eq}} / A_t$  to the thermal inertia  $\sqrt{(\rho c \lambda)}$  of the compartment boundary and that the standard furnace curve could be attained by a ventilation factor of  $0,04 \text{ m}^{0,5}$  and a thermal inertia of  $1160 \text{ Ws/m}^2\text{°C}$ .

Thus the gas temperature  $\theta_g$  can be related to a parametric time base  $t^*$  related to the real time  $t$  (hours) and the ventilation and compartment boundary by the following equation.

For the heating phase

$$\theta_g = 20 + 1325 \left[ 1 - 0,324e^{-0,2t^*} - 0,204e^{-1,7t^*} - 0,472e^{-19t^*} \right] \quad (4.13)$$

where  $t^*$  is defined by

$$t^* = t\Gamma \quad (4.14)$$

with  $\Gamma$  defined as

$$\Gamma = \frac{\left( \frac{O}{\sqrt{\rho c \lambda}} \right)^2}{\left( \frac{0,04}{1160} \right)^2} \quad (4.15)$$

where  $O$  is the opening factor and  $\sqrt{(\rho c \lambda)}$  is the thermal inertia of the compartment boundary.

For the cooling phase,

- for  $t_d^* \leq 0,5$  h

$$\theta_g = \theta_{max} - 625(t^* - xt_{max}^*) \quad (4.16)$$

- for  $0,5 \leq t_d^* \leq 2,0$  h

$$\theta_g = \theta_{max} - 250(3 - t_{max}^*)(t^* - xt_{max}^*) \quad (4.17)$$

- for  $t_d^* > 2,0$  h

$$\theta_g = \theta_{max} - 250(t^* - xt_{max}^*) \quad (4.18)$$

where  $\theta_{max}$  is the maximum temperature reached during the heating phase and  $t_{max}$  ( $=t_{max}^*/\Gamma$ ) is given by

$$t_{max} = \max \left[ \frac{0,2 \times 10^{-3} q_{t,d}}{O\Gamma}; t_{lim} \right] \quad (4.19)$$

where  $t_{lim}$  is dependant upon the growth rate of the fire. Values for  $t_{lim}$  are given in Table 4.4.

**Table 4.4** Values of  $t_{lim}$  (from Table E5, EN 1991-1-2)

Fire growth rate	Occupancy	$t_{lim}$ (min)
Slow	Transport (public space)	25
Medium	Dwelling; Hospital (room); Hôtel (room); Office; School classroom	20
Fast	Library; Shopping centre; Theatre (cinema)	15

Source: Table E5 from EN 1991-1-2

Also if  $t_{max} = t_{lim}$ , then  $t^*$  is defined by  $t^* = t\Gamma_{lim}$  where  $\Gamma_{lim}$  is given by

$$\Gamma_{lim} = \frac{\left[ \frac{0,1 \times 10^{-3} q_{t,d}}{bt_{lim}} \right]^2}{\left( \frac{0,04}{1160} \right)^2} \quad (4.20)$$

If the following limits apply ( $O > 0,04$ ;  $q_{t,d} < 75$  and  $b < 1160$ ), then the value of  $\Gamma_{lim}$  becomes  $k\Gamma_{lim}$ , where  $k$  is given by

$$k = 1 + \frac{O - 0,04}{0,04} \frac{q_{t,d} - 75}{75} \frac{1160 - b}{1160} \quad (4.21)$$

For fuel controlled fires  $t_{max}$  equals  $t_{lim}$ , but for ventilation controlled fires  $t_{max}$  is given by  $0,2 \times 10^{-3} q_{t,d} / O$ . If  $t_{max} > t_{lim}$ ,  $x = 1$  or if  $t_{max} < t_{lim}$ ,  $x = t_{lim}\Gamma / t_{max}^*$ .

Note EN 1991-1-2 places limits on the validity of Eq. (4.15)–(4.19) which are  $0,02 \leq O \leq 0,20$  ( $m^{0,5}$ ),  $50 \leq q_{t,d} \leq 1000$  ( $MJ/m^2$ ) and  $100 \leq \sqrt{(\rho c \lambda)} \leq 2200$  ( $J/m^2 s^{0,5} K$ ).

One anomaly with both approaches is that the rate of increase of temperature in the growth period is independent of the fire load.

It is not always necessary to be able to characterize the complete compartment temperature–time response. It may be sufficient to be able to predict basic data such as maximum temperature or the duration of the fire.

#### 4.4 ESTIMATION OF FIRE CHARACTERISTICS

If the relative amounts of heat flow in Eq. (4.1) are calculated for specific cases, it is possible to draw conclusions on the relative importance of the

**Table 4.5** Relative heat losses in a compartment fire

Opening	Fire load	Relative heat loss (percentage of total)				
		Effluent gases	Boundary	Feedback to fuel	Radiation	Steel
0,5	7,5	67	17	12	3	1
	15,0	67	14	11	6	2
	30,0	65	13	11	9	2
	60,0	61	11	11	13	4
0,25	7,5	56	24	16	2	2
	15,0	55	29	10	4	2
	30,0	52	20	11	11	6
	60,0	53	22	12	9	4
0,125	60,0	47	25	16	7	5

(1) The figure quoted in the column marked 'opening' is the relative area of a full height opening in the longer side of the compartment.

(2) The fire load density is in kg of wood cribs per square metre of floor area.

(3) Although the tests were undertaken to assess protection requirements for fire exposed steelwork, the steelwork adsorbs only a relatively small proportion of the heat so the figures in the above table can be held to refer to a normal compartment.

Source: Heselden (1968) – Building Research Establishment: Crown copyright

terms of Eq.(4.1). Typical data on this are given in Table 4.5 (Heselden, 1968) where it is seen that the largest portion of heat loss is through the effluent gases, and also demonstrates that as the window area decreases the proportion of heat transmitted through the walls of a standard brick or concrete compartment increases. Whilst the total heat output is entirely dependant on the fuel available, its rate of output will be ventilation controlled.

Thus it has been suggested that the rate of burning is proportional to the ventilation factor (Fujita, undated)

$$R = 0,1A_v\sqrt{h_{eq}} \quad (4.22)$$

where  $R$  is the rate of burning (kg/s) and  $A_v\sqrt{h_{eq}}$  is a ventilation factor ( $m^{1,5}$ ). The outflow of heat through the gases escaping through the ventilation sources will also be proportional to  $A_v\sqrt{h_{eq}}$  and that through the walls to  $A_t - A_v$  where  $A_t$  is the total internal area of the compartment. This led to the suggestion that the temperature reached in a compartment fire should be a function of these parameters. The analysis of a large number of fires by Thomas and Heselden (1972), plotted in Fig. 4.6,

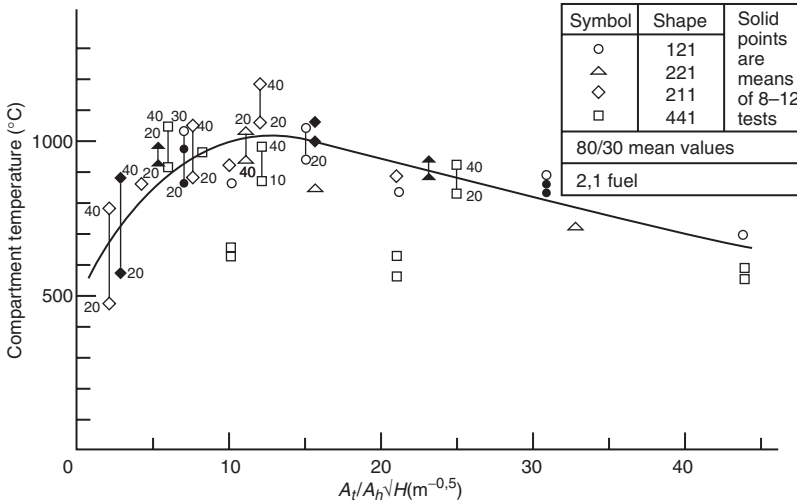


**Figure 4.6** Relationship between maximum compartment temperatures and compartment geometry (Heselden, 1968, by permission of the Building Research Establishment; Crown copyright).

indicates that a parameter  $\eta$  best describes the parametric effect, where  $\eta$  is given by

$$\eta = \frac{A_t - A_v}{A_v \sqrt{h_{eq}}} \quad (4.23)$$

For low values of  $\eta$  (high ventilation areas), the rate of heat loss is greatest but so is the heat loss through the windows, and thus the temperatures are low. For high values of  $\eta$  (low ventilation areas) there is lower heat loss but the rate of heat release is also low hence giving rise to low temperatures. The curve in Fig. 4.6 can be represented by the following equation (Law, 1978).

$$\theta_{f,max} = 6000 \frac{1 - e^{-0,1\eta}}{\sqrt{\eta}} \quad (4.24)$$

The value of  $\theta_{f,max}$  given by Eq. (4.24) is an upper limit which will not be achieved when the fire load is low, and thus the value of  $\theta_{f,max}$  must be modified to allow for this and to enable the maximum fire temperature

$\theta_{max}$  to be calculated as

$$\theta_{max} = \theta_{f,max} \left( 1 - e^{-0,05\psi} \right) \quad (4.25)$$

where  $\psi$  is defined by

$$\psi = \frac{L_{fi,k}}{\sqrt{A_V} (A_f - A_v)} \quad (4.26)$$

where  $L_{fi,k}$  is the total fire load expressed as an equivalent mass of wood having the same calorific value. PD 7974-3 suggests that Eqs (4.24) and (4.25) are valid for  $720 < b < 2500 \text{ J/m}^2\text{s}^{0,5}$ , although it may produce conservative values up to around 25% to high.

The rate of burning  $R$  defines not only the rate of heat release, but it can also be used to define the fire duration  $t_d$  (in seconds) given by

$$t_d = \frac{L_{fi,k}}{R} \quad (4.27)$$

with values of  $R$  taken from Eq. (4.22).

It was recognized by Thomas and Heselden that the rate of burning calculated from Eq. (4.22) was not entirely correct and gave only an approximate value; they found that the rate of burning depended on both the internal area of the compartment and on its geometry. A more accurate estimate (Law, 1983) of the rate of burning is given by

$$R = 0,18A_v \sqrt{h_{eq}} \sqrt{\frac{W}{D}} \left( 1 - e^{-0,036\eta} \right) \quad (4.28)$$

where  $D$  is the depth and  $W$  the width, respectively, of the compartment. Note: Eq. (4.28) only holds for ventilation controlled fires. For fuel controlled fires, the rate of burning depends on the quantity and type of fuel.

Attempts have been made over the years to relate compartment fires to the standard furnace test, as related in Chapter 3. Since all fire testing is performed using a standard temperature–time régime and such tests have provided a substantial amount of data on the performance of structural elements together with design data, it would be useful to enable the data obtained from such tests to be used, in the case where a natural fire

characteristic would be a more reasonable model for the response of a compartment. There have been several attempts to provide this link. They are based either on the concept of fire severity or time equivalence.

## 4.5 FIRE SEVERITY AND TIME EQUIVALENCE

### 4.5.1 Fire severity

The initial ideas in this field were due to Ingberg (1928) who, following a series of compartment tests with known fire loads, suggested that fire severity could be calculated by considering equivalence of the areas under the furnace curve and the compartment curve above a base of either 150 or 300°C (Fig. 4.7). In this way, Ingberg derived a correlation between fire load measured in his tests as load per unit floor area and the standard fire resistance periods. Although this method provided a basis for fire grading as in the Report of the Committee on the Fire Grading of Buildings (Ministry of Works, 1946), it has little theoretical justification and the method also appeared not to consider the effect of ventilation which would also affect the equivalence, in that compartment temperatures are affected both by air supply and fuel supply (Robertson and Gross, 1970). This flaw led to the rejection of Ingberg's ideas and thus alternative approaches needed to be found. Such approaches led to the idea of time equivalence based on equal temperature rise within the element. It must be reiterated that time equivalence only gives a measure

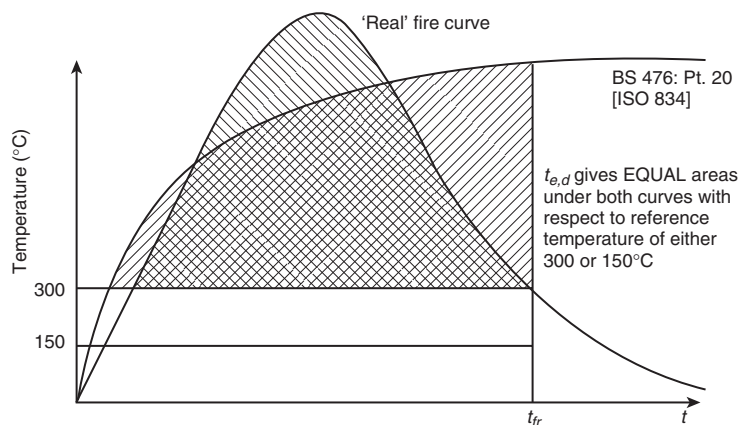


**Figure 4.7** Equivalence of fire severity based on areas beneath the standard and compartment temperature–time curves.

of the total heat input from the fire and does not distinguish between a short high intensity fire and a long low intensity fire (Law, 1997).

#### 4.5.2 Time equivalence

There are two methods available to calculate time equivalence. The first is to consider equivalence based on the same temperature rise in the element and the second is to consider equivalence of heat input. Law (1997) gives much of the background to the determination of time equivalence using temperature rise.

##### 4.5.2.1 Temperature base

The attempt made to correlate the effects of a natural fire and the furnace test on a temperature base was first made by Law (1973). Law calculated the time taken for an insulated steel member to reach a specified temperature of  $550^{\circ}\text{C}$  by being exposed to a natural fire, modelled by assuming its peak temperature to be maintained throughout the fire and the equivalent time taken to reach the same temperature when exposed to the standard furnace test (Fig. 4.8). In the author's view, time equivalence should only be used where the structural element (or structure) behaviour can be characterized by a single temperature. Thus, it is acceptable for protected steelwork, unprotected steelwork (with possible modification) and concrete in flexure where for hogging the fire performance depends on the reinforcing temperature and for sagging the average concrete

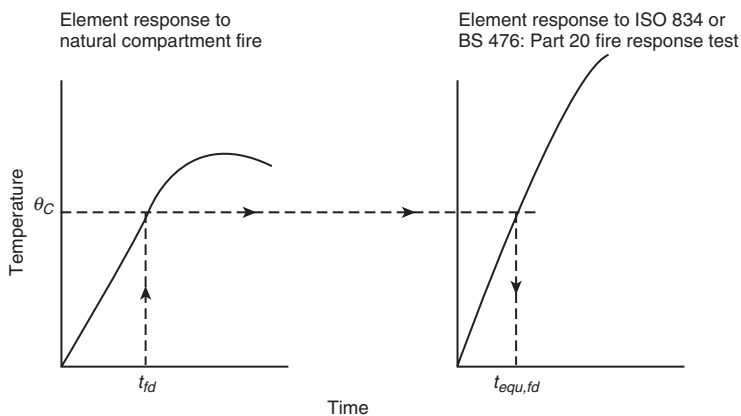


**Figure 4.8** Equivalence of fire severity based on temperatures reached in elements within the compartment.

temperature. For concrete columns when the maximum (average) temperature in the reinforcement and the maximum average temperature in the concrete do not occur at the same time, it is unclear which maximum temperature governs the strength criterion. Time equivalence cannot be used for timber as the controlling phenomenon is char depth and not temperature rise.

Law (1973) found that the required fire resistance was a function of the fire load, internal area of the compartment and the ventilation area

$$t_{e,d} = \frac{KL_{fi,k}}{\sqrt{A_v A_t}} \quad (4.29)$$

where  $t_{e,d}$  is the required equivalent fire resistance (min),  $L_{fi,k}$  is the total fire load (kg of wood equivalent),  $A_v$  is the area of vertical openings ( $m^2$ ) and  $A_t$  the total internal area ( $m^2$ ). The parameter  $K$  has a value of near unity for SI units. Equation (4.29) strictly only holds for insulated steel and should be applied with care to uninsulated steel. Equation (4.29) has gone through three further modifications to improve its accuracy. The first modification was presented at the 1983 CIB W14 Workshop, and took the form

$$t_{e,d} = \frac{0,067q_{t,d}}{\sqrt{\frac{A_v \sqrt{h_{eq}}}{A_t}}} \quad (4.30)$$

where  $q_{t,d}$  is the fire load per unit area of compartment boundary ( $MJ/m^2$ ).

A later, second modification to take account of the effect of compartment thermal boundaries was published by the CIB in 1985 (Thomas, 1986), and took the form

$$t_{e,d} = cwq_{f,d} \quad (4.31)$$

where  $q_{f,d}$  is the fire load per unit floor area,  $c$  is a parameter depending on the construction materials of the compartment walls and  $w$  is related to the compartment geometry by the following equation

$$w = \sqrt{\frac{A_f}{A_v}} \sqrt{\frac{A_f}{A_t \sqrt{h_{eq}}}} \quad (4.32)$$

**Table 4.6** Parameter  $c$  to calculate equivalent fire duration

Compartment thermal absorptivity ( $b$ ) ( $=\sqrt{\rho c \lambda}$ ) ( $\text{Wh}^{0,5}/\text{m}^2\text{K}$ )	$c$ ( $\text{m}^2\text{min}/\text{MJ}$ )
$b \leq 12$	0,09
$12 \leq b \leq 42$	0,07
$b > 42$	0,05

Source: Thomas (ed.), by permission

where  $A_f$  is the floor area ( $\text{m}^2$ ). It should be noted for an area of vertical openings greater than 10% of the floor area,  $w$  can be taken conservatively as 1,5.

The parameter  $c$  may either be taken conservatively as 0,1 or related to the thermal inertia  $\sqrt{(\rho c \lambda)}$ , where  $\rho$  is the density of the boundary material,  $c$  is the specific heat and  $\lambda$  the thermal conductivity of the compartment boundary). Values of the parameter  $c$  are given in Table 4.6.

A third approach is given in the informative Annex F to EN 1991-1-2 where the equivalent fire duration  $t_{e,d}$  is given by

$$t_{e,d} = k_c q_{f,d} k_b w_f \quad (4.33)$$

where  $q_{f,d}$  is the fire load density related to the floor area,  $w_f$  is a ventilation factor given by Eq. (4.32),  $k_b$  is a factor reliant on the thermal properties of the boundary, given in Table 4.7, but may be taken conservatively as 0,07 and  $k_c$  is a correction factor. The correction factor  $k_c$  is taken as 1,0 for protected steel and concrete and 13,70 for unprotected steel. Note the National Annex to EN 1991-1-2 in the UK is likely to recommend that the value of  $k_c$  is taken as 1,0 for all cases, except that time

**Table 4.7** Values of  $k_b$  from EN 1992-1-2 and PD 7974-3

Thermal absorptivity ( $b$ ) ( $\text{J}/\text{m}^2\text{s}^{0,5}\text{K}$ )	$k_b$ ( $\text{min m}^2/\text{MJ}$ )	
	EN 1992-1-2	PD 7974-3
$b > 2500$	0,04	0,050
$720 \leq b \leq 2500$	0,055	0,07
$b > 720$	0,07	0,05

Source: Table F.2 of EN 1991-1-2 and Table 4 of PD 7974-3

equivalence for unprotected steelwork may only be used if  $t_{e,d}$  is less than 60 min (Kirby *et al.*, 2004).

The design fire load  $q_{f,d}$  can be related to the generic fire load  $q_{f,k}$  for a particular occupancy by the following equation

$$q_{f,d} = m\delta_{q1}\delta_{q2}\delta_n q_{f,k} \quad (4.34)$$

where  $\delta_{q1}$  is a partial safety factor dependant upon the danger of fire activation as a function of compartment floor area,  $\delta_{q2}$  is a partial safety factor dependant upon the danger of fire activation and type of occupancy and  $\delta_n$  is a factor allowing for the presence of active fire measures if not considered in the fire model. EN 1991-1-2 recommends a factor of 1,0 for  $\delta_n$ . The values of  $\delta_{q1}$  and  $\delta_{q2}$  are specified in Table E.1. The value of the combustion factor  $m$  should be taken as 0,8 for cellulosic fire loads.

The ventilation factor  $w_f$  subject to a lower limit of 0,5 is given by

$$w_f = \left(\frac{6,0}{H}\right)^{0,3} \left[0,62 + \frac{90(0,4 - \alpha_v)^4}{1 + b_v\alpha_h}\right] \quad (4.35)$$

where  $\alpha_v$  is the ratio between the area of vertical openings and the floor area and should lie between 0,025 and 0,25,  $\alpha_h$  by the ratio between the area of the horizontal openings and the floor area,  $H$  is the compartment height and  $b_v$  is given by

$$b_v = 12,5\left(1 + 10\alpha_v - \alpha_v^2\right) \geq 10,0 \quad (4.36)$$

For small compartments with no roof openings and a floor area less than 100 m<sup>2</sup> and no horizontal openings, the ventilation factor  $w_f$  may be taken as

$$w_f = \frac{A_f}{A_t} O^{-0,5} \quad (4.37)$$

where  $O$  is the opening factor.

#### 4.5.2.2 Normalized heat load base

The theory behind this approach was developed by Harmathy and Mehaffey (1985) and is presented below.

The normalized heat load  $\bar{h}''$  in a furnace test to the standard furnace curve can be related to the duration of the test  $t_{e,d}$  by

$$t_{e,d} = 0,11 + 0,16 \times 10^{-4} \bar{h}'' + 0,13 \times 10^{-9} (\bar{h}'')^2 \quad (4.38)$$

The heat flow from a compartment normalized with respect to the thermal boundaries of the compartment  $\bar{h}'$  is given by

$$\bar{h}' = \frac{(11,0\delta + 1,6) L_{f,d} A_f \times 10^6}{A_t \sqrt{\lambda \rho c} + 935 \sqrt{\Phi L_{f,d} A_f}} \quad (4.39)$$

where  $A_f$  is the floor area,  $A_t$  is the total area of compartment boundaries,  $\sqrt{(\lambda \rho c)}$  is the surface averaged thermal inertia of the compartment boundary,  $\Phi$  is a ventilation factor related to the rate of mass inflow of air into the compartment,  $L_{f,d}$  is the fire load (kg of wood equivalent) per unit area of floor and  $\delta$  is a parameter defining the amount of fuel energy released through the openings and is given by

$$\delta = 0,79 \sqrt{\frac{H^3}{\Phi}} \quad (4.40)$$

where  $H$  is the compartment height.

The value of  $\Phi$  may be taken as its minimum value  $\Phi_{min}$  given by Eq. (4.41) as this produces a conservative answer

$$\Phi_{min} = \rho_{air} A_v \sqrt{g h_{eq}} \quad (4.41)$$

where  $h_{eq}$  and  $A_v$  are the height and area of the window opening respectively,  $\rho_{air}$  is the density of air and  $g$  is acceleration due to gravity (9,81 m/s<sup>2</sup>).

The normalized heat load to the furnace  $\bar{h}''$  can be related to the normalized heat load in a compartment fire  $\bar{h}'$  by the following equation

$$\bar{h}'' = \bar{h}' \exp \left( \beta \sqrt{\left( \frac{\sigma_{\bar{h}''}}{\bar{h}''} \right)^2 + \left( \frac{\sigma_{\bar{h}'}}{\bar{h}'} \right)^2} \right) \quad (4.42)$$

where  $\beta$  is the statistical acceptance/rejection limit on the variables and is 1,64 for a 5% limit, and the ratio of the variance of the normalized heat load to the normalized heat load in the compartment is given by

$$\frac{\sigma_{\bar{h}'}}{\bar{h}'} = \frac{\sigma_{\bar{L}}}{\bar{L}_{f,d}} \frac{A_t \sqrt{\lambda \rho c} + 467,5 \sqrt{\Phi_{\min} \bar{L}_{f,d} A_f}}{A_t \sqrt{\lambda \rho c} + 935 \sqrt{\Phi_{\min} \bar{L}_{f,d} A_f}} \quad (4.43)$$

where  $\sigma_{\bar{L}}/\bar{L}_{f,d}$  is the coefficient of variation in the combustible fire load in the compartment.

The coefficient of variation for the normalized heat input to the furnace is given by

$$\frac{\sigma_{\bar{h}''}}{\bar{h}''} = 0,9 \frac{\sigma_{\bar{t}_{e,d}}}{\bar{t}_{e,d}} \quad (4.44)$$

where  $\sigma_{\bar{t}_{e,d}}/\bar{t}_{e,d}$  is the coefficient of variation in the test results from a furnace and can typically be taken in the order of 0,1.

Thus when values of the fire load and compartment geometry are determined, the equivalent furnace test value can be found.

The alternative methods of determining the behaviour characteristics of a fire compartment are compared in the following example.

#### **Example 4.1: Determination of the behaviour characteristics of a fire compartment**

Consider a compartment 14 m by 7 m by 3 m high with 6 windows each 1,8 m wide by 1,5 m high with a fire load related to floor area of 60 kg/m<sup>2</sup> of wood equivalent.

*Compartment construction:*

$$\text{dense concrete} (\sqrt{\lambda \rho c} = 32 \text{ Wh}^{0,5}/\text{m}^2\text{K})$$

*Total area of windows:*

$$A_v = 6 \times 1,5 \times 1,8 = 16,2 \text{ m}^2$$

$$A_f = 14 \times 7 = 98 \text{ m}^2$$

$$A_t = 2 \times 98 + 2 \times 14 \times 3 + 2 \times 7 \times 3 = 322 \text{ m}^2$$

68 Fire Safety Engineering Design of Structures

Calorific value of fire load = 18 MJ/kg

Fire load per unit surface area  $q_{t,d}$ :

$$q_{t,d} = 60 \times 18 \times A_f / A_t = 60 \times 18 \times 98 / 322 = 329 \text{ MJ/m}^2$$

(This is equivalent to 1080 MJ/m<sup>2</sup> based on floor area)

1. Equivalent fire durations

(a) Equation (4.29):

$$t_{e,d} = \frac{KL_{f,k}}{\sqrt{A_v A_t}} = \frac{1,0 \times 60 \times 98}{\sqrt{16,2 \times 322}} = 81 \text{ min}$$

(b) Equation (4.30):

$$t_{e,d} = \frac{0,067 q_{t,d}}{\sqrt{\frac{A_v \sqrt{h_{eq}}}{A_t}}} = \frac{0,067 \times 329}{\sqrt{\frac{16,2 \times \sqrt{1,5}}{322}}} = 89 \text{ min}$$

(c) CIB method

$$A_f = 98 \text{ m}^2 \quad \text{or} \quad 10\% A_f = 9,8 \text{ m}^2$$

$$A_v = 16,2 \text{ m}^2$$

so  $A_v$  is greater than 10%  $A_f$ , therefore the approximate method may be used.

(i) Exact method:

Determine the value of  $w$  from Eq. (4.32):

$$w = \sqrt{\frac{A_f}{A_v}} \sqrt{\frac{A_f}{A_t \sqrt{h_{eq}}}} = \sqrt{\frac{98}{16,2}} \sqrt{\frac{98}{322 \sqrt{1,5}}} = 1,23$$

Determine the boundary conditions:

$$\sqrt{\rho c \lambda} = 32 \text{ Wh}^{0,5} / \text{m}^2 \text{K}, \text{ hence from Table 4.5, } c = 0,07$$

From Eq. (4.31),

$$t_{e,d} = cwq_{f,d} = 0,07 \times 1,23 \times (60 \times 18) = 93 \text{ min}$$

(ii) Approximate method:

$$w = 1,5 \text{ and } c = 0,1, \text{ hence } t_{e,d} = 162 \text{ min}$$

(d) EN 1991-1-2 Annex F

Take  $k_c = 1,0$ .

From the data in the text with

$$\sqrt{(\rho c \lambda)} = 32 \times 60 = 1920 \text{ J/m}^2\text{s}^{0,5}\text{K}, k_b = 0,055.$$

As there are no horizontal openings, the value of  $b$  is not required.

$$\alpha_v = A_w/A_f = 16,2/98 = 0,165$$

From Eq. (4.35) with  $b = 0$

$$\begin{aligned} w_f &= \left(\frac{6,0}{H}\right)^{0,3} \left[0,62 + \frac{90(0,4 - \alpha_v)^4}{1 + b_v \alpha_h}\right] \\ &= \left(\frac{6,0}{3}\right)^{0,3} \left[0,62 + \frac{90(0,4 - 0,165)^4}{1}\right] = 1,101 \end{aligned}$$

The value of  $w_f$  satisfies the limiting condition of 0,5.

Note: using the approximate Eq. (4.37) for  $w_f$  gives

$$w_f = \frac{A_f}{A_t} O^{-0,5} = \frac{A_f}{A_t} \left(\frac{A_v \sqrt{h_{e,q}}}{A_t}\right)^{-0,5} = \frac{98}{322} \left(\frac{16,2 \sqrt{1,5}}{322}\right)^{-0,5} = 1,23$$

$$q_k = 60 \times 18 = 1080 \text{ MJ/m}^2$$

70 Fire Safety Engineering Design of Structures

From Eq. (4.33)

$$t_{e,d} = q_{f,d} k_b \tau w_f = 0,055 \times 1,101 \times 1080 = 65 \text{ min}$$

The conservative value of  $w_f$  gives  $t_{e,d}$  as 73 min.

Using the  $k_b$  factor value of 0,07 recommended in PD 7974-3 gives values for  $t_{e,d}$  of 83 and 93 minutes, respectively.

(e) Harmathy and Mehaffey

Boundary conditions:

$$\sqrt{(\rho c \lambda)} = 32 \times \sqrt{3600} = 1920 \text{ Js}^{0,5} / \text{m}^2 \text{ degK}$$

$$L_{f,d} = 60 \text{ kg/m}^2; L_{f,d} A_f = 5880 \text{ kg.}$$

From Eq. (4.41) calculate  $\Phi_{min}$ :

$$\Phi_{min} = \rho_{air} A_v \sqrt{g h_{eq}} = 1,21 \times 16,2 \sqrt{9,81 \times 1,5} = 75,2 \text{ kg/s}$$

From Eq. (4.40) calculate  $\delta$ :

$$\delta = 0,79 \left( \frac{H^3}{\Phi_{min}} \right)^{0,5} = 0,79 \left( \frac{3^3}{75,2} \right)^{0,5} = 0,473$$

To ease subsequent calculations:

$$\sqrt{\Phi L_{f,d} A_f} = \sqrt{75,2 \times 60 \times 98} = 665$$

$$A_t \sqrt{(\rho c k)} = 322 \times 1920 = 618240$$

From Eq (4.40) calculate  $\bar{h}'$ :

$$\begin{aligned} \bar{h}' &= \frac{(11,0\delta + 1,6)(L_{f,d} A_f) \times 10^6}{A_t \sqrt{\lambda \rho c} + 935 \sqrt{\Phi L_{f,d} A_f}} \\ &= \frac{(11,0 \times 0,473 + 1,6) 5880 \times 10^6}{618240 + 935 \times 665} \\ &= 32260 \text{ s}^{0,5} \text{ K} \end{aligned}$$

The normalized standard deviation for the fire load will be taken as 0,3. This is reasonable if the data for office loading in Table 4.3 are examined.

From Eq. (4.43), calculate  $\sigma_{\bar{h}'} / \bar{h}'$ :

$$\begin{aligned} \frac{\sigma_{\bar{h}'}}{\bar{h}'} &= \left( \frac{\sigma_{\bar{L}}}{\bar{L}_{f,d}} \right) \left( \frac{A_t \sqrt{\lambda \rho c} + 467,5 \sqrt{\Phi_{\min} \bar{L}_{f,d} A_f}}{A_t \sqrt{\lambda \rho c} + 935 \sqrt{\Phi_{\min} \bar{L}_{f,d} A_f}} \right) \\ &= 0,3 \frac{6\,18\,240 + 467,5 \times 665}{6\,18\,240 + 935 \times 665} = 0,225 \end{aligned}$$

As recommended by Harmathy and Mehaffey,  $\sigma_{t_{e,d}} / \bar{t}_{e,d}$  is taken as 0,1, thus from Eq. (4.44)

$$\frac{\sigma_{\bar{h}''}}{\bar{h}''} = 0,9 \frac{\sigma_{\bar{t}_{e,d}}}{\bar{t}_{e,d}} = 0,9 \times 0,1 = 0,09$$

From Eq. (4.42) calculate  $\bar{h}'' / \bar{h}'$

$$\begin{aligned} \frac{\bar{h}''}{\bar{h}'} &= \exp \left( \beta \sqrt{\left( \frac{\sigma_{\bar{h}''}}{\bar{h}''} \right)^2 + \left( \frac{\sigma_{\bar{h}'}}{\bar{h}'} \right)^2} \right) \\ &= \exp \left( 1,64 \sqrt{0,225^2 + 0,09^2} \right) = 1,488 \end{aligned}$$

or,  $\bar{h}'' = 1,488 \times 32260 = 48003 \text{ s}^{0.5} \text{K}$

From Eq. (4.38) calculate  $t_{e,d}$ :

$$\begin{aligned} t_{e,d} &= 0,11 + 0,16 \times 10^{-4} \bar{h}'' + 0,13 \times 10^{-9} (\bar{h}'')^2 \\ &= 0,11 + 0,16 \times 10^{-4} \times 48003 + 0,13 \times 10^{-9} \times 48003^2 \\ &= 1,18 \text{ h} = 71 \text{ min} \end{aligned}$$

A comparison between the values of  $t_{e,d}$  is presented in Table 4.8, where it is noted that with the exception of the conservative approach adopted by the second of the two CIB approaches the answers are reasonably consistent, but with the method in EN 1991-1-2 giving a lower (therefore unconservative) value than earlier methods.

**Table 4.8** Comparison between calculated equivalent fire durations (Example 4.1)

Method	Equivalent fire duration (min)
Equation (4.29)	81
Equation (4.30)	89
CIB Workshop: Exact	93
Approximate	162
EN 1991-1-2	65 (73)
PD 7974-3	83 (93)
Harmathy and Mehaffey	71

## 2. Maximum temperatures

(a) Equations (4.23) and (4.24)

Calculate  $\eta$  from Eq. (4.23):

$$\eta = \frac{A_t - A_V}{A_v \sqrt{h_{eq}}} = \frac{322 - 16,2}{16,2 \sqrt{1,5}} = 15,4$$

Calculate  $\theta_{f,max}$  for Eq. (4.24)

$$\theta_{f,max} = 6000 \frac{1 - e^{-0,1\eta}}{\sqrt{\eta}} = 6000 \frac{1 - e^{-1,54}}{\sqrt{15,4}} = 1201^\circ\text{C}$$

Correct  $\theta_{f,max}$  for the type of fire:

From Eq. (4.26) calculate  $\psi$ :

$$\psi = \frac{L_{fi,k}}{\sqrt{A_V (A_t - A_v)}} = \frac{60 \times 98}{\sqrt{16,2 (322 - 16,2)}} = 83,5$$

Calculate  $\theta_{max}$  from Eq. (4.25):

$$\theta_{max} = \theta_{f,max} \left(1 - e^{-0,05\psi}\right) = 1201 \left(1 - e^{-0,05 \times 83,5}\right) = 1183^\circ\text{C}$$

(b) Theory due to Lie using Eqs (4.9)–(4.12)

Opening factor,  $O$ :

$$O = A_v \sqrt{h} / A_t = 16,2 \times \sqrt{1,5} / 310 = 0,0616$$

Fire load (in kg/m<sup>2</sup>) of compartment =  $60 \times 98 / 322 = 18,26 \text{ kg/m}^2$

Fire duration  $t_d$  using Eq. (4.11):

$$t_d = L_{fi,k} / (330O) = 18,26 / (330 \times 0,0616) = 0,898 \text{ h} = 53,9 \text{ min}$$

Maximum allowable value of  $t$  using Eq. (4.10):

$$t_{max} = 0,08 / O + 1 = 0,08 / 0,0616 + 1 = 2,30 \text{ h}$$

Thus Eq. (4.9) will hold up to the total fire duration, and is evaluated in Table 4.9 and plotted in Fig. 4.9.

**Table 4.9** Comparison between parametric curves due to Lie and EN 1991-1-2

Time (min)	LIE (°C)	EN 1991-1-2 (°C)
0	20	20
5	568	683
10	768	716
15	844	747
20	877	774
25	895	799
30	910	822
35	925	842
40	939	861
45	954	878
50	970	894
55	951	909
60	895	922
65	840	934
70	784	946
75	729	944

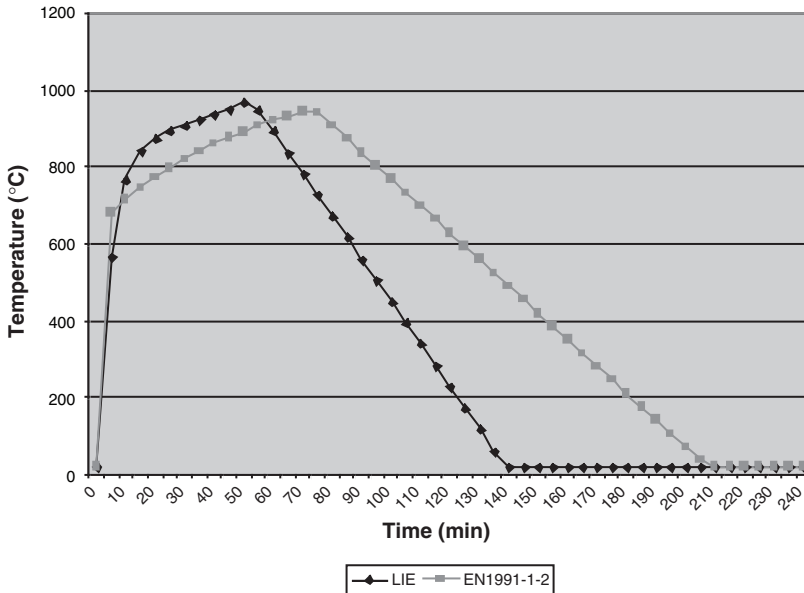
*continued*

Table 4.9—Cont'd

Time (min)	LIE (°C)	EN 1991-1-2 (°C)
80	673	909
85	618	874
90	562	839
95	506	804
100	451	769
105	395	734
110	340	699
115	284	664
120	229	630
125	173	595
130	118	560
135	62	525
140	20	490
145	20	455
150	20	420
155	20	385
160	20	350
165	20	315
170	20	280
175	20	245
180	20	210
185	20	176
190	20	141
195	20	106
200	20	71
205	20	36
210	20	20
215	20	20
220	20	20
225	20	20
230	20	20
235	20	20
240	20	20

The maximum temperature  $\theta_{max}$  attained in the fire is 970°C.

On the decay phase the fire reaches ambient at 2,31 h (139 min), and the temperature profile is linear between the maximum and the point at which ambient is reached.



**Figure 4.9** Comparison between parametric curves due to Lie and EN 1991-1-2.

(c) EN 1991-1-2 using Eq. (4.13)–(4.19):

From Eq. (4.15) calculate  $\Gamma$ :

$$O = 0,0616 \text{ m}^{0,5} \text{ and } \sqrt{(\rho c \lambda)} = 1920 \text{ W s}^{0,5} / \text{m}^2 \text{ } ^\circ\text{C}$$

$$\Gamma = (O / \sqrt{(\rho c \lambda)})^2 / (0,04 / 1160)^2 = 0,866$$

Calculate  $t_{max}$  from Eq. (4.17):

$$t_{max} = 0,20 \times 10^{-3} q_{td} / (O \Gamma) = 1,223 \text{ h} (=74 \text{ min})$$

The values of the increase in gas temperature  $\theta_g$  over ambient may now be calculated up to the design time  $t_d$ . These values are given in Table 4.9 and plotted in Fig. 4.9. The maximum gas temperature  $\theta_{max}$  (above  $0^\circ\text{C}$ ) at a real time of 74 min is  $953^\circ\text{C}$ .

As the fire load density is typical of an office, then from Table 4.4,  $t_{lim}$  is 20 min (0,333 h). This is less than  $t_{max}$ , therefore  $x = 1,0$  in the decay phase.

Since the parametric fire duration is between 0,5 and 2,0 h, Eq. (4.16) is used to calculate the delay phase. The fire decays to a temperature of 20°C at 2,96 h parametric time or 3,42 h real time. It is noticed in Fig. 4.9 that whilst the maximum temperatures are similar, Lie predicts a shorter time period to maximum temperature, a faster cooling rate and a shorter total overall duration of the complete fire of around two-thirds that of EN 1991-1-2.

### 3. Fire duration:

From Eqs (4.27) and (4.28) calculate the rate of burning:

(i) Approximate Eq. (4.27)

$$\text{From Eq. (4.22)} \quad R = 0,1 \times 16,2 \times \sqrt{1,5} = 1,98 \text{ kg/s}$$

$$t_d = L_{f,k} / R = 60 \times 98 / 1,98 = 2970 \text{ s or } 49,5 \text{ min.}$$

(ii) More exact equation, Eq. (4.26):

$$R = 0,18 \times 16,2 \times \sqrt{1,5} \times \sqrt{(14/7)} \times (1 - e^{-0,036 \times 15,4}) = 2,15 \text{ kg/s}$$

thus the fire duration is 46 min.

Table 4.10 gives the maximum temperatures reached in both parametric curves and the value predicted by Eq. (4.21) where it will be observed that both Lie and EN 1991-1-2 predict similar maximum temperatures and that Eq. (4.23) gives a value some 20% higher.

Table 4.11 gives the fire duration predicted by both parametric curves and the value predicted by Eqs (4.25) and (4.26) where it will be observed Lie, Eqs (4.25) and (4.26) predict similar values of around 50 min and EN 1991-1-2 a value around 50% longer.

**Table 4.10** Comparison between maximum fire temperatures

Method	Maximum temperature (°C)
Lie	970
EN 1991-1-2	953
Equation (4.23)	1183

**Table 4.11** Comparison between fire durations

Method	Fire duration (min)
Lie	54
EN 1991-1-2	74
Equation (4.27)	50
Equation (4.28)	46

## 4.6 LOCALIZED FIRES

Two types of localized fires require a brief discussion.

### 4.6.1 Plume fires

This is where there can be a small intense fire at floor level with the flames being spread along any ceiling or floor soffit. Where the possible fire scenario permits localized fires then any structural elements engulfed by such fires should be checked. Plume fires will also permit calculation of smoke release (Annexe C, EN 1991-1-2 or PD 7974-2).

### 4.6.2 5 MW design fire

The design fire has a heat output of 5 MW over an area of 3 m by 3 m and is used to design smoke extract in sprinkler premises. It is not used in structural assessment. The background to the 5 MW design fire is given in Law (1995).

Having established the behaviour of a compartment fire and possible relationships for design purposes between the standard furnace curve and natural fires, it is now pertinent to consider the effect of the fire temperature–time response on structures or structural members either within the compartment or on the boundary of the compartment.

# 5 Properties of materials at elevated temperatures

---

Data on the behaviour of materials at elevated temperatures is needed to allow both the Fourier equation of heat diffusion and the structural simulation to be solved. It is convenient, therefore, to divide this chapter into two distinct sections corresponding to the two stages of the analysis.

The major portion of this chapter will concentrate on steel, both structural and reinforcing, and concrete, since for both these materials, there is a substantial amount of available data which has been published in two RILEM reports (Anderberg, 1983; Schneider, 1986a). It should be noted that these reports are a compendia of the existing data compiled on an *ad hoc* basis using various test methods which are not currently standardized.

In addition, data are given on timber, masonry and aluminium, although in the case of timber there is less need for such data as design methods do not generally need temperature-dependant properties. In the case of masonry, there are no detailed design methods in current use which involve the need for such data.

## 5.1 THERMAL DATA

The Fourier equation of heat transfer is given by

$$\nabla(a(\Delta\theta)) = \dot{\theta} \quad (5.1)$$

where  $\theta$  is the space-dependant temperature and  $a$  is the temperature-dependant thermal diffusivity. It should be noted that the thermal diffusivity is related to the density  $\rho$ , the thermal conductivity  $\lambda$  and the specific heat  $c_v$ :

$$a = \frac{\lambda}{\rho c_v} \quad (5.2)$$

Data for calculating the thermal response are normally required only for concrete, steel and aluminium. Although calculations for the thermal response can be carried out for masonry, it is not generally necessary. For timber, strength calculations are carried out on the core which is either taken to be temperature unaffected, or an allowance is made for the temperature effect by a factor applied to the allowable stresses based on member thickness. Thus, the thermal data are not generally required, although in some cases, where the temperature rise in the core is likely to be significant, a knowledge of the thermal diffusivity is needed.

### 5.1.1 Steel

The values of the properties concerned are sensibly independent on either the use of the steel (structural or reinforcing) or on the strength or grade of the steel.

#### 5.1.1.1 Density

The density of steel may be taken as its ambient value of 7850 kg/m<sup>3</sup> over the normally experienced temperature range.

#### 5.1.1.2 Specific heat

Malhotra (1982a) suggested that the specific heat of steel  $c_a$  (J/kg°C) may be taken as

$$c_a = 475 + 6,010 \times 10^{-4} \theta_a^2 + 9,64 \times 10^{-2} \theta_a^2 \quad (5.3)$$

Equation (5.3) together with test data from Pettersson, Magnusson and Thor (1976) and Stirland (1980) reproduced from Malhotra (1982a) are plotted in Fig. 5.1. It should be noted that owing to the discontinuity in the specific heat of steel at around 750°C, Eq. (5.3) only holds up to this value. EN 1994-1-2 gives equations which hold up to a temperature of 1200°C:

For 20°C ≤  $\theta_a$  ≤ 600°C

$$c_a = 425 + 0,773\theta_a - 1,69 \times 10^{-3} \theta_a^2 + 2,22 \times 10^{-6} \theta_a^3 \quad (5.4)$$

For 600°C =  $\theta_a$  = 735°C

$$c_a = 666 - \frac{1302}{\theta_a - 738} \quad (5.5)$$

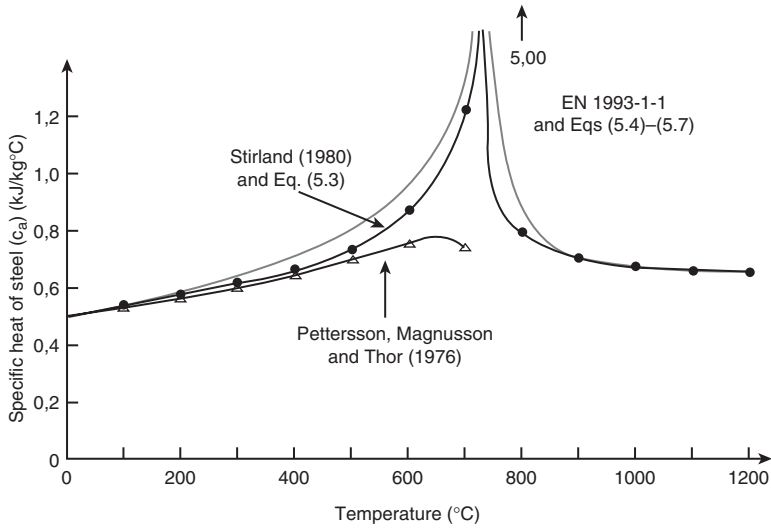


**Figure 5.1** Variation of the specific heat of steel with temperature (Malhotra, 1982a, by kind permission of the author).

For  $735^{\circ}\text{C} \leq \theta_a \leq 900^{\circ}\text{C}$

$$c_a = 545 + \frac{17820}{\theta_a - 731} \quad (5.6)$$

For  $900^{\circ}\text{C} \leq \theta_a \leq 1200^{\circ}\text{C}$

$$c_a = 650 \quad (5.7)$$

Equations (5.4)–(5.7) are also plotted in Fig. 5.1. Note that a constant value for  $c_a$  of 600 J/kgK may be taken in simple calculation models.

### 5.1.1.3 Thermal conductivity

Typical values for the thermal conductivity  $\lambda_a$  of steel ( $\text{W}/\text{m}^{\circ}\text{C}$ ) are given in Fig. 5.2 (Pettersson, Magnusson and Thor, 1976; Malhotra, 1982a). It should be noted that the values of thermal conductivity are slightly dependant on steel strength. The reason for this is not known, but, in any case, it is not very significant. EN 1993-1-2 gives the following equation for  $\lambda_a$  ( $\text{W}/\text{m}^{\circ}\text{C}$ ):

For  $20^{\circ}\text{C} \leq \theta_a \leq 800^{\circ}\text{C}$

$$\lambda_a = 54 - 33,3 \times 10^{-3} \theta_a \quad (5.8)$$

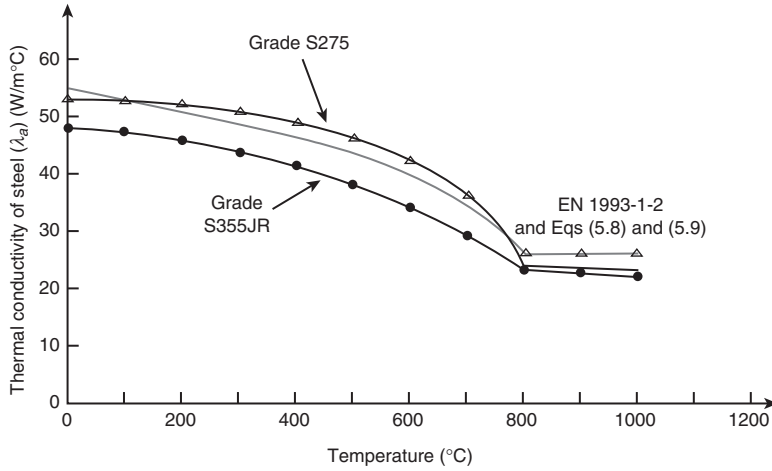


**Figure 5.2** Variation of the thermal conductivity of steel with temperature (Pettersen, Magnusson and Thor, 1976, reproduced by permission, ©Swedish Steel Institute, and Malhotra, 1982a, by kind permission of the author).

For  $\theta_a \geq 800^\circ\text{C}$

$$\lambda_a = 27,3 \tag{5.9}$$

Equations (5.8) and (5.9) are also plotted in Fig. 5.2. Note that, for approximate calculations, it is permissible to take the thermal conductivity of steel as 45 W/mK.

#### 5.1.1.4 Thermal diffusivity

Using the data given in sections 5.1.1.2 and 5.1.1.3 and the standard density values, the thermal diffusivity of steel ( $\text{m}^2/\text{h}$ ) shows a sensibly linear relationship with temperature up to  $750^\circ\text{C}$  according to the following equation (Malhotra, 1982a):

$$a_a = 0,87 - 0,84 \times 10^{-3}\theta_a \tag{5.10}$$

### 5.1.2 Concrete

With concrete, the situation is much more complex, in that values of the thermal parameters required are dependant on the mix proportions, the type of aggregate, the original moisture content of the concrete and

the age of the concrete. The data presented in this section can thus only be taken as representative of typical concretes.

### 5.1.2.1 *Density*

Even though when concrete is heated there will be a loss in weight caused by the evaporation of both free and combined water, this loss is not generally enough to cause substantial changes in density and thus it may be considered accurate enough to take ambient values. However, EN 1992-1-2 suggests that change in density with temperature to be used in thermal calculations may be taken as

For  $20^{\circ}\text{C} \leq \theta_c \leq 115^{\circ}\text{C}$

$$\rho(\theta_c) = \rho(20^{\circ}) \quad (5.11)$$

For  $115^{\circ}\text{C} \leq \theta_c \leq 200^{\circ}\text{C}$

$$\rho(\theta_c) = \rho(20^{\circ}\text{C}) \left( 1 - 0,02 \frac{\theta_c - 115}{85} \right) \quad (5.12)$$

For  $200^{\circ}\text{C} \leq \theta_c \leq 400^{\circ}\text{C}$

$$\rho(\theta_c) = \rho(20^{\circ}\text{C}) \left( 0,98 - 0,03 \frac{\theta_c - 200}{200} \right) \quad (5.13)$$

For  $400^{\circ}\text{C} \leq \theta_c \leq 1200^{\circ}\text{C}$

$$\rho(\theta_c) = \rho(20^{\circ}\text{C}) \left( 0,95 - 0,07 \frac{\theta_c - 400}{800} \right) \quad (5.14)$$

where  $\rho(20^{\circ}\text{C})$  is the ambient density.

For structural calculations the density of concrete must be taken as its ambient value over the whole temperature range.

### 5.1.2.2 *Specific heat*

Figure 5.3 presents values of specific heat for a variety of concretes (Schneider, 1986a), where it will be noted that the type of aggregate has a substantial effect on the values.

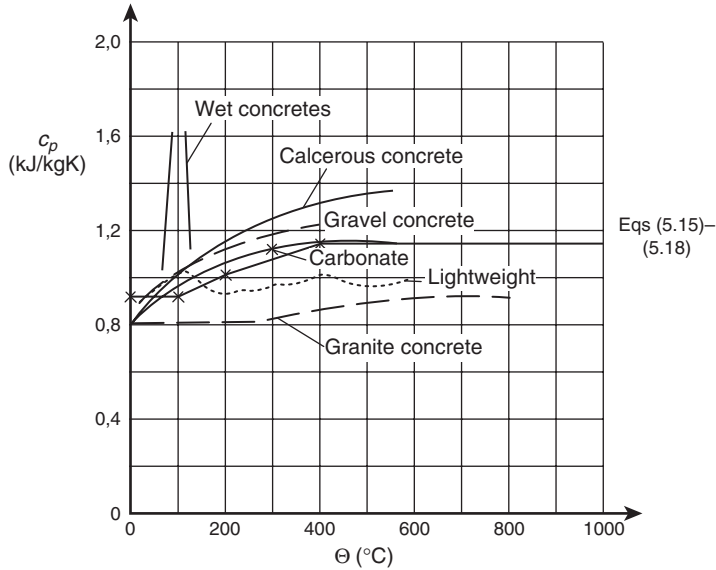


**Figure 5.3** Variation of specific heat of concrete with temperature (Schneider, 1986a, by permission).

EN 1992-1-2 gives the following equations for the specific heat of dry normal-weight concrete (siliceous or calcareous aggregates) (J/kgK):  
 For  $20^{\circ}\text{C} \leq \theta_c \leq 100^{\circ}\text{C}$

$$c_p(\theta_c) = 900 \tag{5.15}$$

For  $100^{\circ}\text{C} \leq \theta_c \leq 200^{\circ}\text{C}$

$$c_p(\theta_c) = 900 + (\theta_c - 100) \tag{5.16}$$

For  $200^{\circ}\text{C} \leq \theta_c \leq 400^{\circ}\text{C}$

$$c_p(\theta_c) = 1000 + \frac{\theta_c - 200}{2} \tag{5.17}$$

For  $400^{\circ}\text{C} \leq \theta_c \leq 1200^{\circ}\text{C}$

$$c_p(\theta_c) = 1100 \tag{5.18}$$

**Table 5.1** Values of  $c_{p,peak}$ 

Moisture content (%)	$c_{p,peak}$ (J/kgK)
0	900
1,5	1470
3,0	2020
10,0	5600

where the moisture content is not explicitly evaluated in the thermal analysis, then a peak  $c_{p,peak}$  is added to Eq. (5.16) at 100–115°C before decaying linearly to 200°C. The values of  $c_{p,peak}$  are given in Table 5.1.

Equations (5.15)–(5.18) are also plotted in Fig. 5.3.

For lightweight concrete a constant value of 840 J/kg°C may be taken (EN 1994-1-2).

### 5.1.2.3 Thermal conductivity

Figure 5.4 presents values of thermal conductivity for various concretes (Schneider, 1986a). It will be observed that the normal-weight aggregate concretes fall into a band with the values for lightweight concrete being substantially lower.

EN 1992-1-2 gives the following equations as limits between which the values of thermal conductivity (W/mK) of siliceous aggregate normal-weight concretes lie:

$$\lambda_c = 2,0 - 0,2451 \left( \frac{\theta_c}{100} \right) + 0,0107 \left( \frac{\theta_c}{100} \right)^2 \quad (5.19)$$

and

$$\lambda_c = 1,36 - 0,136 \left( \frac{\theta_c}{100} \right) + 0,0057 \left( \frac{\theta_c}{100} \right)^2 \quad (5.20)$$

A country's National Annexe is likely to specify which curve is to be used. However, the discrepancy between the analytical curves and the results from Schneider plotted in Fig. 5.4 is not explained.

EN 1994-1-2 indicates that it is permissible to take a constant value of 1,6 W/m°C.

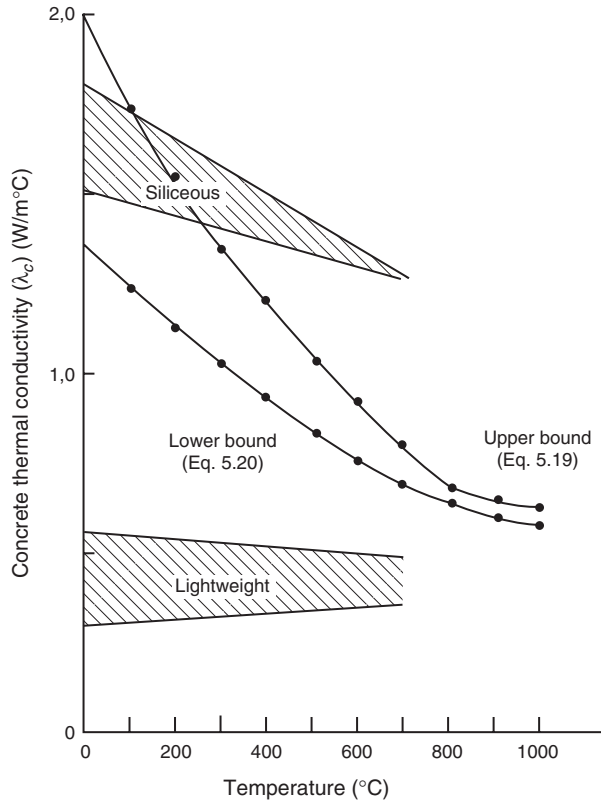


**Figure 5.4** Variation of thermal conductivity of concrete with temperature (Schneider, 1986a, by permission).

For lightweight concrete EN 1994-1-2 gives the following relationship:  
 For  $20^\circ\text{C} \leq \theta_c \leq 800^\circ\text{C}$

$$\lambda_c = 1,0 - \left( \frac{\theta_c}{1600} \right) \quad (5.21)$$

For  $\theta_c > 800^\circ\text{C}$

$$\lambda_c = 0,5 \quad (5.22)$$

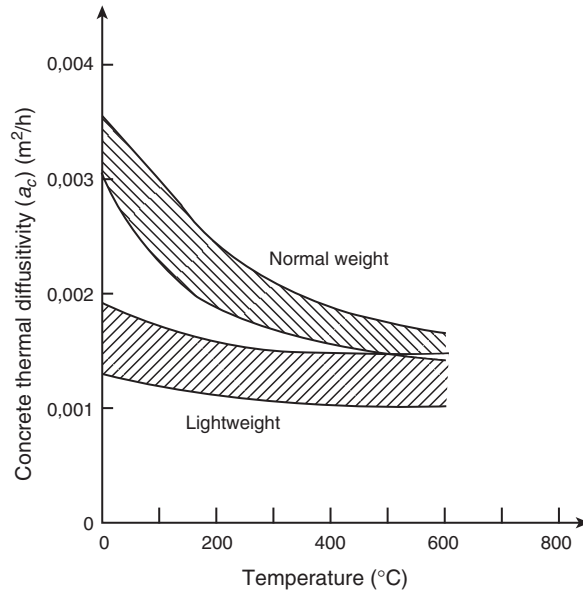


**Figure 5.5** Variation of the thermal diffusivity of concrete with temperature (Schneider, 1986a, by permission).

#### 5.1.2.4 Thermal diffusivity

For the results plotted in Fig. 5.5 it will be observed, as expected, that two distinct bands of results for normal-weight and lightweight concrete exist (Schneider, 1986a).

Using the values of  $\lambda_c = 1,60 \text{ W/mK}$  and  $c_c = 1000 \text{ J/kgK}$  recommended in EN 1993-1-2 for simple calculation methods together with a density  $\rho_c = 2400 \text{ kg/m}^3$ , it is suggested that an approximate value of the thermal diffusivity  $a_c$  can be determined using Eq. (5.2) to give  $a_c = \lambda_c / \rho c_c = 1,6 / (1000 \times 2400) = 0,67 \text{ m}^2/\text{s}$ . This value may be high as Hertz (1988) suggests  $a_c$  may be taken as  $0,35 \times 10^{-6} \text{ m}^2/\text{s}$  for granite (or sea gravel) and  $0,52 \times 10^{-6} \text{ m}^2/\text{s}$  for quartzite concretes, and Wickström (1985a) suggests a value of  $a_c = 0,417 \text{ m}^2/\text{s}$  (see section 5.7 for a further discussion).

### 5.1.3 Masonry

The most significant variable characterizing the high temperature performance of masonry is the density rather than the type of brick (clay or calcium silicate) as the density is a measure of the porosity of the brick.

**5.1.3.1 Density**

Again the density should be taken as the ambient value.

**5.1.3.2 Specific heat**

As shown in Fig. 5.6, the specific heat is sensibly independent of the density of the brick (Malhotra, 1982a). Harmathy (1993) gives the following expression for the specific heat of masonry (kJ/kg°C):

$$c_{pm} = 0,851 = 0,512 \times 10^{-3} \theta_m - \frac{8,676 \times 10^3}{(\theta_m + 273)^2} \quad (5.23)$$

where  $\theta_m$  is the temperature of the masonry.

**5.1.3.3 Thermal conductivity**

As shown in Fig. 5.7, the thermal conductivity of masonry is dependant on the density of the brick with high density bricks having higher values of thermal conductivity (Malhotra, 1982b). Welch (2000) indicates the effect

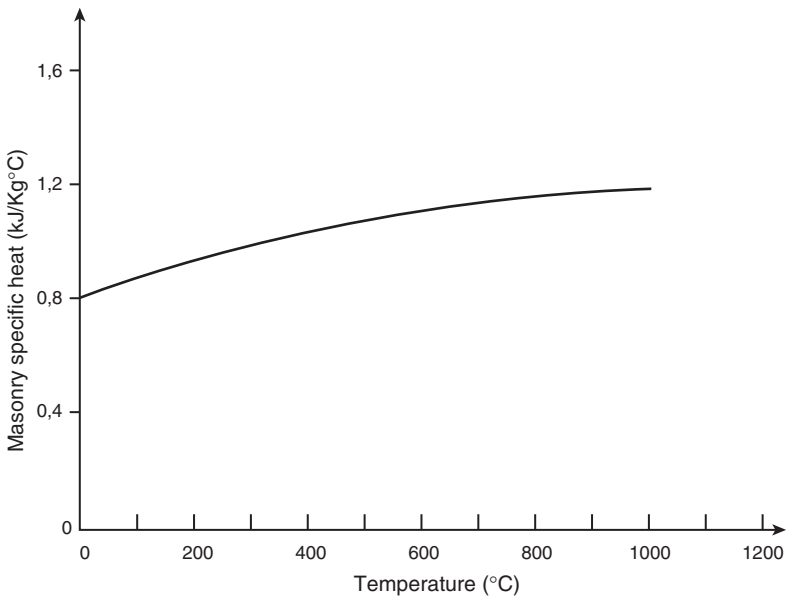


**Figure 5.6** Variation of the specific heat of masonry with temperature (Malhotra, 1982a, by kind permission of the author).

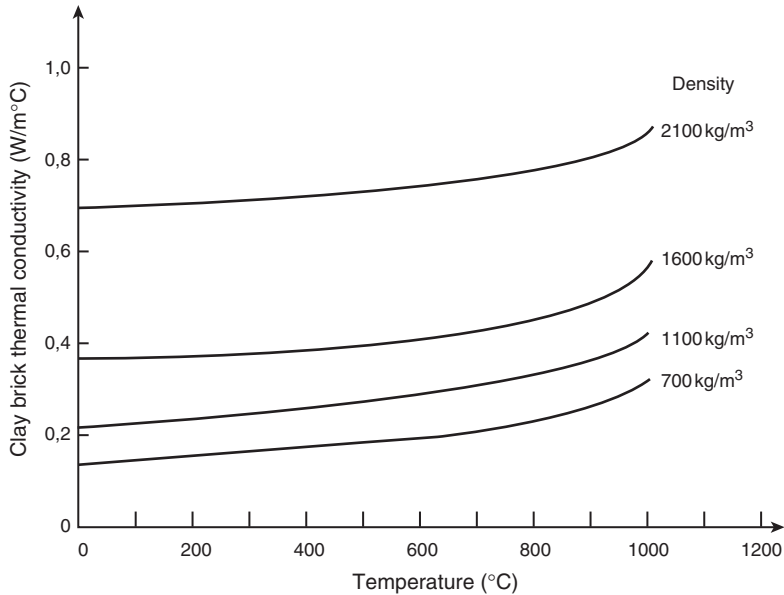


**Figure 5.7** Variation of the thermal conductivity of masonry with temperature (Malhotra, 1982b, by permission Messrs Dunod).

of moisture on the effective thermal conductivity  $\lambda'$  is given by

$$\lambda' = \lambda_0 (1 + M)^{0,25} \quad (5.24)$$

where  $\lambda_0$  is the dry thermal conductivity (W/mK) and  $M$  the moisture content (%).

#### 5.1.4 Timber

As mentioned in the introduction to this section, generally, the only thermal property needed to determine temperatures within the uncharred core is either the thermal diffusivity ( $\text{mm}^2/\text{s}$ ) which is given in Schaffer (1965) as

$$a_w = 0,2421 - 0,1884S \quad (5.25)$$

where  $S$  is the specific gravity of the timber or, the thermal conductivity ( $\text{W}/\text{m}^\circ\text{C}$ )

$$\lambda_w = (2,41 + 0,048M)S + 0,983 \quad (5.26)$$

where  $M$  is the moisture content in per cent by weight.

It appears that both the thermal diffusivity and the thermal conductivity are independent of temperature whereas the specific heat of oven dry wood given in White and Schaffer (1978) is temperature dependant and is given in  $\text{kJ}/\text{kg}^\circ\text{C}$  as

$$c_{pw} = 1,114 + 0,00486\theta_w \quad (5.27)$$

where  $\theta_w$  is the temperature of the wood.

### 5.1.5 Aluminium

Owing to the lower softening and melting points of aluminium compared with steel materials data are required over a more limited temperature range, i.e. up to  $300^\circ\text{C}$ . This is true for aluminium in both its pure state and when alloyed.

#### 5.1.5.1 Density

The density used in calculations may be taken as that pertaining at ambient conditions (i.e.  $2700 \text{ kg}/\text{m}^3$ ).

#### 5.1.5.2 Specific heat

Touloukian and Ho (1973) and Conserva, Donizelli and Trippodo (1992) suggest that over the temperature range  $0\text{--}300^\circ\text{C}$  the specific heat may be taken as constant with a value between  $90$  and  $100 \text{ J}/\text{kg}^\circ\text{C}$  with the slight scatter in the values being due to the effect of the various amounts, and identity, of the trace elements used in the various alloys. ENV 1999-1-2 gives the following equation for specific heat  $c_{al}$  ( $\text{J}/\text{kg}^\circ\text{C}$ ) for an aluminium temperature  $\theta_{al}$  for  $0^\circ\text{C} < \theta_{al} < 500^\circ\text{C}$

$$c_{al} = 0,41\theta_{al} + 903 \quad (5.28)$$

#### 5.1.5.3 Thermal conductivity

Touloukian and Ho (1973) and Conserva, Donizelli and Trippodo (1992) suggest that over the temperature range  $0\text{--}300^\circ\text{C}$  the thermal conductivity may be taken as constant with a value of  $180\text{--}240 \text{ W}/\text{m}^\circ\text{C}$ . The scatter in the values quoted is again due to both the effect of the various amounts

and identity of the trace elements used in the various alloys and there is also a very slight temperature dependence. ENV 1999-1-2 gives two equations for the thermal conductivity of aluminium  $\lambda_{al}$  (W/m°C) dependant upon the alloy:

For alloys in the 1000, 3000 and 6000 series,

$$\lambda_{al} = 0,07\theta_{al} + 190 \quad (5.29)$$

For alloys in the 2000, 4000, 5000 and 7000 series,

$$\lambda_{al} = 0,1\theta_{al} + 140 \quad (5.30)$$

## 5.2 MATERIALS DATA

In order to, be able to, determine the structural response in a fire, it is necessary to, be able to, formulate constitutive laws for the mechanical behaviour of the relevant materials at elevated temperatures. A complete formulation is required only where a full analysis is undertaken in order to calculate the deformations and displacements. Where it is only necessary to calculate load capacity, then a more limited data set can be utilized. Indeed, much early work on evaluating material behaviour was directed to determining specific properties such as tensile strength of steel or compressive strength of concrete at elevated temperatures. It was only much later that the need for constitutive models was appreciated.

It should be noted that, whereas at ambient conditions there are standard test procedures laid down by organizations such as British Standards, there are no such standards in force for testing at elevated temperatures, although there are proposals for such standards being considered by Comité Européen de Normalisation (CEN) . It should be recognized that as creep (or relaxation) is much higher at elevated temperatures, then the rate of loading (stress) or strain used in elevated temperature testing has a far more significant role than at ambient conditions. The rate of heating used to condition the test specimen will also affect the final test results.

### 5.2.1 Testing régimes

Most of, if not all, the early experimental investigations were carried out using steady-state testing régimes whereby the specimen was heated at a uniform rate of temperature rise in a furnace, allowed to condition by soaking for a pre-determined period at the test temperature in order to

allow the specimen to attain constant temperature through the cross section before being loaded to determine the required property. Strength evaluation was generally carried out using a constant rate of stress loading whether for tensile tests on steel or compressive tests on concrete. A disadvantage of the method using constant rate of stress loading is that, the complete stress–strain curve for concrete cannot be obtained. If, however, the test is carried out at a constant rate of deformation then the resultant loads can be measured and the complete stress–strain curve can be obtained, provided the test rig used is stiff enough. Classical creep tests are performed by loading the heated specimen at constant load and measuring the resultant strains over a suitable period of time.

Observations on specimens heated under constant stress indicated a behaviour pattern that could not be explained purely from the results of steady-state tests. It thus became necessary to consider transient testing in which the temperature was allowed to change during the test. The complete range of possible testing régimes is shown in Fig. 5.8 (Malhotra, 1982b). Similar to the thermal data, it is convenient to consider each material separately. Following the presentation of typical

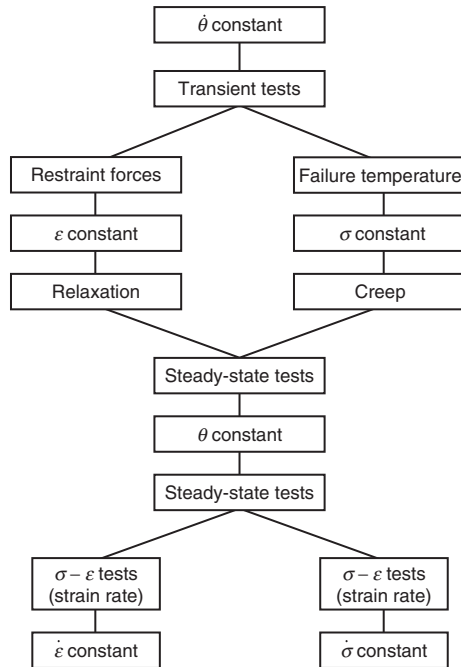


**Figure 5.8** Testing régimes to determine the mechanical behaviour of materials at elevated temperatures (Malhotra, 1982b, by permission Messrs Dunod).

experimental data, analytical models derived from such results will be considered in section 5.3.

## 5.2.2 Steel

The primary thrust on determining the effect of temperature on the properties of steel was strength behaviour characterized by the yield, or proof, strength and then followed by the complete stress–strain curve.

### 5.2.2.1 Strength characteristics

A typical set of stress–strain curves for an American Grade A36 steel (yield strength 300 MPa) is shown in Fig. 5.9. This shows that the strength loss at elevated temperatures is substantial even though at relatively low temperatures there is a slight strength gain (Harmathy and Stanzak, 1970). It should also be noted that, both at ambient and at temperatures only slightly above ambient, a distinct yield plateau is observed whereas at much higher temperatures there is no yield plateau and the curve resembles that for high yield steel. Reinforcing and pre-stressing steels follow very similar patterns (Fig. 5.10) (Harmathy and Stanzak, 1970;

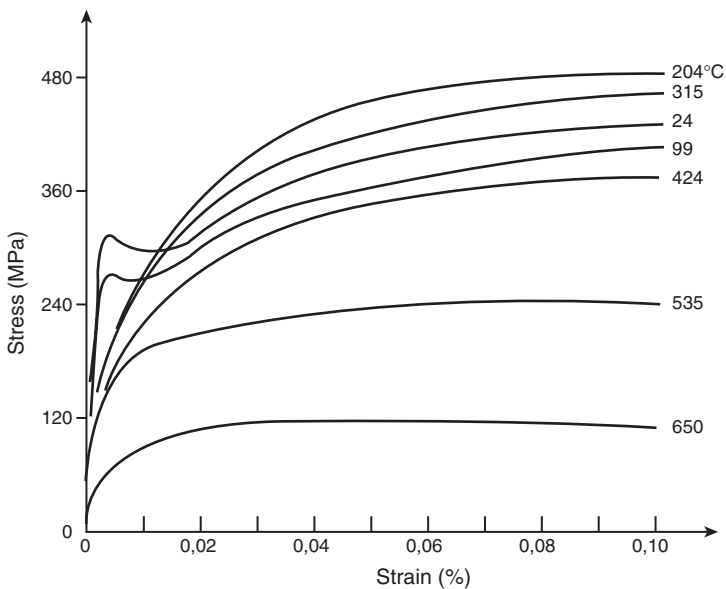


**Figure 5.9** Stress–strain curves for structural steel at elevated temperatures (Harmathy and Stanzak, 1970, by permission).

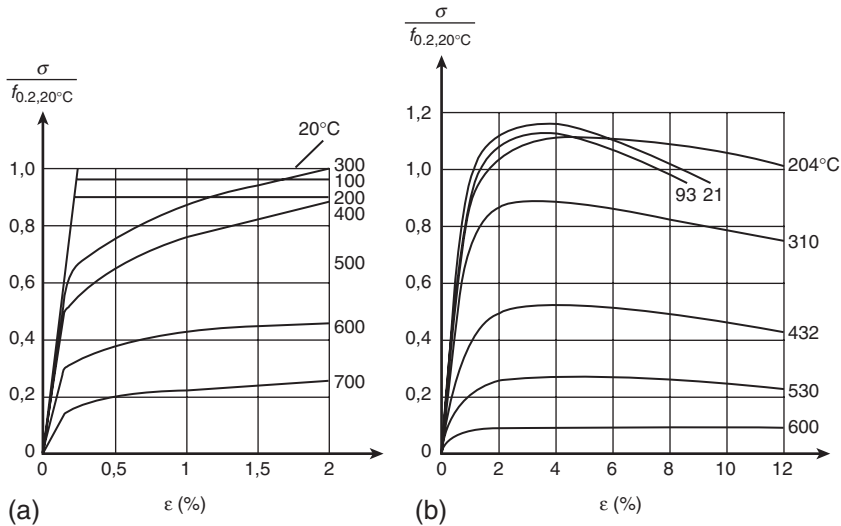


**Figure 5.10** Stress–strain curves for (a) reinforcing and (b) pre-stressing steels at elevated temperatures (Anderberg, 1978a, and Harmathy and Stanzak, 1970, by permission).

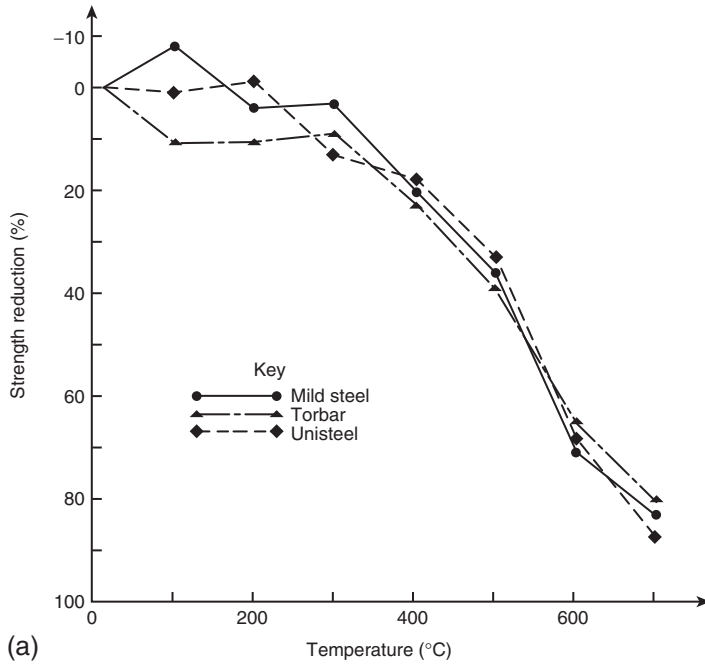
Anderberg, 1978a). It should be noted that owing to the large strains exhibited at elevated temperatures in fire affected members, it is more usual to quote the 1,0 or 2,0%, or in exceptional cases 5,0%, proof stress rather than the conventional ambient value of 0,2% proof stress. It should be noted that where the variation of proof strength, after normalizing the results with respect to the ambient strength for either reinforcing steels or pre-stressing steels is considered, then the resultant strength loss is approximately above 350°C which is sensibly independent of the steel type (Figs 5.11(a) and 5.11(b)) (Holmes *et al.*, 1982).

**5.2.2.2 Unrestrained thermal expansion**

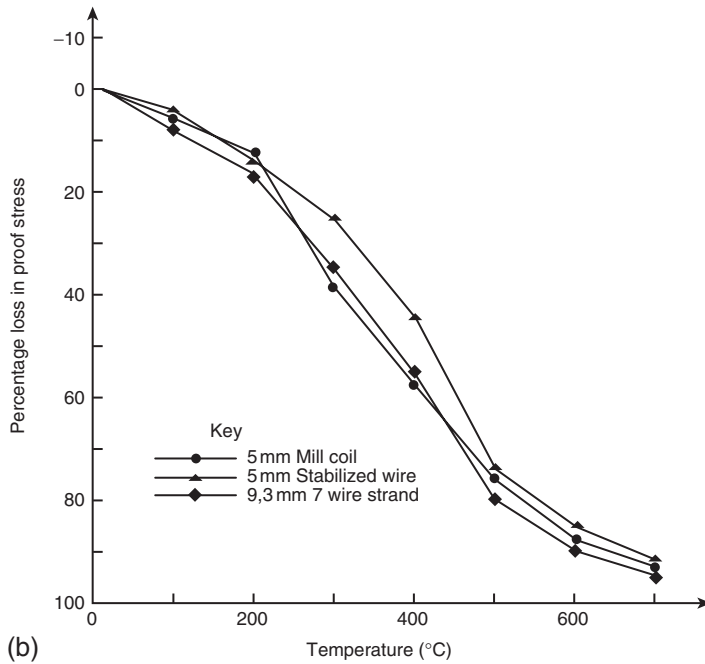
The free thermal expansion of steel is relatively independent of the type of steel (Fig. 5.12) (Anderberg, 1983). EN 1992-1-2 gives the following expressions:

For structural and reinforcing steels:  
 $20^{\circ}\text{C} \leq \theta_s \leq 750^{\circ}\text{C}$

$$\epsilon_s(\theta_s) = -2,416 \times 10^{-4} + 1,2 \times 10^{-5}\theta_s + 0,4 \times 10^{-8}\theta_s^2 \quad (5.31)$$



(a)



(b)

**Figure 5.11** Variation of normalized strength of (a) reinforcing and (b) pre-stressing steels with temperature (Holmes *et al.*, 1982).

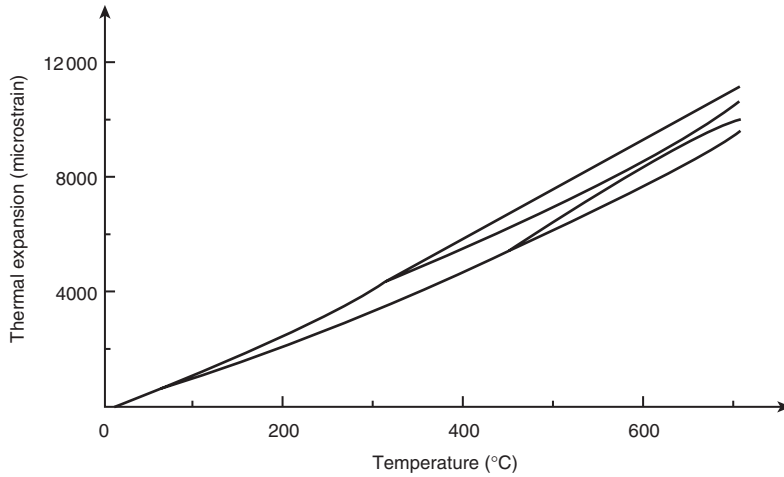


Figure 5.12 Thermal expansion of steel (Anderberg, 1983, by permission).

For  $750^{\circ}\text{C} \leq \theta_s \leq 860^{\circ}\text{C}$

$$\varepsilon_s(\theta_s) = 11 \times 10^{-3} \quad (5.32)$$

For  $860^{\circ}\text{C} \leq \theta_s \leq 1200^{\circ}\text{C}$

$$\varepsilon_s(\theta_s) = -6,2 \times 10^{-4} + 10^{-5}\theta_s + 0,4 \times 10^{-8}\theta_s^2 \quad (5.33)$$

For pre-stressing steel

$20^{\circ}\text{C} \leq \theta_s \leq 12000^{\circ}\text{C}$

$$\varepsilon_s(\theta_s) = -2,016 \times 10^{-4} + 10^{-5}\theta_s + 0,4 \times 10^{-8}\theta_s^2 \quad (5.34)$$

Note that EN 1993-1-2 uses  $\Delta l/l$  as the symbol for thermal strain rather than  $\varepsilon_s(\theta_s)$ . EN 1994-1-2 indicates that for simple calculation methods (see Fig. 5.12) the thermal strain can be determined from

$$\varepsilon_s(\theta_s) = 14 \times 10^{-6} (\theta_s - 20) \quad (5.35)$$

**5.2.2.3 Isothermal creep**

For steel, isothermal creep (i.e. creep measured at constant stress and constant temperature) only tends to become significant approximately above 450°C when both reinforcement and structural steel is approaching its limiting carrying capacity. Typical data on the isothermal creep of steels are given in Fig. 5.13 (Anderberg, 1988).

It is a general practice to analyze the creep data using the Dorn temperature compensated time approach with the secondary creep related to the Zener–Hollomon parameter (section 5.3.1.2). It should be noted that it is very difficult owing to the nature of the test to get repeatable or consistent values of the parameters used to analyze the steel creep data, and thus any values must be treated with caution.

To alleviate this problem, the practice has evolved of using strength data derived from anisothermal creep tests in which the creep is included implicitly in those data.

**5.2.2.4 Anisothermal creep data**

In this test, the specimen is pre-loaded with a given stress, heated to failure at a known temperature rate with the resultant strains being measured. Typical data for British structural steels of Grade S275 (originally 43A) and Grade S355JR (originally 50B) are given in Fig. 5.14

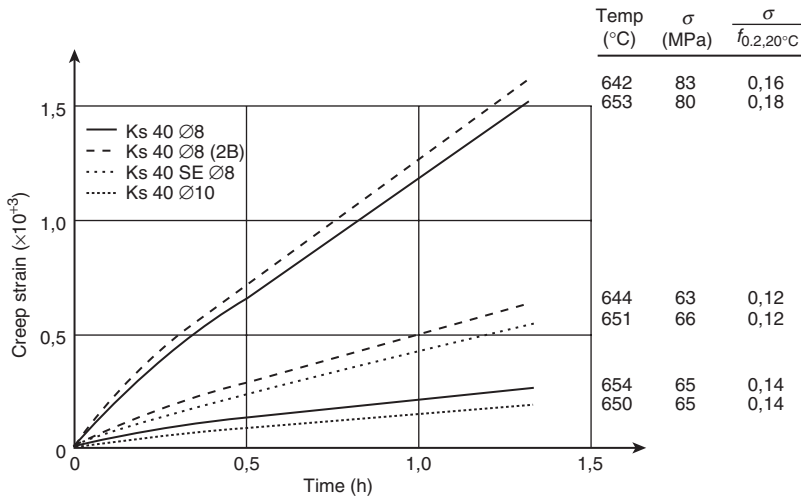


**Figure 5.13** Isothermal creep strains for reinforcing steels at elevated temperature (Anderberg, 1993, by permission).

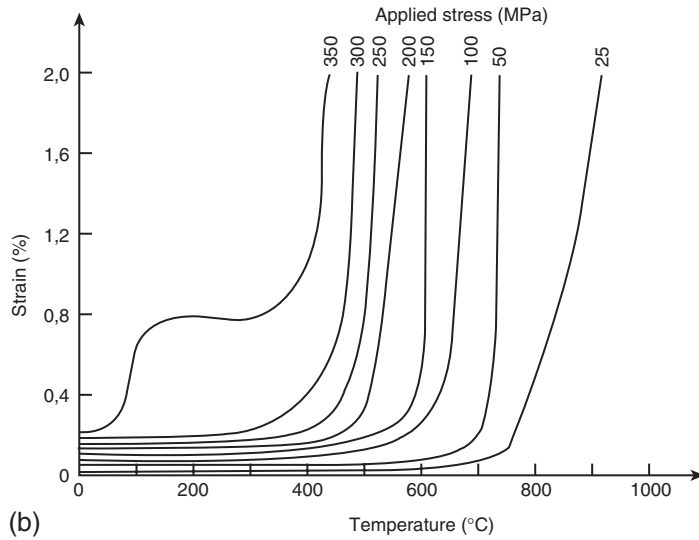
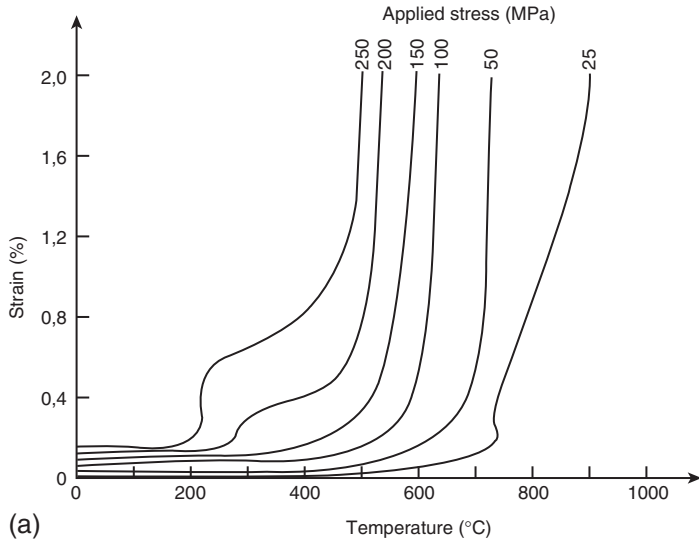


**Figure 5.14** Anisothermal creep strain data for structural steels: (a) grade S275 and (b) grade S355JR (Kirby and Preston, 1988, by permission).

(Kirby, 1986; Kirby and Preston, 1988). It should be noted that the results from anisothermal creep tests are also very sensitive to the exact composition of the steel, thus other steels whilst giving similar trends to those illustrated in Fig. 5.14 exhibit differing values (Anderberg, 1983).

### 5.2.3 Concrete

It is impossible in a text such as this to provide complete data on concrete behaviour owing to the very wide variations in concrete due to mix proportions, aggregate type, age, etc. thus only representative results will be presented.

#### 5.2.3.1 Stress–strain data

Early researchers tended to be interested in measuring specific properties such as compressive strength or elastic modulus rather than obtaining the complete stress–strain characteristic. Although most work tended to be performed on specimens which were heated with no applied load, it was soon established that heating under an applied stress (or pre-load) substantially smaller strength reductions were observed from such specimens (for example, Malhotra, 1956; Abrams, 1968). Data from Malhotra and Abrams are plotted in Fig. 5.15. It was also noted that where different researchers had used different test methods, e.g. for measuring elastic modulus using cylinders in compression (Maréchal, 1970; Schneider, 1976), dynamic modulus (Philleo, 1958) or cylinders in torsion (Cruz, 1966), the absolute values of the results were different, but the trends in the results were similar (Fig. 5.16). The first

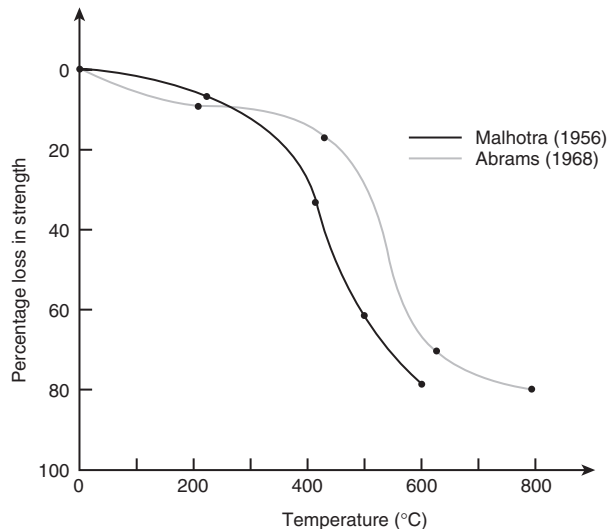


**Figure 5.15** Variation of concrete strength with temperature (Malhotra, 1956, by permission of the Building Research Establishment: Crown copyright and Abrams, 1968, by permission).

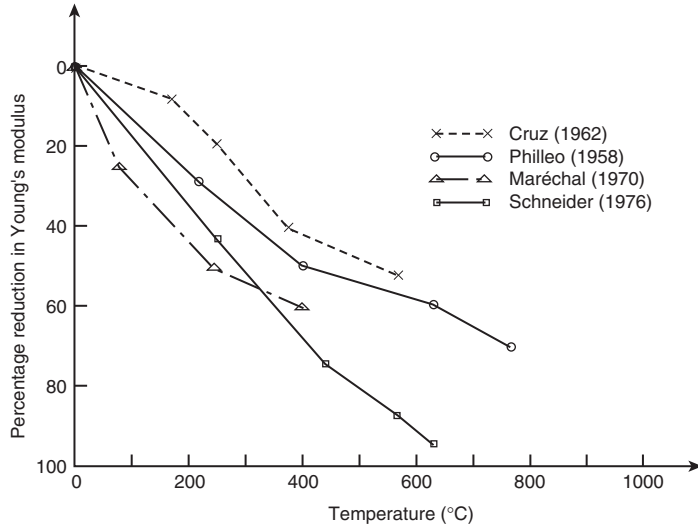


**Figure 5.16** Variation in Young's modulus for concrete with temperature (Philleo, 1958; Cruz, 1962; Maréchal, 1970 and Schneider, 1976, by permission).

researcher to establish the complete stress–strain curve for concrete was Furamura (1966), whose results showed that, besides the compressive stress and elastic modulus being reduced, the slope of the descending branch of the curve also reduced (Fig. 5.17). Baldwin and North (1973) demonstrated that if Furamura's results were non-dimensionalized with respect to the peak (or maximum) compressive stress and the strain value at peak stress (often referred to as the peak strain), then the curves reduced to one single curve which could be curve fitted by the following equation:

$$\frac{\sigma_c}{\sigma_{0,c}} = \frac{\varepsilon_c}{\varepsilon_{0,c}} \exp\left(1 - \frac{\varepsilon_c}{\varepsilon_{0,c}}\right) \quad (5.36)$$

where  $\sigma_c$  and  $\varepsilon_c$  are the stress and strain respectively and  $\sigma_{0,c}$  is the maximum or peak value of stress and  $\varepsilon_{0,c}$  is the strain corresponding to the peak stress value. It should be noted that although Eq. (5.36) is specific to Furamura's data the principle of normalization holds on any set of stress–strain curves for a given concrete. A derivation of Eq. (5.36) is also given in Furamura *et al.* (1987).

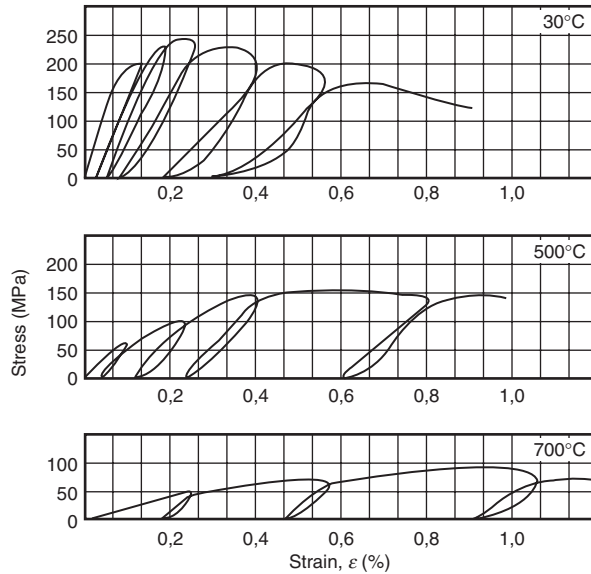


**Figure 5.17** Stress–strain curves for concrete with no pre-load at elevated temperatures (Furamura, 1966).

A more general equation that can be fitted to any concrete stress–strain curve is due to Popovics (1973),

$$\frac{\sigma_c}{\sigma_{0,c}} = \frac{\varepsilon_c}{\varepsilon_{0,c}} \frac{n}{n - 1 + \left(\frac{\varepsilon_c}{\varepsilon_{0,c}}\right)^n} \tag{5.37}$$

In order to fit Eq. (5.37) to any test data, only a single parameter  $n$  is needed. This is determined from Eq. (5.38)

$$\frac{1}{n} = 1 - \frac{\sigma_{0,c}}{\varepsilon_{0,c} E_c} \tag{5.38}$$

Popovics suggested that  $n$  was only dependant on the concrete strength, but it seems likely from the analysis by the author of experimental stress–strain curves obtained during tests at elevated temperatures, that  $n$  is also likely to be dependant on the aggregate size and the aggregate-cement ratio (or the volume fraction of the aggregate) since this will also affect the non-linearity of the stress–strain curve (Table 5.2). The parameter  $n$  can be interpreted as a measure of the degree of non-linearity

**Table 5.2** Variation of stress–strain curve parameter  $n$  with concrete mix

Reference	Mix details	$w/c$ ratio	Pre-load <sup>(*)</sup>	$n$
Furamura (1966)	Quartzite a/s/c <sup>(†)</sup> : 2,9/2,8/1	0,70	0	1,58
Anderberg and Thelandersson (1972)	Quartzite (20 mm) a/s/c <sup>(†)</sup> : 1,92/2,88/1	0,60	0	2,00
Purkiss (1972)	Quartzite (10 mm) a/s/c <sup>(†)</sup> : 1,2/1/1	0,454	0	6,90
Schneider (1976)	Quartzite OPC 240 kg/m <sup>3</sup>	0,8	0	3,57
			0,10	2,44
			0,30	2,22
Bali (1984)	Quartzite (10 mm) a/s/c <sup>(†)</sup> : 3,5/2,5/1	0,65	0	7,25
			0,20	2,31
			0,60	2,68

(\*) The pre-load is defined as the stress applied during heating to the concrete strength.

(†) a/s/c is the aggregate/sand/cement ratio.

in the stress–strain curve which is affected by the aggregate-cement ratio and aggregate size (Hughes and Chapman, 1966).

When the specimen is pre-loaded during the heating cycle and the stress–strain characteristic obtained, it is noted that the characteristics are affected much less by temperature as seen in Fig. 5.18 (Purkiss and Bali, 1988). This is almost certainly due to the effect of the pre-load (or stress) keeping the cracks that would otherwise have formed due to any thermal incompatibility between the aggregate and the matrix closed or at least reduced. This postulate, at least for residual crack density measurements, is confirmed by Guise (1997).

### 5.2.3.2 Creep

The creep of concrete at elevated temperatures is very much greater than that at ambient conditions. Since creep can be considered as an Arrhenius-type phenomenon, then the creep rate is proportional to  $\exp(-U/\Theta)$  where  $U$  is the activation energy and  $\Theta$  is the absolute temperature. Over the time period considered in most creep tests at elevated temperatures of 5 h or less, the variation of creep strains with time can be represented by a power law. Normally only primary and secondary creeps are observed, although at very high temperatures and stresses increasing creep rates can be observed, thereby indicating the possibility that incipient creep

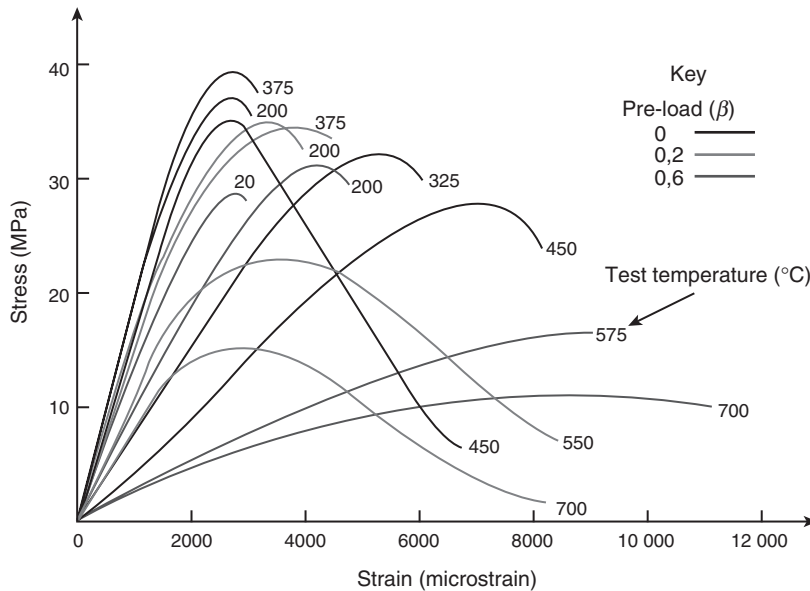


**Figure 5.18** Stress–strain curves for concrete with pre-load at elevated temperatures (Purkiss and Bali, 1988).

rupture could occur. Typical creep data for concrete are given in Fig. 5.19 (Anderberg and Thelandersson, 1976).

### 5.2.3.3 Free thermal expansion

The free thermal expansion is predominantly affected by the aggregate type. The free thermal expansion is not linear with respect to temperature as shown in Fig. 5.20 (Schneider, 1986a).

This non-linear behaviour is in part due to chemical changes in the aggregate (e.g. the breakdown of limestone at around 650°C), or physical changes in the aggregate (e.g. the  $\alpha$ – $\beta$  quartz phase transformation at around 570°C in siliceous aggregates) and in part due to thermal incompatibilities between the aggregate and the matrix. The presence of free moisture will affect the results below 150°C since the water being driven off may cause net shrinkage. EN 1992-1-2 gives the following equations for the free thermal strain of normal-weight concrete:

Siliceous aggregate:

For  $20^\circ\text{C} \leq \theta_c \leq 700^\circ\text{C}$

$$\varepsilon_{th,c} = -1,8 \times 10^{-4} + 9 \times 10^{-6}\theta_c + 2,3 \times 10^{-11}\theta_c^3 \quad (5.39)$$

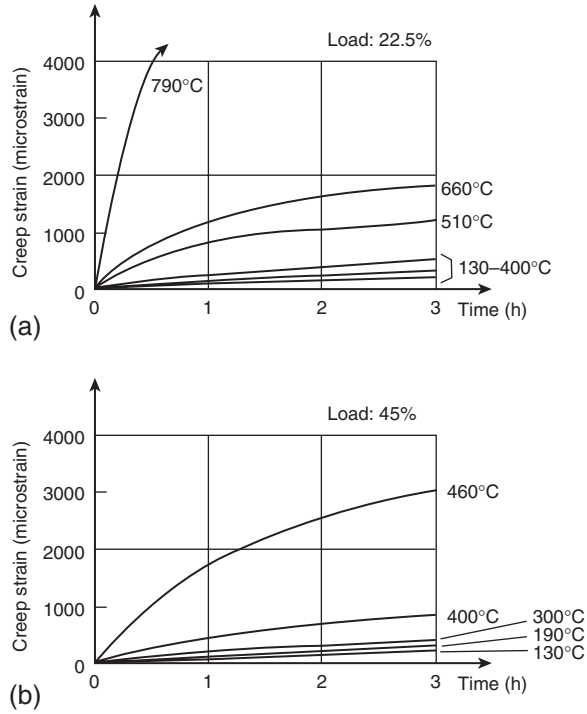


**Figure 5.19** Isothermal creep data for concrete at elevated temperatures (Anderberg and Thelandersson, 1976, by permission).

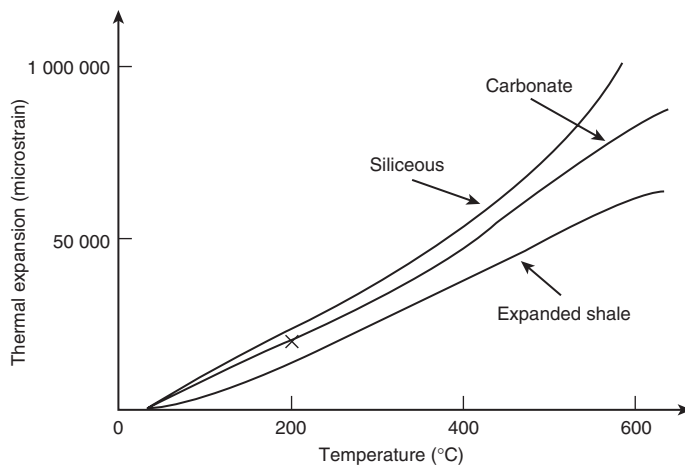


**Figure 5.20** Thermal expansion of concrete (Schneider, 1986a, by permission).

For  $700^{\circ}\text{C} \leq \theta_c \leq 1200^{\circ}\text{C}$

$$\varepsilon_{th,c} = 14 \times 10^{-3} \quad (5.40)$$

Calcareous aggregate concrete:

For  $20^{\circ}\text{C} \leq \theta_c \leq 805^{\circ}\text{C}$

$$\varepsilon_{th,c} = -1,2 \times 10^{-4} + 6 \times 10^{-6}\theta_c + 1,4 \times 10^{-11}\theta_c^3 \quad (5.41)$$

For  $805^{\circ}\text{C} \leq \theta_c \leq 1200^{\circ}\text{C}$

$$\varepsilon_{th,c} = 12 \times 10^{-3} \quad (5.42)$$

For approximate calculations the coefficients of thermal strains may be taken as

For siliceous aggregate

$$\varepsilon_{th}(\theta_c) = 18 \times 10^{-6}(\theta_c - 20) \quad (5.43)$$

For calcareous aggregate

$$\varepsilon_{th}(\theta_c) = 12 \times 10^{-6}(\theta_c - 20) \quad (5.44)$$

For lightweight concrete EN 1994-1-2 gives the following expression:

$$\varepsilon_{th}(\theta_c) = 8 \times 10^{-6}(\theta_c - 20) \quad (5.45)$$

#### 5.2.3.4 *Transient tests*

If a concrete specimen is heated at a constant rate under constant applied stress and the strains are measured, it is observed that these strains are a function of the applied stress as shown in Fig. 5.21 (Anderberg and Thelandersson, 1976) with the strains being recorded as tensile initially, then compressive as the temperature continues to increase and finally the strain rate becomes very high close to failure. At very high stress levels, the strains may be compressive over the whole temperature range. The magnitude of the measured strains is a function of the heating rate, the concrete mix (including aggregate type, although most tests have been conducted on siliceous aggregate) and the stress level.

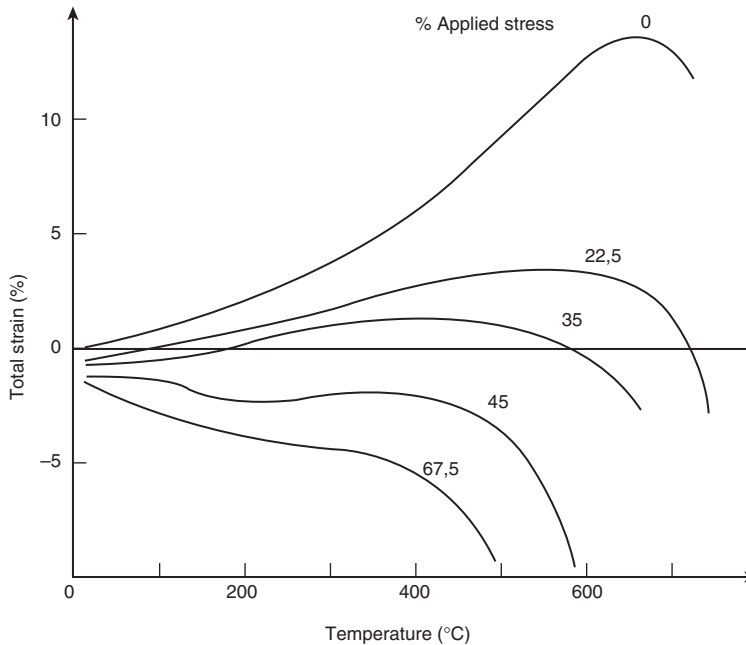


**Figure 5.21** Variation of total strain with temperature for concrete heated under load (Anderberg and Thelandersson, 1976, by permission).

If an attempt be made to calculate these total strains from the free thermal expansion strains, the instantaneous elastic strains and the strains derived from classical creep tests, it is then found that an additional term, known as the transient strain, needs to be incorporated in the calculation to give the requisite strain balance. This transient strain is essentially due to stress modified and thermally induced incompatibilities between the aggregate and the cement–mortar matrix. It should be noted that these transient strains are only exhibited on the first heating cycle, but not the first cooling cycle. Any subsequent heating and cooling cycle does not exhibit such strains. It should also be noted that these transient strains can only be determined from measurements of the total strain, free thermal strain and elastic strains. These transient strains were first identified by Anderberg and Thelandersson (1976). A substantial amount of data on transient strains has also been reported following work at Imperial College (London) (Khoury, Grainger and Sullivan, 1985a, b, 1986; Khoury, 1992) where work was carried out on the effect of applied stress and aggregate type together with heating rate. Although Khoury *et al.* produced master transient strain curves, at that time they did not make any attempt to predict the amount of transient strain after the elastic

strain on first loading is taken into account. The prediction of transient strains is covered in section 5.3.2.

#### **5.2.3.5 Tensile strength of concrete at elevated temperature**

There are only limited data available on tensile strength whether based on direct tensile strength or splitting strength. Felicetti and Gambarova (2003) indicate that for direct tension tests, the tensile strength drops roughly linearly to around 0,25 times the ambient strength at 600°C. They also indicate that the ratio between splitting tensile strength and direct tensile strength for any concrete is around 1,2–1,6 in the temperature range 20–750°C, although there is no consistent pattern to the exact values.

#### **5.2.3.6 Bond strength**

As would be expected, the bond strength between the concrete and steel, whether reinforcing or pre-stressing, decreases with increasing temperature. The magnitude of the loss is a function of the reinforcement (smooth or deformed) and of the type of concrete. The exact results obtained will also be dependant on the test method used, as there is no standardized test procedure. Some typical results are given in Fig. 5.22 (Schneider, 1986a). Bond strength is rarely critical in reinforced concrete as the reinforcement in the bottom face of a beam or slab will be carrying only a small proportion of the applied load, and the reinforcement at the support will only be slightly temperature affected and thus able to carry full bond stresses. Bond is likely to be more critical in pre-stressed concrete, although few, if any, failures have directly occurred due to loss of bond.

#### **5.2.3.7 High-strength (HSC) and self-compacting (SCC) concretes**

High-strength concrete (HSC) is one whose cylinder strength is greater than 60 MPa and self-compacting concrete (SCC) can be considered together as SCC currently is produced with strengths similar to those of HSC.

- **High-performance concrete**

Phan and Carino (1998) provide an excellent overview of the variation of strength properties with temperature. Their summary of loss in strength for both normal-weight and lightweight concretes are given in Figs 5.23(a) and 5.23(b), and loss in elastic modulus in Fig. 5.23(c). It will be noted that the performance of HSCs is erratic, in that some perform similarly to normal strength concretes (NSCs) whereas others perform substantially worse, in that there is a strength loss of around 40% at 200–300°C before a slight regain of strength at

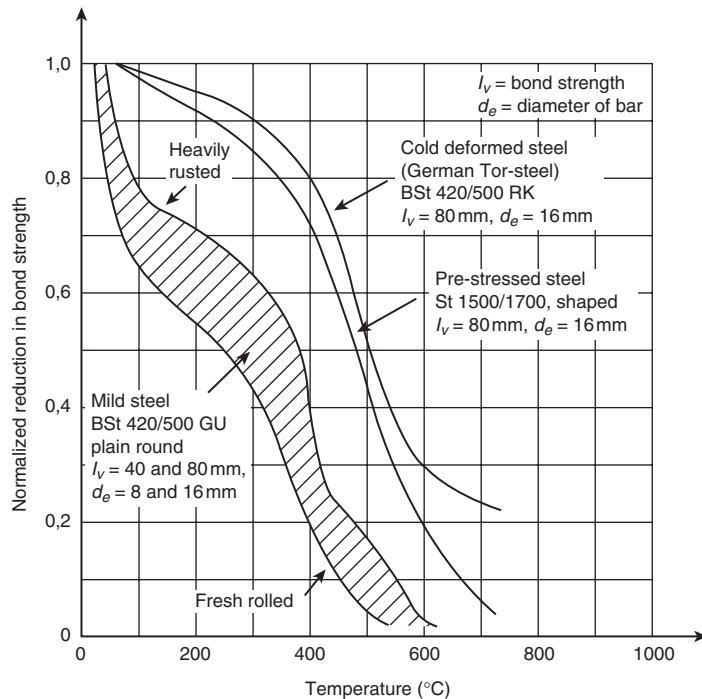


**Figure 5.22** Variation of bond strength between reinforcement and concrete at elevated temperatures (Schneider, 1986a, by permission).

around 400–450°C. After this there is a little difference between HSC and normal concrete. The degradation in elastic modulus is similar to that of normal concrete. Purkiss (2000) suggested that the effect of age was probably a factor in the behaviour of HSC at elevated temperatures due probably to moisture content. Castillo and Durani (1990) indicate that pre-loading specimens before heating exacerbates the strength loss below 400°C although at around 500°C there is a strength increase of around 20% (Fig. 5.24). They too indicate little difference in behaviour of elastic modulus between HSC and NSC. Gillen (1997) indicates there is little difference between the behaviour of normal aggregate HSC and lightweight aggregate HSC. Fu *et al.* (2005) provide data on the complete stress–strain curve for various HSCs for both stressed and unstressed conditions. Their results appear slightly anomalous, in that the concretes heated under stress appear to perform similarly or worse with regard to strength than those heated unstressed. The effect on the elastic modulus of heating under load appears erratic, but with the normalized modulus from the stressed specimens dropping off

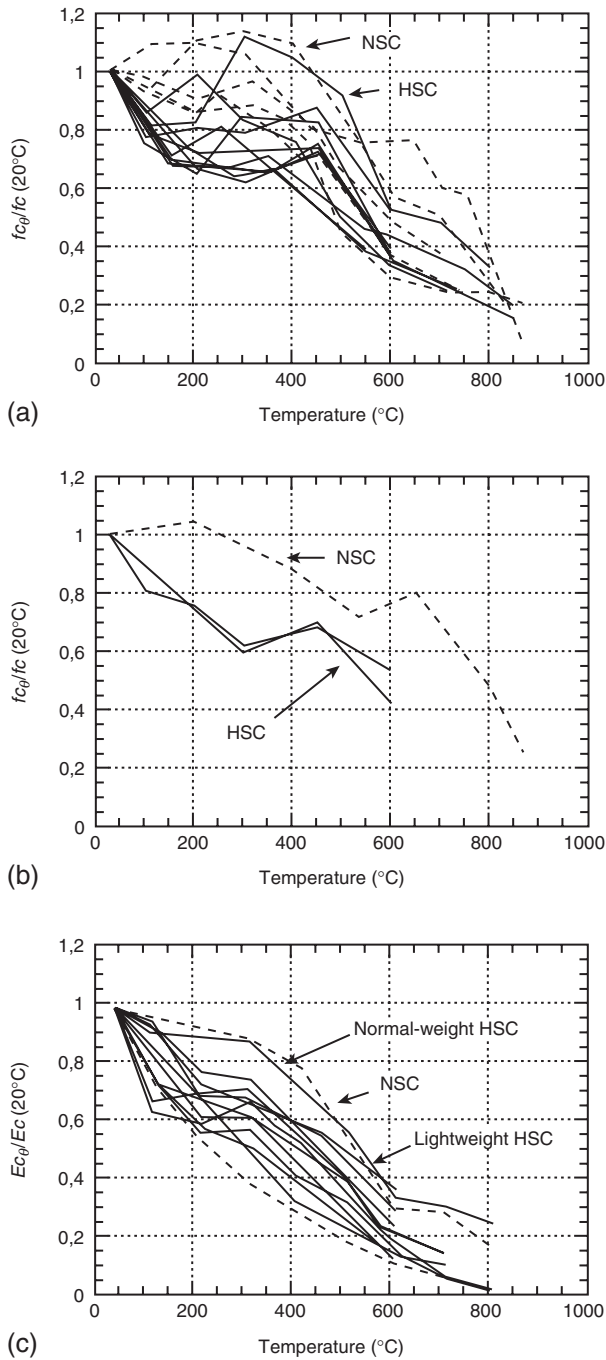


**Figure 5.23** Compressive strength–temperature relationships for: (a) NWA concretes; (b) LWA concretes as obtained by unstressed tests and (c) modulus of elasticity–temperature relationships for NWA and LWA concretes from unstressed test results.

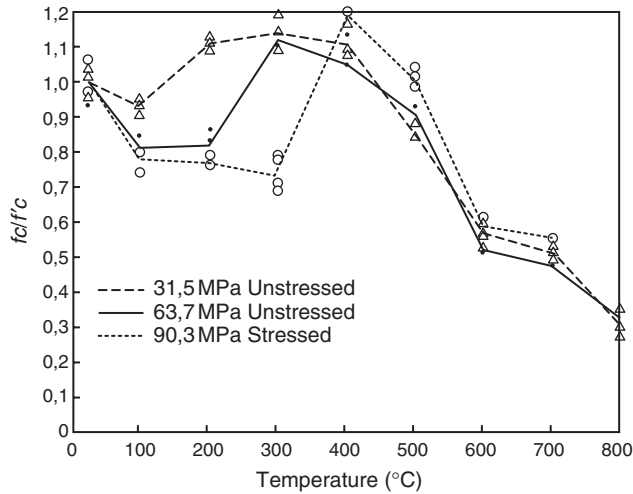


**Figure 5.24** Variation of compressive strength with increase in temperature (Castillo and Durani, by permission).

more slowly. Schneider (1986b, 1988) indicates that for NSC, the elastic modulus increases when the concrete is heated under load. Hassen and Colina (2006) provide some transient strain data for high performance concretes.

- **Self-compacting concrete**

Persson (2003) provides much of the available data on SCC of strengths between 15 and 60 MPa which can be summarized by the following formulae:

Compressive strength:

$$\frac{\sigma_{c,\theta}}{\sigma_{c,20}} = -0,0000012\theta_c^2 - 0,000131\theta_c + 0,99 \quad (5.46)$$

Elastic modulus:

$$\frac{E_{c,\theta}}{E_{c,20}} = 0,0000013\theta_c^2 - 0,00221\theta_c + 1,04 \quad (5.47)$$

Strain at peak stress:

$$\frac{\varepsilon_{c,\theta}}{\varepsilon_{c,20}} = -0,0000022\theta_c^2 - 0,00279\theta_c + 0,95 \quad (5.48)$$

Tests on dynamic and static moduli (Persson, 2003) give the following relationships between temperature and concrete strength and the relevant modulus.

Dynamic modulus  $E_{dyn,\theta}$  (GPa)

$$E_{dyn,\theta} = (0,837 - 0,00079\theta_c) \sigma_{c,20} \quad (5.49)$$

Static modulus  $E_{stat,\theta}$  (GPa)

$$E_{stat,\theta} = \left(0,00211 + 37,4 \times 10^{-6}\theta_c - 91,6 \times 10^{-9}\theta_c^2\right) \sigma_{c,20}^2 \quad (5.50)$$

subject to  $5 \text{ MPa} \geq \sigma_{c,20} \leq 60 \text{ MPa}$ .

Persson also indicates that when polypropylene fibres are introduced, the strength drops by 2,3% per  $\text{kg/m}^3$  for fibre dosages of 0–4  $\text{kg/m}^3$ . This is roughly in agreement with the figure of 5% for a dosage of 3,0  $\text{kg/m}^3$  quoted by Clayton and Lennon (1999) for high performance concrete.

#### 5.2.3.8 *Fibre concretes*

- **Steel fibre concrete**

Lie and Kodur (1995, 1996) give the following set of equations for thermal conductivity (W/mK) for steel fibre-reinforced siliceous aggregate concrete:

For  $0^\circ\text{C} \leq \theta_c \leq 200^\circ\text{C}$

$$\lambda_c = 3,22 - 0,007\theta_c \quad (5.51)$$

For  $200^\circ\text{C} \leq \theta_c \leq 400^\circ\text{C}$

$$\lambda = 2,24 - 0,0021\theta_c \quad (5.52)$$

For  $400^\circ\text{C} \leq \theta_c \leq 1000^\circ\text{C}$

$$\lambda = 1,40 \quad (5.53)$$

For fibre-reinforced carbonate concrete, the values of thermal conductivity become:

For  $0^\circ\text{C} \leq \theta_c \leq 500^\circ\text{C}$

$$\lambda_c = 2,00 - 0,001775\theta_c \quad (5.54)$$

For  $500^{\circ}\text{C} \leq \theta_c \leq 1000^{\circ}\text{C}$

$$\lambda_c = 1,402 - 0,00579\theta_c \quad (5.55)$$

The values for steel fibre-reinforced concrete are only slightly higher than those for non-fibre concrete.

The data provided by Lie and Kodur for specific heat indicate that except for small peaks at around 100 and 420°C, the specific heat for siliceous aggregate can be taken as 1000J/kgC over the temperature range 0–1000°C. This is also true for carbonate aggregate up to 600°C after which a severe peak of 8000J/kgC occurs at 700°C after which the earlier value re-occurs.

Lie and Kodur provide the following data on coefficients of thermal expansion,  $\alpha_c$ :

Siliceous aggregate:

$0^{\circ}\text{C} \leq \theta_c \leq 530^{\circ}\text{C}$

$$\alpha_c = -0,00115 + 0,000016\theta_c \quad (5.56)$$

$530^{\circ}\text{C} \leq \theta_c \leq 600^{\circ}\text{C}$

$$\alpha_c = -0,0364 + 0,000083\theta_c \quad (5.57)$$

$600^{\circ}\text{C} \leq \theta_c \leq 1000^{\circ}\text{C}$

$$\alpha_c = 0,0135 \quad (5.58)$$

Calcareous aggregate:

$0^{\circ}\text{C} \leq \theta_c \leq 750^{\circ}\text{C}$

$$\alpha_c = -0,00115 + 0,00001\theta_c \quad (5.59)$$

$750^{\circ}\text{C} \leq \theta_c \leq 1000^{\circ}\text{C}$

$$\alpha = -0,05187 + 0,000077\theta_c \quad (5.60)$$

Purkiss (1987) notes that the fibres reduce the thermal expansion by around 20% for temperatures up to 500°C, but after which there is

little difference, and this effect is sensibly independent of fibre volume fraction.

Lie and Kodur also give the following formulation for stress–strain curves.

Independent of the aggregate, the stress–strain curves are given by:

For  $\varepsilon_c \leq \varepsilon_{0,\theta}$

$$\frac{\sigma_{c,\theta}}{\sigma_{c,0}} = 1 - \left( \frac{\varepsilon_{0,\theta} - \varepsilon_c}{\varepsilon_{0,\theta}} \right)^2 \quad (5.61)$$

and, for  $\varepsilon_c > \varepsilon_{0,\theta}$

$$\frac{\sigma_{c,\theta}}{\sigma_{c,0}} = 1 - \left( \frac{\varepsilon_{0,\theta} - \varepsilon_c}{3\varepsilon_{0,\theta}} \right)^2 \quad (5.62)$$

where the strain at maximum stress  $\varepsilon_{0,\theta}$  is given by

$$\varepsilon_{0,\theta} = 0,003 + \left( 7,0\theta_c + 0,05\theta_c^2 \right) \times 10^{-6} \quad (5.63)$$

and the strength reduction factors  $\sigma_{c,0}/\sigma_{c,0,20}$  are given by  $0^\circ\text{C} \leq \theta_c \leq 150^\circ\text{C}$

$$\frac{\sigma_{c,0,\theta}}{\sigma_{c,0}} = 1 + 0,000769 (\theta_c - 20) \quad (5.64)$$

$150^\circ\text{C} \leq \theta_c \leq 400^\circ\text{C}$

$$\frac{\sigma_{c,0,\theta}}{\sigma_{c,0}} = 1,1 \quad (5.65)$$

$\theta_c > 400^\circ\text{C}$

$$\frac{\sigma_{c,0,\theta}}{\sigma_{c,0}} = 2,011 - 2,353 \frac{\theta_c - 20}{1000} \quad (5.66)$$

Fairyadh and El-Ausi (1989) present data on the splitting tensile strength at elevated temperatures of both glass and steel fibre-reinforced concrete. They indicate that the splitting tensile strength of

concrete with no fibres reduces to zero at 700°C. When normalized, the results for 1,0% fibres show less degradation than those for 0,7 and 0,5% which are sensibly similar. All the steel fibre concretes retain around 25% of their strength at 800°C. The glass fibre results are anomalous in that, the mix with 0,5% fibres show less degradation than those with 1,0 or 0,7%. The strength retention at 800°C is around 14%.

- **Refractory concretes and slurry infiltrated fibre concrete (SIFCON)**  
Robbins and Austen (1992) carried out tests on fibre-reinforced refractory concretes at elevated temperatures and report loss in strength of around 60% at 850°C. The influence of fibre type is more marked at higher fibre contents, although the fibre content would appear not to be of primary importance when the results are normalized.

SIFCON effectively is a slurry concrete with maximized fibre contents of around 10%. Purkiss, Maleki-Toyserkani and Short (2001) report data on both thermal diffusivity and thermal expansion. They indicate that from 20 to 100°C the thermal diffusivity varies linearly with temperature with a value of 2 mm<sup>2</sup>/s at 20°C to a value of 0,5 mm<sup>2</sup>/s for SIFCON and 0,7 mm<sup>2</sup>/s for the matrix which remain constant thereafter. This behaviour is similar to that of normal fibre-reinforced concrete with fibre contents up to 3% (Purkiss, 1987). The thermal expansion of SIFCON is sensibly constant over a temperature range of 20–800°C at a value of 22–23 μstrain/°C. The matrix expands by 2000 μstrain at 100° and remains constant this value thereafter.

#### **5.2.3.9 Multi-axial behaviour**

The landersson (1982) attempted to formulate a multi-axial constitutive model for concrete at elevated temperatures using the volumetric thermal strain as a scalar damage parameter. He was able to obtain reasonable correlation between the model and uniaxial test results. He also pointed out that many more data were required in order to improve and validate the model. To this Author's awareness this has not been carried forward. It should be noted that such testing is complex and therefore expensive. It is perhaps fortuitous that most modelling, except possibly, for spalling can be carried out using uniaxial data.

#### **5.2.4 Timber**

The situation with timber is different when compared to either steel or concrete, in that when timber is subject to a fire, the outer layer of the timber member chars losing all strength while retaining a role as an insulating layer which prevents excessive temperature rise in the core. The central core is slightly temperature affected with some small loss of strength

and elasticity. Only three properties are thus required to determine the fire performance of timber; namely the rate of charring, and both the strength and elasticity loss in the central core.

#### 5.2.4.1 *Rate of charring*

It has already been pointed out in section 3.2.6 that the result from a standard furnace test is very much affected by the furnace characteristics, notably the heat flux falling on the specimen. This is even more relevant for measurements on the rate of charring of timber which is very much affected by heat flux rather than the absolute rate of temperature rise. For example, Hadvig (1981) reports results in which the charring on the bottom face of a beam is up to 20% higher than that on the side faces. However, it is observed that when timber members are exposed to the standard furnace temperature–time curve, the charring rate on a given face of the member is sensibly constant up to 90 min. This rate is dependent on the timber type (or the density of the timber). After 90 min, tests on timber exposed to the standard furnace curve seem to indicate that there is then a substantial rise in the rate of charring leading to a rapid loss of section. This effect is likely to be exacerbated by the fact that in most tests, the size of timber member used is such that after 90 min there is little of the central core remaining. Values of charring rates from a wide range of tests are given in Table 5.3 where it will be noted that there is a consistency in the data which for design purposes allow the various timbers to be placed in a relatively small number of categories. It should be noted that tests on panels can produce higher charring rates than those on beams or columns. The charring rates are, however, dependant to a limited extent on both the moisture content and the density. Schaffer (1967) gave equations relating the charring rate  $\beta_0$  (mm/min), the moisture content  $M$  (per cent by weight) and the dry specific gravity  $S$  for three different timber types.

For Douglas fir:

$$\frac{1}{\beta_0} = 0,79 [(28,76 + 0,578M)S + 4,187] \quad (5.67)$$

For southern pine:

$$\frac{1}{\beta_0} = 0,79 [(5,832 + 0,120M)S + 12,286] \quad (5.68)$$

For white oak:

$$\frac{1}{\beta_0} = 0,79 [(20,036 + 0,403M)S + 7,519] \quad (5.69)$$

**Table 5.3** Experimentally derived timber char rates

Reference	Type of specimen	Timber type	Char rate (mm/min)
Wardle (1966)	Beam	Spruce	0,5–0,6
		Douglas fir	0,6
		Baltic fir (laminated)	0,6
	Column	Fir	0,55
		Fir (Glulam)	0,66
Schaffer (1967)	Panel	Douglas fir	0,68
		Southern pine	
		White oak	
Rogowski (1969)	Column	Hemlock	0,55 (par) 0,67 (perp)
		Fir	0,64 (par) 0,78 (perp)
		Redwood	0,71 (par) 0,74 (perp)
		Cedar	0,71 (par) 0,85 (perp)
Tenning (1969)	Beam	Glulam	0,62
		Laminated pine	0,5–0,66
		Oak	0,4
		Teak	0,35
Ödeen (1969)	Beam	Fir	0,6–0,62
		Oak	0,4
		Teak	0,37
Fredlund (1988)	Slab	Spruce	0,265
		Pine	0,339
		Chipboard	0,167

For the results from Rogowski, two values are quoted as the tests were carried out on laminated timber columns and the values quoted as (par) are those parallel to the laminations and (perp) are those perpendicular to the laminations. None of the other tests on laminated sections appear to differentiate between the rates in the two directions.

#### 5.2.4.2 *Strength and elasticity loss*

There are few data on strength loss in timber subject to fire, partly because it is recognized that at the charred boundary temperatures drop rapidly in the core to near ambient. Such data as exist indicate that both the strength and elasticity losses are low (Fig. 5.25) (Gerhards, 1982).

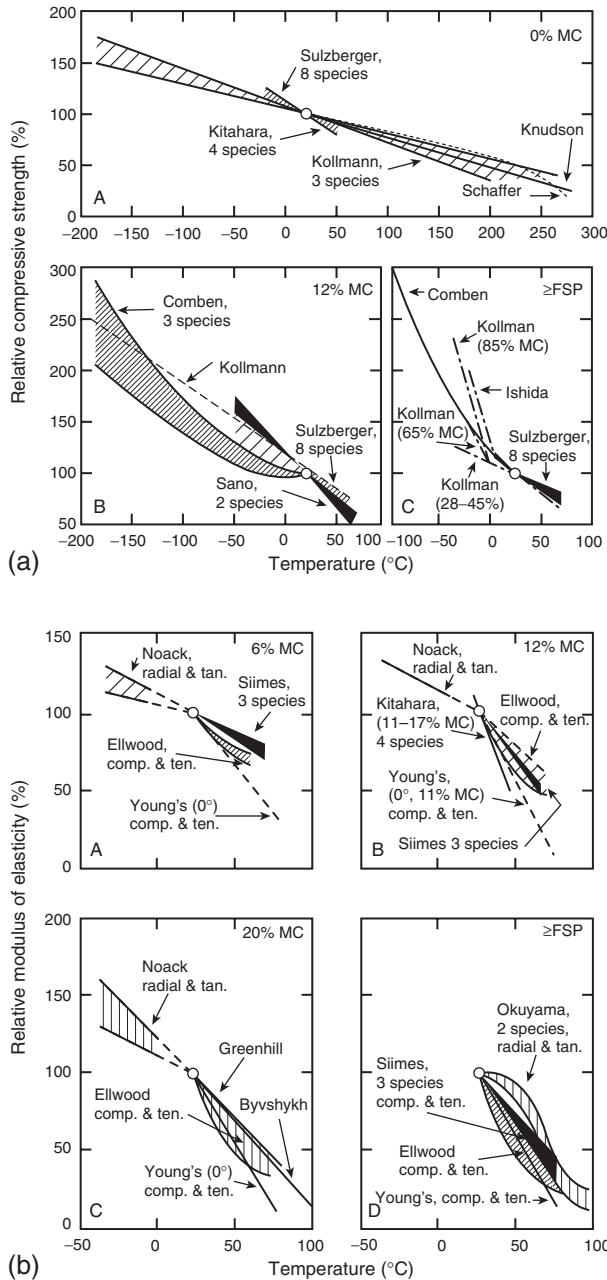


**Figure 5.25** Variation of (a) strength and (b) Young's modulus for timber at elevated temperature (Gerhards, 1982, by permission of society of Wood Science and Technology).

It also seems that the reduction per unit rise in temperature is sensibly independent of the timber type as Sano (1961) reported the following strength results (MPa) for compression parallel to the grain on two timbers tested at temperatures between  $-60^{\circ}\text{C}$  and  $+60^{\circ}\text{C}$ .

For spruce:

$$\sigma_{par} = 49,3 - 0,424\theta_w \quad (5.70)$$

For ash:

$$\sigma_{par} = 57,4 - 0,392\theta_w \quad (5.71)$$

where  $\theta_w$  is the temperature in the wood.

### 5.2.5 Masonry

There appears to be little data on the strength of masonry at elevated temperatures although some data are also available on residual properties (section 13.3.1.5). The residual property data suggest that the strength degradation in the mortar is likely to be the controlling factor in strength performance of masonry, but this has not yet been demonstrated by test as far as the author is aware.

There are some limited data on the thermal expansion of lightweight masonry units utilizing scoria aggregate. Such data are given for three different types of masonry units in Fig. 5.26, where it is noted that in certain cases the coefficient of thermal expansion is negative (Gnanakrishnan and Lawther, 1989).

### 5.2.6 Aluminium

#### 5.2.6.1 Strength data

Owing to the relatively lower temperatures reached in aluminium before collapse ensues, there appears little need for creep data as insignificant creep will have occurred and it will be sufficiently accurate to consider basic stress-strain behaviour with some account being taken of creep in the actual results. Typical data for the reduction in proof strength of aluminium is given in Fig. 5.27 (Bayley, 1992) where it will be noted that the strength loss is dependant upon the alloy. It should be further noted that although alloying will increase the strength at any particular temperature there can also be a concurrent loss in ductility and total elongation to failure (Hammad, Ramadan and Nasr, 1989). It also should be noted

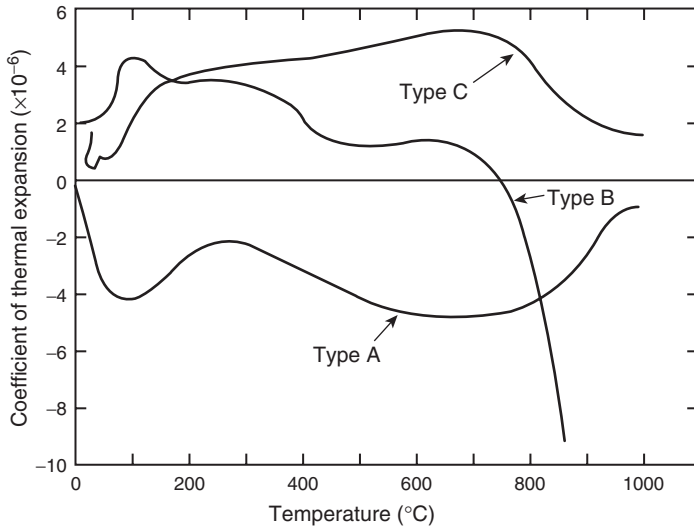


**Figure 5.26** Thermal expansion of masonry (Gnanakrishnan and Lawther, 1989).

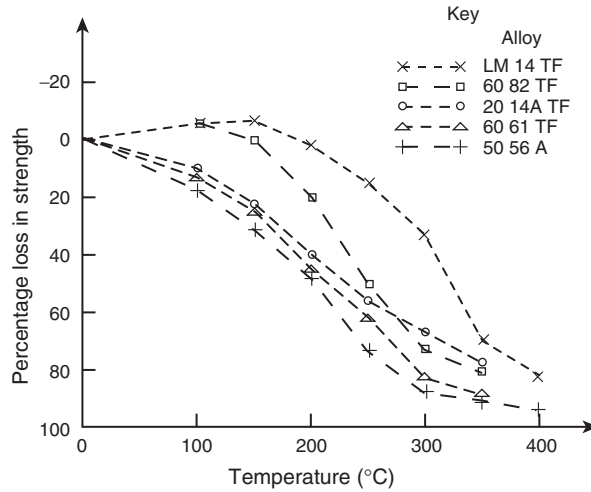


**Figure 5.27** Variation of normalized strength loss for various aluminium alloys with temperature (from Bayley, 1992, reproduced by permission of the Council of the Institution of Mechanical Engineers).

that the strain rate also affects the reduction in proof stress and ultimate tensile strength (Hammad and Ramadan, 1989a, b). The strength data from ENV 1999-1-2 are plotted in Fig. 5.28(a) and Young's modulus data in Fig. 5.28(b).

Depending upon the alloy, a limiting temperature for a strength loss of 30%, which represents an equivalent partial safety factor of around 1,4, is between 150 and 300°C. This means that any design method must take account of the exact nature of the alloy and, unlike steel, a single limiting temperature independent of strength grade cannot be established. It should also be noted that on cooling, some alloys will tend to exhibit brittle rather than ductile failure (Zacharia and Aidun, 1988).

### 5.2.6.2 Thermal expansion

Conserva, Donizelli and Trippodo (1992) suggest that over the temperature range 0–300°C the unrestrained thermal strain is sensibly linear with respect to temperature and therefore a constant coefficient of thermal expansion of between 24 and 26  $\mu\text{strain}/^\circ\text{C}$  may be adopted. The slight scatter in the values is due to the effect of the alloying elements. ENV 1999-1-2 gives the following expression for  $0^\circ\text{C} < \theta_{al} < 500^\circ\text{C}$

$$\frac{\Delta l}{l} = 0,1 \times 10^{-7} \theta_{al}^2 + 22,5 \times 10^{-6} \theta_{al} - 4,5 \times 10^{-4} \quad (5.72)$$

or slightly less accurately

$$\frac{\Delta l}{l} = 2,5 \times 10^{-5} (\theta_{al} - 20) \quad (5.73)$$

## 5.3 CONSTITUTIVE STRESS–STRAIN LAWS

In order to carry out computer analyses of either steel or concrete elements or structures exposed to fire, it is necessary to be able to formulate constitutive stress–strain models for both steel and concrete. These models may either be established using fundamental principles or by curve fitting on established data on an empirical approach. Whilst the former is clearly the more preferable, it is often necessary to resort to the latter owing to either the paucity of data needed to establish a fundamental model or practical aspects in that the model is not required to be portable, but applicable to a single identified material, e.g. a single steel strength (or grade). It is essential to be aware of potential limitations when using any model.

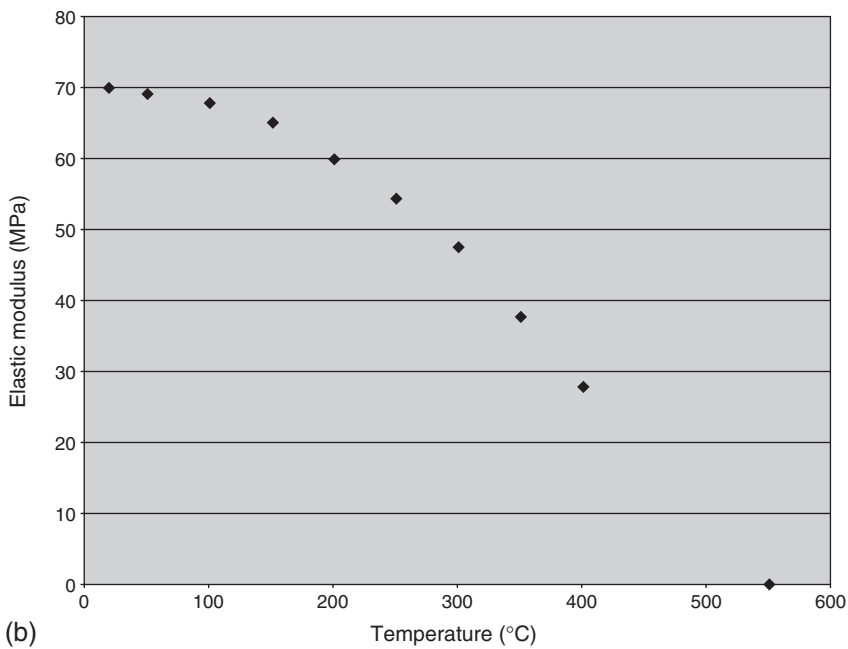
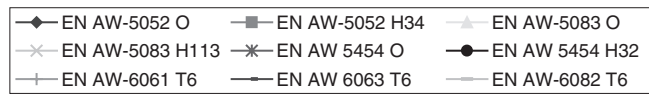
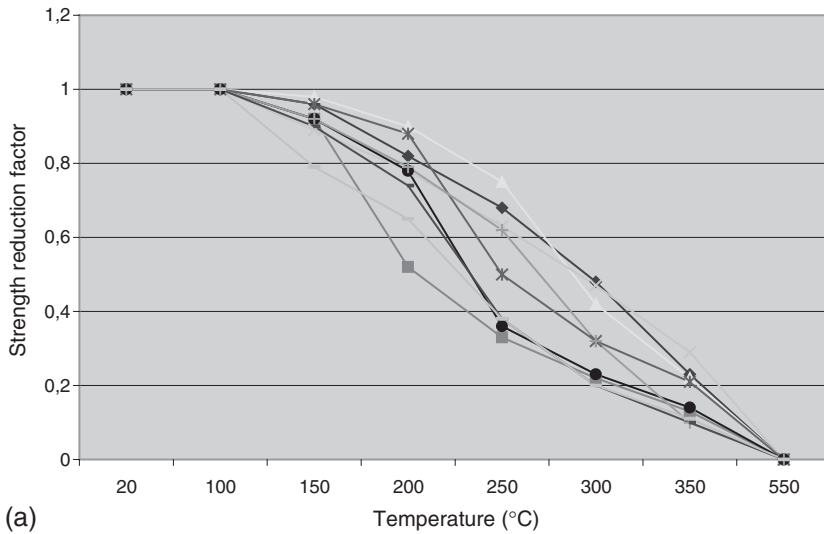


**Figure 5.28** (a) Aluminum strength data from ENV 1999-1-2 and (b) variation of elastic modulus with temperature.

Following Anderberg and Thelandersson (1976), the total strain  $\varepsilon_{tot}$  can be decomposed into three components:

1. the free thermal strain  $\varepsilon_{th}$ ,
2. the stress related strain  $\varepsilon_{\sigma}$ ,
3. the transient creep strain  $\varepsilon_{tr}$ ,

such that

$$\varepsilon_{tot} = \varepsilon_{th} + \varepsilon_{\sigma} + \varepsilon_{tr} \quad (5.74)$$

Additional subscripts 's' and 'c' will be used for steel and concrete respectively, as it is necessary to cover each material separately. The free thermal strain terms in Eq. (5.74) have already been covered in sections 5.2.2.2 and 5.2.3.3, and the remaining terms may now be considered.

### 5.3.1 Steel

#### 5.3.1.1 Elastic strain

The mathematical model used for the instantaneous elastic strain is dependant upon the characterization used for the stress–strain curve. Common models are as follows.

##### 1. Linear elastic perfectly plastic

In this case (Fig. 5.29(a)), the behaviour is taken as elastic up to yield, then plastic post-yield, or,  
for  $0 < \varepsilon_{\sigma,s} < \varepsilon_{y,s,\theta}$

$$\sigma_{s,\theta} = E_{s,\theta} \varepsilon_{\sigma,s} \quad (5.75)$$

and for  $\varepsilon_{\sigma,s} > \varepsilon_{y,s,\theta}$

$$\sigma_{s,\theta} = \sigma_{y,s,\theta} \quad (5.76)$$

where  $\varepsilon_{\sigma,s}$  is the stress-related strain,  $\varepsilon_{y,s,\theta}$  is the temperature-dependant yield strain,  $\sigma_{s,\theta}$  is the temperature-dependant stress,  $\sigma_{y,s,\theta}$  is the temperature-dependant yield stress and  $E_{s,\theta}$  is the temperature-dependant modulus of elasticity.

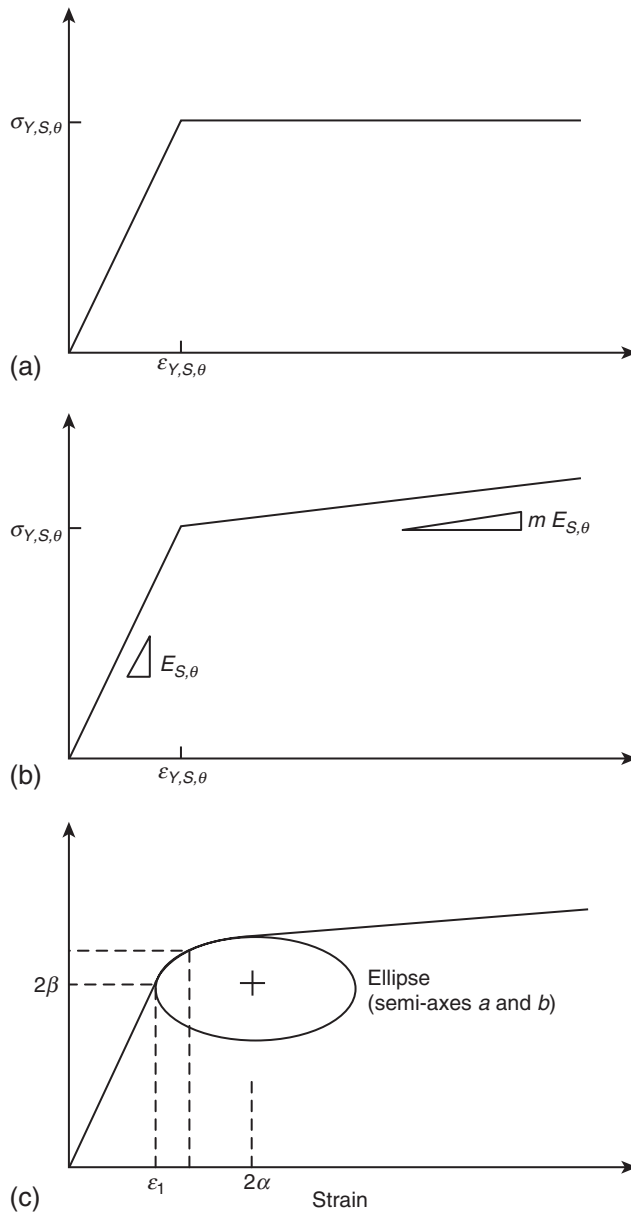


**Figure 5.29** Idealization of stress–strain behaviour for steel at elevated temperatures: (a) linear elastic perfectly plastic; (b) linear elastic, linear strain hardening and (c) Dounas and Golrang model.

Note that the yield strain, yield stress and modulus of elasticity are not independent since

$$E_{s,\theta} = \frac{\sigma_{y,s,\theta}}{\varepsilon_{y,s,\theta}} \quad (5.77)$$

This model has the advantage of being simple but, may not be very accurate close to the yield point and in the post-yield phase. The latter inaccuracy can be ameliorated by adopting a linear elastic, strain hardening model.

**2. Linear elastic, strain hardening model**

In the elastic range, the model is identical to the above, but introduces post-yield strain hardening (Fig. 5.29(b)), but with a post-yield gradient of  $m_\theta E_{s,\theta}$  where  $m_\theta$  is the strain hardening parameter and typically can be taken in the range 0,1–0,15. Thus the governing equation for post-yield behaviour is modified to

$$\sigma_{s,\theta} = \sigma_{y,s,\theta} + m_\theta E_{s,\theta} (\varepsilon_{s,\theta} - \varepsilon_{y,s,\theta}) \quad (5.78)$$

The use of a strain-hardening model, while providing a better model for post-yield behaviour, does not totally overcome the problem of inaccuracies close to the yield point. Dounas and Golrang (1982) proposed that a combination of straight lines for pre- and post-yield and a quarter ellipse at the yield point could be used (Fig. 5.29(c)). This complexity, however, is probably unnecessary when a much simpler, single expression model due to Ramberg and Osgood (1943) exists.

**3. Ramberg–Osgood model**

This model was originally proposed for the behaviour of aluminium which does not possess a definite yield plateau. It is thus also applicable to steel. The Ramberg–Osgood equation in its simplest form is given by

$$\varepsilon_{s,\theta} = \frac{\sigma_{s,\theta}}{E_{s,\theta}} + K \left( \frac{\sigma_{s,\theta}}{E_{s,\theta}} \right)^n \quad (5.79)$$

where  $K$  and  $n$  are the parameters defining the fit of the equation to experimental data. These parameters will be temperature dependant. Burgess, El-Rimawi and Plank (1990) give a temperature modified form of the Ramberg–Osgood equation.

A disadvantage of the Ramberg–Osgood equation is that it gives the strain in terms of the stress, and that an explicit equation cannot be derived for the stress in terms of the strain.

**5.3.1.2 Creep**

As mentioned in section 5.2.2.3, steel creep is generally analyzed in terms of the Dorn (1954) temperature-compensated time approach, where the real time  $t$  is transformed into a temperature-compensated time  $\Theta$  using Eq. (5.80)

$$\Theta = \int_0^t \exp\left(\frac{-\Delta H}{R(\theta_a + 273)}\right) dt \tag{5.80}$$

where  $\Delta H/R$  is the activation energy and  $\theta_a$  is the temperature in the steel ( $^{\circ}\text{C}$ ).

When creep data are plotted to a base of temperature-compensated time, two creep periods can be identified (Fig. 5.30):

**1. Primary creep**

Over this portion, the creep is non-linear, and be taken as parabolic (Harmathy, 1967), with the creep strain  $\varepsilon_{cr,s}$  given by

$$\varepsilon_{cr,s} = \frac{\varepsilon_{cr,s,0}}{\ln 2} \cosh^{-1}\left(2 \frac{Z\Theta}{\varepsilon_{cr,s,0}}\right) \tag{5.81}$$

where  $\varepsilon_{cr,s,0}$  is the intercept of the secondary creep line with strain axis, and  $Z$  is the Zener–Hollomon parameter. Equation (5.81) is valid up

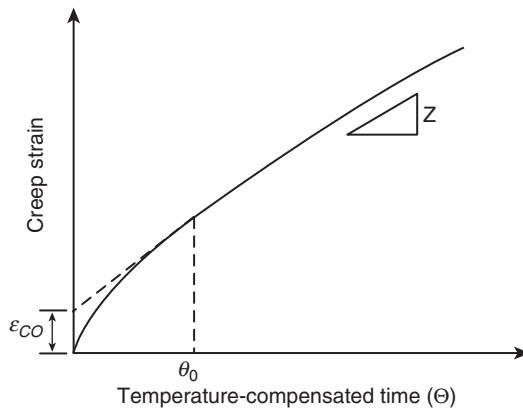


**Figure 5.30** Idealization of isothermal creep data for steel.

to a temperature-compensated time of  $\Theta_0$  given by

$$\Theta_0 = \frac{\varepsilon_{cr,s,0}}{Z} \quad (5.82)$$

## 2. Secondary creep

This is generally taken as a straight line with a slope of  $Z$ .

Alternative creep equations have been proposed by Plem (1975) and Anderberg (1978a). It should be noted that values of  $\Delta H/R$  are very sensitive to the metallurgical characteristics of the steel as are values of  $Z$  and  $\varepsilon_{cr,s,0}$ . The latter two parameters are functions of the stress in the steel and can be calculated from the following equations:

$$\varepsilon_{cr,s,0} = A\sigma_s^B \quad (5.83)$$

For  $\sigma_s \leq \text{SIG1}$

$$Z = C\sigma_s^D \quad (5.84)$$

For  $\sigma_s > \text{SIG1}$

$$Z = He^{F\sigma_s} \quad (5.85)$$

Typical values of  $\Delta H/R$ ,  $\text{SIG1}$ ,  $A$ ,  $B$ ,  $C$ ,  $D$ ,  $H$  and  $F$  are given in Table 5.4. Note that great care should be taken in using any particular set of values from this table to set up a creep model for steel, as the parameters appear very sensitive to the type of steel and thus if applied to a steel not in the table erroneous results may be given.

It is possible to set up empirical equations to give the strain induced in steel, excluding the unrestrained thermal strain at constant temperature and under constant stress by analyzing existing data (Fields and Fields, 1989). It is however necessary to be aware of the procedure used to determine the empirical constants and any limitations adopted, since often log-log plots of data are used. This method compresses the data and may give the appearance of a better fit than actually exists.

**Table 5.4** Steel creep parameters

Steel	$f_{0,s,20}$ (MPa)	$\Delta H/R$ (K)	$A$	$B$	$SIG1$ (MPa)	$D$	$C$ (/min)	$H$ (/min)	$F$
1312	254	55 800	$5,56 \times 10^{-6}$	1,722	108	7,804	$6,083 \times 10^9$	$1,383 \times 10^{23}$	0,0578
1312	263	53 900	$2,66 \times 10^{-6}$	2,248	108	7,644	$8,95 \times 10^8$	$5,10 \times 10^{21}$	0,0601
1411	340	66 000	$3,52 \times 10^{-7}$	2,08	118	8,402	$6,767 \times 10^{12}$	$4,417 \times 10^{27}$	0,0603
A36-66	304	38 900	$4,07 \times 10^{-6}$	1,75	103	4,70	$6,217 \times 10^6$	$2,10 \times 10^{14}$	0,0434
2172	331	50 000	$2,085 \times 10^{-8}$	2,30	108	5,38	$1,33 \times 10^{10}$	$1,083 \times 10^{19}$	0,0446
G40-12	333	36 100	$1,766 \times 10^{-7}$	1,00	103	3,35	$4,733 \times 10^7$	$6,17 \times 10^{12}$	0,0319
A421-65	1470	30 600	$9,262 \times 10^{-5}$	0,67	172	3,00	$3,253 \times 10^6$	$1,368 \times 10^{12}$	0,0145
Ks40 $\phi$ 10	483	45 000	$2,85 \times 10^{-8}$	1,037	84	4,70	$1,16 \times 10^9$	$4,3 \times 10^{16}$	0,0443
Ks40 $\phi$ 8	456	40 000	$3,39 \times 10^{-7}$	0,531	90	4,72	$7,6 \times 10^9$	$1,25 \times 10^{13}$	0,0512
Ks40 $\phi$ 8	504	47 000	$1,99 \times 10^{-5}$	1,28	120	7,26	$4,05 \times 10^4$	$5,00 \times 10^{17}$	0,0384
Ks40SE $\phi$ 8	558	40 000	$3,86 \times 10^{-8}$	1,117	96	3,83	$5,8 \times 10^7$	$4,113 \times 10^{13}$	0,0414
Ks60 $\phi$ 8	710	40 000	$2,06 \times 10^{-6}$	0,439	90	2,93	$8,517 \times 10^8$	$2,65 \times 10^{14}$	0,0313
Ps50 $\phi$ 5	500	40 000	$1,10 \times 10^{-6}$	0,557	100	4,47	$9,783 \times 10^6$	$2,133 \times 10^{15}$	0,0368
Ps50 $\phi$ 8	749	41 000	$1,28 \times 10^{-7}$	0,844	133	3,94	$1,367 \times 10^8$	$1,02 \times 10^{15}$	0,0265

Source: Anderberg (1983) by permission

**5.3.1.3 Design curves**

In order to standardize the parameters required in design, EN 1992-1-2, EN 1993-1-2 and EN 1994-1-2 give a stress–strain curve for both reinforcing and structural steels (Fig. 5.31).

The relationship between the various parameters of the mathematical model given in Fig. 5.31 are given in Table 5.5, and the variation of strength or elastic modulus in Table 5.6. These stress–strain parameters include an allowance for creep.

Hertz (2004) gives an equation which can be used for both hot and residual strength properties for both reinforcing and pre-stressing steels,

$$\xi(\theta) = k + \frac{1 - k}{1 + \frac{\theta}{\theta_1} + \left(\frac{\theta}{\theta_2}\right)^2 + \left(\frac{\theta}{\theta_8}\right)^8 + \left(\frac{\theta}{\theta_{64}}\right)^{64}} \tag{5.86}$$

where  $\theta_1, \theta_2, \theta_8$  and  $\theta_{64}$  are experimentally determined parameters and  $k$  is the ratio between the minimum and maximum values of the property

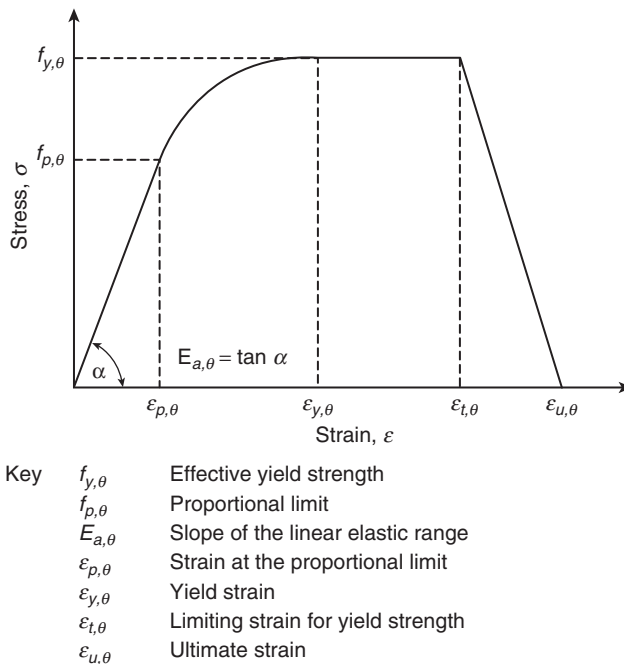


**Figure 5.31** Stress–strain relationship for carbon steel at elevated temperatures, from EN 1993-1-2.

**Table 5.5** Relation between the various parameters of the mathematical model in Fig. 5.31

Strain range	Stress ( $\sigma$ )	Tangent modulus
$\varepsilon < \varepsilon_{p,\theta}$	$\varepsilon E_{a,\theta}$	$E_{a,\theta}$
$\varepsilon_{p,\theta} < \varepsilon < \varepsilon_{y,\theta}$	$f_{p,\theta} - c + \frac{b}{a} \left[ a^2 - (\varepsilon_{y,\theta} - \varepsilon) \right]^{0,5}$	$\frac{b (\varepsilon_{y,\theta} - \varepsilon)}{a \left[ a^2 - (\varepsilon_{y,\theta} - \varepsilon) \right]^{0,5}}$
$\varepsilon_{y,\theta} < \varepsilon < \varepsilon_{t,\theta}$	$f_{y,\theta}$	0
$\varepsilon_{t,\theta} < \varepsilon < \varepsilon_{u,\theta}$	$f_{y,\theta} \left[ 1 - \frac{\varepsilon - \varepsilon_{t,\theta}}{\varepsilon_{u,\theta} - \varepsilon_{t,\theta}} \right]$	-
$\varepsilon = \varepsilon_{u,\theta}$	0,00	-

where

$$a^2 = (\varepsilon_{y,\theta} - \varepsilon_{p,\theta}) \left( \varepsilon_{y,\theta} - \varepsilon_{p,\theta} + \frac{c}{E_{a,\theta}} \right)$$

$$b^2 = c (\varepsilon_{y,\theta} - \varepsilon_{p,\theta}) E_{a,\theta} + c^2$$

$$c = \frac{(f_{y,\theta} - f_{p,\theta})^2}{(\varepsilon_{y,\theta} - \varepsilon_{p,\theta}) E_{a,\theta} - 2 (f_{y,\theta} - f_{p,\theta})}$$

with  $\varepsilon_{y,\theta} = 0,02$ ;  $\varepsilon_{t,\theta} = 0,15$  and  $\varepsilon_{u,\theta} = 0,20$

and

$$\varepsilon_{p,\theta} = \frac{f_{p,\theta}}{E_{a,\theta}}$$

Source: Fig. 3.3 of EN 1992-1-2

being considered. For hot strengths  $k = 0$ , but for residual strengths  $k$  is greater than 0.

Hertz (2004) also gives strength reduction functions  $\xi_{s,02}(\theta_s)$  for the 0,2% proof strength,  
For  $0^\circ\text{C} \leq \theta_s \leq 600^\circ\text{C}$

$$\xi_{s,02}(\theta_s) = 1 + \frac{\theta_s}{767 \ln \left( \frac{\theta_s}{1750} \right)} \tag{5.87}$$

For  $600^\circ\text{C} \leq \theta_s \leq 1000^\circ\text{C}$

$$\xi_{s,02}(\theta_s) = 0,108 \frac{1000 - \theta}{\theta - 440} \tag{5.88}$$

**Table 5.6** Structural carbon steel strength data

Steel temperature ( $\theta_a$ ) (°C)	Reduction factors		
	Yield strength ( $k_{y,\theta}$ )	Proportional limit ( $k_{p,\theta}$ )	Elastic modulus ( $k_{E,\theta}$ )
20	1,000	1,000	1,000
100	1,000	1,000	1,000
200	1,000	0,807	0,900
300	1,000	0,613	0,800
400	1,000	0,420	0,700
500	0,780	0,360	0,600
600	0,470	0,180	0,310
700	0,230	0,075	0,130
800	0,110	0,050	0,090
900	0,060	0,0375	0,0675
1000	0,040	0,0250	0,0450
1100	0,020	0,0125	0,0250
1200	0,000	0,000	0,000

Source: Table 3.1 of EN 1993-1-2

### 5.3.2 Concrete

There is still much debate as to the most reliable approach to formulating the stress–strain section of the constitutive model. The original research in this field was carried out by Anderberg and Thelandersson (1976), but the basis of their analysis has been questioned by Schneider (1982, 1986b, 1988). An alternative approach based on Anderberg and Thelandersson for calculating the transient strain was proposed by Diederichs (1987). A further model using the concept of plastic hardening for determining the elastic response was developed by Khennane and Baker (1993). It is the author’s firm view that the transient strain component, however calculated, cannot be ignored or neglected. This is clearly demonstrated by Mustapha (1994) and Purkiss and Mustapha (1996) with the analysis of reinforced concrete columns heated on three sides with the load applied axially and eccentrically. The results from the computer analysis, together with the experimental data from Haksever and Anderberg (1981/2) are presented in Fig. 5.32. The annotation of the material’s models is M1 (slightly modified Anderberg and Thelandersson with variable slope to the descending branch of the stress–strain curve), M2 (Schneider) and M3 (no transient strain). Where the compression zone of the concrete is relatively cool (column C2), all three models predict very similar trends

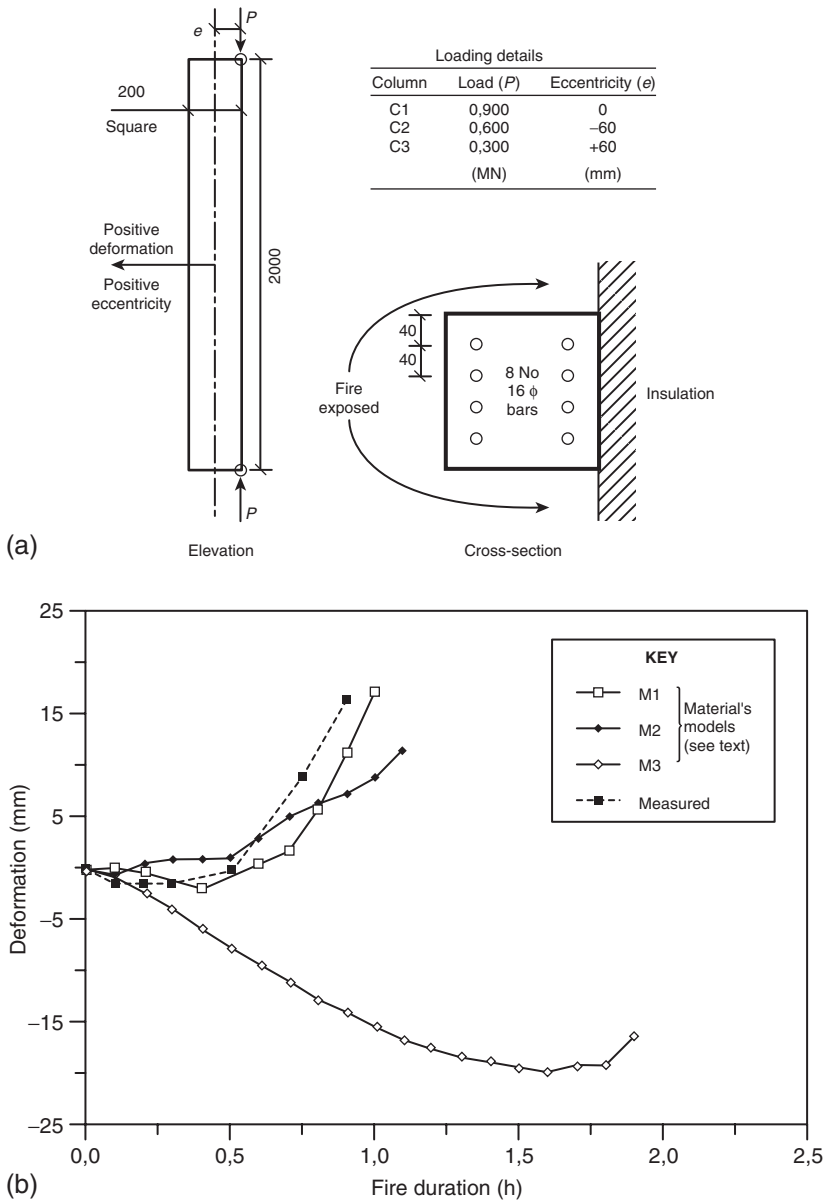


**Figure 5.32** Comparison between experimental and calculated behaviour of columns in a fire for varying materials models (Mustapha and Purkiss): (a) general details; (b) column C1; (c) column C2 and (d) column C3.

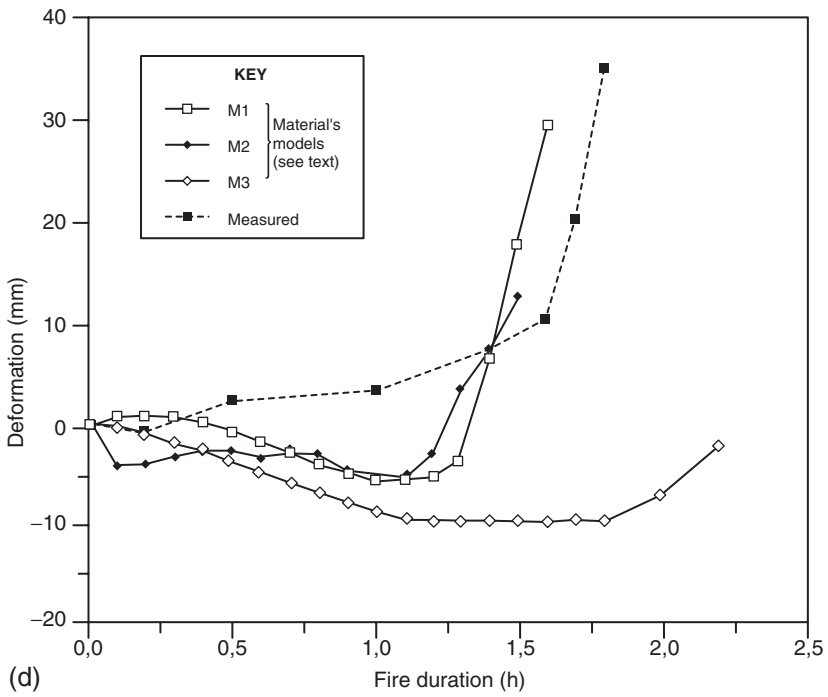
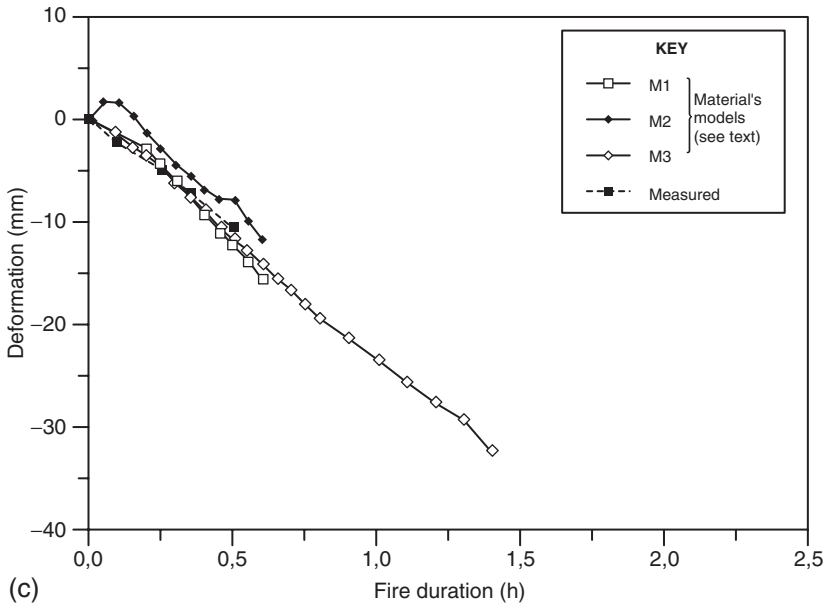


Figure 5.32 Continued.

except that the fire endurance period if no transient strain is included is overestimated by a factor of around 2–2.5. For columns C1 and C3, where the compression zone of the column is under the full heating effects of the furnace, the effect of ignoring transient strain is unacceptable. In column C1 the predicted horizontal deflection is of the wrong sign and overpredicts the fire endurance by a factor of 2. For column C3, the three models predict similar trends in horizontal deflection up to around an hour and a quarter before the predictions with transient strain follow the test results, whilst the prediction with no transient strain continues to produce deflections of the same sign until very close to failure. It should be observed that the quantitative correlation between experimental results and prediction is the least good for column C3. This is almost certainly due to the situation that the moment due to the thermal gradient and the eccentric load are of opposite sign. At the start of the test or simulation, the moment due to the eccentric load will control behaviour before being overtaken later in the test by the opposite sense thermal gradient. In the simulation this could produce temporary instability.

Rather than discuss the formulation of the individual terms of each constitutive model, it is more convenient to consider the individual models as entities.

### 5.3.2.1 *Anderberg and Thelandersson*

Anderberg and Thelandersson proposed that the stress-related component of the total strain  $\varepsilon_{tot,c} - \varepsilon_{th,c}$  can be decomposed into three components:

$$\varepsilon_{tot,c} - \varepsilon_{th,c} = \varepsilon_{\sigma,c} + \varepsilon_{cr,c} + \varepsilon_{tr,c} \quad (5.89)$$

where  $\varepsilon_{tot,c}$  is total concrete strain,  $\varepsilon_{th,c}$  is the free thermal strain,  $\varepsilon_{\sigma,c}$  is the instantaneous stress-related strain,  $\varepsilon_{cr,c}$  is the classical creep strain and  $\varepsilon_{tr,c}$  is the transient strain.

The instantaneous stress-related strain was calculated assuming a parabolic stress–strain profile for strains beyond the peak and then a linear descending portion with a fixed (i.e. temperature independent), slope  $E_c^*$ . Thus the complete stress–strain relationship (Fig. 5.33) is given by:

For  $0 \leq \varepsilon_{\sigma,c} \leq \varepsilon_{1,c}$

$$\frac{\sigma_c}{\sigma_{0,c}} = \frac{\varepsilon_{\sigma,c}}{\varepsilon_{0,c}} \left( 2 - \frac{\varepsilon_{\sigma,c}}{\varepsilon_{0,c}} \right) \quad (5.90)$$

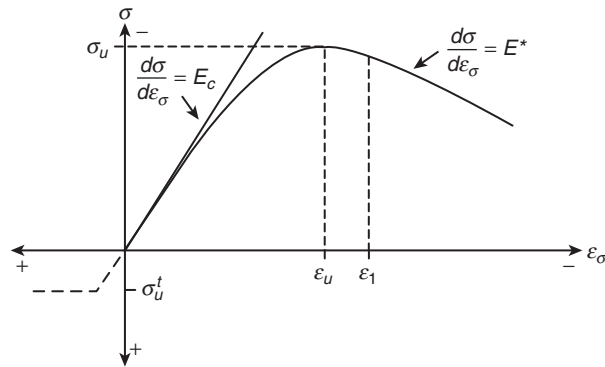


**Figure 5.33** Stress–strain curves for concrete with a constant descending (unloading) branch (Anderberg and Thelandersson, 1976, by permission).

For  $\varepsilon_{\sigma,c} \geq \varepsilon_{1,c}$

$$\sigma_c = \varepsilon_{\sigma,c} E_c^* + \sigma_{0,c} \left(1 - \frac{E_c^*}{E_c}\right)^2 \quad (5.91)$$

where

$$\frac{\varepsilon_{1,c}}{\varepsilon_{0,c}} = 1 - \frac{E_c^*}{E_c} \quad (5.92)$$

The assumption of a temperature-independent slope for the descending branch is questionable when the experimental data on stress–strain behaviour are examined.

The equation to analyze the creep data was obtained by curve fitting the creep results rather than working from basic fundamental principles. The equation finally obtained is given by:

$$\varepsilon_{cr,c} = 0,00053 \frac{\sigma_c}{\sigma_{0,c,\theta}} \left(\frac{t}{180}\right)^{0,5} e^{0,00304(\theta_c - 20)} \quad (5.93)$$

where  $\sigma_c$  is the applied stress,  $\sigma_{0,c,\theta}$  is the strength at temperature  $\theta_c$  (°C) and  $t$  is the time in minutes.

To calculate the total creep strains occurring during a transient test, the accumulated creep strains were calculated using fictitious times and

stresses at the previous time step. The transient strains can be calculated once the instantaneous stress-related strains and the accumulated creep strains are known.

It remained to attempt to relate the resultant transient strains to some known parameter and it was discovered that at temperatures below 550°C for the siliceous aggregate concrete used in the experimental investigation, the transient strain could be related to the free thermal strain, thus giving the following relationship:

$$\varepsilon_{tr,c} = -k_2 \frac{\sigma_c}{\sigma_{0,c,20}} \varepsilon_{th,c} \quad (5.94)$$

where  $\sigma_c/\sigma_{0,c,20}$  is the ratio of the concrete stress to the ambient strength and  $k_2$ , an experimentally determined parameter. Note the minus sign is needed since the transient strain and thermal strain are of opposite sign. Anderberg and Thelandersson report a value of 2,35 for  $k_2$ , whereas other analyses reported in the same publication on different data give values of 1,8 and 2,0. It should be noted that Purkiss and Bali (1988) report that for their tests there appeared to be no significant correlation between the transient and thermal strains.

Above 550°C the picture is less clear, but it appears that from Anderberg and Thelandersson that the temperature-dependant rate of transient strain is constant

$$\frac{\partial \varepsilon_{tr,c}}{\partial \theta} = 0,0001 \frac{\sigma_c}{\sigma_{0,c,20}} \quad (5.95)$$

### 5.3.2.2 *Diederichs*

Diederichs adopts a similar analysis, except that the classical creep strain is ignored and the instantaneous elastic strain calculated using the ambient modulus of elasticity. Thus the transient strain  $\varepsilon_{tr,c}$  is given by:

$$\varepsilon_{tr,c} = \frac{\varepsilon_{c,\theta} - \frac{\sigma_c}{E_{c,20}} - \varepsilon_{th,c}}{\frac{\sigma_c}{\sigma_{0,20,c}}} \quad (5.96)$$

The Diederichs model calculates the transient strain by a simple expression, but the model gave no guide to the determination of the values of transient strain. Subsequently Li and Purkiss (2005) curve fitted

Diederich's data to give

$$\varepsilon_{tot,c} - \varepsilon_{th,c} = \varepsilon_{\sigma,c} + \varepsilon_{tr,c} + \varepsilon_{cr,c} = \frac{\sigma_c}{E_{c,20}} \left[ 1 - \frac{E_{c,20}}{\sigma_{0,20}} f(\theta_c) \right] \quad (5.97)$$

where  $f(\theta_c)$  is given by

$$f(\theta_c) = 0,0412 (\theta_c - 20) - 0,172 \times 10^{-4} (\theta_c - 20)^2 + 0,33 \times 10^{-6} (\theta_c - 20)^3 \quad (5.98)$$

### 5.3.2.3 *Khoury and Terro*

In his experimental results, Khoury, Grainger and Sullivan (1985b) defined the elastic strain as  $\sigma_c/E_{0,20}$ , thus the transient strain, called by Khoury load-induced thermal strain (LITS) (which includes any classical creep strain) is given by

$$LITS(\theta_c, \sigma) = \varepsilon_{tot,c} - \varepsilon_{th,c} - \frac{\sigma_c}{E_{0,20}} \quad (5.99)$$

Initially Terro (1998) fitted the master curve at a stress level of  $0,3\sigma_{0,20}$  to give:

$$\begin{aligned} LITS(\theta_c, 0,3\sigma_{0,20}) = & 43,87 \times 10^{-6} - 2,73 \times 10^{-6} \theta_c - 6,35 \times 10^{-8} \theta_c^2 \\ & + 2,19 \times 10^{-10} \theta_c^3 - 2,77 \times 10^{-13} \theta_c^4 \end{aligned} \quad (5.100)$$

For other stress levels, the transient strain is given by

$$LITS(\theta_c, \sigma_c) = LITS(\theta_c, 0,3\sigma_{0,20}) \left( 0,032 + 3,226 \frac{\sigma_c}{\sigma_{0,20}} \right) \quad (5.101)$$

For siliceous aggregate, Eq. (5.100) needs to be modified

$$\begin{aligned} LITS(\theta_c, 0,3\sigma_{0,20}) = & 1,48 \times 10^{-6} \left( 1098,5 - 39,21\theta_c + 0,43\theta_c^2 \right) \\ & - 1,48 \times 10^{-9} \left( 2,44\theta_c^3 - 6,27 \times 10^{-3} \theta_c^4 + 5,95 \times 10^{-6} \theta_c^5 \right) \end{aligned} \quad (5.102)$$

Additionally the values of LITS may be corrected for volume fractions of aggregate  $V_a$  other than the original 65% by using the following equation:

$$LITS(\theta_c, \sigma_c)|_{V_a} = LITS(\theta_c, \sigma_c)|_{65\%} \frac{V_a}{0,65} \quad (5.103)$$

It should be noted that the model only holds up to temperatures of 590°C.

**5.3.2.4 Khennane and Baker**

Khennane and Baker (1993) take as a starting point the model developed by Anderberg and Thelandersson. However, they determine the instantaneous stress-related strain using a stress–strain curve which is initially linear to a yield value which may be taken as 0,45 times the peak concrete strength and then the remainder of the characteristic is taken as a part of a quarter ellipse (Fig. 5.34) with the following equation

$$\frac{(\sigma_{c,\theta} - \sigma_{1,c,\theta})^2}{(\sigma_{0,c,\theta} - \sigma_{1,c,\theta})^2} + \frac{(\Delta p - \varepsilon_{p,c,\theta})^2}{(\Delta p)^2} = 1 \quad (5.104)$$

The final stress–strain law is in the form of an incremental rule

$$\Delta \varepsilon_{tot,c} = A \Delta \sigma_c - B \sigma_c + \Delta \varepsilon_{tr,c} + \Delta \varepsilon_{th,c} \quad (5.105)$$

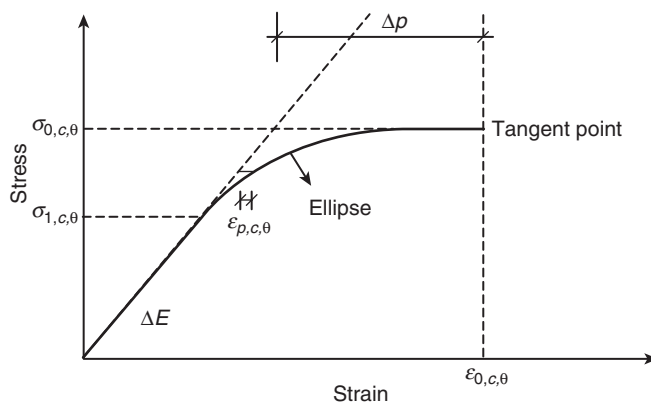


**Figure 5.34** Linear elastic-elliptical plastic idealization of the stress–strain curve for concrete (after Khennane and Baker, 1993).

where  $\Delta\varepsilon_{tot,c}$  is the increment in total strain,  $\sigma_c$  is the stress,  $\Delta\sigma_c$  is the increment in stress over the time step,  $\Delta\varepsilon_{th,c}$  is the increment of thermal strain,  $\Delta\varepsilon_{tr,c}$  is the increment in transient strain defined in the same manner as Anderberg and Thelandersson and  $A$  and  $B$  are parameters defined by the following equations

$$A = \frac{E_t}{(E_t + \beta\Delta E_t)^2} + \frac{H_t}{(H_t + \beta\Delta H_t)^2} + \beta \frac{k_2}{\sigma_{0,c,20}} \frac{\partial \varepsilon_{th,c}}{\partial \theta} \Delta\theta \quad (5.106)$$

and

$$B = \frac{\Delta E_t}{(E_t + \beta\Delta E_t)^2} + \frac{\Delta H_t}{(H_t + \beta\Delta H_t)^2} \quad (5.107)$$

where  $\theta$  is the temperature,  $E_t$  is the slope of the linear portion of the stress–strain curve, i.e. the initial tangent modulus,  $\Delta E_t$  is the change in tangent modulus at time  $t$  to  $t + \Delta t$ , and  $H_t$  and  $\Delta H_t$  are the values of the strain hardening parameter and the change in the strain-hardening parameter,  $\beta$  is an interpolation parameter taking a value between zero and unity and  $\Delta\theta$  is the temperature rise. Khennane and Baker found that the best value for  $\beta$  was 0,5.

The equivalent plastic strain  $\varepsilon_{p,c,\theta}$  (determined from Eq. (5.105)) and the strain-hardening parameter  $H$  are both dependant upon the current stress state. The latter parameter is given by

$$H = \frac{(\sigma_{0,c,\theta} - \sigma_{1,c,\theta})^2}{(\Delta p)^2} \frac{\Delta p - \varepsilon_{p,c,\theta}}{\sigma_{c,\theta} - \sigma_{1,c,\theta}} \quad (5.108)$$

This model does not appear to allow for the instantaneous strain in the concrete to exceed the peak value and the formulation for transient strain valid for temperatures above 550°C also appears not to be considered. This latter point may be critical since Khennane and Baker appear to produce excellent correlation between experimental results and prediction below temperatures of 550°C but far poorer correlation at temperatures above this value. Further, the value of  $\Delta H_t$  needs to be estimated as it depends on the stress at the end of the incremental time step. The authors also indicate that an elaborate algorithm is needed to allow for the situation when both the temperature and the stress vary during an incremental step. It should be noted that this is likely case in a full structural analysis of fire affected concrete members.

### 5.3.2.5 *Schneider*

The model used by Schneider is based on a unit stress compliance function, i.e. the creep is considered to be linear with respect to stress. The general background to this approach is detailed in Bažant (1988) and the specific formulation for high temperatures is given in Bažant (1983). An important simplification to the general compliance function approach that can be made for creep in a fire is that the duration of between a half and four hours is short compared with the age of the concrete and thus any time dependence in the model can be ignored. The full background to Schneider's model is given in Schneider (1986b, 1988), and only the results will be presented.

The unit stress compliance function  $J(\theta, \sigma)$  can be written as

$$J(\theta_c, \sigma_c) = \frac{1 + \kappa}{E_{c,\theta}} + \frac{\Phi}{E_{c,\theta}} \quad (5.109)$$

where  $E_{c,\theta}$  is the temperature-dependant modulus of elasticity and  $\kappa$  is a parameter allowing for non-linear stress-strain behaviour for stresses above about half the concrete strength and is given by Eq. (5.110) which is derived from Popovics (1973) (Eq. (5.37)),

$$\kappa = \frac{1}{n - 1} \left( \frac{\varepsilon_{\sigma,c,\theta}}{\varepsilon_{0,c,\theta}} \right)^n \quad (5.110)$$

with  $n$  taking a value of 2,5 for lightweight concrete and 3,0 for normal-weight concrete. An alternative formulation for  $\kappa$  is given by

$$\kappa = \frac{1}{n - 1} \left( \frac{\sigma(\theta_c)}{\sigma_{0,\theta}} \right)^5 \quad (5.111)$$

The value of  $E_{c,\theta}$  is given by

$$E_{c,\theta} = gE_{c,0} \quad (5.112)$$

where the parameter  $g$  is given by the following equation

$$g = 1 + \frac{f_{c,\theta}}{\sigma_{0,c,20}} \frac{\theta_c - 20}{100} \quad (5.113)$$

where  $\theta_c$  is the concrete temperature ( $^{\circ}\text{C}$ ),  $f_{c,\theta}/\sigma_{0,c,20}$  is the ratio of the initial stress under which the concrete is heated to the ambient strength and the creep function  $\Phi$  is given by

$$\Phi = g\phi + \frac{f_{c,\theta}}{\sigma_{0,c,20}} \frac{\theta_c - 20}{100} \tag{5.114}$$

with  $\phi$  being given by

$$\phi = C_1 \tanh \gamma_w (\theta_c - 20) + C_2 \tanh \gamma_0 (\theta_c - \theta_g) + C_3 \tag{5.115}$$

with  $\gamma_w$  defined by

$$\gamma_w = 0,001 (0,3w + 2,2) \tag{5.116}$$

where  $w$  is the moisture content in per cent by weight.

It should be reiterated that the stress used in the definition of  $g$  and  $\Phi$  is that *initially* applied at the start of the heating period.

The values of  $C_1$ ,  $C_2$ ,  $C_3$ ,  $\theta_g$  and  $\gamma_0$  proposed by Schneider are given in Table 5.7. There is however some evidence that these parameters are likely to be functions of the concrete mix proportions since Purkiss and Bali (1988) report values of 2,1 and 0,7 for  $C_2$  and  $C_3$ . A further unpublished analysis by the author of Bali's original data (Bali, 1984) gives slightly different values of 1,5 and 0,95, respectively. An analysis by the author of Anderberg and Thelandersson's data gives values for  $C_2$  and  $C_3$  of 3,27 and 1,78, respectively, for the tests with a heating rate of  $1^{\circ}\text{C}/\text{min}$ .

It should be noted that the formulation by Anderberg and Thelandersson, whilst not justifiable on theoretical grounds has been successfully used as a model in computer simulations as has the Schneider model.

**Table 5.7** Concrete stress-strain model parameters

Concrete type	Parameter				
	$C_1$	$C_2$	$C_3$	$\gamma_0$ ( $^{\circ}\text{C}$ )	$\theta_g$ ( $^{\circ}\text{C}$ )
Quartzite	2,60	1,40	1,40	0,0075	700
Limestone	2,60	2,40	2,40	0,0075	650
Lightweight	2,60	3,00	3,00	0,0075	600

Source: Schneider (1985) by permission

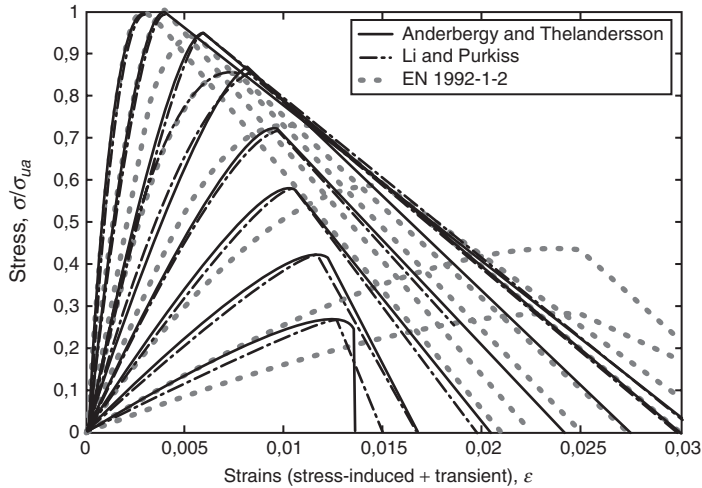


**Figure 5.35** Comparisons of full stress–strain curves at temperatures 40, 100, 200, 300, 400, 500, 600 and 700°C.

#### 5.3.2.6 Li and Purkiss

Li and Purkiss (2005) have demonstrated that it is possible to determine a numerical apparent stress–strain curve which explicitly includes the transient strain. These curves are given in Fig. 5.35 with a comparison between Anderberg and Thelandersson and EN 1992-1-2 where it will be observed that there is a close correlation with Anderberg and Thelandersson and EN 1992-1-2 at low temperatures but an increasing divergence from EN 1992-1-2.

*En passant* Li and Purkiss noted that Khoury and Diederichs predict lower (but similar) transient strains than Schneider or Anderberg and Thelandersson.

### 5.3.3 Design code provisions for stress–strain behaviour

Full stress–strain temperature relationships are only needed when a full elastoplastic analysis is needed to determine the fire performance of a concrete structure. Where an ‘end point’ calculation is sufficient, a stress–strain curve that allows for some creep may be used. EN 1992-1-2 and EN 1994-1-2 give such a set of curves providing data for a stress–strain relationship which may be used for the analysis of concrete sections. The analytical form of the curve is the same as that proposed by Popovics (Eq. (5.37)) with  $n = 3$  for normal-weight concrete. The parametric variation of data with respect to temperature is given in Table 5.8.

**Table 5.8** Variation of concrete strength parameters with temperature

Temperature $\theta_c$ (°C)	Strength reduction factor [ $k_c(\theta_c)$ ]			$\varepsilon_{c1,\theta}$	$\varepsilon_{cu1,\theta}$
	Siliceous	Calcareous	Lightweight		
20	1,000	1,000	1,000	0,0025	0,0200
100	1,000	1,000	1,000	0,0040	0,0225
200	0,950	0,970	1,000	0,0055	0,0250
300	0,850	0,910	1,000	0,0070	0,0275
400	0,750	0,850	0,880	0,0100	0,0300
500	0,600	0,740	0,760	0,0150	0,0325
600	0,450	0,600	0,640	0,0250	0,0350
700	0,300	0,430	0,520	0,0250	0,0375
800	0,150	0,270	0,400	0,025	0,0400
900	0,080	0,150	0,280	0,0250	0,0425
1000	0,040	0,060	0,160	0,0250	0,0450
1100	0,010	0,020	0,04	0,0250	0,0475
1200	0,000	0,000	0,000	-	-

The values of  $\varepsilon_{c1,\theta}$  and  $\varepsilon_{cu1,\theta}$  only apply to normal-weight concrete.  
 Source: Table 3.1 (EN 1992-1-2) and Table 3.3 of EN 1994-1-2

However, it should be noted that the strain values at the peak are far higher than those for simple stress–strain curves. It is thought that these higher values allow for transient strain. Li and Purkiss (2005) note that after 400°C, these peak strains are up to around twice the values allowing for transient strains. Anderberg (2005) also notes the values of peak strain if used in a structural analysis where axial loads exist may give erroneous results. Although EN 199-1-2 provides the strength data in a tabular form, Hertz (2005) provides equations for both the hot condition when the concrete is at its weakest and the cold condition when the reinforcement is at its weakest. The equation used is Eq. (5.85) but with suitable ‘concrete’ parameters (and with  $k = 0$ ).

This chapter is only intended to provide an overview of the thermal and mechanical behaviour of the main structural materials, before the succeeding chapters and the calculation on the performance of structural elements and structures could be undertaken.

# 6 Calculation approach\*

---

The analysis of structural fire resistance is a complicated process because it involves many variables such as fire growth and duration, temperature distribution in structural members, interaction between structural members, changes in material properties and the influence of loads on the structural system. The process generally includes three distinct components: fire hazards analysis to identify fire scenarios and determine the impact of each scenario on adjacent structural members; thermal analysis to calculate temperature history in each member and structural analysis to determine forces and stresses in each member and whether local or progressive structural collapse would occur during any of the fire hazard scenarios. The primary objective to conduct such analyses is to determine the length of time that the structure will be able to resist collapse during exposure to a fire, or the strength at a pre-determined time, or the time lapse in achieving a certain strength reduction, or the time to achieve a given temperature when the structure or structural member is exposed to gas temperatures generated from either a natural fire or the standard furnace test. The integrity of an element, i.e. its ability to resist the passage of flame through gaps in the structure, is not normally calculated; this is best determined using the standard furnace test since this form of failure is mostly applicable to elements such as fire doors or other closure systems. The limit state of integrity will not therefore be considered further as far as calculations are concerned.

For the fire hazards analysis, it is generally not important whether the fire exposure is determined from that induced in the standard furnace test or from the effects of a natural or compartment fire. It is sufficient that the compartment temperature–time response is known either as a continuous function or as a series of discrete temperature–time values.

Also, as pointed out in Chapter 2, the calculation of the temperature response in a member in a structure can be generally decoupled from

---

\*This chapter is contributed by Long-Yuan Li, School of Engineering and Applied Science, Aston University, Birmingham, UK.

the determination of the structural response provided that the geometry of the structure does not have significant changes during the period that is concerned. For steelwork, the boundaries of steel members are not subject to any possible changes during the fire exposure except that there is a total or partial loss of the insulation and therefore it is acceptable to decouple the calculation of the temperature response from that of the structure response. For concrete, however, the decoupling approach is often not acceptable because spalling of the concrete is likely to occur. Spalling will change the boundaries of concrete members due to the concrete cover being lost, and is then likely to expose reinforcement to the full effects of the fire, producing a rapid rise of the temperature in the reinforcement, and thus a greater loss in strength (Purkiss and Mustapha, 1996). The problems associated with spalling are covered in more details in Chapter 7. Since, currently at least, the mechanism of spalling is not completely understood and its occurrence cannot be quantified, it is not possible to allow for the effects of spalling in the calculation approach. Thus an approach, which decouples the calculations of the temperature response and the structural response, will of necessity have to be used.

## 6.1 THERMAL ANALYSIS

The procedure described for the thermal analysis in this section is mainly for concrete, steel or steel–concrete composite members or structures. A much simplified approach is available for timber which will be discussed in section 6.2. Since the temperature–time curves in fire have been addressed in Chapter 3, this section will be focussed on only the transfer of heat from the fire to the structural member.

### 6.1.1 Governing equation and boundary conditions

The analysis of temperature response in a structural member can be subdivided into two parts. One is the heat transfer across the boundary from the furnace or fire into the surface of the structural member, which is through the combination of convection and radiation and is usually treated as boundary conditions; the other is the heat transfer within the structural member, which is through conduction and is treated as governing equation expressed by the Fourier equation of heat transfer.

Heat conduction is the transfer of thermal energy from one place to another through a solid or fluid due to the temperature difference between the two places. The transfer of thermal energy occurs at the molecular and atomic levels without net mass motion of the material. The rate equation

describing this heat transfer mode is Fourier law, expressed by

$$\mathbf{q} = -\lambda \nabla \theta \quad (6.1)$$

where  $\mathbf{q}$  is the vector of heat flux per unit area,  $\lambda$  is the thermal conductivity tensor and  $\theta$  is the temperature. For an isotropic solid such as steel, concrete or masonry,  $\lambda = \lambda \mathbf{I}$ , where  $\lambda$  is the thermal conductivity that may be a function of the temperature and  $\mathbf{I}$  is the identity matrix. The conservation of energy with Fourier's law requires

$$\rho c \frac{\partial \theta}{\partial t} = -\nabla \cdot \mathbf{q} + Q \quad (6.2)$$

where  $\rho$  is the density,  $c$  is the specific heat,  $t$  is the time and  $Q$  is the internal heat generation rate per unit volume. The specific heat may be temperature dependent. Substituting Eq. (6.1) into Eq. (6.2) yields

$$\rho c \frac{\partial \theta}{\partial t} = \nabla \cdot (\lambda \nabla \theta) + Q \quad (6.3)$$

Equation (6.3) is the heat conduction equation and is solved subject to an initial condition and appropriate boundary conditions. The initial condition consists of specifying the temperature throughout the solid at an initial time. The boundary conditions may take the following several forms.

- (1) The fire exposed surface – The surface of the structural member is exposed to a fire on which the heat transfer involves both convection and radiation, although it is generally accepted that the radiation component is the more dominant after the very early stages of the fire. The net heat flux to the surface of the structural member thus is expressed as

$$\dot{h}_{net} = \dot{h}_{net,c} + \dot{h}_{net,r} \quad (6.4a)$$

in which,

$$\begin{aligned} \dot{h}_{net,c} &= \alpha_c (\theta_g - \theta_m) = \text{net convective heat flux per unit surface} \\ \dot{h}_{net,r} &= \Phi \varepsilon_m \varepsilon_f \sigma [(\theta_g + 273)^4 - (\theta_m + 273)^4] = \text{net radiative heat flux} \\ &\quad \text{per unit surface} \end{aligned}$$

where  $\alpha_c$  is the coefficient of heat transfer by convection,  $\theta_g$  is the gas temperature in the vicinity of the fire exposed surface,  $\theta_m$  is the surface temperature of the structural member,  $\Phi$  is the configuration factor,  $\varepsilon_m$  is the surface emissivity of the structural member,  $\varepsilon_f$  is the emissivity of the fire and  $\sigma = 5,67 \times 10^{-8} \text{ W/m}^2\text{K}^4$  is the Stephan–Boltzmann constant.

- (2) The no heat-flow surface – The surface is a thermal symmetric plane or has a large degree of insulation and thus can be assumed as thermally insulated having no heat flow through it. Therefore, the net heat flux to the surface of the structural member can be simply expressed as

$$\dot{h}_{net} = 0 \quad (6.4b)$$

- (3) The ambient exposed surface – The surface is exposed to ambient conditions and thus can be treated similarly to that exposed to a fire but replacing the fire temperature with the ambient temperature,  $\theta_a$ , that is,

$$\dot{h}_{net} = \alpha_c(\theta_a - \theta_m) + \Phi\varepsilon_m\varepsilon_f\sigma[(\theta_a + 273)^4 - (\theta_m + 273)^4] \quad (6.4c)$$

- (4) The fixed temperature surface – The surface temperature of the structural member is specified to be constant or a function of a boundary coordinate and/or time.

The boundary condition for the surface types (1)–(3) is called *Neumann* boundary condition which specifies the normal derivative of the temperature, that is,

$$\lambda \frac{\partial \theta_m}{\partial n} = \dot{h}_{net} \quad (6.5a)$$

where  $n$  is the normal of the surface. The boundary condition for the surface type (4) is called *Dirichlet* boundary condition which specifies the function of the temperature, that is,

$$\theta_m = \bar{\theta}(t) \quad (6.5b)$$

where  $\bar{\theta}(t)$  is the prescribed temperature at the boundary.

Convection is the transfer of thermal energy through a fluid due to motion of the fluid. The energy transfer from one fluid particle to

another occurs by conduction, but thermal energy is transported by the motion of the fluid. However, the convection heat transfer coefficient is not a property of the fluid. It is an experimentally determined parameter whose value depends on all the variables influencing convection such as the surface geometry, the nature of fluid motion, the properties of the fluid and the bulk fluid velocity. In EN 1991-1-2, it has been suggested that  $\alpha_c = 25 \text{ W/m}^2\text{K}$  for the fire exposed surface when the standard temperature–time curve is used and  $\alpha_c = 9 \text{ W/m}^2\text{K}$  for the ambient exposed surface when assuming it contains the effects of heat transfer by radiation.

Unlike the convection which requires a medium to transfer the heat, the radiation is the transfer of thermal energy between two locations by an electromagnetic wave which requires no medium. The radiation term used here in Eq. (6.4) is the traditional one that has been used in textbooks and also implemented in computer packages (Becker, Bizri and Bresler, 1974; Iding, Bresler and Nizamuddin, 1977a). In literature several different radiation expressions have been suggested. For example, Mooney (1992) proposed a radiation expression based on the concept of the surface radiant energy balance in the fire environment, which uses the representative temperature and representative emissivity, instead of the traditionally used fire temperature and fire emissivity. It should be noted that, however, whichever expression is used experimental data are always required to validate the expression and determine the parameters involved in the expression. To allow for varying radiative heat flux levels while keeping the surface and fire emissivities as constants, a configuration factor is introduced in the radiative heat flux expression. A conservative choice for the configuration factor is  $\Phi = 1$ . A lower  $\Phi$  value may be obtained from the calculation based on the fraction of the total radiative heat leaving a given radiating surface that arrives at a given receiving surface, as given in EN 1991-1-2, to take account of so called position and shadow effects. The theory behind the calculation of the configuration factor is given by Drysdale (1998). Figure 6.1 shows a typical example of the variation of the resultant emissivity in the prediction of temperatures within a steel column when the configuration factor is taken as  $\Phi = 1$ , i.e.  $\varepsilon_{res} = \Phi\varepsilon_m\varepsilon_f = \varepsilon_m\varepsilon_f$  (Chitty *et al.*, 1992). It should be noted that the variation of  $\varepsilon_{res}$  shown in Fig. 6.1 can be interpreted as the variation of configuration factor due to the difference in positions while taking  $\varepsilon_m$  and  $\varepsilon_f$  as constants.

It should be stated here that both the governing, Eq. (6.3) and boundary condition, Eq. (6.5) are non-linear. The former is due to the thermal conductivity and specific heat that are temperature dependent, as shown in Chapter 5, and the latter is due to the radiative boundary condition which involves a non-linear term of the temperature. Thus the closed form solution to governing, Eq. (6.3) with boundary conditions, Eq. (6.5) is not

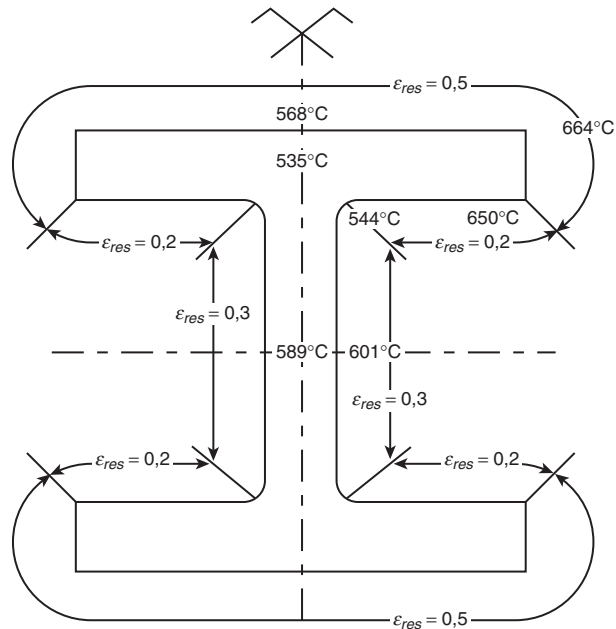


**Figure 6.1** Variation of resultant emissivity in the prediction of temperatures within a steel column. The temperatures given correspond to the temperature field calculated at 46 min (temperatures around profile correspond to the centre of the discretized border elements of 10 mm thickness). (Copy with permission from Chitty *et al.*, 1992).

possible for even the simplest geometry. Numerical methods such as finite element methods are usually required to solve this kind of heat transfer problems.

### 6.1.2 Finite element solution of the heat transfer problem

The finite element method is a numerical analysis technique for obtaining approximate solutions to engineering problems. It offers a way to solve a complex continuum problem by allowing it to be subdivided into a series of simpler interrelated problems and gives a consistent technique for modelling the whole as an assemblage of discrete parts. The 'whole' may be a body of matter or a region of space in which some phenomenon of interest is occurring.

In the heat transfer problem, temperature field is the field variable which is the function of each generic point in the body or solution region.

Consequently, the problem is one with an infinite number of unknowns. Finite element analysis reduces the problem to one of a finite number of unknowns by dividing the solution region into elements and by expressing the temperature field in terms of assumed interpolation functions within each element. The interpolation functions are defined in terms of the values of the temperature field at specified points called nodes. The nodal values of the temperature field and the interpolation functions for the elements completely define the behaviour of the temperature field within the elements. For the finite element representation of the heat transfer problem the nodal values of the temperature field become the unknowns. The matrix equations expressing the properties of the individual elements are determined from the governing equation by using the weighted residual approach. The individual element matrix equations are then combined to form the global matrix equations for the complete system. Once the boundary conditions have been imposed, the global matrix equations can be solved numerically. Once the nodal values of the temperature field are found, the interpolation functions define the temperature field throughout the assemblage of elements.

Assume that the solution domain  $\Omega$  is divided into  $M$  elements and each element has  $n$  nodes. Thus, the temperature within each element can be expressed as follows

$$\theta(x, y, z, t) = \sum_{i=1}^n N_i(x, y, z)\theta_i(t) = \mathbf{N}(x, y, z)\boldsymbol{\theta}_e(t) \quad (6.6)$$

where  $N_i(x, y, z)$  is the interpolation function defined at node  $i$ ,  $\theta_i$  is the value of the temperature at node  $i$ ,  $\mathbf{N}(x, y, z)$  is the interpolation matrix and  $\boldsymbol{\theta}_e(t)$  is the vector of element nodal temperatures. The element matrix equation is obtained from the governing Eq. (6.3) by using the method of weighted residuals in which the weighting function is assumed to be the same as the interpolation function, that is,

$$\int_{\Omega_e} \mathbf{N}^T \left\{ \rho c \mathbf{N} \frac{\partial \boldsymbol{\theta}_e}{\partial t} - [\nabla \cdot (\lambda \nabla \mathbf{N} \boldsymbol{\theta}_e)] - Q \right\} d\Omega = 0 \quad (6.7)$$

where  $\Omega_e$  is the domain of element  $e$ . Using Gauss's theorem, for element domain  $\Omega_e$  of boundary  $\Gamma_e$  the following expression may be derived

$$\int_{\Omega_e} \mathbf{N}^T [\nabla \cdot (\lambda \nabla \mathbf{N})] d\Omega = \int_{\Gamma_e} \mathbf{N}^T [(\lambda \nabla \mathbf{N}) \cdot \hat{\mathbf{n}}] d\Gamma - \int_{\Omega_e} (\nabla \mathbf{N})^T \cdot (\lambda \nabla \mathbf{N}) d\Omega \quad (6.8)$$

where  $\hat{\mathbf{n}}$  is the normal of the element boundary  $\Gamma_e$ . Using Eq. (6.8), Eq. (6.7) can be simplified as follows:

$$\begin{aligned} & \int_{\Omega_e} (\mathbf{N}^T \rho c \mathbf{N}) \frac{\partial \boldsymbol{\theta}_e}{\partial t} d\Omega + \int_{\Omega_e} (\nabla \mathbf{N}^T \lambda \nabla \mathbf{N}) \boldsymbol{\theta}_e d\Omega \\ &= \int_{\Gamma_e} \mathbf{N}^T (\lambda \nabla \mathbf{N} \boldsymbol{\theta}_e \cdot \hat{\mathbf{n}}) d\Gamma + \int_{\Omega_e} \mathbf{N}^T Q d\Omega \end{aligned} \quad (6.9)$$

After some manipulation the resulting element matrix equation becomes

$$\mathbf{C}_e \frac{\partial \boldsymbol{\theta}_e}{\partial t} + \mathbf{K}_{ce} \boldsymbol{\theta}_e = \mathbf{R}_{qe} + \mathbf{R}_{Qe} \quad (6.10)$$

in which,

$$\mathbf{C}_e = \int_{\Omega_e} \mathbf{N}^T \rho c \mathbf{N} d\Omega = \text{element capacitance matrix}$$

$$\mathbf{K}_{ce} = \int_{\Omega_e} \nabla \mathbf{N}^T \lambda \nabla \mathbf{N} d\Omega = \text{element conductance matrix}$$

$$\begin{aligned} \mathbf{R}_{qe} &= \int_{\Gamma_e} \mathbf{N}^T [(\lambda \nabla \mathbf{N} \boldsymbol{\theta}_e) \cdot \hat{\mathbf{n}}] d\Gamma \\ &= - \int_{\Gamma_e} \mathbf{N}^T (\mathbf{q} \cdot \hat{\mathbf{n}}) d\Gamma = \text{element nodal vector of heat flow} \end{aligned}$$

$$\mathbf{R}_{Qe} = \int_{\Omega_e} (\mathbf{N}^T Q) d\Omega = \text{element nodal vector of internal heat source}$$

Equation (6.10) is the general formulation of element matrix equation for transient heat conduction in an isotropic medium. Note that the element nodal temperatures cannot be solved from the element matrix Eq. (6.10). This is because the nodal vector of heat flow in the right-hand side of Eq. (6.10) is also an unknown. However, this unknown will be eliminated during the assembly of the element matrix equations or can be identified when applying boundary conditions. Therefore, the integration in calculating  $\mathbf{R}_{qe}$  can apply only to the boundaries with

the prescribed heat flux. The global finite element matrix equation is obtained by the assembly of element matrix equations, which can be expressed as

$$\mathbf{C} \frac{\partial \boldsymbol{\theta}(t)}{\partial t} + \mathbf{K}_c \boldsymbol{\theta}(t) = \mathbf{R}_q + \mathbf{R}_Q \quad (6.11)$$

in which,

$$\mathbf{C} = \sum_{e=1}^M \mathbf{C}_e = \text{global capacitance matrix}$$

$$\mathbf{K}_c = \sum_{e=1}^M \mathbf{K}_{ce} = \text{global conductance matrix}$$

$$\mathbf{R}_q = \sum_{e=1}^M \mathbf{R}_{qe} = \text{global nodal vector of heat flow}$$

$$\mathbf{R}_Q = \sum_{e=1}^M \mathbf{R}_{Qe} = \text{global nodal vector of internal heat source}$$

where the summation implies correct addition of the matrix elements in the global coordinates and degrees of freedom. Note that,  $\mathbf{R}_q$  is other than zero only when it is in the position corresponding to the node that is on a boundary. For a boundary that has prescribed temperatures,  $\mathbf{R}_q$  is unknown but  $\boldsymbol{\theta}$  is known; whereas for a boundary that has prescribed heat fluxes  $\boldsymbol{\theta}$  is unknown but  $\mathbf{R}_q$  is known. Thus, the total number of unknowns in the global finite element equation is always equal to the total number of nodes. It should be noted that, for the prescribed heat flux boundary condition the expression of  $\mathbf{R}_{qe}$  may involve the unknown surface temperatures which need to be decomposed out from  $\mathbf{R}_{qe}$ . According to the definition of  $\mathbf{R}_{qe}$  in Eq. (6.10) and noticing that,  $-(\mathbf{q} \cdot \hat{\mathbf{n}}) = \dot{h}_{net} = \dot{h}_{net,c} + \dot{h}_{net,r}$ ,  $\mathbf{R}_{qe}$  may be rearranged into

$$\mathbf{R}_{qe} = - \int_{\Gamma_e} \mathbf{N}^T (\mathbf{q} \cdot \hat{\mathbf{n}}) d\Gamma = \int_{\Gamma_e} \mathbf{N}^T \dot{h}_{net} d\Gamma = \int_{\Gamma_e} \mathbf{N}^T \alpha_{eff} (\theta_g - \theta_m) d\Gamma \quad (6.12)$$

in which,

$$\begin{aligned}\alpha_{eff} &= \frac{\dot{h}_{net}}{\theta_g - \theta_m} \\ &= \alpha_c + \Phi \varepsilon_m \varepsilon_f \sigma [(\theta_g + 273)^2 + (\theta_m + 273)^2] [(\theta_g + 273) + (\theta_m + 273)]\end{aligned}$$

where  $\alpha_{eff}$  is the combined convection and radiation coefficient which is temperature dependent. Let,

$$\mathbf{R}_{qe} = \mathbf{R}_{q\theta e} - \mathbf{K}_{q\theta e} \boldsymbol{\theta}_e \quad (6.13)$$

in which,

$$\begin{aligned}\mathbf{R}_{q\theta e} &= \int_{\Gamma_e} \mathbf{N}^T \alpha_{eff} \theta_g d\Gamma \\ \mathbf{K}_{q\theta e} \boldsymbol{\theta}_e &= \int_{\Gamma_e} \mathbf{N}^T \alpha_{eff} \theta_m d\Gamma = \int_{\Gamma_e} \mathbf{N}^T \alpha_{eff} \mathbf{N} \boldsymbol{\theta}_e d\Gamma\end{aligned}$$

Similarly, the global nodal vector of heat flow can be rewritten into

$$\mathbf{R}_q = \mathbf{R}_{q\theta} - \mathbf{K}_{q\theta} \boldsymbol{\theta} \quad (6.14)$$

in which,

$$\begin{aligned}\mathbf{R}_{q\theta} &= \sum_{e=1}^M \mathbf{R}_{q\theta e} \\ \mathbf{K}_{q\theta} &= \sum_{e=1}^M \mathbf{K}_{q\theta e}\end{aligned}$$

Thus, Eq. (6.11) becomes

$$\mathbf{C} \frac{\partial \boldsymbol{\theta}(t)}{\partial t} + (\mathbf{K}_c + \mathbf{K}_{q\theta}) \boldsymbol{\theta}(t) = \mathbf{R}_{q\theta} + \mathbf{R}_Q \quad (6.15)$$

Equation (6.15) is the finite element formulation of non-linear transient heat transfer problems, in which  $\mathbf{C}$ ,  $\mathbf{K}_c$ ,  $\mathbf{K}_{q\theta}$  and  $\mathbf{R}_{q\theta}$  are all

temperature dependent. The temperature dependence of  $\mathbf{C}$  is due to the specific heat that is the function of temperature; the temperature dependence of  $\mathbf{K}_c$  is due to the conductivity that is the function of temperature; while temperature dependence of  $\mathbf{K}_{q\theta}$  and  $\mathbf{R}_{q\theta}$  is due to the boundary conditions involving radiation. To solve Eq. (6.15), time integration techniques must be employed.

Integration techniques for transient non-linear solutions are typically a combination of the methods for linear transient solutions and steady-state non-linear solutions (Huebner, Thornton and Byrom, 1995; Zienkiewicz and Taylor, 2000). The transient solution of the non-linear ordinary differential equations is computed by a numerical integration method with iterations at each time step to correct for non-linearities. Explicit or implicit one-parameter  $\beta$  schemes are often used as the time integration method, and Newton–Raphson or modified Newton–Raphson methods are used for the iteration. Let  $t_k$  denote a typical time in the response so that  $t_{k+1} = t_k + \Delta t$ , where  $k = 0, 1, 2, \dots, N$ . A general family of algorithms results by introducing a parameter  $\beta$  such that  $t_\beta = t_k + \beta \Delta t$  where  $0 \leq \beta \leq 1$ . Equation (6.15) at time  $t_\beta$  can be written as

$$\mathbf{C}(\boldsymbol{\theta}_\beta) \frac{\partial \boldsymbol{\theta}_\beta}{\partial t} + \mathbf{K}(\boldsymbol{\theta}_\beta, t_\beta) \boldsymbol{\theta}_\beta = \mathbf{R}(\boldsymbol{\theta}_\beta, t_\beta) \quad (6.16)$$

where  $\mathbf{K} = \mathbf{K}_c + \mathbf{K}_{q\theta}$ ,  $\mathbf{R} = \mathbf{R}_{q\theta} + \mathbf{R}_Q$  are defined at temperature  $\boldsymbol{\theta}_\beta$  and time  $t_\beta$ , and the subscript  $\beta$  indicates the temperature vector  $\boldsymbol{\theta}_\beta$  at time  $t_\beta$ . By using the following approximations

$$\begin{aligned} \boldsymbol{\theta}_\beta &= (1 - \beta) \boldsymbol{\theta}_k + \beta \boldsymbol{\theta}_{k+1} \\ \frac{\partial \boldsymbol{\theta}_\beta}{\partial t} &= \frac{\boldsymbol{\theta}_{k+1} - \boldsymbol{\theta}_k}{\Delta t} \\ \mathbf{R}(\boldsymbol{\theta}_\beta, t_\beta) &= (1 - \beta) \mathbf{R}(\boldsymbol{\theta}_k, t_k) + \beta \mathbf{R}(\boldsymbol{\theta}_{k+1}, t_{k+1}) \end{aligned} \quad (6.17)$$

Equation (6.16) can be rewritten into

$$\begin{aligned} &\left( \beta \mathbf{K}(\boldsymbol{\theta}_\beta, t_\beta) + \frac{1}{\Delta t} \mathbf{C}(\boldsymbol{\theta}_\beta) \right) \boldsymbol{\theta}_{k+1} \\ &= \left( (\beta - 1) \mathbf{K}(\boldsymbol{\theta}_\beta, t_\beta) + \frac{1}{\Delta t} \mathbf{C}(\boldsymbol{\theta}_\beta) \right) \boldsymbol{\theta}_k + (1 - \beta) \mathbf{R}(\boldsymbol{\theta}_k, t_k) + \beta \mathbf{R}(\boldsymbol{\theta}_{k+1}, t_{k+1}) \end{aligned} \quad (6.18)$$

where  $\boldsymbol{\theta}_{k+1}$  and  $\boldsymbol{\theta}_\beta$  are unknowns and  $\boldsymbol{\theta}_k$  is known from the previous time step.

Equation (6.18) represents a general family of recurrence relations; a particular algorithm depends on the value of  $\beta$  selected. If  $\beta = 0$ , the algorithm is the forward difference method in which if the capacitance matrices are further lumped, it becomes explicit and reduces to a set of uncoupled algebraic equations; if  $\beta = 1/2$ , the algorithm is the Crank–Nicolson method; if  $\beta = 2/3$ , the algorithm is the Galerkin method; and if  $\beta = 1$ , the algorithm is the backward difference method.

For a given  $\beta$ , Eq. (6.18) is a recurrence relation for calculating the vector of nodal temperatures  $\theta_{k+1}$  at the end of time step from known values of  $\theta_k$  at the beginning of the time step. For  $\beta > 0$ , the algorithm is implicit and requires solution of a set of coupled algebraic equations using iterations because the coefficient matrices  $\mathbf{K}$ ,  $\mathbf{C}$  and nodal heat vector  $\mathbf{R}$  are functions of  $\theta$ . The Newton–Raphson iteration method is often used to solve the non-linear equations at each time step.

Hughes (1977) shows the algorithm to be unconditionally stable for  $\beta \geq 1/2$  as in the corresponding linear algorithm. For  $\beta < 1/2$  the algorithm is only conditionally stable, and the time step must be chosen smaller than a critical time step given by

$$\Delta t_{cr} = \frac{2}{1 - 2\beta} \frac{1}{\lambda_m} \quad (6.19)$$

where  $\lambda_m$  is the largest eigenvalue of the current eigenvalue problem. The explicit and implicit algorithms have the same trade-offs as occur for linear transient solutions. The explicit algorithm requires less computational effort, but it is conditionally stable; the implicit algorithm is computationally expensive, but it is unconditionally stable. The non-linear implicit algorithm requires even greater computational effort than in linear implicit solutions because of the need for iterations at each time step. Thus the selection of a transient solution algorithm for a non-linear thermal problem is even more difficult than in linear solutions.

There are a number of finite element computer codes that can be used to solve the non-linear heat transfer equation with the fire boundary condition. Three of the most commonly used are FIRES-T3 from National Institute of Standards and Technology, USA (Iding, Bresler and Nizamuddin, 1977a), SAFIR from the University of Liège, Belgium (Franssen, 2003) and TASEF from Lund Institute of Technology, Sweden (Sterner and Wickström, 1990). In addition to these special codes developed for structures exposed to fire, there are some general finite element programs such as ABAQUS, ANSYS, DIANA and Comsol Multiphysics which can also be used to conduct the heat transfer analysis.

## 6.2 CALCULATION OF TEMPERATURE IN TIMBER ELEMENT

The situation for timber is much simpler in that the temperature within a timber element is dependent only on the rate of charring (which defines the depth of charring), the thermal conductivity and the temperature at the wood-char boundary (Schaffer, 1965). The temperature  $\theta$  within a semi-infinite element is given by

$$\frac{\theta - \theta_0}{\theta_{cw} - \theta_0} = \exp\left(\frac{\beta_0 x}{a_w}\right) \quad (6.20)$$

where the depth  $x$  is measured from the wood-char interface,  $\theta_0$  is the initial wood temperature which is generally taken as  $20^\circ\text{C}$ ,  $\theta_{cw} = 288^\circ\text{C}$  is the temperature at the wood-char interface,  $a_w$  is the thermal diffusivity of wood which represents how fast heat diffuses through wood material and is defined as  $a_w = \lambda/(\rho c)$  and  $\beta_0$  is the rate of charring taken as constant.

## 6.3 STRUCTURAL ANALYSIS

The analysis of the response of a structure to a fire can be accomplished using the established principles of engineering mechanics. The analysis, however, needs to consider the continuing changes in material properties due to rising temperatures. Those properties that are most significant to structural performance include yield strength, modulus of elasticity and coefficient of thermal expansion. The development of numerical techniques and an enhanced knowledge of the thermal and mechanical properties of materials at elevated temperatures have made it possible to determine the fire resistance of various structural members by calculations. It should be emphasized that the structural analysis should examine the fire safety of the whole structure. The response of each member is calculated and local failures are identified. But then it is important to continue the calculations in order to determine whether these local failures could lead to progressive collapse of the whole structure. Note that, during the course of the fire, plastic deformations may develop in the materials of structural members. Therefore, the structural analysis should be time dependent although the inertia and damping forces may not necessarily be involved in the analysis. The analysis with history dependent based on time steps but without considering the inertia and damping forces is called the quasi-static analysis.

### 6.3.1 Calculation of structural responses using simple approaches

For some simple structural members such as beams and columns if the fire scenarios are identical or very much similar along the longitudinal direction of the member, then the temperature field can be assumed to be independent of the longitudinal coordinate and determined based on a two-dimensional heat transfer problem within the cross section of the member. Once the temperature field has been determined, the response of the member to the applied loading can be calculated based on the simple bending theory of Bernoulli beams.

The main assumption of the Bernoulli beam is the linear distribution of the axial strain in the cross section. Under this assumption, the axial strain at any coordinate point of the cross section can be expressed as the sum of a membrane strain and two bending strains as follows

$$\varepsilon(y, z) = \varepsilon_0 + y\kappa_{xy} + z\kappa_{xz} \quad (6.21)$$

where  $\varepsilon_0$  is the membrane strain,  $\kappa_{xy}$  and  $\kappa_{xz}$  are the curvatures of the beam in the  $xy$ - and  $xz$ -planes, respectively. On the other hand, the total strain can be decomposed in terms of the components generated by individual actions (Li and Purkiss, 2005)

$$\varepsilon(y, z) = \varepsilon_\sigma(\sigma, \theta) + \varepsilon_{cr}(\sigma, \theta, t) + \varepsilon_{tr}(\sigma, \theta) + \varepsilon_{th}(\theta) \quad (6.22)$$

where  $\sigma$  is the stress,  $\theta$  is the temperature,  $t$  is the time,  $\varepsilon_\sigma$  is the stress-induced strain which is the function of stress and temperature,  $\varepsilon_{cr}$  is the classical creep strain which is the function of stress, temperature and time,  $\varepsilon_{tr}$  is the transient strain which is the function of stress and temperature and exists only for concrete material and  $\varepsilon_{th}$  is the thermal strain which is the function of temperature. Expressions for  $\varepsilon_\sigma$ ,  $\varepsilon_{cr}$ ,  $\varepsilon_{tr}$  and  $\varepsilon_{th}$  for steel and concrete materials can be found in Chapter 5. It is known that, when the strain involves the plastic strain, the stress-strain relation is usually expressed in the increment form. According to Eq. (6.22), the increment of the axial strain can be expressed as

$$\Delta\varepsilon = f_\sigma(\sigma, \theta, t)\Delta\sigma + f_\theta(\sigma, \theta, t)\Delta\theta + f_t(\sigma, \theta, t)\Delta t \quad (6.23)$$

in which,

$$\begin{aligned} f_\sigma(\sigma, \theta, t) &= \frac{\partial\varepsilon}{\partial\sigma} = \frac{\partial\varepsilon_\sigma}{\partial\sigma} + \frac{\partial\varepsilon_{cr}}{\partial\sigma} + \frac{\partial\varepsilon_{tr}}{\partial\sigma} \\ f_\theta(\sigma, \theta, t) &= \frac{\partial\varepsilon}{\partial\theta} = \frac{\partial\varepsilon_\sigma}{\partial\theta} + \frac{\partial\varepsilon_{cr}}{\partial\theta} + \frac{\partial\varepsilon_{tr}}{\partial\theta} + \frac{\partial\varepsilon_{th}}{\partial\theta} \\ f_t(\sigma, \theta, t) &= \frac{\partial\varepsilon}{\partial t} = \frac{\partial\varepsilon_{cr}}{\partial t} \end{aligned}$$

where  $\Delta\varepsilon$ ,  $\Delta\sigma$ ,  $\Delta\theta$  and  $\Delta t$  are the increments of strain, stress, temperature and time, respectively. Similarly, the increment form of Eq. (6.21) can be expressed as,

$$\Delta\varepsilon = \Delta\varepsilon_0 + y\Delta\kappa_{xy} + z\Delta\kappa_{xz} \quad (6.24)$$

where  $\Delta\varepsilon_0$  is the increment of membrane strain,  $\Delta\kappa_{xy}$  and  $\Delta\kappa_{xz}$  are the increments of curvatures. Substituting Eq. (6.23) into Eq. (6.24) yields

$$\Delta\sigma = \frac{1}{f_\sigma}(\Delta\varepsilon_0 + y\Delta\kappa_{xy} + z\Delta\kappa_{xz} - f_\theta\Delta\theta - f_t\Delta t) \quad (6.25)$$

Let  $N_x$  be the axial membrane force and  $M_y$  and  $M_z$  be the bending moments about  $y$ - and  $z$ -axes. Their increments thus can be expressed as

$$\begin{aligned} \Delta N_x &= \int_A \Delta\sigma dA \\ \Delta M_z &= \int_A y\Delta\sigma dA \\ \Delta M_y &= \int_A z\Delta\sigma dA \end{aligned} \quad (6.26)$$

Substituting Eq. (6.25) into Eq. (6.26) yields,

$$\begin{aligned} \Delta N_x &= K_{11}\Delta\varepsilon_0 + K_{12}\Delta\kappa_{xy} + K_{13}\Delta\kappa_{xz} - \Delta F_1 \\ \Delta M_z &= K_{12}\Delta\varepsilon_0 + K_{22}\Delta\kappa_{xy} + K_{23}\Delta\kappa_{xz} - \Delta F_2 \\ \Delta M_y &= K_{13}\Delta\varepsilon_0 + K_{23}\Delta\kappa_{xy} + K_{33}\Delta\kappa_{xz} - \Delta F_3 \end{aligned} \quad (6.27)$$

in which,

$$\begin{aligned} K_{11} &= \int_A \frac{1}{f_\sigma} dA, & K_{12} &= \int_A \frac{y}{f_\sigma} dA, & K_{13} &= \int_A \frac{z}{f_\sigma} dA, & \Delta F_1 &= \int_A \frac{f_\theta\Delta\theta + f_t\Delta t}{f_\sigma} dA \\ K_{22} &= \int_A \frac{y^2}{f_\sigma} dA, & K_{23} &= \int_A \frac{yz}{f_\sigma} dA, & \Delta F_2 &= \int_A \frac{y(f_\theta\Delta\theta + f_t\Delta t)}{f_\sigma} dA \\ K_{33} &= \int_A \frac{z^2}{f_\sigma} dA, & \Delta F_3 &= \int_A \frac{z(f_\theta\Delta\theta + f_t\Delta t)}{f_\sigma} dA \end{aligned}$$

Equation (6.27) can be rewritten into the matrix relationship between the increments of generalized strains and generalized forces

$$\begin{bmatrix} K_{11} & K_{12} & K_{13} \\ K_{12} & K_{22} & K_{23} \\ K_{13} & K_{23} & K_{33} \end{bmatrix} \begin{Bmatrix} \Delta \varepsilon_0 \\ \Delta \kappa_{xy} \\ \Delta \kappa_{xz} \end{Bmatrix} = \begin{Bmatrix} \Delta F_1 \\ \Delta F_2 \\ \Delta F_3 \end{Bmatrix} + \begin{Bmatrix} \Delta N_x \\ \Delta M_z \\ \Delta M_y \end{Bmatrix} \quad (6.28)$$

Equation (6.28) is the generalized form of the bending equation of Bernoulli beams, in which the increments of generalized forces  $\Delta N_x$ ,  $\Delta M_z$  and  $\Delta M_y$  can be expressed in terms of the increments of externally applied mechanical loads and reaction forces at boundaries (if it is a statically indeterminate structure) through the use of equilibrium equations. The increments  $\Delta F_1$ ,  $\Delta F_2$  and  $\Delta F_3$  are generated due to the temperature and time increments. In the case of ambient temperature,  $\Delta F_1$ ,  $\Delta F_2$  and  $\Delta F_3$  remain zero and thus Eq. (6.28) reduces to the conventional incremental form of the bending equation of beams. Further, if the material constitutive equation is linear, then the stiffness coefficients  $K_{ij}$  will be independent of stresses and strains and thus the relationship between generalized strains and generalized forces will be the same as that between their increments.

In the case where the temperature and internal forces are independent of the longitudinal coordinate, Eq. (6.28) can be solved directly based on increment steps. Examples of this include the column subjected to pure compression and the beam subjected to pure bending. Otherwise, the membrane strain and curvatures must be solved by considering the compatibility along the longitudinal direction of the member with imposed or calculated end conditions (Purkiss and Weeks, 1987; Purkiss, 1990a). Note that

$$\Delta \varepsilon_0 = \frac{d(\Delta u)}{dx}, \Delta \kappa_{xy} = -\frac{d^2(\Delta v)}{dx^2}, \Delta \kappa_{xz} = -\frac{d^2(\Delta w)}{dx^2} \quad (6.29)$$

$$\Delta q_x = \frac{d(\Delta N_x)}{dx}, \Delta q_y = \frac{d^2(\Delta M_z)}{dx^2}, \Delta q_z = \frac{d^2(\Delta M_y)}{dx^2} \quad (6.30)$$

where  $\Delta u$  is the increment of axial displacement,  $\Delta v$  and  $\Delta w$  are the increments of deflections in  $y$ - and  $z$ -directions,  $\Delta q_x$  is the increment of axial distributed load ( $q_x$  is positive if it is in  $x$ -axis direction),  $\Delta q_y$  and  $\Delta q_z$  are the increments of transverse distributed loads in  $y$ - and  $z$ -directions ( $q_y$  and  $q_z$  are positive if they are in  $y$ - and  $z$ -axis directions). For statically determinate beams,  $\Delta N_x$ ,  $\Delta M_z$  and  $\Delta M_y$  can be

determined from Eq. (6.30) or from static equilibrium equations directly. For statically indeterminate beams,  $\Delta N_x$ ,  $\Delta M_z$  and  $\Delta M_y$  cannot be determined directly from static equilibrium equations and will involve some of unknown reaction forces, which need to be determined from displacement boundary conditions. Substituting Eq. (6.29) into Eq. (6.28) yields

$$\begin{bmatrix} K_{11} & K_{12} & K_{13} \\ K_{12} & K_{22} & K_{23} \\ K_{13} & K_{23} & K_{33} \end{bmatrix} \begin{Bmatrix} \frac{d(\Delta u)}{dx} \\ -\frac{d^2(\Delta v)}{dx^2} \\ -\frac{d^2(\Delta w)}{dx^2} \end{Bmatrix} = \begin{Bmatrix} \Delta F_1 \\ \Delta F_2 \\ \Delta F_3 \end{Bmatrix} + \begin{Bmatrix} \Delta N_x \\ \Delta M_z \\ \Delta M_y \end{Bmatrix} \quad (6.31)$$

Equation (6.31) can be solved using various discrete methods along the longitudinal direction to convert the differentiation equations into algebraic equations. Because of the non-linearity involved in the material constitutive equation, the stiffness coefficient  $K_{ij}$  in Eq. (6.31) are not only temperature dependent but also stresses and strains dependent. Thus, iterations are required in solving the equations at each time step to correct for non-linearities. This finally leads to a complete deformation time history for the given externally applied loads. Such calculations are only amenable to computer analysis, examples of which include FIRES-RC (Becker and Bresler, 1972), CEFFICOS (Schleich, 1986, 1987), CONFIRE (Forsén, 1982). Figure 6.2 provides a flowchart for this kind of calculations. The method can be applied to steel, concrete and composite steel-concrete members. For timber, which chars substantially when subjected to heat leaving a relatively unaffected core, calculations can be undertaken using normal ambient methods with the use of temperature-reduced strengths if considered appropriate on the core after the parent section has been reduced by the appropriate depth of charring. Hosser, Dorn and Richter (1994) provided a very useful overview and assessment of some of available simplified, i.e. non-computer code, design methods.

### 6.3.2 Calculation of structural responses using finite element analysis packages

The simple approach described in section 6.3.1 can be applied only to very simple structural members with uniaxial stress state. For frame structures or structural members in which stresses are not uniaxial, structural analysis packages based on finite element approaches should be used. There are many structural analysis software packages commercially

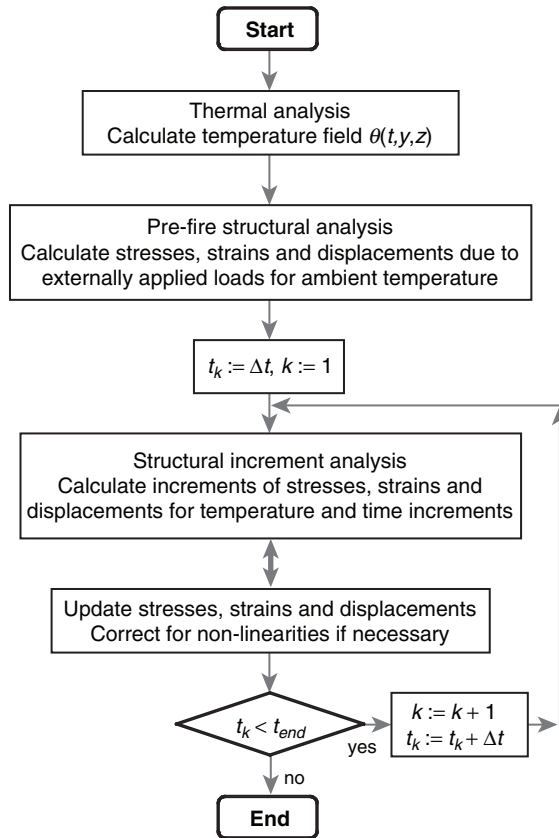


Figure 6.2 Overall calculation procedure for the structural behaviour of fire affected members.

available nowadays. However, since the fire involves high temperatures, the software packages to be used must be able to take into account the special characteristics of materials at high temperatures and the non-linearity both in geometry and material. Several computer packages were specially designed for modelling high-temperature phenomena, including FIRES-RC II (Iding, Bresler and Nizamuddin, 1977b), FASBUS II (Iding and Bresler, 1987, 1990), SAFIR (Nwosu *et al.*, 1999) and VULCAN (Huang, Burgess and Plank, 2003a, b). The VULCAN is capable of modelling the global three-dimensional behaviour of composite steel-framed buildings under fire conditions. The analysis considers the whole frame action and includes geometrical and material non-linearities within its beam-column and slab elements. It also includes the ability to represent semi-rigid connections that degrade with temperature and partial

interaction between the steel section and slab. In addition to these specific software packages, other non-linear finite element structural analysis programs such as ABAQUS, ANSYS and DIANA can also be utilized for conducting the fire analysis of structures (Sanad *et al.*, 1999).

Most finite element programs require data to be entered on the stress-strain temperature behaviour of steel whether reinforcing, pre-stressing or structural and/or concrete as appropriate. Since the thermal strain is treated separately in most structural analysis programs, the strain used to define the stress-strain temperature behaviour required as an input in the program thus is the sum of all other strains. For steel this includes the classical creep strain and the strain induced by the mechanical stress. In the case where the classical creep strain is negligible, this reduces to just the strain induced by the mechanical stress and therefore the stress-strain temperature behaviour can be simply represented by the temperature-dependent stress-strain equations as described in Chapter 5. For concrete, however, the transient strain is not negligible and the strain used to define the stress-strain temperature behaviour thus must include both the transient strain and the strain induced by the mechanical stress. Therefore, the temperature-dependent stress-strain equations must be modified to include the transient strain before they can be as the input to the program (Li and Purkiss, 2005).

Although there are many computer simulation results published in literature, there have been limited comparative, or benchmark, tests commissioned for both thermal response and, more importantly, structural response. The latter is very much affected by materials models and the exact formulation of the analysis techniques used. Sullivan, Terro and Morris (1993/4) gave some results following a survey of available computer software packages both for thermal and structural analyses. For the thermal analysis programs, particularly for steel structures, it seems that most packages gave comparable answers and that these answers were also in reasonable agreement with experimental data. However, for concrete structures, particularly at temperatures of around 100–200°C, agreement was less acceptable for the reason that the packages examined did not fully consider moisture transport. It was also noted that the fit between experimental and predicted temperatures was often improved by adjusting the values of the parameters defining the thermal diffusivity and/or the thermal boundary conditions such as emissivity.

For the structural analysis packages investigated, a greater spread of acceptability was found. This spread was, in part, due to the fact that some of the packages investigated were developed for research (and thus did not have adequate documentation or were user unfriendly), in part due to the assumptions made within the analysis algorithms (such as no allowance for large displacements) and in part due to inadequate materials models (especially for concrete where either transient strain

or the effect of stress history was ignored). It appeared that many of the programs predicted correct trends but that the absolute results did not agree with experimental data. It was also noted that the effect of classical creep on the behaviour of steel was neglected.

### 6.4 EXAMPLES

The first example presented here is a circular steel tube filled with concrete subjected to pure compression and its outside surface is exposed to a fire. The problem was solved using the simple approach described in section 6.3.1 by Yin, Zha and Li (2006). Because of the axial symmetry of the problem, the temperature and axial compressive stress are axial symmetric. Figure 6.3 shows the temperature distributions along the radial direction at various different times when the composite column is exposed to the fire, the temperature of which is defined by the standard fire curve. As is seen in Fig. 6.3, the variation of the temperature is much smaller in the steel tube than in the concrete core. This is because steel has a much greater thermal diffusivity than concrete. The high temperature in the steel tube together with the non-uniform temperature distribution in the concrete core leads to a complicated distribution of the axial

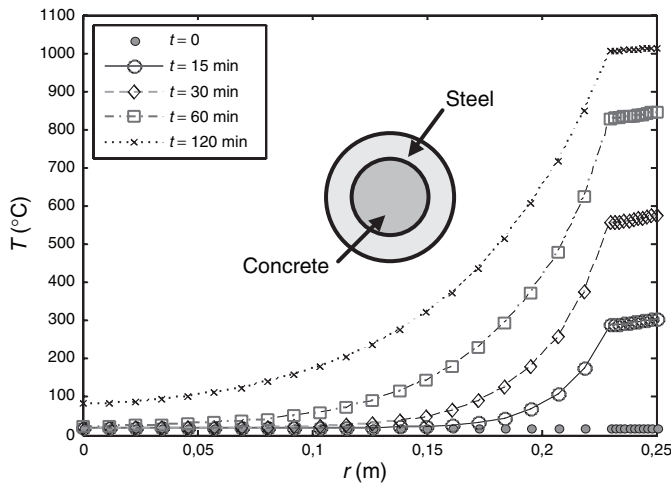


**Figure 6.3** Temperature distribution profiles of the circular steel tube filled with concrete (column diameter  $D = 500$  mm, steel tube thickness  $h_c = 20$  mm, conductivity and specific heat are temperature dependent for both steel and concrete, the standard fire curve is used for the fire temperature, Yin, Zha and Li, 2006).

compressive stress, as demonstrated in Fig. 6.4. Note that the reduction in stress in the steel tube when fire-exposure time increases is due to the strength reduction caused by high temperature. Figure 6.5 shows the load–displacement curves of the composite column at various different fire-exposure times. The fire resistance of the column can be obtained by plotting the maximum loads of the load–displacement curves against the fire-exposure times.

The second example is a two-bay I-section steel frame with columns fixed at the base and beams uniformly loaded on the top. The analysis was

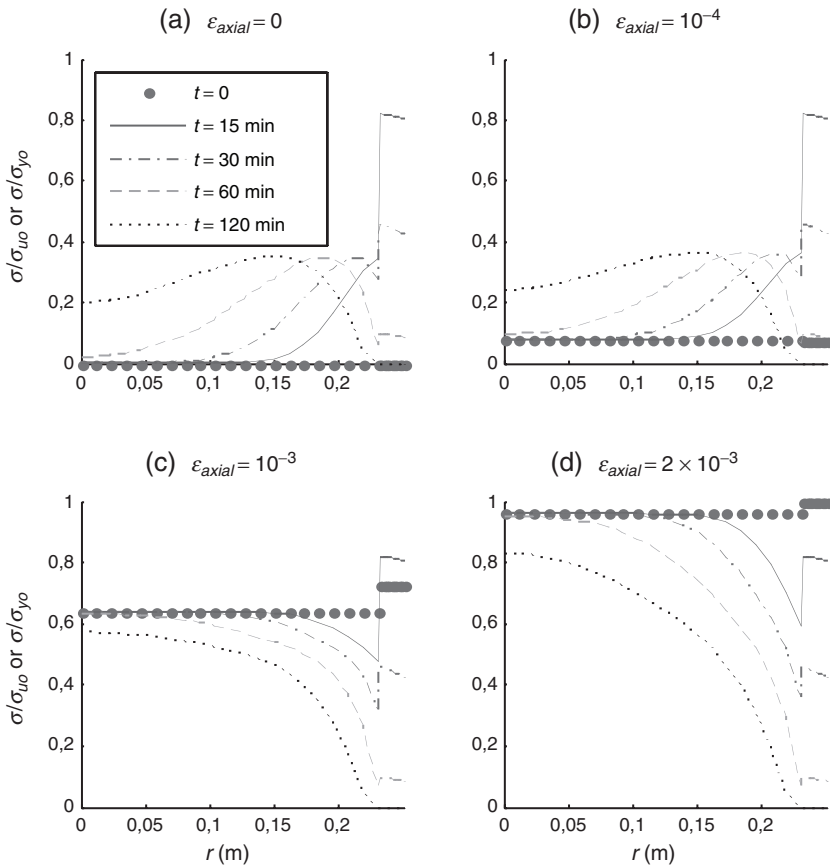


**Figure 6.4** Stress distribution profiles along the radial direction at various times for different compressive strains ( $\sigma_{u0}$  is the concrete peak compressive stress at ambient temperature and  $\sigma_{y0}$  is the steel yield stress at ambient temperature, Yin, Zha and Li, 2006).

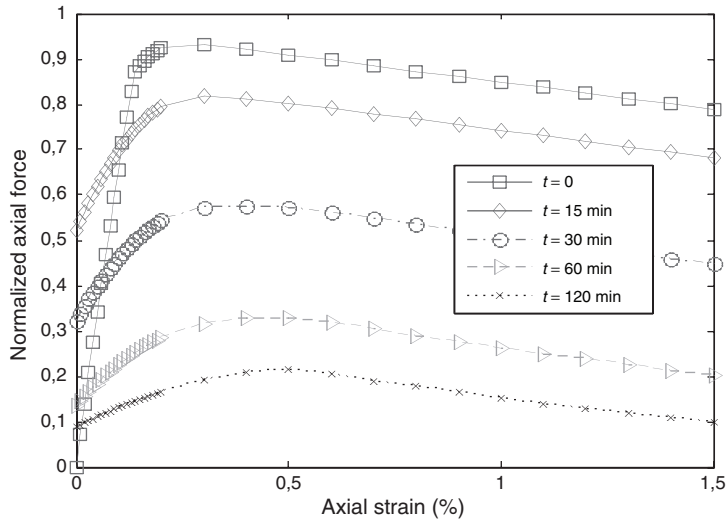


**Figure 6.5** Load–displacement curves with temperature effects (Yin, Zha and Li, 2006).

performed using the non-linear finite element analysis package ABAQUS by Ali, Senseny and Alpert (2004). Two main steps were followed in the analysis procedure. In the first step, the frame was analyzed under the applied load at room temperature to establish the pre-fire stress and deformation in the frame. In the second step, the history of fire temperature was calculated and was imposed on the deformed and loaded structure causing the steel to expand and the mechanical properties to degrade. Both geometric and material non-linearities were included in the simulations to account for the expected large displacements, plastic deformations and creep. Five different fire scenarios were investigated. The highly non-linear problem was solved using iterative procedures with automatic time stepping.

Figure 6.6 shows the simulation results. It is seen that the frame expands slowly toward the wall until it reaches its maximum lateral displacement followed by rapid change in displacement direction and collapse away from the fire wall. The time to collapse is about 45 min. When the fire covers at least one bay of the frame, the time to collapse is largely unaffected by the fire scenario because the plastic hinges and the excessive deformations in the span close the wall very much control the failure. The required space between the wall and steel depends on the extent of fire. The minimum clearance required between the frame and the wall increases with the length of the fuel burning. This behaviour is consistent with the simple case of uniformly heated steel members that are restrained

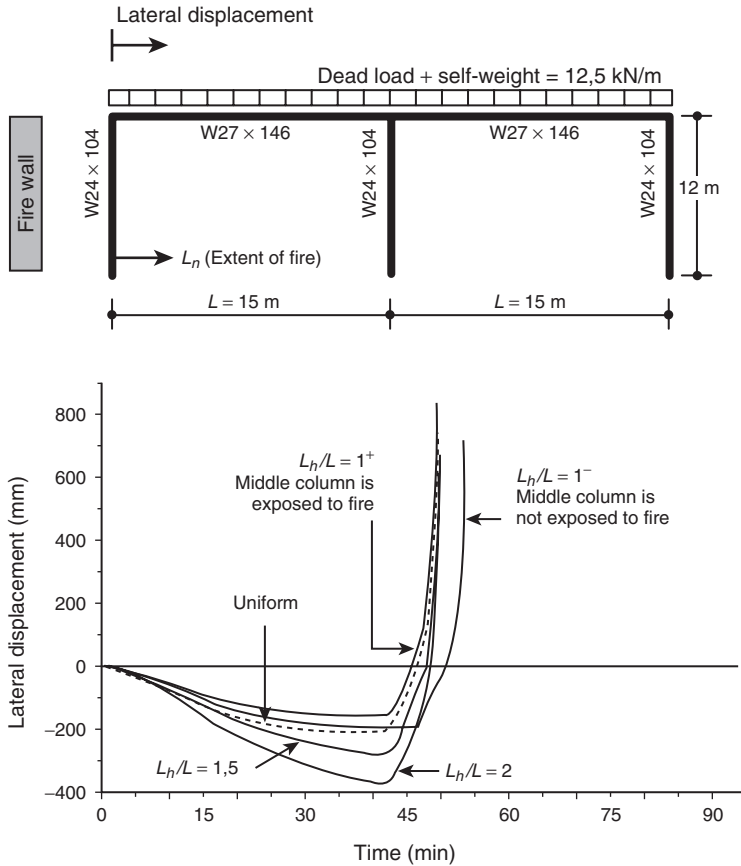


**Figure 6.6** Lateral displacement histories for a two-bay steel frame.  $L_h/L = 1^-$  – fire is localized to the bay closest to the firewall excluding the middle column.  $L_h/L = 1^+$  – the bay closest to the wall is exposed to fire including the middle column.  $L_h/L = 1.5$  – fire is extended beyond the first bay to cover half of the second bay.  $L_h/L = 2$  – the two bays are heated except for the far column. Uniform – the fire heats all columns and girders of the frame.  $L_k$  ( $0 \leq L_h \leq 2L$ ) is the length of the fuel burning measured from the firewall to anywhere within the two bay. (Copy with permission from Ali, Senseny and Apert, 2004).

only at one end in which longitudinal thermal expansion is proportional to the heated length of the member. A significant difference in lateral expansion is noticed between the two-bay fire scenario ( $L_h/L = 2$ ) and the uniform fire case. The uniform fire scenario is mathematically equivalent to a fixed girder at the middle column, and results in lateral displacements similar to the one-bay fire case ( $L_h/L = 1$ ).

Figure 6.7 is an example that shows how the moisture influences the heat transfer and thus the temperature distribution in the concrete structural member. The problem shown here is a simple concrete wall of 400 mm thick. The wall has an initial porosity of 0.08 and the corresponding initial moisture content is 2% of concrete weight. The wall is subject to double-side fire exposure. The temperature results for the case where the moisture transfer is considered are taken from Tenchev, Li and Purkiss (2001b). The experimental data are taken from Ahmed and Hurst (1997). The two temperature curves for the case where the moisture transfer is not considered are corresponding to different specific heat expressions, both of which are given in EN 1992-1-2 (one is recommended to use together with considering moisture transfer and the other is recommended to use without considering the moisture transfer). The comparisons of temperature distribution profiles between different models demonstrate that the

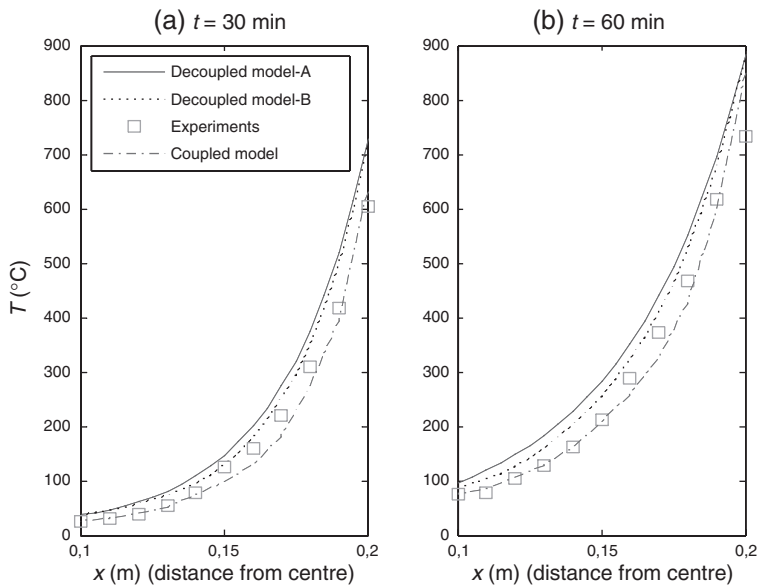
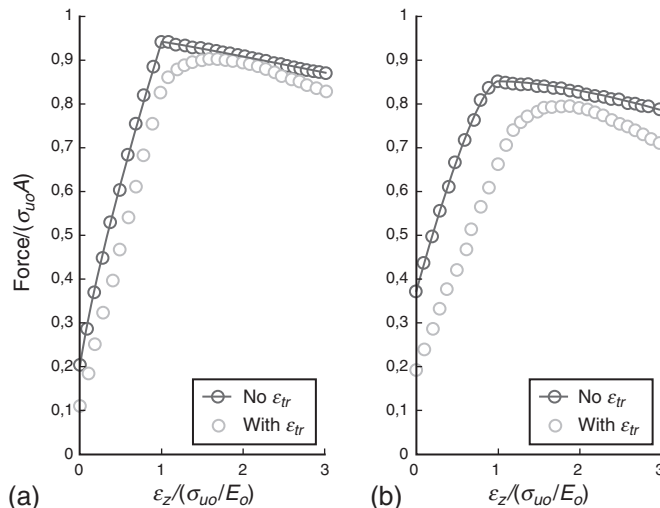


**Figure 6.7** Temperature distribution profiles of the concrete wall (400 mm) with moisture content 2% of the concrete weight at fire exposure times of 30 and 60 min, obtained from different models. Decoupled model-A uses the specific heat of dry concrete. Decoupled model-B uses the specific heat recommended in EN 1992-1-2 to take account the effects of moisture. Experimental data are taken from Ahmed and Hurst (1997). Coupled model considers the transfer of both heat and moisture and the results are taken from Tenchev, Li and Purkiss (2001b).

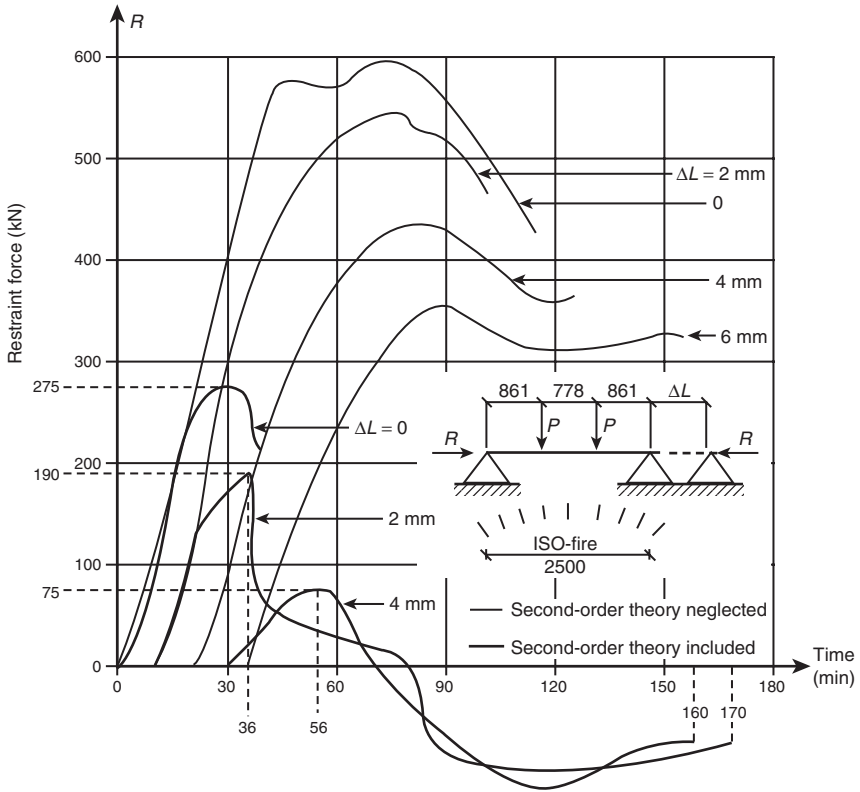
coupled moisture and heat transfer model provides more accurate results, while the model using an equivalent specific heat to take into account the moisture influence on the heat transfer can slightly improve the prediction but not completely.

Figure 6.8 gives an example that shows how the transient strain influences the fire performance of concrete structures. The problem is the same as that shown in Fig. 6.7 except for an additional uniform distributed compressive load which is applied on the wall (Li and Purkiss, 2005). The two sets of results shown in Fig. 6.8 correspond to two models; one ignores the transient strain and the other includes the transient strain in the stress-strain temperature behaviour model. Thus, the difference between the two sets of results reflects the influence of the transient strain. It is seen from the figure that, for short time exposure, the influence of the transient strain on the load-displacement curve is not very significant and thus it has a little influence on the fire performance of the wall. However, when the exposure time is not short, in which case the temperature in the concrete is high, the influence of the transient strain on the load-displacement curve becomes very significant and thus it has considerable influence on the fire performance of the wall.

Figure 6.9 shows another example which demonstrates the importance of considering geometric non-linearity or the second-order



**Figure 6.8** Compressive load-displacement curves of the concrete wall (400 mm) (a) at 20 min and (b) at 60 min ( $A$  is the cross section area,  $\sigma_{u0}$  is the concrete peak compressive stress, Li and Purkiss, 2005).



**Figure 6.9** The influence of second-order effects on the calculated displacements, in the analysis of the fire affected concrete beam. (Copy with permission from Forsén, 1982).

effects (Forsén, 1982). Both steel and concrete structures can undergo large displacements during the fire. This is simply due to the high temperature that weakens the stiffness of the structural member. Therefore, the geometric non-linearity or the second-order effect, i.e. the additional moments caused by large deflections or displacements, can substantially affect the results of calculations, or in the treatment of support conditions, as demonstrated in Fig. 6.9.

# 7

## Design of concrete elements

---

The design of concrete elements affected by exposure to fire may be undertaken in one of two ways; a prescriptive approach or a calculation approach. The prescriptive approach, in which tables of minimum dimensions, minimum axis distance, etc. corresponding to a given standard fire endurance are consulted, has been covered in Chapter 3 and will not be discussed further, except to note that even in the calculation approach minimum dimensions are conveniently determined using such tables when the exposure is taken as the standard furnace temperature–time curve. It should be noted that the minimum axis distance required for adequate fire resistance for low periods of fire resistance is likely to be less than that required for durability, and thus a calculation approach may not be viable.

Because of the complexity of the stress–strain relationships involved for concrete in compression where the elastic strains, unrestrained thermal expansion and transient strains need to be taken into account, it is not generally possible in simple design methods to consider the deformation history of the structural element. It is normally sufficient to consider only the resistance to the applied forces and thus the analytical approach reduces to an ‘end-point’ calculation, where the inequality between the resistance effect and the load effect is determined at a given time. However, using numerical stress–strain curves such as those proposed by Li and Purkiss (2005), it may be possible to determine deformation history using spreadsheets. The time to failure for a structural element may be determined by calculating the moment capacity or axial capacity at a series of discrete time steps.

The previous chapter has dealt with matrix techniques for both temperature distribution and stresses within structural elements, this chapter will concentrate on hand methods, although the use of spreadsheets may be found to be advantageous. The methods presented will assume that the thermal analysis and the structural analysis may be decoupled.

## **7.1 CALCULATION OF TEMPERATURES**

The basic theory for calculating the temperature distribution in any element was given in Chapter 6, but it should be noted that empirical or graphical solutions are available as a design tool. It is generally accurate enough to use such data for the end-point design of concrete members. Where exposure is to a parametric or real fire curve, the temperatures within a concrete element, including therefore those of any steel reinforcement, continue to rise for a period after the maximum fire, or gas, temperature has been reached. Thus the mechanical response or resistance of any concrete element so exposed will need calculation during the early stages of the cooling period as the critical design strength may be attained after the maximum fire temperature has occurred.

### **7.1.1 Graphical data**

There are three main sources of graphical data.

#### **7.1.1.1 *The ISE and Concrete Society design guide (1978)***

This publication gives temperature profiles for both flat soffit slabs and beams exposed to the standard furnace temperature–time response. Note that although the flat soffit slab data in the design guide are given for both normal and lightweight concrete, the beam data are for siliceous aggregate normal-weight concrete only. However, the guide suggests that for lightweight concrete beams, the temperatures may be taken as 80% of those for normal-weight concrete.

#### **7.1.1.2 *FIP/CEB report (1978)***

This gives temperature data on more varied types of concrete, including limestone aggregates, but only for exposure to the standard furnace curve.

#### **7.1.1.3 *EN 1992-1-2***

Temperature profiles for standard fire resistance periods slabs and beam/column sections cast from normal-weight concrete are given in Annex A of EN 1992-1-2. Annex A implies that these profiles are a result of calculation. It is not, however, known whether these profiles have been calibrated against actual test data.

### 7.1.2 Empirical methods

These in general are based either on curve fitting techniques on data derived from furnace tests, or on the superposition of simple solutions to the Fourier heat transfer equation. There are two such available methods.

The first proposed by Wickström (1985a, 1986) is based on the analysis of results from TASEF-2 and the second is proposed by Hertz (1981a, b). Both methods can be applied to exposure to either an actual compartment temperature–time curve, provided that for Wickström’s method the parametric curve in EN 1991-1-2 (Annex A) is used, or the standard furnace test curve. Both methods are applicable to different concretes as the thermal diffusivity is entered as data. Both methods give the temperature rise  $\Delta\theta$  above ambient. The presentation of both methods, given below, is limited to exposure to the standard furnace curve.

#### 7.1.2.1 Wickström’s method

The temperature rise in a normal-weight concrete element  $\Delta\theta$  is given by: For uniaxial heat flow

$$\Delta\theta = n_x n_w \Delta\theta_f \quad (7.1)$$

or, for biaxial heat flow

$$\Delta\theta_{xy} = (n_w (n_x + n_y - 2n_x n_y) + n_x n_y) \Delta\theta_f \quad (7.2)$$

where  $n_w$  is given by

$$n_w = 1 - 0,0616t^{-0,88} \quad (7.3)$$

and assuming constant thermal properties  $n_x$  (or  $n_y$  with  $y$  substituted for  $x$ ) by

$$n_x = 0,18 \ln u_x - 0,81 \quad (7.4)$$

where

$$u_x = \frac{a}{a_c} \frac{t}{x^2} \quad (7.5)$$

and  $a$  is the thermal diffusivity of the concrete under consideration and  $a_c$  is a reference value of  $0,417 \times 10^6 \text{ m}^2/\text{s}$ . For  $a = a_c$ , Eq. (7.4) reduces to

$$n_x = 0,18 \ln \frac{t}{x^2} - 0,81 \quad (7.6)$$

with  $x$  (or  $y$ ) subject to the limit

$$x \geq 2h - 3,6\sqrt{0,0015t} \quad (7.7)$$

where  $t$  is the time (h),  $x$  and  $y$  are the depths into the member (m) and  $h$  is the overall depth of the section (m). The  $\Delta\theta_g$  is given by the rise in furnace temperature above ambient at time  $t$ . Note that the temperature rise above ambient on the surface of the element is given by  $n_w\Delta\theta_g$ .

### 7.1.2.2 Hertz's method

The unidimensional time-dependant temperature  $\theta(x, t)$  is given by

$$\Delta\theta(x, t) = f_1(x, t) + f_2(x, t) + f_3(x, t) \quad (7.8)$$

where the functions  $f_1(x, t)$ ,  $f_2(x, t)$  and  $f_3(x, t)$  are solutions to the heat transfer equation for specific boundary conditions. These functions are given by

$$f_1(x, t) = E \left( 1 - \frac{x}{3,363\sqrt{at}} \right)^2 \quad (7.9)$$

$$f_2(x, t) = D e^{-x\sqrt{\frac{\pi}{2Ca}}} \sin \left( \frac{\pi t}{C} - x\sqrt{\frac{\pi}{2Ca}} \right) \quad (7.10)$$

and

$$f_3(x, t) = \frac{D + E}{2(e^{LC} - 1)} \left( 1 - e^{\left( L(t-C) - x\sqrt{\frac{L}{a}} \right)} \right) \quad (7.11)$$

where  $a$  is the thermal conductivity.

Note that  $f_1$  is set equal to zero if

$$1 - \frac{x}{3,363\sqrt{at}} \leq 0 \quad (7.12)$$

$f_2$  is set equal to zero if

$$\frac{\pi t}{C} - x\sqrt{\frac{\pi}{2Ca}} \leq 0 \quad (7.13)$$

$f_3$  is set equal to zero if

$$L(t - C) - x\sqrt{\frac{L}{a}} \leq 0 \quad (7.14)$$

The parameters  $E$ ,  $D$  and  $C$  are dependant upon the heating régime and  $L$  is dependant on the temperature curve during cooling, and is given by

$$L = \frac{2}{C} \ln \left( \frac{3D}{E - 2D} \right) \quad (7.15)$$

Note if  $E - 2D$  is negative, then  $E - 2D$  is set equal to 0,02. The temperature rise on the surface during heating is given by  $D + E$ . Note that for exposure to the standard furnace, temperature–time curve  $L$  does not need calculation, since  $f_3$  is always zero.

For exposure to the standard furnace curve, values of  $C$ ,  $D$  and  $E$  are given in Table 7.1. It should be noted that  $C$  is equal to twice the required time period. For the values of these parameters when exposure is to a parametric compartment, temperature–time response reference should be made to Hertz.

For two-dimensional heat flow, the above method needs modification in that the temperature  $\theta(x, y, t)$  is given by:

$$\Delta\theta(x, y, t) = \Delta\theta_0 (\xi_{\theta,x} + \xi_{\theta,y} - \xi_{\theta,x}\xi_{\theta,y}) \quad (7.16)$$

where  $\Delta\theta_0$  is the surface temperature rise at time  $t$  and  $\xi_{\theta,x}\Delta\theta_0$  is the temperature rise at the point being considered assuming unidimensional heat flow on the  $x$ -direction and  $\xi_{\theta,y}\Delta\theta_0$  is the temperature rise for heat flow on the  $y$ -direction.

**Table 7.1** Parameters required for temperature analysis of concrete members under standard conditions

Time (h)	C (h)	D (°C)	E (°C)
0,5	1,0	150	600
1,0	2,0	220	600
1,5	3,0	310	600
2,0	4,0	360	600
3,0	6,0	410	600
4,0	8,0	460	600

Where the element at the top of the fire compartment concerned has a web narrower than the bottom flange, the values of *D* and *E* should be multiplied by 0,9.

Source: Hertz (1981b) by permission

**Table 7.2** Comparison of surface temperature rise between Wickström, Hertz and EN 1992-1-2

Standard fire duration (h)	Surface temperatures (°C)			
	Furnace temperature	Wickström	Hertz	EN 1992-1-2 (Fig. A2)
0,5	842	749	770	730
1,0	945	888	840	880
1,5	1006	963	930	950
2,0	1049	1015	980	1010
3,0	1110	1084	1030	1080
4,0	1153	1132	1080	1120

It is instructive to compare the surface temperature predicted by Wickström, Hertz and EN 1991-1-2 (Fig. A2). This comparison is carried out in Table 7.2, where it is noted that all three sets of results are within around 40°C of each other. Thus it would appear acceptable to use any of the methods to predict temperature rise.

### 7.1.3 Values of thermal diffusivity

Both calculations of internal temperatures require the value of thermal diffusivity. EN 1992-1-2 does not give any guidance on this.

EN 1993-1-2 gives values of the thermal conductivity  $\lambda_c$  and specific heat  $c_c$  that may be used in simple calculations. These are  $\lambda_c = 1,6$  W/mK and  $c_c = 1000$  J/kgK. If a value of  $\rho_c$  of  $2400$  kg/m<sup>3</sup> is assumed, then from Eq. (5.2)

$$a_c = \frac{\lambda_c}{\rho_c c_c} = \frac{1,6}{1000 \times 2400} = 0,67 \times 10^{-6} \text{ m}^2/\text{s}$$

Hertz (1981b) quotes values of  $0,35 \times 10^{-6}$  m<sup>2</sup>/s for Danish sea gravel or granite concrete and  $0,52 \times 10^{-6}$  m<sup>2</sup>/s for a quartzite concrete. Wickström (1986) gives a value of  $0,417 \times 10^{-6}$  m<sup>2</sup>/s for normal-weight concrete.

It would therefore appear that for siliceous aggregate concretes  $a_c$  should lie in the range  $0,417$ – $0,67 \times 10^{-6}$  m<sup>2</sup>/s.

#### 7.1.4 Position of the 500°C isotherm

This is required for the method first proposed by Anderberg (1978b). From Wickström (1985a, 1986), for uniaxial heat flow, the position  $x$  for a temperature rise  $\Delta\theta_x$  at time  $t$  and furnace temperature rise  $\Delta\theta_f$  is given by:

$$x = \left[ \frac{\frac{a}{0,417 \times 10^{-6}} t}{\exp\left(4,5 + \frac{\Delta\theta_x}{0,18 n_w \Delta\theta_f}\right)} \right]^{0,5} \quad (7.17)$$

For the 500°C isotherm,  $\Delta\theta_x = 480^\circ\text{C}$  and  $x = x_{500}$ . Values of  $x_{500}$  were determined for values of  $a_c$  of  $0,415$ ;  $0,52$  and  $0,67 \times 10^{-6}$  m<sup>2</sup>/s.

A closed form solution cannot be obtained from Hertz, thus a spreadsheet was used to obtain values of  $x_{500}$  for the same values of  $a_c$ . Additionally, values of  $x_{500}$  obtained from Fig. A2 of EN 1992-1-2 are tabulated in Table 7.3.

It would appear from Table 7.3 that Wickström overestimates the value of  $x_{500}$  for all values of  $a_c$  with the least differences for  $a_c = 0,417 \times 10^{-6}$  m<sup>2</sup>/s. Hertz consistently overpredicts the value of  $x_{500}$  and is thus conservative. In all calculations for the 500°C isotherm, Wickström's approximation will be adopted with a value of  $a_c = 0,417 \times 10^{-6}$  m<sup>2</sup>/s.

**Table 7.3** Comparisons between the depth of the 500°C isotherm (mm) determined using Wickström, Hertz and EN 1992-1-2

Time (h)	Thermal diffusivity ( $\times 10^6$ m <sup>2</sup> /s)						
	Wickström			Hertz		EN 1992-1-2	
	0,417	0,52	0,67	0,417	0,52	0,67	
0,5	12	13	14	17	18	21	10
1,0	23	25	29	27	30	34	21
1,5	31	35	40	36	41	46	30
2,0	39	44	49	44	49	56	37
3,0	52	58	66	57	63	72	48
4,0	64	71	81	68	76	86	60

## 7.2 SIMPLE CALCULATION METHODS

### 7.2.1 Calculation of load effects

This section applies to whichever method is used to determine section capacity. There are two ways that the load effect may be calculated either using load combinations and load factors given in EN 1990 may be used to determine the effect of the actions on the structure, or the actions to be considered during a fire may be taken as  $\eta_{fi}$  times those at the ultimate limit state.

#### 7.2.1.1 Direct calculation

The combination of loading is determined from the unfavourable (and favourable) permanent actions with a partial safety factor of 1,0 and the variable actions multiplied by  $\psi_2$  from EN 1990 (cl 4.3.1(2), EN 1991-1-2). From Table A1.1 (EN 1990),  $\psi_2$  takes a value of 0,3 for domestic, residential, offices and high level traffic areas, 0,6 for shopping or congregation areas or low level traffic areas and 0,8 for storage areas.

#### 7.2.1.2 Indirect calculation

The design effect in fire  $E_{d,fi}$  should be taken as  $\eta_{fi}E_d$ , where  $E_d$  is the design effect at ambient and  $\eta_{fi}$  is given by:

$$\eta_{fi} = \frac{G_k + \psi_{fi}Q_{k,1}}{\gamma_G G_k + \gamma_{Q,1} Q_{k,1}} \quad (7.18)$$

$$\eta_{fi} = \frac{G_k + \psi_{fi} Q_{k,1}}{\gamma_G G_k + \gamma_{Q,1} \psi_{0,1} Q_{k,1}} \quad (7.19)$$

$$\eta_{fi} = \frac{G_k + \psi_{fi} Q_{k,1}}{\xi \gamma_G G_k + \gamma_{Q,1} Q_{k,1}} \quad (7.20)$$

depending upon which set of combination rules has been used to determine  $E_d$ .

As a conservative simplification a value of  $\eta_{fi} = 0,7$  may be adopted.

## 7.2.2 Materials' partial safety factors

The recommended value for material strength partial safety factors  $\gamma_{M,fi}$  is 1,0 for both steel and concrete.

## 7.2.3 Methods of determining section capacity

EN 1992-1-2 allows two methods for determining section resistance: the 500°C isotherm method (Anderberg, 1978b) and the method of slices by Hertz (1981a, 1981b, 1985, 1988).

### 7.2.3.1 Reduced section method (500°C isotherm)

This method was proposed by Anderberg (1978b), following the analysis of a number of fire tests carried out on flexural reinforced concrete elements. There are some limitations placed on the use of the method and comprise minimum thicknesses for either standard exposure times or fire load densities (Table B1: EN 1992-1-2). If used with parametric curves then the opening factor must be greater than 0,14 m<sup>1/2</sup>.

The calculations are carried out by assuming:

- (1) The concrete within the 500°C isotherm remains unaffected by heat.
- (2) The reduction factors for the reinforcement (assuming Class N) are for:
  - Compression reinforcement and tension reinforcement with the strain in the reinforcement  $\varepsilon_{s,fi} < 2\%$  (cl 4.2.4.3)
  - 20° ≤ θ ≤ 100°C

$$k_s(\theta) = 1,0 \quad (7.21)$$

$$100^{\circ}\text{C} \leq \theta \leq 400^{\circ}\text{C}$$

$$k_s(\theta) = 0,7 - 0,3 \frac{\theta - 400}{300} \quad (7.22)$$

$$400^{\circ}\text{C} \leq \theta \leq 500^{\circ}\text{C}$$

$$k_s(\theta) = 0,57 - 0,13 \frac{\theta - 500}{100} \quad (7.23)$$

$$500^{\circ}\text{C} \leq \theta \leq 700^{\circ}\text{C}$$

$$k_s(\theta) = 0,1 - 0,47 \frac{\theta - 700}{200} \quad (7.24)$$

$$700^{\circ}\text{C} \leq \theta \leq 1200^{\circ}\text{C}$$

$$k_s(\theta) = 0,1 \frac{1200 - \theta}{500} \quad (7.25)$$

- Tension reinforcement with  $\varepsilon_{s,fi} > 2\%$  (Table 3.2a, EN 1992-1-2)  
 $20^{\circ}\text{C} \leq \theta \leq 400^{\circ}\text{C}$

$$k_s(\theta) = 1,0 \quad (7.26)$$

$$400^{\circ}\text{C} \leq \theta \leq 500^{\circ}\text{C}$$

$$k_s(\theta) = 0,78 - 0,22 \frac{\theta - 500}{200} \quad (7.27)$$

$$500^{\circ}\text{C} \leq \theta \leq 600^{\circ}\text{C}$$

$$k_s(\theta) = 0,47 - 0,31 \frac{\theta - 600}{100} \quad (7.28)$$

$$600^{\circ}\text{C} \leq \theta \leq 700^{\circ}\text{C}$$

$$k_s(\theta) = 0,23 - 0,24 \frac{\theta - 700}{100} \quad (7.29)$$

$$700^{\circ}\text{C} \leq \theta \leq 800^{\circ}\text{C}$$

$$k_s(\theta) = 0,11 - 0,12 \frac{\theta - 800}{100} \quad (7.30)$$

$$800^{\circ}\text{C} \leq \theta \leq 1200^{\circ}\text{C}$$

$$k_s(\theta) = 0,11 \frac{1200 - \theta}{400} \quad (7.31)$$

- (3) In accordance with EN 1992-1-1, the depth of the stress block is taken as  $\lambda x$ , where  $x$  is the depth to the neutral axis, where  $\lambda$  is given by:

$$\lambda = 0,8 - \frac{f_{ck} - 50}{200} \leq 0,8 \quad (7.32)$$

and the concrete strength is taken as  $\eta f_{cd}$ , where  $\eta$  is given by:

$$\eta = 1,0 - \frac{f_{ck} - 50}{200} \leq 1,0 \quad (7.33)$$

- (4) All concrete in tension is ignored.  
 (5) In both methods the value of the load duration factor  $\alpha_{cc}$  is taken as 1,0, and therefore will not be included in the calculations.

The moment capacity of the section  $M_u$  is given by:

$$M_u = M_{u1} + M_{u2} \quad (7.34)$$

where  $M_{u1}$  is due to the tension reinforcement and  $M_{u2}$  is due to the compression reinforcement and its balancing tension reinforcement.  $M_{u1}$  is given by:

$$M_{u1} = A_{s1} f_{sd,fi}(\theta_m) z \quad (7.35)$$

and the mechanical reinforcement ratio  $\omega_k$  is given by:

$$\omega_k = \frac{A_{s1} f_{sd,fi}(\theta_m)}{b_{fi} d_{fi} f_{cd,fi}(20)} \quad (7.36)$$

$M_{u2}$  is given by:

$$M_{u2} = A_{s2} f_{sd,fi}(\theta_m) z' \quad (7.37)$$

The total tension steel area  $A_s$  is given by:

$$A_s = A_{s1} + A_{s2} \quad (7.38)$$

Symbols are defined in Fig. 7.1.

The values of  $f_{scd,fi}(\theta_m)$  and  $f_{sd,fi}(\theta_m)$  are the temperature reduced strengths of the reinforcement at a mean temperature  $\theta_m$  in a given layer. Where the reinforcement is in layers then the mean temperature reduced strength  $k(\phi)f_{sd,fi}$  is given by:

$$k(\phi) f_{sd,fi} = \frac{\sum [k_s(\theta_i) f_{sd,i} A_i]}{\sum A_i} \quad (7.39)$$

and the effective axis distance  $a$  by:

$$a = \frac{\sum [a_i k_s(\theta_i) f_{sd,i} A_i]}{k_s(\theta_i) f_{sd,i} A_i} \quad (7.40)$$

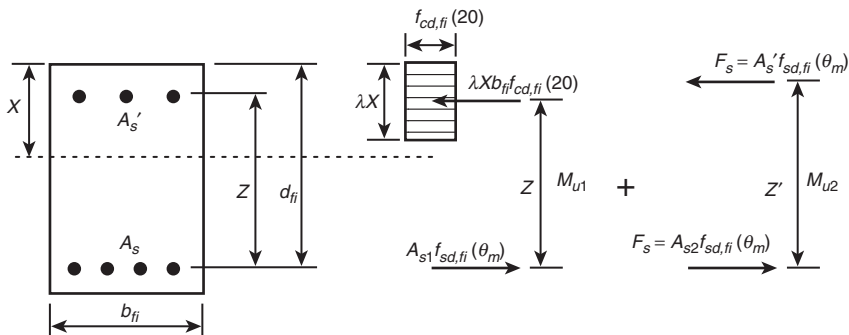


**Figure 7.1** Stress distribution at ultimate limit state for a rectangular concrete cross section with compression reinforcement, from EN 1992-1-2.

For the more usual case where all the reinforcement has the same strength then Eqs (7.30) and (7.40) reduce to:

$$k(\phi) = \frac{\sum [k_s(\theta_i) A_i]}{\sum A_i} \quad (7.41)$$

and the effective axis distance  $a$  to:

$$a = \frac{\sum [a_i k_s(\theta_i) A_i]}{\sum k_s(\theta_i) A_i} \quad (7.42)$$

### 7.2.3.2 *Method of slices (zone method)*

The heat affected concrete is divided into a series of slices and the temperature  $\theta$  determined at the mid-depth of each slice. The concrete strength reduction factor for siliceous aggregate concrete  $k_c(\theta)$  is given by (Table 3.1, EN 1992-1-2):

$20^\circ\text{C} \leq \theta \leq 100^\circ\text{C}$

$$k_c(\theta) = 1,0 \quad (7.43)$$

$100^\circ\text{C} \leq \theta \leq 200^\circ\text{C}$

$$k_c(\theta) = 0,95 - 0,05 \frac{\theta - 200}{100} \quad (7.44)$$

$200^\circ\text{C} \leq \theta \leq 400^\circ\text{C}$

$$k_c(\theta) = 0,75 - 0,2 \frac{\theta - 400}{200} \quad (7.45)$$

$400^\circ\text{C} \leq \theta \leq 800^\circ\text{C}$

$$k_c(\theta) = 0,15 - 0,6 \frac{\theta - 800}{400} \quad (7.46)$$

$800^\circ\text{C} \leq \theta \leq 900^\circ\text{C}$

$$k_c(\theta) = 0,08 - 0,07 \frac{\theta - 900}{100} \quad (7.47)$$

$900^{\circ}\text{C} \leq \theta \leq 1000^{\circ}\text{C}$

$$k_c(\theta) = 0,04 - 0,04 \frac{\theta - 1000}{100} \quad (7.48)$$

$1000^{\circ}\text{C} \leq \theta \leq 1100^{\circ}\text{C}$

$$k_c(\theta) = 0,01 - 0,03 \frac{\theta - 1100}{100} \quad (7.49)$$

$1100^{\circ}\text{C} \leq \theta \leq 1200^{\circ}\text{C}$

$$k_c(\theta) = 0,1 \frac{1200 - \theta}{100} \quad (7.50)$$

The mean concrete strength reduction factor  $k_{c,m}$  is given by:

$$k_{c,m} = \frac{1 - \frac{0,2}{n}}{n} \sum_{i=1}^n k_c(\theta_i) \quad (7.51)$$

The factor  $1 - 0,2/n$  in Eq. (7.51) is to compensate for the fact that  $k_c(\theta_i)$  is determined at the centre of a strip.

The effective width of a uniform stress block is determined by calculating the width of the damage zone  $a_z$  given by:

- For columns

$$a_z = w \left[ 1 - \left( \frac{k_{c,m}}{k_c(\theta_M)} \right)^{1,3} \right] \quad (7.52)$$

- For beams and slabs

$$a_z = w \left[ 1 - \left( \frac{k_{c,m}}{k_c(\theta_M)} \right) \right] \quad (7.53)$$

The strength reduction factor  $k_c(\theta_M)$  is determined at the centre of the member and  $w$  is the half width for exposure on opposite faces and the width (thickness of a slab). For columns,  $2w$  is the

lesser cross-sectional dimension. EN 1992-1-2 provides graphical data for reduction of concrete strength and section width in Annex B (Fig. B.5).

The reinforcement strength reduction factors are the same as those used in the 500°C isotherm method, and the method of analysis for beams is also similar.

EN 1992-1-2 imposes a restriction on the zone method, that it may only be used for exposure to the standard furnace curve. The reason for this is unclear as Hertz implies there is not restriction as he tabulated mean strength and damage zone width parameters for exposure to parametric fire curves. In all subsequent examples, a value,  $a_c = 0,417 \times 10^{-6} \text{ m}^2/\text{s}$  will be used where appropriate.

**Example 7.1: Concrete slab design**

A simply supported slab in a multi-span structure has been designed and detailed in Fig. 7.2. Continuity steel in the top face has been provided purely to resist the effect of cracking over the support. The cover provided is that to satisfy durability only. The slab is to be checked for a 2 h fire resistance period when exposed to the standard furnace test. Assume the usage of the structure is as an office, then the structural loading in the fire limit state is given by:

$$0,125 \times 25 + 1,0 + 0,3 \times 2,5 = 4,875 \text{ kPa}$$

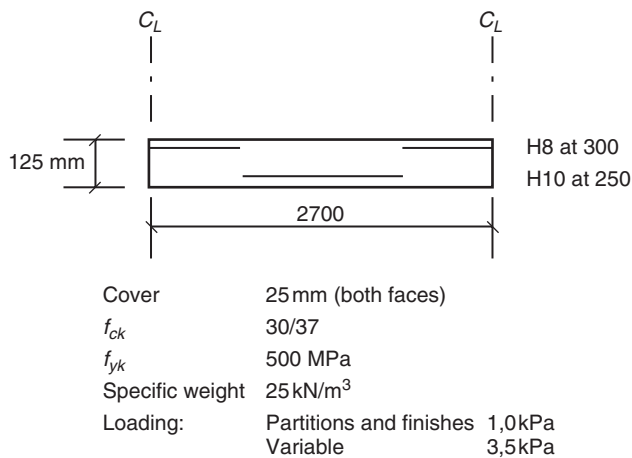


**Figure 7.2** Design data for a reinforced concrete slab (Example 7.1).

The  $\psi$  factor has been taken as 0,3, but the partition loading has been treated as totally permanent.

$$M_{Ed,fi} = 4,875 \times 2,7^2 / 8 = 4,44 \text{ kNm/m}$$

(a) 500°C isotherm method

The 500°C is approximately 40 mm from the bottom of the slab, thus for sagging moments the concrete strength is unaffected (Table 7.3, Wickström). Use Wickström, Eqs (7.1)–(7.6) to determine temperatures.

Temperature in the steel:

The centroid of the reinforcement is at  $20 + 10/5 = 25$  mm.

$$n_w = 1 - 0,0616t^{-0,88} = 1 - 0,0616 \times 2^{-0,88} = 0,967$$

$$n_x = 0,18 \ln(t/x^2) - 0,81 = 0,18 \ln(2/0,025^2) - 0,81 = 0,643$$

$$\Delta\theta_g = 345 \log(480t + 1) = 345 \log(480 \times 2 + 1) = 1029^\circ\text{C}$$

$$\Delta\theta = n_x n_w \Delta\theta_g = 0,643 \times 0,967 \times 1029 = 640^\circ\text{C, or}$$

$$\theta_s = 640 + 20 = 660^\circ\text{C}$$

(Assuming an ambient temperature of 20°C).

As the strength reduction will be high (and the neutral axis depth small), use the values of strength reduction factors for  $\varepsilon_{s,fi} > 2\%$ .

From Eq. (7.29):

$$\begin{aligned} k_s(\theta) &= 0,23 - 0,24(\theta - 700)/100 \\ &= 0,23 - 0,24(660 - 700)/100 = 0,326 \end{aligned}$$

Tension force,  $F_s$ :

$$F_s = 0,326 \times 500 \times 314 = 51182 \text{ N}$$

For Grade 30/37 concrete,  $\lambda = 0,8$  and  $\eta = 1,0$ , so

$$F_c = \eta f_{cd,fi}(20) \lambda x b = 0,8(30/1,0) \times 0,8x \times 1000 = 19200x$$

Equating  $F_s$  and  $F_c$  gives  $x = 2,67$  mm. If  $\varepsilon_{cu} = 3500 \mu\text{strain}$ , then clearly  $\varepsilon_s > 2\%$ .

$$\begin{aligned} M_{u1} &= F_s(d - 0,5\lambda x) = 51182(125 - 25 - 0,5 \times 0,8 \times 2,67) \\ &= 5,06 \text{ kNm/m} \end{aligned}$$

The moment capacity of 5,06 kNm/m exceeds the applied moment of  $M_{Ed,fi}$  of 4,44 kNm/m. Thus the slab is satisfactory.

Where a factor of  $\eta_{fi}$  of 0,7 to be taken,  $M_{Ed}$  would be  $0,7(0,125 \times 25 + 1,0 + 2,5) \times 2,7^2/8 = 4,23$  kNm/m, which would also be satisfactory. The reason the use of  $\eta_{fi} = 0,7$  produces a slightly lower value of  $M_{Ed,fi}$  is due to the relatively low value of the variable load of 2,5 kPa.

(b) Zone method

Under sagging moments the concrete strength is unaffected as the neutral axis depth is small.

Using Hertz's method, Eqs (7.8)–(7.10), to determine the temperature in the reinforcement gives  $\theta_s = 689^\circ\text{C}$ . From Eq. (7.29),  $k_s(\theta) = 0,256$ .

$$\begin{aligned} k_s(\theta) &= 0,23 - 0,24(\theta - 700)/100 \\ &= 0,23 - 0,24(660 - 700)/100 = 0,326 \end{aligned}$$

Tension force,  $F_s$ :

$$F_s = 0,256 \times 500 \times 314 = 40192 \text{ N}$$

For Grade 30/37 concrete,  $\lambda = 0,8$  and  $\eta = 1,0$ , so

$$F_c = \eta f_{cd,fi}(20)\lambda x b = 0,8(30/1,0) \times 0,8x \times 1000 = 19200x$$

Equating  $F_s$  and  $F_c$  gives  $x = 2,09$  mm. If  $\varepsilon_{cu} = 3500 \mu\text{strain}$ , then clearly  $\varepsilon_s > 2\%$ .

$$\begin{aligned} M_{u1} &= F_s(d - 0,5\lambda x) = 40192(125 - 25 - 0,5 \times 0,8 \times 2,09) \\ &= 3,99 \text{ kNm/m} \end{aligned}$$

The moment capacity of 3,99 kNm/m is less than applied moment of  $M_{Ed,fi}$  of 4,44 kNm/m. Thus the top steel needs to be capable of mobilizing a moment of  $4,44 - 3,99 = 0,45$  kNm/m.

**Table 7.4** Temperatures and strength reduction factors for Example 7.1

$x$ (mm)	$\theta_c$ (°C)	$k_c(\theta)$
12,5	828	0,130
37,5	562	0,507
62,5	352	0,798
87,5	199	0,951
112,5	101	1,0
$\sum k_c(\theta)$		3,386

From Fig. B.5(a) (EN 1992-1-2),  $k_c(\theta_M) = 1,0$  for a 125 mm thick slab at 120 min exposure.

Divide the slab into 5 slices (Table 7.4)

From Eq. (7.49),

$$k_{c,m} = \frac{1 - \frac{0,2}{n}}{n} \sum_{i=1}^n k_c(\theta_i) = \frac{1 - \frac{0,2}{5}}{5} 3,386 = 0,650$$

From Eq. (7.53),

$$a_z = w \left[ 1 - \left( \frac{k_{c,m}}{k_c(\theta_M)} \right) \right] = 125 \left[ 1 - \frac{0,650}{1,0} \right] = 44 \text{ mm}$$

Fig. B.5(b) (EN 1992-1-2) gives a much lower value of around 33 mm. The depth of the slab now becomes  $125 - 44 = 81$  mm, and the effective depth,  $d = 81 - 20 - 8/2 = 57$  mm.

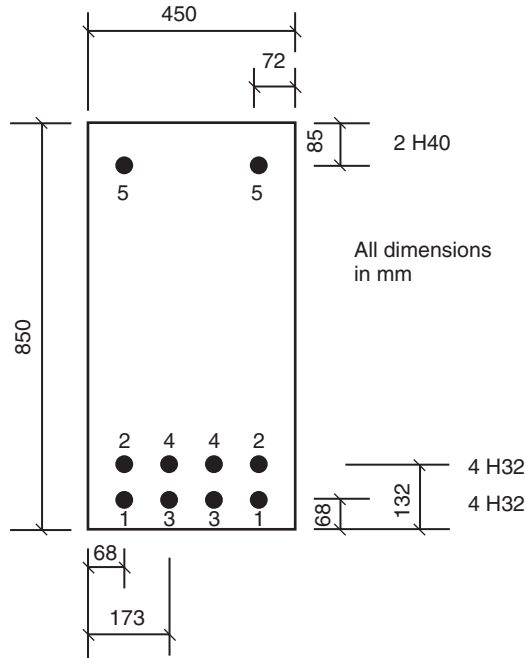
$$F_s = 500 \times 168 = 84\,000 \text{ N}$$

$$F_c = \eta f_{cd,fi}(20) \lambda x b = 0,8(30/1,0) \times 0,8x \times 1000 = 19\,200x$$

Equating  $F_s$  and  $F_c$  gives  $x = 4,4$  mm. If  $\varepsilon_{cu} = 3500 \mu\text{strain}$ , then clearly  $\varepsilon_s > 2\%$ .

$M_{u1} = F_s(d - 0,5\lambda x) = 84\,000(57 - 0,5 \times 0,8 \times 4,4) = 4,64 \text{ kNm/m}$ . The  $x/d$  ratio of  $4,4/57 (=0,077)$  is well within the range of that for a singly reinforced section.

This is well in excess of that required (0,45 kNm/m). Thus the slab is satisfactory, but only if the top steel is mobilized.



$f_{yk} = 500\text{MPa}$   
 Concrete grade c 30/37  
 Span 11 m  
 Specific weight  $25\text{kN/m}^3$   
 Variable loading  $2 \times 260\text{kN}$  at 4 m from support

**Figure 7.3** Design data for a concrete beam (Example 7.2).

**Example 7.2: Concrete beam design**

Determine the load-carrying capacity history over the complete range of standard furnace exposures, and check the duration the beam can last.

The data for the example are given in Fig. 7.3.

Permanent load =  $0,45 \times 0,85 \times 25 = 9,56 \text{ kNm/m}$

Permanent load moment =  $9,56 \times 11^2/8 = 145 \text{ kNm}$

Assuming office loading, then  $\psi_2 W = 0,3 \times 260 = 78 \text{ kN}$

Moment due to the variable loading is  $78 \times 4 = 312 \text{ kNm}$

Total applied moment ( $M_{Ed,fi}$ ) =  $145 + 312 = 457 \text{ kNm}$ .

(a) 500°C isotherm method

The position of the 500°C isotherm is only needed parallel to the side faces. These values are obtained from Table 7.3 and the reduced width is then given by  $450 - 2x_{500}$ .

Determination of reinforcement temperatures (Tables 7.5, 7.6).  
 As all the reinforcement is the same size, Eq. (7.41) reduces to:

$$k(\phi) = \frac{1}{n} \sum k_s(\theta_i) \tag{7.54}$$

Equation (7.54) expands to:

$$k(\phi) = \frac{k_s(\theta_1) + k_s(\theta_2) + k_s(\theta_3) + k_s(\theta_4)}{4}$$

and Eq. (7.42) reduces to:

$$a = \frac{\sum [a_i k_s(\theta_i)]}{\sum k_s(\theta_i)} \tag{7.55}$$

**Table 7.5** Values of temperature parameters and strength reduction factors for Bar 5

t (h)	$n_w$		$n_x$		Bar 5		
	72	68	132	173	$\theta_s$ (°C)	$k_s(\theta)$	
0,5	0,887	0,012	0,033	0	0	29	1,0
1,0	0,938	0,137	0,158	0	0	139	0,961
1,5	0,957	0,210	0,231	0	0	218	0,882
2,0	0,967	0,262	0,283	0,044	0	281	0,819
3,0	0,977	0,335	0,356	0,117	0,019	376	0,724
4,0	0,982	0,380	0,407	0,169	0,071	450	0,547

**Table 7.6** Temperatures and strength reduction factors for Bars 1–4

t (h)	Bar 1 (68,68)		Bar 2 (68,132)		Bar 3 (68,173)		Bar 4 (132,173)	
	$\theta_s$ (°C)	$k_s(\theta)$	$\theta_s$ (°C)	$k_s(\theta)$	$\theta_s$ (°C)	$k_s(\theta)$	$\theta_s$ (°C)	$k_s(\theta)$
0,5	67	1,0	44	1,0	44	1,0	20	1,0
1,0	273	1,0	157	1,0	157	1,0	20	1,0
1,5	408	0,881	238	1,0	238	1,0	20	1,0
2,0	506	0,761	333	1,0	302	1,0	64	1,0
3,0	646	0,360	480	0,802	412	0,878	163	1,0
4,0	744	0,177	586	0,513	520	0,718	274	1,0

Equation (7.55) expands to:

$$a = \frac{68 [k_s (\theta_1) + k_s (\theta_3)] + 132 [k_s (\theta_2) + k_s (\theta_4)]}{4k (\phi)}$$

$$b_{fi} = b - 2x_{500} = 400 - 2x_{500}$$

$$F_s = A_{sfsd,fi}(\theta_m) = A_{sc}k(\theta_5)f_{yk} = 2513 \times 500k(\theta_5) = 12\,56\,500k(\theta_5)$$

$$A_{sifs,fi}(\theta) = A_{sfsd,fi}(\theta_m) - F_{sc} = 6434 \times 500k(\phi) = 3,217k(\phi) \text{ MN}$$

$$x = A_{sifs,fi}(\theta) / (0,8 \times f_{cd}(20) \times b_{fi})$$

$$= A_{sifs,fi}(\theta) / (0,8 \times 30 \times b_{fi}) = A_{sifs,fi}(\theta) / (24 \times b_{fi})$$

$$M_{u1} = A_{sifs,fi}(\theta)[h - a - 0,4x] = A_{sifs,fi}(\theta)[850 - a - 0,4x]$$

$$M_{u2} = F_{sc}[h - a - 85] = F_{sc}[765 - a]$$

The values of  $M_{u1}$ ,  $M_{u2}$  and  $M$  are determined in Table 7.7.

(b) Method of slices

In this method, nine vertical strips of 50 mm width are taken parallel to the vertical faces of the beam cross section and the temperatures determined at the mid-depth of each strip using Eqs (7.8)–(7.10). The results are given in Table 7.8.

The sum of the concrete strength reduction factors  $\sum k_c(\theta)$  is given by:

$$\sum k_c(\theta) = 2k_c(\theta_1) + 2k_c(\theta_2) + 2k_c(\theta_3) + 2k_c(\theta_4) + k_c(\theta_5)$$

**Table 7.7** Determination of  $M_{u1}$ ,  $M_{u2}$  and  $M$

$t$ (h)	$k(\phi)$	$a$ (mm)	$b_{fi}$ (mm)	$F_s$ (MN)	$F_{s,tot}$ (MN)	$F_{s1}$ (MN)	$x$ (mm)	$M_{u1}$ (kNm)	$M_{u2}$ (kNm)	$M$ (kNm)
0,5	1,0	100	426	1,257	3,217	1,960	192	1319	836	2155
1,0	1,0	100	404	1,143	3,217	2,074	214	1378	760	2138
1,5	0,97	101	388	1,108	3,120	2,012	216	1333	736	2069
2	0,94	102	372	1,029	3,204	2,175	244	1415	682	2097
3	0,76	106	346	0,910	2,445	1,535	185	1028	600	1628
4	0,60	109	322	0,687	1,930	1,243	161	975	451	1426

**Table 7.8** Determination of concrete temperatures, strength reduction factors and section width reduction

$t$ (h)	Strip no (x)										$\sum k_c(\theta)$	$a_z$ (mm)
	1		2		3		4		5			
	25	75	125	175	225							
	$\theta_1$ (°C)	$k_c(\theta_1)$	$\theta_2$ (°C)	$k_c(\theta_2)$	$\theta_3$ (°C)	$k_c(\theta_3)$	$\theta_4$ (°C)	$k_c(\theta_4)$	$\theta_5$ (°C)	$k_c(\theta_5)$		
0,5	385	0,765	41	1,00	20	1,00	20	1,00	20	1,00	8,530	16
1,0	516	0,576	128	0,986	21	1,00	20	1,00	20	1,00	8,124	26
1,5	620	0,420	201	0,949	48	1,00	20	1,00	20	1,00	7,738	35
2	689	0,317	268	0,882	82	1,00	22	1,00	20	1,00	7,398	44
3	773	0,191	371	0,779	139	0,981	50	1,00	20	1,00	6,902	56
4	842	0,121	452	0,672	198	0,951	85	1,00	31	1,00	6,488	66

and  $k_{c,m}$  by:

$$k_{c,m} = \frac{1 - \frac{0,2}{n}}{n} \sum k_c(\theta_1) = \frac{1 - \frac{0,2}{9}}{9} \sum k_c(\theta_1) = 0,109 \sum k_c(\theta_i)$$

The value of  $k_c(\theta_M)$  is given by  $k_c(\theta_5)$  which equals 1,0 for all time steps.

The value of  $a_z$  is given by:

$$a_z = w \left[ 1 - \frac{k_{c,m}}{k_c(\theta_M)} \right] = \frac{450}{2} \left[ 1 - \frac{0,109 \sum k_c(\theta_i)}{1,0} \right]$$

The next stage is to determine the  $\xi_{\theta,x}$  (or  $\xi_{\theta,y}$ ) factors to determine the steel temperatures. The temperatures corresponding to depths of 68, 132 and 173 mm are given in Table 7.10, together with the  $\xi_{\theta,x}$  values derived from the calculated temperatures.

The determination of reinforcement temperatures and strength reduction factors are tabulated in Tables 7.9 and 7.10.

The values of  $k(\phi)$  and  $a$  are calculated as before and are given in Table 7.11.

In conclusion, it should be noted that there is little difference in the results from Anderberg (500°C isotherm method) and Hertz (zone method) up to 2 h, but then Hertz indicates a slightly more rapid decrease after 2 h. However, in both cases the beam will last for more than 4 h.

**Table 7.9** Determination of temperature factors and strength reduction factors for Bar 5

$t$ (h)	$\xi_{\theta,x}$				Bar 5		
	$D + E(^{\circ}\text{C})$	72 (mm)	68 (mm)	132 (mm)	173 (mm)	$\theta_s(^{\circ}\text{C})$	$k_s(\theta)$
0,5	750	0,038	0,055	0	0	49	1,0
1,0	820	0,146	0,168	0	0	140	0,960
1,5	910	0,219	0,246	0,020	0	219	0,881
2,0	960	0,278	0,305	0,050	0,002	287	0,813
3,0	1010	0,367	0,393	0,102	0,032	390	0,710
4,0	1060	0,426	0,451	0,144	0,064	471	0,539

**Table 7.10** Temperatures and strength reduction factors for Bars 1–4

$t$ (h)	Bar 1 (68,68)		Bar 2 (68,132)		Bar 3 (68,173)		Bar 4 (132,173)	
	$\theta_s(^{\circ}\text{C})$	$k_s(\theta)$	$\theta_s(^{\circ}\text{C})$	$k_s(\theta)$	$\theta_s(^{\circ}\text{C})$	$k_s(\theta)$	$\theta_s(^{\circ}\text{C})$	$k_s(\theta)$
0,5	100	1,0	41	1,0	41	1,0	20	1,0
1,0	272	1,0	158	1,0	158	1,0	20	1,0
1,5	413	0,876	258	1,0	244	1,0	20	1,0
2,0	516	0,730	346	1,0	314	1,0	70	1,0
3,0	658	0,331	479	0,803	437	0,849	152	1,0
4,0	761	0,157	582	0,526	535	0,671	231	1,0

**Table 7.11** Determination of  $M_{u1}$ ,  $M_{u2}$  and  $M$

$t$ (h)	$k(\phi)$	$a$ (mm)	$b_{fi}$ (mm)	$F_s$ (MN)	$F_{s,tot}$ (MN)	$F_{s1}$ (MN)	$x$ (mm)	$M_{u1}$ (kNm)	$M_{u2}$ (kNm)	$M$ (kNm)
0,5	1,0	100	418	1,257	3,217	1,960	195	1317	836	2155
1,0	1,0	100	398	1,206	3,217	2,011	211	1339	802	2141
1,5	0,969	101	380	1,107	3,117	2,010	220	1329	735	2066
2,0	0,933	102	362	1,022	3,001	1,979	228	1300	678	1978
3,0	0,748	106	338	0,892	2,406	1,514	187	1013	588	1601
4,0	0,589	109	318	0,677	1,895	1,218	160	825	444	1269

### 7.3 COLUMNS

Only the case where columns are not subjected to bending moments or where buckling need not be considered are covered herein.

EN 1992-1-2 Annex B3 gives a method of handling this situation, but it is iterative as the column curvature(s) need to be taken into account. Also if buckling is not critical at the normal ambient limit state it need not be considered at the fire limit state. This is in contradiction to Hertz (1985) who used the Rankine equation to determine the load capacity of any column under the fire limit state.

#### Example 7.3: Concrete column

Determine the fire resistance of a short reinforced concrete column 400 mm by 800 mm with 8 H25 bars having a cover of 35 mm (Fig. 7.4). The concrete is Grade 50/60.

$$A_c = 320\,000 \text{ mm}^2, A_s = 3927 \text{ mm}^2.$$

At ambient the load-carrying capacity  $N_{Rd}$  is given as

$$N_{Rd} = A_c \frac{\alpha_{cc} f_{ck}}{\gamma_m} + A_s \frac{f_{yk}}{\gamma_m} = 320\,000 \frac{0,85 \times 50}{1,5} + 3927 \frac{500}{1,15} = 10,77 \text{ MN}$$

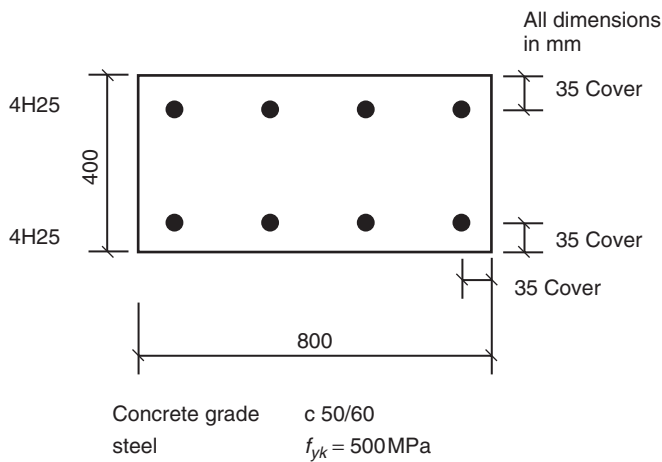


Figure 7.4 Design data for a concrete column (Example 7.3).

As the use of the structure is not known, nor the relative magnitudes of permanent and variable load, take the fire loading as  $\eta_{fi}N_{Ed}$ , so

$$N_{Ed,fi} = \eta_{fi}N_{Ed} = 0,7 \times 10,77 = 7,54 \text{ MN}$$

Although EN 1992-1-2 suggests the method of slices is more accurate, use both methods as an illustration.

(a) 500°C isotherm method

Figure B.1 (EN 1992-1-2) suggests that either rounding of the isotherm at corners should be considered or that a rectangular area equal to that contained within rounding at the corners should be taken.

As an approximation, take a 45° line through the point producing 500°C through bi-directional heating (Fig. 7.5).

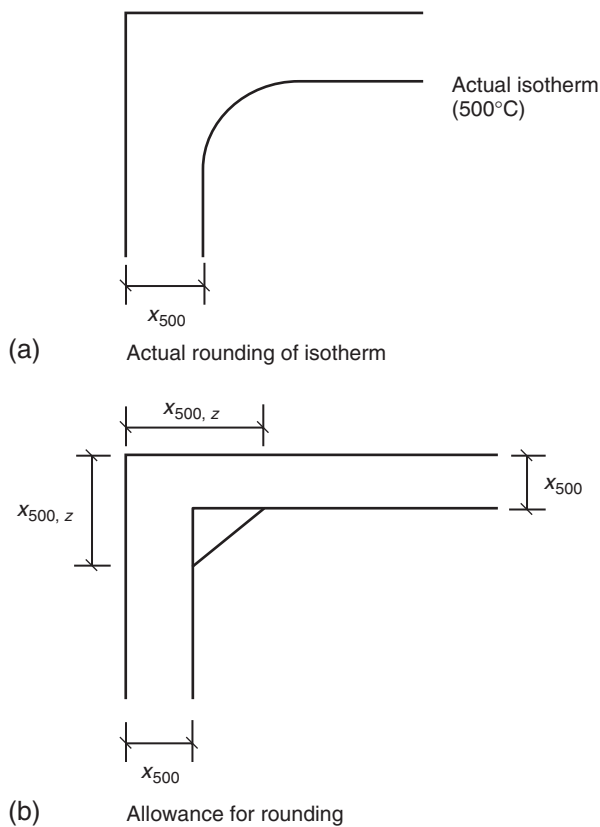


**Figure 7.5** Approximation of isotherm position at a corner.

With  $a_c = 0,417 \times 10^{-6} \text{ m}^2/\text{c}$ , the distance from the face  $x_{500,2}$  is given from Eqs (7.1)–(7.6) as:

$$x_{500,2} = \sqrt{\frac{t}{\exp\left[\frac{n_w - \sqrt{n_w^2 - (2n_w - 1)\frac{\Delta\theta}{\Delta\theta_g}}}{0,18(2n_w - 1)} + 4,5\right]}} \quad (7.56)$$

The loss of area at each corner  $A_{c,loss}$  is given by:

$$A_{c,loss} = 2(x_{500,2} - x_{500})^2 \quad (7.57)$$

and the total loss  $A_{c,loss,total}$  by:

$$A_{c,loss,total} = 8(x_{500,2} - x_{500})^2 \quad (7.58)$$

This represents a lower bound as the actual loss of area is less than this. The values of the loss in concrete area due isotherm rounding are given in Table 7.12.

Carry out the calculations twice, first not considering loss of area due to isotherm rounding and secondly with consideration of isotherm rounding.

*Ignoring rounding:*

The values of  $x_{500}$  are taken from Table 7.3.

To determine the temperatures in the reinforcement  $x(=y) = 35 + 25/2 = 47,5 \text{ mm}$ . The results of the calculation are given in Table 7.13.

**Table 7.12** Determination of loss in area due to isotherm rounding

$t$ (h)	$x_{500}$ (mm)	$x_{500,2}$ (mm)	$A_{c,loss,total}$ (mm <sup>2</sup> )
0,5	12	25	1352
1,0	23	43	3200
1,5	31	57	5408
2,0	39	69	7200
3,0	52	89	10 952
4,0	64	107	14 792

**Table 7.13** Determination of reinforcement temperatures and strength reduction factor

$t$ (h)	$n_w$	$\Delta\theta_g$ (°C)	$n_x$	Bar 1		Bar 2	
				$\theta$ (°C)	$k_s(\theta)$	$\theta$ (°C)	$k_s(\theta)$
0,5	0,887	822	0,162	138	0,962	239	0,861
1,0	0,938	925	0,287	269	0,831	451	0,548
1,5	0,957	1006	0,360	360	0,740	594	0,349
2,0	0,967	1049	0,412	429	0,557	690	0,124
3,0	0,977	1090	0,485	536	0,485	808	0,078
4,0	0,982	1133	0,536	617	0,295	899	0,060

**Table 7.14** Determination of load-carrying capacity

$t$ (h)	$x_{500}$ (mm)	$b_{fi}$ (mm)	$d_{fi}$ (mm)	$N_{c,fi}$ (kN)	$N_{s,fi}$ (kN)	$N_{Rd,fi14}$ (kN)
0,5	12	376	776	14,59	1,79	16,38
1,0	23	354	754	13,35	1,16	14,51
1,5	31	338	738	12,47	1,10	13,57
2,0	39	322	722	11,62	0,67	12,29
3,0	52	296	696	10,30	0,55	10,85
4,0	64	272	672	9,14	0,35	9,49

The results of the determination of load-carrying capacity are to be found in Table 7.14

As both  $\alpha_{cc}$  and  $\gamma_{mc}$  are equal to 1,0 in the fire limit state, the concrete capacity in compression effectively becomes:

$$N_{c,fi} = b_{fi}d_{fi}f_{ck} \quad (7.59)$$

The compression capacity of the reinforcement with  $\gamma_{m,s} = 1,0$  becomes:

$$N_{s,fi} = 1964 \times 500 (k_s(\theta_1) + k_s(\theta_2)) = 982\,000 (k_s(\theta_1) + k_s(\theta_2)) \quad (7.60)$$

The structural fire load  $N_{\bar{f},Ed}$  is 7,54 MN, thus column would last more than 4 h.

The results, considering rounding of the isotherms, are given in Table 7.15.

**Table 7.15** Load-carrying capacity allowing for isotherm rounding

$t$ (h)	$x_{500}$ (mm)	$b_{fi}$ (mm)	$d_{fi}$ (mm)	$A_{c,loss,total}$ (mm <sup>2</sup> )	$N_{c,fi}$ (kN)	$N_{s,fi}$ (kN)	$N_{Rd,fi}$ (kN)
0,5	12	376	776	1352	14,52	1,79	16,31
1,0	23	354	754	3200	13,19	1,16	14,35
1,5	31	338	738	5408	12,20	1,10	13,30
2,0	39	322	722	7200	11,26	0,67	11,83
3,0	52	296	696	10 952	9,75	0,55	10,30
4,0	64	272	672	14 792	8,40	0,35	8,75

As both  $\alpha_{cc}$  and  $\gamma_{mc}$  are equal to 1,0 in the fire limit state, the concrete capacity in compression effectively becomes:

$$N_{c,fi} = (b_{fi}d_{fi} - A_{c,loss,total})f_{ck} \quad (7.61)$$

The compression capacity of the reinforcement is determined using Eq. (7.60).

The structural axial fire load  $N_{fi,Ed}$  is 7,54 MN, so the column would still last more than 4 h. It should be noted the effect of corner rounding is not significant until around 2 h, and even at 4 h the axial capacity is only reduced by around 8%.

(b) Zone method

Use 50 mm wide slices (i.e. four per half width). Note, as the number of strips is even the mean concrete temperature at the centre will need calculation separately. The heat transfer is considered through the narrower dimension of 400 mm and the results are given in Table 7.16.

**Table 7.16** Concrete zone temperatures and strength reduction factors

$t$ (h)	$x = 25$ mm		$x = 75$ mm		$x = 125$ mm		$x = 175$ mm		$x = 200$ mm	
	$\theta$ (°C)	$k_c(\theta)$								
0,5	385	0,765	41	1,00	20	1,00	20	1,00	20	1,00
1,0	516	0,576	128	0,986	21	1,00	20	1,00	20	1,00
1,5	620	0,420	201	0,949	48	1,00	20	1,00	20	1,00
2,0	689	0,317	268	0,883	82	1,00	22	1,00	20	1,00
3,0	773	0,191	371	0,779	139	0,981	50	1,00	27	1,00
4,0	842	0,121	452	0,672	198	0,951	85	1,00	52	1,00

**Table 7.17** Determination of reinforcement temperatures and strength loss

$t$ (h)	$D + E$ (°C)	$\xi_{\theta,x} n_x$	Bar 1		Bar 2	
			$\theta$ (°C)	$k_s(\theta)$	$\theta$ (°C)	$k_s(\theta)$
0,5	750	0,189	162	0,938	277	0,823
1,0	820	0,338	297	0,803	481	0,535
1,5	910	0,414	397	0,703	618	0,293
2,0	960	0,469	470	0,540	709	0,098
3,0	1010	0,546	571	0,403	822	0,076
4,0	1060	0,594	650	0,218	905	0,059

Strictly for the point  $x = 200$ , the heat flow is bi-directional, but considering uniaxial flow is satisfactory as the temperature rises are small (Table 7.16).

The mean concrete strength reduction factor  $k_{c,m}$  is given by

$$k_{c,m} = \frac{1 - \frac{0,2}{n}}{n} \sum_1^4 k_c(\theta_i) = \frac{1 - \frac{0,2}{4}}{4} \sum_1^4 k_c(\theta_i) = 0,2375 \sum_1^4 k_c(\theta_i) \quad (7.62)$$

The temperatures and strength reduction factors are given in Table 7.17 (noting the centroid of the reinforcement is at 47,5 mm from the surface).

As  $k_c(\theta_M) = 1,0$  for all cases, Eq. (7.52) reduces to:

$$a_z = w \left[ 1 - k_{c,m}^{1,3} \right] = 200 \left[ 1 - k_{c,m}^{1,3} \right] \quad (7.63)$$

The determination of the load-carrying capacity using Eqs (7.59) and (7.60) is carried out in Table 7.18.

Using the zone method, the column would just last 4 h as  $N_{Ed,fi} = 7,54$  MN.

#### 7.4 COMPARISONS BETWEEN THE METHODS OF CALCULATION

For the three examples carried out herein, the zone method would appear slightly more conservative than the 500°C isotherm method, although this may in part be due to the different methods of calculating temperature rise as the method derived by Hertz produces slightly higher temperatures than derived by Wickström.

**Table 7.18** Determination of load-carrying capacity

$t$ (h)	Strips 1-4							
	$\sum k_c(\theta_i)$	$k_{c,m}$	$a_z$ (mm)	$b_{fi}$ (mm)	$d_{fi}$ (mm)	$N_{c,fi}$ (kN)	$N_{s,fi}$ (kN)	$N_{Rd,fi}$ (kN)
0,5	3,765	0,894	27	346	746	12,91	1,73	14,64
1,0	3,562	0,846	39	322	722	11,62	1,31	12,93
1,5	3,369	0,800	50	300	700	10,50	0,98	11,48
2,0	3,200	0,760	60	280	680	9,52	0,63	10,15
3,0	2,951	0,701	74	252	652	8,22	0,47	8,69
4,0	2,744	0,652	85	230	630	7,25	0,27	7,54

## 7.5 DESIGN AND DETAILING CONSIDERATIONS

### 7.5.1 Shear

For simply supported or continuous reinforced concrete construction, shear is rarely a problem (Krampf, undated). However, this will not be the case for pre-stressed concrete due to the moments induced in the section by the pre-stress. Bobrowski and Bardhan-Roy (1969) indicated that the critical section for shear was between 0,15 and 0,2L from the support, where  $L$  is the span. Shear is unlikely to be critical in conventional pre-cast pre-stressed concrete floor units (Lennon, 2003; van Acker, 2003/4; Fellingner, 2004) provided the pre-cast units are constrained to act as a diaphragm by being adequately tied in the plane of the floor. The tests reported by Lennon (2003) were to a natural fire of a time equivalent of approximately 1 h and indicated no spalling.

### 7.5.2 Bond

This also is generally not a problem even though bond strengths are severely reduced in a fire. The problem is more likely to be worse in pre-stressed concrete construction where bond in the anchorage length is needed to transfer the pre-stress force into the concrete. However, there appears to have been few, if any, failures in pre-stressed concrete directly attributable to loss in bond. It is not a general practice to check bond strengths in fire design. Fellingner (2004) indicates it can be considered a good practice to insulate floor units over the transfer length of the pre-stressing.

### 7.5.3 Spalling

Spalling occurs in one of two forms in a fire. The first is explosive spalling which occurs very early in a fire and is likely to lead to loss of cover to the main reinforcing and hence to more rapid rises in temperature and resultant strength loss leading to reduced fire performance. The second form is known as sloughing, whereby the concrete gradually comes away due to loss of effective bond and strength loss. This mode tends to occur toward the end of a fire or late on in the standard furnace test and is rarely critical. The magnitude of the effects of spalling is demonstrated both by actual test results and computer simulation. Results are given by Aldea, Franssen and Dotreppe (1997) (quoted in Table 3.1) and Purkiss, Morris and Connolly (1996) who recorded the results from two sets of tests carried out by the Fire Research station 1964–1976. Most of the columns suffered a loss of around 30% of the cross-sectional area and failed to achieve levels of fire endurance that would have been anticipated from relevant design guides. A computer simulation (Mustapha, 1994; Purkiss and Mustapha, 1995) indicates that a loss of cross-sectional area can lead to reduction of fire endurance of around 40–50%.

The exact mechanism of explosive spalling is still not understood, but it is affected by the following factors (Malhotra, 1984; Connolly, 1995, 1997):

#### 7.5.3.1 *Moisture content*

A concrete with a high moisture content is more likely to spall since one of the possible mechanisms of spalling is due to the build up of high vapour pressures near the surface causing tensile failures in the concrete caused by moisture clog (Shorter and Harmathy, 1965). However, it is now recognized that the critical isotherm for pore pressure build up is the 200°C isotherm and not the 100°C (Khalafallah, 2001). The blanket limit of a moisture content of 3%, below which EN 1992-1-2 indicates spalling will not occur, should be questioned. The original proposal by Meyer-Ottens (1975) also suggested stress limits.

#### 7.5.3.2 *Concrete porosity and permeability*

A more porous concrete, and therefore one with a high permeability, will allow the dissipation of vapour pressure, and thus relieve any build up within the section. However, it must be pointed out that a porous concrete will give a poor performance with respect to durability. It has also become clear that it is a combination of moisture content and permeability is critical (Tenchev and Purnell, 2005). This is indicated in Fig. 7.6 from Techev and Purnell. The values of water content  $W$  (in Fig. 7.6) are defined in respect of an initial water content of 80 kg/m<sup>3</sup> at  $W = 50\%$ . The water

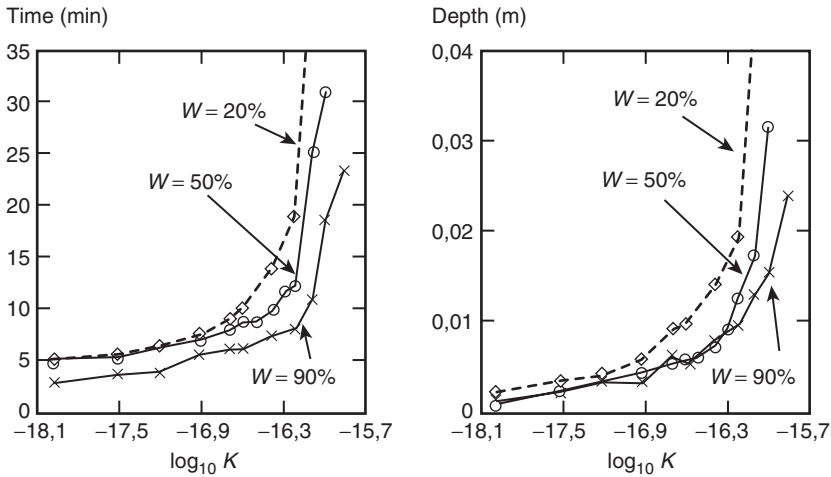


**Figure 7.6** Time and depth of spalling as function of permeability  $K$  ( $\text{m}^2$ ) for three levels of initial free water content  $\rho_L$ . (Tenchev and Purnell, 2005, by permission).

content of  $80 \text{ kg/m}^3$  is equivalent to a percentage moisture content by weight of 3,3. It is possible for a homogenous concrete to determine pore pressures using a coupled heat and mass transfer model (Tenchev, Li and Purkiss, 2001a, b; Tenchev *et al.*, 2001) and as a result to predict levels and times to spalling. The following results are given in Tenchev, Purkiss and Li (2001c). The time to spalling  $t_{spall}$  and the depth of spalling  $x_{spall}$  are given by:

$$t_{spall} = (382 - 3,34S + 0,00538S^2 - 0,00054S^3)p_{or} \quad (7.64)$$

$$x_{spall} = (1,09 - 0,0085S)p_{or} \quad (7.65)$$

where  $p_{or}$  is the porosity of the concrete and  $S$  is the initial water saturation in per cent. In deducing Eqs (7.64) and (7.65), it has been assumed that an initial porosity of 0,08 corresponds to an initial permeability of  $8 \times 10^{-17} \text{ m}^2$ .

### 7.5.3.3 Stress conditions

From evidence of fire tests and observations in fires, it has been noted that spalling is likely to be more severe in areas where the concrete cross section is in compression, i.e. areas of hogging moments in beams or

slabs, or in columns. This can partly be explained by the fact that in areas of compressive stresses, cracks cannot open up to relieve internal pressures. This does not mean that spalling cannot occur in areas of sagging moments where tensile cracks exist, since it is possible that pressure build up will still occur as in general tension cracks are discrete and not part of a continuum.

#### **7.5.3.4 Aggregate type**

The evidence available suggests that the aggregate most likely to give spalling is siliceous aggregate, with limestone producing less spalling and lightweight concrete the least. This is likely to be linked to the basic porosity of the aggregate, in that siliceous aggregate is impermeable compared to the others and that moisture transport has to occur through the mortar matrix. However, there is now some evidence that limestone and lightweight aggregates may give problems, especially in younger concretes as the pore structure of the aggregate may provide convenient reservoir storage for free water (Connolly, 1995).

#### **7.5.3.5 Section profile and cover**

There is some evidence to suggest that sharp profiles will produce more spalling than rounded or chamfered edges. Spalling is also exacerbated in thin sections, partly since the depth of spalling is a greater proportion of the section dimension and hence proportionally worse, and partly due to the fact that there is less of a cool reservoir for any moisture to migrate toward (Khalafallah, 2001).

High covers are also likely to produce greater amounts of spalling. Thus, design codes frequently place restrictions when high covers are needed at high fire resistance periods in order to maintain low temperatures in the reinforcing. These restrictions often concern the placement of a light mesh with 4 mm wires at a spacing of 100 mm at the surface of the concrete cover when the axis distance exceeds 70 mm, in order to retain the cover (EN 1992-1-2). In many cases this supplementary mesh is difficult to place, and indeed on site it is often omitted, and tests have shown that even with high covers it is not absolutely necessary to give fire resistance periods of up to 4 h (Lawson, 1985).

#### **7.5.3.6 Heating rate**

The higher the heat flux, the less chance pore pressures have to dissipate to the relatively cool internal regions of a concrete element. The rate of heating is therefore critical to an assessment of the likelihood of spalling. A hydrocarbon-type curve will therefore be far more critical than a cellulosic-type fire. The influence of heating rate

was demonstrated in tests on high strength concrete columns by Ali, O'Connor and Abu-Tair (2001) who demonstrated that the level of spalling was lower at low heating rates compared to high rates, and moreover that this effect appeared not to depend on load level. The high heating rate in the tests corresponded to BS 476 Part 20 with the low heating rate corresponding to BS 476 up to a temperature of around 300°C and then approximately linear with a rate of 75°C/min.

#### 7.5.3.7 Concrete strength

In spite of the above, normal strength concretes ( $f_{ck} \leq 60$  MPa) may not spall. However, if a concrete although designed as normal strength has a much higher strength than that designed for, problems may ensue. In the Cardington fire test on the concrete frame structure, the floor slab with flint aggregate was designed to be Grade C30/37. The actual strength at the time of test was 61 MPa (cube) or approximately 50 MPa (cylinder). With a moisture content of 3,8% and a permeability of  $6,75 \times 10^{-17}$  m<sup>2</sup>, the slab suffered severe spalling in the test (Bailey, 2002). The problems are exacerbated for high strength concretes.

#### 7.5.4 High strength concrete and self-compacting concrete

These concretes can produce worse symptoms of spalling as the pore structure is such that the porosity is lower (i.e. the permeability is lower), therefore the build up of pore pressures is much greater. The higher tensile strengths of such concretes do not remove the problem as tiny pores will act as stress raisers and hence reduce the effective tensile strength.

EN 1992-1-2 allows a number of methods to reduce the effect of spalling on high strength concrete. However, the most effective is to add 2% of polypropylene fibres to the concrete (Lennon and Clayton, 1999; Clayton and Lennon, 2000; Boström, 2002, 2004; Persson, 2003; Jansson and Boström, 2004). It is not recommended to use steel fibres to attempt to control spalling as Hertz (1992) found they had little or no effect.

#### 7.5.5 Detailing

Where beams and slabs are designed to act as continuous members in a fire or where advantage, as in Example 7.1, is taken of anti-crack steel to give continuity in a fire but not at ambient, then it is absolutely essential that the hogging reinforcement is detailed so that anchorage

forces needed to generate those hogging moments are capable of being sustained. It is thus essential that such reinforcement should be fully anchored beyond the point of contraflexure. For continuous members, the ISE/Concrete Society Report (1978) and EN 1992-1-2 both give detailing requirements which ought to be adhered to.

# 8 Design of steel elements

---

The determination of the thermal response and the structural response may be decoupled in a similar manner to that adopted in the design of concrete elements. The calculations may be simplified even further for steelwork as the temperature gradient across a member may be neglected and as there is no transient strain component; it is possible to use empirically modified steady state stress–strain data to allow for the effects of classical creep. As the thermal properties of steel are sensibly independent of the steel strength it is also possible to utilize empirical equations to determine the temperature rise within an element. The simplifications due to thermal gradient and stress behaviour mean that it is possible to consider calculation methods for steelwork over a broader base than concrete.

This chapter covers both the calculation of temperatures within an element and the methods by which the load-carrying capacity at elevated temperatures may be determined.

## 8.1 CALCULATION OF TEMPERATURES

### 8.1.1 Basic principles

As stated above, it is possible to ignore the effect any thermal gradient through the member which means that the temperature rise is entirely a function of time. Account is however taken of the proportion of the element exposed to the effects of the fire, i.e. a column or stanchion exposed on four sides or a beam element on three sides.

Since the temperature régime is independent of the spatial coordinate system, the Fourier heat diffusion is much simplified. The resultant heat flow  $\dot{h}_{net}$  is now given by:

$$\dot{h}_{net} = KF (\theta_t - \theta_{a,t}) \quad (8.1)$$

where  $K$  is the coefficient of total heat transfer,  $F$  is the surface area of the element exposed to the fire,  $\theta_{a,t}$  is the temperature of the steel and  $\theta_t$  is the gas temperature at time  $t$ .

The coefficient of total heat transfer has three components due to convection, radiation and insulation, respectively. A full discussion of the evaluation of the convection and radiation boundary conditions is given in Chapter 6.

However, for steelwork there are three components (including that due to the insulation). Each of the three components of the heat flow boundary conditions may be discussed in turn:

(1) Convection ( $\alpha_c$ )

This mode other than in the very early stages of a fire is not dominant and  $\alpha_c$  may be taken as  $25 \text{ W/m}^2\text{C}$  for cellulosic fires and  $50 \text{ W/m}^2\text{C}$  for hydrocarbon fires;

(2) Radiation ( $\alpha_r$ )

This is calculated using the Stefan–Boltzmann law for radiation

$$\alpha_{cr} = \phi \left( \frac{5,67 \times 10^{-8} \varepsilon_{res}}{(\theta_g + 273) - (\theta_a + 273)} \right) \left( (\theta_g + 273)^4 - (\theta_a + 273)^4 \right) \quad (8.2)$$

where  $\phi$  is the configuration factor which conservatively takes a value of unity and  $\varepsilon_{res}$  is the resultant emissivity which may be taken as  $\varepsilon_f \varepsilon_m$ , where  $\varepsilon_f$  is the emissivity of the fire compartment and  $\varepsilon_m$  is the surface emissivity. For all furnace tests, the emissivity of the fire compartment  $\varepsilon_f$  equals 1,0, and for steel (and concrete) the surface emissivity  $\varepsilon_m$  equals 0,7, thus the resultant emissivity  $\varepsilon_{res}$  is also 0,7.

(3) Insulation

This is given by  $d_p/\lambda_p$ , where  $d_p$  is the thickness of the insulation (m) and  $\lambda_p$  is the effective thermal conductivity of the insulation ( $\text{W/m}^\circ\text{C}$ ). The effective thermal conductivity of the insulation is temperature dependant, but it is a usual practice to adopt a constant value which is correct at around  $550^\circ\text{C}$ .

The total coefficient of heat transfer  $K$  is given by:

$$K = \frac{1}{\frac{1}{\alpha_c + \alpha_r} + \frac{d_p}{\lambda_p}} \quad (8.3)$$

The rate of heat flow into the element may also be written in incremental form as:

$$\dot{h}_{net} = c_a \rho_a V_i \frac{\Delta \theta_{a,t}}{\Delta t} \quad (8.4)$$

where  $c_a$  is the specific heat of steel,  $\rho_a$  is the density of steel and  $V_i$  is the volume per unit length.

Equating the values of heat flow in Eqs (8.1) and (8.4) give:

$$\Delta \theta_{a,t} = \frac{K}{c_a \rho_a} \frac{F}{V_i} (\theta_t - \theta_{a,t}) \Delta t \quad (8.5)$$

Changing notation from  $F/V_i$  to  $A_m/V$  gives Eq. (8.5) as:

$$\Delta \theta_{a,t} = \frac{K}{c_a \rho_a} \frac{A_m}{V} (\theta_t - \theta_{a,t}) \Delta t \quad (8.6)$$

The calculation of the heated perimeter per unit volume of steelwork  $A_m/V$  is considered in section 8.1.6.

Modifications to Eq. (8.6) may now be made to deal with the specific cases of uninsulated and insulated steelwork.

### 8.1.2 Heat flow in uninsulated steelwork

With no insulation, Eq. (8.6) reduces to:

$$\Delta \theta_{a,t} = \frac{\alpha_c + \alpha_r}{c_a \rho_a} \frac{A_m}{V} (\theta_t - \theta_{a,t}) \Delta t \quad (8.7)$$

where  $\theta_{a,t}$  is the steel temperature,  $\theta_t$  is the gas temperature at time  $t$  and  $A_m/V$  is the exposed surface area per unit volume.

EN 1993-1-2 cl 4.2.5.1 (5) indicates that  $\Delta t$  should not exceed 5 s. However, this is likely to be conservative and Eq. (8.11) should be noted. Example 8.1 indicates the difference between using a  $\Delta t$  of 5 s and a value calculated from Eq. (8.11). The use of Eq. (8.7) is demonstrated in Examples 8.1 and 8.2.

### 8.1.3 Heat flow in insulated steelwork

In the early work published by the ECCS (1983, 1985) the heat flow to insulated steelwork was subdivided into the cases where the insulation had either negligible or substantial heat capacity. The reason for this subdivision was that the equation used for calculations where the insulation had substantial heat capacity was unstable when the other situation was operative. It was later shown by Melinek and Thomas (1987) and Melinek (1989) that the ECCS method for heavy insulation could not be justified on theoretical grounds. However, for historical completeness the ECCS method is included.

#### 8.1.3.1 ECCS method of calculation

As indicated above, both the cases need consideration. The first is where the insulation has negligible heat capacity as it is either relatively thin or dry. The external face of the steelwork may then be considered to have the same temperature as the furnace gases. The second case is where the insulation has substantial heat capacity or there may also be a substantial moisture content. The insulation temperature can then be taken as the mean of the steel temperature and the gas temperature.

The insulation is deemed to have a substantial heat capacity when the parameter  $\Phi$  is greater than 0,50, where  $\Phi$  is defined by:

$$\Phi = \frac{c_p \rho_p}{c_a \rho_a} d_p \frac{A_m}{V} \quad (8.8)$$

where  $c_p$  is the specific heat of the insulation and  $\rho_p$  its density.

In both these cases, the heat transfer term due to the insulation is dominant and thus the component of the total heat transfer coefficient due to convection and radiation may be neglected and  $K$  can be taken equal to  $\lambda_p/d_p$ . The derivation of the European Community for Coal and Steel (ECCS) equations Eqs (8.9) and (8.10) is given in Malhotra (1982a).

#### (1) Heat flow in insulated members with negligible heat capacity

In this case Eq. (8.6) is rewritten as:

$$\Delta\theta_{a,t} = \frac{\lambda_p}{c_a \rho_a} \frac{A_m}{V} (\theta_t - \theta_{a,t}) \quad (8.9)$$

(2) Heat flow in members with substantial heat capacity

In this case Eq. (8.6) is modified to:

$$\Delta\theta_{a,t} = \frac{\lambda_p}{\bar{d}_p} \frac{A_m}{c_a \rho_a V} \frac{(\theta_t - \theta_{a,t}) \Delta t}{1 + \frac{\Phi}{2}} - \frac{\Delta\theta_t}{1 + \frac{2}{\Phi}} \quad (8.10)$$

Note, the original notation of the ECCS equations has been modified to agree with EN 1993-1-2 and EN 1994-1-2.

The ECCS rules give the following equation to determine the critical value of  $\Delta t$  to ensure convergence of the finite difference form of the heat transfer equation

$$\Delta t \leq \frac{25\,000}{\frac{A_m}{V}} \quad (8.11)$$

### 8.1.3.2 EN 1993-1-2 approach

EN 1993-1-2 (and EN 1994-1-2) use the method derived by Wickström (1985b) with the governing equation written as:

$$\Delta\theta_{a,t} = \frac{\lambda_p}{\bar{d}_p} \frac{A_m}{c_a \rho_a V} \frac{(\theta_t - \theta_{a,t}) \Delta t}{1 + \frac{\Phi}{3}} - \left( e^{\left(\frac{\Phi}{10}\right)} - 1 \right) \Delta\theta_t \quad (8.12)$$

EN 1993-1-2 places a limit on the value of  $\Delta t$  as 30 s (cl 4.2.3.2). Wickström, however, suggests that the limit on  $\Delta t$  should be taken as:

$$\Delta t \leq \frac{c_a \rho_a V}{\lambda_p A_m} \left( 1 + \frac{\Phi}{3} \right) < 60 \text{ s} \quad (8.13)$$

Wickström also suggests that a time shift  $\bar{t}$  needs to be introduced at the commencement of heating to allow for the thermal capacity of the insulation and thus improve the accuracy of Eq. (8.12). This time shift is given by:

$$\bar{t} = c_a \rho_a \frac{V}{A_m} \frac{d_p}{\lambda_p} \left( 1 + \frac{\Phi}{3} \right) \frac{\Phi}{8} \quad (8.14)$$

Melinek and Thomas (1987) derive the time shift term differently and give the following equation:

$$\bar{t} = c_a \rho_a \frac{V}{A_m} \frac{d_p}{\lambda_p} \left( 1 + \frac{\Phi}{3} \right) \left( \frac{\Phi}{2\Phi + 6} \right) \quad (8.15)$$

ENV 1993-1-2 makes no direct reference to the time shift to allow for the thermal capacity of the insulation.

The heat flow calculations for an insulated section are covered in Example 8.3.

It should be noted that the calculations for both uninsulated and insulated sections are best performed on a spreadsheet, as is done for the examples in this chapter and the next.

#### 8.1.4 Effect of moisture

As mentioned above, the effect of moisture in the insulation is to slow down the rate of temperature rise and will cause a dwell in temperature rise around 100°C as the water is vapourized. There are two approaches that may be used to deal with this effect.

The first is to use a moisture-dependant effective density for the insulation in the temperature calculations. The second is to introduce a dwell, or delay time,  $t_v$  when the steel temperature reaches 100°C. The latter approach is indicated in EN 1993-1-2, although no explicit method is included but reference is made to EN 13381-4.

##### 8.1.4.1 Effective density of insulation

The effective density of the insulation  $\rho'_p$  is given by Eq. (8.16)

$$\rho'_p = \rho_p (1 + 0,03p) \quad (8.16)$$

where  $p$  is the moisture content in per cent by weight.

##### 8.1.4.2 Delay time

The delay time  $t_v$  in minutes may be calculated from the following equation (ECCS, 1983):

$$t_v = \frac{0,2p\rho_p d_p^2}{\lambda_p} \quad (8.17)$$

It is easier to use an effective density for the insulation than to employ a delay time as this is iterative as the time delay depends on the insulation thickness.

### 8.1.5 Empirical approach for the calculation of temperatures

Equations for such an approach have been derived from a study of experimental results.

#### 8.1.5.1 Bare steelwork

Twilt and Witteveen (1986) give the following equation for the temperature rise on bare steelwork

$$t_{fi,d} = 0,54 (\theta_{a,t} - 50) \left( \frac{A_m}{V} \right)^{-0,6} \quad (8.18)$$

where  $\theta_{a,t}$  is the temperature in the steel reached at a time  $t$  (min). Note that Eq. (8.18) only holds for  $10 \leq t_{fi,d} \leq 80$  min;  $400 \leq \theta_{a,t} \leq 600^\circ\text{C}$  and  $10 \leq A_m/V \leq 300 \text{ m}^{-1}$ .

#### 8.1.5.2 Protected steelwork

A similar curve fitting exercise on test results from the times to failure for steelwork protected with dry insulation found that the time to failure was dependant solely on the term  $(d_p/\lambda_p)(V_i/A_p)$  with the following resultant equation:

$$t_{fi,d} = 40 (\theta_{a,t} - 140) \left( \frac{d_p}{\lambda_p} \frac{V}{A_m} \right)^{0,77} \quad (8.19)$$

This equation was fitted to data that were determined from tests in which the insulation material was light. Thus when the insulation has substantial heat capacity, Eq. (8.18) takes the following form (Wickström, 1985b; Melinek and Thomas, 1987):

$$t_{fi,d} = 40 (\theta_{a,t} - 140) \left( \frac{d_p}{\lambda_p} \left( \frac{V}{A_m} + \frac{d_p \rho_p}{\rho_a} \right) \right)^{0,77} \quad (8.20)$$

Equation (8.19) can be rewritten as:

$$\frac{\rho_p}{\rho_a} \frac{1}{\lambda_p} d_p^2 + \frac{1}{\lambda_p} \frac{V}{A_m} d_p - \left[ \frac{t_{fi,d}}{40(\theta_{a,t} - 140)} \right]^{1,3} = 0 \quad (8.21)$$

or

$$d_p = \frac{-\frac{1}{\lambda_p} \frac{V}{A_m} + \sqrt{\left(\frac{1}{\lambda_p} \frac{V}{A_m}\right)^2 + 4 \frac{\rho_p}{\rho_a} \frac{1}{\lambda_p} \left[ \frac{t_{fi,d}}{40(\theta_{a,t} - 140)} \right]^{1,3}}}{2 \frac{\rho_p}{\rho_a} \frac{1}{\lambda_p}} \quad (8.22)$$

### 8.1.6 Calculation of $A_m/V$

The cross-sectional area  $V$  is always that of the basic steel section. The heated perimeter  $A_m$  will depend on the type of insulation, e.g. sprayed insulation or intumescent paint which is applied to the section profile or board insulation which boxes the section and on the number of sides of the member exposed to the effect of the fire. The calculation of  $A_m/V$  may either be performed using basic principles (Fig. 8.1) or may be determined from data tables such as those published by the Association of Specialist Fire Protection Contractors and Manufacturers (1993) or those in Wainman and Kirby (1988). The units of  $A_m/V$  are  $m^{-1}$  and usually expressed to the nearest  $5 m^{-1}$ .

### 8.1.7 Thermal properties of insulation materials

To apply this method, knowledge of the various thermal properties of the insulation materials is needed. Currently, specific values for any particular material may not be available. However in the absence of specific data, the generic data in Table 8.1 may be used (Malhotra, 1982a). Lawson and Newman (1996) give similar data.

Three examples on calculating temperature rise will be carried out, two on uninsulated steelwork and the other on insulated steelwork.

#### **Example 8.1: Temperature rise on unprotected steelwork exposed to the standard furnace curve**

Calculate the temperature–time response curve for a  $203 \times 203 \times 52$  UC heated to the standard furnace temperature–time curve for 30 min.

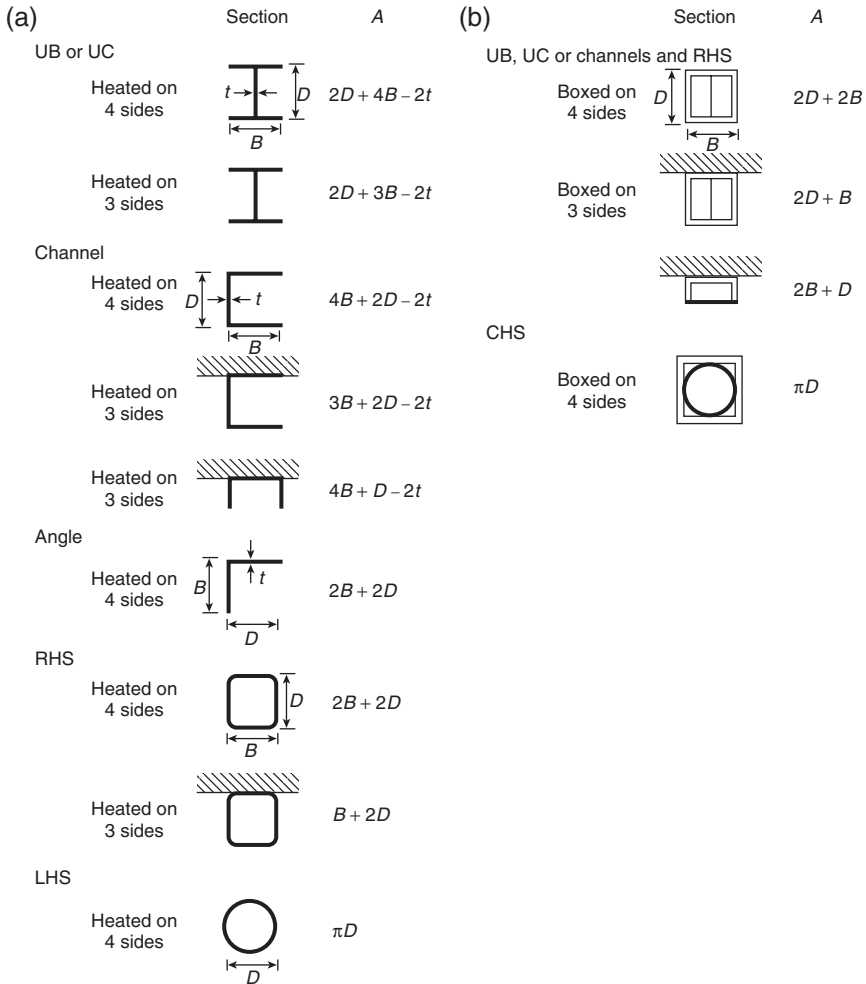


**Figure 8.1** Calculation of the values of the ratio of heated perimeter per unit volume ( $A/V$ ) for steel elements: (a) values of  $A$  for unprotected steelwork or steelwork protected by sprayed insulation or intumescent paint and (b) values of  $A$  for boxed sections.

For a bare  $203 \times 203 \times 52$  UC,  $A_m/V = 180 \text{ m}^{-1}$

The resultant emissivity  $\varepsilon_{res}$  is taken as 0,70.

Calculate maximum value of  $\Delta t$  from Eq. (8.11),

$$\Delta t = 25\,000 / (A_i/V_i) = 25\,000 / 180 = 139 \text{ s}$$

Use  $\Delta t = 2 \text{ min}$  (120 seconds) and a constant value of  $c_a = 600 \text{ J/kgC}$ .

**Table 8.1** Generic thermal data for insulation materials

Material	Density (kg/m <sup>3</sup> )	Specific heat (J/kgC)	Thermal conductivity (W/mC)	Moisture content (per cent by weight)
Sprayed mineral fibre	250–350	1050	0,1	1,0
Vermiculite slabs				
Vermiculite/ gypsum slabs	300 800	1200 1200	0,15 0,15	7,0 15,0
Gypsum plaster	800	1700	0,20	20,0
Mineral fibre sheets	500	1500	0,25	2,0
Aerated concrete	600	1200	0,30	2,5
Lightweight concrete	600	1200	0,80	2,5
Normal-weight concrete	2200	1200	1,70	1,5

Source: Malhotra (1982a), by permission

The heat transfer coefficient  $\alpha$  is given by:

$$\alpha = 25 + \frac{0,7 \times k_{sh} \times 0,56 \times 10^{-8}}{\theta_t - \theta_{a,t}} \left[ (\theta_t + 273)^4 - (\theta_{a,t} + 273)^4 \right]$$

The parameter  $k_{sh}$  is the shielding parameter (equivalent to the configuration factor  $\phi$  in Eq. (8.2)). The value of  $k_{sh}$  will initially be set equal to 1.

The governing equation for this case is Eq. (8.7) which with numerical values substituted for  $c_a$ ,  $\rho_a$ ,  $A_i/V_i$  and  $\Delta t$  becomes

$$\begin{aligned} \Delta\theta_{a,t} &= \frac{\alpha}{c_a \rho_a} \frac{A_m}{V} (\theta_t - \theta_{a,t}) \Delta t \\ &= \frac{\alpha}{600 \times 7850} 180 (\theta_t - \theta_{a,t}) 120 = \frac{\alpha}{218} (\theta_t - \theta_{a,t}) \end{aligned}$$

At  $t = 0$ , the base temperature is taken as 20°C.

The gas temperature  $\theta_t$  is given by the standard curve

$$\theta_t = 20 + 345 \log(8t + 1)$$

The values of  $\theta_t$ ,  $\alpha$ ,  $\theta_t - \theta_{a,t}$  and  $\Delta\theta_a$  are calculated at 1, 3, 5, 7 min etc. with the resultant temperature in the steel  $\theta_{a,t}$  being given at 0, 2, 4 min etc. The calculations are presented in Table 8.2. In addition to the calculations with  $\Delta t = 120$  s, the final calculated results with  $\Delta t = 5$  s as recommended by ENV 1993-1-2: cl 4.2.3.1 are given in Table 8.2. It will be noted that there is little difference between both sets of results.

Also, opportunity was taken to evaluate the effects of using the values of  $c_a$  which vary with temperature, Eqs (5.4)–(5.7), and separately the effect of the shielding factor  $k_{sh}$ .

For I sections, EN 1993-1-2 cl 5.2.5.1 (2) gives the shielding factor  $k_{sh}$  as:

$$k_{sh} = 0,9 \frac{\left[ \frac{A_m}{V} \right]_b}{\frac{A_m}{V}} \quad (8.23)$$

where  $[A_m/V]_b$  is the box value of the section factor.

For a  $203 \times 203 \times 52$  UC,  $[A_m/V]_b = 125 \text{ m}^{-1}$ , thus

$$k_{sh} = 0,9 \frac{\left[ \frac{A_m}{V} \right]_b}{\frac{A_m}{V}} = 0,9 \frac{125}{180} = 0,625$$

The final results from using  $k_{sh}$  with constant  $c_a$  and ignoring the shielding factor but incorporating variable  $c_a$  are also given in Table 8.2. The results are plotted in Fig. 8.2 together with the mean temperatures actually measured in a furnace test (Data Sheet 41 from Wainman and Kirby, 1988). The actual test was terminated at 23 min with an average temperature in the column of  $688^\circ\text{C}$ . The maximum temperature measured at 0,61 m up the column was  $723^\circ\text{C}$  in the flange and  $713^\circ\text{C}$  in the web. It was noted that the furnace temperature was  $23^\circ\text{C}$  below that from the standard furnace curve.

The calculations with a constant specific heat of  $600 \text{ J/kg/}^\circ\text{C}$  gave  $788^\circ\text{C}$ . Calculations with variable specific heat of steel a temperature of  $761^\circ\text{C}$  was found at 23 min. The results from these calculations are also plotted in Fig. 8.2.

It should be noted that after around 20 min, the predicted temperatures are sensibly independent of assumptions. However, all the calculations

**Table 8.2** Bare steel results

Original calculations						$\Delta t = 5$ (°C)	Variable $c_a$ (°C)	$k_{sh} = 0,625$ (°C)
$t$ (min)	$\theta_t$ (°C)	$\alpha$ (W/m <sup>2</sup> C)	$\theta_t - \theta$ (°C)	$\Delta\theta_{a,t}$ (°C)	$\theta_{a,t}$ (°C)			
0					20	20	20	20
2	349	42,2	329	636	84	77	107	74
4	502	57,7	419	111	195	181	238	163
6	576	74,1	382	130	325	301	372	265
8	626	94,1	301	130	455	421	489	371
10	663	118	208	113	568	525	579	472
12	693	142	125	82	650	607	640	561
14	717	164	68	51	701	666	683	634
16	739	180	38	32	733	708	713	688
18	757	192	25	22	755	738	732	727
20	774	202	20	18	773	760	740	755
22	789	211	16	16	789	779	751	776
24	802	218	14	14	803	794	771	793
26	814	226	12	13	816	808	797	808
28	826	233	11	12	828	821	819	821
30	837	239	10	11	839	832	835	832
32	847	245	9	10	849	843	846	843

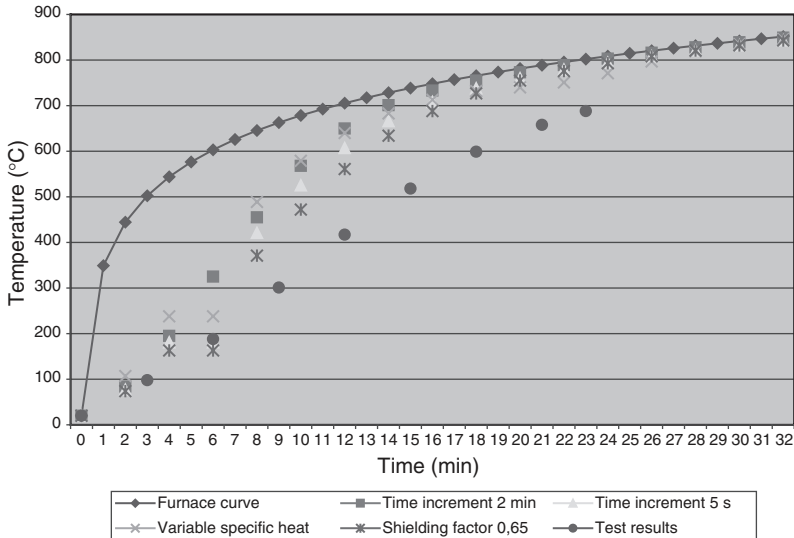


Figure 8.2 Response of unprotected steelwork.

predict temperatures higher than those in the test (Fig. 8.2) with a difference of around  $100^{\circ}\text{C}$ . If the assumption of constant specific heat be made, then a value of  $\varepsilon_{res}k_{sh} = 0,15$  would have to be employed. This would give a temperature of  $692^{\circ}\text{C}$  at 23 min. If  $k_{sh} = 0,625$ , then  $\varepsilon_{res}$  would have to be taken as  $0,24$ . This is not unreasonable if Fig. 6.1 (from Chitty *et al.*, 1992) is examined where resultant emissivities as low as  $0,2$  are required to give reasonable prediction of temperatures in columns.

### Example 8.2: Determination of the temperature response of bare steelwork to a parametric fire curve

Calculate the temperature–time response curve for a  $203 \times 203 \times 52$  UC heated in to the parametric temperature–time curve determined in Example 4.1 for both heating and cooling.

For a bare  $203 \times 203 \times 52$  UC,  $A_i/V_i = 180 \text{ m}^{-1}$

The resultant emissivity  $\varepsilon_{res}$  is taken as  $0,70$  (i.e. the shielding factor is ignored).

The recommended value of  $\Delta t$  of  $5 \text{ s}$  is used.

The governing equation is identical to that of Example 8.1.

The gas temperature  $\theta_t$  is given by the parametric fire curve of Example 4.1 which is plotted in Fig. 4.9.

The results are plotted in Fig. 8.3(a) where it is noted that after around a quarter of an hour the steel and fire temperatures are virtually indistinguishable. On the cooling section of the curve, the steel temperatures lag the fire temperature by around 2–3°C. At the maximum fire temperature the steel is around 0,5°C cooler. The results from the first 15 min of the calculations are plotted in Fig. 8.3(b).

**Example 8.3: Determination of the temperature response on an insulated specimen subjected to the standard furnace curve**

Determine the temperature history for a 203 × 203 × 46 UC with fire protection formed by 30 mm thick mineral fibre boarding encasing the column on all four sides (Fig. 8.4) using the heat transfer equations of ENV 1993-1-2 (Table 8.3).

Material data:

$$\lambda_p = 0.25 \text{ W/m}^\circ\text{C}, \rho_p = 500 \text{ kg/m}^3, p = 2\%, c_p = 1500 \text{ J/kg}^\circ\text{C},$$

$$A_p/V_i = 140 \text{ m}^{-1}, \rho_a = 7850 \text{ kg/m}^3 \text{ and } c_a = 600 \text{ J/kg}^\circ\text{C}$$

From Eq. (8.8)

$$\Phi = \frac{c_p \rho_p d_p A_m}{c_a \rho_a V} = \frac{1500 \times 500 (1 + 0,03 \times 2)}{600 \times 7850} 0,030 \times 140 = 0,709$$

and from Eq. (8.12)

$$\begin{aligned} \Delta\theta_{a,t} &= \frac{\lambda_p}{d_p} \frac{A_m}{c_a \rho_a V} \frac{(\theta_t - \theta_{a,t}) \Delta t}{1 + \frac{\Phi}{3}} - \left( e^{\left(\frac{\Phi}{10}\right)} - 1 \right) \Delta\theta_t \\ &= \frac{\frac{0,25}{0,030}}{600 \times 7850} 140 \frac{30 (\theta_t - \theta_{a,t})}{1 + \frac{0,709}{3}} - \left( e^{\frac{0,709}{10}} - 1 \right) \Delta\theta_t \\ &= 0,00601 (\theta_t - \theta_{a,t}) - 0,0735 \Delta\theta_t \end{aligned}$$

EN 1993-1-2 gives a recommended value of  $\Delta t$  of 30 s which is used in this example. The recommendation by Wickström is 60 s and Eq. (8.11) gives a  $\Delta t$  of 178,6 s (or in practice 3 min).

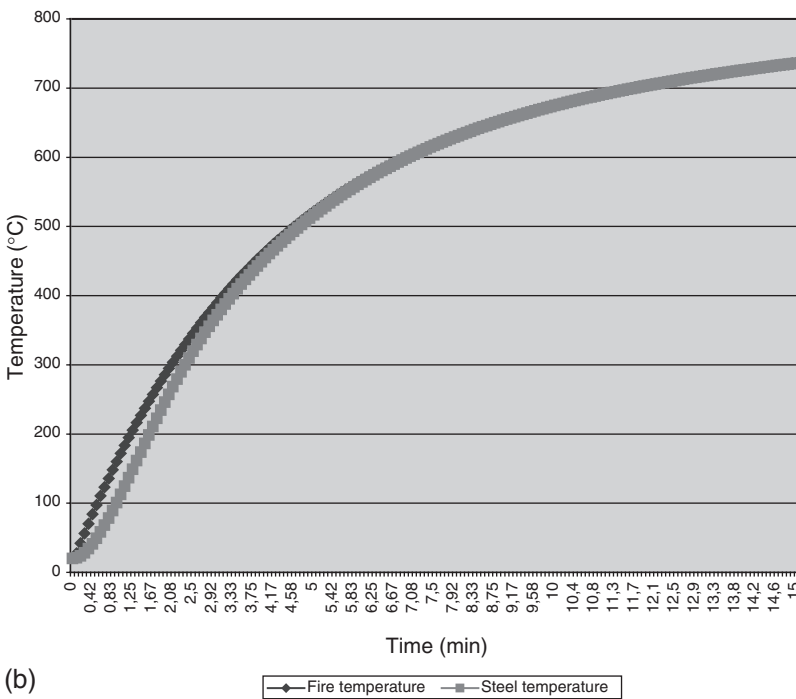
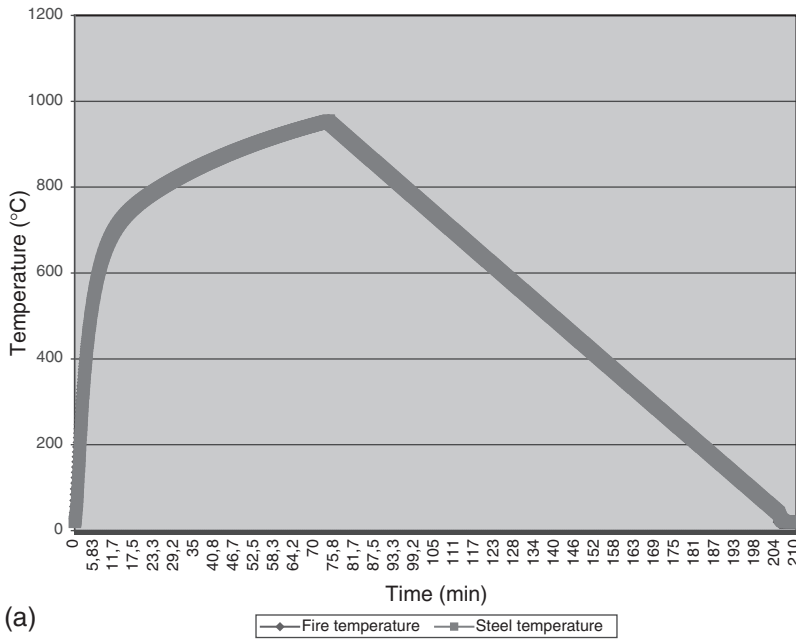
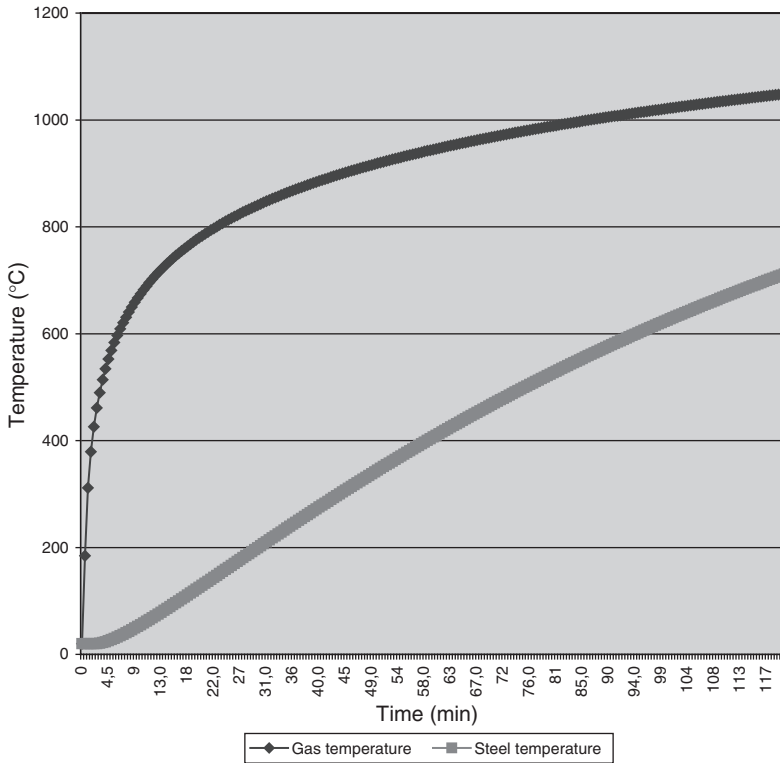


Figure 8.3 (a) Response of bare steelwork to a parametric fire curve and (b) response to a parametric curve for the first 15 min.



**Figure 8.4** Temperature response of a protected member.

As in Example 8.1 the reference temperature is taken as 20°C and the gas temperature  $\theta_t$  calculated from the standard furnace curve.

Note that in the early stages of heating the heat flux is adsorbed by the insulation and thus there appears to be negative heat transfer to the section with  $\Delta\theta_{a,t}$  taking values less than zero. These negative values have been ignored and set equal to zero when calculating the steel temperatures. Typical calculations for the start and end of the heating period are to be found in Table 8.3.

If the time shift calculations are carried out according to Eqs (8.14) and (8.15) a value of 6,9 min is obtained from the formulation proposed by Wickström and 7,5 min from that by Melinek and Thomas. These values are not significantly different, and thus the temperature rise at 120 min can be taken as the value reached in 113 min, i.e. approximately 7 min delay period. The results are plotted in Fig. 8.4.

**Table 8.3** Calculation of the temperature rise of protected steelwork exposed to the standard furnace curve (Example 8.3)

Time (s)	$\theta_t$ (°C)	$\theta_t - \theta_{a,t}$ (°C)	$\Delta\theta_{a,t}$ (°C)	$\theta_{a,t}$ (°C)
0				20,0
30	184,6	164,6	-11,1	20
60	311,6	291,6	-7,6	20,0
90	379,3	359,3	-2,8	20
120	425,8	405,8	-1,0	20,0
150	461,2	441,2	0	20,0
180	489,8	469,7	0,7	20,8
210	513,8	493,1	1,2	22,0
240	534,5	512,6	1,6	23,5
The calculation is continued to				
7080				703,6
7110	1046,2	344,6	2,0	705,7
7140	1046,8	343,2	2,0	707,7
7170	1047,5	340,4	2,0	709,7
7200	1048,7	339,1	2,0	711,7

Having established methods of determining the temperature rise in steelwork, it is now possible to consider the design of such members in a fire. It is convenient because of the different approaches used to consider non-composite and composite construction separately. Composite construction is where a second material, generally concrete, acts in

conjunction with the steelwork in such a manner that each carries part of the load. Concrete floor units sitting on the top flange of a beam are not acting compositely even though the presence of the floor units increases the carrying capacity of the beam by reducing the effect of lateral torsional buckling and by acting as a heat sink so reducing the temperatures attained in the steelwork. Composite steelwork is covered in the next chapter.

## **8.2 DESIGN OF NON-COMPOSITE STEELWORK**

Historically, the results from furnace tests on members loaded to their full design strengths led to the concept of a critical failure temperature of around 550°C for both columns and beams. The latter were tested with concrete slabs resting on the top flange and were non-composite. A research programme was set up in the mid-1980s to evaluate the effects of varying load patterns and partial or total shielding of the web and exposed flanges of members with no additional protection. This research showed that for certain categories of section, the temperatures were below those required to cause failure and that both shielding of the web and exposed flanges, which has the effect of inducing thermal gradients in the section and thus allowing a redistribution of carrying capacity from the hotter to the cooler parts of the section, and reducing the applied stresses had the effect of increasing the inherent fire resistance of unprotected steelwork (Kirby, 1986; Robinson and Latham, 1986; Robinson and Walker, 1987). The complete test data are given in Wainman and Kirby (1988, 1989). Results from unprotected beams and columns with partial or total shielding and varying loadings are given in Figs 8.5 and 8.6.

### **8.2.1 Determination of structural load in the fire limit state**

This follows an identical procedure to that for concrete (section 7.2.1) except that  $\eta_{fi}$  may be taken as 0,65.

### **8.2.2 EN 1993-1-2 approach for the determination of structural fire capacity**

#### **8.2.2.1 Background to the EuroCode method**

The method used here was first formulated in the ECCS recommendations (1983) and the ECCS design guide (1985). The original approach was to calculate the ratio of the required strength at elevated temperature to that at ambient in order to ensure the element would not collapse, thus for

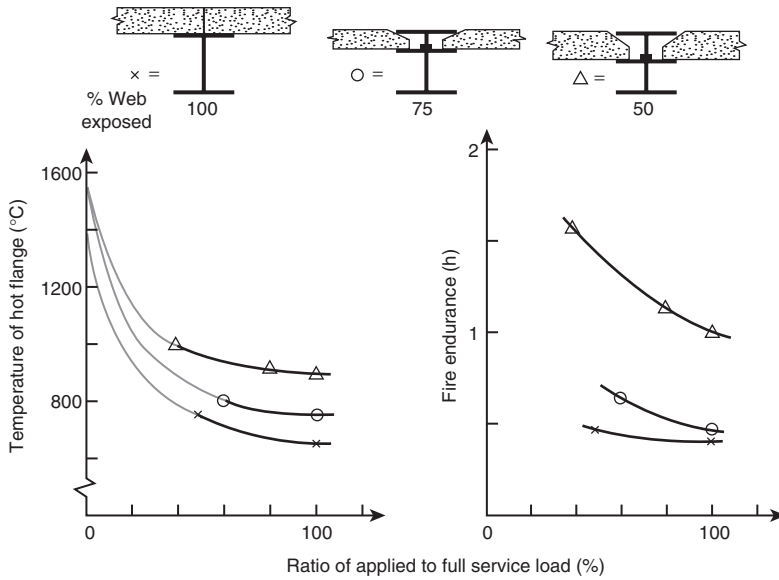


**Figure 8.5** Fire test performance of partially protected beams (Robinson and Latham, 1986, by permission).

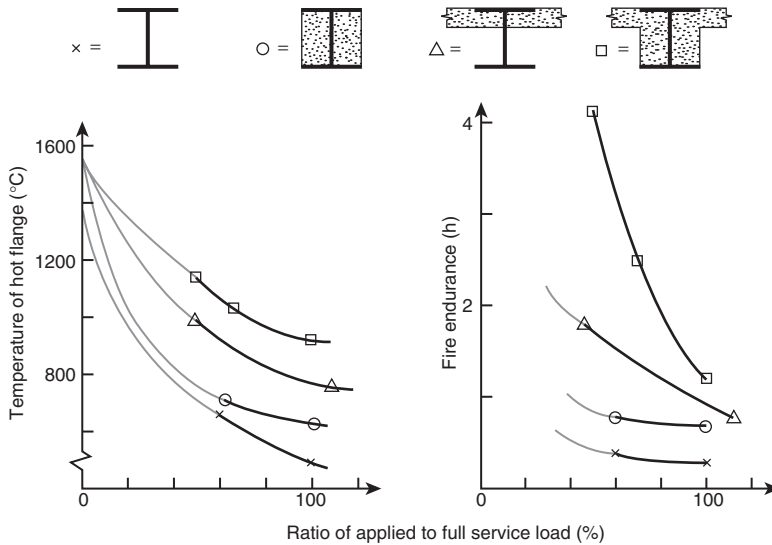


**Figure 8.6** Fire test performance of partially protected columns (Robinson and Latham, 1986, by permission).

beams designed elastically

$$k_{y,\theta} = \frac{f_{a\max,\theta_{cr}}}{f_{ay,20}} = \frac{\kappa}{\theta} \frac{W_{el}}{W_{pl}} \frac{q_{fi,d}}{q_{Sd,el}} \quad (8.24)$$

where  $f_{a\max,\theta_{cr}}/f_{ay,20}$  is the stress ratio ( $=k_{y,\theta}$ ),  $\kappa$  is a factor allowing for the non-uniform temperature distribution, geometric imperfections and strength variations,  $\theta$  is a factor, greater than unity, allowing for redistribution between the elastic ambient moment distribution and the plastic distribution under fire,  $W_{el}/W_{pl}$  is the ratio between the elastic and plastic section moduli (known as the shape factor), and  $q_{fi,d}/q_{Sd,el}$  is the ratio of the design load (action) in the fire to the elastic design load (action).

For beams designed plastically

$$k_{y,\theta} = \frac{f_{a\max,\theta_{cr}}}{f_{ay,20}} = \kappa \frac{q_{fi,d}}{q_{Sd}} \quad (8.25)$$

where  $q_{fi,d}/q_{Sd}$  is the ratio of the fire load (action) to the ultimate design load (action).

As a corollary it should be noted that a beam designed elastically has a greater reserve of strength when exposed to a fire than a beam designed plastically.

The basis behind the derivation of the parameter  $\kappa$  and the values thereof are given in Pettersson and Witteveen (1979/80) who showed how the variation in material strengths, temperature gradient both transversely and longitudinally and any structural imperfections affected the calculated strengths of members based on the simplifying assumption that these variations did not exist.

### 8.2.2.2 EuroCode methods

The EuroCode gives two methods for the design of steelwork members in a fire. The first method is to satisfy the load-carrying criterion and the second is a limiting, or critical, temperature approach.

#### (1) Load-carrying method

This can simply be stated as the satisfaction of the following criterion:

$$E_{fi,d} \leq R_{fi,d,t} \quad (8.26)$$

where  $E_{fi,d}$  is the design value of the internal force to be resisted and  $R_{fi,d,t}$  is the design resistance at time  $t$  and should be calculated in accordance with the principles of EN 1993-1-1.

## (a) Section classification

This should be carried out in accordance with EN 1993-1-1, except the value of  $\varepsilon$  is modified to allow for the effects of temperature increase to

$$\varepsilon = 0,85 \left[ \frac{235}{f_y} \right]^{0,5} \quad (8.27)$$

## (b) Tension members (cl 4.2.21)

With a uniform temperature distribution, the axial tensile capacity  $N_{fi,\theta,Rd}$  may be calculated as:

$$N_{fi,\theta,Rd} = k_{y,\theta} N_{Rd} \left[ \frac{\gamma_{M,1}}{\gamma_{M,fi}} \right] \quad (8.28)$$

Since  $\gamma_{M,1} = \gamma_{M,fi} = 1,0$ , Eq. (8.28) reduces to

$$N_{fi,\theta,Rd} = k_{y,\theta} N_{Rd} \quad (8.29)$$

where  $k_{y,\theta}$  is the normalized strength reduction at a temperature of  $\theta_a$  and  $N_{Rd}$  is the ambient design resistance.

For tension members with a non-uniform temperature distribution, the axial capacity may either be obtained by summing the contributions of incremental areas or conservatively using the maximum steel temperature reached and assuming constant temperature.

## (c) Compression members (Class 1, 2 and 3 cross section) (cl 4.2.3.2)

$$N_{b,fi,t,Rd} = \chi_{fi} A k_{y,\theta} \frac{f_y}{\gamma_{M,fi}} \quad (8.30)$$

where the buckling strength reduction factor  $\chi_{fi}$  is determined from

$$\chi_{fi} = \frac{1}{\phi_\theta + \sqrt{\phi_\theta^2 - \bar{\lambda}_\theta^2}} \quad (8.31)$$

with

$$\phi_{\theta} = 0,5 \left[ 1 + 0,65 \sqrt{\frac{235}{f_y} \bar{\lambda}_{\theta} + \bar{\lambda}_{\theta}^2} \right] \quad (8.32)$$

where the normalized slenderness ratio  $\bar{\lambda}_{\theta}$  is defined as

$$\bar{\lambda}_{\theta} = \bar{\lambda} \left[ \frac{k_{y,\theta}}{k_{E,\theta}} \right]^{0,5} \quad (8.33)$$

where  $k_{E,\theta}$  is the temperature-dependant reduction factor for Young's modulus, and  $\bar{\lambda}$  is the normalized slenderness ratio, except that buckling length for a continuous column at other than the top storey may be taken as 0,5 times the column length (0,7 for the top storey), provided the frame is braced and that the fire resistance of the compartments above and below have a resistance not less than that required for the column.

(d) Beams

- Class 1 or 2 section classification (cl 4.2.3.3)  
With a uniform temperature distribution, the moment capacity  $M_{fi,\theta,Rd}$  with no lateral torsional buckling may be calculated as:

$$M_{fi,\theta,Rd} = k_{y,\theta} M_{Rd} \left[ \frac{\gamma_{M,1}}{\gamma_{M,fi}} \right] \quad (8.34)$$

Since  $\gamma_{M,1} = \gamma_{M,fi} = 1,0$ , Eq. (8.34) reduces to

$$M_{fi,\theta,Rd} = k_{y,\theta} M_{Rd} \quad (8.35)$$

where  $k_{y,\theta}$  is the normalized strength reduction at a temperature of  $\theta_a$  and  $M_{Rd}$  is the ambient design resistance.

For flexural members with a non-uniform temperature distribution, the moment capacity may either be obtained by summing the contributions of incremental areas.

For non-uniform temperature distribution, the design moment of resistance  $M_{fi,t,d}$  may be determined from

$$M_{fi,t,Rd} = \frac{M_{fi,\theta,d}}{\kappa_1 \kappa_2} \quad (8.36)$$

where  $\kappa_1$  allows for non-uniform temperature distribution within the cross section and should be taken as 1,0 for a beam exposed on all four sides, 0,85 for a protected beam exposed on three sides with a composite or concrete slab on the fourth and 0,70 for an unprotected beam exposed on three sides with a composite or concrete slab on the fourth. The parameter  $\kappa_2$  should be taken as 1,0 except at the supports of a statically indeterminate beam when it should be taken as 0,85.

Where lateral torsional buckling can occur, then the moment capacity  $M_{b,fi,t,d}$  is given by

$$M_{b,fi,t,d} = \chi_{LT,fi} W_{pl,y} k_{y,\theta,com} \frac{f_y}{\gamma_{M,fi}} \quad (8.37)$$

where  $k_{y,\theta,com}$  is the strength reduction factor for the temperature in the compression flange (which can be conservatively based on the uniform temperature  $\theta_d$ ), and  $\chi_{LT,fi}$  is determined from

$$\chi_{LT,fi} = \frac{1}{\phi_{LT,\theta,com} + \sqrt{[\phi_{LT,\theta,com}]^2 - [\bar{\lambda}_{LT,\theta,com}]^2}} \quad (8.38)$$

with

$$\phi_{LT,\theta,com} = 0,5 \left[ 1 + 0,65 \sqrt{\frac{235}{f_y} \bar{\lambda}_{LT,\theta,com} + (\bar{\lambda}_{LT,\theta,com})^2} \right] \quad (8.39)$$

and

$$\bar{\lambda}_{LT,\theta,com} = \bar{\lambda}_{LT} \left[ \frac{k_{y,\theta,com}}{k_{E,\theta,com}} \right]^{0,5} \quad (8.40)$$

where  $k_{E,\theta,com}$  is the temperature-dependant reduction factor for Young's modulus for the compression flange, and  $\lambda_{LT}$  is the normalized lateral torsional buckling slenderness ratio.

- Class 3 (cl 4.2.3.4)  
These are dealt with exactly as Class 1 or 2 beams except that the moment capacity  $M_{Rd}$  is determined using the elastic section modulus  $W_{el}$  and not the plastic section modulus  $W_{pl}$ .
- Shear (Class 1,2 or 3)  
The design shear resistance  $V_{fi,t,d}$  is determined from

$$V_{fi,t,d} = k_{y,\theta,web} V_{Rd} \left[ \frac{\gamma_{M,1}}{\gamma_{M,fi}} \right] \quad (8.41)$$

where  $k_{y,\theta,web}$  is the strength reduction factor based on the temperature within the web.

- (e) Members subject to combined bending and axial compression.  
The design buckling resistance  $R_{fi,t,d}$  should satisfy the following interaction equations:

- Class 1 or 2

$$\frac{N_{fi,Ed}}{\chi_{min,fi} A k_{y,\theta} \frac{f_y}{\gamma_{M,fi}}} + \frac{k_y M_{y,fi,Ed}}{W_{pl,y} k_{y,\theta} \frac{f_y}{\gamma_{M,fi}}} + \frac{k_z M_{z,fi,Ed}}{W_{pl,z} k_{y,\theta} \frac{f_y}{\gamma_{M,fi}}} \leq 1,0 \quad (8.42)$$

$$\frac{N_{fi,Ed}}{\chi_{z,fi} A k_{y,\theta} \frac{f_y}{\gamma_{M,fi}}} + \frac{k_{LT} M_{y,fi,Ed}}{\chi_{LT,fi} W_{pl,y} k_{y,\theta} \frac{f_y}{\gamma_{M,fi}}} + \frac{k_z M_{z,fi,Ed}}{W_{pl,z} k_{y,\theta} \frac{f_y}{\gamma_{M,fi}}} \leq 1,0 \quad (8.43)$$

- Class 3

$$\frac{N_{fi,Ed}}{\chi_{min,fi} A k_{y,\theta} \frac{f_y}{\gamma_{M,fi}}} + \frac{k_y M_{y,fi,Ed}}{W_{el,y} k_{y,\theta} \frac{f_y}{\gamma_{M,fi}}} + \frac{k_z M_{z,fi,Ed}}{W_{el,z} k_{y,\theta} \frac{f_y}{\gamma_{M,fi}}} \leq 1,0 \quad (8.44)$$

$$\frac{N_{fi,Ed}}{\chi_{z,fi} A k_{y,\theta} \frac{f_y}{\gamma_{M,fi}}} + \frac{k_{LT} M_{y,fi,Ed}}{\chi_{LT,fi} W_{el,y} k_{y,\theta} \frac{f_y}{\gamma_{M,fi}}} + \frac{k_z M_{z,fi,Ed}}{W_{el,z} k_{y,\theta} \frac{f_y}{\gamma_{M,fi}}} \leq 1,0 \quad (8.45)$$

where

$$k_{LT} = 1 - \frac{\mu_{LT} N_{fi,Ed}}{\chi_{z,fi} A k_{y,\theta} \frac{f_y}{\gamma_{M,fi}}} \leq 1,0 \quad (8.46)$$

with

$$\mu_{LT} = 0,15 \bar{\lambda}_{z,\theta} \beta_{M,LT} - 0,15 \leq 0,9 \quad (8.47)$$

and

$$k_y = 1 - \frac{\mu_y N_{fi,Ed}}{\chi_{y,fi} A k_{y,\theta} \frac{f_y}{\gamma_{M,fi}}} \leq 3,0 \quad (8.48)$$

with

$$\mu_y = (1,2 \beta_{M,y} - 3) \bar{\lambda}_{y,\theta} + 0,44 \beta_{M,LT} - 0,29 \leq 0,8 \quad (8.49)$$

$$k_z = 1 - \frac{\mu_z N_{fi,Ed}}{\chi_{z,fi} A k_{y,\theta} \frac{f_y}{\gamma_{M,fi}}} \leq 3,0 \quad (8.50)$$

with

$$\mu_z = (2 \beta_{M,z} - 5) \bar{\lambda}_{z,\theta} + 0,44 \beta_{M,z} - 0,29 \leq 0,8 \quad (8.51)$$

Equations (8.46)–(8.51) are subject to the limit that  $\bar{\lambda}_{z,\theta} \leq 1,1$ .

Figure 4.2 of EN 1993-1-2 gives values of the equivalent moment factor  $\beta_M$  for various types of moment diagrams due to lateral in plane loading cases, and also for the case of end moments only where  $\beta_M$  is then given by

$$\beta_M = 1,8 - 0,7\psi \quad (8.52)$$

where  $\psi$  is the ratio between the end moments such that  $-1 > \psi > 1$ .

It should be noted there where lateral torsion buckling or strut buckling can occur, the procedure to determine the critical temperature in the member is iterative as the buckling coefficients are also temperature dependant. Where columns carry moments, this situation becomes worse in that some of the coefficients in the interaction equations are also temperature dependant.

The tabular data for  $k_{E,\theta}$  from Table 3.1 of EN 1993-1-2 are given by the following equations:

$$20^{\circ}\text{C} \leq \theta_a \leq 100^{\circ}\text{C}$$

$$k_{E,\theta} = 1,0 \quad (8.53)$$

$$100^{\circ}\text{C} \leq \theta_a \leq 500^{\circ}\text{C}$$

$$k_{E,\theta} = 0,6 - 0,4 \frac{\theta_a - 500}{400} \quad (8.54)$$

$$500^{\circ}\text{C} \leq \theta_a \leq 600^{\circ}\text{C}$$

$$k_{E,\theta} = 0,31 - 0,29 \frac{\theta_a - 600}{100} \quad (8.55)$$

$$600^{\circ}\text{C} \leq \theta_a \leq 700^{\circ}\text{C}$$

$$k_{E,\theta} = 0,13 - 0,18 \frac{\theta_a - 700}{100} \quad (8.56)$$

$$700^{\circ}\text{C} \leq \theta_a \leq 800^{\circ}\text{C}$$

$$k_{E,\theta} = 0,09 - 0,04 \frac{\theta_a - 800}{100} \quad (8.57)$$

$$800^{\circ}\text{C} \leq \theta_a \leq 1100^{\circ}\text{C}$$

$$k_{E,\theta} = 0,0225 - 0,0675 \frac{\theta_a - 1100}{300} \quad (8.58)$$

$$1100^{\circ}\text{C} \leq \theta_a \leq 1200^{\circ}\text{C}$$

$$k_{E,\theta} = 0,0225 \frac{1100 - \theta_a}{100} \quad (8.59)$$

The tabular data for  $k_{y,\theta}$  from Table 3.1 of EN 1993-1-2 are given by the following equations:

$$20^{\circ}\text{C} \leq \theta_a \leq 400^{\circ}\text{C}$$

$$k_{y,\theta} = 1,0 \quad (8.60)$$

$$400^{\circ}\text{C} \leq \theta_a \leq 500^{\circ}\text{C}$$

$$k_{y,\theta} = 0,78 - 0,22 \frac{\theta_a - 500}{100} \quad (8.61)$$

$$500^{\circ}\text{C} \leq \theta_a \leq 600^{\circ}\text{C}$$

$$k_{y,\theta} = 0,47 - 0,31 \frac{\theta_a - 600}{100} \quad (8.62)$$

$$600^{\circ}\text{C} \leq \theta_a \leq 700^{\circ}\text{C}$$

$$k_{y,\theta} = 0,23 - 0,24 \frac{\theta_a - 700}{100} \quad (8.63)$$

$$700^{\circ}\text{C} \leq \theta_a \leq 800^{\circ}\text{C}$$

$$k_{y,\theta} = 0,11 - 0,12 \frac{\theta_a - 800}{100} \quad (8.64)$$

$$800^{\circ}\text{C} \leq \theta_a \leq 900^{\circ}\text{C}$$

$$k_{y,\theta} = 0,06 - 0,05 \frac{\theta_a - 900}{100} \quad (8.65)$$

$$900^{\circ}\text{C} \leq \theta_a \leq 1100^{\circ}\text{C}$$

$$k_{y,\theta} = 0,02 - 0,04 \frac{\theta_a - 1100}{200} \quad (8.66)$$

$$1100^{\circ}\text{C} \leq \theta_a \leq 1200^{\circ}\text{C}$$

$$k_{y,\theta} = 0,02 \frac{1100 - \theta_a}{100} \quad (8.67)$$

(2) Limiting temperature criterion

For a member to perform adequately where deflection or stability (buckling) is not critical in a fire EN 1993-1-2 requires that

$$\theta_a \leq \theta_{a,cr} \quad (8.68)$$

- (a) Determination of the actual steel temperature  $\theta_a$   
 This has already been covered earlier in the chapter and in Examples 8.1–8.3 and will not be discussed further.
- (b) Determination of the design or critical steel temperature  $\theta_{a,cr}$   
 The value of  $\theta_{a,cr}$  is dependant on the degree of utilization  $\mu_0$ . The relationship between  $\theta_{a,cr}$  and  $\mu_0$  has been determined from elementary plasticity theory and the reduction in steel strength with temperature and is given empirically by the following equation:

$$\theta_{a,cr} = 39,19 \ln \left[ \frac{1}{0,9674\mu_0^{3,833}} - 1 \right] + 482 \quad (8.69)$$

subject to the limit  $\mu_0 > 0,013$ .

The degree of utilization is defined as

$$\mu_0 = \frac{E_{fi,d}}{R_{fi,d,0}} \quad (8.70)$$

where  $R_{fi,d,0}$  is the resistance of the member at time  $t = 0$  determined in accordance with the principles outlined above, and  $E_{fi,d}$  is the design effect of the structural fire actions. Alternatively  $\mu_0$  may be defined conservatively as

$$\mu_0 = \eta_{fi} \left[ \frac{\gamma_{M,fi}}{\gamma_{M1}} \right] \quad (8.71)$$

The use of  $\theta_{a,cr}$  only holds for tension members and Class 1, 2 or 3 beams and compression members.

**Example 8.4: Determination of fire protection requirements for a laterally torsionally restrained beam**

A Grade S275 beam is simply supported over a span of 8 m. It carries permanent loading from 125 mm thick pre-cast concrete units (205 kg/m<sup>2</sup>), 40 mm concrete screed, 20 mm wood blocks and a suspended ceiling of mass 40 kg/m<sup>2</sup>. The lightweight partitions comprise 1,0 kN/m<sup>2</sup> and the variable loading is 2,5 kPa. The beams are 457 × 152 × 60 UB's at 3,75 m pitch. Design mineral board protection to give 60 min standard fire resistance.

Permanent load	kg/m <sup>2</sup>	kPa
Beam self-weight	16	
Pre-cast units	205	
Screed (2400 × 0,040)	96	
Wood blocks (900 × 0,020)	18	
Suspended ceiling	40	
Total	375	3,75
Partitions		1,00
Total		4,75

Variable load in the fire limit state is  $0,3 \times 2,5 = 0,75$  kPa

$$M_{fi,Ed} = 3,75(4,75 + 0,75)8^2/8 = 163 \text{ kNm.}$$

$$M_{Rd} = 275 \times 1287 \times 10^{-3}/1,0 = 354 \text{ kNm.}$$

Check section classification:

$$\varepsilon = 0,85 \left[ \frac{235}{f_y} \right]^{0,5} = 0,85 \left[ \frac{235}{275} \right]^{0,5} = 0,786$$

Flange classification:

$$c = 0,5 [b - 2r - t_x] = 0,5 [152,9 - 2 \times 10,2 - 8,1] = 62,6$$

$$\frac{c}{t_f} = \frac{62,6}{13,3} = 4,71$$

Limiting value for Class 1 is  $9\varepsilon = 9 \times 0,786 = 7,07$ . Flange is Class 1

Web check:

$$c = \text{depth between fillets} = 407,6 \text{ mm}$$

$$\frac{c}{t_w} = \frac{407,6}{8,1} = 50,3$$

Limiting value for Class 1 is  $9\varepsilon = 72 \times 0,786 = 56,6$ . Web is Class 1.

(a) Section resistance

Setting  $M_{\bar{f}i,Rd,t}$  equal to  $M_{\bar{f}i,Ed}$  then from Eq. (8.34),

$$k_{y,\theta} = \frac{M_{\bar{f}i,Ed}}{M_{Rd}} = \frac{163}{354} = 0,460$$

As the temperature is non-uniform, this value may be modified by  $1/\kappa_1$  ( $\kappa_2 = 1,0$  as the beam is simply supported). For this case (beam protected on three sides with concrete slab on the top flange,  $\kappa_1 = 0,85$ ), thus from Eq. (8.36) the effective value of  $k_{y,\theta}$  is  $0,46/0,85 = 0,541$ , and from Eq. (8.62)  $\theta_a = 577^\circ\text{C}$ .

Fire protection data:

Mineral fibre boarding as Example 8.3 (i.e.  $\rho_p = 500 \text{ kg/m}^3$ ,  $p = 2\%$ ,  $c_p = 1500 \text{ J/kgC}$ ,  $\lambda_p = 0,25 \text{ W/mC}$ ). For a four-sided box,  $A_m/V = 140 \text{ m}^{-1}$ .

Using Eq. (8.22):

$$\begin{aligned} d_p &= \frac{-\frac{1}{\lambda_p} \frac{V}{A_m} + \sqrt{\left(\frac{1}{\lambda_p} \frac{V}{A_m}\right)^2 + 4 \frac{\rho_p}{\rho_a} \frac{1}{\lambda_p} \left[\frac{t_{\bar{f}i,d}}{40(\theta_{a,t}-140)}\right]^{1,3}}}{2 \frac{\rho_p}{\rho_a} \frac{1}{\lambda_p}} \\ &= \frac{-\frac{1}{0,25 \times 140} + \sqrt{\left(\frac{1}{0,25 \times 140}\right)^2 + 4 \frac{530}{7850 \times 0,25} \left[\frac{60}{40(577-140)}\right]^{1,3}}}{2 \frac{530}{7850 \times 0,25}} = 0,019 \text{ m} \end{aligned}$$

From Eq. (8.12) using the heat transfer equations  $d_p = 0,0195 \text{ m}$  ( $\theta_{a,t} = 576^\circ\text{C}$ ).

(b) Critical temperature approach

$$\begin{aligned} \mu_0 &= \frac{E_{\bar{f}i,d}}{R\bar{f}i,d,0} = \frac{163}{354} = 0,460 \\ \theta_{a,cr} &= 39,19 \ln \left[ \frac{1}{0,9674 \mu_0^{3,833}} - 1 \right] + 482 \\ &= 39,19 \ln \left[ \frac{1}{0,9674 \times 0,46^{3,833}} - 1 \right] + 482 = 598^\circ\text{C} \end{aligned}$$

It should be observed that the two temperatures differ only by around  $20^\circ\text{C}$ .

From Eq. (8.21)

$$d_p = \frac{-\frac{1}{\lambda_p} \frac{V}{A_m} + \sqrt{\left(\frac{1}{\lambda_p} \frac{V}{A_m}\right)^2 + 4 \frac{\rho_p}{\rho_a} \frac{1}{\lambda_p} \left[\frac{t_{fi,d}}{40(\theta_{a,t}-140)}\right]^{1,3}}}{2 \frac{\rho_p}{\rho_a} \frac{1}{\lambda_p}}$$

$$= \frac{-\frac{1}{0,25 \times 140} + \sqrt{\left(\frac{1}{0,25 \times 140}\right)^2 + 4 \frac{530}{7850 \times 0,25} \left[\frac{60}{40(598-140)}\right]^{1,3}}}{2 \frac{530}{7850 \times 0,25}} = 0,018 \text{ m}$$

From Eq. (8.12) using heat transfer calculations,  $d_p = 0,0185 \text{ m}$  ( $\theta_{a,t} = 597^\circ\text{C}$ ).

The use of the quadratic equation for determination of protection thicknesses and the heat transfer calculations give almost identical results. The limiting temperature approach is slightly less conservative, although the resultant differences in fire protection thicknesses are negligible.

### Example 8.5: Design of the fire protection for a beam

Determine the thickness of mineral fibre board protection required to give 90 min fire resistance for a  $406 \times 178 \times 74$  UB (Grade S355 JR) whose design data are given in Fig. 8.7(a).

As the beam can suffer lateral torsional buckling, the critical temperature approach cannot be used. Also it will be assumed conservatively that the compression flange temperature is equal to the uniform temperature.

As the solution to Eq. (8.37) is iterative, a spreadsheet was used in which the temperature was varied until the moment capacity was just greater than the applied moment.

From the ambient design  $\bar{\lambda}_{LT} = 0,715$ .

At a temperature  $\theta_a = 565^\circ\text{C}$ .

From Eq. (8.62)  $k_{y,\theta} = 0,579$ .

From Eq. (8.55)  $k_{E,\theta} = 0,411$ .

Thus from Eq. (8.40)

$$\bar{\lambda}_{Lt,\theta,com} = \bar{\lambda}_{LT} \left[ \frac{k_{y,\theta,com}}{k_{E,\theta,com}} \right]^{0,5} = 0,715 \left[ \frac{0,579}{0,411} \right]^{0,5} = 0,848$$

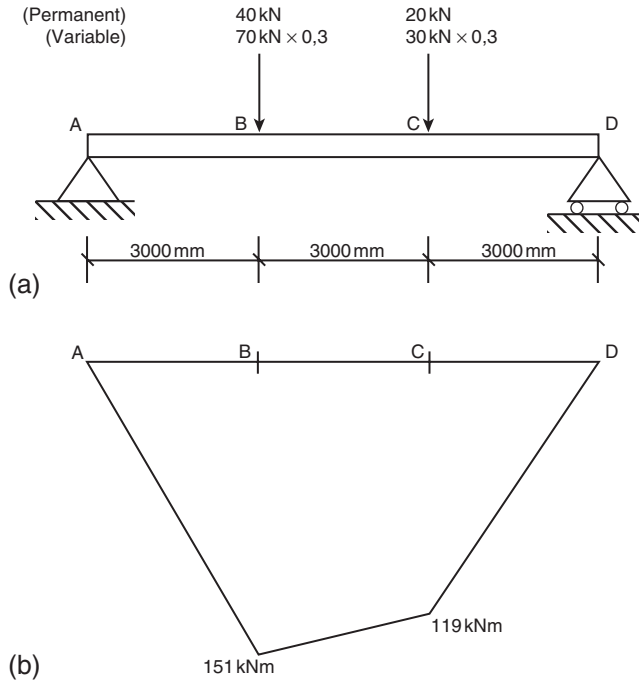


**Figure 8.7** (a) Beam loading data and (b) bending moment diagram for Example 8.4.

From Eq. (8.39)

$$\begin{aligned} \phi_{LT,\theta,com} &= 0,5 \left[ 1 + 0,65 \sqrt{\frac{235}{f_y}} \bar{\lambda}_{LT,\theta,com} + (\bar{\lambda}_{LT,\theta,com})^2 \right] \\ &= 0,5 \left[ 1 + 0,848 \times 0,65 \sqrt{\frac{235}{355}} + 0,848^2 \right] = 1,084 \end{aligned}$$

From Eq. (8.38)

$$\begin{aligned} \chi_{LT,fi} &= \frac{1}{\phi_{LT,\theta,com} + \sqrt{[\phi_{LT,\theta,com}]^2 - [\bar{\lambda}_{LT,\theta,com}]^2}} \\ &= \frac{1}{1,084 + \sqrt{1,084^2 - 0,848^2}} = 0,568 \end{aligned}$$

From Eq. (8.37)

$$\begin{aligned} M_{b,fi,t,d} &= \chi_{Lt,fi} W_{pl,y} k_{y,\theta,com} \frac{f_y}{\gamma_{M,fi}} \\ &= 0,568 \times 1301 \times 0,579 \times 355 \times 10^{-3} = 152 \text{ kNm} \end{aligned}$$

This is greater than the applied moment  $M_{fi,Ed}$  of 151 kNm.

For a three-sided box,  $A/V = 105 \text{ m}^{-1}$ .

From Eq. (8.22)

$$\begin{aligned} d_p &= \frac{-\frac{1}{\lambda_p} \frac{V}{A_m} + \sqrt{\left(\frac{1}{\lambda_p} \frac{V}{A_m}\right)^2 + 4 \frac{\rho_p}{\rho_a} \frac{1}{\lambda_p} \left[\frac{t_{fi,d}}{40(\theta_{a,t}-140)}\right]^{1,3}}}{2 \frac{\rho_p}{\rho_a} \frac{1}{\lambda_p}} \\ &= \frac{-\frac{1}{105 \times 0,25} + \sqrt{\left(\frac{1}{105 \times 0,25}\right)^2 + 4 \frac{530}{7850 \times 0,25} \left[\frac{90}{40(565-140)}\right]^{1,3}}}{2 \frac{530}{7850 \times 0,25}} = 0,025 \text{ m} \end{aligned}$$

From Eq. (8.12),  $d_p = 0,0255 \text{ m}$  ( $\theta_{a,t} = 565^\circ\text{C}$ ).

### Example 8.6: Column heated under an axial load only

A  $254 \times 254 \times 107$  UC Grade 275 carries a permanent load and a variable axial load both equal to 1000 kN at ambient limit state. The effective length of the column is 3,5 m. Design box protection to give 90 min fire performance.

The ambient design gives  $\bar{\lambda} = 0,612$  with  $N_{Rd} = 3112 \text{ kN}$ . At ambient,  $N_{Ed} = 2850 \text{ kN}$ .

Check section classification:

$$\varepsilon = 0,85 \left[ \frac{235}{275} \right]^{0,5} = 0,85 \left[ \frac{235}{275} \right]^{0,5} = 0,786$$

Flange classification:

$$c = 0,5 [b - 2r - t_w] = 0,5 [258,8 - 2 \times 12,7 - 12,8] = 110,3 \text{ mm}$$

$$\frac{c}{t_f} = \frac{110,3}{20,5} = 5,38$$

Limiting value for Class 1 is  $9\varepsilon = 9 \times 0,786 = 7,07$ . Flange is Class 1  
Web check:

$$c = \text{depth between fillets} = 200,3 \text{ mm}$$

$$\frac{c}{t_w} = \frac{200,3}{12,8} = 15,6$$

Limiting value for Class 1 is  $9\varepsilon = 72 \times 0,786 = 56,6$ . Web is Class 1.

As the exact end conditions are not known, take the buckling length in the fire limit state as 3,5 m.

Taking  $\psi = 0,3$  on the variable load gives

$$N_{Ed,fi} = 1,0 \times 1000 + 0,3 \times 1000 = 1300 \text{ kN}$$

For a steel temperature of  $565^\circ\text{C}$ ,

From Eq. (8.62),  $k_{y,\theta} = 0,5785$ .

From Eq. (8.55),  $k_{E,\theta} = 0,4115$ .

From Eq. (8.33)

$$\bar{\lambda}_\theta = \bar{\lambda} \left[ \frac{k_{y,\theta}}{k_{E,\theta}} \right]^{0,5} = 0,612 \left[ \frac{0,5785}{0,4115} \right]^{0,5} = 0,725$$

From Eq. (8.32)

$$\begin{aligned} \phi_\theta &= 0,5 \left[ 1 + 0,65 \sqrt{\frac{235}{f_y}} \bar{\lambda}_\theta + \bar{\lambda}_\theta^2 \right] \\ &= 0,5 \left[ 1 + 0,725 \times 0,65 \sqrt{\frac{235}{275}} + 0,725^2 \right] = 0,981 \end{aligned}$$

From Eq. (8.31)

$$\chi_{fi} = \frac{1}{\phi_\theta + \sqrt{\phi_\theta^2 - \bar{\lambda}_\theta^2}} = \frac{1}{0,981 + \sqrt{0,981^2 - 0,725^2}} = 0,609$$

and from Eq. (8.30)

$$N_{b,fi,t,Rd} = \chi_{fi} A k_{y,\theta} \frac{f_y}{\gamma_{M,fi}} = 0,609 \times 13\,600 \times 0,5785 \times 275 \times 10^{-3} = 1318 \text{ kN}$$

This exceeds the design load  $N_{fi,Ed}$  of 1300 kN and is therefore satisfactory.

For a four-sided box  $A_m/V = 75 \text{ m}^{-1}$ .

From Eq. (8.22),

$$d_p = \frac{-\frac{1}{\lambda_p} \frac{V}{A_m} + \sqrt{\left(\frac{1}{\lambda_p} \frac{V}{A_m}\right)^2 + 4 \frac{\rho_p}{\rho_a} \frac{1}{\lambda_p} \left[\frac{t_{fi,d}}{40(\theta_{a,t} - 140)}\right]^{1,3}}}{2 \frac{\rho_p}{\rho_a} \frac{1}{\lambda_p}}$$

$$= \frac{-\frac{1}{75 \times 0,25} + \sqrt{\left(\frac{1}{75 \times 0,25}\right)^2 + 4 \frac{530}{7850 \times 0,25} \left[\frac{90}{40(565 - 140)}\right]^{1,3}}}{2 \frac{530}{7850 \times 0,25}} = 0,019 \text{ m}$$

From Eq. (8.12),  $d_p = 0,0197 \text{ m}$  ( $\theta_{a,t} = 566^\circ\text{C}$ ).

### Example 8.7: Design the fire protection for a column under moment and axial force

Determine the thickness of plaster board protection required to give 90 min fire resistance for the column ( $305 \times 305 \times 137$  Grade S 275) with an axial force from permanent actions of 600 kN and a moment about the major axis due to variable actions of 300 kNm. The buckling length of the column in both the ambient and fire limit states is 3,5 m.

From the ambient design,  $\bar{\lambda}_y = 0,294$ ;  $\bar{\lambda}_z = 0,514$  and  $\bar{\lambda}_{LT} = 0,276$ .

Although for the ambient design  $\bar{\lambda}_{LT} < 0,4$  which indicates lateral torsional buckling will not occur, there is no indication whether this restriction still applies in the fire limit state, thus the check with and without lateral torsional buckling will be carried out.

Also assume that the column is an edge toward the mid-height of a multi-storey structure when the moments at the ends of the column will be of opposite sign and approximately equal, thus the ratio  $\psi$  can be taken as  $-1$ . Thus from Eq. (8.52)

$$\beta_{M,\psi} = 1,8 - 0,7\psi = 1,8 - 0,7(-1) = 2,5$$

This value will also apply in the determination of  $k_y$ ,  $k_z$  and  $k_{LT}$ .

For a value of  $\theta_a = 640^\circ\text{C}$ .

From Eq. (8.63),  $k_{y,\theta} = 0,374$ .

From Eq. (8.56),  $k_{E,\theta} = 0,238$ .

From Eq. (8.33)

$$\bar{\lambda}_{\theta,y} = \bar{\lambda}_y \left[ \frac{k_{y,\theta}}{k_{E,\theta}} \right]^{0,5} = 0,294 \left[ \frac{0,374}{0,238} \right]^{0,5} = 0,369$$

From Eq. (8.32)

$$\begin{aligned} \phi_{\theta,y} &= 0,5 \left[ 1 + 0,65 \sqrt{\frac{235}{f_y}} \bar{\lambda}_{\theta} + \bar{\lambda}_{\theta}^2 \right] \\ &= 0,5 \left[ 1 + 0,369 \times 0,65 \sqrt{\frac{235}{275}} + 0,369^2 \right] = 0,679 \end{aligned}$$

From Eq. (8.31)

$$\chi_{fi,y} = \frac{1}{\phi_{\theta} + \sqrt{\phi_{\theta}^2 - \bar{\lambda}_{\theta}^2}} = \frac{1}{0,679 + \sqrt{0,679^2 - 0,369^2}} = 0,801$$

From Eq. (8.33)

$$\bar{\lambda}_{\theta,z} = \bar{\lambda}_z \left[ \frac{k_{y,\theta}}{k_{E,\theta}} \right]^{0,5} = 0,514 \left[ \frac{0,374}{0,238} \right]^{0,5} = 0,644$$

From Eq. (8.32)

$$\begin{aligned} \phi_{\theta,z} &= 0,5 \left[ 1 + 0,65 \sqrt{\frac{235}{f_y}} \bar{\lambda}_{\theta} + \bar{\lambda}_{\theta}^2 \right] \\ &= 0,5 \left[ 1 + 0,644 \times 0,65 \sqrt{\frac{235}{275}} + 0,644^2 \right] = 0,901 \end{aligned}$$

From Eq. (8.31)

$$\chi_{fi,z} = \frac{1}{\phi_{\theta} + \sqrt{\phi_{\theta}^2 - \bar{\lambda}_{\theta}^2}} = \frac{1}{0,901 + \sqrt{0,901^2 - 0,644^2}} = 0,653$$

$$\chi_{fi,min} = 0,653$$

From Eq. (8.40)

$$\bar{\lambda}_{LT,\theta,com} = \bar{\lambda}_{LT} \left[ \frac{k_{y,\theta,com}}{k_{E,\theta,com}} \right]^{0,5} = 0,276 \left[ \frac{0,374}{0,238} \right]^{0,5} = 0,346$$

From Eq. (8.39)

$$\begin{aligned} \phi_{LT,\theta,com} &= 0,5 \left[ 1 + 0,65 \sqrt{\frac{235}{f_y}} \bar{\lambda}_{LT,\theta,com} + (\bar{\lambda}_{LT,\theta,com})^2 \right] \\ &= 0,5 \left[ 1 + 0,346 \times 0,65 \sqrt{\frac{235}{275}} + 0,346^2 \right] = 0,664 \end{aligned}$$

From Eq. (8.38)

$$\begin{aligned} \chi_{LT,\bar{f}_i} &= \frac{1}{\phi_{LT,\theta,com} + \sqrt{[\phi_{LT,\theta,com}]^2 - [\bar{\lambda}_{LT,\theta,com}]^2}} \\ &= \frac{1}{0,664 + \sqrt{0,664^2 - 0,346^2}} = 0,813 \end{aligned}$$

From Eq. (8.47)

$$\mu_{LT} = 0,15 \bar{\lambda}_{z,\theta} \beta_{M,LT} - 0,15 = 0,15 \times 0,644 \times 2,5 - 0,15 = 0,092$$

This is less than 0,9, therefore satisfactory.

From Eq. (8.46)

$$k_{LT} = 1 - \frac{\mu_{LT} N_{\bar{f}_i,Ed}}{\chi_{z,\bar{f}_i} A k_{y,\theta} \frac{f_y}{\gamma_{M,\bar{f}_i}}} = 1 - \frac{0,092 \times 600 \times 10^3}{0,653 \times 17\,400 \times 0,374 \times 275} = 0,953$$

This is less than 1,0 and therefore satisfactory.

From Eq. (8.49)

$$\begin{aligned} \mu_y &= (1,2 \beta_{M,y} - 3) \bar{\lambda}_{y,\theta} + 0,44 \beta_{M,y} - 0,29 = 0,368 (1,2 \times 2,5 - 3) \\ &\quad + 0,44 \times 2,5 - 0,29 = 0,81 \end{aligned}$$

As this is greater than the limiting value of 0,8,  $\mu_y = 0,8$ .

From Eq. (8.48)

$$k_y = 1 - \frac{\mu_y N_{fi,Ed}}{\chi_{y,fi} A k_{y,\theta} \frac{f_y}{\gamma_{M,fi}}} = 1 - \frac{0,8 \times 600 \times 10^3}{0,801 \times 17\,400 \times 0,374 \times 275} = 0,665$$

This is less than the limiting value of 3.

From Eq. (8.51)

$$\begin{aligned} \mu_z &= (2\beta_{M,z} - 5)\bar{\lambda}_{z,\theta} + 0,44\beta_{M,z} - 0,29 \\ &= 0,644(2 \times 2,5 - 5) + 0,44 \times 2,5 - 0,29 = 0,81 \end{aligned}$$

As this is greater than the limiting value of 0,8,  $\mu_z = 0,8$ .

From Eq. (8.50)

$$k_z = 1 - \frac{\mu_z N_{fi,Ed}}{\chi_{z,fi} A k_{y,\theta} \frac{f_y}{\gamma_{M,fi}}} = 1 - \frac{0,8 \times 600 \times 10^3}{0,653 \times 17\,400 \times 0,374 \times 275} = 0,589$$

Check the interaction Eqs (8.42) and (8.43)

Equation (8.42):

$$\begin{aligned} &\frac{N_{fi,Ed}}{\chi_{min,fi} A k_{y,\theta} \frac{f_y}{\gamma_{M,fi}}} + \frac{k_y M_{y,fi,Ed}}{W_{pl,y} k_{y,\theta} \frac{f_y}{\gamma_{M,fi}}} + \frac{k_z M_{z,fi,Ed}}{W_{pl,z} k_{y,\theta} \frac{f_y}{\gamma_{M,fi}}} \\ &= \frac{600 \times 10^3}{0,653 \times 17\,400 \times 0,374 \times 275} + \frac{0,665 \times 90 \times 10^3}{2297 \times 0,374 \times 275} + 0 = 0,767 \end{aligned}$$

Equation (8.43)

$$\begin{aligned} &\frac{N_{fi,Ed}}{\chi_{z,fi} A k_{y,\theta} \frac{f_y}{\gamma_{M,fi}}} + \frac{k_{LT} M_{y,fi,Ed}}{\chi_{LT,fi} W_{pl,y} k_{y,\theta} \frac{f_y}{\gamma_{M,fi}}} + \frac{k_z M_{z,fi,Ed}}{W_{pl,z} k_{y,\theta} \frac{f_y}{\gamma_{M,fi}}} \\ &= \frac{600 \times 10^3}{0,653 \times 17\,400 \times 0,374 \times 275} + \frac{0,953 \times 90 \times 10^3}{0,813 \times 2297 \times 0,374 \times 275} + 0 = 0,96 \end{aligned}$$

It will be seen that in this case the check including lateral torsional buckling is critical.

From Eq. (8.22)

$$d_p = \frac{-\frac{1}{\lambda_p} \frac{V}{A_m} + \sqrt{\left(\frac{1}{\lambda_p} \frac{V}{A_m}\right)^2 + 4 \frac{\rho_p}{\rho_a} \frac{1}{\lambda_p} \left[\frac{t_{fi,d}}{40(\theta_{a,t}-140)}\right]^{1,3}}}{2 \frac{\rho_p}{\rho_a} \frac{1}{\lambda_p}}$$

$$= \frac{-\frac{1}{70 \times 0,25} + \sqrt{\left(\frac{1}{70 \times 0,25}\right)^2 + 4 \frac{530}{7850 \times 0,25} \left[\frac{90}{40(640-140)}\right]^{1,3}}}{2 \frac{530}{7850 \times 0,25}} = 0,015 \text{ m}$$

From Eq. (8.12)  $d_p = 0,0152 \text{ m}$  ( $\theta_{a,t} = 641^\circ\text{C}$ ).

### 8.3 OTHER STEELWORK CONSTRUCTIONS

#### 8.3.1 External steelwork

It may be necessary in certain structures for the steel frame to be external to the cladding, i.e. outside the main envelope of the structure. Thus the design of the steelwork must consider the effects of a fire escaping from a compartment rather than the fire being within a compartment. Methods are therefore needed that can be used to calculate the temperatures in external steelwork, since it is possible if the temperatures attained are low enough that no protection need be applied to the steelwork. The problem therefore is one of temperature calculation rather than strength response. To carry out the calculations necessary, the reader is referred to Law (1978) or Law and O'Brien (1989) where the theoretical basis behind the calculations and typical examples are given. It should be noted that the Annex in EN 1993-1-2 on bare external steelwork is directly adapted from Law and O'Brien.

#### 8.3.2 Shelf angle floors

It should be noted that only BS 5950: Part 8 gives an explicit method to cope with shelf angle floors, and it is concerned with the actual calculation of moment capacity. EN 1993-1-2 allows direct calculation of moment capacity but gives no guidance on the calculation of the temperature field within shelf angle floors. Further information including design charts to enable a simple check to be carried out on the sufficiency of shelf angle floors is given in Newman (1993).

It should be noted that BS 5950: Part 8 places some limitations on shelf angle floors which are:

- (1) The connections at the end of the beam to any stanchions should either be within the depth of the slab or protected to the same standard as the supporting member.
- (2) The supporting angles should be checked that their moment capacity, based on the elastic section modulus of the leg, in a fire is sufficient to resist the loads applied from the pre-cast units. A strength reduction factor corresponding to 1,5% proof strain should be used.
- (3) The weld on the upper face of the angle should be designed to resist both the applied vertical shear and the longitudinal shear. The weld on the underside of the angle is to be neglected.

(a) Calculation of the temperature response

The beam is divided up into a series of zones corresponding to the bottom flange, the exposed web, the exposed part of the shelf angles and that part of the web and vertical legs of the shelf angles which attain temperatures of above 300°C. The temperature zones and the alternative positions of the 300°C isotherm are given in Fig. 8.8.

The temperature of the bottom flange  $\theta_1$  is determined from Table 10 of BS 5950: Part 8. The remaining temperatures are determined from  $\theta_1$  using Table C.1 of the Code (Table 8.4). The position of the 300°C isotherm  $x_{300}$  above the top surface of the horizontal leg of the shelf angle is determined from a reference temperature  $\theta_R$  by the following equation

$$x_{300} = \frac{\theta_R - 300}{G} \quad (8.72)$$

where  $G$  takes values of 2,3, 3,8 or 4,3°C/mm for fire resistance periods of 30, 60 or 90 min, respectively.

The temperatures of blocks 4,5 and 6 are calculated from the following equation

$$\theta_x = \theta_R - Gx \geq 300^\circ\text{C} \quad (8.73)$$

(b) Calculation of moment capacity

With steel strengths reduced by factors determined for a 1,5% strain level, conventional plastic analysis is used to determine the moment capacity with the beam and angles replaced by rectangles with the fillets ignored.

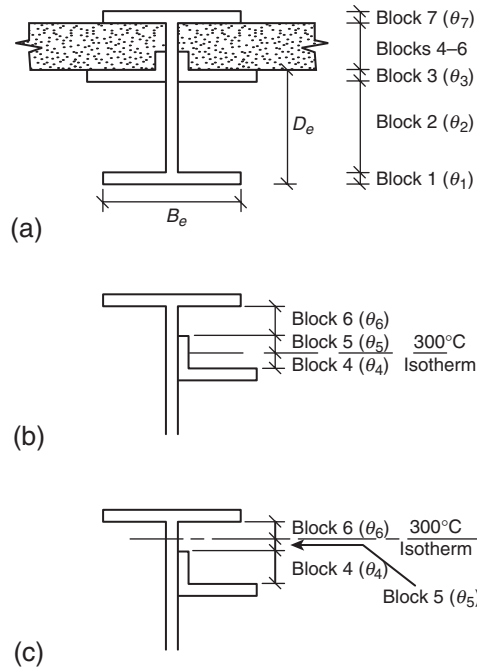


**Figure 8.8** Temperature block definitions for shelf angle floor beams: (a) layout of blocks and corresponding temperatures ( $\theta$ ); (b) 300 isotherm in flange of angle and (c) 300 isotherm in web of beam above angle.

**Table 8.4** Block temperatures

Aspect ratio	Block temperatures for a given fire endurance period (min)								
	30			60			90		
	$\theta_2$ (°C)	$\theta_3$ (°C)	$\theta_R$ (°C)	$\theta_2$ (°C)	$\theta_3$ (°C)	$\theta_R$ (°C)	$\theta_2$ (°C)	$\theta_3$ (°C)	$\theta_R$ (°C)
$\frac{D_e}{B} \leq 0,6$	$\theta_1 - 140$	475	350	$\theta_1 - 90$	725	600	$\theta_1 - 60$	900	775
$0,6 < \frac{D_e}{B} \leq 0,8$	$\theta_1 - 90$	510	385	$\theta_1 - 60$	745	620	$\theta_1 - 30$	910	785
$0,8 < \frac{D_e}{B} \leq 1,1$	$\theta_1 - 45$	550	425	$\theta_1 - 30$	765	640	$\theta_1$	925	800
$1,1 < \frac{D_e}{B} \leq 1,5$	$\theta_1 - 25$	500	425	$\theta_1$	765	640	$\theta_1$	925	800
$1,5 < \frac{D_e}{B}$	$\theta_1$	5550	425	$\theta_1$	765	640	$\theta_1$	925	800

Source: Table C.1 BS 5950: Part 8

**Example 8.8: Design of a shelf angle floor**

Determine the moment capacity after a 30 min exposure to the standard furnace test for a shelf angle floor fabricated from a  $406 \times 178 \times 54$  Grade S275 UB with  $125 \times 75 \times 12$  Grade S355 angles with upper face of the long leg of the angles 282 mm above the soffit of the beam.

The example chosen is that reported in Data sheet No 35 in Wainman and Kirby (1988). It should be noted that the fire endurance test was terminated at a limiting deflection of span/30. Thus the beam would still have had the ability to resist the applied moment for slightly longer than the time period quoted in the test report.

## (a) Determination of steel temperatures

The flange thickness of the beam is 10,9 mm. Thus from Table 10 (BS 5950 Part 8),  $\theta_1 = 760^\circ\text{C}$  (flange thickness of 11 mm).

The ratio  $D_e/B_e = 282/177,7 = 1,59$ .

From Table C.1 (Table 8.4),

$\theta_2 = \theta_1 = 760^\circ\text{C}$ ;  $\theta_3 = 550^\circ\text{C}$ ;  $\theta_R = 425^\circ\text{C}$ .

From Eq. (8.72) calculate  $x_{300}$ ,

$$x_{300} = \frac{\theta_R - 300}{G} = \frac{425 - 300}{2,3} = 54,3 \text{ mm}$$

This falls within the vertical leg of the angle and the upper portion of the angle and web are at temperatures below  $300^\circ\text{C}$ .

Calculate the temperature  $\theta_4$  using Eq. (8.73) at the mid-height of the angle:

$$\theta_4 = \theta_R - Gx = 425 - 2,3 \times (54,3/2) = 363^\circ\text{C}$$

The relevant strength reduction factors are to be found in Table 1 of BS 5950: Part 8. The relevant zones and dimensions for calculating temperatures are given in Fig. 8.9.

## (b) Calculation of moment capacity

The simplest way to carry out this is to determine the total force on the section by summing the strengths of the individual zones. Then by calculating the tension, or compression, force resultant as half this value, the resultant position of the plastic neutral axis may be determined and hence moments may be taken about the soffit of the beam to determine the temperature reduced strength capacity.

The calculations are carried out for one-half the beam in Table 8.5.

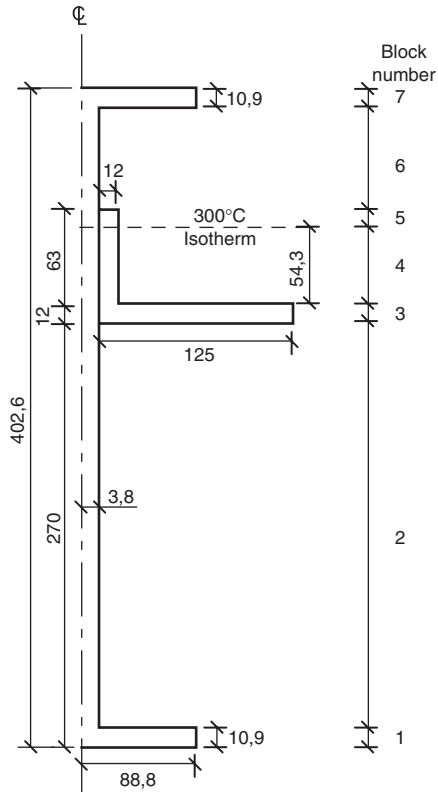


**Figure 8.9** Temperature block data and section dimensions for Example 8.6.

The total force on the section is 1051,58 kN, thus the compressive or tensile force is numerically equal to  $0,5\sum P_i$  (= 525,79 kN).

$$P_1 + P_2 + P_3 = 403,06 \text{ kN,}$$

$$P_1 + P_2 + P_3 + P_4 = 681,76 \text{ kN.}$$

Thus the neutral axis lies within Zone 4.

$$0,5\sum P_i - P_1 + P_2 + P_3 = 525,79 - 403,06 = 122,73 \text{ kN.}$$

$$x = \frac{122,73 \times 10^3}{0,965 (12 \times 355 + 3,85 \times 275)} = 23,91 \text{ mm}$$

Zone 4 is partially in tension and partially in compression, thus dividing it into two sections as per column 6 of Table 8.6. Moments can then be taken about the soffit of the beam to determine  $\sum M_i$ .

**Table 8.5** Calculation of moment capacity

Zone	$f_{yk}$ (MPa)	$\theta$ (°C)	$k_{y,\theta}$	$P_i$ (kN)		$l_a$ (mm)	$M_i$ (kNm)
1	275	760	0,143	37,94		5,45	0,207
2	275	760	0,143	39,23		140,45	5,510
3a	355	550	0,612	325,89		276,0	89,946
3b	275	550	0,612	7,78		276,0	2,147
4a	355	363	0,965	223,22	98,29( <i>t</i> )	293,40	28,838
					124,93( <i>c</i> )	321,11	-40,116
4b	275	363	0,965	55,48	24,43( <i>t</i> )	293,40	7,168
					31,05( <i>c</i> )	321,11	-9,970
5a	355	< 300	1,0	37,06		340,65	-12,624
5b	275	< 300	1,0	9,21		340,65	-3,137
6	275	< 300	1,0	49,44		368,35	-18,211
7	275	< 300	1,0	266,33		397,15	-105,773
			$\sum P_i$	1051,58		$\sum M_i$	-56,015

*c* = compression; *t* = tension.

**Table 8.6** Comparison between assumed and measured temperatures (°C)

Zone	Position	Measured	Assumed
1	Bottom flange	733	760
2	Exposed web	715	760
3	Underside of shelf angle	571	550
4	Upstand of shelf angle	368	363
5	Unexposed web	167	<300
6	Top flange	97	<300

For half the beam,  $\sum M_i$  is numerically equal to 56,015 kNm, thus the total capacity of the beam is 112 kNm.

The actual test reported in Wainman and Kirby lasted for 29 min with a deflection of  $L/30$ , with the beam carrying a total udl of 271,4 kN on a span of 4,5 m giving an applied moment of 152,7 kNm. Part of the discrepancy is due to the temperatures measured in the test and the assumed values in the calculations. These are summarized in Table 8.6, where it is noted that the test temperatures are lower in the bottom flange and web, thus increasing the values of  $P_i$ , but slightly higher in the underside and

upstand of the shelf angle, thus decreasing the values of  $P_i$ . The latter will have a lesser effect on the moment capacity as they are closer to the centroidal axis.

Wainman and Kirby also reported that the actual strengths were for the Grade 275 beam 280 MPa and for the Grade 355 shelf angle 381 MPa. These actual strengths would also increase the capacity of the section, thus overall the calculated moment capacity is acceptable.

## 8.4 STAINLESS STEEL

The principles of the design of stainless steel in fire are similar to those of normal carbon steel (Baddoo and Burgan, 2001). The major difference is in the determination of the strength reduction factors in that these are dependant upon the grade of stainless steel and that if strength loss corresponding to 2% strain, then an additional factor  $g_{2,\theta}$  is required as

$$p_{2,\theta} = p_{0,2proof,\theta} + g_{2,\theta} (U_{s,\theta} - p_{0,2proof,\theta}) \quad (8.74)$$

where  $p_{0,2proof,\theta}$  is 0,2% proof strain at a temperature  $\theta$  and  $U_{s,\theta}$  is ultimate strength.

The values of  $k_{p0,2proof,\theta}$  ( $= p_{0,2proof,\theta} / p_y$ ) and  $k_{s,\theta}$  ( $= U_{s,\theta} / U_s$ ) are tabulated. For the strength loss at 1% strain, the factor  $g_{2,\theta}$  in Eq. (8.74) is replaced by  $0,5g_{2,\theta}$ .

## 8.5 METHODS OF PROTECTION

### 8.5.1 Types of protection

There are essentially five basic methods of fire protecting steelwork; board systems, spray systems, intumescent paints, brickwork/blockwork and concrete encasement.

#### 8.5.1.1 Board systems

These are now the most common, certainly within the UK, as they are quick and easy to fix and also produce relatively little mess as it is a dry process. Essentially the boards, which are mineral fibre or plaster-board, are either secured together to form a box system in the case of column protection or are fixed to wood battens inserted between the flanges on beam systems. A further advantage of board systems is that they can have the building finishes directly applied, thus speeding up building execution.

#### **8.5.1.2 Spray protection**

In this case, the protection in the form of a gunite-type material is wet sprayed on to the member. It is a process which can produce considerable mess and if it is used on exposed steelwork it will require additional finishing by plastering or boarding to achieve the standard required for decorating. Generally spray systems are limited to beams where there are false ceilings.

#### **8.5.1.3 Intumescent paints**

These are paint systems which when exposed to heat foam up and provide insulation in the form of aerated carbon similar to the char layer that forms on timber. The advantage with intumescent paints is that they may be used to provide the final architectural finish to exposed steelwork. The drawbacks are those of maintenance in that continual inspection is needed to examine the integrity of the paint layer and a fire actually occurring when the paint layer will subsequently need replacing. Intumescent paints will also resist the effects of blast and hydrocarbon fires (Allen, 2006).

#### **8.5.1.4 Brickwork/blockwork**

This may be used as a convenient way of providing fire protection to either freestanding stanchions or stanchions partially or totally built into masonry walls. The non-loadbearing masonry effectively acts as a heat sink and thus reduces the average temperatures within the steelwork. Freestanding stanchions with non-structural infilling to the webs are capable of providing 30–60 min fire resistance (Building Research Establishment, 1986). It is possible to provide structural infill to assist in load carrying, i.e. the steel column acts compositely with the infill. The design of such columns is covered in Chapter 9.

#### **8.5.1.5 Concrete encasement**

This method is now essentially obsolete partly owing to the large additional permanent loading imposed on the structure and partially because it is a long slow process to carry out. Since formwork is needed for the concrete together with some reinforcement and the need for curing time, it is probably more economic to use full reinforced concrete construction. Some of the problems can be mitigated by the use of pre-cast concrete protection, but concrete will still need to be cast around the beam-to-column (or beam-to-beam connections).

### 8.5.1.6 Manufacturer's data

A compendium of manufacturer's data is provided in the UK by the Association for Specialist Fire Protection (ASFP/SCI/FTSG (2004)). The thermal behaviour of insulation is conventionally determined using a 'failure' temperature of 550°C for columns with normal protection materials, 620°C for beams supporting concrete floors over a limited range of section sizes. Thus manufacturer's design data imply such a failure temperature. It is known that this approach is conservative and that steel members can achieve higher temperatures than these at failure.

To allow test data to be extrapolated over a greater range of section sizes, an approach using linear regression was evolved (Barnfield, 1986; ASFP, 2004). The standard fire resistance period  $t_{fi}$  is given by:

$$t_{fi} = a_0 + a_1 \frac{V}{A_m} + a_2 d_p \quad (8.75)$$

where  $a_0$ ,  $a_1$  and  $a_2$  are parameters relating to a given protection material.

Equation (8.81) may be rewritten as:

$$d_p = \frac{t_{fi} - a_0 - a_1 \frac{V}{A_m}}{a_2} \quad (8.76)$$

These equations may then be used to predict values of  $d_p$  required on sections other than those tested.

EN 13381-4 allows a similar, but more complex, approach as it also includes the temperature of the steel, and  $t_{fi}$  is now given by

$$t_{fi} = a_0 + a_1 d_p + a_2 \frac{d_p}{\frac{A_m}{V}} + a_3 \theta + a_4 d_p \theta + a_5 d_p \frac{\theta}{\frac{A_m}{V}} + a_6 \frac{\theta}{\frac{A_m}{V}} + \frac{a_7}{\frac{A_m}{V}} \quad (8.77)$$

where  $a_0$ – $a_7$  are regression coefficients and  $\theta$  is the steel temperature.

Equation (8.77) may be rewritten as:

$$d_p = \frac{t_{fi} - a_0 - a_3 \theta - a_6 \frac{\theta}{\frac{A_m}{V}} - \frac{a_7}{\frac{A_m}{V}}}{a_1 + a_4 \theta + \frac{a_2}{\frac{A_m}{V}} + a_5 \frac{\theta}{\frac{A_m}{V}}} \quad (8.78)$$

It also needs to be noted that generally tests are on I or H sections and modifications need to be made under certain circumstances.

- Structural hollow sections  
The thicknesses  $d_p$  obtained from manufacturer's data need to be increased to  $d_{p,mod}$  as follows:  
 $A/V < 250$

$$d_{p,mod} = d_p \left( 1 + 0,001 \frac{A}{V} \right) \quad (8.79)$$

$$250 \leq A/V \leq 310$$

$$d_{p,mod} = 1,25d_p \quad (8.80)$$

- Castellated beams and beams with circular web openings  
The issue with both these types of beam is that the web may heat up faster than the bottom flange and thus cause instability problems. Indeed the web temperature may exceed the bottom flange temperature.

For castellated beams, tabulated fire protection thicknesses of normal protection materials and intumescent should be increased by 20% with the  $A/V$  value obtained from the parent beam section (ASFP, 2004). For beams with circular web openings, the 20% rule applies only to conventional protection materials. Newman, Dowling and Simms (2005) indicate that tabular data provided in SCI Advisory Desk note AD 269 (SCI, 2003) are limited to cases where the diameter of the circular openings is limited to 0,8 times the beam depth, the end post widths are at least 0,3 times the diameter of the openings, the spacing of openings to the opening diameter is greater than 0,4 and the beams are subject to typical office building loads. AD 269 states that the  $A_m/V$  ratio for three-sided heating should be based on the  $A_m/V$  ratio of the bottom T at the centreline of the circular web opening. Table 1 of AD 269 then gives multiplication factors for increase of protection thicknesses.

### 8.5.2 Connections

The resistance of connections should be checked by using temperature reduced design values for bolts whether in shear or tension and for welds. The appropriate strength reduction factors are given in Annex D of EN 1993-1-2. The temperature of a connection may be assessed using the local  $A/V$  values of parts forming the connection. As an approximation a uniform temperature may be assumed calculated on the basis of the maximum value of  $A/V$  value of the members framing into the connection.

For beam-to-beam or beam-to-column connections where the beams are supporting any type of concrete floor, then the temperature of the bottom flange of the beam at mid-span may be used to determine the temperature in the connection.

The temperature distribution  $\theta_h$  within the connection can be determined as follows:

$D < 400$  mm

$$\theta_h = 0,88\theta_0 \left[ 1 - 0,3 \frac{h}{D} \right] \quad (8.81)$$

$D > 400$  mm

$h < D/2$

$$\theta_h = 0,88\theta_0 \quad (8.82)$$

$h > D/2$

$$\theta_h = 0,88\theta_0 \left[ 1 + 0,2 \left( 1 - \frac{2h}{D} \right) \right] \quad (8.83)$$

where  $h$  is the height measured from the soffit,  $D$  is the depth of the beam and  $\theta_0$  is the temperature of the bottom flange remote from the connection.

### 8.5.3 Ageing of and partial loss of protection

All the above calculation methods assume that any insulating material remains in place, shows no deterioration in properties with age, and is effective for the whole of the fire resistance period required. Clearly there exists the requirement to ensure that the standard of workmanship for the execution of fire protection work is as high as the standard imposed for the remainder of the execution of the works.

#### 8.5.3.1 Ageing effects

A series of tests carried out over a period of some six years by Kruppa (1992) indicates that for any of the common methods of fire protection to structural steelwork there is little evidence of any deterioration in the insulation properties with time.

**8.5.3.2 Partial loss of protection**

The effect of loss of protection during a fire is to reduce substantially the fire performance of the structure. This has been observed in situations where a fire has occurred in partially protected structures such as Broadgate Phase 8 (SCI, 1991) and also in simulation studies (Tomacek and Milke, 1993) where it was found that although a reduction of standard fire test performance is observed for any loss of fire protection, the effect is far more marked for longer fire resistance periods. Tomacek and Milke determined that for a 3 h design fire resistance period, an 18% loss of protection to the column flanges reduced the fire resistance of a column to around 40–60 min and that the reduction was sensibly independent of the column size, whereas for a 1 h design, the effect from an 18% loss was a reduction to a fire resistance of around 30–40 min.

A further effect of partial loss of protection is that any structural deformations during a fire will be increased as the steel attains higher temperatures with subsequent decreases in Young's modulus. The effect on cooling will be to maintain the increased deformations even though there will be little resultant effect on the residual strength of the steelwork (section 13.3.1.2).

Having thus considered non-composite steelwork elements, it is necessary to turn to composite steel–concrete construction.

# 9 Composite construction

---

This chapter is divided into three sections; composite slabs with profile sheet steel decking, composite beams where the composite action is achieved through shear studs welded to the top flange of the beam with or without the use of sheet steel profiled decking to support the concrete slabs and composite concrete filled steel columns.

## 9.1 COMPOSITE SLABS

It is not a general practice to apply any fire protection to the soffit of a composite slab. This means that the profile sheet steel decking is exposed directly to the fire and therefore loses its strength very rapidly. From furnace tests it was found that simply supported composite slabs are inherently capable of providing 30 min fire resistance when exposed to the standard furnace test, and the decking may be assumed to retain about 5% of its original strength (Cooke, Lawson and Newman, 1988). However, most calculation methods are conservative in ignoring this residual strength and determine the strength of the slab system purely on contributions of the concrete slab and any flexural reinforcement. As with reinforced concrete construction the slab is required to satisfy both the load-bearing capacity and insulation limit states. The latter is generally satisfied by specifying overall slab depths.

### 9.1.1 Insulation requirement

There are two approaches that are able to be used (Annex D). The first is a calculation method and the second is a simple approach based on effective thickness.

**9.1.1.1 Calculation approach**

The time to failure of the insulation limit state  $t_i$  is given by

$$t_i = a_0 + a_1 h_1 + a_3 \Phi + a_3 \frac{A}{L_r} + a_4 \frac{1}{l_3} + a_5 \frac{A}{L_r} \frac{1}{l_3} \tag{9.1}$$

where  $a_0$  to  $a_5$  are coefficients given in Table D.1 (EN 1994-1-2),  $A/L_r$  is a rib geometry factor,  $\Phi$  is the view factor for the upper flange and  $l_3$  is the width of the upper flange (Fig. 9.1).

$A/L_r$  is given by

$$\frac{A}{L_r} = \frac{h_2 \frac{l_1+l_2}{2}}{l_2 + 2\sqrt{h_2^2 + \left(\frac{l_1-l_2}{2}\right)^2}} \tag{9.2}$$

and  $\Phi$  is given by

$$\Phi = \frac{\sqrt{h_2^2 + \left(l_3 + \frac{l_1-l_2}{2}\right)^2} - \sqrt{h_2^2 + \left(\frac{l_1-l_2}{2}\right)^2}}{l_3} \tag{9.3}$$

**9.1.1.2 Effective thickness**

This is satisfied by the determination of a minimum effective thickness  $h_{eff}$  which is given as: for  $h_2/h_1 \leq 1,5$  and  $h_1 > 40$  mm

$$h_{eff} = h_1 + 0,5h_2 \frac{l_1 + l_2}{l_1 + l_3} \tag{9.4}$$

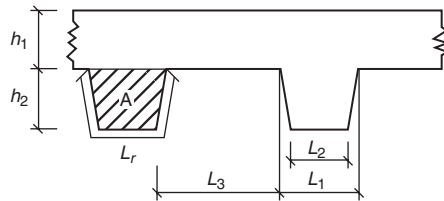


**Figure 9.1** Rib geometry for calculation of  $A/L_r$  (from Fig. D.1 of EN 1994-1-2).

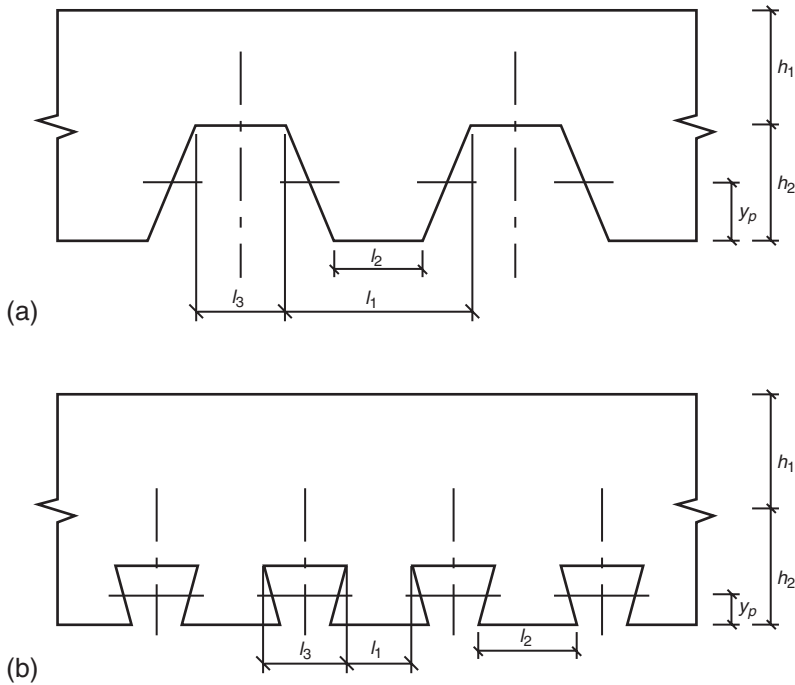


**Figure 9.2** Definition of the dimensions to determine the insulation requirements of a composite deck (from Fig. 4.1 of ENV 1994-1-2): (a) trapezoidal section and (b) dovetail section.

and for  $h_2/h_1 > 1,5$  and  $h_1 > 40$  mm

$$h_{eff} = h_1 \left( 1 + 0,75 \frac{l_1 + l_2}{l_1 + l_3} \right) \quad (9.5)$$

where  $h_1$ ,  $h_2$ ,  $l_1$ ,  $l_2$  and  $l_3$  are defined in Fig. 9.2. If  $l_3 > 2l_1$ ,  $h_{eff} = h_1$ .

The required values of  $h_{eff}$  for normal-weight concrete are given in Table 9.1. For lightweight concrete these values should be reduced by 10%.

### 9.1.2 Load-bearing capacity

The slab should be analysed assuming the formation of plastic hinges at mid-span and the supports where appropriate. For end spans where

**Table 9.1** Values of effective thickness

Standard fire resistance	Minimum effective thickness
R30	$60-h_3$
R60	$80-h_3$
R90	$100-h_3$
R120	$120-h_3$
R180	$150-h_3$
R240	$175-h_3$

Note:  $h_3$  is thickness of the screed layer if present.

Source: Table D.6 of EN 1994-1-2

continuity exists at one support only, it is sufficiently accurate to assume the hinge in the sagging régime occurs at mid-span.

### 9.1.2.1 Calculation of moment capacity

#### (1) Mid-span (sagging moments)

The strength of the concrete should be taken as its ambient strength. This is not unreasonable as the depth of the concrete stress block will be small since the tensile force in the reinforcement that the concrete in compression is required to balance is low. This means that it is very unlikely that the concrete strength will be affected by excessive temperature rise.

The temperature  $\theta_a$  in the bottom flange, web or top flange of the decking is given by

$$\theta_a = b_0 + b_1 \frac{1}{l_3} + b_2 \frac{A}{L_r} + b_3 \Phi + b_4 \Phi^2 \quad (9.6)$$

where  $b_0$  to  $b_4$  are coefficients dependant upon the type of concrete and the fire resistance period and are given in Table D.2 of EN 1994-1-2.

The temperature of the reinforcement  $\theta_s$  is given by

$$\theta_s = c_0 + c_1 \frac{u_3}{h_1} + c_2 z + c_3 \frac{A}{L_r} + c_4 \alpha + c_5 \frac{1}{l_3} \quad (9.7)$$

where  $c_0$  to  $c_5$  are coefficients dependant upon the fire period and concrete type and are given in Table D.3 (of EN 1994-1-2),

$u_3$  and  $z$  characterize the position of the reinforcing bar and  $\alpha$  is the angle of the web (in degrees).

The parameter  $z$  is given by

$$\frac{1}{z} = \frac{1}{\sqrt{u_1}} + \frac{1}{\sqrt{u_2}} + \frac{1}{\sqrt{u_3}} \quad (9.8)$$

where  $u_1$ ,  $u_2$  and  $u_3$ , measured in mm, are defined in Fig. 9.3. For a re-entrant profile where perpendicular distances  $u_2$  and  $u_3$  are undefined owing to the position of the rebar, then  $u_2$  and  $u_3$  are taken to the nearest corner of the dovetail.

The moment capacity is then determined using conventional reinforced concrete theory.

(2) Supports (hogging moments) Method 1

The contribution of the steel decking may be ignored (as it is small). Only the concrete cross section with temperatures less than a limiting

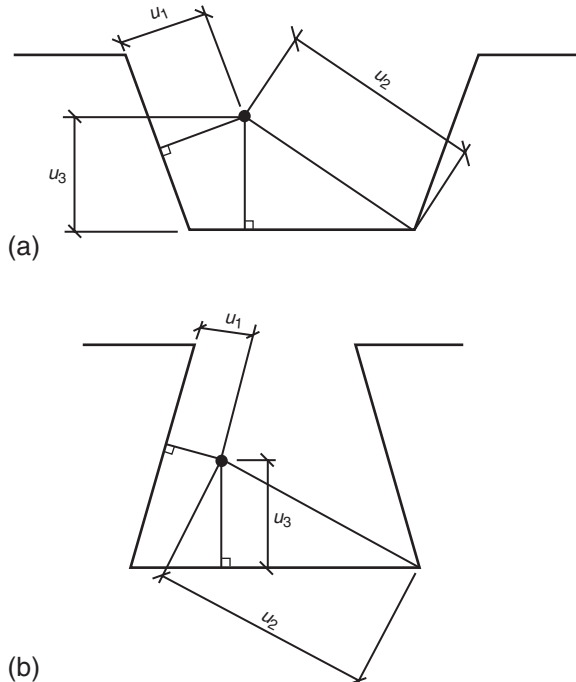


**Figure 9.3** Definition of the parameters required to determine the reinforcement temperatures within a profiled deck (Fig. D.2 of EN 1994-1-2): (a) trapezoidal section and (b) dovetail section.

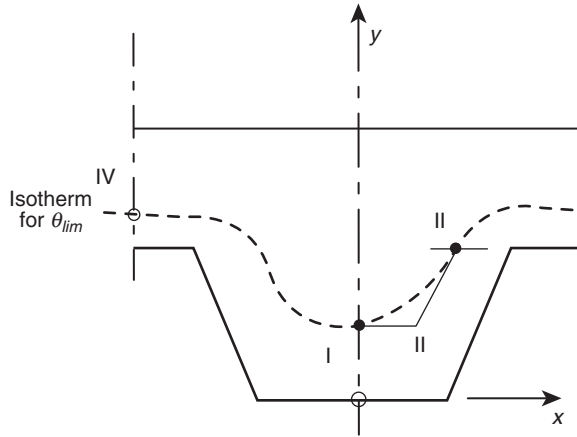


**Figure 9.4** Idealization of isotherm for  $\theta_{lim}$  (from Figs D.3(a) and D.3(b) of EN 1994-1-2).

value of  $\theta_{lim}$  are considered as contributing to the moment capacity (see Fig. 9.4).

$$\theta_{lim} = d_0 + d_1 N_s + d_2 \frac{A}{L_r} + d_3 \Phi + d_4 \frac{1}{l_3} \quad (9.9)$$

where  $d_0$  to  $d_4$  are coefficients given in Table D.3.3 of EN 1994-1-2, and  $N_s$  is the force in the hogging reinforcement.

The positions I–VI are defined by the following coordinates

$$X_I = 0 \quad (9.10)$$

$$Y_I = Y_{II} = \frac{1}{\left(\frac{1}{z} - \frac{4}{\sqrt{l_1+l_3}}\right)^2} \quad (9.11)$$

$$X_{II} = \frac{l_2}{2} + \frac{Y_I}{\sin \alpha} (\cos \alpha - 1) \quad (9.12)$$

$$X_{III} = \frac{l_1}{2} - \frac{b}{\sin \alpha} \quad (9.13)$$

$$Y_{III} = h_2 \quad (9.14)$$

$$X_{IV} = \frac{l_1}{2} \quad (9.15)$$

$$Y_{IV} = h_2 + b \quad (9.16)$$

where

$$\alpha = \arctan \left( \frac{2h_2}{l_1 - l_2} \right) \quad (9.17)$$

$$a = \left( \frac{1}{z} - \frac{1}{\sqrt{h_2}} \right) l_1 \sin \alpha \quad (9.18)$$

$$b = \frac{l_1}{2} \sin \alpha \left( 1 - \frac{\sqrt{a^2 - 4ac}}{a} \right) \quad (9.19)$$

and for  $a \geq 8$

$$c = -8 \left( 1 + \sqrt{1 + a} \right) \quad (9.20)$$

for  $a < 8$

$$c = 8 \left( 1 + \sqrt{1 + a} \right) \quad (9.21)$$

The value of  $z$  should be determined using Eq. (9.7) with  $\theta_R = \theta_{lim}$  and  $u_3/h_2 = 0,75$ . If  $Y_I > h_2$ , then the concrete in the ribs may be ignored.

A conservative approach to determine the position of isotherms in a 100 mm thick normal-weight concrete is given in Table 9.2 (from Table D.5 of EN 1994-1-2) (for lightweight concrete the temperatures in Table D.5 may be reduced by 10%).

(2) Supports (hogging moments) Method 2

The profiled concrete slab is replaced by a flat slab having a depth equal to  $h_{eff}$  measured from the top of the slab excluding any structural screed. The temperature profile in the concrete is given by the isotherm values in Table 9.2, where the depth is measured from the bottom of the equivalent deck. The strength reduction factors for normal-weight concrete are given in Table 6.6.

Where appropriate, the reinforcement strength should be reduced using the concrete temperature at the level of the reinforcement. The moment capacity must then be calculated using basic theory, but with an iterative procedure as the depth of the neutral axis is not known *a priori*.

**Example 9.1: Fire engineering design of a composite slab**

The composite slab detailed in Fig. 9.5 is to be checked under a 90 min fire resistance period. The concrete is Grade 25/30 normal-weight

**Table 9.2** Concrete temperature distribution in a slab

Depth $x$ (mm)	Temperature $\theta_c$ (°C) for a fire duration (min) of					
	30	60	90	120	180	240
5	535	705				
10	470	642	738			
15	415	581	681	754		
20	350	525	627	697		
25	300	469	571	642	738	
30	250	421	519	591	689	740
35	210	374	473	542	635	700
40	180	327	428	493	590	670
45	160	289	387	454	549	645
50	140	250	345	415	508	550
55	125	200	294	369	469	520
60	110	175	271	342	430	495
80	80	140	220	270	330	395
100	60	100	160	210	260	305

Source: Table D.5 of EN 1994-1-2

concrete with structural mesh over the supports to resist hogging moments. The profiled deck is Richard Lee's Super Holorib deck which is of dovetail profile.

(a) Insulation

EN 1994-1-2 allows two approaches. In this example both will be used, although clearly in practice only one is necessary. The dimensions of the deck and sheeting are given in Fig. 9.5.

(1) Effective depth approach (cl)

Determine  $h_2/h_1$ :

$h_2/h_1 = 51/59 < 1,5$  and  $h_1 > 40$  mm, so use Eq. (9.4):

$$h_{eff} = h_1 + 0,5h_2 \frac{l_1 + l_2}{l_1 + l_3} = 59 + 0,5 \times 51 \frac{112 + 138}{112 + 38} = 101 \text{ mm}$$

From Table 9.1 with no screed (i.e.  $h_3 = 0$ ), the minimum value of  $h_{eff}$  is 100 mm, i.e. the slab just satisfies the insulation requirement.

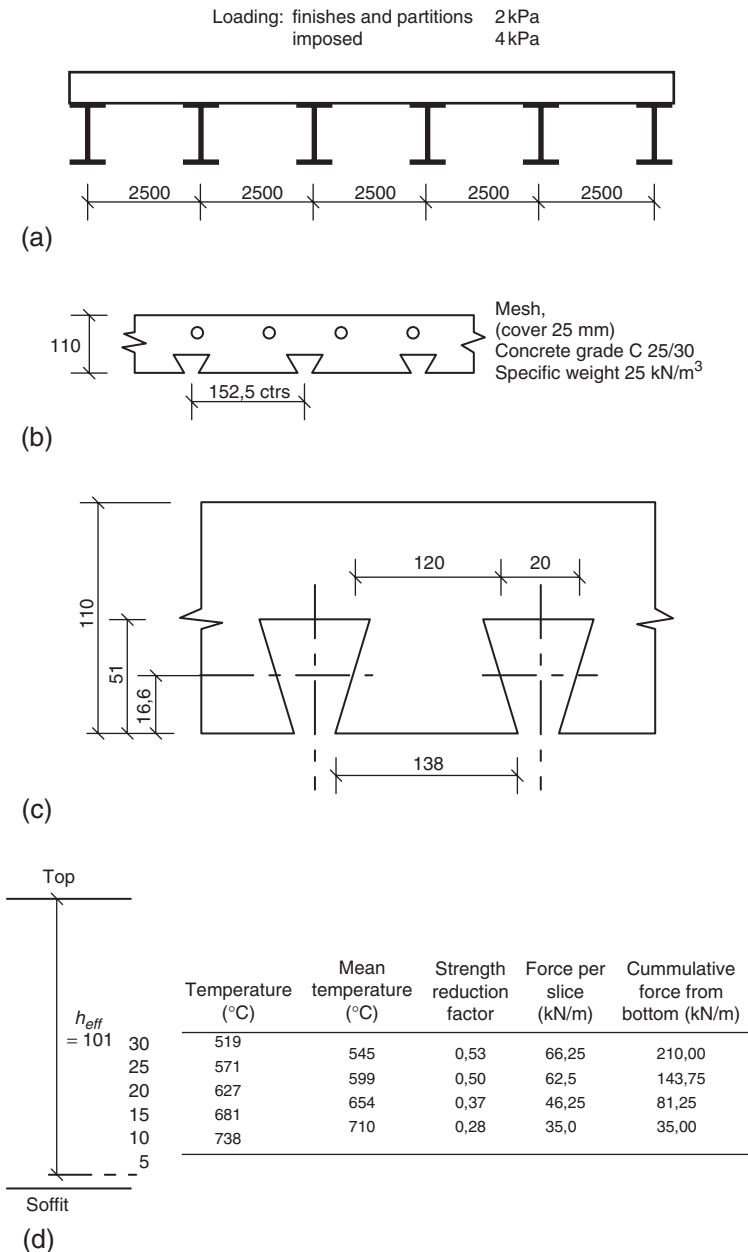


**Figure 9.5** Design data for the determination of the fire performance of a composite deck (Example 9.1): (a) longitudinal view; (b) cross section; (c) calculation of  $h_{eff}$  and (d) calculation of compressive force.

(2) Calculation approach (cl D.1)

Determine parameter  $A/L_r$  from Eq. (9.2)

$$\frac{A}{L_r} = \frac{h_2 \frac{l_1+l_2}{2}}{l_2 + 2\sqrt{h_2^2 + \left(\frac{l_1-l_2}{2}\right)^2}} = \frac{51 \frac{138+112}{2}}{138 + 2\sqrt{51^2 + \left(\frac{112-138}{2}\right)^2}} = 26,2 \text{ mm}$$

Determine  $\Phi$  from Eq. (9.3):

$$\begin{aligned} \Phi &= \frac{\sqrt{h_2^2 + \left(l_3 + \frac{l_1-l_2}{2}\right)^2} - \sqrt{h_2^2 + \left(\frac{l_1-l_2}{2}\right)^2}}{l_3} \\ &= \frac{\sqrt{51^2 + \left(38 + \frac{112-138}{2}\right)^2} - \sqrt{51^2 + \left(\frac{112-138}{2}\right)^2}}{38} = 0,11 \end{aligned}$$

With the values of  $a_0$  to  $a_5$  taken from Table D.1 of EN 1994-1-2, Eq. (9.1) is evaluated as

$$\begin{aligned} t_i &= a_0 + a_1 h_1 + a_3 \Phi + a_3 \frac{A}{L_r} + a_4 \frac{1}{l_3} + a_5 \frac{A}{L_r} \frac{1}{l_3} \\ &= -28,8 + 1,55 \times 59 - 12,6 \times 0,11 + 0,33 \times 26,2 - 735 \times \frac{1}{38} \\ &\quad + 48 \times \frac{26,2}{38} = 84 \text{ min} \end{aligned}$$

This is less than the required 90 min (albeit by a small margin). It would possibly be expected that the effective thickness approach would have been more conservative!

(b) Strength

Using  $\psi$  values from EN 1990 applied to the variable load,

$$M_{fi,Ed} = (0,11 \times 25 + 2,0) + 0,3 \times 4,0 \times 2,5^2/8 = 4,65 \text{ kNm/m}$$

(i) Interior span

Replace the dovetail profile slab by a slab of depth  $h_{eff}$  measured from the top of the slab (Fig. 9.5).

The temperature at  $h_{eff}$  minus centroidal distance to top steel, i.e. at  $102 - 30 = 72$  mm is around  $240^\circ\text{C}$  (Table 9.2). From Table 5.4, the reinforcement suffers no strength reduction.

Two options can be considered: design and detail the mesh such that no bottom reinforcement is required to carry any sagging moments, or design and detail the mesh such that bottom reinforcement is only required in the end span.

Although the former is more economic and more practical on site, both solutions will be investigated here in order to demonstrate the principles involved.

Method A (no bottom reinforcement):

Supply B283 Mesh;

Force in the reinforcement  $F_t = 283 \times 500 = 141,5$  kN.

This must be balanced by the force in the strength reduced concrete. Take a series of 5 mm deep strips in the concrete, determine the concrete temperatures at 0, 10, 15 mm etc. up from the soffit, calculate the temperatures at the mid-point of the strips together with the strength reduction factors to enable the concrete force in each strip to be determined. Then, take sufficient 5 mm strips to balance the concrete and steel force.

This calculation has been carried out in Fig. 9.5, where the bottom 10 mm of concrete has been ignored since there are no data for 0 and 5 mm in Table 9.2 for concrete temperatures at 90 min exposure.

Assuming that where a partial depth strip occurs, the concrete strength reduction factor is taken as that for the whole 5 mm strip, then the total depth of the concrete  $x$  required to balance the tensile force in the steel is given by

$$x = 25 + \frac{(141,5 - 81,25) \times 10^3}{1000 \times 0,50 \times 25} = 24,82 \text{ mm}$$

Taking moments about the reinforcement,  $M_{fi,Rd-}$  is given as

$$\begin{aligned} M_{fi,Rd-} &= 35,0(72 - 12,5) + 81,25(72 - 17,5) + 60,25 \left( 72 - 20 - \frac{4,82}{2} \right) \\ &= 9,5 \text{ kNm/m} \end{aligned}$$

This is around double the free bending moment of  $4,65$  kNm/m, and thus will be adequate over all the spans, including the end span.

Method B (bottom reinforcement in end span):

Supply B196 Mesh;

Force in the reinforcement  $F_t = 196 \times 500 = 98 \text{ kN}$ .

This must be balanced by the force in the strength reduced concrete. Take a series of 5 mm deep strips in the concrete, determine the concrete temperatures at 0, 10, 15 mm etc. up from the soffit, calculate the temperatures at the mid-point of the strips together with the strength reduction factors to enable the concrete force in each strip to be determined. Then take sufficient 5 mm strips to balance the concrete and steel force.

This calculation has been carried out in Fig. 9.5, where the bottom 10 mm of concrete has been ignored since there are no data for 0 and 5 mm in Table 9.2 for concrete temperatures at 90 min exposure.

Assuming that where a partial depth strip occurs, the concrete strength reduction factor is taken as that for the whole 5 mm strip, then the total depth of the concrete  $x$  required to balance the tensile force in the steel is given by:

$$x = 20 + \frac{(98 - 81,25) \times 10^3}{1000 \times 0,50 \times 25} = 21,34 \text{ mm}$$

Taking moments about the reinforcement,  $M_{fi,Rd^-}$  is given as

$$\begin{aligned} M_{fi,Rd^-} &= 35,0(72 - 12,5) + 81,25(72 - 17,5) + 16,75 \left( 72 - 20 - \frac{1,34}{2} \right) \\ &= 7,37 \text{ kNm/m} \end{aligned}$$

This is greater than the free bending moment of 4,65 kNm/m, and thus will be adequate for internal spans.

If the hinge occurs in the centre of the end span, the required moment is approximately  $4,65 - 7,41/2 \approx 1 \text{ kNm/m}$ .

It will be conservative to ignore any contribution of the decking, then the sagging reinforcement can be designed as if for a slab, but with the steel strength taken as  $k_y(\theta)f_y$ .

Place the required reinforcement level with the top of the dovetail, i.e. the effective depth is  $h_1$  or 59 mm.

Determine  $\theta_s$  using Eq. (9.7)

Determination of  $z$ ;

$$u_1 = 51 \text{ mm}$$

$$u_2 = u_3 = 0,5(150 - 38) = 56 \text{ mm}$$

From Eq. (9.8)  $1/z$  is given by

$$\frac{1}{z} = \frac{1}{\sqrt{u_1}} + \frac{1}{\sqrt{u_2}} + \frac{1}{\sqrt{u_3}} = \frac{1}{\sqrt{51}} + \frac{1}{\sqrt{56}} + \frac{1}{\sqrt{56}} = 0,407$$

or  $z = 2,46$

$$\begin{aligned} \theta_s &= c_0 + c_1 \frac{u_3}{h_1} + c_2 z + c_3 \frac{A}{L_r} + c_4 \alpha + c_5 \frac{1}{l_3} \\ &= 1342 - 256 \frac{51}{51} - 235 \times 2,56 - 5,3 \times 26,2 + 1,39 \times 104 - \frac{1267}{38} = 483^\circ\text{C} \end{aligned}$$

From Table 5.6,  $k_y(\theta) = 0,817$ .

Noting that for reinforced concrete design in the fire limit state the values of  $\gamma_c$ ,  $\gamma_s$  and  $\alpha_{cc}$  are all 1,0, and that for  $f_{ck} = 25$  MPa,  $\eta = 1,0$  and  $\lambda = 0,8$ , Eq. (6.15) of Martin and Purkiss (2006) reduces to

$$\frac{A_s k_y(\theta) f_y}{b d f_{ck}} = 1,0 - \sqrt{1 - 2 \frac{M}{b d^2 f_{ck}}}$$

$$M/bd^2 f_{ck} = 1,0 \times 10^6 / (1000 \times 59^2 \times 25) = 0,0115 \text{ and}$$

$$A_s k_y(\theta) / b d f_{ck} = 0,0116, \text{ or}$$

$$A_s = 0,0116 \times 1000 \times 59 \times 25 / (0,817 \times 500) = 42 \text{ mm}^2/\text{m}.$$

Supply H6 bars in alternate ribs, i.e.  $A_s = 95 \text{ mm}^2/\text{m}$ .

$$A_s k_y(\theta) / b d f_{ck} = 95 \times 0,817 \times 500 / (1000 \times 59 \times 25) = 0,0263.$$

From Eq. (6.11) (Martin and Purkiss, 2006)

$$\frac{x}{d} = 1,25 \frac{A_s k_y(\theta) f_y}{b d f_{ck}} = 1,25 \times 0,0263 = 0,033$$

From Eq. (6.12) (Martin and Purkiss, 2006)

$$\begin{aligned} M_{Rd} &= A_s k_y(\theta) (d - 0,4x) = 95 \times 0,817 \times 500 (59 - 0,4 \times 0,033 \times 59) \\ &= 2,26 \text{ kNm/m} \end{aligned}$$

Check the capacity of the end span using the equation proposed by Cooke, Lawson and Newman (1988),

$$M_{\bar{f}_i, Rd^+} + 0,5 M_{\bar{f}_i, Rd^-} \left( 1 - \frac{M_{\bar{f}_i, Rd^-}}{8 M_{\bar{f}_i, Ed}} \right) \geq M_{\bar{f}_i, Ed} \quad (9.22)$$

where  $M_{fi,Rd+}$  and  $M_{fi,Rd-}$  are the sagging and hogging moments and  $M_{fi,Ed}$  is the free bending moment.

$$M_{fi,Rd+} + 0,5M_{fi,Rd-} \left( 1 - \frac{M_{fi,Rd-}}{8M_{fi,Ed}} \right) = 2,26 + 0,5 \times 7,37 \left( 1 - \frac{7,37}{8 \times 4,65} \right) \\ = 5,21 \text{ kNm/m}$$

This is greater than the free bending moment of 4,65 kNm/m and is therefore satisfactory.

## 9.2 COMPOSITE BEAMS

Figure 9.6 gives the basic configuration of composite beam that will be considered. The two types of deck can generically be described as trapezoidal and dovetail. It is also important to distinguish the relative direction of the beam span and deck span as this may affect the temperatures within the steelwork (Newman and Lawson, 1991).

The case where beams are infilled or encased in concrete will not be considered as these are covered by a tabular approach. For the determination of structural behaviour EN 1994-1-2 adopts one of two approaches concerned with the calculation of either a critical temperature or the full moment capacity. In both cases, the calculation of temperatures uses the equations for non-composite steelwork which assume no thermal gradients.

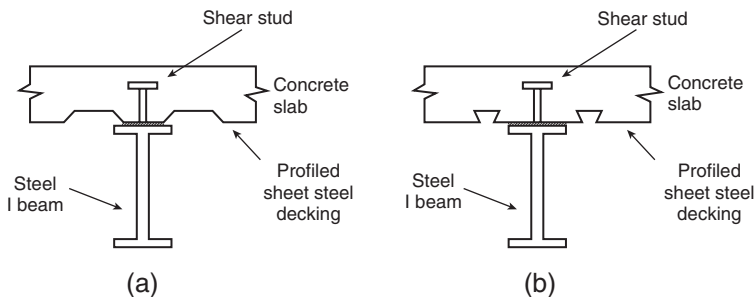


**Figure 9.6** Typical steel–concrete composite beam details. Composite construction with: (a) trapezoidal profile steel decking and (b) dovetail profile steel decking.

### 9.2.1 Critical temperature approach

This may only be used where the beam depth is less than 500 mm, the slab depth  $h_c$  is greater than 120 mm and that the composite beam system is simply supported under sagging moments only.

The critical temperature  $\theta_{cr}$ , for a fire resistance period of R30, is determined corresponding to a critical steel strength  $f_{ay,\theta_{cr}}$  and is given by

$$0,9\eta_{fi,t} = f_{ay,\theta_{cr}}/f_{ay} \quad (9.23)$$

and for all other cases

$$1,0\eta_{fi,t} = f_{ay,\theta_{cr}}/f_{ay} \quad (9.24)$$

where  $f_{ay}$  is the ambient yield or characteristic strength, and the load level  $\eta_{fi,t}$  is given by

$$\eta_{fi,t} = \frac{E_{fi,d,t}}{R_d} \quad (9.25)$$

The temperature rise in the steel section may be determined using the  $A_m/V$  factor for the lower flange.

### 9.2.2 Full moment calculation

Plastic theory is used to determine the moment capacity for all but Class 4 sections. If shear connectors are provided the compression flange may be taken as Class 1. This may only be used to determine the sagging moment capacity. Calculations are made of the steel temperatures, assuming the web and both flanges are at uniform temperatures and the compression zone of the concrete slab is unaffected by temperature. The notation used is given in Fig. 9.7.

To determine the temperatures in the flanges for either unprotected members or members with contour protection, the section factor  $A/V_i$  is calculated as follows:

- (a) Top flange when at least 85% of the concrete slab is in contact with the upper flange and any voids are filled with

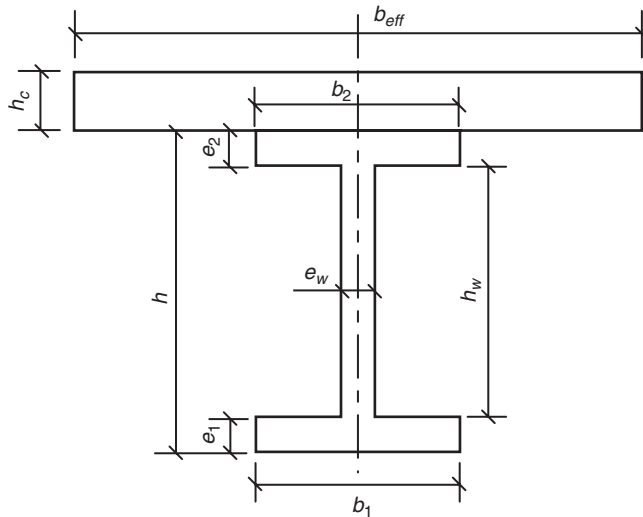


**Figure 9.7** Definition of symbols for the moment capacity method of EN 1994-1-2.

non-combustible materials:

$$\frac{A}{V} = \frac{b_2 + 2e_2}{b_2e_2} \quad (9.26)$$

(b) Top flange when less than 85% of the deck is in contact

$$\frac{A}{V} = 2 \frac{b_2 + e_2}{b_2e_2} \quad (9.27)$$

(c) Bottom flange

$$\frac{A}{V} = 2 \frac{b_1 + e_1}{b_1e_1} \quad (9.28)$$

where  $b_1$ ,  $e_1$ ,  $b_2$  and  $e_2$  are the widths and thicknesses of the bottom and top flanges, respectively. Note, that where the overall beam depth is less than 500 mm, the web temperature may be taken equal to that in the bottom flange.

For box-protection, a uniform temperature over the whole section may be assumed with the  $A/V$  value taken as that for the box.

For unprotected composite steel beams, Eq. (8.7) is used but with a shadow factor  $k_{shadow}$  introduced in the equation to give

$$\Delta\theta_{a,t} = k_{shadow} \frac{\alpha}{c_a \rho_a} \frac{A}{V} (\theta_t - \theta_{a,t}) \Delta t \quad (9.29)$$

where  $k_{shadow}$  is given by

$$k_{shadow} = [0,9] \frac{e_1 + e_2 + \frac{b_1}{2} + \sqrt{h_w^2 + \frac{(b_1 - b_2)^2}{4}}}{h_w + b_1 + \frac{b_2}{2} + e_1 + e_2 - e_w} \quad (9.30)$$

The 0,9 factor is a nationally determined parameter.

Annex E details the model that may be used to determine both the sagging and hogging moment resistances of composite beams. Only the former will be considered here, thus the superscript '+' will be omitted.

The tensile capacity of the steel beam  $T$  calculated using temperature reduced steel strengths (Table 5.6), and is given by

$$T = \frac{f_{ay,\theta 1} b_1 e_1 + f_{ay,\theta w} b_w e_w + f_{ay,\theta 2} b_2 e_2}{\gamma_{M,fi,a}} \quad (9.31)$$

where  $f_{ay,\theta 2}$ ,  $f_{ay,\theta w}$  and  $f_{ay,\theta 1}$  are the temperature reduced stresses in the top flange, web and bottom flange respectively,  $\gamma_{M,fi,a}$  is the materials partial safety factor applied to the steel section and  $h_w$  and  $e_w$  are the height and thickness of the web, respectively.

The tensile force  $T$  acts at a distance  $y_T$  from the bottom of the beam which is calculated from

$$y_T = \frac{f_{ay,\theta 1} \frac{b_1 e_1^2}{2} + f_{ay,\theta w} b_w e_w \left( e_1 + \frac{h_w}{2} \right) + f_{ay,\theta 2} b_2 e_2 \left( h - \frac{e_2}{2} \right)}{T \gamma_{M,fi,a}} \quad (9.32)$$

where  $h$  is the overall depth of the beam.

The tensile force  $T$  is limited to

$$T \leq NP_{fi,Rd} \quad (9.33)$$

where  $N$  is the number of shear connectors in any critical length of the beam and  $P_{fi,Rd}$  is temperature reduced capacity of the shear connectors.

The tensile force  $T$  is resisted by the force from the compression block in the concrete where the depth of the concrete block  $h_u$  is given by

$$h_u = \frac{T}{\frac{b_{eff} f_{ck}}{\gamma_{M,f,c}}} \quad (9.34)$$

where  $b_{eff}$  is the effective width of the slab taken as the ambient design condition and  $f_{ck}$  is the ambient strength of the concrete.

If  $h_c - h_u > h_{cr}$ , the temperature of the concrete is below 250°C and may be taken at full strength.

If  $h_c - h_u < h_{cr}$ , then some layers of the concrete are at temperatures greater than 250°C. The calculation of  $T$  is then iterative and is based on using 10 mm thick layers in the temperature affected zone, and  $T$  is then given by

$$T = \frac{b_{eff} (h_c - h_{cr}) f_{ck} + \sum_{i=2}^{n-1} 10 b_{eff} f_{cf,\theta i} + h_{u,n} b_{eff} f_{ck,\theta n}}{\gamma_{M,f,c}} \quad (9.35)$$

where

$$h_u = (h_c - h_{cr}) + 10(n - 2) + h_{u,n} \quad (9.36)$$

where  $n$  is the total number of layers of concrete including the top concrete layer with a temperature less than 250°C. The position of  $h_{cr}$  and the elemental temperatures should be taken from Table D.5.

The point of application of the compression force  $y_F$  is given by

$$y_F = h + h_c - \frac{h_u}{2} \quad (9.37)$$

and the moment capacity of the section  $M_{f_i,Rd}$  is given by

$$M_{f_i,Rd} = T \left( h + h_c - y_T - \frac{h_u}{2} \right) \quad (9.38)$$

The shear stud capacity must also be checked in that the stud capacity  $P_{\bar{f}_i,Rd}$  is given as the lesser of

$$P_{\bar{f}_i,Rd} = 0,8k_{u,\theta} P_{Rd} \quad (9.39)$$

or

$$P_{fi,Rd} = k_{c,\theta} P_{Rd} \quad (9.40)$$

where  $k_{u,\theta}$  is the temperature reduction on the ultimate strength of steel and  $k_{c,\theta}$  is the concrete strength reduction factor. The values of  $P_{Rd}$  should be calculated in accordance with EN 1994-1-1 except that the partial safety factor  $\gamma_v$  should be replaced by  $\gamma_{M,fi,v}$ . The temperature  $\theta_v$  in the shear studs may be taken as 0,8 of the temperature in the top flange of the steel beam, and the temperature in the concrete  $\theta_c$  as 0,4 of that in the top flange.

### Example 9.2: Determination of the required fire protection for a composite beam

Determine the thickness of sprayed Gypsum plaster to give a beam 90 min fire resistance. The design data for the composite beam are given in Fig. 9.8, when it should be noted that the dovetail decking (Richard Lee's Super Holorib) is running normal to the span of the beam.

Although no specific recommendations are made in EN 1994-1-2 for the effects of the loss of concrete in the deck, the effective thickness will be used for structural calculations.

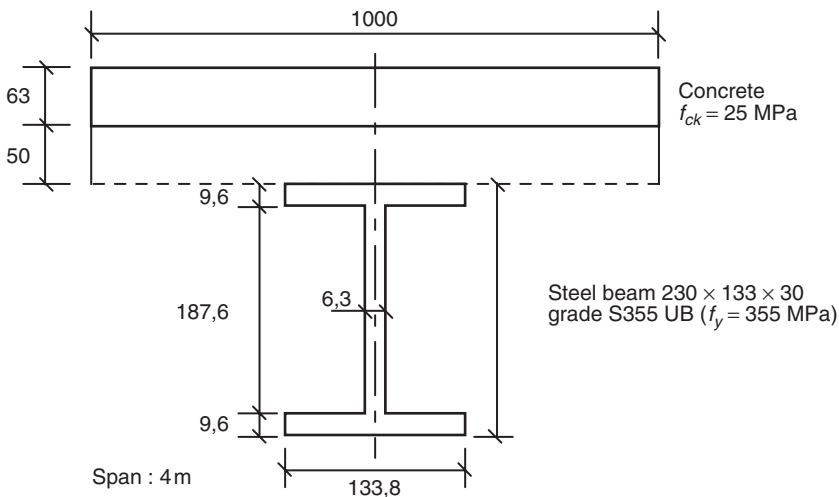


**Figure 9.8** Design data for the determination of the fire performance of a composite steel beam (Example 9.2).

Applied loading (actions):

Imposed (variable): 4 kPa  
 Dead (permanent): 2,75 kPa  
 Finishes (permanent): 2,0 kPa.

The beam is at an internal support of a composite deck system. From the ambient structural analysis of the decking, the application of a udl of  $q$  to the deck, gives a beam reaction per unit run of beam is  $2,98q$ .

Actions in the fire limit state:

Per unit area:

$$q_{fi} = (25 \times 0,11 + 2,0) + 0,3 \times 4 = 5,95 \text{ kPa}$$

Per unit run:

$$q_{fi} = 2,98 \times 5,95 = 16,66 \text{ kN/m}$$

$$M_{fi,Ed} = 16,66 \times 4^2/8 = 33,3 \text{ kNm}$$

(a) Moment capacity approach

This solution is also iterative for both the temperature determination and the resultant moment capacity calculations. Only the final result is given here and not previous invalid determinations.

Calculation of  $A_p/V_i$  values:

Note: To comply with the units in the heat transfer equations, all dimensions are in metres. Bottom flange from Eq. (9.28):

$$A/V = 2(b_1 + e_1)/b_1e_1 = 223 \text{ m}^{-1}$$

Top flange, from Eq. (9.26), when at least 85% of the profile deck is in contact with the beam;

$$A/V = (2e_2 + b_2)/b_2e_2 = 119 \text{ m}^{-1}$$

The beam depth is less than 500 mm, so the web temperature can be taken as the lower (bottom) flange temperatures.

It was found that an insulation thickness of 15,4 mm produced the following temperatures and strength reduction factors:

Bottom flange (and web): 834°C and 0,093

Top flange: 691°C and 0,253.

From Eq. (9.31)

$$\begin{aligned} T &= \frac{f_{ay,\theta 1} b_1 e_1 + f_{ay,\theta w} b_w e_w + f_{ay,\theta 2} b_2 e_2}{\gamma_{M,f_i,a}} \\ &= 355 \frac{0,093 \times 9,6 \times 133,8 + 0,093 \times 187,6 \times 6,3 + 0,253 \times 9,6 \times 133,8}{1,0} \\ &= 196,8 \text{ kN} \end{aligned}$$

Determine  $y_T$  from Eq. (9.32)

$$\begin{aligned} y_T &= \frac{f_{ay,\theta 1} \frac{b_1 e_1^2}{2} + f_{ay,\theta w} b_w e_w \left( e_1 + \frac{h_w}{2} \right) + f_{ay,\theta 2} b_2 e_2 \left( h - \frac{e_2}{2} \right)}{T \gamma_{M,f_i,a}} \\ &= \frac{355 \left( 0,093 \frac{133,8 \times 9,6^2}{2} + 0,093 \times 6,3 \times 187,6 \left( 9,6 + \frac{187,6}{2} \right) \right. \\ &\quad \left. + 0,253 \times 133,8 \times 9,6 \left( 9,6 + 187,6 + \frac{9,6}{2} \right) \right)}{196,8 \times 10^3 \times 1,0} \end{aligned}$$

As in the ambient design, the effective width of the concrete flange  $b_{eff}$  is 1000 mm, thus from Eq. (9.33) the depth of the compression block  $h_u$  (assuming the concrete temperatures are below 250°C) is given by

$$h_u = \frac{T}{\gamma_{M,f_i,c} \frac{b_{eff} f_{ck}}{1,0}} = \frac{196,8 \times 10^3}{\frac{1000 \times 25}{1,0}} = 7,87 \text{ mm}$$

Interpolating the values in Table 9.2 gives  $h_{cr} = 68 \text{ mm}$  for a temperature of 250°C.

The value of  $h_{eff} = 101 \text{ mm}$  (from Example 9.1).

Thus the allowable depth of the compression block before concrete strength loss needs to be considered is  $h_{eff} - h_{cr} = 101 - 68 = 37 \text{ mm}$ ,  $h_u$  is less than this critical value.

The moment capacity  $M_{f_i,Rd}$  is given by Eq. (9.38),

$$\begin{aligned} M_{f_i,Rd} &= T \left( h + h_c - y_T - \frac{h_u}{2} \right) = 196,8 \left( 187,6 + 2 \times 9,6 + 110 - 140 - \frac{7,87}{2} \right) \\ &= 34 \text{ kNm} \end{aligned}$$

This is greater than the applied moment of 33,3 kNm.

Calculation of shear stud capacity:

In the ambient design, 19 mm studs were placed in each trough giving 13,3 (or in practice 14) studs per half span of the beam at a spacing of 150 mm.

The temperature in the stud is taken as 80% of the top flange temperature, i.e.  $0,8 \times 691 = 553^\circ\text{C}$  and the concrete temperature as 40%, i.e.  $0,4 \times 691 = 276^\circ\text{C}$ .

From Table 5.8,  $k_{c,\theta} = 0,874$ ; and from Table 3.2 of EN 1994-1-2,  $k_{u,\theta} = 0,616$ .

Temperature reduced ultimate shear capacity,  $P_{fi,Rd}$  (Eq. (9.39)):

$$P_{fi,Rd} = 0,8k_{u,\theta} \left[ \frac{0,8f_u \frac{\pi d^2}{4}}{\gamma_{M,fi,v}} \right] = 0,8 \times 0,616 \left[ \frac{0,8 \times 450 \frac{\pi 19^2}{4}}{1,0} \right] = 50,3 \text{ kN}$$

Temperature reduced crushing capacity (Eq. (9.40)):

From Table 3.1 of EN 1992-1-1,  $E_{cm} = 33 \text{ GPa}$  for concrete grade C30.

$$P_{fi,Rd} = k_{c,\theta} \frac{0,29\alpha d^2 \sqrt{f_{ck} E_{cm}}}{\gamma_{M,fi,v}} = 0,874 \frac{0,29 \times 1,0 \times 19^2 \sqrt{25 \times 33 \times 10^3}}{1,0} \\ = 83,1 \text{ kN}$$

as the stud layout is such that  $\alpha = 1,0$ .

Minimum fire capacity of the shear studs is 50,3 kN.

The value of  $T$  is limited to a value of  $T_{lim}$  given by

$$T_{lim} = NP_{fi,Rd} = \frac{13,3}{2} 50,3 = 334 \text{ kN}$$

The actual value of  $T$  is 196,8 kN, and therefore the section capacity is not limited by the shear stud capacity.

(b) Limiting temperature approach

Note: Strictly the example is outside the limits where the critical temperature approach may be used as the slab is *only* 110 mm thick and is therefore 10 mm below the lower limit of 120 mm. However, rather than to use another example, the calculations that follow are *illustrative* only.

The design moment of resistance of the composite beam is 200 kNm, so from Eq. (9.25)

$$\eta_{fi,t} = \frac{E_{fi,t,d}}{R_d} = \frac{33,3}{200} = 0,167$$

$$k_{y,\theta} = 0,167, \text{ or } \theta_{cr} = 753^\circ\text{C (from Table 5.6)}$$

The heat transfer calculations were carried out on a spreadsheet and gave a protection thickness of 0,0183 m with a temperature of 752°C.

### 9.3 COMPOSITE STEEL AND CONCRETE COLUMNS

#### 9.3.1 Concrete filled rolled hollow steel columns

The concrete filled rolled hollow section column can also be designed at ambient conditions as composite. The effect at elevated temperatures is that the concrete core acts as a heat sink and that the steel section heats up more slowly and that the loading is transferred to the concrete core which may be either plain concrete, steel–fibre reinforced concrete or contain conventional reinforcement.

##### 9.3.1.1 EN 1994-1-2

Annex H details simple calculation methods for concrete filled hollow sections:

$$N_{fi,Rd} = N_{fi,cr} \leq N_{fi,pl,Rd} \quad (9.41)$$

$$N_{fi,cr} = \left(\frac{\pi}{l_\theta}\right)^2 [E_{a,\theta,\sigma} I_a + E_{c,\theta,\sigma} I_c + E_{s,\theta,\sigma} I_s] \quad (9.42)$$

where  $I_a$ ,  $I_c$  and  $I_r$  are second moments of area of the steel section, the concrete and reinforcement, and  $E_{a,\theta,\sigma}$ ,  $E_{c,\theta,\sigma}$  and  $E_{r,\theta,\sigma}$  the *Tangent* moduli calculated at the stress level  $\sigma$  and temperature level  $\theta$  for each of the constituent materials. Note that for the concrete and, possibly the reinforcement it will be necessary to determine the total flexural stiffness by summing incremental stiffnesses over the area.

The plastic capacity,  $N_{fi,pl,Rd}$ , is given by

$$N_{fi,pl,Rd} = A_a \frac{\sigma_{a,\theta}}{\gamma_{M,fi,a}} + A_c \frac{\sigma_{c,\theta}}{\gamma_{M,fi,c}} + A_s \frac{\sigma_{s,\theta}}{\gamma_{M,fi,s}} \quad (9.43)$$

where  $A_a$ ,  $A_c$  and  $A_r$  are the respective areas of the steel section, the concrete and the reinforcement,  $\sigma_{a,\theta}$ ,  $\sigma_{c,\theta}$  and  $\sigma_{r,\theta}$  are the temperature affected stresses in the steel, concrete and reinforcement, respectively, calculated on the condition that the strains in all three components are equal. It will be necessary to sum the contributions of the concrete and reinforcement incrementally.

The thermal analysis should be carried out using appropriate methods, almost certainly necessitating the use of finite element analysis (FEA).

If the loading is eccentric, the eccentricity should not exceed  $0,5b$  or  $0,5d$ . The equivalent axial load  $N_{equ}$  is given by

$$N_{equ} = \frac{N_{fi,Sd}}{\phi_s \phi_\delta} \quad (9.44)$$

where  $\phi_s$  allows for the presence of reinforcement (with no reinforcement  $\phi_s = 0,4$ ) and  $\phi_\delta$  allows for the effects of eccentricity. Values of  $\phi_s$  and  $\phi_\delta$  are obtained from Figs H.1 and H.2 (of EN 1994-1-2), respectively.

For column in continuous construction where local buckling did not occur, then the buckling length may be taken as  $0,55$  times the actual length (Bailey, 2000). Where local buckling is included in the analysis, then the factor should be increased to  $0,75$ . For column continuous only at one end the buckling factor is increased further to  $0,8$ .

### 9.3.1.2 Empirical methods

Kodur and Lie (1995) and Kodur (1999) have suggested that following tests and a parametric investigation that fire endurance  $t_{fi,Rd}$  of a square or circular concrete filled hollow section could be expressed as:

$$t_{fi,Rd} = f_1 \frac{f_{ck} + 20}{l_\theta - 1000} \frac{D^{2,5}}{\sqrt{N_{fi,Ed}}} \quad (9.45)$$

where  $f_{ck}$  is the characteristic concrete strength (MPa),  $l_\theta$  is the buckling length (mm),  $D$  is the diameter of a circular column or side length of a square column (mm),  $N_{fi,Ed}$  is the applied load in the fire limit state (kN), and  $f_1$  is a factor (Table 9.3) which allows for type of concrete (plain or non-fibre) and for the level of reinforcement.

Wang (2000) provides an empirical approach whereby the squash load  $N_{fi,Rd}$  at a time  $t_{fi}$  (min) for a protected circular column of diameter  $D$  (mm) is given by:

For  $t_{fi} < D$ ,

$$N_{fi,Rd} = \frac{t_{fi}}{D} (N_{fi,\theta,const} - N_{fi,\theta,a}) + N_{fi,\theta,a} \quad (9.46)$$

**Table 9.3** Values of  $f_1$ 

Aggregate type	Column type	Plain concrete	Fibre concrete	Reinforcement ratio and cover			
				<3%		>3%	
				<25	>25	<25	>25
Siliceous	CHS	0,07	0,075	0,075	0,08	0,08	0,085
	SHS	0,06	0,065	0,065	0,07	0,07	0,075
Carbonate	CHS	0,08	0,07	0,085	0,09	0,09	0,095
	SHS	0,06	0,065	0,075	0,08	0,08	0,085

Source: Kodur (1999)

For  $t_{fi} > D$

$$N_{\bar{f}_i, Rd} = N_{\bar{f}_i, \theta, const} \quad (9.47)$$

where  $N_{\bar{f}_i, \theta, d}$  is the column squash load with the steelwork and concrete at the same constant temperature and  $N_{\bar{f}_i, \theta, const}$  is squash load when the steelwork is at maximum temperature and the concrete is considered as cold (20°). For unprotected columns, the contribution of the concrete will need to be determined incrementally.

An alternative form of composite column is to use a standard column or beam section with the web infilled.

### 9.3.2 Web-infilled columns

In these columns the areas contained between the webs and the flanges of a normal I or H section are infilled with concrete so that the concrete acts compositely with the steel. Composite action is provided using proprietary shot fired shear connectors.

Data reported by Newman (1992) indicate that such columns are capable of attaining a 60 min fire test rating, provided there is no possibility of premature failure at the ends of the column and that the original section is designed as totally non-composite. Newman also provides design tables for UK sections. EN 1994-1-2 gives design charts for European sections to Grade 355 and a concrete grade of 40/50.

# 10 Design of timber elements

Unlike the situation where the design of concrete, steel or steel–concrete composite construction is concerned, the calculation procedure is much simplified since there is no explicit requirement to calculate the temperature distribution within the element as the strength calculation is carried out on the residual section after the depth of charring is removed from the original section. There is also generally no need to consider any strength reduction in the residual section as any temperature rise can be considered small and therefore ignored. This chapter considers fire design to EN 1995-1-2 and various empirical methods.

## 10.1 DESIGN TO EN 1995-1-2

The design process is a two stage process, the first is to calculate the depth of charring and the second is to determine the strength of the residual section.

### 10.1.1 Depth of charring

Two cases need to be considered, namely exposure to the standard furnace curve or to a real or parametric fire.

#### 10.1.1.1 Exposure to the standard furnace curve

EN 1995-1-2 gives two values of charring rates,  $\beta_0$  for single face exposure and  $\beta_n$  for multi-face exposure. The values of  $\beta_n$  include an allowance for aris rounding. Values of  $\beta_0$  and  $\beta_n$  for timber are given in Table 10.1.

To calculate the depth of charring there are two cases to be considered:

- (a) Single face exposure

In this case the depth of charring  $d_{char,0}$  is given by

$$d_{char,0} = \beta_0 t \quad (10.1)$$

**Table 10.1** Charring rates from EN 1995-1-2

Timber type	Charring rate (mm/min)	
	$\beta_0$	$\beta_n$
Softwood and beech		
Glulam ( $\rho \geq 290 \text{ kg/m}^3$ )	0,65	0,70
Solid ( $\rho \geq 290 \text{ kg/m}^3$ )	0,65	0,80
Hardwood		
Solid or glulam ( $\rho = 290 \text{ kg/m}^3$ )	0,65	0,70
Solid or glulam ( $\rho > 450 \text{ kg/m}^3$ )	0,50	0,55

Notes: For solid hardwoods, except beech, the charring rates for densities between 240 and  $450 \text{ kg/m}^3$  may be obtained using linear interpolation. Beech should be treated as a softwood.

Source: Table 3.1 of EN 1995-1-2 (abridged)

(b) Multi-face exposure

There are two ways to determine this: either by the use of  $\beta_n$  or by using  $\beta_0$  and modifying values

$$d_{char,n} = \beta_n t \quad (10.2)$$

or if the value of the minimum width of the section  $b_{min}$  satisfies the following relationships,  $\beta_0$  may be used, but then arris rounding with a radius of  $d_{char,0}$  must be taken into account.

For  $d_{char,0} > 13 \text{ mm}$

$$b_{min} = 2d_{char,0} + 80 \quad (10.3)$$

For  $d_{char,0} < 13 \text{ mm}$

$$b_{min} = 8,15d_{char,0} \quad (10.4)$$

**10.1.1.2 Charring to parametric exposure (Annex A)**

The equations needed to calculate the charring depth  $d_{char}$  for timber exposed to natural fires were developed by Hadvig (1981) following a series of tests:

For  $0 \leq t \leq t_0$

$$d_{char} = \beta_{part} t \quad (10.5)$$

For  $t_0 \leq t \leq 3t_0$

$$d_{char} = \beta_{par} \left( 1,5t_0 - \frac{t^2}{4t_0} - \frac{t_0}{4} \right) \quad (10.6)$$

and for  $3t_0 \leq t \leq 5t_0$

$$d_{char} = 2\beta_{par}t_0 \quad (10.7)$$

where  $t$  is the time in minutes,  $t_0$  is a parameter which determines the time to maximum charring and is dependant upon the characteristics of the fire and the compartment and is defined by

$$t_0 = 0,009 \frac{q_{t,d}}{O} \quad (10.8)$$

where  $q_{t,d}$  is the design fire load density with respect to the total compartment area ( $\text{MJ}/\text{m}^2$ ) and  $O$  is the ventilation factor defined as  $A_v \sqrt{h_{eq}} / A_t$ , where  $A_t$  is the total area of the compartment ( $\text{m}^2$ ),  $A_v$  and  $h_{eq}$  are the area ( $\text{m}^2$ ) and height (m) of the openings, respectively, and  $\beta_{par}$  ( $\text{mm}/\text{min}$ ) is defined by

$$\beta_{par} = 1,5\beta_n \frac{0,2\sqrt{\Gamma} - 0,04}{0,16\sqrt{\Gamma} + 0,08} \quad (10.9)$$

where  $\Gamma$  accounts for the thermal properties of the compartment and is given by

$$\Gamma = \frac{\left( \frac{O}{\sqrt{\rho c \lambda}} \right)^2}{\left( \frac{0,04}{1160} \right)^2} \quad (10.10)$$

where  $\sqrt{\rho c \lambda}$  is the thermal inertia of the compartment.

This method may only be used if  $t \leq 40$  min and  $d_{char}$  is less than both  $b/4$  and  $d/4$ .

### 10.1.2 Calculation of structural capacity

The strength and stiffness properties for the fire limit are based not on the usual 5% fractile values used at ambient limit state but 20% fractiles. The design values of strength  $f_k$  and stiffness  $S_{05}$  are multiplied by a factor  $k_{fi}$  which has values of 1,25 for solid timber and 1,15 for glulam.

The background to the determination of cross-sectional resistance determination is given in Kersken-Bradley (1993). The first design method uses an increased charring depth to allow for potential strength loss in the core and is known as the Effective Section Method, whereas the second uses a lower char depth together with factors to allow for the reduction of properties with temperature.

#### 10.1.2.1 Effective section method

The total depth of section reduction  $d_{ef}$  is given as the sum of two components  $d_{char,n}$  and an additional factor  $k_0 d_0$  such that

$$d_{ef} = d_{char,n} + k_0 d_0 \quad (10.11)$$

where  $d_0$  is taken as 7 mm, and  $k_0$  is given by  $t < 20$  min

$$k_0 = \frac{t}{20} \quad (10.12)$$

For  $t > 20$  min,

$$k_0 = 1,0 \quad (10.13)$$

The values of  $\gamma_{M,fi}$  are taken as 1,0.

#### 10.1.2.2 Reduced strength and stiffness method

The reduction in section dimensions is taken as due only to the charring.

For  $t > 20$  min, the strengths and Young's modulus are reduced by modification factors  $f_{mod,f}$  which are for:

(a) Bending strength:

$$k_{mod,fi} = 1,0 - \frac{1}{200} \frac{p}{Ar} \quad (10.14)$$

(b) Compressive strength:

$$k_{mod,fi} = 1,0 - \frac{1}{125} \frac{p}{A_r} \quad (10.15)$$

(c) Tension strength and Young's modulus:

$$k_{mod,fi} = 1,0 - \frac{1}{330} \frac{p}{A_r} \quad (10.16)$$

where  $p/A_r$  is the section factor in  $\text{m}^{-1}$  defined as heated perimeter/cross-sectional area for the reduced section.

For  $t < 20$  min, the modification factors are obtained using linear interpolation between those for Eqs (10.14)–(10.16) and a value of  $k_{mod,fi}$  of 1,0 at  $t = 0$ .

All design examples will be done using Grade C22 timber for which  $f_{m,k} = 22$  MPa,  $E_{mean} = 10$  kPa,  $E_{0,05} = 6,7$  kPa,  $f_{v,k} = 2,4$  MPa.

Determine values of 20% fractile strength and elasticity values are as follows:

$$f_{m,20} = k_{fi} f_{m,k} = 1,25 \times 22 = 27,5 \text{ MPa}$$

$$f_{v,20} = k_{fi} f_{v,k} = 1,25 \times 2,4 = 3,0 \text{ MPa}$$

$$E_{20} = k_{fi} E_{0,05} = 1,25 \times 6,7 = 8,5 \text{ kPa}$$

$$f_{c,20} = k_{fi} f_{c,0,k} = 1,25 \times 20 = 25 \text{ MPa}$$

### Example 10.1: Determination of the fire performance of a beam

The timber beam is 250 mm deep by 75 mm wide and is simply supported over a span of 4,5 m. The beam system is at 600 mm spacing and carries a permanent load of 0,2 kN/m and a total variable load of 2,5 kPa. The required fire endurance period is 30 min.

With a  $\psi$  factor of 0,3, the load in the fire limit state is  $0,3 \times (0,6 \times 2,5) + 0,2 = 0,65$  kN/m.

Maximum bending moment,  $M_{Ed,fi} = 0,65 \times 4,5^2 / 8 = 1,65$  kNm.

(a) Effective cross section method

From Table 10.1 the charring rate  $\beta_n$  is 0,80 mm/min, for a softwood of density greater than 290 kg/m<sup>3</sup>.

The depth of charring  $d_{char,n}$ :

$$d_{char,n} = 30 \times 0,80 = 24 \text{ mm}$$

As  $t > 20 \text{ min}$   $k_0 = 1,0, k_0 d_0 = 7 \text{ mm}$ ,

$$\text{so } d_{ef} = 24 + 7 = 31 \text{ mm}$$

$$\text{Reduced width, } b = B - 2d_{ef} = 75 - 2 \times 31 = 13 \text{ mm}$$

$$\text{Reduced depth, } d = D - d_{ef} = 250 - 31 = 219 \text{ mm}$$

(i) Flexure

Elastic section modulus,  $W_{el} = bd^3/6 = 13 \times 219^3/6 = 104 \times 10^3 \text{ mm}^3$ .

$f_{m,20} = 27,5 \text{ MPa}$ , so  $M_{Rd,fi} = 27,5 \times 104 \times 10^{-3} = 2,86 \text{ kNm}$ .

$M_{Ed,fi} = 1,65 \text{ kNm}$ , so the beam is satisfactory.

(ii) Shear

Maximum shear force is  $0,65 \times 4,5/2 = 1,46 \text{ kN}$ .

$V_{Rd,fi} = 1,5bd_{fv,20} = 1,5 \times 13 \times 219 \times 3,0 \times 10^{-3} = 12,8 \text{ kN}$ , which is satisfactory.

Although there appears no specific requirement to check deflection, it is worthwhile to carry out the check.

(iii) Deflection

$$I = bd^3/12 = 13 \times 219^3/12 = 11,4 \times 10^6 \text{ mm}^4$$

$$\delta_b = 5ML^2/48EI = 5 \times 1,65 \times 10^3 \times 4,5^2 / (48 \times 8,5 \times 10^{-6} \times 11,4 \times 10^6) = 0,035 \text{ m, or}$$

a span/deflection ratio of  $4,5/0,035 = \text{span}/130$  which is satisfactory.

(b) Reduced strength and stiffness method

From Table 10.1 the charring rate is  $0,80 \text{ mm/min}$ , hence the depth of charring  $d_{char} = 30 \times 0,80 = 24 \text{ mm}$

$$\text{Reduced width, } b = B - 2d_{char} = 75 - 2 \times 24 = 27 \text{ mm}$$

$$\text{Reduced depth, } d = D - d_{char} = 250 - 24 = 226 \text{ mm}$$

$$\text{Residual area, } A_r = 226 \times 27 = 6102 \text{ mm}^2$$

Residual perimeter calculated for the fire exposed faces only,

$$p_r = 2 \times 226 + 27 = 479 \text{ mm}$$

$$p/A_r = 479/6102 = 0,078 \text{ mm}^{-1} = 78 \text{ m}^{-1}.$$

(i) Flexure

Elastic section modulus,  $W_{el} = bd^2/6 = 230 \times 10^3 \text{ mm}^3$

For flexure  $k_{mod,fi}$  is given by Eq. (10.14),

$$k_{mod,fi} = 1 - (1/200)p/A_r = 1 - (-78/200) = 0,61$$

$$M_{Rd,fi} = k_{mod,fi} W_{el} f_{20} = 0,61 \times 0,230 \times 27,5 = 3,86 \text{ kNm}$$

$M_{Ed,fi} = 1,65 \text{ kNm}$ . The beam is therefore satisfactory.

(ii) Reduction factors are not given for shear, but given the large margin in (a), this should not be a problem.

## (iii) Deflection

$$I = bd^3/12 = 27 \times 226^3/12 = 26,0 \times 10^6 \text{ mm}^4$$

Modification factor for Young's modulus is calculated from Eq. (10.16),

$$k_{mod,fi} = 1 - (1/330)p/A_r = 1 - 78/330 = 0,766$$

$$E_{f,d} = k_{mod,f} E_{mean} / \gamma_{m,s} = 0,766 \times 8500 = 6511 \text{ MPa}$$

$$\delta_b = 5ML^2/48E_{f,d}I = 5 \times 1,65 \times 10^3 \times 4,5^2 / (48 \times 6,511 \times 10^{-6} \times 26,0 \times 10^6) = 0,021 \text{ m, or a span-deflection ratio} = 4,5/0,021 = 214$$

which is satisfactory.

**Example 10.2: Check the fire performance of 150 mm square 3 m high column to last 30 min carrying an axial load in the fire limit state of 45 kN**

In both methods, assume the column is isolated and that the effective length may be taken as 3 m. The buckling strength is then determined using the methods of EN 1995-1-1 but with values of strength and stiffness appropriate to the fire limit state. As the column is square, suffices relating to axes will be omitted from symbols where appropriate.

## (a) Effective section method

The charring rate  $\beta_n$  is taken as 0,80 mm/min.

$$d_{char,n} = 0,80 \times 30 = 24 \text{ mm}$$

$$k_0 = 1,0 \text{ (} t > 20 \text{ min)}, \text{ so } k_0 d_0 = 7 \text{ mm, and } d_{ef} = 24 + 7 = 31 \text{ mm.}$$

$$d = D - 2d_{ef} = 150 - 2 \times 31 = 88 \text{ mm.}$$

$$\lambda = \frac{L}{i} = \frac{L}{\frac{d}{2\sqrt{3}}} = \frac{3000}{\frac{88}{2\sqrt{3}}} = 118$$

$$\lambda_{rel} = \frac{\lambda}{\pi} \sqrt{\frac{f_{c,20}}{E_{20}}} = \frac{118}{\pi} \sqrt{\frac{25}{8,5 \times 10^3}} = 2,04$$

$$k = 0,5 \left[ 1 + \beta_c (\lambda_{rel} - 0,3) + \lambda_{rel}^2 \right]$$

$$= 0,5 \left[ 1 + 0,2 (2,04 - 0,3) + 2,04^2 \right] = 2,75$$

( $\beta_c = 0,2$  for solid timber)

$$k_c = \frac{1}{k + \sqrt{k^2 - \lambda_{rel}^2}} = \frac{1}{2,75 + \sqrt{2,75^2 - 2,04^2}} = 0,218$$

$$N_{Rd,fi} = k_c f_{c,20} A_c = 0,218 \times 25 \times 88^2 \times 10^{-3} = 42 \text{ kN}$$

This is less than the applied load, thus the load carrying capacity at Ultimate Limit State should be reduced to  $42/0,7 = 60 \text{ kN}$ . Thus the carrying capacity at the fire limit state controls the performance of the column.

(b) Reduced strength and stiffness method

$$d_{char,n} = 0,80 \times 30 = 24 \text{ mm}$$

$$d = D - 2d_{char,n} = 150 - 2 \times 24 = 102 \text{ mm}$$

For a column heated on four sides,  $p/A_r = 4/d$ , so  $p/A_r = 4/0,102 = 39,2 \text{ m}^{-1}$

Assume the column is isolated and that the effective length may be taken as 3 m.

The buckling strength is then determined using the methods of EN 1995-1-1 but with values of strength and stiffness appropriate to the fire limit state. As the column is square, suffices relating to axes will be omitted from symbols where appropriate.

$$\lambda = \frac{L}{i} = \frac{L}{\frac{d}{2\sqrt{3}}} = \frac{3000}{\frac{102}{2\sqrt{3}}} = 102$$

$$\lambda_{rel} = \frac{\lambda}{\pi} \sqrt{\frac{f_{c,20}}{E_{20}}} = \frac{102}{\pi} \sqrt{\frac{25}{8,5 \times 10^3}} = 1,76$$

$$\begin{aligned} k &= 0,5 \left[ 1 + \beta_c (\lambda_{rel} - 0,3) + \lambda_{rel}^2 \right] \\ &= 0,5 \left[ 1 + 0,2 (1,76 - 0,3) + 1,76^2 \right] = 2,19 \end{aligned}$$

( $\beta_c = 0,2$  for solid timber)

$$k_c = \frac{1}{k + \sqrt{k^2 - \lambda_{rel}^2}} = \frac{1}{2,19 + \sqrt{2,19^2 - 1,76^2}} = 0,286$$

The modification factor for compressive strength is given by

$$k_{mod,fi} = 1,0 - \frac{1}{125} \frac{p}{A_r} = 1,0 - \frac{39,2}{125} = 0,686$$

$$\begin{aligned} N_{Rd,fi} &= k_{mod,fi} k_c f_{c,20} A_c \\ &= 0,686 \times 0,286 \times 25 \times 102^2 \times 10^{-3} = 51 \text{ kN} \end{aligned}$$

This is less than the applied load, thus the load-carrying capacity at Ultimate Limit State should be reduced to  $51/0,7 = 73$  kN. Thus the carrying capacity at the fire limit state controls the performance of the column.

For both the beam and column example, the reduced properties method is less conservative than the reduced cross section method.

## 10.2 EMPIRICAL APPROACHES

A number of empirical approaches to the assessment of the fire performance of timber elements have been developed by Ödeen (1969), Lie (1977) and Stiller (1983). It is convenient to consider these in historical order.

### 10.2.1 Approach developed by Ödeen

For members heated on four sides, Ödeen (1969) proposed the following empirical equations to determine the fire endurance  $t_{fi,d}$  of timber members with a constant charring rate exposed to the standard furnace curve,

$$t_{fi,d} = \left(1 - \frac{d}{D}\right) \frac{D}{2\beta} \quad (10.17)$$

where the depth of the residual section  $d$  is determined from

$$\left(\frac{k}{\alpha}\right) \left(\frac{\frac{B}{D}}{\frac{d}{D} - \left(1 - \frac{B}{D}\right)}\right) = \left(\frac{d}{D}\right)^2 \quad (10.18)$$

where  $k$  is the ratio between the maximum stress induced by the loading before the fire to the ultimate strength of the timber,  $\alpha$  is the ratio between the ultimate strength of the timber in its temperature affected state to its ambient strength,  $B$  and  $D$  are the original width and depth of the section,  $d$  is the fire affected depth,  $t_{fi,d}$  is the required fire resistance given by standard ratings and  $\beta$  is the appropriate rate of charring.

For a beam heated on three sides, the equations are modified to

$$t_{fi,d} = \left(1 - \frac{d}{D}\right) \frac{D}{\beta} \quad (10.19)$$

$$\left(\frac{k}{\alpha}\right) \left(\frac{\frac{B}{D}}{\frac{B}{D} - 2\left(1 - \frac{d}{D}\right)}\right) = \left(\frac{d}{D}\right)^2 \quad (10.20)$$

Ödeen suggests that the value of the strength reduction factor with temperature  $\alpha$  should lie between 0,85 and 0,9. Following Malhotra (1982a), the value of  $\alpha$  is taken as 0,87 in all the ensuing examples.

In the original work, the value of  $k$  was defined as the ratio between the maximum bending stress before the fire to the ultimate bending strength before the fire. At that point in time, timber was generally designed using working (or serviceability) loads, and it would have been assumed that the structural loading in the fire limit state was the normal design loading. Given that the variable portion of the fire loading may be reduced by  $\psi$  factors, it is more appropriate to use the structural fire load to determine the value of  $k$ . Also, the determination of the load level to calculate over-design parameter  $f$  should be based on structural fire loading (not service loading).

**Example 10.3: Check the fire performance of the beam in Example 10.1 using Ödeen's approach**

Using the modified definition of  $k$ :

From Example 10.1, the design fire moment  $M_{Ed,fi} = 1,65 \text{ kNm}$ .

$$F_{Ed,fi} = 1,65 \times 10^6 / (75 \times 250^2 / 6) = 2,11 \text{ MPa.}$$

Design strength (assuming medium-term loading) is  $0,8 \times 22 / 1,3 = 13,54 \text{ MPa}$ .

$$k = 2,11 / 13,54 = 0,156.$$

From Eq.(10.20),

$$\left(\frac{k}{\alpha}\right) \left(\frac{\frac{B}{D}}{\frac{B}{D} - 2\left(1 - \frac{d}{D}\right)}\right) - \left(\frac{d}{D}\right)^2 = 0 = \left(\frac{0,156}{0,87}\right) \left(\frac{\frac{75}{250}}{\frac{75}{250} - 2\left(1 - \frac{d}{D}\right)}\right) - \left(\frac{d}{D}\right)^2$$

or,

$$\left(\frac{d}{D}\right)^2 \left(0,3 - 2\left(1 - \frac{d}{D}\right)\right) = 0,052$$

or,

$$d/D = 0,883$$

Take the charring rate as  $\beta_n$  as arris rounding has not been taken into account in the formulae.

So from Eq. (10.19)

$$t_{fi,d} = \frac{D}{\beta} \left( 1 - \frac{d}{D} \right) = \frac{250}{0,8} (1 - 0,883) = 37 \text{ min}$$

thus the beam would last in excess of 30 min.

### 10.2.2 Approach developed by Lie for beams

For a beam heated on three sides, Lie (1977) proposed a much simpler equation which gives a direct evaluation of the fire resistance

$$t_{fi,d} = 0,1fB \left( 4 - \frac{B}{D} \right) \tag{10.21}$$

where  $f$  is a factor allowing for effective over-design due to the availability of timber sizes, and all dimensions are in millimetres. Equation (10.7) implies a charring rate of 0,6 mm/min. Values of the parameter  $f$  are given in Table 10.2.

#### Example 10.4: Check the performance of the beam of Example 10.1 using Lie’s formula

Determination of  $f$ :

$k = 0,156$  as above (Example 10.3), so from Table 10.2,  $f = 1,3$ .

**Table 10.2** Values of over-design factor  $f$

Load ratio ( $\lambda$ ) (% of allowable)	Member type		
	Beam	Column	
		$L/D > 10$	$L/D \leq 10$
$\lambda \geq 75$	1,0	1,0	1,2
$75 > \lambda \geq 50$	1,1	1,1	1,3
$\lambda \leq 50$	1,3	1,3	1,5

Source: Lie (1977), by permission of National Research Council of Canada

From Eq. (10.21)

$$t_{fi,d} = 0,1fB \left( 4 - \frac{B}{D} \right) = 0,1 \times 1,3 \times 75 \left( 4 - \frac{75}{250} \right) = 36 \text{ min}$$

Lie's equation was derived for a charring rate of 0,6 mm/min, thus the time of 36 min will be an overestimate.

### 10.2.3 Empirical determination of fire endurance for columns

For short timber columns, where the strength is determined by the pure compressive strength of the timber (i.e. there is no buckling), then the following equation can be derived for the relationship between the pre- and post-fire dimensions

$$\left( \frac{k}{\alpha} \right) \left( \frac{\frac{B}{D}}{\frac{d}{D} - \left( 1 - \frac{B}{D} \right)} \right) = \left( \frac{d}{D} \right) \quad (10.22)$$

For extremely slender columns, when the strength is dependant entirely on buckling, the load capacity can then be derived from the basic Euler equation for buckling strength. The equation relating to section dimensions, assuming the effective length of column is the same in both the ambient and fire limit states and that the temperature dependence of the modulus of elasticity of the timber can be taken as that for loss in strength, is then given by

$$\left( \frac{k}{\alpha} \right) \left( \frac{\frac{B}{D}}{\frac{d}{D} - \left( 1 - \frac{B}{D} \right)} \right) = \left( \frac{d}{D} \right)^3 \quad (10.23)$$

The assumption of similar behaviour with respect to temperature for both the modulus of elasticity and compressive strength is reasonable when deriving an empirical equation (Gerhards, 1982).

However, most columns are neither short nor extremely slender but have a slenderness ratio such that failure is by a combination of squashing and buckling. Lie (1977) thus suggested that for the general case, the relationship between the column dimensions in the determination of

the fire resistance of an axially loaded column when subjected to fire on all four sides could be taken as

$$\left(\frac{k}{\alpha}\right) \left(\frac{\frac{B}{D}}{\frac{d}{D} - \left(1 - \frac{B}{D}\right)}\right) = \left(\frac{d}{D}\right)^n \quad (10.24)$$

where  $k$  is the ratio between the load applied during a fire to the column strength at ambient allowing for the enhancement of allowable stresses,  $\alpha$  is the reduction in compressive strength of the residual section, and  $n$  is a parameter with limiting values of 1 for short columns and 3 for long columns. Lie suggested that for most practical columns, a value of  $n = 2$  could be taken. The fire resistance  $t_{fi,d}$  based on standard classification is then calculated from

$$t_{fi,d} = \frac{D}{2\beta} \left(1 - \frac{d}{D}\right) \quad (10.25)$$

For square columns,  $B/D$  equals unity, and Eq. (10.24) reduces to

$$\frac{d}{D} = \left(\frac{k}{\alpha}\right)^{\frac{1}{n+1}} \quad (10.26)$$

and the fire performance  $t_{fi,d}$  is then given directly by

$$t_{fi,d} = \frac{D}{2\beta} \left(1 - \left(\frac{k}{\alpha}\right)^{\frac{1}{n+1}}\right) \quad (10.27)$$

A simplified empirical relationship, also due to Lie, gives the fire resistance directly for axially loaded columns as

$$t_{fi,d} = 0,10fD \left(3 - \frac{D}{B}\right) \quad (10.28)$$

where  $f$  is a factor dependant upon the level of loading and the slenderness ratio and is given in Table 10.2, and the dimensions are in millimetres with the charring rate taken as 0,6 mm/min.

For a square column, Eq. (10.28) reduces to

$$t_{fi,d} = 0,20fD \quad (10.29)$$

**Example 10.5: Check the performance of the column of Example 10.2 using both Lie's approaches**

Determination of  $k$ :

The ultimate load-carrying capacity assuming medium-term duration load is 150 kN, the load in the fire limit state is 45 kN,  $k = 45/150 = 0,30$ . As the column is over medium slenderness ( $\lambda \approx 100$  (Example 10.2)), take  $n = 2$ . With  $\alpha = 0,87$ , Eq. (10.27) becomes

$$t_{fi,d} = \frac{D}{2\beta} \left( 1 - \left( \frac{k}{\alpha} \right)^{\frac{1}{1+n}} \right) = \frac{150}{2 \times 0,8} \left( 1 - \left( \frac{0,3}{0,87} \right)^{\frac{1}{1+2}} \right) = 28 \text{ min}$$

The column does therefore not achieve 30 min – this is in line with the result from the reduced cross section method.

Lie's approximate method: Eq. (10.29)

As the load level is below 50%,  $k = 1,3$  (Table 10.2).

$$t_{fi,d} = 0,20fD = 0,2 \times 1,3 \times 150 = 39 \text{ min}$$

This result will be conservative as the charring rate is assumed as 0,6 mm/min, rather than 0,8 in the calculations.

#### 10.2.4 Approach developed by Stiller

The full analytical work behind the equations developed by Stiller (1983) will not be covered here except to comment that the equations derived are based on a large amount of research which attempted to fit calculated results for the performance of timber beams and axially columns to the results from a large number of tests. The equations to determine the loss of section which allow the rounding of arrises and any strength losses in the core to be ignored were determined using regression analyses on various hypotheses until acceptable fits were found.

**10.2.4.1 Beams**

Stiller gives the depth of charring  $d_{char,s}$  in millimetres after an exposure of  $t_{fi,d}$  in minutes to the standard furnace curve on the side faces of the beam as

$$d_{char,s} = 0,753t_{fi,d} + 8,92 \quad (10.30)$$

and the depth of charring on the upper or lower face  $d_{char,b}$  as

$$d_{char,b} = 1,472d_{char,s} - 0,12 \quad (10.31)$$

The elastic section modulus of the section is calculated on the original section reduced by the charring depths calculated from Eqs (10.30) and (10.31) and the bending strength determined on the reduced section.

**10.2.4.2 Columns**

For axially loaded columns exposed on all four sides, the charring depth  $d_{char,col}$  is given by

$$d_{char,col} = 0,59t_{fi,d} + 6,4 \quad (10.32)$$

The load-carrying capacity is then determined using the residual section with the axial compressive strength  $\sigma_{w,t}$  determined using a strut buckling interaction equation which is given by

$$\frac{\sigma_{w,t}}{\sigma_d} = \frac{1}{2} + \frac{1 + \eta}{2} \frac{\sigma_E}{\sigma_d} - \sqrt{\left(\frac{1}{2} + \frac{\sigma_E}{\sigma_d} \frac{1 + \eta}{2}\right)^2 - \frac{\sigma_E}{\sigma_d}} \quad (10.33)$$

where  $\sigma_d$  is the design compressive strength of the timber,  $E$  is Young's modulus,  $\sigma_E$  is the Euler buckling stress calculated using the slenderness ratio  $\lambda$  determined on the reduced section and the imperfection factor  $\eta$  is given by

$$\eta = 0,1 + \frac{\lambda}{200} \quad (10.34)$$

**Example 10.6: Determination of the fire performance of the beam in Example 10.1 using the approach proposed by Stiller**

The timber beam (Grade C22) is 250 mm deep by 75 mm wide and is simply supported over a span of 4,5 m. The beam system is at 600 mm spacing and carries a permanent load on the beam of 0,2 kN/m and a total variable load of 2,5 kPa. The required fire resistance is 30 min.

Load in the fire limit state is  $0,3 \times (0,6 \times 2,5) + 0,2 = 0,65$  kN/m

Maximum bending moment,  $M_{Ed,fi} = 0,65 \times 4,5^2/8 = 1,65$  kNm.

Calculate the loss of section for the side faces from Eq. (10.30)

$$d_{char,s} = 0,753 \times 30 + 8,92 = 31,5 \text{ mm}$$

Calculate the loss of section from the bottom face from Eq. (10.31)

$$d_{char,b} = 1,472 \times 31,5 - 0,12 = 46,2 \text{ mm}$$

Reduced width,  $b = B - 2d_{char,s} = 75 - 2 \times 31,5 = 12$  mm

Reduced depth,  $d = D - d_{char,b} = 250 - 46,2 = 203,8$  mm

(i) Flexure

Elastic section modulus,  $W_{el} = bd^2/6 = 0,083 \times 10^3$  mm<sup>3</sup>.

Use the 20% fractile strengths and stiffnesses determined in Example 10.1.

So,  $M_{Rd,fi} = 0,083 \times 27,5 = 2,28$  kNm, which exceeds  $M_{Ed,fi}$ .

(ii) Shear

$$V_{Rd,fi} = 1,5f_{v,20}bd = 1,5 \times 3,0 \times 12 \times 203,8 = 11,0 \text{ kN} \quad (V_{Ed,fi} = 1,46 \text{ kN})$$

(iii) Deflection

$$I = 8,46 \times 10^6 \text{ mm}^4$$

$$\delta_b = 5ML^2/48EI = 5 \times 1,65 \times 4,5^2/(48 \times 8,5 \times 10^{-6} \times 8,46 \times 10^6) = 0,048 \text{ m}$$

Span-deflection ratio =  $4,5/0,048 = 94$ . Although this is low it would be acceptable in an accidental limit state.

**Example 10.7: Column design using Stiller**

Check the fire performance of 150 mm square 3 m high column to last 30 min carrying an axial load in the fire limit state of 45 kN.

Use Eq. (10.32) to determine the charring depth.

$$d_{char,col} = 0,59 \times 30 + 6,4 = 24,1 \text{ mm}$$

$$d = D - 2d_{char,col} = 150 - 2 \times 24,1 = 101,8 \text{ mm}$$

$$i = d/2\sqrt{3} = 29,4 \text{ mm}$$

$$\lambda = L_e/i = 3000/29,4 = 102$$

$$\sigma_E = \frac{\pi^2 E_{20}}{\lambda^2} = \frac{8,5 \times 10^3 \pi^2}{102^2} = 8,06 \text{ MPa}$$

Take the design compressive stress  $\sigma_d$  as 20 MPa.

Use Eq. (10.33) to calculate  $\sigma_{w,t}/\sigma_D$ .

From Eq. (10.34),

$$\eta = 0,1 + \frac{\lambda}{200} = 0,1 + \frac{102}{200} = 0,61$$

and

$$\begin{aligned} \frac{\sigma_{w,t}}{\sigma_d} &= \frac{1}{2} + \frac{1 + \eta}{2} \frac{\sigma_E}{\sigma_d} - \sqrt{\left(\frac{1}{2} + \frac{\sigma_E}{\sigma_d} \frac{1 + \eta}{2}\right)^2 - \frac{\sigma_E}{\sigma_d}} \\ &= \frac{1}{2} + \frac{1,61}{2} \frac{8,06}{20} - \sqrt{\left(\frac{1}{2} + \frac{8,06}{20} \frac{1,61}{2}\right)^2 - \frac{8,06}{20}} = 0,298 \end{aligned}$$

or  $\sigma_{w,t} = 0,298 \times 20 = 5,96$  MPa. Multiply this by 1,25 to give the 20% fractile, so

$$N_{Rd,fi} = 1,25 \times \sigma_{w,t} d^2 = 1,25 \times 5,96 \times 101,8^2 = 77,2 \text{ kN}$$

This exceeds the design fire load.

### 10.3 TIMBER FLOORS AND PROTECTED TIMBER SYSTEMS

#### 10.3.1 Timber floors

Where the joists of timber floors are directly exposed to fire, the methods outlined in the previous sections of this chapter may be used. Where there is plasterboard or other similar protection to the underside of the floor or where there is additional insulation between the joists, the above methods are not applicable, and either the method mentioned in the following section should be used or reference made to a publication on the fire protection of timber floors by the Association of Specialist Fire Protection Contractors and Manufacturers (1993). This later reference is also useful where existing floors need to be upgraded or checked for increased fire resistance periods.

#### 10.3.2 Protected timber systems

The earliest available data on the performance of stud walls is given in Meyer-Ottens (1967) which includes details of German fire resistance tests.

The results from these tests produced the concept that the contribution of various parts of the system produced additive contributions to the fire performance.

For timber members in unfilled voided construction, the start of charring is delayed by a time  $t_{ch}$  given by

$$t_{ch} = t_f \quad (10.35)$$

where  $t_f$  is given by

- For fire protective claddings and wood-based panels, thickness  $h_p$

$$t_f = \frac{h_p}{\beta_0} - 4 \quad (10.36)$$

- For type A and H gypsum, plasterboard for walls or with floors with joist spacing less than 400 mm

$$t_f = 2,8h_p - 11 \quad (10.37)$$

- For type A and H gypsum plasterboard for walls or with floors with joist spacing between 400 and 600 mm

$$t_f = 2,8h_p - 12 \quad (10.38)$$

For the separating function of wall and floor assemblies to be satisfied,  $t_{ins} > t_{req}$ .

$$t_{ins} = \sum_i t_{ins,0,i} k_{pos} k_j \quad (10.39)$$

where  $t_{ins,0,i}$  is the basic insulation value of layer  $i$ ,  $k_{pos}$  is a position coefficient and  $k_j$  is a joint coefficient.

The values of  $t_{ins,0,i}$  are given for a number of materials or finishes:

- Plywood ( $\rho \geq 450 \text{ kg/m}^3$ )

$$t_{ins,0,i} = 0,95h_p \quad (10.40)$$

- Particleboard or fibreboard ( $\rho \geq 600 \text{ kg/m}^3$ )

$$t_{ins,0,i} = 1,1h_p \quad (10.41)$$

- Wood panelling ( $\rho \geq 400 \text{ kg/m}^3$ )

$$t_{ins,0,i} = 0,5h_p \quad (10.42)$$

- Gypsum plasterboard types A, F, R and H

$$t_{ins,0,i} = 1,4h_p \quad (10.43)$$

If cavities are completely or partially filled to an insulation thickness of  $h_{ins}$ , then

- Rock fibre

$$t_{ins,0,i} = 0,2h_{ins}k_{dens} \quad (10.44)$$

- Glass fibre

$$t_{ins,0,i} = 0,1h_{ins}k_{dens} \quad (10.45)$$

The values of  $k_{dens}$  are related to the material type and density and are given in Table 10.3.

For a void cavity with depths from 45 to 200 mm,  $t_{ins,0}$  is taken as 5,0 min.

The position coefficient  $k_{pos}$  are taken as appropriate from Tables E.3–E.5 of EN 1995-1-2.

**Table 10.3** Values of  $k_{dens}$

Material	Density ( $\text{kg/m}^3$ )			
	15	20	26	50
Glass fibre	0,9	1,0	1,2	
Rock fibre			1,0	1,1

Source: Table E2 of EN 1995-1-2

# 11

## Masonry, aluminium, plastics and glass

---

This chapter covers the design of structural elements or structures fabricated from or involving the use of masonry, aluminium or plastics. The term plastics also cover the use of plastic-based composites. Notes are also included on the behaviour of glass.

### 11.1 MASONRY

There has been little development in the calculation of the performance of masonry in a fire, partly because one of the main uses of masonry is to act as non-loadbearing fire separating walls to form isolated compartments within a large open plan structure. Often where masonry is used as external cladding, again the wall is carrying no applied vertical load, but only has to resist the effect of horizontal wind loading. In the UK, at least, load-bearing masonry, i.e. designed to carry imposed vertical loads, is either used in housing (where the fire resistance requirements are low) or in single-storey structures such as sports halls (where the wall is often of diaphragm- or fin-type construction which will have far greater stability than conventional cavity wall systems and therefore tends not to be a problem). The other reason why there appears to be little calculation on the effect of fire on masonry is the paucity of test data on either the compressive or tensile strength of masonry at elevated temperatures. The general use of masonry is to act as a separating element and therefore to ensure the temperature on the unexposed face does not exceed the limit prescribed in the standard fire test of 140°C.

#### 11.1.1 Insulation requirements of masonry construction

Tabulated requirements for the insulation limit state of insulation for masonry are given by specifying the wall thickness needed for a given

type of brick and finish, e.g. plaster. Data on these requirements may be found in EN 1996-1-2. It is possible under certain circumstances to propose either interaction formulae between individual layers or to allow for the effects of coatings (de Vekey, 2004).

One such equation for interaction (ASCE/SFPE, 2003) for the fire resistance  $R$  (hours) of an assembly is given by

$$R = \left( R_1^{0,59} + R_2^{0,59} + \dots + R_n^{0,59} + A_s \right)^{1,7} \quad (11.1)$$

where  $R_1$ ,  $R_2$ , to  $R_n$  are the resistances of individual layers of each leaf, and  $A_s$  is taken as 0,3 for each continuous air space of width between 12,6 and 89 mm.

It has also been proposed by de Vekey that for type 1 concrete masonry (density less than 1100 kg/m<sup>3</sup>), the fire resistance  $R$  (hours) can be given by

$$R = (0,026 + 0,01P) t_{eff} \quad (11.2)$$

where  $t_{eff}$  is the equivalent thickness of the wall (mm),  $P$  is a coating factor taken as 0 for bare walls and 1 for plastered or rendered walls with a minimum layer thickness of 12 mm.

It should be remembered that most fire resistance tests are carried out under a heating regime determined by the standard furnace curve and are performed on limited panel sizes often unloaded, thus providing little or no information on load-carrying capacity. Also it should be noted that whereas a wall panel, typically some 3 m square, when tested is likely to be stable, extrapolation of stability and any resultant reduction in load-carrying capacity cannot be made to larger panel sizes found in normal building construction. Even where panels are loaded during the test, the loading is axial, i.e. applied through the centroid of the section. This loading pattern is not the most severe and may not represent the loading pattern actually present in structures, since the loading from joists, either built into the walls or attached using joist hangers, will be eccentric to the centroidal axis (Foster, 1975). Also such results assume that the wall construction does not allow the passage of flame between the joints in successive panels. Movement between panels for unloaded masonry is likely as a certain amount of bowing occurs due to the thermal gradients across a leaf of masonry (Fisher, 1975).

### 11.1.2 Thermal bowing

When a wall is subjected to temperature gradient across its thickness, then the wall may be considered as a one-dimensional member

(i.e. there is no lateral boundary affecting the unrestrained bowing), the amount of bowing is given by (Cooke, 1987a, b; Cooke and Morgan, 1988):

(a) for a cantilever

$$\delta_{bow,c} = \frac{\alpha_m h_{wall}^2 \Delta\theta}{2d_{wall}} \quad (11.3)$$

where  $\delta_{bow,c}$  is the deflection of the cantilever,  $\Delta\theta$  is the temperature gradient across the leaf,  $d_{wall}$  is the thickness,  $\alpha_m$  is the coefficient of thermal expansion and  $h_{wall}$  is the height of the wall and,

(b) for a simply supported beam

$$\delta_{bow,b} = \frac{\alpha_m h_{wall}^2 \Delta\theta}{8d_{wall}} \quad (11.4)$$

where  $\delta_{bow,b}$  is the central deflection of the beam.

It will thus be noted that for a cantilever element, the deflection is four times that for a beam element with the same temperature gradient, thickness and coefficient of thermal expansion. Ideally, therefore, separating walls should be held at the top and bottom by the supporting structure. However, the deflections calculated from either Eq. (11.3) or (11.4) are seldom likely to be attained in practice; the aspect ratio of a tall fire separating wall is likely to be such that the vertical restraint along the sides of wall (where it is restrained by the supporting structure) will be such as to cause the wall to span horizontally and so reduce the deflection substantially. A wall with no vertical or top restraint will show some bowing, although this will be reduced in the initial stages by the effects of any vertical loading applied to the wall. The vertical load is only likely to cause problems after a substantial period when the wall may tend to become laterally unstable with the vertical load inducing high tensile stresses owing to the moments induced by the lateral deformations. The Design Guide issued in 1992 by the Canadian Concrete and Masonry Codes Council provides information on the forces to be resisted by horizontal members in resisting any sagging effects caused by the bowing of walls during a fire.

### 11.1.3 Load-bearing cavity walls

The largest amount of work on the testing and analysis of loaded cavity walling appears to have been carried out in Australia, although more recent work has been carried out at Ulster University (Lavery, Nadjai

**Table 11.1** Experimental results from fire tests on cavity walls

Wall type*	Loading <sup>†</sup>		Maximum deflection (mm)	Time to failure (min)
	Internal	External		
230/90	125	0	74	68
230/90	75	0	87	47 <sup>‡</sup>
230/90	25	0	87	39 <sup>‡</sup>
230/90	160	0	58	22
230/90	125	125	60	183 <sup>§</sup> /240 <sup>‡</sup>
230/90	0	160	18	240
270/110	0	240	–	300
270/110	80	0	75	50
270/110	100	0	70	34

\* The first figure in the wall-type is the overall thickness (mm) and the second is the thickness (mm) of each leaf built from clay bricks.

<sup>†</sup> The loading is given as a percentage of the working (or service) loading.

<sup>‡</sup> Indication that failure occurred by excessive deflection.

<sup>§</sup> Indicates initial failure of the internal leaf before the whole wall failed.

*Source:* Gnanakrishnan, Lawrence and Lowther, 1988

and O'Connor, 2000/1; Nadjai, Laverty and O'Gara, 2001) where it was observed that the effect of increasing load (i.e. increasing the compressive stress levels) may offset the potential deleterious effect of increasing slenderness.

A comprehensive series of tests on 230-mm and 270-mm thick with various load levels were carried out in Australia (Gnanakrishnan, Lawrence and Lawther, 1988). The results are given in Table 11.1, where it is observed that loading on the leaf adjacent to the fire appears far more critical than load levels on the unheated or external leaf. The application of loading on the hot leaf reduces lateral deflection or thermal bowing. The application of loading on the external or cold leaf appears to stabilize the wall and also has the effect of reducing the deflections. Temperature measurements during the tests indicated that the temperature rises in the external leaf were relatively low with a substantial gradient across the 50-mm cavity. Some attempt was also made to model the behaviour of the cavity walls but, due to the assumptions made and the paucity of high strength data on masonry, the results appear only to show the correct trends.

## 11.2 ALUMINIUM

The calculation procedure given in ENV 1999-1-2 to determine the fire performance of aluminium closely follows that for steelwork since the

assumption of no significant temperature gradient across the thickness of the specimen holds for both materials.

Thus the temperature within an aluminium section can be calculated using the equations given in Chapter 8 using the relevant properties given in Chapter 5. The only difficulty is that the values of the thermal conductivity of the insulation must be those applicable at the limiting temperature for aluminium. The values of insulation properties given in Chapter 8 cannot be used since these are only valid at temperatures of around 550–600°C. Owing to the extensive use of aluminium in the off-shore industry, it may also be necessary to consider the use of the hydrocarbon curve rather than the standard cellulosic curve to give the gas temperature.

The limiting temperature for aluminium is around 200°C (Bayley, 1992) as above this temperature the strength loss is such that any factor of safety in the ambient design is completely eroded. The limiting temperature is taken as a function of the exact aluminium alloy in use as the temperature-related strength loss is very dependant on the amounts and type of alloying constituents.

### **11.3 PLASTICS AND PLASTIC-BASED COMPOSITES**

Plastics and especially plastic-based composites are structurally very efficient in terms of their weight strength ratio but poor when exposed to the effects of fire. This therefore means that such materials need extensive levels of protection in order to retain load-carrying capacity at elevated temperatures. This therefore means that the insulation thicknesses need to ensure that the temperatures within the plastic element need to be kept close to ambient. There is an additional problem in that some plastics decompose with temperature and emit highly inflammatory or toxic gases.

Bishop and Sheard (1992) report some tests carried out under exposure to the hydrocarbon rather than the cellulosic standard curve on fire protection of poltruded phenolic resin systems and note that even though the levels of protection needed are higher than those for steelwork, the resultant strength weight ratio is still favourable for resins compared to steel. Unfortunately the temperature levels for which the insulation was designed when applied to the extruded sections is not stated. Wong (2003) reports some test results on Glass Fibre-Reinforced Polymer (GFRP) stringer wall systems and material properties. The compressive strength drops from around 275 MPa at ambient to around 85 MPa at 90°C and 20 MPa at 250°C. The values of Young's modulus at the same temperatures are 22,25 GPa, 15,6 GPa and 6,6 GPa, respectively. Results comparing the elevated temperature tensile strengths of Carbon Fibre-Reinforced plastic (CFRP) and Glass Fibre-Reinforced Plastic are also presented.

Both materials give a strength loss at 500°C of around 84%, although in absolute terms CFRP is stronger, also there appears to be no size effect on GFRP between 9,5 and 12,7 mm diameter specimens.

#### **11.4 GLASS**

Conventional glass softens at around 700–800°C although shattering can occur below these temperatures where load is applied to the glass through expansion of the system used to support any glazing. It is generally considered that any glazing will fail in the very early stages of fire and thus any openings normally glazed can be considered as an effective ventilation source and in the case of roof lights will allow the fire to vent. Where glass is required to resist the effects of fire, for example, in fire doors (although the amount of glazing is limited), the glazing unit should either be assembled from specially toughened glass or wired glass is used.

# 12 Frames

---

Whereas the previous chapters have dealt with the design aspects of isolated structural elements when exposed to the effects of fire, this chapter is concerned with how those elements behave when connected together to form part of a structure and how the continuity effects that are generated when elements are connected together can be taken advantage of, in a design. Rather than to repeat the material produced recently in a considerable number of papers, tests on the various frames at Cardington are posted here so that the emphasis is placed on discussing the implications for design. Additionally, the performance of connections and portal frames will be highlighted.

## 12.1 TESTS ON ISOLATED FRAMES AND CONNECTIONS

### 12.1.1 Frame tests

The earliest large-scale test reported by Cooke and Latham (1987) was on a frame heated by a natural compartment fire. The frame was of unprotected steelwork except that the stanchion webs were filled in by non-loadbearing blockwork. Such non-loadbearing blockwork had already been shown to increase the fire resistance of bare steelwork (Building Research Establishment, 1986; Robinson and Latham, 1986). The stanchions had a pinned feet and were  $203 \times 203 \times 52$  UC (3,53 m long), and the rafter which was laterally unrestrained was connected to the columns by flexible end plates was a  $406 \times 178 \times 54$  UB (4,55 m long). Both the members were of Grade 43A (S275) steel and carried a full service loading comprising 39,6 kN vertical loads applied at fifth points on the rafter, and axial loads of 552 kN applied at the top of each stanchion. The test had to be terminated due to the inability of the load to be applied as excessive deflections occurred after 22 min in a natural fire deemed to be equivalent to 32,5 min of a standard furnace test. The column alone had a fire resistance of 36 min and the beam, which failed by the occurrence

of plastic hinges, had a fire resistance of 22 min. It was surely this test which started to demonstrate the beneficial effects of continuity that was the seed corn that produced the concept of testing on a full-sized multi-storey, multi-bay structure at Cardington. However, before continuing to discuss Cardington, it is perhaps worthwhile to examine the tests on beam–column connection behaviour which was also highlighted by the Cooke and Latham test.

### 12.1.2 Fire tests on beam and column assemblies

Tests were carried out on stub beams (305×165×40 UB Grade S275) bolted with varying types of connections to stub columns (203×203×52 UC Grade S275) with the beams loaded to give shear forces and hogging moments typical of those in conventional construction (Lawson, 1990a, b).

The tests utilized varying types of structural fire protection. Where full protection was envisaged, a spray protection designed to give 60 min fire resistance at a critical steel temperature of 550°C was used. In certain cases, the column web was infilled with non-loadbearing concrete blockwork and in others no protection was applied to the column. The results from the tests are given in Table 12.1. The results show that the connections are capable of adsorbing a high degree of moment before undue deformations occurred and thus a significant transfer of moment could occur from the beam into the column during a fire. It should be noted that the tests were on assemblies which modelled internal columns where the net moment on the column would sensibly be zero owing to the balanced nature of the loading. This will not be the case for an external column where, if moment transfer from the beam is allowed during a fire, either substantially higher amounts of fire protection or a larger column for a given amount of fire protection will be needed as the load ratio on the column is increased. The tests also provided data on the temperatures reached in the bolted connections. These data enable capacity checks to be carried out on the connection. Owing to the local buckling observed close to the ends of beams in the Cardington tests, the method of enhancement of fire performance using moment transfer at beam–column connections should be limited to slim floor beams or partially encased beams or situations where thermal expansion is not restrained (Bailey, Newman and Simms, 1999).

Unfortunately, these tests were carried out only at a single load level and could not therefore be used to determine moment–rotation characteristics for connections subject to variable load levels as would be needed for computer analysis of fire-affected steel frameworks. Experimental work (Leston-Jones *et al.*, 1997) suggested that the moment–curvature relationship for flush end-plate connections could be expressed using an

**Table 12.1** Results from tests on unrestrained connections to establish moment transfer characteristics

Connection details	Moment capacity	Test moment	Lever arm (m)	Fire performance	
				Target (min)	Actual (min)
Extended endplate (UB)	0,66 $M_{pl}$	0,4 $M_{pl}$	0,98	30	45
		0,3 $M_{pl}$			50
Flush endplate (UB)	0,30 $M_{pl}$	0,2 $M_{pl}$	0,49	30	29
Extended endplate (U)	0,66 $M_{pl}$	0,2 $M_{pl}$	0,49	60	97
Flush endplate (P)	0,30 $M_{pl}$	0,2 $M_{pl}$	0,49	90	126
Web cleat (P)	0,10 $M_{pl}$	0,1 $M_{pl}$	0,49	90	115
Composite flush endplate (P)	0,4 $M_{pl}$	0,4 $M_{pl}$	0,98	90	100
		0,3 $M_{pl}$			113
Composite web cleat (P)	0,20 $M_{pl}$	0,2 $M_{pl}$	0,49	90	112
Shelf-angle flush endplate (UB)	0,30 $M_{pl}$	0,2 $M_{pl}$	0,49	60	70
		0,1 $M_{pl}$			90

$M_{pl}$  refers to the moment capacity of the beam.

P indicates that both the beam and column were protected to 60 min, U both the beam and column were unprotected, and B the web of the column was blocked in with lightweight concrete blocks.

Three of the tests were carried out under the influence of the higher of the two moments in the above table until failure was imminent when the moments were then reduced to the lower values until actual failure.

Source: Lawson (1990a)

equation similar to the Ramberg-Osgood (1943) equation for the ductile stress-strain curve, i.e.

$$\phi = \frac{M}{A} + 0,01 \left( \frac{M}{B} \right)^n \quad (12.1)$$

where  $\phi$  is the rotation under a moment  $M$ ,  $A$  is related to the stiffness of the connection,  $B$  to its strength and  $n$  defines the non-linear shape of the curve.

## 12.2 TESTS ON THE LARGE FRAME STRUCTURES AT CARDINGTON

### 12.2.1 Timber frame structure

The timber frame structure at Cardington had two fire tests carried out. The first one was effectively designed to evaluate the fire spread

(and compartmentation) and the second one to evaluate the performance of stairs subject effectively to arson.

In the first test, a timber crib fire was ignited in a corner flat on the level 3 storey. Peak temperatures reached at around 1000°C in the compartment. The fire lasted for around 64 min including a pre-flashover period of 24 min, and was terminated after the fixity of the ceiling boards was lost and the joists were subjected to direct fire exposure for around 8 min. However, during this time, the temperatures outside the fire compartment did not exceed 50°C except for some areas in the cavities which reached 100°C. The results from this test allowed a relaxation in the England and Wales Building Regulations on timber frame construction, and allowed the Scotland and Northern Ireland Regulations to be brought into line.

Preliminary tests in a purpose-built test rig, demonstrated that the stair system would need fire-retardant treatment (i.e. raw timber burnt out too quickly). The actual test demonstrated no fire spread from the ignition sources with the fire lasting for 31 min and the stairs were perfectly reusable (Enjily, 2003).

### **12.2.2 Concrete frame structures**

Only one concrete frame structure was constructed. It was of a slightly unusual format, in that it was a flat slab with diagonal steel flats acting as bracing. Also, the columns were kept at the same size throughout the structure with the concrete strength being increased in the columns in the lower storeys. The structure was designed to investigate the optimization of the execution process rather than necessarily to investigate fire performance although fire tests were envisaged from the initiation of the project (Chana and Price, 2003).

The structure was a seven-storey structure with five sets of columns in one direction and four in the other, all at 7,5 m spacing. Each storey was 3750 mm high from soffit to soffit. The slab was 250 mm thick (Grade C37 concrete with a flint type aggregate). The internal columns were 400 mm square and the external 400 mm × 250 mm. The columns in the lower storeys were constructed using Grade 85 high strength concrete with limestone aggregate and microsilica. They also contained 2,7 kg/m<sup>3</sup> polypropylene fibres.

The test was carried out in September 2001 shortly before the Cardington Test Facility was closed. The technical data are taken from Bailey (2002). Since the author was present at the test and was able to inspect the structure shortly after the test, the interpretations of the results are those of the author.

The compartment chosen for the fire test involved 4 bays of the lowest storey of the frame surrounding one of the square internal columns. The design fire was a parametric fire with an opening factor of  $0,08 \text{ m}^{0,5}$  and an insulation factor of  $1104 \text{ J/m}^2 \text{ s}^{0,5} \text{ K}$  which gives a maximum temperature of around  $1050^\circ\text{C}$  at about 35 min. The fire load was  $40 \text{ kg/m}^2$  timber cribs, equivalent to  $720 \text{ MJ/m}^2$ .

At 18 min, the instrumentation failed when the ceramic blanket, which was shot-fired to the soffit of the slab, at the top of the blockwork and plasterboard came out owing to the severe spalling of the slab. This is part of the reason why the slab spalled was of the aggregate type (flint); but this was exacerbated by the high strength of the concrete (61 MPa cube strength, or around 50 MPa cylinder strength at 28 days), the high moisture content of 3,8% by weight and a permeability of  $6,75 \times 10^{-17} \text{ m}^2$ . The structure was around three- and-a-half years old at the time of the test, thus using strength gain data for normal cements from EN 1992-1-2, the cylinder strength at the time of test may have been around  $1,35 \times 50 = 67 \text{ MPa}$ . This would put the slab concrete into the category of high strength concrete. From Fig. 9 in Tenchev and Purnell (2005) spalling in the slab would be expected at around 8–10 min with a depth of 10 mm if the fire exposure were to the standard furnace curve. In the actual test, spalling commenced at around 6–7 min after ignition. The actual depth of spalling was around 20–25 mm as much of the bottom reinforcement was exposed. The test also indicates the possible need to consider maximum as well as minimum strength requirements for concrete.

It should be noted that the central column (Grade C85) with a cube strength of 103 MPa (cylinder strength 80 MPa) at 28 days did not spall. The moisture content was 4,4%, the permeability  $1,92 \times 10^{-19} \text{ m}^2$ , with an estimated cylinder strength at the time of test of slightly over 100 MPa. After the test, cracking was observed at the corners of the column – it is not known when all this had occurred. It needs to be noted that the moisture contents were high as the building was unable to dry out as would occur in a structure built in an open air.

The structural variable fire load was 3,25 kPa above the fire compartment. This gave a load of 925 kN in the central column and 463 kN in the edge column.

At the time of failure of the instrumentation, the slab deflections were between 10 and 60 mm, with the higher values generally in the centres of the slabs or where severe spalling had occurred. The residual deflections in the slab on an average were around 60 mm.

More worrying was the lateral deflection of the edge column which caused buckling of the steel flats forming the bracing. The maximum deflection during the test was in excess of 100 mm. The residual deflection

of this column at first floor level was 67 mm. Cracking was also observed at the column–slab interface at first floor level.

Although the Cardington test was useful, in that it showed that the type of frame tested could satisfactorily resist a compartment fire, there are a number of issues unresolved:

- (1) A single fire test is inadequate to allow full calibration of any computer simulation. This is in part due to the unfortunate loss of temperature and deformation data in the test and in part due to the need to consider other fire scenarios of severity or position.
- (2) The fact that the structure was reasonably flexible in the horizontal direction may have alleviated the effects of spalling in the slab. A much stiffer structure with lift shafts and stairwells may have induced higher compressive stresses into the slab and hence increased the spalling levels.

### 12.2.3 Composite steel frames

The structure is eight storeys high, with a plan of 5 bays each 9 m long by 3 bays wide each of 6 m wide surrounding a central bay of 9 m with an approximate floor area of 945 m<sup>2</sup>. The soffit to soffit height was 4 m. The primary beams were 356×171×51 UB Grade S355 on the 6 m span and 610×229×101 UB Grade S275 on the 9 m spans, the secondary beams are 305×165×40 UB Grade S755 (all 9 spans), the perimeter beams were also 356×171×51 UB Grade S355 and the columns 254×254×89 UC Grade S355 on the upper storeys and 305×305×137 UC Grade S355. The composite deck was lightweight concrete (cube strength 47 MPa, cylinder strength 38 MPa).

There were six main tests carried out with applied loading in each test of 2663 kPa (Moore and Lennon, 1997). The summary below is in part taken from Moore and Lennon, but with additional information from Bailey, Lennon and Moore, 1999; Izzuddin and Moore, 2002; O'Connor, Kirby and Martin, 2003; Newman, Robinson and Bailey, 2006.

#### **Test 1: Restrained beam**

The test was carried out on one of the secondary composite beams with a gas-fired furnace surrounding the central 8 m of the 9 m span of a beam at level 7 with a floor area of 24 m<sup>2</sup>. The heating rate was 3–10°C/min. At a maximum temperature of 875°C in the lower flange, a maximum vertical displacement of 232 mm was recorded. The residual deflection was 133 mm. Local buckling of the bottom flange at the ends of the beam and failure of the end-plate connection at both ends was observed. It would

appear that the failure of the end-plates was gradual and was due to the high tensile forces induced during cooling.

### **Test 2: Plane frame**

This test was conducted on a complete plane frame across the structure at level 4 with a floor area of  $53\text{ m}^2$  using a purpose-built furnace measuring 21 m long by 3 m high. The floor beams and connections were unprotected. The columns were protected within 200 mm below the connections. At a steel temperature of  $800^\circ\text{C}$ , a maximum vertical displacement of 445 mm was recorded. This test also produced distortional buckling of the column heads with the columns shortening by around 200 mm. This led to the columns and connections being fire protected in later tests. The secondary beams were heated over a length of around 1 m. An inspection after the test indicated bolts in the fin plate connections had sheared. Again, this was due to high tensile forces induced during cooling.

### **Test 3: Corner compartment no. 1**

This was conducted under a natural fire regime with timber cribs providing a fire load of  $45\text{ kg/m}^2$  with ventilation being controlled by a moveable shutter on one face. The opening factor was initially  $0,031\text{ m}^{0,5}$  and subsequently increased slightly to  $0,034\text{ m}^{0,5}$ . It was estimated that the heating regime had a time equivalent of around 85 min. This was at level 2 with a floor area of  $76\text{ m}^2$ . The internal compartment wall was placed slightly eccentric to the 9 m internal beam, but under the 6 m internal beam. In each case, a 15 mm deflection allowance was inbuilt. Little damage to the blockwork compartment walls was observed. The perimeter beams and columns were fire protected but the internal beams were left bare. Temperatures in excess of  $1000^\circ\text{C}$  were recorded with an associated maximum displacement of 425 mm. The maximum slab deflection was 269 mm in the centre of the compartment. After cooling, this deflection had recovered to 160 mm.

### **Test 4: Corner compartment no. 2**

This was carried out on a corner compartment  $9\text{ m} \times 6\text{ m}$  at level 3 with a fire load of  $40\text{ kg/m}^2$ . The compartment walls were constructed using fire-resistant boarding running between the boundary columns. The columns were fire protected up to and including the connections. One external face (length 9 m) was formed using double-glazed aluminium screen. The fire initially did not flashover owing to lack of oxygen and two panes of glass needed to be removed sequentially to achieve flashover. Finally, the maximum compartment temperature was around  $1050^\circ\text{C}$  with the

temperature recorded on the lower flange of the unprotected beam being 903°C. The maximum slab deflection was 270 mm. The stud walls suffered severe damage owing to the beam deflections. Additionally, local buckling of the beams at the connections and end-plate fracture in the connections caused during cooling were observed. A substantial amount of cracking in upper surface of the composite slab around the column was also observed.

#### **Test 5: Large compartment**

The compartment was designed to be representative of an open plan office with dimensions of 18 m × 21 m at level 3. The fire load was 40 kg/m<sup>2</sup> timber cribs. The compartment was bounded by erecting a fire-resistant wall across the whole structure. The lift shaft was also provided with additional protection. Double glazing was installed on two sides of the building with the middle-third of the open area on each side left open for ventilation. All the beams were left unprotected whilst internal and external columns were protected up to and including the connections. The fire started sluggishly, but because of a cross draught the maximum temperatures were reduced. The recorded maximum was 760°C, with the steelwork some 60°C lower. The maximum slab deflection was 557 mm which recovered to 481 mm after cooling. After the test, it was observed that extensive local buckling occurred at the beam to beam connections with a number of failures in the end plates. One case of a complete fracture between the beam web and end plate was noted. The shear was then carried by the composite floor above the connection causing large cracks, but no collapse, in the floor.

#### **Test 6: Demonstration compartment**

The compartment had an area of 180 m<sup>2</sup> at level 2 and was filled with office furniture (and timber cribs) to give a fire load of 45 kg/m<sup>2</sup> timber equivalent. Ventilation was provided by a combination of blank openings and widows. All the beams were left unprotected whilst internal and external columns were protected up to and including the connections. At around 10 min the temperature at the rear of the compartment had risen to over 900°C with an eventual maximum of 1213°C. The recorded maximum steel temperatures were in excess of 1100°C in the loor beams, and between 1012 and 1055°C in the primary beams. The maximum deflections were around 640 mm on one of the secondary beams. The residual deflection after cooling was 540 mm. Cracking of the floor around one of the column heads was also observed. This was in part due the mesh in the top of the slab being inadequately lapped.

Observations from the tests:

- (1) It is very obvious that the overall behaviour of members in a frame is far superior to that predicted by isolated furnace tests. This is in part due to continuity and in part due to alternative load paths or load-carrying mechanisms.
- (2) Temperature levels were far higher than those that would be permitted by design codes, even allowing for the load levels under applied variable loads of around 1/3rd the ambient variable imposed load (O'Connor, Kirby and Martin, 2003).
- (3) These were high but did not cause failure. The values attained only confirm that the deflection limits imposed in the standard furnace test are not applicable to structural behaviour.
- (4) The values of residual deflections are high, i.e. the deflections in the test are effectively plastic, and hence irrecoverable. It should be noted that part of the residual deflections of the slabs will be due to the beams. Photographic evidence from the tests indicates that there may be large residual deflections of the beam system.
- (5) Whilst the connections performed well during the heating phase, it is clear that the cooling phase may cause problems due to high tensile forces being induced into the beam systems. These tensile forces may cause failure of the end plates, welds or bolt shear.

The performance of the frame under test conditions clearly has implications for design, but these implications can only be realized if it is understood how the frame is actually behaving. This can only be achieved through computer simulation. Much effort has been expended on this to the extent that the results from the Cardington Tests can be reproduced (e.g. Bailey, Burgess and Plank, 1996; Plank, Burgess and Bailey, 1997; Bailey, 1998; Huang, Burgess and Plank, 1999; Sanad *et al.*, 2000).

One immediate conclusion was that secondary beams could go unprotected subject to limits on position and fire endurance (Bailey and Newman, 1998; Newman, Robinson and Bailey, 2006). This work also led to the identification of additional possible load-carrying mechanisms – namely that beside acting in flexure, the slab was also generating, membrane action (Bailey and Moore, 2000a, b; Huang, Burgess and Plank, 2003a, b). The membrane action is generated by a compression ring around the edges of the slab and a central tension zone. A design guide presenting a simplified approach was produced by Bailey (2001) and full design approach by Bailey (2003).

The approach can be outlined as follows. The total load capacity is due to any of the unprotected beam within the area being considered plus that due to the slab determined by yield-line response. However, the yield-line load capacity may be enhanced due to membrane action.

Thus, the total load  $q_{p\theta}$  that may be carried is given by

$$q_{p\theta} = e \left( \frac{WD_{slab,int}}{WD_{floor,ext}} \right) + \frac{WD_{beam,int}}{WD_{floor,ext}} \quad (12.2)$$

where  $WD_{slab,int}$  is the internal work done by the slab,  $WD_{beam,int}$  is the internal work done by the beams,  $WD_{floor,ext}$  is the work done by the loading.

This can be simplified to

$$q_{p\theta} = eq_{p\theta,slab} + q_{p\theta,udl} \quad (12.3)$$

where  $q_{p\theta,slab}$  is load carried by the slab and  $q_{p\theta,udl}$  is the udl (per unit area) supported by the beam.

From conventional yield-line analysis of a rectangular slab under sagging moments  $q_{p\theta,slab}$  is given by

$$q_{p\theta,slab} = \frac{24m_{p\theta}}{(\alpha L)^2 \left[ \sqrt{3 + \alpha^2} - \alpha \right]^2} \quad (12.4)$$

where  $L$  is the longer side of the slab,  $\alpha$  is the aspect ratio of the slab ( $<1,0$ ) and  $m_{p\theta}$  is the temperature-reduced value of the sagging moment which may be based solely on the loss in strength of the reinforcement as the concrete temperature will be relatively low (as the neutral axis depth is small), and any contribution from the profile sheet steel decking is ignored.

The value of  $q_{p\theta,beam}$  over the area supported by an internal beam is determined using a temperature-modified flexural strength  $M_\theta$  based on the temperature of the lower flange and that the beams may be treated as simply supported, i.e.

$$q_{p\theta,beam} = \frac{8M_\theta}{L^2} \quad (12.5)$$

The enhancement factor  $e$  is a function of the vertical displacement to effective depth ratio ( $w/d$ ), the inverse of the aspect ratio ( $1/\alpha$ ) and

a parameter  $g_0$  which is related to the depth of the compression block  $d_c$

$$g_0 = 1 - \frac{2d_c}{d} \quad (12.6)$$

where  $d$  is the effective depth of the slab.

The maximum allowable vertical deflection  $w$  is given by

$$w = \frac{\alpha_c (\theta_2 - \theta_1) l^2}{19,2h} + \sqrt{\frac{3L^2}{8} \frac{0,5f_{y,20}}{E_{s,20}}} \leq \frac{\alpha_c (\theta_2 - \theta_1) l^2}{19,2h} + \frac{l}{30} \quad (12.7)$$

where  $\alpha_c$  is the coefficient of thermal expansion of concrete ( $18 \times 10^{-6}/^\circ\text{C}$  for normal-weight concrete and  $8 \times 10^{-6}/^\circ\text{C}$  for lightweight concrete),  $\theta_2 - \theta_1$  the temperature difference between top and bottom of the slab (for design  $770^\circ\text{C}$  for up to 90 min fire resistance and  $900^\circ\text{C}$  for 120 min),  $L$  and  $l$  are the longer and shorter spans of the slab, and  $h$  is the thickness which may be taken from the mid-height of trough decking and the overall height for dovetail decking.

### Example 12.1: Composite slab with membrane action

A composite slab 110 mm thick (concrete Grade 25/30) with Richard Lees Holorib decking and has H10 bars at 150 mm centres in each direction. The slab element is  $4\text{ m} \times 5\text{ m}$  and is bounded by protected beams on the perimeter and is supported by an unprotected single beam at the mid-point of the 5 m side (Fig. 12.1).

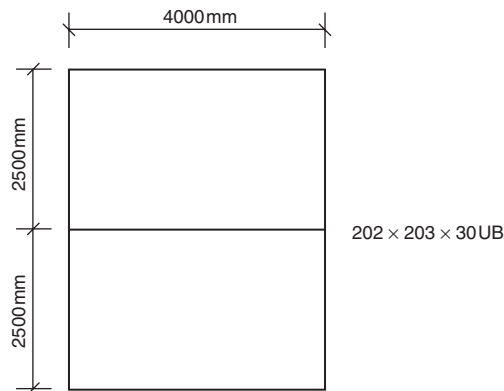


Figure 12.1 Slab and beam layout for Example 12.1.

Determination of the load-carrying capacity for a standard fire exposure of 60 min.

(a) Beam capacity

A 203×133×30 has a flange thickness of 9,6 mm. Use data for 10 mm flange from Table 10 of BS 5950: Part 8 to give a lower flange temperature of 938°C. From Table 5.6,  $k_{y,\theta} = 0,0524$ .

$$M_{\theta} = k_{y,\theta} M_{pl,Rd} = 0,0524 \times 200 = 10,48 \text{ kNm}$$

From Eq. (12.5),

$$q_{p\theta,beam} = \frac{8M_{\theta}}{L^2} = \frac{8 \times 10,48}{4^2} = 5,24 \text{ kN/m}$$

This carries a udl over a width of 2,5 m, thus  $q_{p\theta,udl} = q_{p\theta,beam}/2,5 = 5,24/2,5 = 2,10 \text{ kPa}$ .

Determination of the temperature-reduced moment capacity  $m_{p\theta}$  of the slab:

It will be conservative to ignore the contribution of the decking, then the sagging reinforcement can be designed as if for a slab, but with the steel strength taken as  $k_y(\theta)f_y$ .

Place the required reinforcement level with the top of the dovetail, i.e. the effective depth is  $h_1$  or 59 mm.

Determination of  $\theta_s$  using Eq. (9.7):

The values of  $A/L_r$ ,  $u_3$ ,  $z$ ,  $h_1$ ,  $l_3$  and  $\alpha$  are taken from Example 9.1, thus

$$\begin{aligned} \theta_s &= c_0 + c_1 \frac{u_3}{h_1} + c_2 z + c_3 \frac{A}{L_r} + c_4 \alpha + c_5 \frac{1}{l_3} \\ &= 1191 - 250 \frac{51}{51} - 240 \times 2,56 - 5,01 \times 26,2 + 1,04 \\ &\quad \times 104 - \frac{925}{38} = 279^\circ\text{C} \end{aligned}$$

From Table 5.6,  $k_y(\theta) = 1,0$ ,  $A_s = 524 \text{ mm}^2/\text{m}$ .

It can be noted that for reinforced concrete design in the fire limit state the values of  $\gamma_c$ ,  $\gamma_s$  and  $\alpha_{cc}$  are all 1,0.

From Eq. (6.11) of Martin and Purkiss (2006),

$$\frac{A_s k_y (\theta) f_y}{b d f_{ck}} = \frac{524 \times 1,0 \times 500}{1000 \times 59 \times 25} = 0,178$$

From Eq. (6.11) of Martin and Purkiss (2006),

$$\frac{x}{d} = 1,25 \frac{A_s k_y (\theta) f_y}{b d f_{ck}} = 1,25 \times 0,178 = 0,223$$

From Eq. (6.12) of Martin and Purkiss (2006),

$$\frac{M_{Rd}}{b d^2 f_{ck}} = \frac{A_s k_y (\theta) f_y}{b d f_{ck}} \left(1 - \frac{0,8 x}{2 d}\right) = 0,178 (1 - 0,4 \times 0,223) = 0,162$$

or

$$M = 0,162 b d^2 f_{ck} = 0,162 \times 1000 \times 59^2 \times 25 = 14,1 \text{ kNm/m}$$

Determination of  $q_{p\theta,slab}$  from Eq. (12.4), with  $\alpha = 0,8$  and  $L = 5 \text{ m}$ ,

$$q_{p\theta,slab} = \frac{24 m_{p\theta}}{(\alpha L)^2 \left[ \sqrt{3 + \alpha^2} - \alpha \right]^2} = \frac{24 \times 14,1}{(0,8 \times 5)^2 \left[ \sqrt{3 + 0,8^2} - 0,8 \right]^2} = 17,2 \text{ kPa}$$

Depth of the compression block is  $0,8x = 0,8 \times 0,223 \times 59 = 10,5 \text{ mm}$ .  
From Eq. (12.6),

$$g_0 = 1 - \frac{2d_c}{d} = 1 - \frac{2 \times 10,5}{59} = 0,64$$

Determination of the deflection  $w$  from Eq. (12.7)

$$\begin{aligned} w &= \frac{\alpha_c (\theta_2 - \theta_1) l^2}{19,2h} + \sqrt{\frac{3L^2}{8} \frac{0,5f_{y,20}}{E_{s,20}}} \\ &= \frac{18 \times 10^{-6} \times 770 \times 4^2}{19,2 \times 0,110} + \sqrt{\frac{3 \times 5^2}{8} \frac{0,5 \times 500}{210 \times 10^3}} = 0,211 \text{ m} \end{aligned}$$

(b) Limiting value:

$$w = \frac{\alpha_c (\theta_2 - \theta_1) l^2}{19,2h} + \frac{l}{30} = \frac{18 \times 10^{-6} \times 770 \times 4^2}{19,2 \times 0,11} + \frac{4}{30} = 0,238 \text{ m}$$

The calculated deflection is less than that of the limiting value, hence  $w/d = 0,211/0,059 = 3,6$ .

The aspect ratio  $1/\alpha = 1/0,8 = 1,25$ . From Bailey (2001),  $e = 1,77$ . From Eq. (12.3),

$$q_{p\theta} = e q_{p\theta,slab} + q_{p\theta,udl} = 1,77 \times 17,2 + 5,1 = 35,5 \text{ kPa}$$

### 12.3 PITCHED ROOF PORTALS

There is no explicit requirement in EN 1993-1-2 to check if a portal frame when erected close to a boundary will collapse inwards rather than outwards causing damage to adjacent property or injury to firefighters and other persons, although it is required in the UK by regulatory authorities.

The rafters of a single-storey portal frame are generally unprotected and lose their strength rapidly in a fire. This means that they are both unable to carry any of the remaining dead load from the roof and to supply any propping restraint for the stanchions or external cladding. Since the eaves connection at ambient conditions is rigid, any attempt by the rafters to deflect will cause rotation and lateral movement to the tops of the stanchions. This lateral movement must not be sufficient to cause the stanchion to topple outwards (Fig. 12.2). The principle is to ensure that when movement occurs the stanchion will rotate about its foot into the space occupied by the structure. This means that although the base of the stanchion was designed to be pinned at ambient conditions there must be some degree of fixity during the fire to ensure some degree of stability. The full background to the calculations is given in Simms and Newman (2002).

At collapse hinges will tend to occur at either side of the apex connection and in the rafter at the end of the haunch. With these assumed positions of plastic hinges, it is then possible to determine the moment and other forces required to provide stability at the foot of the stanchion (Fig. 12.3). To carry out the calculations, assumptions are also needed to be made on the resultant frame geometry in the fire.

The vertical reaction  $V_{Sd}$  is given by,

$$V_{Sd} = F_1 + F_2 \quad (12.8)$$

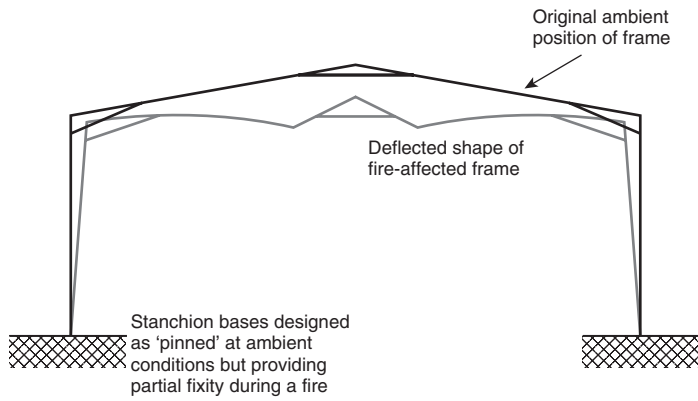


**Figure 12.2** Schematic collapse behaviour of a pitched roof portal frame in a fire.

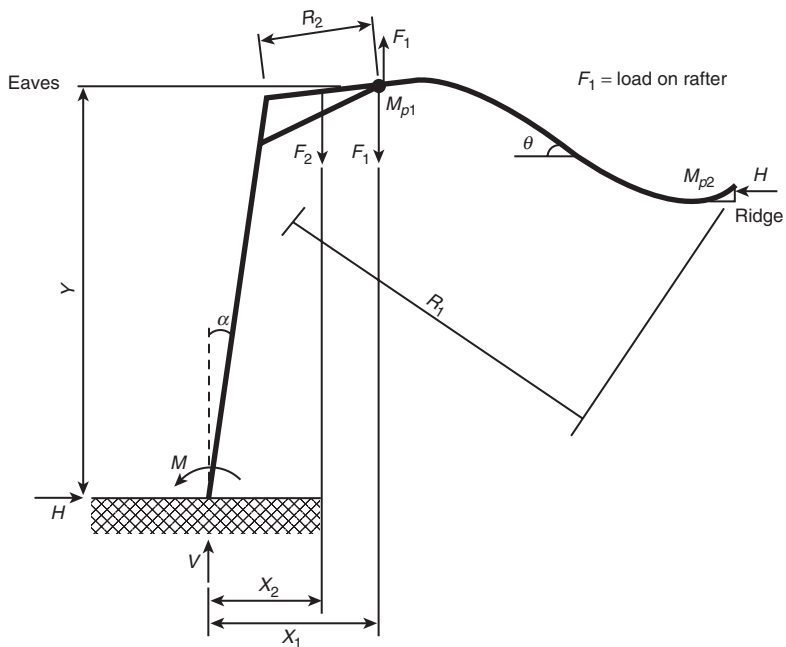


**Figure 12.3** The geometry of a portal frame in a fire together with the actions on the frame.

where  $F_1$  is the force on the main rafter of length  $R_1$  between haunches and  $F_2$  on the length  $R_2$  equal to the haunch length.

The horizontal reaction  $H_{Sd}$  is given by

$$H_{Sd} = \frac{F_1 R_1 \cos \theta - 2(M_{pl,1} + M_{pl,2})}{2R_1 \sin \theta} = \frac{F_1}{2 \tan \theta} - \frac{M_{pl,1} + M_{pl,2}}{R_1 \sin \theta} \quad (12.9)$$

From consideration of the loading,

$$F_1 = 0,4q_f SG \quad (12.10)$$

where  $q_f$  is the load on the rafter,  $S$  is the frame spacing and  $G$  is the distance between haunches,  $M_{pl,1}$  and  $M_{pl,2}$  are the temperature-reduced plastic moments of the rafter at the end of the haunch and the rafter, respectively and  $\theta$  is the slope of the rafter at collapse.

$R_1$  can be determined in terms of  $G$ , initial rafter pitch  $\theta_0$  and elongation, and is given by

$$R_1 = 1,02 \frac{G}{2 \cos \theta_0} \quad (12.11)$$

where an elongation of 2% has been assumed.

If  $M_{pl,1}$  and  $M_{pl,2}$  are both taken as  $0,065 M_{pl,rafter}$ , then  $H_{Sd}$  becomes:

$$H_{Sd} = \frac{q_f SG}{4 \tan \theta} - \frac{0,255 M_{pl,rafter} \cos \theta_0}{G \sin \theta} \quad (12.12)$$

and the moment at the base of the stanchion  $M_{Sd}$  by

$$M_{Sd} = H_{Sd} Y + F_1 X_1 + F_2 X_2 + M_{pl,1} \quad (12.13)$$

where  $Y$  is the height to the end of the haunch.

For a column rotation angle of around  $1^\circ$ ,

$$X_1 \approx \frac{Y}{60} + \frac{L - G}{2} \quad (12.14)$$

and

$$X_2 \approx \frac{Y}{60} + \frac{L - G}{4} \quad (12.15)$$

Thus,

$$F_1X_1 + F_2X_2 = q_fSGY \left( \frac{L}{120G} + \frac{L^2 - G^2}{8GY} \right) \quad (12.16)$$

and

$$HY = \frac{q_fSGY}{4 \tan \theta} - M_{pl,rafter} \left( \frac{0,255Y \cos \theta_0}{G \sin \theta} \right) \quad (12.17)$$

If the haunch length is around 10% of the span, then as a further approximation

$$\frac{L}{120G} = \frac{1}{96} \quad (12.18)$$

The rafter sag angle  $\theta$  is given for single bay portal frames by

$$\theta = \arccos \left( \frac{L - 2X_1}{2R_1} \right) \quad (12.19)$$

or

$$\theta = \arccos \left( \frac{\left( G - \frac{Y}{30} \right) \cos \theta_0}{1,02G} \right) \quad (12.20)$$

A parametric study has indicated that Eq. (12.20) can be simplified to:

$$\theta = \arccos (0,97 \cos \theta_0) \quad (12.21)$$

The value of  $M_{Sd}$  may be further simplified to:

$$M_{Sd} = q_fSGY \left( A + \frac{B}{Y} \right) - M_{pl,rafter} \left( \frac{CY}{G} - 0,065 \right) \quad (12.22)$$

where,

$$A = \frac{1}{4 \tan \theta} + \frac{1}{96} \quad (12.23)$$

$$B = \frac{L^2 - G^2}{8G} \quad (12.24)$$

and

$$C = 0,255 \frac{\cos \theta_0}{\sin \theta} \quad (12.25)$$

The horizontal reaction  $H_{Sd}$  is then given by

$$H_{Sd} = q_f SGA - \frac{CM_{pl,rafter}}{G} \quad (12.26)$$

The applied loading  $q_f$  should be taken as the dead load of the roofing material and purlins less any combustible material. Further guidance on this is also given in Simms and Newman (Table 2.1).

There are some further considerations which need to be covered before undertaking an example set of calculations:

- (1) Provision must also be made for longitudinal stability, and *any* one of the following conditions may be satisfied:
  - (a) the provision of 4 equal-sized holding down bolts in each base plate, symmetrically distributed about the section in the longitudinal direction at a minimum spacing of 70% of the width of the stanchion flange,
  - (b) the provision of a masonry wall properly tied to the stanchion restraining the column in the plane of the wall of a height not less than 75% of the height to eaves,
  - (c) the provision of a suitably designed horizontal restraint members which will require to be fire protected,
  - (d) the provision of any protected area of wall horizontal steel members having a combined tensile strength of

$$0,25 V_{Sd} \sum (\text{height of unprotected area})/(\text{height to eaves})$$

where the summation is taken over all the frames.

### Example 12.2: Portal frame stability check

The portal frame illustrated in Fig. 12.4 is to be checked for the stability requirement as it is adjacent to a boundary.

Assume that all the cladding is non-combustible, then the fire load per unit area is 0,42 kPa (which includes the weight of the frame).

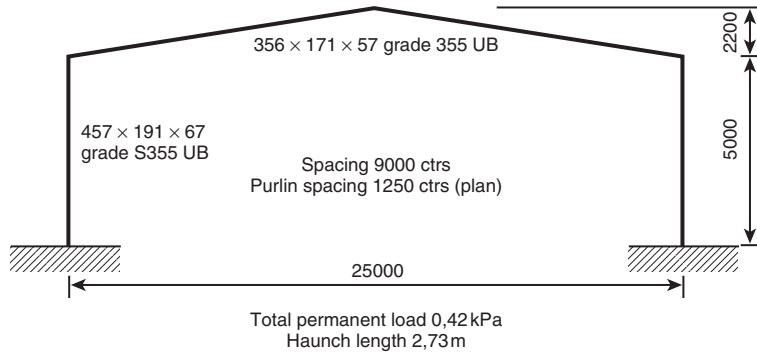


**Figure 12.4** Design data for the determination of the fire performance of a portal frame (Example 12.2).

Fire load per unit run,  $q_f = 9 \times 0,42 = 3,78 \text{ kN/m}$ .

The length between haunches,  $G = 25 - 2 \times 2,73 = 19,54 \text{ m}$ .

The height to the end of the haunch,  $Y = 5 + 2,73 \tan 10 = 5,48 \text{ m}$ .

From Eq. (12.20),

$$\theta = \arccos \left( \frac{\left( G - \frac{Y}{30} \right) \cos \theta_0}{1,02G} \right) = \arccos \left( \frac{\left( 19,54 - \frac{5,48}{30} \right) \cos 10}{1,02 \times 19,54} \right) = 17,0^\circ$$

The approximate equation, Eq. (12.21) gives

$$\theta = \arccos (0,97 \cos \theta_0) = \arccos (0,97 \cos 10) = 17,2^\circ$$

When the angles are almost identical, use the value of  $\theta = 17^\circ$ .

Determination of the parameters  $A$ ,  $B$  and  $C$ :

From Eq. (12.23),

$$A = \frac{1}{4 \tan \theta} + \frac{1}{96} = \frac{1}{4 \tan 17} + \frac{1}{96} = 0,828$$

From Eq. (12.23),

$$B = \frac{L^2 - G^2}{8G} = \frac{25^2 - 19,54^2}{8 \times 19,54} = 1,56$$

and from Eq. (12.24),

$$C = 0,255 \frac{\cos \theta_0}{\sin \theta} = 0,255 \frac{\cos 10}{\sin 17} = 0,859$$

$$M_{pl,rafter} = W_{pl} f_y = 1010 \times 355 \times 10^{-3} = 359 \text{ kNm}$$

From Eq. (12.22),

$$M_{Sd} = q_f S G Y \left( A + \frac{B}{Y} \right) - M_{pl,rafter} \left( \frac{C Y}{G} - 0,065 \right)$$

$$= 0,42 \times 9 \times 19,58 \times 5,48 \left( 0,828 + \frac{1,56}{5,48} \right)$$

$$- 359 \left( \frac{0,859 \times 5,48}{19,58} - 0,065 \right) = 388,3 \text{ kNm}$$

The minimum value of the overturning moment  $M_{Sd,min}$  should be  $M_{pl,column}/10$ , so

$$M_{Sd,min} = \left( 1471 \times 355 \times 10^{-3} \right) / 10 = 52,2 \text{ kNm}$$

Determination of the horizontal reaction from Eq. (12.26),

$$H_{Sd} = q_f S G A - \frac{C M_{pl,rafter}}{G} = 0,42 \times 9 \times 19,54 \times 0,828 - \frac{0,859 \times 359}{19,54} = 45,4 \text{ kN}$$

The minimum value of  $H_{Sd,min}$  is  $M_{pl,column}/10Y$ , so

$$H_{Sd,min} = \left( 1471 \times 355 \times 10^{-3} \right) / (10 \times 5) = 10,4 \text{ kN}$$

Again this condition is satisfied. The vertical reaction is simply half the load on the frame.

The preceding chapters have considered the design of elements or frames under the effects of fire. It remains to consider the evaluation of structures after damage due to fire.

# 13

## Assessment and repair of fire-damaged structures

---

Often the initial response when looking over a fire-damaged structure is one of despair and horror at the extent of damage. This situation is exacerbated by the amount of non-structural debris lying around together with the acrid smell of many combustion products. In most cases, the damage is not as severe as is initially thought, even though immediate decisions must be taken on the short-term safety of the structure and whether any temporary propping is necessary or, indeed, whether some demolition work is necessary. This decision will often need to be taken very quickly after the fire and will generally be based on a visual survey and expert judgement. It should be pointed out that the assessment of fire-damaged structures is very much a 'black art' in that it relies heavily on experience. It is also to be noted that it is at this point that the owner's, or occupier's, insurance company will become involved, as even if the structure is capable of being saved, it will be a matter of economics as to whether there should be repair or demolition and complete rebuild. This question can often be answered after a thorough visual inspection has been carried out.

### 13.1 VISUAL INSPECTION

The aim of the visual inspection is to determine:

1. the short-term stability of the structure and
2. the extent and severity of the fire.

#### 13.1.1 Stability

If possible, the original drawings for the structure should be consulted at this stage. These allow assessment of how the structure transmits the

applied loading and enables the principal load carrying members to be identified, as well as those providing structural stability. The inspection needs to check any excessive deformation, deflection or cracking in the main load-carrying members and integrity at the connections between the main members. It is also necessary to consider the stability if excessive bowing has occurred in any masonry cladding or internal compartment walls. In the case of concrete construction, attention should be given to damage due to spalling on beams and columns as this may reduce the load-carrying capacity of the member due to excessive temperature rise in any reinforcement. Where the fire has only affected part of the structure, it is essential that the inspection also extends to any part of the structure not damaged directly by the fire; it is possible that a substantial redistribution of forces can occur into the unaffected part of the structure. This redistribution of forces has been noted from theoretical work on concrete frames by Kordina and Krampf (1984) where moments in the frame remote from the fire affected compartment exceeded the design moments, and also in the Broadgate fire (SCI, 1991) when the structure behaved during the fire in a totally different manner to the way it was designed, in that forces were redistributed away from the fire by columns acting in tension to transmit forces to the relatively cool upper stories of the structure.

### **13.1.2 Estimation of fire severity**

The first method of obtaining a rough estimate of the fire severity is by the use of the fire brigade records in terms of the number of appliances called out, the length of time taken to fight the fire, the length of time between the fire being noted and the arrival of the brigade, the operation of any automatic fire detection or fire-fighting equipment and the degree of effort required to fight the fire.

The second approach is to estimate the temperature reached in the fire by a study of the debris caused by the fire. It is thus important that no debris is removed until such a study is carried out; otherwise, vital evidence may be lost. Provided the materials generating the debris can be identified, the knowledge may be used to give an indication of temperature reached, since most materials have known specific melting or softening temperatures; some typical data are given in Table 13.1 (Parker and Nurse, 1956). Care should, however, be exercised when using these data as the temperature varies over the height of a fire compartment, thus the original position of a particular artefact is important. Also, this method only gives an indication that particular temperatures were reached and not the duration of exposure to that temperature.

A third method that is available to give an estimate in terms of either the standard furnace test duration or a known fire, is to measure the

**Table 13.1** Melting point data

Material behaviour	Approximate temperature (°C)
Softening or collapse of polystyrene	120
Shrivelling of polythene	120
Melting of polythene	150
Melting of polystyrene	250
Darkening of cellulose	200–300
Soldered plumbing adrift	250
Lead plumbing melts or softens	300–350
Aluminium softens	400
Aluminium melts	650
Softening of glass	700–800
Melting point of brass	800–1000
Melting point of silver	950
Melting point of copper	1100
Melting point of cast iron	1100–1200

*Source:* Parker and Nurse (1956) Building Research Establishment: Crown Copyright

charring depth on any substantial piece of timber known to have been exposed to the fire from the start of the fire. The charring depth can be related back to the standard furnace exposure since timber of known, or established, density can be assumed to char at a constant rate between 30 and 90 min standard exposure (section 5.2.4). The position of the timber specimen in the compartment should also be noted. An estimate of actual fire exposure can be obtained using Eqs (10.5)–(10.10).

A fourth method is to calculate the fire severity from estimates of the compartment size, the fire load density and the area of openings (ventilation factor) using the equations presented in section 4.4. It should be remembered that these equations assume the whole fire load ignites instantaneously and that the whole ventilation is available from the start of the fire, and thus may not be totally accurate for a large compartment fire.

In practice, no one of the above methods is completely reliable and therefore a combination of methods must be used to give a reasonable answer.

The visual inspection, once carried out, will have identified those areas which must be either immediately demolished (where the damage is beyond that capable of being repaired) or those areas which may be capable of being repaired if sufficient strength can be attained. The inspection will also identify where there is no, or only very superficial, damage. This last category merits no further discussion. The problems arising

when demolition is necessary are considered in section 13.5. If repair is considered feasible, then a much more thorough investigation is required to ascertain the exact extent and severity of any damage and the residual strength of the structure. To do this, it is first necessary to clear all debris from the structure and to clean as much smoke damage as possible to allow an unimpeded examination of all surfaces.

## **13.2 DAMAGE ASSESSMENT**

This needs carrying out in a series of stages. The first stage involves a complete fully detailed survey of the structure. The second stage ascertains the residual strength of both the individual members and of the complete structure.

### **13.2.1 Structural survey**

For all structures, the first stage is to carry out, where appropriate, a full line and level survey. This is needed to assess the residual deformations and deflections in the structure. The measured deflections should be compared with those for which the structure was designed. Care should be taken to note the effect of any horizontal movements due to thermal actions during the fire. Such effects of horizontal movement are often apparent away from the seat of the fire (Malhotra, 1978; Beitel and Iwankiw, 2005).

Other observations needed in the survey depend on the main structural material: steel, concrete or masonry.

In concrete structures, it is necessary to note the existence of spalling and therefore exposed reinforcement. It should be noted that large amounts of spalling do not necessarily imply that the reinforcement, or the structure, is substantially weakened since spalling may occur late in a fire due to the action of cold water from firemen's hoses. It is likely that where the exposed surfaces are smoke blackened, spalling occurred early in the fire. It is useful to note the colour of the exposed concrete face as this can give an indication of the temperature to which the element was exposed; care is needed, though, because spalling may nullify the observation, and some aggregates do not exhibit colour changes. Note should also be made of the formation of cracks. Cracking is unlikely to be deleterious in the tension zones of reinforced concrete beams, but will indicate the existence of severe problems should it occur in the compression zones of beams or slabs or in columns. The fire test on the concrete frame at Cardington demonstrated the ability of that particular frame to remain intact in spite of large degrees of spalling, but it also suffered

large horizontal deformations at the top of the fire test compartment (Bailey, 2002).

In steel structures, since most structural steels regain more strength on cooling (see section 13.3.1), there will be a slight loss in strength. However, the resultant deformations are likely to indicate the state of the structure. In this case, it is important to assess the integrity of the connections; it is possible that bolts could have failed within the connection or could have become unduly deformed. Where the floors comprise profile sheet steel decking and *in situ* concrete, examination should be made for any separation between the decking and the beams. This separation can still occur even if thorough deck stud welding was used. Another potential point of failure is the shear bond between the decking and the *in situ* concrete. Even with substantial damage of the types mentioned above, the structure may still be intact as demonstrated after the fire tests on the steel frame structures at Cardington (Bailey, 2004a).

Masonry is either used in low-rise load-bearing structures or as cladding to framed structures. The major cause of distress to masonry walls is expansion or movement in the structure caused by thermal action on the frame or flooring. This is less likely in low-rise construction where substantial amounts of timber are likely to be used. Note should therefore be made of any areas where there are signs of punching failure or excess deflections on the outer leaf of a cavity wall. If the damage is restricted to the inner leaf it may be possible to retain the external leaf and rebuild only the inner leaf, provided the wall ties are still reusable.

Whilst carrying out the visual survey, attention should be given to the need for carrying tests on the structural materials to ascertain their residual strengths. The testing methods used may either be non-destructive or involve the taking of samples from damaged portions on the structure, together with control specimens from undamaged areas.

## 13.2.2 Materials testing

### 13.2.2.1 Concrete

The only common destructive test is to take concrete cores usually 40 mm diameter from the fire-damaged zone and test the cores in compression according to the relevant standard, e.g. BS 1881: Part 120: 1983, and then relate the measured strength to an equivalent cube strength using appropriate empirical formulae. Great care is needed with the use of cores to assess residual strengths as it is necessary to attempt to extract cores free from any reinforcement, although the presence of reinforcement can be allowed for in assessing equivalent strengths. A further problem in heavily damaged structures is the ability to obtain cores of sufficient integrity to be tested. It is also necessary to obtain cores from an undamaged part

of the structure where concrete of a similar specified grade was used. To aid the assessment of loss of strength, it is useful if at all possible to obtain the original cube or cylinder control test records when the structure was built. It is also useful if any colour changes in the concrete along the length of the core are noted, as this can help assess the residual strength of parts of the structure where it may not be possible to extract cores.

There are a series of non-destructive test methods available (discussed below), although they all have problems.

#### 13.2.2.1.1 *Ultrasonic pulse velocity (UPV) measurements*

Although the apparatus for this is conveniently portable, the results obtained are not very sensitive and have the disadvantage of being comparative in that a reference is needed to establish base values of strength and pulse velocity. The test may either be carried out by measuring the time taken to transmit a signal through the member or by measuring the time taken for a reflected signal to travel from transmitter to receiver (Fig. 13.1). In the former case, it is necessary to be able to gain access to both sides of a member, together with the further limitation that the thickness cannot exceed about 200 mm. In the latter case, the surface must be good enough to allow a series of readings to be taken and that a similar procedure is used for the reference value. Provided reference values of both the pulse velocity and strength are known, then it is possible to estimate the loss in strength if the loss in UPV is known. It has been demonstrated from test results that the loss in strength  $(1 - \sigma_{c,\theta}/\sigma_{c,20})$  is related linearly to the loss in pulse velocity  $(1 - U_\theta/U_{20})$  by an equation of the form

$$\left(1 - \frac{\sigma_{c,\theta}}{\sigma_{c,20}}\right) = k_1 \left(1 - \frac{U_\theta}{U_{20}}\right) + k_2 \quad (13.1)$$

where  $\sigma_{c,\theta}$  and  $U_\theta$  are the compressive strength and UPV at a temperature  $\theta$  and  $\sigma_{c,20}$  and  $U_{20}$  are the reference strength and UPV, respectively, and  $k_1$  and  $k_2$  are dependant on the concrete age and composition (Purkiss, 1984, 1985). Benedetti (1998) proposed a rather complex method capable of determining the loss in elastic modulus within the fire-damaged zone using the reflection method. Benedetti suggests that a linear degradation model of elastic modulus with temperature is adequate. The method does rely on a relatively undamaged surface.

#### 13.2.2.1.2 *Schmidt hammer*

This will only measure the properties of the concrete in the surface layer and requires a clean smooth surface to give reliable results. It also needs

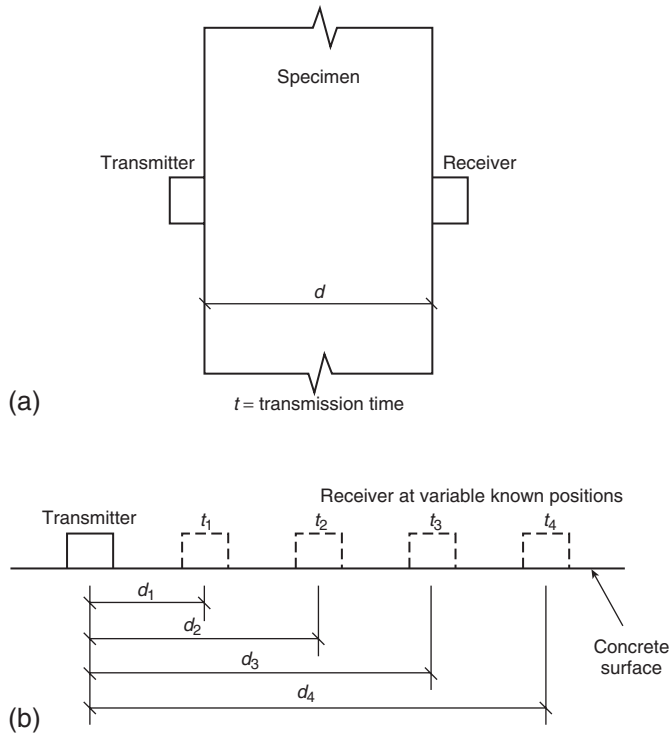


**Figure 13.1** Methods of carrying out UPV measurements: (a) direct method ( $V = d/t$ ) and (b) indirect method (velocity given as slope of distance–time graph).

calibrating for a given concrete and is not suitable where knowledge of the concrete properties are required within the element.

#### 13.2.2.1.3 Windsor probe and pull out test

These have been placed together since they both require a reasonable surface to enable the test to be carried out. Nene and Kavle (1992) report the use of the Windsor probe to assess the *in situ* strength of fire-damaged concrete but give few details on the results obtained.

#### 13.2.2.1.4 Thermoluminescence test

This test only requires very small samples of mortar obtained using very small diameter cores to be subjected to a thermoluminescence test. By studying changes to the silica within the sample, it is possible to determine the temperature that has been reached by the concrete (Placido, 1980;

Smith and Placido, 1983). It also, however, requires very specialist equipment that may not be readily available.

#### 13.2.2.1.5 *Differential thermal analysis and thermogravimetric analysis*

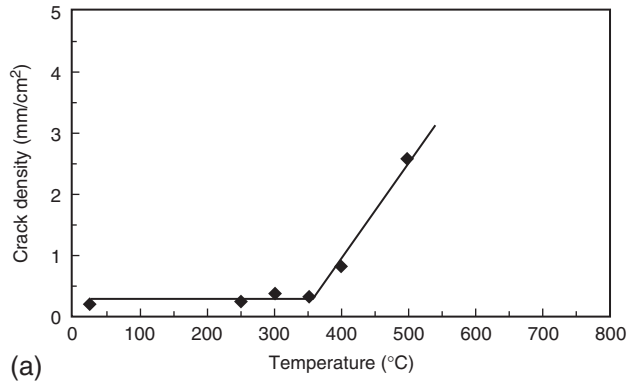
Both differential thermal analysis (DTA) and thermogravimetric analysis (TGA) can be used to evaluate changes in the structure of a concrete when exposed to heating as pattern of the responses change with temperature owing to physicochemical changes in the cement (Handoo, Agarwal and Maiti, 1991). Short, Purkiss and Guise (2000) indicate that DTA/TGA is only satisfactory on unblended cements. Cements with pulverized fuel ash (PFA) or ground granulated blast-furnace slag (GGBS) do not show any or very little change in response when heated.

#### 13.2.2.1.6 *Petrographic analysis*

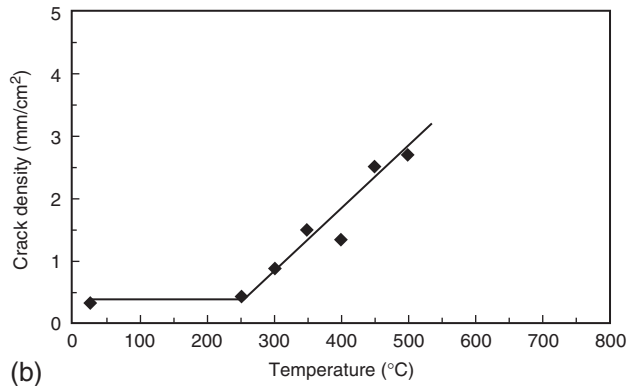
In this technique, thin slices from cores are examined under a microscope and the isotropy, density and type of cracking are observed. Riley (1991) suggests that when the temperature exceeds 500°C the cement paste appears anisotropic under polarized light. The crack patterns also change: below 300°C, the cracks form between the boundaries of the aggregate and the mortar matrix, whereas above 500°C the cracks will also tend to pass through the matrix. More recently it has been demonstrated (Short, Purkiss and Guise, 2002; Short and Purkiss, 2004) that it is possible to quantify the relationship between crack density and temperature reached due to heating (Fig. 13.2). With the unexplained exception of siliceous aggregate concrete containing PFA, the correlation between temperature  $\theta_{cd}$  at which the crack density increases above base value and the temperature  $\theta_{cs}$  at which compressive strength loss starts to occur is good (Table 13.2). The ability of change in crack density to predict the position of the 325°C isotherm (at which compressive strength loss starts to occur) is illustrated in Fig. 13.3.

#### 13.2.2.1.7 *Stiffness damage test*

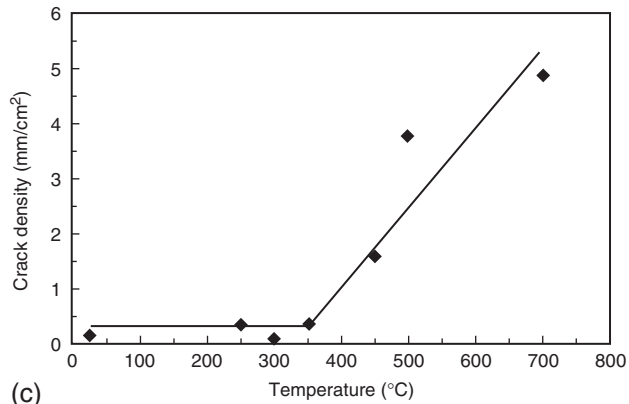
This is a type of compression test carried out on cylindrical specimens 175 mm long and 75 mm diameter under a limited stress range of 0 to around 4.5 MPa under cyclic loading with the strains being measured over the central 67 mm (Nassif, Burley and Rigden, 1995; Nassif, Rigden and Burley, 1999; Nassif, 2000). Measurements are then taken for variously defined elastic moduli and of hysteresis between the loading cycles. The test results from concrete uniformly heated up to temperatures of 470°C confirm data on residual Young's modulus and may provide an alternative method of performance assessment at moderate temperatures.



(a)



(b)



(c)

**Figure 13.2** The development of crack density with temperature for concretes made with siliceous aggregate and: (a) Ordinary Portland Cement (OPC); (b) OPC/PFA; (c) OPC/GGBS cements; (d) limestone and (e) granite. (From Short, Purkiss and Guise, 2002).

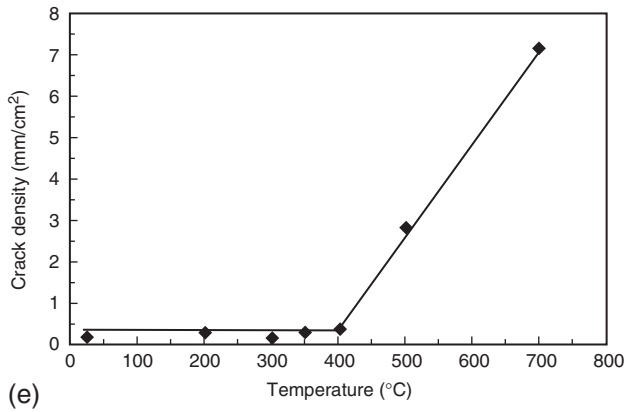
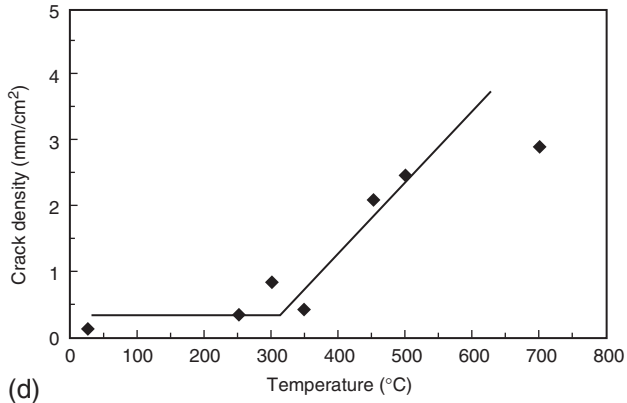
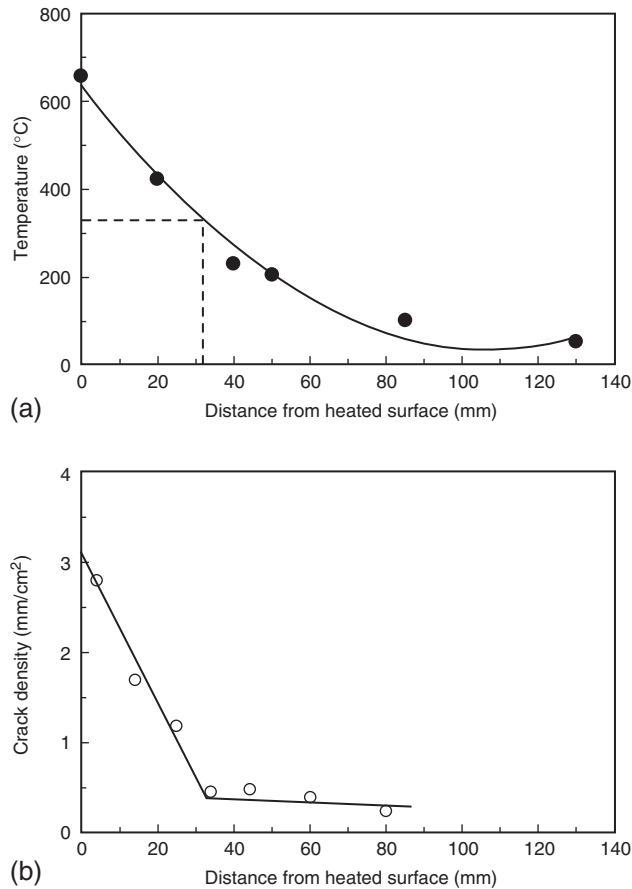


Figure 13.2 Continued.

Table 13.2 Values of initial crack density and strength transition temperatures

Concrete type	Initial crack density ( $C_0$ ) mm/cm <sup>2</sup>	$\theta_{cd}$ (°C)	$\theta_{cs}$ (°C)
OPC/Siliceous	0,29	350	325
OPC/PFA/Siliceous	0,36	250	325
OPC/GGBS/Siliceous	0,26	350	350
OPC/Limestone	0,31	300	325
OPC/Granite	0,24	400	400

Source: Short, Purkiss and Guise (2002)



**Figure 13.3** (a) Temperature distribution and (b) crack density for an OPC-siliceous aggregate concrete cylinder heated from one end.

It is not clear what the effect of a temperature gradient along the specimen would have on the results.

*13.2.2.1.8 Surface permeability*

Montgomery (1997) proposed the use of air permeability and water sorpity tests on heated concrete to ascertain damage measured by surface pull-off tensile strength using an epoxy bonded 50 mm diameter steel disc. The 150 mm cube specimens were heated by an imposed flame for two hours at a prescribed surface temperature. The tensile strengths will be those of the surface (as will the air permeability and water sorpity), but the cube strengths will to some extent be a function of the

temperature distribution in the specimen. However, in spite of the limited data reported, the method appears to give reasonable correlation between air permeability, API and pull-off tensile strength,  $f_{t,\theta}$

$$\left(1 - \frac{f_{t,\theta}}{f_{t,20}}\right) = -0,00814 \left(1 - \frac{API_{\theta}}{API_{20}}\right) \quad (R^2 = 0,826) \quad (13.2)$$

Similar equations can be determined for the other parameters but the values of  $R^2$  in each case are around 0,5 which indicates a poorer fit.

#### 13.2.2.1.9 *Fire behaviour test (FB test)*

dos Santos, Branco and de Brito (2002) proposed a test in which a core taken from a fire-damaged structure is sliced into 15 mm thick discs and the water adsorption is measured. They reported that close to the fire-damaged face the water adsorption is high, but that away from the face it dropped to a sensibly constant value, and that the percentage increase in water adsorption ( $WA$ ) over the mean value with respect to temperature  $\theta$  could be given by the following equation

$$WA = 0,5 + \frac{4}{300} (\theta - 200) \quad (R^2 = 0,831) \quad (13.3)$$

A similar pattern emerged for measurements of split cylinder strengths on the discs, and that the decrease in splitting tensile strength against temperature is given by,

$$f_{t,20} - f_{t,\theta} = 1,35 + 3,5 \times 10^{-3} (\theta - 200) \quad (13.4)$$

or using their reported ambient value of  $f_{t,20}$  of 2,4 MPa, Eq. (13.4) becomes

$$f_{t,\theta} = 1,75 - 3,5 \times 10^{-3} (\theta - 200) \quad (13.5)$$

Equation (13.5) implies zero tensile strength at 500°C, which may be slightly low.

*13.2.2.1.10 Hammer and chisel*

Although not a scientific method in the generally accepted sense of the word, this method is probably the best to give a very quick, albeit crude, assessment of concrete quality and strength.

An overview of traditional non-destructive testing on fire-damaged concrete is given in Muenow and Abrams (1987).

For reinforcement, similar techniques are available to structural steel. It should, however, be noted that where specimens are taken from either tensile steel in beams or compressive steel in columns, the elements or structure must be propped since removal of the specimen will reduce the strength of the member. It may be possible to remove samples from shear links at the mid-point of a beam or a column without propping.

**13.2.2.2 Steel**

There are essentially two approaches that may be used to assess residual steel strengths for steel.

The first is to remove test coupons or samples and subject those specimens to a standard tensile test. Care should be taken in removing test specimens in that the damaged structure is not further weakened, and that again any necessary propping should be used.

The second is to use non-destructive tests of which the most suitable is a hardness indentation test usually measuring the Brinell hardness. There is a direct, sensibly linear, relationship between the Brinell hardness number (BHN) and tensile strength (Fig. 13.4) (Kirby, Lapwood and Thompson, 1986). It is important that care is taken in using this test since a number of results are needed before the strength estimates are statistically reliable.

**13.3 STRENGTH ASSESSMENT OF THE STRUCTURE**

This can either be performed using materials strength data derived from testing regimes described in the foregoing section, or by assessment of the temperatures within the structural element and knowledge of residual, i.e. post-heating and cooling, properties of materials. Often, it should be noted that combination of these two approaches will be needed. Effectively, any strength assessment of an element of a structure can be undertaken using the same basic approaches as outlined in previous chapters for the assessment of structural performance at elevated temperatures. Use can also be made of experimental results from residual strength tests on fire affected members. Such results should be used with care, since for example, data on the residual strengths of fire affected columns were obtained from tests where the columns were heated with

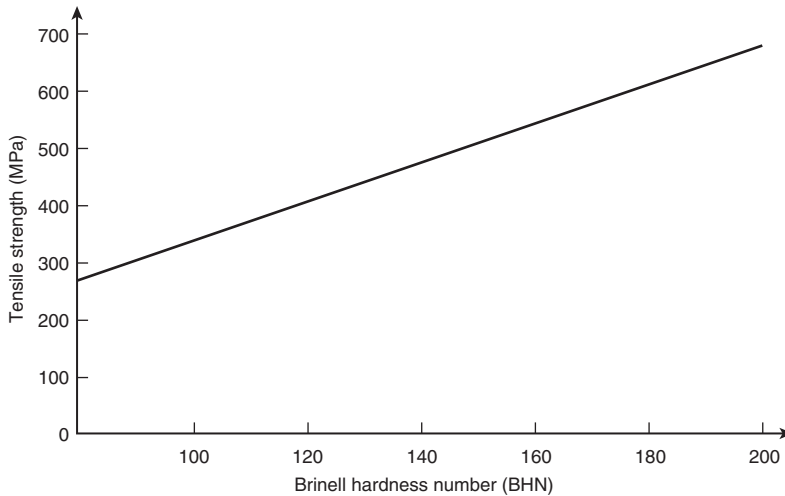


**Figure 13.4** Relationship between steel strengths and Brinell hardness number (BHN) (Kirby, Lapwood and Thompson, 1986, by permission).

no applied load (unloaded) which is not the case in a fire (Lie, Rowe and Lin, 1986; Lin, Chen and Hwang, 1989).

### 13.3.1 Residual properties

Besides the residual properties of concrete and steel, it is also necessary to consider materials of a more historical nature such as wrought or cast iron, as fire damage is no respecter of history!

#### 13.3.1.1 Concrete

The only essential property of concrete required for the assessment of fire damage is the residual compressive strength. Typical strength data for normal strength concrete from Malhotra (1954), Abrams (1968) and Purkiss (1984, 1985) are plotted in Fig. 13.5. From the plotted data, it may be observed that older, historical concretes appear to give a worse performance than more modern concretes. Chan, Peng and Anson (1999) and Poon *et al.* (2001) both support the data by Purkiss, in that, normal strength concrete loses about 25% of its strength at 400°C, 60% at 600°C and 85% at 800°C. The residual strength of concrete is lower than that strength measured at elevated temperatures as there is further degradation on cooling caused by differing thermal properties between the aggregate and the cement matrix. This difference appears to be affected

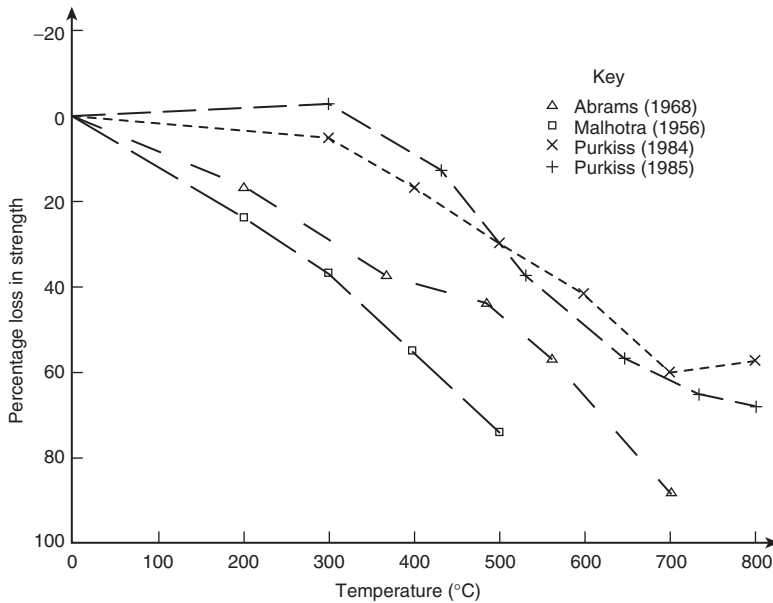


**Figure 13.5** Variation of residual strengths of concrete with temperature (Malhotra, 1956, by permission of the Building Research Establishment: Crown Copyright; Abrams, 1968, by permission; Purkiss, 1984, 1985).

also by the type of post-firing cooling in that quenched values are lower than those obtained by air cooling (Nassif, Rigden and Burley, 1999). However, it is not usual to take account of any pre-load applied to specimens as it is conservative not to. Equally, although various researchers have reported strength gain where the temperatures to which the concrete has been heated are relatively low (around 200°C) it is prudent to ignore such rises in analysis of concrete elements.

- **High performance concrete**  
Phan, Lawson and Davis (2001) present data on residual compressive strength loss on high performance concretes with and without silica fume. The concretes with silica fume behaved better than those without. The mixes with silica fume retained between 75 and 100% of their ambient strengths between 20 and 300°C with the concrete having a lower water/cement ratio behaving appreciably better. The two concretes without silica fume dropped to a strength retention of 70% at 100°C, remaining at similar values until 300°C when a further drop to 55% occurred at 450°C. Phan, Lawson and Davis also demonstrate there is no real difference in the degradation of Young's modulus in

normal and high-strength concretes in that both lose around 70–75% of their elastic modulus at a temperature of 450°C in a sensibly linear fashion. Poon *et al.* (2001) report a 10% gain in residual strength at 200°C, around 5% loss at 400°C, 45% at 600°C and 75% at 800°C. Gowripalan (1998) reports tests on residual strength properties of high-strength concrete subject to varying heating and cooling régimes (3 and 24 h exposure and tested dry or wet). The effect on heating régime for specimens tested dry was negligible at 250 or 1000°C, but was significant at 500°C where heating for 24 h produced a strength loss of 70% compared with a loss of 55% when heated for 3 h. The effect of water immersion on specimens heated for 24 h was negligible compared to specimens tested dry. Gowripalan also reports that residual splitting tensile strength drops to around 25% of ambient at 750°C. For concretes of strength around 50 MPa, the effect on the compressive residual strength is that the addition of silica fume increases the residual strength at a given temperature but that the pattern does not appear consistent (Saad *et al.*, 1996). Overall, though, the results are similar in that strength loss does not seem to occur until around 300–350°C. If their splitting tensile strength results are normalized, there would appear little difference between the concretes with an almost linear degradation to 25% of ambient at 600°C. The effect of varying PFA dosage on residual compressive strength is not marked when results are normalized, although a strength gain at 200°C is noted. At around 350°C the strength is that at ambient before it drops to around 20% at 800°C (Xu *et al.*, 2001).

- Self-compacting concrete

Persson (2003) provides much of the available data on residual properties of self-compacting concrete of strengths between 15 and 60 MPa which can be summarized by the following formulae:

Residual compressive strength:

$$\frac{\sigma_{\theta,0}}{\sigma_{20,0}} = -0,0000005\theta_c^2 - 0,000729\theta_c + 1,01 \quad (13.6)$$

Residual elastic modulus:

$$\frac{E_{\theta,0}}{E_{20,0}} = -0,0000008\theta_c^2 - 0,00196\theta_c + 1,04 \quad (13.7)$$

Residual strain at peak stress:

$$\frac{\varepsilon_{\theta,0}}{\varepsilon_{20,0}} = -0,0000035\theta_c^2 - 0,000301\theta_c + 1,0 \quad (13.8)$$

Persson also provides the following formula relating residual static modulus to concrete strength

$$E_{stat,res} = f_{c,20}(90,507 - 0,000263\theta - 0,00152f_{c,20}) \quad (13.9)$$

subject to the limit  $5 \leq f_{c,20} \leq 60$  MPa.

- Fibre concretes

Chen and Liu (2004) report residual compressive strength behaviour of high performance concretes reinforced with various combinations of steel, carbon and polypropylene fibres. All the concretes retained their normalized compressive strength at 200°C. Most of the concretes then showed an almost linear drop off to a loss of 60–70% at 800°C. The two exceptions were plain high performance which dropped to 55% at 400°C and 90% loss at 800°C and high performance concrete only with polypropylene fibres which dropped to around 50% at 400°C and about 35% at 800°C (similar to the other fibre concretes). Purkiss (1984) and El-Refal, Kamal and Bahnasawy (1992) provide data on the residual strength performance of steel fibre concrete.

Purkiss, Maleki-Toyserkani and Short (2001) report that slurry infiltrated concrete (SIFCON) retains around one-third of its flexural tensile strength after cooling from 600°C compared to an almost total loss of strength for the matrix. Residual toughness indices show an approximately linear drop from ambient to 400°C, after which they are sensibly constant. The drop is around 70%. The residual dynamic modulus drops approximately linearly to around 10% of its ambient value at 800°C, compared to the matrix which shows a slower and less dramatic decline to around 50% at 800°C. The residual compressive strength of the particular mix used shows an increase at 200°C before dropping to around one-third of the ambient strength at 800°C. The matrix again shows a less serious decline to about two-thirds of ambient at 800°C, with a slight increase at 200°C. It is thought that the peak is due to the presence of PFA in the mix. The effect is also noted by Short, Purkiss and Guise (2002).

### 13.3.1.2 Structural steel

All the results quoted here are taken from Kirby, Lapwood and Thompson (1986). For Grade 43A (S275) steel there is no residual strength loss based on the 0,2% proof stress when the steel is heated to temperatures up to 600°C but a 30% reduction at a temperature of 1000°C. The variation in residual strength between these temperatures is sensibly linear. The pattern for Grade 50D (S355 J2) steel is similar except that the strength loss at 1000°C is only about 15%. Kirby, Lapwood and Thompson also

quote results on an American ASTM A572 Grade 50 steel (equivalent to S355) which is similar to a UK Grade 50B (S355 JR) steel. Here, yet again, there is no reduction below 600°C but at 800°C a 30% reduction occurred. However, at 1000°C the strength reduction was only around 12%.

It should be noted that in all the tests, except for the American steel at 800°C, the measured tensile strengths exceeded the minimum guaranteed yield strength. COR-TEN B structural steel behaved similarly to the American Grade 50 steel.

### **13.3.1.3 Reinforcing and pre-stressing steels**

Data on such steels are presented in Fig. 13.6 (Holmes *et al.*, 1982), where it is seen that the yield strength for reinforcing steel shows an increase above ambient strength at temperatures below about 550°C, but a decrease at temperatures above 550°C. Pre-stressing steels show no change in strength below 300°C, but a substantial drop after this point such that at 800°C only around 50% of strength remains.

### **13.3.1.4 Cast and wrought iron**

Wrought iron appears to show a marginal strength increase at temperatures up to 900°C and thus appears able to perform well in a fire provided

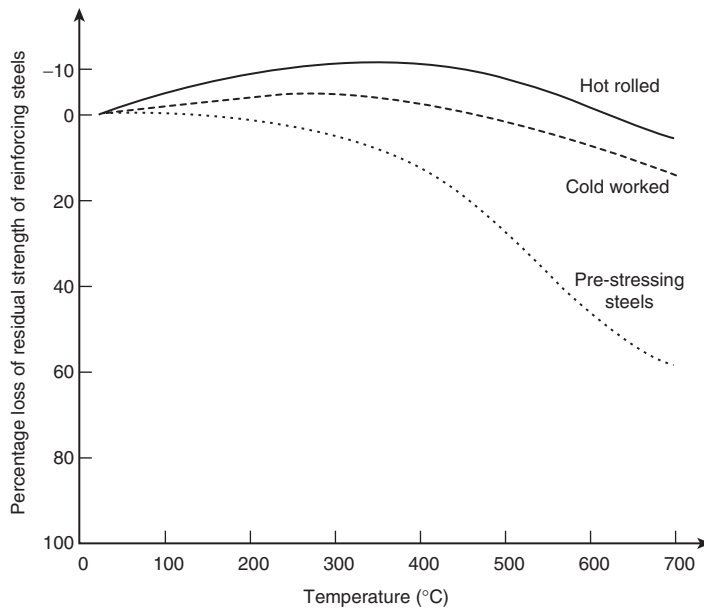


**Figure 13.6** Variation of residual strengths of reinforcing and pre-stressing steels with temperature (Holmes *et al.*, 1982).

however, that excessive deformations do not occur (Kirby, Lapwood and Thompson, 1986).

Cast iron will also perform reasonably well unless undue large bending moments are applied to the member during the fire. The good fire performance in real structures is in part due to the very low stresses to which cast iron members were subjected in design. One problem that can occur is that brittle failure is possible if cast iron is quenched by cold water from firemen's hoses whilst still red-hot, or if additional loads are induced during the fire (Barnfield and Porter, 1984).

#### **13.3.1.5 Masonry**

There are few data on the residual strength of masonry, but those that are available indicate that clay bricks lose virtually no strength at 1000°C, whereas concrete and calcium silicate bricks lose around 75% of their strength and mortar has no residual strength at 1000°C (Lawrence and Gnanakrishnan, 1988a, b). Türker, Erdoğan and Erdoğan (2001) report test data on residual strengths of mortar which indicate that for limestone or quartzite mortars the strength loss is around 20% at 500°C, 65% at 700°C and 80% at 850°C. For lightweight aggregate (pumice) mortars, the figures are no loss, 40% and 50%.

### **13.3.2 Determination of temperatures within an element**

The methods used here are exactly the same as used to assess the performance of structures during a fire. If standard solutions based on exposure to the standard furnace test are used, then the fire equivalent time will need calculating to enable such methods to be used to give realistic answers. Bessey (1956) and Ahmed, Al-Shaikh and Arafat (1992) report visually observed colour changes in heated concrete. However, such changes can be difficult to observe by eye alone often due to the type of aggregate. The application of colour image analysis techniques can overcome this problem. By determining the change in hue when concrete is heated, there is an obvious change in the frequency of occurrence of red (Short, Purkiss and Guise, 2001). The other primary colours yellow and green appear to have little impact (Fig. 13.7(a)). When a temperature range of 20–500°C is examined, it is noticed that an increase in hue values occurs at temperatures of around 250–300°C (Fig. 13.7(b)). For situations where there is a thermal gradient, the onset of change in hue values corresponds with a temperature level of around 300°C. The original work by Short, Purkiss and Guise was carried out using an Olympus polarizing microscope and a Sight Systems Ltd. workstation. Felicetti (2004)

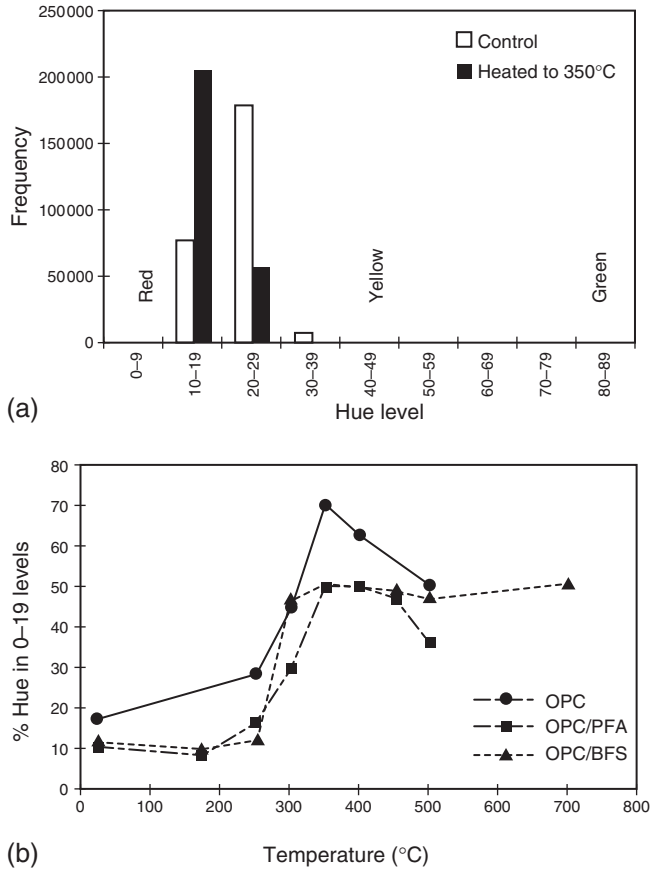


**Figure 13.7** Colour changes on heated concrete: (a) frequency of the occurrence for the levels of hue from 0–89 (control and fired samples) and (b) hue measurements for samples heated to equilibrium temperature (siliceous aggregate). (From Short, Purkiss and Guise, 2001).

has successfully demonstrated that a similar technique can be adapted to digital photography which makes the analysis much easier.

However, the absence of colour change should not be taken as an indication of exposure to only comparatively low temperatures, since the colour change is dependant on certain impurities in the aggregates which may not, in a specific case, be present. Some sources of siliceous aggregates may not produce any colour change. The results from the work of Bessey on siliceous aggregates and Ahmed, Al-Shaikh and Arafat on limestone aggregates are given in Table 13.3.

**Table 13.3** Colour changes in heated concrete

Concrete type	Colouration	Temperature (°C)	Condition
Siliceous	Normal	0–300	Normal strength
	Pink	300–600	Loss in strength
	Whitish-grey	600–900	Weak and friable
	Buff	above 900	Weak and friable
Limestone	Grey	0–200	Normal strength
	Light pink	200–400	Loss in strength
	Dull grey	400–600	Poor

*Note:* Not all siliceous or limestone aggregate concretes will show these changes, as they may be due to impurities in the sand as well as the aggregate. Absence of or a different colour change to those noted above should be treated with care.

*Sources:* Bessey (1956) Building Research Establishment: Crown Copyright and Ahmed, Al-Shaikh and Arafat (1992) by permission Thomas Telford Publications

Following the structural assessment when it determined that the residual structure is either strong enough to carry the imposed loads or that only minor strengthening is required, attention must be given to methods of repair. However, before these are chosen, the economics of the situation must be considered. Thus, estimates should be prepared of the cost and duration of both repair and demolition and rebuild must be made. On complex or important structures, such a process should start immediately after the fire.

It is likely that if only minor repairs are required, albeit with some minor demolition and replacement, repairing the structure will be much more economic. Further information on the assessment of repairability, together with additional references, is given in a CIB Report (Schneider and Nägele (eds), 1989).

#### 13.4 METHODS OF REPAIR

As far as steelwork is concerned, any repair will be in the form of partial replacement where the original structure has deformed beyond the point at which it can be reused. Where the steelwork is still intact, it is almost certain that the fire protection system used will need partial or total replacement. Any intumescent paint systems will certainly need renewing. For further information on the reinstatement of steel structures reference should be made to Smith *et al.* (1981).

In the case of masonry, where there is only superficial damage, it may well be sufficient to apply a cosmetic repair with plaster-based products

although the integrity of any cavity insulation should be checked before considering this. In any other case replacement of either or both leaves is likely to be necessary.

Timber structures will generally need total replacement. This will certainly be true of modern roofing systems where the member thicknesses are small and will have no residual section. In the case of older and more historic structures, timber roofing and flooring systems will be far more substantial and thus repair may be feasible (Dixon and Taylor, 1993).

Concrete structures generally provide the greatest scope for repair and strengthening. There are a large number of choices available to the engineer in such cases. It is only intended here to give an overview of the situation. More detailed guidance is given in a Concrete Society Report (1990). Any repair must satisfy all the original design criteria for the structure including strength, deflection, durability and fire resistance. Where the structure needs strengthening, it is essential that the new sections of the structure are not only capable of carrying the forces within the new sections, but must also be capable of transmitting the forces from the existing sections of the structure. This will mean that, for example, it will be necessary to ensure that there is sufficient lap length between existing and new reinforcement. Repair can be effected by concrete spraying (guniting), resin repairs or overcladding.

For guniting repairs, it is essential that all exposed concrete faces are thoroughly cleaned to ensure that the guniting bonds fully to the existing concrete. It will often be necessary to place very light mesh within the depth of the repair to aid integrity unless the repaired area is very small (Fig. 13.8).

Resin repairs are usually only applicable to lightly damaged areas where spalling is shallow. There are some problems in that most resins soften at around 80°C, and thus their integrity in a fire may be suspect (CIRIA, 1987). Plecnik, Foggerty and Kurfees (1986) confirm that from tests epoxy repaired beams lose strength and stiffness rapidly at uniform temperatures above 120°C. It is thus necessary to be very careful when specifying resin repairs, with consideration being given to the provision of additional fire protection using plaster finishes.

Overcladding can take two forms: for walls or slab soffits where the damage is slight, the damage can be covered by the use of plasterboard and battens; for columns, glass reinforced cement panels can be used with the gap between the panels and the original column being filled with either mortar or concrete.

Case studies on the assessment, repair and reinstatement of a fire-damaged concrete building structures are provided in Morales (1992) or Nene and Kavle (1992) and for a concrete bridge structure (part of which needed demolition) in Boam and Cropper (1994).

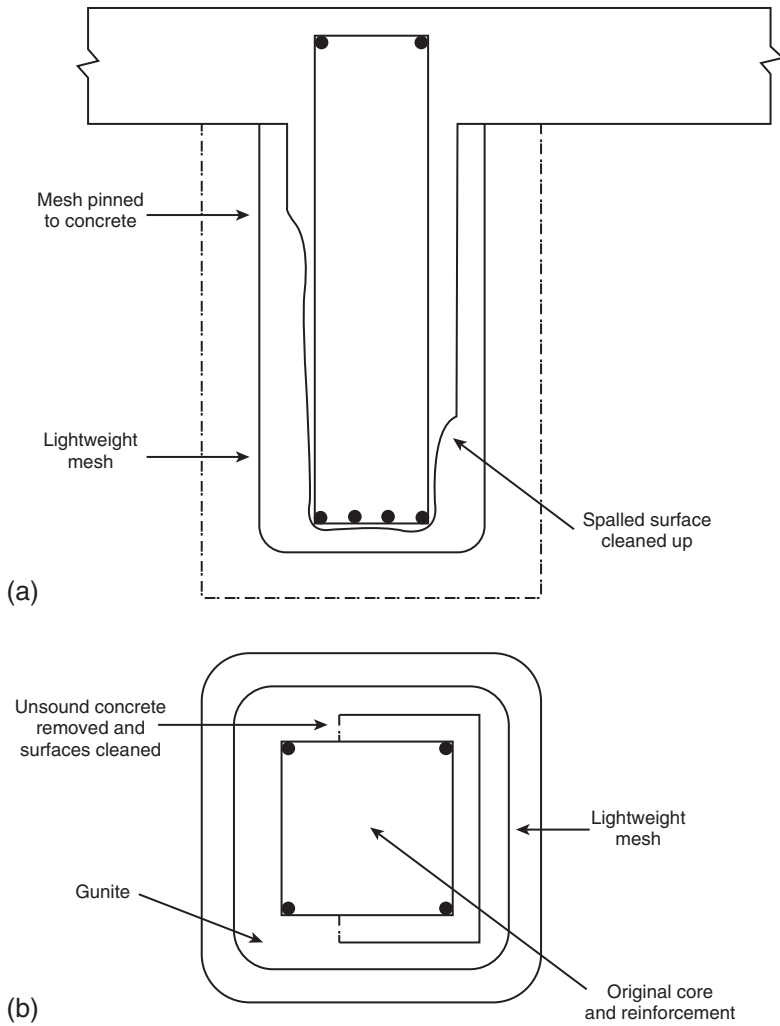


**Figure 13.8** Gunite repairs to fire-damaged concrete: (a) typical beam repair and (b) typical column repair.

### 13.5 DEMOLITION OF FIRE-DAMAGED STRUCTURES

Clearly, the same safety hazards that exist for structures being demolished for reasons other than fire damage exist for those so damaged, except that problems of stability are exacerbated for fire-damaged structures as the structure itself is inherently weaker, often to such an extent

that little physical effort may be needed for demolition. There are however additional aspects that warrant consideration (Purkiss, 1990b).

The first is that some of the products of combustion may be toxic and that the structure may need clearing and fully venting before any demolition can take place.

The second is that in some structures, asbestos will be present either as lagging to hot water pipes and tanks, or in older steel structures as fire protection to beams. In both cases, the asbestos will need specialist handling before demolition can start.

The third problem is that where the structure has basements, these are likely to be partially or fully filled with water following fire fighting. Thus the basements will need pumping out, but it should be noted that due to possible toxic combustion products care will need taking as to where such effluents can be discharged.

# 14 Postscript

---

The book, to this point, has presented the current situation at which structural fire safety engineering finds itself and outlines its ability to provide conceptually accurate, and scientifically and numerically sound calculation procedures for the design of structural elements or, in some cases, complete structures to resist the effects of fire. It needs to be reiterated, however, that relatively simple solutions including prescriptive rules based either on traditional test methods or parametric calculation studies are likely to be adequate and sufficient for the majority of routine structures. It is only in either the special, non-standard cases that complex and complete engineering solutions will be necessary or where the expense of a fully engineered approach can be justified in terms of the economics of savings in the protection measures needed or in certain circumstances the avoidance of any protection systems.

Since the first edition of the book, there has been much progress in the field of fire safety engineering. The prime example of this is the indication following the large frame tests on the composite steel frame at Cardington that fire performance of members in a frame is substantially enhanced over that predicted using simple member design methods. It should however be reiterated that whilst computer analysis is able to predict (or rather mimic) the response of the Cardington frame with a high degree of accuracy, such analysis methods should not be applied to frames whose geometry is significantly different to that of Cardington. This is due to the possibility of alternative failure mechanisms or second order effects becoming far more critical.

The single fire test on the concrete frame at Cardington was interesting, but it should not necessarily be concluded from the test on a flat slab structure with diagonal steel bracing that the result can be extrapolated to other more traditional forms of concrete construction, nor to construction using partially or totally pre-cast concrete elements. It is essential that further full scale tests are carried out on the existing concrete frame together with tests on a more conventional beam and column frame, a pre-cast frame and an *in-situ* frame with pre-cast floor units. In each case lateral restraint should be provided by stairwells and lift shafts.

It would be ideal if test results were available on steel–concrete composite frames with larger spans than those of the frame previously utilized. Tests on steel frames with pre-cast concrete floor units are less of a need as there is unlikely to be the level of enhancement of fire performance shown by the composite frame, although there is likely to be some gain over isolated element behaviour owing to the floor plate, if properly tied, acting as a diaphragm.

Given that the tests on the frames at Cardington put the UK at the forefront of fire safety engineering, the author deplores the fact that the test facility at Cardington is now closed, seemingly permanently. He equally accepts that this was due to financial reasons in part due to the misguided privatization of building research establishment (BRE), but he still feels that the facility must be reopened and supported in full by government and, where necessary, industry.

That there is greater interest in structural fire safety engineering is in part due to the two guides produced by the ISE (ISE, 2003, 2006), the BRE reference guide (Chitty and Fraser-Mitchell, 2003), the digests produced by BRE (Bailey, 2004b; Bregulla, Enjily and Lennon, 2004; Lennon, 2004a, b, c; de Vekey, 2004; Welch, 2004). There is also a set of design guides from BRE due in the near future.

Whilst relatively straightforward structures can be within the remit of structural engineers, it is felt by the author that with respect to very large or unorthodox structures that this is likely to remain a very specialist area as the requirements for the design-analysis synthesis will remain complex and demand substantial computing to enable solutions to be achieved, with such undertakings only able to be carried out by engineers with authoritative experience in the field of fire safety engineering.

Fire safety engineering still has a very promising and potentially rewarding future provided it is not fettered by prescriptive or legislative rules which prevent the engineer from taking properly argued engineering judgements. It is feared that decisions based on emotive responses may control or overturn those based on full scientific principles. This situation is one which must not be allowed to happen as it could impose unnecessary and unwelcome restrictions on the discipline of the fire safety engineering. Any emotive response based on the events of 11 September 2001 should not be allowed to straitjacket performance-based fire safety engineering.

Fire safety engineering design of structures must be considered of equal importance within the overall process of design as either the conventional ambient structural design, whether at ultimate or serviceability limit states, or the effects of other accidental actions such as earthquake or explosion. It is hoped that the contents of this book have helped to explain and clarify the importance of fire safety engineering.

## References

---

- Abrams, M.S. (1968) Compressive strength of concrete up to 1600°F (871°C), in *Temperature and Concrete*, Special Publication SP-25, American Concrete Institute, Detroit, pp. 33–58.
- Ahmed, G.N. and Hurst, J.P. (1997) An analytical approach for investigating the cases of spalling of high-strength concrete at elevated temperatures. *International Workshop on Fire Performance of High-Strength Concrete*, NIST Gaithersburg, MD, Feb. 13–14, paper B.6, pp. 95–108.
- Ahmed, A.E., Al-Shaikh, A.H. and Arafat, T.I. (1992) Residual compressive and bond strengths of limestone aggregate concrete subjected to elevated temperatures. *Magazine of Concrete Research*, **44**, 117–25.
- Aldea, C.-M., Franssen, J.-M. and Dotreppe, J.-C. (1997) Fire test on normal and high strength reinforced concrete columns. *International Workshop on Fire Performance of High-Strength Concrete* (eds L.T. Phan, N.J. Carino, D. Duthinh and E. Garboczi), Gaithersburg (Feb. 13–14), NIST, pp. 109–124.
- Ali, F.A., O'Connor, D. and Abu-Tair, A. (2001) Explosive spalling of high-strength concrete columns in fire. *Magazine of Concrete Research*, **53** (3), 197–204.
- Ali, H.M., Senseny, P.E. and Alpert, R.L. (2004) Lateral displacement and collapse of single-storey steel frames in uncontrolled fires. *Engineering Structures*, **26**, 593–607.
- Allen, B. (2006) Intumescent fire protection of tall buildings. *New Steel Construction*, **14** (1), 24–8.
- Anderberg, Y. (1978a) *Armeringsståls Mekaniska Egenskaper vid Höga Temperaturer*, Bulletin 61, University of Lund, Sweden.
- Anderberg, Y. (1978b) *Analytical fire engineering design of reinforced concrete structures based on real fire characteristics*, in Proceedings of the Eighth Congress of the Fédération Internationale de la Précontrainte, London, 1978, Concrete Society, London, pp. 112–23.
- Anderberg, Y. (1983) *Properties of Materials at High Temperatures-Steel*, RILEM Report, University of Lund, Sweden.

- Anderberg, Y. (1988) Modelling steel behaviour. *Fire Safety Journal*, **13**, 17–26.
- Anderberg, Y. (2005) The effects of the constitutive models on the prediction of concrete mechanical behaviour and on the design of concrete structures exposed to fire, in *Fire Design of Concrete Structures: What Now? What Next?* (eds P.G. Gamberova, R. Felicetti, A. Meda and P. Riva), Proceedings of a Workshop, Politecnico di Milano, Dec. 2–3, 2004, Starrylink Editrice, pp. 37–48.
- Anderberg, Y. and Thelandersson, S. (1976) *Stress and Deformation Characteristics of Concrete, 2 – Experimental Investigation and Material Behaviour Model*, Bulletin 54, University of Lund, Sweden.
- Anon (1973) The Summerland fire. *Fire Prevention*, 1–16.
- Anon (1980) Report of the Woolworth's fire, Manchester. *Fire Prevention*, **138**, 13–24.
- Anon (1983) An FPA review of the official report on the Stardust disco fire. *Fire Prevention*, **158**, 12–20.
- Anon (1985) Fire tragedy at football stadium. *Fire Prevention*, **81**, 5–6.
- Anon (1986) News scene. *Fire Prevention*, **188**, 5.
- Anon (1987) King's cross tragedy. *Fire Prevention*, **205**, 5–6.
- Anon (1988) Fenell report finds fundamental errors made by senior underground management. *Fire Prevention*, **215**, 12.
- Anon (1990) Birmingham fire may force rebuild. *New Civil Engineer*, Sept. 6, 11.
- Anon (1993) Goodnight Vienna. *Fire Prevention*, **257**, 40–1.
- Arup (2005) Madrid Windsor Fire: the Arup view. <http://www.arup.com/fire/feature.cfm?pageid=6150>
- ASCE/SFPE (2003) *Standard Calculation Methods for Structural Fire Protection*, American Society of Civil Engineers.
- ASFP/SCI/FTSG (2004) *Fire Protection for Structural Steel in Buildings (Third Edition)*, Association for Specialist Fire Protection.
- Ashton, L.A. (1966) Effect of restraint of longitudinal deformation or rotation, in *Feuerwiderstandsfähigkeit von Spannbeton* (Braunschweig, 1965), Bauerlag Gmb H, Braunschweig, pp. 15–9.
- Ashton, L.A. and Bate, S.C.C. (1960) The fire-resistance of prestressed concrete beams. *Proceedings of the Institution of Civil Engineers*, **17**, 15–38.
- Association of Specialist Fire Protection Contractors and Manufacturers (1993) *Fire protection of timber floors*, ASFPCM, Aldershot.
- Babrauskas, V. and Williamson, R.B. (1978a) The historical basis of fire resistance testing-I. *Fire Technology*, **14**, 184–94 and 205.
- Babrauskas, V. and Williamson, R.B. (1978b) The historical basis of fire resistance testing-II. *Fire Technology*, **14**, 304–16.
- Baddoo, N.R. and Burgan, B.A. (2001) *Structural design of stainless steel*, Publication P291, SCI.

- Bahrends, J.F.B. (1966) Brandversuche an durchlaufenden Spannbetonbauteilen, in *Feuerwiderstandsfähigkeit von Spannbeton* (Braunschweig, 1965), Bauerlag Gmb H, Braunschweig, pp. 2023.
- Bailey, C.G. (1998) Development of computer software to simulate the structural behaviour of steel-framed building in fire. *Computers and Structures*, **67**, 421–38.
- Bailey, C.G. (2000) Effective lengths of concrete-filled steel square hollow sections in fire. *Proceedings of the Institution of Civil Engineers, Structures and Buildings*, **140**, 169–78.
- Bailey, C.G. (2001) *Steel Structures Supporting Composite Floor Slabs: Design for Fire*, Digest 462, BRE.
- Bailey, C.G. (2002) Holistic behaviour of concrete buildings in fire. *Proceedings of the Institution of Civil Engineers, Buildings and Structures*, **152** (3), 199–212.
- Bailey, C.G. (2003) *New Fire Design Method for Steel Frames with Composite Floor Slabs*, FBE Report 5, BRE.
- Bailey, C.G. (2004a) Structural fire design: core or specialist subject. *Structural Engineer*, **82** (9) 32–8.
- Bailey, C.G. (2004b) *Structural Fire Engineering Design: Materials Behaviour-Steel*, Digest 487 Part 2, BRE.
- Bailey, C.G. and Moore, D.B. (2000a) The structural behaviour of steel frames with composite floorslabs subject to fire: Part 1: Theory. *The Structural Engineer*, **78** (11), 19–27.
- Bailey, C.G. and Moore, D.B. (2000b) The structural behaviour of steel frames with composite floorslabs subject to fire: Part 1: Design. *The Structural Engineer*, **78** (11), 28–33.
- Bailey, C.G. and Newman, G.M. (1998) The design of steel framed buildings without applied fire protection. *Structural Engineer*, **76** (5), 77–81.
- Bailey, C.G., Burgess, I.W. and Plank, R.J. (1996) Computer simulation of a full-scale structural fire test. *Structural Engineer*, **74**, 93–100.
- Bailey C.G., Lennon, T. and Moore, D.B. (1999) The behaviour of full-scale steel-framed buildings subjected to compartment fires. *Structural Engineer*, **77** (8), 15–21.
- Bailey, C.G., Newman, G.M. and Simms, W.I. (1999) *Design of Steel Framed Buildings without Applied Fire Protection*, Publication 186, SCI.
- Baldwin, R. (1975) *Structural fire protection – the economic option*, in Proceedings of the Jubilee Conference of the Midlands Branch of the Institution of Structural Engineers – Structural Design for Fire Resistance, Birmingham, 1975, ISE, pp. 115–37.
- Baldwin, R. and North, M.A. (1973) A stress strain relationship for concrete at high temperature. *Magazine of Concrete Research*, **24**, 99–101.

- Baldwin, R. and Thomas, P.H. (1973) *Passive and Active Fire Protection – the Optimum Combination*, Fire Research Note 963/1973, Joint Fire Research Organisation (now BRE).
- Bali, A. (1984) The transient behaviour of plain concrete at elevated temperatures. PhD Thesis, University of Aston, Birmingham, England.
- Barnfield, J.R. (1986) *The UK procedure for the appraisal of fire protection to structural steelwork*, EGOLF Seminar, Brussels, Nov. 1986.
- Barnfield, J.R. and Porter, A.M. (1984) Historic buildings and fire; fire performance of cast-iron structural elements. *Structural Engineer*, **62A**, 373–80.
- Bayley, M.J. (1992) *The fire protection of aluminium in offshore structures*, in Proceedings of IMechE Conference, Materials and Design against Fire, London, 1992, Paper No C438/019/92, Mechanical Engineering Publications, London, pp. 113–20.
- Bažant, Z.P. (1983) Mathematical Model for Creep and Thermal Shrinkage of Concrete at High Temperatures. *Nuclear Engineering and Design*, **76**, 183–91.
- Bažant, Z.P. (ed.) (1988) *Mathematical Modelling of Creep and Shrinkage of Concrete*, John Wiley and Sons Ltd, Chichester, England.
- Becker, J. and Bresler, B. (1972) *FIRES-RC A Computer Program for the Fire Response of Structures-Reinforced Concrete Frames*, Report No UCB-FRG 74-3, Department of Civil Engineering, University of Berkeley, California.
- Becker, J., Bizri, H. and Bresler, B. (1974) *Fires-T2 A Computer Programme for the Fire Response of Structures – Thermal*, Report No UCB-FRG 74-1, Department of Civil Engineering, University of Berkeley, California.
- Beitel, J.J. and Iwankiw, N.R. (2005) Historical survey of multi-storey building collapses in fire. *International Fire Protection*, (24), 43–6.
- Benedetti, A. (1998) On the ultrasonic pulse propagation into fire damaged concrete. *ACI Structural Journal*, **95** (3), 259–71.
- Bessey, G.E. (1956) *Investigations into Building Fires: Part 2 – Visible Changes in Concrete and Mortar Exposed to High Temperature*, Technical Paper No 4, National Building Studies, HMSO, pp. 6–18.
- Bishop, P. (1991) Blaze adds to insurer unease. *New Civil Engineer*, Aug. 15, 4.
- Bishop, G.R. and Sheard, P.A. (1992) Fire-resistant composites for structural sections. *Composite Structures*, **21**, 85–9.
- Boam, K. and Cropper, D. (1994) Midlands link motorway viaducts: Rehabilitation of a fire damaged structure. *Proceedings of the Institution of Civil Engineers: Structures and Buildings*, **104**, 111–23.
- Bobrowski, J. and Bardhan-Roy, B.K. (1969) A method of calculating the ultimate strength of reinforced and prestressed concrete beams in combined flexure and shear. *Structural Engineer*, **47**, 3–15.

- Boström, L. (2002) *The Performance of Some Self Compacting Concretes When Exposed to Fire*, SP Swedish National Testing and Research Institute, Report No 2002:23.
- Boström, L. (2004) *Innovative Self-compacting Concrete – Development of Test Methodology for Determination of Fire Spalling*, SP Swedish National Testing and Research Institute, Report No 2004:06.
- Bregulla, J., Enjily, V. and Lennon, T. (2004) *Structural Fire Engineering Design: Materials Behaviour-Timber*, Digest 487 Part 4, BRE.
- BS 476: Part 3: 1975 Fire tests on building materials and structures; Part 3 External fire exposure roof test, British Standards Institution.
- BS 476: Part 6: 1989 Fire tests on building materials and structures; Part 6 Method of test for fire propagation for products, British Standards Institution.
- BS 476: Part 7: 1987 Fire tests on building materials and structures; Part 7 Method for classification of the surface spread of flame of products, British Standards Institution.
- BS 476: Part 8: 1972 Fire tests on building materials and structures; Part 8 Test methods and criteria for the fire resistance of elements of building construction, British Standards Institution.
- BS 476: Part 20: 1987 Fire tests on building materials and structures; Part 20 Method for the determination of the fire resistance of elements of construction (general principles), British Standards Institution.
- BS 476: Part 21: 1987 Fire tests on building materials and structures; Part 21 Methods for the determination of the fire resistance of loadbearing elements of construction, British Standards Institution.
- BS 476: Part 22: 1987 Fire tests on building materials and structures; Part 22 Methods for the determination of the fire resistance of non-loadbearing elements of construction, British Standards Institution.
- BS 1881: Part 120: 1983 Methods of testing concrete; Part 120 Method for the determination of the compressive strength of concrete cores, British Standards Institution.
- BS 5588: Fire precautions in the design and construction of buildings: buildings, British Standards Institution.
- BS 5950: Part 8 Structural use of steelwork in buildings; Part 8 Code of Practice for fire resistant design, British Standards Institution.
- Buchanan, A.H. (2001) *Structural Design for Fire Safety*, John Wiley and Sons, Ltd, Chichester.
- Building Employers Confederation and Loss Prevention Council (1992) *Fire Prevention on Construction Sites*. National Contractors Group, Coventry, England.
- Building Research Establishment (1986) *Fire Resistant Steel Structures: Free Standing Blockwork Filled Columns and Stanchions*, Digest 317, BRE, Garston.

- Building Research Establishment (1987) *Smoke Control in Buildings: Design Principles*, Digest 260, BRE, Garston.
- Burgess, I.W., El-Rimawi, J.A. and Plank, R.J. (1990) Analysis of beams with non-uniform temperature profile due to fire exposure. *Journal of Constructional Steelwork Research*, **16**, 169–92.
- Byrd, T. (1992a) Sprinklers dry as Expo burned. *New Civil Engineer*, Feb. 27, 5.
- Byrd, T. (1992b) Burning question. *New Civil Engineer*, Feb. 27, 12–13.
- Canadian Concrete and Masonry Codes Council (1992) *Firewalls, a Design Guide*, CCMCC, Ottawa.
- Canter, D. (1985) *Studies of Human Behaviour in Fire: Empirical Results and their Implication for Education and Design*, BRE, Garston.
- Castillo, C. and Durani, A.J. (1990) Effect of transient high temperature on high-strength concrete. *ACI Materials Journal*, **87** (1), 47–53.
- Castle, G.K. (1974) The nature of various fire environments and the application of modern material approaches for fire protection of exterior structural steel. *Journal of Fire and Flammability*, **5**, 203–22.
- Chan, Y.N., Peng, G.F. and Anson, M. (1999) Residual strength and pore structure of high-strength concrete and normal strength concrete after exposure to high temperatures. *Cement and Concrete Composites*, **21**, 23–7.
- Chana, P. and Price, W. (2003) The Cardington fire test. *Concrete*, **37** (1), 28 and 30–3.
- Chen, B. and Liu, J. (2004) Residual strength of hybrid-fiber-reinforced high strength concrete after exposure to high temperatures. *Cement and Concrete Research*, **34**, 1065–9.
- Chitty, R. and Fraser-Mitchell, J. (2003) *Fire Safety Engineering – A Reference Guide*, BRE.
- Chitty, R., Cox, G., Fardell, P.J. and Morris, W.A. (1992) *Mathematical Fire Modelling and its Application to Fire Safety Design*, Report BR 223, BRE, Garston.
- CIB W14 Report (1983) A conceptual approach towards a probability based design guide on structural fire safety. *Fire Safety Journal*, **6**, 1–79.
- Clayton, N. and Lennon, T. (2000) High-grade concrete columns in fire. *Concrete*, **34** (3), 51.
- Cockroft, D. (1993) An architect's perspective on the Windsor Castle fire. *Fire Prevention*, **22** (4), 4–7.
- Concrete Society (1990) *Assessment and Repair of Fire Damaged Concrete Structures*. Technical Report 33, Concrete Society, Wexham Springs.
- Connolly, R.J. (1995) The spalling of concrete in fires, PhD Thesis, University of Aston.
- Connolly, R.J. (1997) The spalling of concrete. *Fire Engineers Journal*, January, 38–40.

- Conserva, M., Donzellii, G. and Trippodo, R. (1992) *Aluminium and its Applications*, EDIMET SPA, Italy.
- Construction Industry Research and Information Association (1987) *Fire Tests on Ribbed Concrete Slabs*, Technical Note 131, CIRIA, London.
- Cooke, G.M.E. (1987a) Fire engineering of tall fire separating walls (Part 1). *Fire Surveyor*, **16** (3), 13–29.
- Cooke, G.M.E. (1987b) Fire engineering of tall fire separating walls (Part 2). *Fire Surveyor*, **16** (4), 19–29.
- Cooke, G.M.E. and Latham, D.J. (1987) The inherent fire resistance of a loaded steel framework. *Steel Construction Today*, **1**, 49–58.
- Cooke, G.M.E. and Morgan, P.B.E. (1988) *Thermal Bowing in Fire and How it Affects Building Design*, Information Paper IP21/88, BRE, Garston.
- Cooke, G.M.E., Lawson, R.M. and Newman, G.M. (1988) Fire resistance of composite deck slabs. *Structural Engineer*, **66**, 253–61 and 267.
- Cruz, C.R. (1962) An optical method of determining the elastic constants of concrete. *Journal of the Portland Cement Association Research and Development Laboratories*, May, 24–32.
- Day, T. (1994) Fire safety in major retail outlets. *Fire Safety Engineering*, **1** (5), 18–20.
- Department of the Environment (1991) *Standard Fire Precautions for Contractors*, HMSO.
- Department of the Environment (1992a) *Building Regulations: Approved Document B, Fire Safety*, HMSO.
- Department of the Environment (1992b) *Building Regulations and Fire Safety: Procedural Guidance*, DoE, London.
- Diederichs, U. (1987) Modelle zur Beschreibung der Betonverformung bei instantionären Temperaturen, in *Abschlusskolloquium – Bauwerke unter Brandeinwirkung*, Technische Universität, Braunschweig, pp. 25–34.
- Dixon, R. and Taylor, P. (1993) Hampton Court: restoration of the fire-damaged structure. *Structural Engineer*, **71**, 321–5.
- Dorn, J.E. (1954) Some fundamental experiments on high temperature creep. *Journal of the Mechanics and Physics of Solids*, **3**, 86–116.
- dos Santos, J.R., Branco, F.A. and Brito de, J. (2002) Assessment of concrete structures subjected to fire – the FBTest. *Magazine of Concrete Research*, **54**, 203–8.
- Dotreppe, J.-C., Franssen, J.-M. and Vanderzeypen, Y. (1995) *A straightforward calculation method for the fire resistance of reinforced concrete columns*. Poster Paper. First European Symposium on Fire Safety Science, Institute for Structural Engineering, Zurich (Aug. 21–23).
- Dougill, J.W. (1966) The relevance of the established method of structural fire testing to reinforced concrete. *Applied Materials Research*, **5**, 235–40.
- Dounas, S. and Golrang, B. (1982) *Ståhls Mekaniska Egenskaper vid Höger Temperaturer*, University of Lund, Sweden.

- Dowling, J. (2005) Steel in fire: the latest news. *New Steel Construction*, **13** (8), 30–2.
- Drysdale, D. (1998) *An Introduction to Fire Dynamics (Second Edition)*, John Wiley and Sons, Ltd., Chichester.
- ECCS (1983) *Calculation of the Fire Resistance of Load Bearing Elements and Structural Assemblies Exposed to the Standard Fire*, Elsevier Applied Science, Amsterdam.
- ECCS (1985) *Design Manual on the European Recommendations for the Fire Safety of Steel Structures*, ECCS Technical Committee 3, Brussels.
- Ehm, H. (1967) *Ein Beitrag zur reichnerische Bemessung von brandbeanspruchten balkenartigen Stahlbetonbauteilen*, Technische Hochschule Braunschweig.
- Ehm, H. and von Postel, R. (1966) Versuche an Stahlbetonkonstruktionen mit Durchlaufwirkung unter Feuerangriff, in *Feuerwiderstandsfähigkeit von Spannbeton* (Braunschweig, 1965), Bauerlag Gmb H, Braunschweig, pp. 24–31.
- El-Refal, F.E., Kamal, M.M. and Bahnasawy, H.H. (1992), Effect of high temperature on the mechanical properties of fibre reinforced concrete cast using superplasticizer, in *Fibre Reinforced Cement and Concrete* (ed. R.N. Swamy), E&FN Spon, pp. 749–63.
- EN 1363. Fire Resistance Tests, Comité Européen de Normalisation/British Standards Institution.
- EN 1363-1. Fire resistance Tests – Part 1: General Requirements.
- EN 13381-4. EN 13881: Part 4 Test method for determining the contribution to the fire resistance of structural members: by applied protection to steel structural elements, Comité Européen de Normalisation/British Standards Institution.
- EN 13501. Fire Classification of Construction Products and Building Elements, Comité Européen de Normalisation/British Standards Institution.
- EN 1990: Eurocode: Basis for structural design, Comité Européen de Normalisation/British Standards Institution.
- EN 1991-1-2: Eurocode 1: Basis of design and actions on structures. Part 1.2: Actions on structures exposed to fire, Comité Européen de Normalisation/British Standards Institution.
- EN 1992-1-1: Eurocode 2: Design of concrete structures. Part 1.1: General rules and rules for buildings, Comité Européen de Normalisation/British Standards Institution.
- EN 1992-1-2: Eurocode 2: Design of concrete structures. Part 1.2: Supplementary rules for structural fire design, Comité Européen de Normalisation/British Standards Institution.
- EN 1993-1-1: Eurocode 3: Design of steel structures. Part 1.2: General rules and rules for buildings, Comité Européen de Normalisation/British Standards Institution.

- EN 1993-1-2: Eurocode 3: Design of steel structures. Part 1.2: Supplementary rules for structural fire design, Comité Européen de Normalisation/British Standards Institution.
- EN 1994-1-1: Eurocode 4: Design of composite steel and concrete structures. Part 1.1: General rules and rules for buildings, Comité Européen de Normalisation/British Standards Institution.
- EN 1994-1-2: Eurocode 4: Design of composite steel and concrete structures. Part 1.2: Supplementary rules for structural fire design, Comité Européen de Normalisation/British Standards Institution.
- EN 1995-1-1: Eurocode 5: Design of timber structure – Part 1.1: General Common rules and rules for buildings, Comité Européen de Normalisation/British Standards Institution.
- EN 1995-1-2: Eurocode 5: Design of timber structures. Part 1.2: Supplementary rules for structural fire design, Comité Européen de Normalisation/British Standards Institution.
- ENV 1996-1-2: Eurocode 6: Design of masonry structures. Part 1.2: Supplementary rules for structural fire design, Comité Européen de Normalisation/British Standards Institution.
- EN 1999-1-2 Eurocode 9: Design of aluminium structures – Part 1.1 General rules – Structural fire design.
- Enjily, V. (2003) *The fire performance of a six-storey timber frame building at BRE Cardington*. Paper presented at ‘Guidance for Structural Fire Engineering’ at ISE, Feb. 13, 2003.
- Fackler, J.P. (1959) Concernant la résistance au feu des éléments de construction. *Cahiers du Centre Scientifique et Technique du Bâtiment*, **37**, 1–20.
- Fairyadh, F.I. and El-Ausi, M.A. (1989) Effect of elevated temperature on splitting tensile strength of fibre concrete. *International Journal of Cement Composites and Lightweight Concrete*, **11** (3), 175–8.
- Fédération Internationale de la Précontrainte and Comité Euro-International du Béton (1978) *FIP/CEB Report on Methods of Assessment of the Fire Resistance of Concrete Structural Members*, Cement and Concrete Association, Wexham Springs.
- Felicetti, R. (2004) Digital Camera Colorimetry for the assessment of fire-damaged concrete, in *Fire Design of Concrete Structures: What Now? What Next?* (eds P.G. Gambarova, R. Felicetti, A. Meda and P. Riva), Politecnico di Milano, Dec. 2–3, 2004, Starrylink Editrice, pp. 211–20.
- Felicetti, R. and Gambarova, P.G. (2003) Heat in concrete: Special issues in materials testing. *Studies and Researches*, Politecnico di Milano, **24**, 121–38.
- Fellinger, J.H.H. (2004) *Shear and Anchorage Behaviour of Fire Exposed Hollow Core Slabs*, DUP Science, Delft.

- Fields, B.A. and Fields, R.J. (1989) *Elevated Temperature Deformation of Structural Steel*, NISTIR 88-3899, United States National Institute of Standards and Technology, Gaithersburg.
- Fisher, K. (1975) *The performance of brickwork in fire resistance tests*, in Proceedings of the Jubilee Conference of the Midlands Branch of the Institution of Structural Engineers – Structural Design for Fire Resistance, Birmingham, 1975, ISE, pp. 314–38.
- Forsén, N.E. (1982) *A Theoretical Study on the Fire Resistance of Concrete Structures*, Cement and Concrete Research Institute, Norwegian Institute of Technology, Trondheim, Report STF A82062.
- Foster, D. (1975) *The design of brickwork against fire with regard to building regulations*, in Proceedings of the Jubilee Conference of the Midlands Branch of the Institution of Structural Engineers – Structural Design for Fire Resistance, Birmingham, 1975, ISE, pp. 282–313.
- Fowler, D. and Doyle, N. (1992) Stability probe leads castle salvage. *New Civil Engineer*, Nov. 26, 4–5.
- Franssen, J.M. (2003) *SAFIR – a thermal/structural program modeling structures under fire*, in Proceedings of the NASCC Conference, American Institute for Steel Construction, Baltimore.
- Fredlund, B. (1988) *A Model for Heat and Mass Transfer in Timber Structures during a Fire – A Theoretical, Numerical and Experimental Study*, Report No LUTUDG/CTVBB-1003, Lund Institute of Technology, Sweden.
- Fu, Y.F., Wong, Y.L., Poon, C.S. and Tang, C.A. (2005) Stress-strain behaviour of high-strength concrete at elevated temperatures. *Magazine of Concrete Research*, **57** (9), 535–44.
- Fujita, K. (undated) *Characteristics of a Fire in a Non-Combustible Room and Prevention of Fire Damage*, Japanese Ministry of Construction Building Research Institute Report No 2(2), Tokyo.
- Furamura, F. (1966) Stress-strain curve of concrete at high temperatures. *Transactions of the Architectural Institute of Japan*, Abstract No 7004, p. 686.
- Furamura, F., Oh, C.H., Ave, T. and Kim, W.J. (1987) Simple formulation for stress-strain relationship of normal concrete at elevated temperature. *Report of the Research Laboratory of Engineering Materials, Tokyo Institute of Technology*, **12**, 155–72.
- Gerhards, C.C. (1982) Effect of moisture content and temperature on the mechanical properties of wood: an analysis of immediate effects. *Wood and Fiber*, **14**, 4–36.
- Gillen, M.P. (1997) The behaviour of high performance lightweight concrete at elevated temperatures, in *Third Canment/ACI International Symposium on Advances in Concrete Technology* (ed. V.M. Malhotra), ACI SP 171-5, 131–55.

- Gnanakrishnan, N. and Lawther, R. (1989) *Some aspects of the fire performance of single leaf masonry construction*, in Proceedings of International Symposium on Fire Engineering for Building Structures and Safety, Melbourne, 1989, Institution of Engineers Australia, Melbourne, pp. 93–9.
- Gnanakrishnan, N., Lawrence, S.J. and Lawther, L. (1988) *Behaviour of cavity walls exposed to fire*, in Proceedings of the 8th International Brick/Block Masonry Conference, Dublin, 1988, pp. 981–90.
- Gowripalan, N. (1998) Mechanical properties of high-strength concrete subjected to high temperatures, in *Concrete under Severe Conditions 2* (eds O.E. Gjry, K. Sakai and N. Banthia), Troms, June 21–24, E&FN Spon, pp. 774–84.
- Guise, S.E. (1997) The use of colour image analysis for assessment of fire damaged concrete. PhD thesis, Aston University, Birmingham.
- Hadvig, S. (1981) *Charring of Wood in Building Fires – Practice, Theory, Instrumentation, Measurement*. Laboratory of Heating and Air Conditioning, Technical University of Denmark, Lyngby.
- Haksever, A. and Anderberg, Y. (1981/2) Comparison between measured and computed structural response of some reinforced concrete columns in fire. *Fire Safety Journal*, **4**, 293–7.
- Hammad, A.-H.M. and Ramadan, K.K. (1989a) Mechanical properties of Al-Mg alloys at elevated temperatures. Part 2: Correlation between strength, ductility and structural changes for Al-3% Mg. *Zeitschrift fr Metallkunde*, **80**, 178–85.
- Hammad, A.-H.M. and Ramadan, K.K. (1989b) Mechanical properties of Al-Mg alloys at elevated temperatures. Part 3: Deformation behaviour of quenched and aged Al-3% Mg. *Zeitschrift fr Metallkunde*, **80**, 431–8.
- Hammad, A.-H.M., Ramadan, K.K. and Nasr, M.A. (1989) Mechanical properties of Al-Mg alloys at elevated temperatures. Part 1: High temperature deformation of pure Al and Al-Mg. *Zeitschrift fr Metallkunde*, **80**, 173–7.
- Handoo, S.K., Agarwal, S. and Maiti, S.C. (1991) *Application of DTA/TGA for the assessment of fire damaged concrete structures*, 8th Proceedings National Symposium on Thermal analysis, Indian Thermal Analysis, Mumbai, pp. 437–43.
- Hansell, G.O. and Morgan, H.P. (1994) *Design Approaches for Smoke Control in Atrium Buildings*, Report BR258, BRE, Garston, England.
- Harmathy, T.Z. (1967) Deflection and failure of steel supported floors and beams in fire, in *Symposium on Fire Test Methods – Restraint and Smoke*, (1966), American Society of Testing Materials, STP 422, pp. 40–62.
- Harmathy, T.Z. (1969) Design of fire test furnaces. *Fire Technology*, **5**, 140–50.
- Harmathy, T.Z. (1993) *Fire Safety Design and Concrete*. Longman Scientific and Technical, Harlow, England.

- Harmathy, T.Z. and Mehaffey, J.R. (1985) Design of buildings for prescribed levels of structural fire safety, in *Fire Safety: Science and Engineering* (ed. T.Z. Harmathy), ASTM STP 882, Philadelphia, pp. 160–73.
- Harmathy, T.Z. and Stanzak, W.W. (1970) Elevated temperature tensile and creep properties of some structural and prestressing steels, in *Symposium on Fire Test Performance, American Society of Testing and Materials*, STP 464, pp. 186–208.
- Hassen, S. and Colina, H. (2006) Transient thermal creep of concrete in accidental conditions up to 400°C. *Magazine of Concrete Research*, **58** (4), 201–8.
- Hertz, K. (1981a) *Stress Distribution Factors*, Report No 158 (reissued as 2nd edn Report 190, 1988), Institute of Building Design, Technical University of Denmark.
- Hertz, K. (1981b) *Simple Temperature Calculations of Fire Exposed Concrete Constructions*, Report No 159, Institute of Building Design, Technical University of Denmark.
- Hertz, K. (1985) *Analyses of Prestressed Concrete Structures Exposed to Fire*, Report No 174, Institute of Building Design, Technical University of Denmark.
- Hertz, K.D. (1992) Danish investigations on silica fume concretes at elevated temperatures. *ACI Materials Journal*, **89** (4), 345–7.
- Hertz, K.D. (2004) Reinforcement data for fire safety design. *Magazine of Concrete Research*, **56** (8), 453–9.
- Hertz, K.D. (2005) Concrete strength for fire safety design. *Magazine of Concrete Research*, **57** (8), 445–3.
- Hertz, K.D. (2006) Quenched reinforcement exposed to fire. *Magazine of Concrete Research*, **58** (1), 43–8.
- Heselden, A.J.M. (1968) Parameters determining the severity of fire, in *Symposium No. Behaviour of Structural Steel in Fire* (London 1968), HMSO, pp. 19–28.
- Heselden, A.J.M. (1984) *The Interaction of Sprinklers and Roof Venting in Industrial Buildings: The Current Knowledge*, BRE, Garston.
- Hinkley, P.L. and Illingworth, P.M. (1990) *The Ghent Fire Tests: Observations on the Experiments*, Colt International, Havant, Hampshire, England.
- Hinkley, P.L., Hansell, G.O., Marshall, N.R. and Harrison, R. (1992) Sprinklers and vents interaction. *Fire Surveyor*, **21** (5), 18–23.
- Holmes, M., Anchor, R.D., Cooke, G.M.E., and Crook, R.N. (1982) The effects of elevated temperatures on the strength properties of reinforcing and prestressing steels. *Structural Engineer*, **60B**, 7–13.
- Hopkinson, J.S. (1984) *Fire Spread in Buildings*, Paper IP 21/84, BRE, Garston.

- Hosser, D., Dorn, T. and Richter, E. (1994) Evaluation of simplified calculation methods for structural fire design. *Fire Safety Journal*, **22**, 249–304.
- Huang, Z., Burgess, I.W. and Plank, R.J. (1999) Three-dimensional modelling of two full-scale fire tests on a composite building. *Proceedings of the Institution of Civil Engineers: Structures and Buildings*, **134**, 243–55.
- Huang, Z., Burgess, I.W. and Plank, R.J. (2003a) Modelling membrane action of concrete slabs in composite buildings in fire. I: Theoretical development. *ASCE Journal of Structural Engineering*, **129** (8), 1093–102.
- Huang, Z., Burgess, I.W. and Plank, R.J. (2003b) Modelling membrane action of concrete slabs in composite buildings in fire. II: Validations. *ASCE Journal of Structural Engineering*, **129** (8), 1103–12.
- Huebner, K.H., Thornton, E.A. and Byrom, T.G. (1995) *The Finite Element Method for Engineers (Third Edition)*, John Wiley & Sons, Inc. New York.
- Hughes, T.R.J. (1977) Unconditionally stable algorithm for nonlinear heat conduction. *Computer Methods in Applied Mechanical Engineering*, **10**, 135–9.
- Hughes, B.P. and Chapman, G.P. (1966) Deformation of concrete and microconcrete in tension and compression. *Magazine of Concrete Research*, **18**, 19–24.
- Iding, R.H. and Bresler, B. (1987) *FASBUS II User's Manual Prepared for the American Iron and Steel Institute*, Wiss, Janney, Elstner Associates, Inc.
- Iding, R.H. and Bresler, B. (1990) Effect of restraint conditions on fire endurance of steel-framed construction. *Proceedings of the 1990 National Steel Construction Conference*, AISC, Chicago IL.
- Iding, R.H., Bresler, B. and Nizamuddin, Z. (1977a) *FIRES-T3 A Computer Program for the Fires Response of Structures – Thermal*, Report No UCB-FRG 77-15, University of Berkeley, California.
- Iding, R.H., Bresler, B. and Nizamuddin, Z. (1977b) *FIRES-RC II – Structural Analysis Program for the Fire Response of Reinforced Concrete Frames*, UCB-FRG Report 77-8, Fire Research Group, Department of Civil Engineering, University of California, Berkeley.
- Ingberg, S.H. (1928) Tests of the severity of building fires. *US National Fire Protection Quarterly*, **22**, 43–61.
- ISE (2002) *Safety in Tall Buildings and Other Buildings with Large Occupancy*, Institution of Structural Engineers.
- ISE (2003) *Introduction to the Fire Safety Engineering of Structures*, Institution of Structural Engineers.
- ISE (2006) *Advanced Fire Safety Engineering of Structures*, Institution of Structural Engineers (to be published).
- Institution of Structural Engineers (ISE) and Concrete Society (1978) *Design and Detailing of Concrete Structures for Fire Resistance*, Institution of Structural Engineers, London.

- ISO 834: 1975 *Fire Resistance Tests – Elements of Building Construction*, International Organization for Standardization, Switzerland.
- Issen, L.A., Gustaferrero, A.H. and Carlson, C.C. (1970) *Fire tests of concrete members: improved method of estimating thermal restraint forces*, American Society for Testing and Materials Publication SP 464, pp. 153–65.
- Izzuddin, B.A. and Moore, D.B. (2002) Lessons from a full-scale fire test. *Proceedings of the Institution of Civil Engineers, Structures and Buildings*, **152** (4), 319–29.
- Jansson, R. and Boström, L. (2004) Experimental investigation on concrete spalling in fire, in *Fire Design of Concrete Structures: What Now? What Next?* (eds P.G. Gamberova, R. Felicetti, A. Meda and P. Riva), Proceedings of a Workshop, Politecnico di Milano, Dec. 2–3, 2004, Starrylink Editrice, pp. 109–14.
- Kawagoe, K. (1958) *Fire Behaviour in Rooms*, Report No 27, Building Research Institute, Tokyo.
- Kersken-Bradley, M. (1986) Probabilistic concepts in fire engineering, in *Design of Structures against Fire* (eds R.D. Anchor, H.L. Malhotra and J.A. Purkiss), Elsevier Applied Science, London, pp. 21–39.
- Kersken-Bradley, M. (1993) *EuroCode 5, Part 10 Structural Fire Design*, in Proceedings of the Oxford Fire Conference, Oxford, July 1–2, 1993, Timber Research and Development Association, Princess Risborough, England.
- Khalafallah, B.H. (2001) Coupled heat and mass transfer in concrete exposed to fire, PhD Thesis, University of Aston.
- Khennane, A. and Baker, G. (1993) Uniaxial model for concrete under variable temperature and stress. *American Society of Civil Engineers, Journal of Engineering Mechanics*, **119**, 1507–25.
- Khoury, G.A. (1992) Compressive strength of concrete at high temperatures: a reassessment. *Magazine of Concrete Research*, **44**, 291–309.
- Khoury, G.A., Grainger, B.N. and Sullivan, P.J.E. (1985a) Transient thermal strain of concrete: literature review, conditions within the specimen and behaviour of individual constituents. *Magazine of Concrete Research*, **37**, 131–44.
- Khoury, G.A., Grainger, B.N. and Sullivan, P.J.E. (1985b) Strain of concrete during first heating to 600°C under load. *Magazine of Concrete Research*, **37**, 195–215.
- Khoury, G.A., Grainger, B.N. and Sullivan, P.J.E. (1986) Strain of concrete during first cooling from 600°C under load. *Magazine of Concrete Research*, **38**, 3–12.
- Kirby, B.R. (1986) Recent developments and applications in structural fire engineering design – a review. *Fire Safety Journal*, **11**, 141–79.
- Kirby, B.R. (2004) Calibration of Eurocode 1: Actions on structures – Part 1.2: Actions on structures exposed to fire. *Structural Engineer*, **82** (19), 38–43.

- Kirby, B.R. (undated) *Fire Engineering in Sports Stands*, British Steel Technical, Cleveland.
- Kirby, B.R. and Preston, R.R. (1988) High temperature properties of hot-rolled structural steels for use in fire engineering design studies. *Fire Safety Journal*, **13**, 27–37.
- Kirby, B.R., Lapwood, D.J. and Thompson G. (1986) *The Reinstatement of Fire Damaged Steel and Iron Framed Structures*. British Steel Technical (Swinden Laboratories), Rotherham.
- Kirby, B.R., Newman, G.M., Butterworth, N., Pagan, J. and English, C. (2004) A new approach to specifying fire resistance periods. *Structural Engineer*, **82** (19), 34–7.
- Kirby, B.R., Wainman, D.E., Tomlinson, L.H., Kay, T.R. and Peacock, B.N. (1994) *Natural Fires in Large Scale compartments – A British Steel Technical*, Fire Research Station Collaborative Project, British Steel (now Corus) Technical Swinden Laboratories.
- Kodur, V.K.R. (1999) Performance based fire resistance design of concrete filled steel columns. *Journal of Constructional Steel Research*, (51), 21–36.
- Kodur, V.K.R. and Lie, T.T. (1995) Fire performance of concrete-filled hollow steel columns. *Journal of Fire Protection Engineering*, **7** (3), 89–98.
- Kordina, K. and Henke, V. (1987) *Sicherheitstheoretische Untersuchungen zur Versagenwahrscheinlichkeit von brandbeanspruchten Bauteilen bzw. Bauwerksabschnitten*, Sonderforschungsbereich 148, Technische Universität, Braunschweig.
- Kordina, K. and Krampf, L. (1984) Empfehlungen für brandschutztechnisch richtiges Konstruieren von Betonbauwerkern. *Deutscher Ausschuss für Stahlbeton*, **352**, 9–33.
- Krampf, L. (undated) *Investigations on the Shear Behaviour of Reinforced Concrete Beams Exposed to Fire*, Institut für Baustoffkunde und Stahlbetonbau, Technische Universität Braunschweig, Germany.
- Kruppa, J. (1992) *Ageing effect of fire insulation of steel structures*. Proceedings of IMechE Conference on Materials and Design against Fire (London, 1992), Paper No C438/007/92, Mechanical Engineering Publications, London, pp. 129–34.
- Latham, D.J., Kirby, B.R. and Thompson, G. (1987) The temperatures attained by unprotected structural steelwork in experimental natural fires. *Fire Safety Journal*, **12**, 139–52.
- Laverty, D., Nadjai, A. and O'Connor, D.J. (2000/1) Modelling of thermo-structural response of concrete masonry walls subjected to fire. *Journal of Applied Fire Science*, **10** (1), 3–19.
- Law, M. (1973) Prediction of Fire Resistance, in *Symposium No 5 Fire Resistance Requirements for Buildings – A New Approach* (London, 1971), HMSO, pp. 16–29 .
- Law, M. (1978) Fire safety of external building elements. *Engineering Journal of the American Institute of Steel Construction*, 59–74.

- Law, M. (1983) A basis for the design of fire protection of building structures. *Structural Engineer*, **61A**, 25–33.
- Law, M. (1995) The origins of the 5 MW Fire. *Fire Safety Engineering*, April, 17–20.
- Law, M. (1997) *A review of formulae for T-equivalent*. Proceedings of Fifth International Symposium on Fire Safety Science, Melbourne Australia, Mar. 3–7, unpaginated.
- Law, M. and O'Brien, T. (1989) *Fire Safety of Bare External Structural Steel*, Report No SCI-P-009, Steel Construction Institute, Ascot.
- Lawrence, S.J. and Gnanakrishnan, N. (1988a) *The fire resistance of masonry walls – an overview*. Proceedings of the First National Structural Engineering Conference, Melbourne, 1987, Institution of Engineers, Australia, pp. 431–7.
- Lawrence, S.J. and Gnanakrishnan, N. (1988b) *The Fire Resistance of Masonry Walls*. Technical Record 531, National Building Technology Centre, Chatswood, New South Wales.
- Lawson, R.M. (1985) *Fire Resistance of Ribbed Concrete Floors*, Report No 107, Construction Industry Research and Information Association, London.
- Lawson, R.M. (1990a) Behaviour of steel beam to column connections in fire. *Structural Engineer*, **68**, 263–71.
- Lawson, R.M. (1990b) *Enhancement of Fire Resistance of Beams by Beam to Column Connections*, Report TR-086, Steel Construction Institute, Ascot.
- Lawson, R.M. and Newman, G.M. (1996) *Structural Fire Design to EC3 and EC4, and Comparison with BS 5950*, Technical Report 159, SCI.
- Lennon, T. (2003) *Precast hollowcore slabs in fire*, Information Paper IP 5/03, BRE.
- Lennon, T. (2004a) *Structural Fire Engineering Design: Introduction*, Digest 484, BRE.
- Lennon, T. (2004b) *Structural Fire Engineering Design: Fire Development*, Digest 485, BRE.
- Lennon, T. (2004c) *Structural Fire Engineering Design: Materials Behaviour – Concrete*, Digest 487 Part 1, BRE.
- Lennon, T. and Clayton, N. (1999) *Fire tests on high grade concrete with polypropylene fibres*. 9th Concrete Communications Conference, British Cement Association, pp. 255–64.
- Leston-Jones, L.C., Burgess, I.W., Lennon, T. and Plank, R.J. (1997) Elevated temperature tests moment-rotation tests on steelwork connections. *Proceedings of the Institution of Civil Engineers, Structures and Buildings*, **122**, 410–19.
- Li, L.-Y. and Purkiss, J.A. (2005) Stress-strain constitutive equations of concrete at elevated temperatures. *Fire Safety Journal*, **40**, 669–86.
- Lie, T.T. (1974) Characteristic temperature curves for various fire severities. *Fire Technology*, **10**, 315–26.

- Lie, T.T. (1977) A method of assessing the fire resistance of laminated timber beams and columns. *Canadian Journal of Civil Engineering*, **4**, 161–9.
- Lie, T.T. and Kodur, V.K.R. (1995) *Effect of temperature on thermal and mechanical properties of steel fibre-reinforced concrete*, National Research Council Canada, Report 695.
- Lie, T.T. and Kodur, V.K.R. (1996) Thermal and mechanical properties of steel fibre-reinforced concrete at elevated temperatures. *Canadian Journal of Civil Engineering*, **23**, 511–17.
- Lie, T.T., Rowe, T.J. and Lin, T.D. (1986) *Residual strength of fire-exposed reinforced concrete columns*, Special Publication SP92-9, American Concrete Institute, Detroit, pp. 153–74.
- Lin, C.-H., Chen, S.-T. and Hwang, T.-Z. (1989) Residual strength of reinforced concrete columns exposed to fire. *Journal of the Chinese Institute of Engineers*, **12**, 557–65.
- LPC, ABI, FPA (2000) *The LPC Design Guide for the Fire Protection of Buildings – A Code of Practice for the Protection of Business*, Fire Protection Association.
- Malhotra, H.L. (1956) Effect of temperature on the compressive strength of concrete. *Magazine of Concrete Research*, **8**, 85–94.
- Malhotra, H.L. (1978) *Some noteworthy fires in concrete structures*. Proceedings of the 8th Congress of the Fédération Internationale de la Précontrainte, London, 1978, Concrete Society, Wexham Springs, pp. 86–98.
- Malhotra, H.L. (1982a) *Design of Fire-Resisting Structures*, Surrey University Press, Glasgow.
- Malhotra, H.L. (1982b) Report on the work of technical committee 44PHT 'Properties of materials at high temperatures'. *Matériaux et Constructions*, **15**, 161–70.
- Malhotra, H.L. (1984) *Spalling of Concrete in Fires*, Technical Note No 118, Construction Industry Research and Information Association, London.
- Malhotra, H.L. (1986) A survey of fire protection developments for buildings, in *Design of Structures against Fire* (eds R.D. Anchor, H.L. Malhotra and J.A. Purkiss), Elsevier Applied Science, London, pp. 1–13.
- Malhotra, H.L. (1987) *Fire Safety in Buildings*, BRE, Garston.
- Malhotra, H.L. (1993) Fire compartmentation: needs and specification. *Fire Surveyor*, **22** (2), 4–9.
- Malhotra, H.L. (1994) What is fire resistance? *Fire Safety Engineering*, **1** (1), 19–22.
- Maréchal, J.-C. (1970) Influence des températures sur la résistance, sur le fluage, sur la déformation plastique du béton. *Annales de L'Institute Technique du Bâtiment et des Travaux Publics*, **23**, October, 123–46.
- Marshall, N.R. (1992) *Smoke Control in Large Stores: an Extended Calculation Method for Slit Extraction Design*, Occasional Paper OP51, BRE, Garston.

- Marshall, N.R. and Morgan, H.P. (1992) User's guide to BRE spill plume calculations. *Fire Surveyor*, **21** (8), 14–9.
- Martin, L.H. and Purkiss, J.A. (2006) *Concrete Design to EN 1992*, Butterworth Heinemann, London.
- Melinek, S.J. (1989) Prediction of the fire resistance of insulated steel. *Fire Safety Journal*, **14**, 127–34.
- Melinek, S.J. and Thomas, P.H. (1987) Heat flow to insulated steel. *Fire Safety Journal*, **12**, 1–8.
- Meyer-Ottens, C. (1969) The behaviour of load bearing and non-loadbearing internal and external walls of wood and wood based materials under fire exposure, in *Symposium No 3 Fire and Structural Use of Timber* (London, 1967), HMSO, pp. 77–89.
- Meyer-Ottens, C. (1975) *Zur Frage der Abplatzungen an Bauteilen aus Beton bei Brandbeanspruchungen*, Deutsche Ausschluß für Stahlbeton, Heft 248.
- Ministry of Works (1946) *Fire Grading of Buildings: Part I General Principles and Structural Precautions*, Post-War Building Studies No 20, HMSO (reissued by BRE, 1992).
- Ministry of Works (1952) *Fire Grading of Buildings: Part II Fire Fighting Equipment; Part III Personal Safety; Part IV Chimneys and Flues*, Post War Building Studies, No 29, HMSO (reissued by BRE, 1992).
- Mlakar, P.F., Dusenberry, D.O., Harris, J.R., Haynes, G., Phan, L.T. and Sozen, M.A. (2003) Pentagon Building Performance Report. *Civil Engineering*, **73** (2), 43–55.
- Montgomery, F.R. (1997) Surface permeability measurement as a means of assessing fire damage of concrete, in *The Concrete Way to Development*, (Vol. 2), FIP Symposium, Johannesburg, Mar. 9–12, 1997, Concrete Society of South Africa, pp. 821–8.
- Mooney, J. (1992) Surface radiant energy balance for structural thermal analysis. *Fire and Materials*, **6**, 61–6.
- Moore, D.B. and Lennon, T. (1997) Fire engineering design of steel structures. *Progress in Structural Engineering and Materials*, **1** (1), 4–9.
- Morales, E.M. (1992) Rehabilitation of a fire damaged building, in *Evaluation and Rehabilitation of Concrete Structures and Innovations in Design* (Hong Kong, 1991), Special Publication SP-128, American Concrete Institute, Detroit, pp. 1457–72.
- Morgan, H.P. (1993) Combining sprinklers and vents: an interim approach. *Fire Surveyor*, **22** (2), 10–4.
- Morgan, H.P. and Gardner, J.P. (1991) *Design Principles for Smoke Ventilation in Enclosed Shopping Centres*, Report BR 186, BRE, Garston, England.
- Morris, B. and Jackman, L.A. (2003) An examination of fire spread in multi-storey building via glazed curtain wall façades. *Structural Engineer*, May 6, 22–6.

- Morris, W.A., Read, R.E.H. and Cooke, G.M.E. (1988) *Guidelines for the Construction of Fire-Resisting Structural Elements (Second Edition)* HMSO, London.
- Muenow, R.A. and Abrams, M.S. (1987) Non-destructive testing methods for evaluating damage and repair of concrete exposed to fire, in *Repair and Rehabilitation of Concrete Structures*, Publication SCM-16, American Concrete Institute, Detroit, pp. 284–95.
- Muirhead, J. (1993) Making it safely through construction. *Fire Surveyor*, **22** (1), 5–7.
- Mustapha, K.N. (1994) Modelling the effects of spalling on the failure modes of concrete columns in fire, PhD Thesis, University of Aston.
- Nadjai, A., Laverty, D. and O’Gara, M. (2001) Behaviour of compartment masonry walls in fire situations, in *Civil and Structural Engineering Computing, 2001* (ed. B.H.V. Topping), Saxe-Coburg Publications, pp. 407–31.
- Nassif, A.Y. (2000) A new classification system for fire-damaged concrete based on the strain energy dissipated in a hysteresis loop. *Magazine of Concrete Research*, **52**, 287–95.
- Nassif, A.Y., Burley, E. and Rigden, S. (1995) A new quantitative method of assessing fire damage to concrete structures. *Magazine of Concrete Research*, **47**, 271–8.
- Nassif, A.Y., Rigden, S. and Burley, E. (1999) The effects of rapid cooling by water quenching on the stiffness properties of fire-damaged concrete. *Magazine of Concrete Research*, **51**, 255–61.
- Nene, R.L. and Kavle, P.S. (1992) Rehabilitation of a fire damaged structure, in *Evaluation and Rehabilitation of Concrete Structures and Innovations in Design*, (Vol. 2), American Concrete Society Special Publication SP-128, Detroit, pp. 1195–211.
- Newman, G.M. (1992) *The Fire Resistance of Web-Filled Steel Columns*, Publication No 124, Steel Construction Institute, Ascot.
- Newman, G.M. (1993) *The Fire Resistance of Shelf Angle Floor Beams to BS 5950: Part 8*, Publication No 126, Steel Construction Institute, Ascot.
- Newman, G.M. and Lawson, R.M. (1991) *Fire Resistance of Composite Beams*, Technical Report SCI-P-109, Steel Construction Institute, Ascot.
- Newman, L.C., Dowling, J. and Simms, W.I. (2005) *Structural Fire Design: Off-site Applied Thin Film Intumescent Coatings (Second Edition)*, Publication P 160, SCI.
- Newman, G.M., Robinson, J.T. and Bailey, C.G. (2006) *Fire Safe Design: A New Approach to Multi-Storey Steel-Frame Buildings (Second Edition)*, Publication P 288, SCI.
- Nwosu, D.I., Kodur, V.K.R., Franssen, J.M. and Hum, J.K. (1999) *User Manual for SAFIR: A Computer Program for Analysis of Structures at*

- Elevated Temperature Conditions*, National Research Council Canada, int. Report 782.
- O'Connor, M.A., Kirby, B.R. and Martin, D.M. (2003) Behaviour of a multi-storey composite steel frame building in fire. *Structural Engineer*, **81** (2), 27–36.
- Ödeen, K. (1969) Fire resistance of glued laminated timber structures, in *Symposium No 3 Fire and Structural Use of Timber in Buildings* (London 1967), HMSO, London, pp. 7–15.
- Parker, T.W. and Nurse, R.W. (1956) *Investigations into Building Fires: Part 1 – The Estimation of the Maximum Temperatures attained in Building Fires from Examination of the Debris*, Technical Paper No 4, National Building Studies, HMSO, pp. 1–5.
- PD 7974-2 Application of fire safety engineering principles to the design of buildings – Part 2: Spread of smoke and toxic gases within and beyond the enclosure of origin (Sub-system 2).
- PD 7974-3 Application of fire safety engineering principles to the design of buildings – Part 3: Structural response and fire spread beyond the enclosure of origin (Sub-system 3).
- Persson, B. (2003) *Self-Compacting Concrete at Fire Temperatures*, Report TVMB-3110, Lund Institute of Technology, Lund University.
- Pettersson, O. and Witteveen, J. (1979/80) On the fire resistance of structural steel elements derived from standard fire tests or by calculation. *Fire Safety Journal*, **2**, 73–87.
- Pettersson, O., Magnusson, S.E. and Thor, J. (1976) *Fire Engineering Design of Steel Structures*, Publication No 50, Swedish Institute of Steel Construction.
- Phan, L.T. and Carino, N.J. (1998) Review of mechanical properties of HSC at elevated temperatures. *American Society of Civil Engineers, Journal of Materials in Civil Engineering*, **10** (1), 58–64.
- Phan, L.T., Lawson, J.R. and Davis, F.L. (2001) Effects of elevated temperature exposure on heating characteristics, spalling, and residual properties of high performance concrete. *Matériaux et Constructions*, **34**, 83–91.
- Philleo, R. (1958) Some physical properties of concrete at high temperatures. *Proceedings of the American Concrete Institute*, **54**, 857–64.
- Placido, F. (1980) Thermoluminescence test for fire-damaged concrete. *Magazine of Concrete Research*, **32**, 112–16.
- Plank, R.J., Burgess, I.W. and Bailey, C.G. (1997) Modelling the behaviour of steel-framed building structures by computer, in *Fire, Static and Dynamic Tests of Building Structures* (eds G.S.T. Armer and T. O'Dell), Proceedings of the Second Cardington Conference, Mar. 12–14, 1996, E&FN Spon.
- Plecnik, J.M., Plecnik, J.M., Fogerty, J.H. and Kurfees, J.R. (1986) Behavior of epoxy repaired beams under fire. *ASCE Journal of Structural Engineering*, **112** (4), 906–22.

- Plem, E. (1975) *Theoretical and experimental investigations of point set structure*, Document D9, Swedish Council for Building Research, Copenhagen.
- Poon, C.-S., Azhar, S., Anson, M. and Wong, Y.-L. (2001) Comparison of the strength and durability performance of normal- and high-strength pozzolanic concretes at elevated temperatures. *Cement and Concrete Research*, **31**, 1291–300.
- Pope, R. (2006) Lessons from Madrid. *New Steel Construction*, **14** (3), 26–8.
- Popovics, S. (1973) A numerical approach to the complete stress-strain curve of concrete. *Cement and Concrete Research*, **3**, 583–99.
- Proulx, G. (1994) Human response to fires. *Fire Research News*, (National Research Council, Canada), **71**, 1–3.
- Purkiss, J.A. (1972) A study of the behaviour of concrete heated to high temperatures under restraint or compressive loading. PhD Thesis, University of London, England.
- Purkiss, J.A. (1984) Steel fibre reinforced concrete at elevated temperature. *International Journal of Cement Composites and Lightweight Concrete*, **6**, 179–84.
- Purkiss, J.A. (1985) Some mechanical properties of glass fibre reinforced concrete at elevated temperatures, in *Composites – 3* (ed. I.H. Marshall), Elsevier Applied Science, London, pp. 230–41.
- Purkiss, J.A. (1987) Thermal expansion of steel fibre reinforced concrete up to 800°C, in *Composites – 4* (ed. I.H. Marshall), Elsevier Applied Science, London, pp. 404–15.
- Purkiss, J.A. (1988) A systems approach to fire safety engineering, in *Structural Safety Evaluation Based on System Identification Approaches* (eds H.G. Natke and J.T.P. Yao), F. Vieweg und Sohn Verlag mbH, Braunschweig, pp. 394–413.
- Purkiss, J.A. (1990a) Computer modelling of concrete structural elements exposed to fire, in *Interflam '90* (ed. C.A. Franks), Interscience Communications Ltd., London, pp. 67–75.
- Purkiss, J.A. (1990b) The decommissioning of fire damaged building structures, in *Decommissioning and Demolition* (ed. I.L. Whyte), Thomas Telford Ltd., pp. 68–72.
- Purkiss, J.A. (2000) High-strength concrete and fire. *Concrete*, **34** (3), 49–50.
- Purkiss, J.A. and Bali, A. (1988) *The transient behaviour of concrete at temperatures up to 800°C*, in Proceedings of the 10th Ibausil (Weimar 1988), Hochschule für Architektur und Bauwesen, Weimar, Section 2/1, pp. 234–9.
- Purkiss, J.A. and Mustapha, K.N. (1995) A study of the effect of spalling on the failure modes of concrete columns in a fire, in *Concrete 95, Toward Better Concrete Structures*, Concrete Institute of Australia and Fédération de la Précontrainte, Brisbane, pp. 263–72.
- Purkiss, J.A. and Mustapha, K.N. (1996) An investigation into the influence of concrete constitutive models on the behaviour of

- reinforced concrete columns exposed to fire. *Journal of the Institution of Engineers, Malaysia*, **57** (3), 23–32.
- Purkiss, J.A. and Weeks, N.J. (1987) A computer study of the behaviour of reinforced concrete columns in a fire. *Structural Engineer*, **65B**, 22–8.
- Purkiss, J.A., Claridge S.L. and Durkin P.S. (1989) Calibration of simple methods of calculating the fire resistance of flexural reinforced concrete members. *Fire Safety Journal*, **15**, 245–63.
- Purkiss, J.A., Morris, W.A. and Connolly, R.J. (1996) Fire resistance of reinforced concrete columns – correlation of analytical methods with observed experimental behaviour, in *Interflam 96* (eds C. Franks and S. Grayson), Interscience Communications, pp. 531–41.
- Purkiss, J.A., Maleki-Toyserkani, M. and Short, N.R. (2001) *Thermal and residual mechanical behaviour of SIFCON subjected to elevated temperatures*, 11th Concrete Communications Conference, BCA, pp. 357–66.
- Ramberg, W. and Osgood, W. (1943) *Description of Stress-Strain Curves by Three Parameters*, Technical Note TN902, National Advisory Committee on Aeronautics, United States of America.
- Rasbash, D.J. (1984/5) Criteria for acceptability for use with quantitative approaches to fire safety. *Fire Safety Journal*, **8**, 141–58.
- Read R.E.H. (ed.) (1991) *External Fire Spread: Building Separation and Boundary Distances*, BRE, Garston.
- Read, R.E.H. (1985) *Trade-Offs Between Sprinklers and Passive Fire Protection*, Personal communication.
- Read, R.E.H. and Morris W.A. (1993) *Aspects of Fire Precautions in Buildings (Third Edition)*, Department of the Environment, London.
- Redfern, B. (2005) Lack of fire stops blamed for speed of Madrid tower inferno. *New Civil Engineer*, Feb. 17, 5–7.
- Riley, M.A. (1991) Possible new method for the assessment of fire-damaged concrete. *Magazine of Concrete Research*, **43**, 87–92.
- Robbins, J. (1990) Baptism of fire. *New Civil Engineer*, July 12, 17–19.
- Robbins, J. (1991) Running repair. *New Civil Engineer*, Aug. 15, 17–18.
- Robbins, P.J. and Austen, S.A. (1992) Flexural testing of steel fibre reinforced refractory concrete at elevated temperatures, in *Fibre Reinforced Cement and Concrete* (ed. R.N. Swamy), E&FN Spon, 153–65.
- Robertson, A.F. and Gross, D. (1970) Fire load, fire severity, and fire endurance, in *Symposium on Fire Test Performance*, American Society of Testing and Materials, STP 464, pp. 3–29.
- Robinson, J.T. and Latham, D.J. (1986) Fire resistant steel design – the future challenge, in *Design of Structures against Fire* (eds R.D. Anchor, H.L. Malhotra and J.A. Purkiss), Elsevier Applied Science, London, pp. 225–36.
- Robinson, J.T. and Walker, H.B. (1987) Fire safe structural design. *Construction and Building Materials*, **1**, 40–50.

- Rogowski, B.F.W. (1969) Charring of timber in fire tests, in *Symposium No 3 Fire and Structural Use of Timber in Buildings* (London, 1967), HMSO, London, pp. 52–9.
- Rosato, C. (1992) London Underwriting Centre. *Fire Prevention*, **248**, 33–5.
- Rubert, A. and Schaumann, P. (1986) Structural steel and plane frame assemblies under fire action. *Fire Safety Journal*, **10**, 173–84.
- Saad, M., Abo-El-Enein, S.A., Hanna, G.B. and Kotkata, M.F. (1996) Effect of temperature on physical and mechanical properties of concrete containing silica fume. *Cement and Concrete Research*, **26** (5), 669–75.
- Sanad, A.M., Lamont, S., Usmani, A.S. and Rotter, J.M. (2000) Structural behaviour in fire compartment under different heating regimes – Part 1 (slab thermal gradients). *Fire Safety Journal*, **35**, 96–116.
- Sanad, A.M., Rotter, J.M., Usmani, A.S. and O'Connor, M.A. (1999) *Finite element modeling of fire tests on the Cardington composite building*, Proceedings of Interflam '99, Interscience Communications, London.
- Sano, C. (1961) Effect of temperature on the mechanical properties of wood, I – compression parallel to the grain. *Journal of the Japanese Wood Research Society*, **7**, 147–50.
- Schaffer, E.L. (1965) An approach to the mathematical prediction of temperature rise within a semi-infinite wood slab subjected to high temperature conditions. *Pyrodynamics*, **2**, 117–32.
- Schaffer, E.L. (1967) *Charring Rate of Selected Woods – Transverse to Grain*, FPL 69, US Department of Agriculture, Forest Service, Forest Products Laboratory, Madison, Wisconsin.
- Schleich, J.B. (1986) Numerical simulations, a more realistic fire safety approach in structural stability, in *New Technology to Reduce Fire Losses and Costs* (eds S.J. Grayson and D.A. Smith), Elsevier Applied Science, London, pp. 203–10.
- Schleich, J.B. (1987) Fire design of steel structures. *Steel Construction*, **3**, 20–1.
- Schneider, U. (1976) Behaviour of concrete under thermal steady state and non-steady state conditions. *Fire and Materials*, **1**, 103–15.
- Schneider, U. (1982) Creep effects under transient temperature conditions, in *Fundamental Research on Creep and Shrinkage of Concrete* (ed. F.H. Wittmann), Martinus Nijhoff, den Hag, pp. 193–202.
- Schneider, U. (1986a) *Properties of Materials at High Temperatures – Concrete (Second Edition)*, RILEM Report, Gesamthochschule Kassel, Germany.
- Schneider, U. (1986b) Modelling of concrete behaviour at high temperatures, in *Design of Structures against Fire* (eds R.D. Anchor, H.L. Malhotra and J.A. Purkiss), Elsevier Applied Science, London, pp. 53–70.
- Schneider, U. (1988) Concrete at high temperatures – a general review. *Fire Safety Journal*, **13**, 55–68.

- Schneider, U. and Nägele, E. (eds) (1989) *Repairability of Fire Damaged Structures*, CIB W14 Report Publication No 111, Gesamthochschule Kassel, Germany.
- SCI (1991) *Structural Fire Engineering: Investigation into the Broadgate Phase 8 Fire*. Steel Construction Institute, Ascot.
- SCI (2003) AD 269 – The use of intumescent coatings for the fire protection of beams with circular web openings. *New Steel Construction*, Nov./Dec., 33–4.
- Selvaggio, S.L. and Carlson, C.C. (1963) *Effects of Restraint on the Fire Resistance of Prestressed Concrete*, PCA Research Bulletin No 164, Portland Cement Association, Illinois.
- Shields, T.J. (1993) *Fire and Disabled People in Buildings*, Report BR 231, BRE, Garston.
- Short, N.R. and Purkiss, J.A. (2004) Petrographic analysis of fire-damaged concrete, in *Fire Design of Concrete Structures: What Now? What Next?* (eds P.G. Gambarova, R. Felicetti, A. Meda and P. Riva), Politecnico di Milano, Dec. 2–3, 2004, Starrylink Editrice, pp. 221–30.
- Short, N.R., Purkiss, J.A. and Guise, S.E. (2000) *Assessment of fire damaged concrete*, 10th Concrete Communications Conference, Birmingham, BCA, pp. 245–54.
- Short, N.R., Purkiss, J.A. and Guise, S.E. (2001) Assessment of fire damaged concrete using colour image analysis. *Construction and Building Materials*, **15**, 9–15.
- Short, N.R., Purkiss, J.A. and Guise, S.E. (2002) Assessment of fire damaged concrete using crack density measurements. *Structural Concrete*, **3** (3), 137–43.
- Shorter, G.W. and Harmathy, T. (1965) Moisture clog spalling. *Proceedings of the Institution of Civil Engineers*, **20**, 75–90.
- Simms, W.I. and Newman, G.M. (2002) *Single Storey Steel Frame Buildings in Fire Boundary Conditions*, Publication P313, SCI.
- Smith, L.M. and Placido, F. (1983) Thermoluminescence: a comparison with the residual strength of various concretes, in *Fire Safety of Concrete Structures* (ed. M.S. Abrams), Publication SP-80, American Concrete Institute, Detroit, pp. 293–304.
- Smith, C.I., Kirby, B.R., Lapwood, D.G., Cole, K.J., Cunningham, A.P. and Preston, R.R. (1981) The reinstatement of fire damaged steel framed structures. *Fire Safety Journal*, **4**, 21–62.
- Sterner, E. and Wickström, U. (1990) *TASEF – Temperature Analysis of Structures Exposed to Fire*, SP Report 1990:05, Swedish National Testing and Research Institute, Borås.
- Stiller, J. (1983) Berechnungsmethode für brandbeanspruchte Holzstützen und Holzbalken aus brett-schichtverleimtem Nadelholz, in *Arbeitsbericht 1981-1983*, SFB 148 Brandverhalten von Bauteilen, Technische Universität Braunschweig, pp. 219–76.

- Stirland, C. (1980) *Steel Properties at Elevated Temperatures for Use in Fire Engineering Calculations*, Report No T/RS/11/80C, Teesside Laboratory, British Steel Technical, Middlesborough.
- Stirland, C. (1981) *Sprinklers and the Building Regulations: the Case for Trade-offs*, Report T/RS/1189/22/81/C, Teesside Laboratory, British Steel Technical, Middlesborough.
- Sullivan, P.J.E., Terro, M.J. and Morris, W.A. (1993/4) Critical review of fire-dedicated thermal and structural computer programs. *Applied Fire Science*, **3**, 113–35.
- Tenchev, R. and Purnell, P. (2005) An application of a damage constitutive model to concrete at high temperature and prediction of spalling. *International Journal of Solids and Structures*, (42), 6550–65.
- Tenchev, R.T., Li, L.Y. and Purkiss, J.A. (2001a) *Numerical analysis of temperature and pore pressure in intensely heated concrete*, in Proceedings 9th Annual ACME Conference (ed. A.H.C. Chan), Birmingham University, Apr. 8–10, pp. 5–8.
- Tenchev, R.T., Li, L.Y. and Purkiss, J.A. (2001b) Finite element analysis of heat and moisture transfer in concrete subject to fire. *Numerical Heat Transfer*, (39), 685–710.
- Tenchev, R.T., Purkiss, J.A. and Li, L.Y. (2001) *Numerical analysis of thermal spalling in a concrete column*, in Proceedings 9th National Congress on Theoretical and Applied Mechanics (eds Y.A. Ivanov, A. Baltov and E. Manoach), Varna Sept. 19–22, Bulgarian Academy of Science, Vol. 1, pp. 604–9.
- Tenchev, R.T., Li, L.Y., Purkiss, J.A. and Khalafallah, B.H. (2001) Finite element analysis of coupled heat and moisture transfer in concrete when it is in fire. *Magazine of Concrete Research*, (53), 117–25.
- Tenning, K. (1969) Glued laminated timber beams: fire tests and experience in practice, in *Symposium No 3 Fire and Structural Use of Timber in Buildings* (London, 1967), HMSO, London, pp. 1–6.
- Terro, M.J. (1998) Numerical modeling of the behavior of concrete structures in fire. *ACI Structural Journal*, **95** (2), 183–93.
- Thelandersson, S. (1982) On the multiaxial behaviour of concrete exposed to high temperature. *Nuclear Engineering and Design*, **75**, 271–82.
- Thomas, F.G. and Webster, C.T. (1953) *Fire resistance of reinforced concrete columns*. National Building Studies Research Paper No 18, HMSO, London.
- Thomas, P.H. (ed.) (1986) Design guide – structural fire safety (CIB W14 Workshop). *Fire Safety Journal*, **10**, 75–154.
- Thomas, P.H. and Heselden, A.J.M. (1972) *Fully Developed Fires in Single Compartments* (CIB Report 20), Joint Fire Research Organization Fire Research Note 923, HMSO.

- Tomacek, D.V. and Milke, J.A. (1993) A study on the effect of partial loss of protection on the fire resistance of steel columns. *Fire Technology*, **29**, 3–21.
- Touloukian, Y.S. and Ho, C.Y. (eds) (1973) *Properties of Aluminum and Aluminum Alloys*, TPRC Report 21, Thermophysical Properties Research Center, Purdue University.
- Türker, P., Erdoğan, K. and Erdoğan, B. (2001) *Investigation of fire-damaged concrete with different types of aggregate*, in Proceedings of the 23rd International Conference on Cement Microscopy, Albuquerque, April 29–May 4, International Cement Microscopy Association, pp. 193–212.
- Twilt, L. and Witteveen, J. (1986) Calculation methods for fire engineering design of steel and composite structures, in *Design of Structures against Fire* (eds R.D. Anchor, H.L. Malhotra and J.A. Purkiss), Elsevier Applied Science, London, pp. 155–76.
- van Acker, A.V. (2003/4) Shear resistance of prestressed hollow core floors exposed to fire. *Structural Concrete, Journal of the fib*, **2**, June 2003.
- Varley, N. and Both, C. (1999) Fire protection of concrete linings in tunnels. *Concrete*, May, 27–30.
- Vekey de, R. (2004) *Structural Fire Engineering Design: Materials Behaviour-Masonry*, Digest 487 Part 3, BRE.
- Wainman, D.E. and Kirby, B.R. (1988) *Compendium of UK Standard Fire Test Data – Unprotected Structural Steelwork – 1*, Report No RS/RSC/S10328/1/87/B, British Steel Technical, Swinden Laboratories, Rotherham.
- Wainman, D.E. and Kirby, B.R. (1989) *Compendium of UK Standard Fire Test Data – Unprotected Structural Steelwork – 2*, Report No RS/R/S1198/8/88/B, British Steel Technical, Swinden Laboratories, Rotherham.
- Wang, Y.C. (2000) A simple method for calculating the fire resistance of concrete-filled CHS columns. *Journal of Constructional Steel Research*, (54), 365–86.
- Wardle, T.M. (1966) *Fire Resistance of Heavy Timber Construction*, Information Series No 53, New Zealand Forest Service, Wellington.
- Welch, S. (2000) *Developing a model for thermal performance of masonry exposed to fire*, First International workshop 'Structures in fire' Copenhagen, June 19–20, 117–34.
- Welch, S. (2004) *Structural Fire Engineering Design: Fire and Thermal Response*, Digest 488 Part 1, BRE.
- White, R.H. and Schaffer, E.L. (1978) Application of CMA program to wood charring. *Fire Technology*, **4**, 279–90 and 296.
- Wickström, U. (1981/2) Temperature calculation of insulated steel columns exposed to natural fire. *Fire Safety Journal*, **4**, 219–25.

- Wickström, U. (1985a) Application of the standard fire curve for expressing natural fires for design purposes, in *Fire Safety: Science and Engineering* (ed. T.Z. Harmathy), STP 882, American Society of Testing and Materials, pp. 145–59.
- Wickström, U. (1985b) Temperature analysis of heavily-insulated steel structures exposed to fire. *Fire Safety Journal*, **9**, 281–85.
- Wickström, U. (1986) A very simple method for estimating temperatures in fire exposed structures, in *New Technology to Reduce Fire Losses and Costs* (eds S.J. Grayson and D.A. Smith), Elsevier Applied Science, London, pp. 186–94.
- Williams-Lier, G. (1973) Analytical equivalents of standard fire temperature curves. *Fire Technology*, **9**, 132–36.
- Witteveen, J. (1983) Trends in design methods for structural fire safety, in *Three Decades of Structural Fire Safety* (Boreham Wood, 1983), BRE, Garston, pp. 21–30.
- Witteveen, J. and Twilt, L. (1981/2) A critical review on the results of standard fire resistance tests on steel columns. *Fire Safety Journal*, **4**, 259–70.
- Wong, P. (2003) Performance of GRP composite structures at ambient and elevated temperatures. *Structural Engineer*, **81** (15), 10 and 12.
- Xu, Y., Wong, Y.L., Poon, C.S. and Anson, M. (2001) Impact of high temperatures on PFA concrete. *Cement and Concrete Research*, **31**, 1065–73.
- Yin, J., Zha, X.X. and Li, L.Y. (2006) Fire resistance of axially loaded concrete filled steel tube columns. *Journal of Construction Steel Research*, **62** (7), 723–9.
- Zacharia, T. and Aidun, D.K. (1988) Elevated temperature mechanical properties of Al-Li-Cu-Mg Alloy. *Welding Journal*, **67**, 281–8.
- Zienkiewicz, O.C. and Taylor, R.L. (2000) *The Finite Element Method (Fifth Edition)*, Butterworth Heinemann, Oxford.

**This page intentionally left blank**

## Author index

---

- Abo-el-Enein, S.A., 338  
Abrams, M.S., 98, 335–337  
Abu-Tair, A., 201  
Agarwal, S., 330  
Ahmed, A.E., 341–343  
Ahmed, G.N., 165  
Aidun, D.K., 119  
Aldea, C.-M., 31, 198  
Ali, F.A., 201  
Ali, H.M., 163, 164  
Allen, B., 248  
Al-Shaikh, A.H., 341–343  
Apert, R.L., 163, 164  
Anchor, R.D., 93, 94, 340  
Anderberg, Y., 78, 93, 95–97,  
101–105, 121, 125, 126, 129,  
132–134, 137, 139–141, 174, 176,  
189, 196  
Anson, M., 336, 338  
Arafat, T.I., 341  
Ashton, L.A., 33, 35  
Austen, S.A., 113  
Ave, T., 99  
Azhar, S., 336, 338
- Babrauskas, V., 26  
Baddoo, N.R., 247  
Bahnasawy, H.H., 339  
Bahrends, J.F.B., 33  
Bailey, C.J., 201, 276, 304, 306, 308,  
311, 316, 327, 348  
Baker, G., 129, 136, 137  
Baldwin, R., 24, 99
- Bali, A., 101, 102, 134, 139  
Bardhan-Roy, B.K., 197  
Barnfield, J.R., 249, 341  
Bate, S.C.C., 35  
Bayley, M.J., 117, 118, 301  
Bažant, Z.P., 138  
Becker, J., 40, 146, 158  
Beitel, J.J., 36, 326  
Benedetti, A., 328  
Bessey, G.E., 341–343  
Bishop, G.R., 301  
Bishop, P., 12  
Bizri, H., 40, 146  
Boam, K., 344  
Bobrowski, J., 197  
Boström, L., 201  
Both, C., 30  
Branco, F.A., 334  
Bregulla, J., 348  
Bresler, B., 40, 146, 153, 158, 159  
Buchanan, A.H., 51  
Burgan, B.A., 247  
Burgess, I.W., 123, 159, 304, 311  
Burley, E., 330, 337  
Butterworth, N., 11, 25, 65  
Byrd, T., 12  
Byrom, T.G., 152
- Canter, D., 5  
Carino, N.J., 106  
Carlson, C.C., 33, 34  
Castillo, C., 107, 109  
Castle, G.K., 37

- Chan, Y.N., 336  
 Chana, P., 306  
 Chapman, B.P., 101  
 Chen, B., 339  
 Chen, S.-T., 336  
 Chitty, R., 146, 215, 348  
 Claridge, S.L., 19  
 Clayton, N., 110, 201  
 Cockcroft, D., 12  
 Cole, K.J., 343  
 Colina, H., 109  
 Connolly, R.J., 31, 198, 200  
 Conserva, M., 89, 119  
 Cooke, G.M.E., 33, 40, 94, 253, 265,  
     299, 303, 304, 340  
 Cox, G., 146, 215  
 Crook, R.N., 93, 94, 340  
 Cropper, D., 344  
 Cruz, C.R., 98, 99  
 Cunningham, A.P., 343
- Davis, F.L., 337  
 Day, T., 9  
 de Brito, J., 334  
 de Vekey, R., 298, 348  
 Diederichs, U., 129, 134, 140  
 Dixon, R., 344  
 Donizelli, G., 89, 119  
 Dorn, J.E., 124  
 Dorn, T., 158  
 dos Santos, J.R., 334  
 Dotreppe, J.-C., 31, 36, 198  
 Dougill, J.W., 35  
 Dounas, S., 122, 123  
 Dowling, J., 3, 11  
 Doyle, N., 12  
 Drysdale, D., 45, 47, 146  
 Durani, A.J., 107, 109  
 Durkin, P.S., 19  
 Dusenberry, D.O., 11
- Ehm, H., 33, 40  
 El-Ausi, M.A., 112  
 El-Refal, F.E., 339
- El-Rimawi, J.A., 123  
 English, C., 11, 25, 65  
 Enjily, V., 306, 348  
 Erdoğan, B., 341  
 Erdoğan, K., 341
- Fackler, J.P., 28  
 Fairyadh, F.I., 112  
 Fardell, P.J., 146, 215  
 Felicetti, R., 106, 341  
 Fellingner, J.H.H., 197  
 Fields, B.A., 125  
 Fields, R.J., 125  
 Fisher, K., 298  
 Foggerty, J.H., 344  
 Forsén, N.E., 158, 167  
 Foster, D., 298  
 Fowler, D., 12  
 Franssen, J.-M., 31, 36, 153,  
     159, 198  
 Fraser-Mitchell, J., 348  
 Fredlund, B., 115  
 Fu, Y.F., 107  
 Fujita, K., 58  
 Furamura, F., 99, 100
- Gambarova, P.G., 106  
 Gardner, J.P., 7, 8  
 Gerhards, C.C., 115, 116, 289  
 Gillen, M.P., 107  
 Gnanakrishnan, N., 117, 118,  
     300, 341  
 Golrang, B., 122, 123  
 Gowripalan, N., 338  
 Grainger, B.N., 105, 135  
 Guise, S.E., 101, 330–332, 339, 341  
 Gustaferro, A.H., 33, 34
- Hadvig, S., 114, 279  
 Haksever, A., 129  
 Hammad, A.-H.M., 117, 119  
 Handoo, S.K., 330  
 Hanna, G.B., 338  
 Hansell, G.O., 8, 9

- Harmathy, T.Z., 37, 44, 65, 70, 72, 87, 92, 93, 198
- Harris, J.R., 11
- Harrison, R., 9
- Hassen, S., 109
- Henke, V., 19
- Hertz, K., 86, 127, 128, 141, 170–176, 182, 184, 189, 191, 196, 201
- Heselden, A.J.M., 9, 58–60
- Hinkley, P.L., 9
- Ho, C.Y., 89
- Holmes, M., 93, 94, 340
- Hopkinson, J.S., 3
- Hosser, D., 158
- Huang, Z., 159, 311
- Huebner, K.H., 152
- Hughes, B.P., 101
- Hughes, T.R.J., 153
- Hum, J.K., 159
- Hurst, J.P., 165
- Hwang, T.-Z., 336
- Iding, R.H., 146, 153, 159
- Illingworth, P.M., 9
- Ingberg, S.H., 61
- Issen, L.A., 33, 34
- Iwankiw, N.R., 36, 326
- Izzuddin, B.A., 308
- Jackman, L.A., 10
- Jansson, R., 201
- Kamal, M.M., 339
- Kavle, P.S., 329, 344
- Kawagoe, K., 45
- Kay, T.R., 50
- Kersken-Bradley, M., 23, 281
- Khalafallah, B.H., 198–200
- Khennane, A., 129, 136, 137
- Khoury, G.A., 105, 135, 140
- Kim, W.J., 99
- Kirby, B.R., 11, 24, 25, 45, 50, 65, 97, 210, 213, 220, 243, 246, 247, 308, 311, 335, 336, 339, 341, 343
- Kodur, V.K.R., 110–112, 159, 276
- Kordina, K., 19, 324
- Kotkata, M.F., 338
- Krampf, L., 197, 324
- Kruppa, J., 251
- Kurfees, J.R., 344
- Lamont, S., 311
- Lapwood, D.G., 343
- Lapwood, D.J., 335, 336, 339, 341
- Latham, D.J., 33, 35, 45, 220, 221, 303, 304
- Lavery, D., 299, 300
- Law, M., 59, 60, 62, 63, 77, 241
- Lawrence, S.J., 300, 341
- Lawson, J.R., 337
- Lawson, R.M., 33, 210, 253, 265, 266, 304, 305
- Lawther, D., 300
- Lawther, R., 117, 118
- Lennon, T., 110, 197, 201, 304, 308, 348
- Leston-Jones, L.C., 304
- Li, L.-Y., 134, 140, 141, 155, 160–163, 165, 166, 168, 199
- Lie, T.T., 21, 54, 55, 73, 75, 76, 110–112, 276, 288–291, 336
- Lin, C.-H., 336
- Lin, T.D., 336
- Liu, J., 339
- Magnusson, S.E., 46, 48–55, 79, 81
- Maiti, S.C., 330
- Maleki-Toyserkani, M., 113, 339
- Malhotra, H.L., 1, 10, 12, 26, 36, 79–81, 87, 88, 91, 98, 198, 206, 210, 212, 287, 326, 336, 337
- Maréchal, J.-C., 98, 99
- Marshall, N.R., 8, 9
- Martin, D.M., 308, 311
- Martin, L.H., 265, 315

- Mehaffey, J.R., 65, 70, 72  
 Melinek, S.J., 206, 208, 209, 218  
 Meyer-Ottens, C., 198, 294  
 Milke, J.A., 252  
 Mlakar, P.F., 11  
 Montgomery, F.R., 333  
 Mooney, J., 146  
 Moore, D.B., 308, 311  
 Morales, E.M., 344  
 Morgan, H.P., 7–9  
 Morgan, P.B.E., 299  
 Morris, B., 10  
 Morris, W.A., 5, 31, 40, 146, 160,  
     198, 215  
 Muenow, R.A., 335  
 Muirhead, J., 12  
 Mustapha, K.N., 129, 130, 143, 198  
  
 Nadjai, A., 299, 300  
 Nägele, E., 343  
 Nasr, M.A., 117  
 Nassif, A.Y., 330, 337  
 Nene, R.L., 329, 344  
 Newman, G.M., 11, 25, 65, 210,  
     241, 253, 265, 266, 277, 304, 308,  
     311, 316  
 Nizamuddin, Z., 146, 153, 159  
 North, M.A., 99  
 Nurse, R.W., 324, 325  
 Nwosu, D.I., 159  
  
 O'Brien, T., 241  
 O'Connor, D.J., 201, 300  
 O'Connor, M.A., 160, 308, 311  
 Ödeen, K., 115, 286, 287  
 O'Gara, M., 300  
 Oh, C.H., 99  
 Osgood, W., 123  
  
 Pagan, J., 11, 25, 65  
 Parker, T.W., 324, 325  
 Peacock, B.N., 50  
 Peng, G.F., 336  
 Persson, B., 109, 110, 201, 338  
  
 Pettersson, O., 46, 48–55, 79,  
     81, 222  
 Phan, L.T., 11, 106, 337  
 Philleo, R., 98, 99  
 Placido, F., 329, 330  
 Plank, R.J., 123, 304, 311  
 Plecnik, Joseph M., 344  
 Plecnik, John M., 344  
 Plem, E., 125  
 Poon, C.S., 107, 336, 338  
 Pope, R., 3, 12  
 Popovics, S., 100, 138, 140  
 Porter, A.M., 341  
 Preston, R.R., 97, 343  
 Price, W., 306  
 Proulx, G., 5, 6  
 Purkiss, J.A., 19, 23, 31, 101, 102,  
     107, 111, 113, 129, 130, 134,  
     139–141, 143, 155, 157, 160, 165,  
     166, 168, 198, 199, 265, 315, 328,  
     330–332, 336, 337, 339, 341, 346  
 Purnell, P., 198, 199, 307  
  
 Ramadan, K.K., 117, 119  
 Ramberg, W., 123  
 Rasbash, D.J., 18  
 Read, R.E.H., 5, 10, 11, 40  
 Redfern, B., 3  
 Richter, E., 158  
 Rigden, S., 330, 337  
 Riley, M.A., 330  
 Robbins, J., 1, 12  
 Robbins, P.J., 113  
 Robertson, A.F., 61  
 Robinson, J.T., 35, 220, 221, 303,  
     308, 311  
 Rogowski, B.F.W., 115  
 Rosato, C., 12  
 Rotter, J.M., 160, 311  
 Rowe, T.J., 336  
  
 Saad, M., 338  
 Sanad, A.M., 160, 311  
 Sano, C., 117

- Schaffer, E.L., 88, 89, 114, 115, 154  
 Schleich, J.B., 158  
 Schneider, U., 78, 82–86, 98, 99,  
 101–103, 106, 107, 109, 129,  
 138–140, 343  
 Selvaggio, S.L., 33, 34  
 Senseny, P.E., 163, 164  
 Sheard, P.A., 301  
 Shields, T.J., 5  
 Short, N.R., 113, 330–332, 339, 341  
 Shorter, G.W., 198  
 Simms, W.I., 304, 316  
 Smith, C.I., 343  
 Smith, L.M., 330  
 Sozen, M.A., 11  
 Stanzak, W.W., 92, 93  
 Sterner, E., 153  
 Stiller, J., 286, 291–293  
 Stirland, C., 8, 9, 24, 79  
 Sullivan, P.J.E., 105, 135, 160
- Tang, C.A., 107  
 Taylor, P., 344  
 Taylor, R.L., 152  
 Tenchev, R.T., 165, 198, 199, 307  
 Tenning, K., 115  
 Terro, M.J., 135, 160  
 Thelandersson, S., 101–105, 113,  
 121, 129, 132–134, 137, 139, 140  
 Thomas, F.G., 35  
 Thomas, P.H., 24, 58, 60, 63, 206,  
 208, 209, 218  
 Thompson, G., 45, 335, 336,  
 339, 341  
 Thor, J., 46, 48–55, 79, 81  
 Thornton, E.A., 152  
 Tomacek, D.V., 252  
 Tomlinson, L.H., 50
- Touloukian, Y.S., 89  
 Trippodo, R., 89, 119  
 Türker, P., 341  
 Twilt, L., 36, 209
- Usmani, A.S., 160, 311
- van Acker, A., 197  
 Vanderzeypen, Y., 36  
 Varley, N., 30  
 von Postel, R., 33
- Wainman, D.E., 50, 210, 213, 220,  
 243, 246, 247  
 Walker, H.B., 35, 220  
 Wang, Y.C., 276  
 Wardle, T.M., 115  
 Webster, C.T., 35  
 Weeks, N.J., 157  
 Welch, S., 87, 348  
 White, R.H., 89  
 Wickström, U., 55, 86, 153, 170,  
 173–175, 183, 206, 207, 209, 216,  
 218  
 Williams-Leir, G., 28  
 Williamson, R.B., 26  
 Witteveen, J., 20, 36, 209, 222  
 Wong, P., 301  
 Wong, Y.-L., 107, 336, 338
- Xu, Y., 338
- Yin, J., 161–163
- Zacharia, T., 119  
 Zha, X.X., 161–163  
 Zienkiewicz, O.C., 152

**This page intentionally left blank**

# Subject index

---

- Aluminium
  - density, 89
  - Elastic modulus, 120
  - fire protection, 300
  - specific heat, 89
  - strength data, 117, 120
  - thermal conductivity, 89
  - thermal expansion, 119
- Assessment models
  - general, 20
  - level 1, 20
  - level 2, 21
  - level 3, 21
- Beams, steel
  - structural fire load, 220
  - utilization ratio, 230
- Bond behaviour, 106, 197
- Cardington Test Facility, 305, 347
- Cast iron, residual behaviour, 340
- Charring rate
  - natural fires, 279
  - standard furnace exposure, 114, 279
- Colour changes (concrete), 343
- Colour image analysis, 341
- Columns
  - composite, 275
  - concrete, 191
  - steel, 223, 235
  - timber, 284, 289, 292
  - web infilled, 277
- Compartment temperature–time response
  - assumptions in behaviour, 47
  - calculation of, 47
  - compartment construction, 51
  - heat flow terms, 47
  - horizontal openings, 50
  - multiple vertical openings, 50
  - solution, 48
- Compartmentation, 9
- Composite beams
  - load ratio, 267
  - moment capacity, 267
  - shear stud strength, 270
- Composite columns, 275, 277
- Composite slabs
  - effective thickness, 254
  - insulation, 253
  - membrane action, 311
  - moment capacity, 256
- Compression members, 223, 226
- Computer techniques
  - structural, 158, 311
  - thermal, 143
- Concrete
  - bond, 196, 197
  - classical creep behaviour, 101, 133
  - constitutive models, 132
  - continuity, 33
  - density, 82
  - design stress–strain curves, 140
  - detailing, importance of, 201

Concrete (*continued*)

- fibres concretes, 110, 339
- flexural capacity, 176
  - 500°C isotherm, 176
  - zone method, 180
- frame behaviour, 306
- high strength concrete, 106, 201, 337
- instantaneous stress–strain behaviour, 99, 112, 132, 136, 140
- multi-axial behaviour, 113
- prescriptive approach to fire resistance, 39
- residual strength, 336 *et seq*
- self-compacting concrete, 109, 201, 338
- shear, 197
- spalling, 31, 198 *et seq*, 307, 326
- specific heat, 82
- strength reduction factors
  - fibres concretes, 112, 339
  - high performance concrete, 108, 337
  - normal concrete, 141, 337
  - self-compacting concrete, 109, 338
- temperature calculations, 147, 165, 169
- tensile strength, 106
- thermal conductivity
  - fibres concrete, 110
  - non-fibre concrete, 84
- thermal diffusivity
  - fibres concretes, 113
  - normal concrete, 86, 173
- thermal expansion
  - fibres concretes, 110, 113
  - non-fibre concretes, 111
- transient creep behaviour, 104, 109, 129, 133 *et seq*, 155, 160
- LITS, 135

- unit stress compliance function, 138

Connections,  
design, 250

- moment transfer of, 304

Constitutive stress–strain laws

- basic principles, 119
- concrete
  - Anderberg and Thelandersson, 132
  - Deiderichs, 134
  - general principles, 130
  - Khennane and Baker, 136
  - Khoury and Terro, 135
  - Li and Purkiss, 140
  - Schneider, 138
- steel, 121

Continuity (concrete), 33, 40

Creep

- concrete (classical), 103
- concrete (transient), 104, 109
- steel (anisothermal), 97
- steel (isothermal), 96, 124

Critical (limiting) temperature of steelwork, 229, 267

Deformation limits (fire test), 31

Demolition of structures, 345

Density

- aluminium, 89
- concrete, 82
- insulation, 208, 210, 212
- masonry, 87
- steel, 79

Detailing of reinforced concrete, 201

Dynamic modulus (concrete), 98, 110

Elastic (Static) modulus

- aluminium, 120
- concrete, 97, 108, 109, 110, 338, 339
- timber, 116

- Element temperatures
  - composite beams, 267
  - composite slabs, 256, 259
  - concrete, 143 *et seq*, 169 *et seq*
  - determination of, 143
  - fire damage, 341
  - shelf angle floors, 242
  - steel, 143 *et seq*
  - timber, 154
- Emissivity
  - configuration (shadow) factor, 146, 204, 269
  - flame (or furnace), 146, 204
  - resultant, 146, 204
  - surface (material), 146, 204
- Equivalent fire duration, 21, 62 *et seq*
- Explosive spalling, 198, 307
- External steelwork, 241
  
- Fire characteristics
  - estimation of, 57
  - maximum temperature, 59
  - rate of burning, 58, 60
- Fire damage, 326
- Fire design criteria, 22
- Fire detection, 6
- Fire-fighting systems, 8
- Fire (fuel) load, calculation of, 51
- Fire, localized, 77
- Fire, natural or real, 43
- Fire, parametric, 43
- Fire resistance (performance)
  - composite, 253 *et seq*
  - concrete, 39, 168 *et seq*
  - masonry, 41, 297
  - prescriptive determination, 37
  - steelwork, 40, 204 *et seq*
  - tests on frames, 304 *et seq*
  - timber, 41, 278 *et seq*
- Fire safety engineering
  - definition, 1
  - design concerns, 2
  - design philosophies, 14
- Fire safety management, 4
- Fire severity, 61, 324
- Fire spread, 10
- Fire testing, 27
  - deformation limits, 31
- Flexural capacity, calculation of
  - composite beams, 267
  - composite slabs, 256
  - reinforced concrete
    - reduced section, 176
    - zone method, 180
  - steelwork, 224, 242
  - timber beams, 281, 292
- Frames, high temperature
  - performance
    - composite, 308
    - concrete, 306
    - portal, 316
    - timber, 305
- Fuel controlled fire, 45
  
- Glass, 10, 302
  
- Heat flow in steelwork
  - effective density of
    - insulation, 208
  - insulated, 206
  - moisture effect, 208
  - time shift, 207
  - uninsulated, 205
- Heat transfer
  - basic equations for
    - steelwork, 203
  - computer packages, 153
  - convergence, 153
  - Crank–Nicolson method, 153
  - Dirichlet boundary, 145
  - explicit algorithm, 153
  - finite element, 147, 150, 151
  - finite element (matrix)
    - formulation, 147
  - Fourier equation, 78
  - Galerkin method, 153
  - Gauss's theorem, 148

- Heat transfer (*continued*)
  - implicit algorithm, 153
  - interpolation function, 148
  - Neumann boundary, 145
  - Newton–Raphson, 152, 153
  - thermal analysis, 143
- Heat transfer co-efficients
  - configuration (shadow) factor, 146, 204, 269
  - convection, 144, 204
  - effective (net or total), 144, 204
  - insulation, 204
  - radiation, 144, 204
- High strength (performance)
  - concrete, 106, 201, 307, 337
- Insulation
  - ageing of, 251
  - calculation of requirements, 209, 222
  - manufacturer's data, 249
  - partial loss of, 252
  - thermal properties, 210
  - types of, 247
- Limit state
  - serviceability, 14
  - ultimate, 14
- Limit state design
  - ambient, 14
  - fire, 16
- Limit states of
  - insulation, 18, 30
  - integrity, 17, 30
  - load-bearing capacity, 17, 30
- Limiting (critical) temperature of
  - steelwork, 230
- Load ratio (utilization factor), 230, 267
- Localized fires
  - 5 MW, 77
  - Plume, 77
- Masonry
  - cavity wall behaviour, 299
  - density, 87
  - insulation, 297
  - prescriptive approach, 41
  - residual strength, 341
  - specific heat, 87
  - thermal bowing, 298
  - thermal conductivity, 87
  - thermal expansion, 117
- Materials testing, 90, 327
- Means of escape, 4
- Membrane action, 311
- National Annexes, 19
- Natural or compartment fires, 43
  - decay, 45
  - factors affecting growth, 45
  - post-flashover period, 44
  - pre-flashover period, 43
- Opening (ventilation) factor, 48, 50, 54, 56, 280
- Parametric fire, 43
- Parametric temperature–time
  - curves, 29, 53
- Partial safety factors
  - determination of, 18
  - general, 15
  - loading
    - concrete, 176
    - general, 175
    - steel, 220
  - materials
    - concrete, 176
    - steel, 223
    - timber, 281
- Plastics, 301
- Probability of failure, 16, 18
- Provisions for fire safety
  - active, 13
  - passive, 13

- Regulatory control, 11, 23
- Repairability, 343
- Residual section, determination of, 281, 292
- Residual strength assessment
  - methods
  - concrete
    - cores, 327
    - DTA, TGA, 330
    - fire behaviour test, 334
    - hammer and chisel, 335
    - petrographic analysis, 330
    - pull out test, 329
    - Schmidt hammer, 328
    - Stiffness damage test, 330
    - Surface permeability, 333
    - thermoluminescence test, 329
    - ultrasonic pulse velocity, 328
    - Windsor probe, 329
  - steel
    - Brinell hardness, 335
    - direct testing, 335
- Residual strengths, 336
- Restraint or continuity, effect of, 33, 304
- Section factor ( $A/V$ ), 205, 210, 267
- Self-compacting concrete, 109, 201, 338
- Serviceability limit state, 15
- Shear
  - concrete, 197
  - connections, 327
- Shear studs (composite construction), 270, 327
- Shelf angle floors, 241
- Sloughing (spalling), 198
- Smoke control, 7
- Spalling of concrete, 198, 324, 326
- Specific heat
  - aluminium, 89
  - concrete, 82
  - insulation, 212
  - masonry, 87
  - steel, 79
  - timber, 89
- Stability of fire-damaged structures, 323
- Standard fire gradings, 23, 24
- Standard fire (furnace) test, 26
  - deformation (deflection) control, 31
  - drawbacks, 32
  - failure criteria, 30, 35
  - furnace design and characteristics, 37
  - general, 27
  - reasons for carrying out, 31
- Standard temperature–time curve
  - cellulosic, 28
  - external, 30
  - hydrocarbon, 30
- Steel
  - anisothermal creep behaviour, 96
  - creep strain component, 124 *et seq*
  - critical (limiting) temperature, 229
  - density, 79
  - design stress–strain curves, 127
  - elastic strain component, 121 *et seq*
  - external members, 241
  - isothermal creep behaviour, 96
  - isothermal strength data, 92
  - portal frames, 316
  - prescriptive approach to design, 40
  - residual properties, 339
  - section factor ( $A/V$ ), 205, 210, 267
  - shelf angle floors, 241
  - specific heat, 79
  - strength capacity (flexure), 224

- Steel (*continued*)
  - strength loss data for
    - reinforcement, 94, 176
  - temperature calculations, 143, 203, 267
  - thermal conductivity, 80
  - thermal diffusivity, 81
  - thermal expansion, 93
  - total strain, 121
  - utilization factor, 230
- Steel fibre concrete, 110
- Strength assessment, 335
- Strength loss data
  - aluminium, 117
  - concrete, 141, 180
  - steel (reinforcement), 94, 176
  - steel (structural), 92,
  - timber, 115
- Stress–strain curves for design
  - concrete, 140
  - steel, 127
- Stress–strain experimental data
  - concrete, 100, 112
  - steel (isothermal), 92
- Stress–strain models
  - concrete
    - Anderberg and Thelandersson, 132
    - Diederich, 134
    - Khoury and Terro, 135
    - Khennane and Baker, 136
    - Li and Purkiss, 140
    - Schneider, 138
  - steel, 121
- Structural fire actions,
  - determination of, 19
- Structural response, calculation of
  - Bernoulli beams, 155, 157
  - finite element, 158, 160, 163
  - quasi-static analysis, 154
  - statically indeterminate
    - beams, 158
  - structural analysis, 154
- Structure collapse, 10
- Temperature determination
  - (post fire), 341
- Tension members, 223
- Testing procedures, 90, 327 *et seq*
- Thermal boundary conditions
  - convection, 144, 204
  - general, 144
  - radiation, 144, 204
- Thermal bowing of
  - masonry, 298
- Thermal conductivity
  - aluminium, 89
  - concrete, 84
  - insulation, 212
  - masonry, 87
  - steel, 80
  - timber, 89
- Thermal diffusivity
  - concrete, 86, 173
  - steel, 81
  - timber, 88
- Thermal expansion
  - aluminium, 119
  - concrete, 102
  - masonry, 116
  - steel, 93
  - steel fibre concretes, 111
- Timber
  - beams, 281, 286, 292
  - columns, 284, 289, 292
  - empirical methods, 286, 291
  - prescriptive approach to fire resistance, 41
  - rate of charring (natural fires), 279
  - rate of charring (standard test), 114, 279
  - residual section, 211, 291
  - specific heat, 89
  - strength and elasticity loss, 115, 281, 287
  - stud walls or floors, 294

- Timber (*continued*)
  - temperature calculations, 154
  - thermal conductivity, 89
  - thermal diffusivity, 88
- Trade-off, 24
- Transient creep behaviour of
  - concrete, 129, 134, 135, 137, 138
- Ultimate limit state, 14
- Ventilation controlled fire, 45, 57
- Web-infilled columns, 277
- Wrought iron, residual properties, 340
- Young's modulus (*see* Elastic modulus)

**This page intentionally left blank**